The collapse of shallow coal mine workings

Garrard, G. F. G.

THE COLLAPSE OF SHALLOW

COAL MINE WORKINGS

A Thesis submitted for the Degree of

Doctor of Philosophy

in the

University of Durham

by

G.F.G. GARRARD M.Sc.

July 1981

The Collapse of Shallow Coal Mine Workings

by G.F.G. Garrard

The present study was undertaken to investigate the mechanism of void migration and the collapse characteristics of old shallow surface (< 50m), pillar and stall coal mine workings. Simple stereo-photographic techniques have been employed to record these structures where they occur in the high walls of NCB and private opencast coal sites. Several relationships have been identified from this data, and the investigation concludes that the crushing of coal pillars at depth is rare and that the principal mechanism of failure involves the collapse of the roof material into the working.

A classification of failure mechanisms based on the frequency and spacing of horizontal and vertical discontinuities relative to the span of the working is proposed. Two distinct situations for analysis are recognised. The first involves the stability of the immediate roof, while the second is concerned with the stability of the 'arch' that develops when the immediate roof beam collapses. Continuous roof beams have been found to be rare in Coal Measures rocks and therefore simple beam analysis is considered to be of little use. Where discontinuities are present Voussoir beam analysis may be appropriate, and Voussoir beam theory has been corrected and extended to overcome some of the problems recognised with the technique.

Bulking and arching have been recognised as the 'normal' limiting factors on the height of collapse and are considered as complimentary failure mechanisms. For a 'typical coal mine collapse' situation arching is shown to be the dominant control. However, a review of arching has shown that in general all the theories underestimate the height of collapse. Thus, a statistically derived relationship of (collapse height = 2.68 x span of working) has been proposed as the limiting height for arching situations. Existing bulking relationships have been shown to be rather simplistic and appropriate corrections to the theories are suggested. An analysis of bulking factors derived from colliery discard has shown that a regional variation in this parameter is likely.

Acknowledgements.

I would like to acknowledge with thanks the help of those individuals and organisations who have helped and encouraged me throughout the pursuance of this project. In particular I am grateful to:-

N.E.R.C. for financial support during the first two years of the project.

The NCB. Opencast Executive and especially their site agents and surveying staff for assisting me with and during my field work.

The BSC. Surveyors department at Ibstock for providing me with open access to their abandonment and hazard plans.

The NCB. Civil Engineering department, Doncaster for access to the NCB.- Durham data base system.

Professor M.H.P. Bott and the staff and technicians of the Department of Geological Sciences for their general assistance, and to Professor P.B. Attewell in particular for the use of the facilities in the Engineering Geology Laboratories, Durham University.

I would also like to extend my sincerest thanks to my supervisor Dr. R.K. Taylor for initially conceiving the project but more particularly for his continued support and advice throughout the years. Without his subtle blend of encouragement and coercement this thesis would not have been written. I am also grateful to my present employer Mr. G. Walton for his patience, and for allowing me time off work to complete the thesis and to his secretary Liz for her help with the typing of tables and references.

Finally I would like to acknowledge the tremendous support and help afforded to me by my Parents and friends. I am particularly grateful to my fiancée Gill who in the past six months has spent much of her free time correcting my spelling, editing text, and drawing diagrams. The assistance of everyone who has been involved is greatly appreciated.

This thesis is dedicated to:-

My Grandfather for kindling my interest in old mines, and to my Parents for their continued support and encouragement over the years.

C O N T E N T S

LIST OF FIGURES

LIST OF TABLES

LIST OF PLATES

CHAPTER 1

INTRODUCTION.

1.1 INTRODUCTION

Many of the large industrial towns and cities of this country owe their development to the presence of underlying mineral seams. Most of these cities are still underlain by unrecorded and often unsuspected shafts and shallow mine workings.

In Britain, over 70,000 old mine workings have been charted in coal alone, and there are still an estimated 30,000 unrecorded mine workings yet to be found (Littlejohn, 1979). Over the years it is estimated that from these mines in excess of 20,000 million tonnes of coal has been extracted, together with related ironstones and fireclays (Willis, 1980). Access to many of these abandoned mines was by shaft and there are still an estimated 80,000 old shafts remaining in Britain. Once again some thousands of these are uncharted.

The problem posed by abandoned shallow mine workings is colossal but is not restricted to Great Britain. Virtually every developed and many third world countries are facing similar problems. Indeed it is pertinent to remember that subsidence engineering developed in response to this concern and was not a British development. The earliest practitioners of this 'art' were Belgian and French nationals (Shadbolt, 1977) and these countries are still facing significant problems from old mine workings. Today the USA has severe problems from collapsing mine workings over large areas of Pennsylvania and Appalachia (Gray et al., 1977, Beck et al., 1975). India (Singh et al. 1982) and Japan (Nishida et al., 1981) are among many countries for which ancient (and not so ancient) uncharted coal workings are now posing problems.

This thesis is concerned with the mode of failure that develops in shallow surface pillar and stall coal mines. However, the term shallow is rather vague with no clear definition. Piggott and Eynon (1977) suggested that, at its simplest, it could be said to be the depth from the surface beyond which the

influence of past mining has no effect, either at the surface or on any surface development.

This definition implies a 'safe depth', at or beyond which no surface subsidence will take place. This is an old and hotly disputed concept which seems to have originated as a result of subsidence in Liege, Belgium, in the late 1820's (Shadbolt, 1977). The accepted official opinion at that time was that no surface subsidence would occur if the workings were more than 100m deep.

Since this date a number of other depth 'cut-offs' have been suggested. This thesis is primarily concerned with workings at a depth of less than about 40 to 50m. Beyond this depth there is a significant possibility that the mine pillars will have crushed out or that the floor will have heaved into the workings. No evidence of pillar failure was seen in any of the opencast sites visited during the fieldwork and therefore, in the remainder of this thesis, this mode of failure will not be considered further.

Shallow mine workings can cause problems in a number of ways. Possibly the greatest risk to surface structures comes from the development of crown holes. These are depressions or holes which develop rapidly and unexpectedly at the surface and have their origin in the collapse of a mine roof possibly tens of metres below the surface. The progressive deterioration and collapse of the mine roof into the old working leads to the slow movement of a void or zone of loose or uncompacted material towards the surface (void migration, Plate 4). Where such a zone breaks the surface beneath a structure it can obviously cause problems (Plate 2). However, shallow mine workings can cause problems in other ways. For example it has been estimated that about 10% of all slope failures in opencast coal mines are related to the presence of old mine workings in, or just beneath, the high wall (Plate 2).

In an urban environment workings can be stabilised by grouting techniques. These techniques are extremely expensive, especially for the deeper workings. However, it is a well established observation that the incidence of crown holes generally decreases as the depth of the workings from the surface increases.

Therefore, in critical areas a decision frequently has to be made on whether to grout up the workings, or to leave them alone and hope that no surface subsidence will take place. Such a decision obviously involves an element of 'risk analysis' in which the cost of stabilising the workings is weighed up against the risk (and hence cost) of the collapse of the structure.

Over the years a number of rules of thumb have emerged to help an engineer to make such a decision. These 'rules' are partly based on observation and experience, and partly based on semi-analytical techniques (see Walton and Taylor, 1976, Piggott and Eynon, 1977, Carter, 1984). The purpose of this project was therefore to :-

1. Gather and analyse data on the collapse of shallow old mine workings.

2. To evaluate and review the methods of analysis that are currently, or could in the future be used to analyse the problem.

In Britain old mine workings for coal undoubtedly represent the greatest hazard and are the main concern of this thesis. However, many other minerals and rocks in every geological system and in just about every county, have at some stage or another been worked by partial extraction systems. The problems associated with the collapse of workings in such minerals are often identical to those posed by workings in coal. For this reason, and where such studies are pertinent to the development of the subject, old workings in minerals other than coal have been included.

Minerals other than coal worked by partial extraction methods include :- flint and chert, ironstone, brick and pottery clays, fireclays, China clay, ganisters, sandstone for building purposes, limestones including chalk, oil shales, salt, anhydrite and gypsum, potash, allum, slate, igneous rocks (eg Cleveland Dyke), Fuller's earth, iron oxides or ochre, jet and metal ores such as lead and copper from stratified mineral deposits.

It is also worth remembering that in many instances coal was not the most valuable mineral worked from a 'coal mine'. Table 1.1 presents a comparison of the value of some of the economic minerals from the Upper Carboniferous as recorded in Glasgow between 1804 and 1805 (Allen et al., 1984). These values give some idea of the financial incentives to mine minerals other than coal.

Table 1.1. VALUE OF ECONOMIC MINERALS IN GLASGOW BETWEEN 1804 AND 1805.

Rock or mineral	Price	Relative value (units)
1 cubic yard of good sandstone	1 shilling	12
1 ton of Airdrie blackband ironstone	2 shillings	24
1 ton of limestone	6d	6
1 ton of coal	5d	5
1 ton of fireclay	5-40 shillings depending on purity	60-480

1.2 LOCATION AGE AND SIZE OF THE PROBLEM.

1.2.1. DEVELOPMENT OF THE COALFIELDS.

The factors affecting the development of the different coalfields in the British Isles are numerous and extremely complex. Somewhat surprisingly the major milestones are not technological but rather political and economic. However, this is not to say that there were not severe technical problems that needed to be overcome. The principle technological problems facing the mines were drainage, ventilation, geology, haulage/winding and explosions.

The late 17th Century saw the start of a massive increase in the demand for coal. Neff (1932) saw this increase, and the development of the coalfields in general, as falling broadly into four main periods (Fig. 1.1).

1. A period prior to the middle of the 16th Century when demand for coal, and hence output, was governed by the populations attitude towards the fuel. During this period coal was used by the poor and by artisans who used it as a cheap and noxious alternative to wood. This period is characterised by bell pits and crop workings, and although important sociologically, is not of great significance with respect to present day stability problems. (see Taylor, 1975 for a

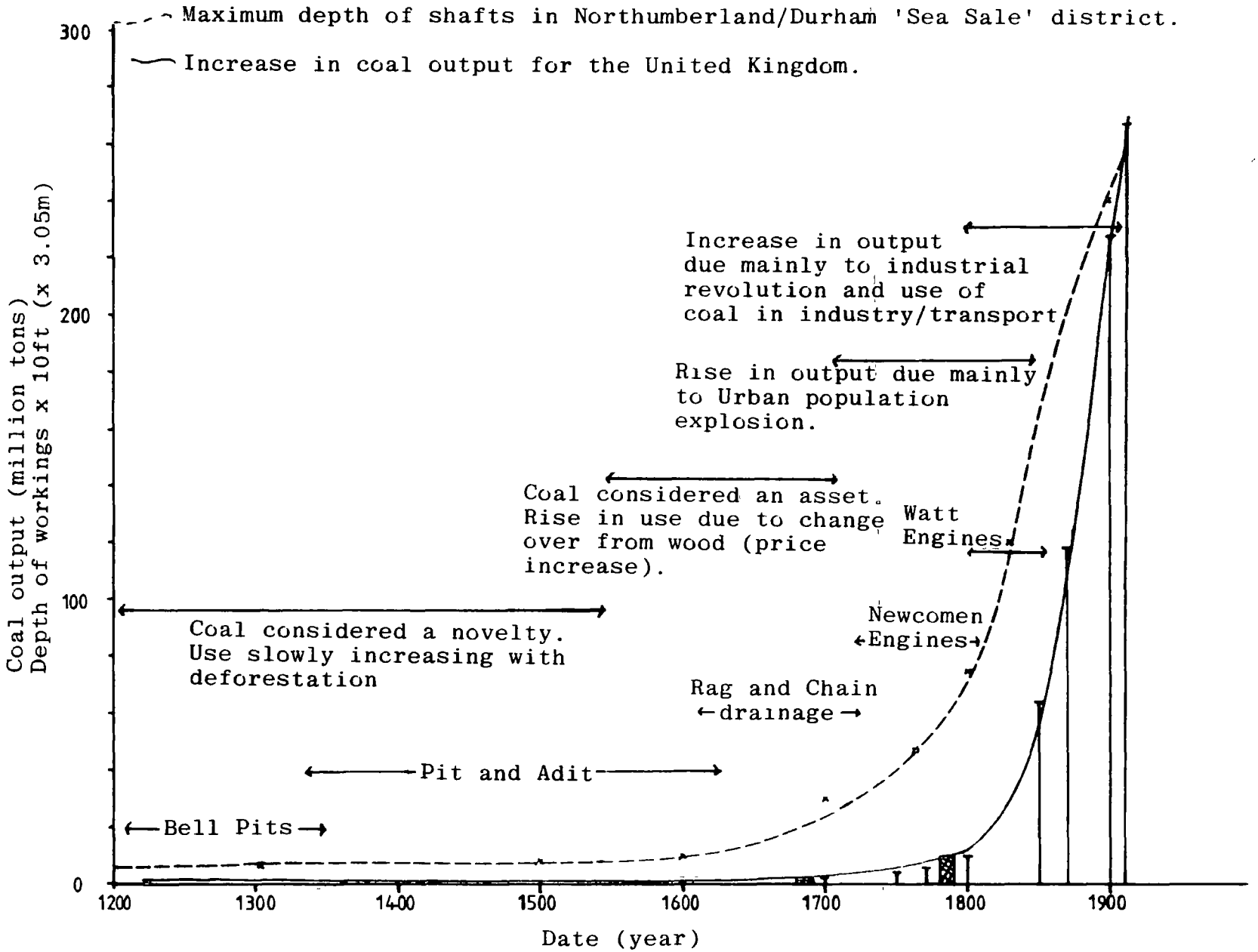

Figure 1.1 Generalised development of the coalfields.

description of bell pits, Fig. 1.2).

2. A period from roughly the middle of the 16th Century to the end of the 17th Century when wood was becoming increasingly costly and scarce (Medieval energy crisis, Humphrey et al., 1979) and coal was beginning to be seen as an asset. During this period coal became acceptable as a household fuel partly as a result of the accession of James 1st to the throne. (Scotland had been using coal for many years because of the scarcity of wood). Old workings from this period are occasionally encountered in inner city areas, or in other centres of population or development, but are generally not important geotechnically.

3. A shorter period lasting from the beginning of the 18th Century through to the end of the 19th Century when there was a phenomenal increase in coal demand, mostly accounted for by a rapid rise in the urban population. This period saw the diversification of mining systems and marks the beginning of the major stability problems of today.

4. A period from the beginning of the 19th Century through to the present day, which marked the change in society from predominately agricultural to industrial. This was characterised by a further increase in the demand for coal from the manufacturing industries and transport. The majority of shallow coal workings that today are creating problems are represented by the early part of this period.

An alternative method of viewing the development of the coalfields was suggested by Galloway (1835). He approached the subject from a mining technology viewpoint. However, this viewpoint is also essentially economic as 'necessity was the mother of invention' especially in the coal industry! Galloway (1835) used the development of drainage systems for the mines as the basis for his classification and differentiated five main periods or eras :- (Fig. 1.1)

1. A period prior to the middle of the 14th Century when little or no drainage was required and bell pits were the normal methods of coal production (Fig. 1.2).

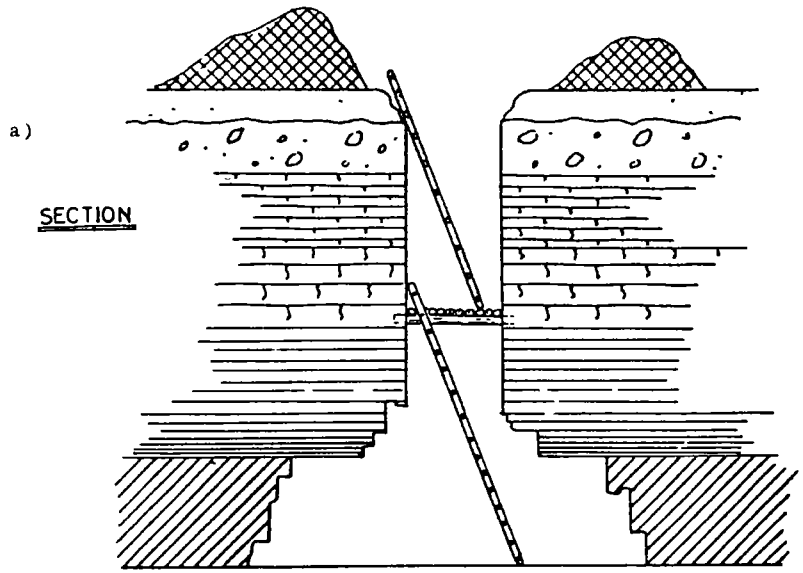

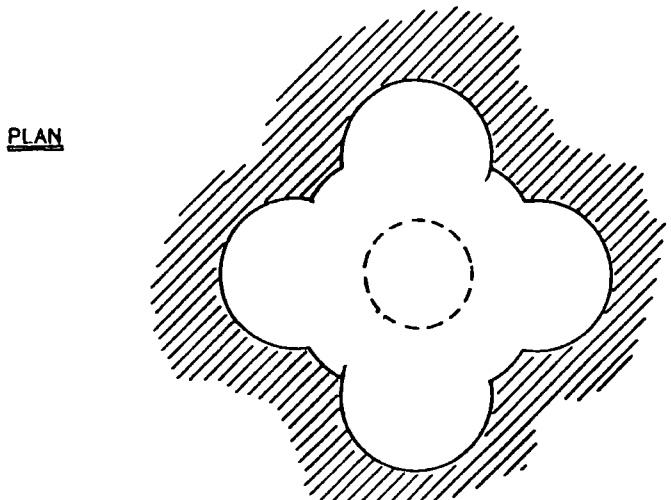

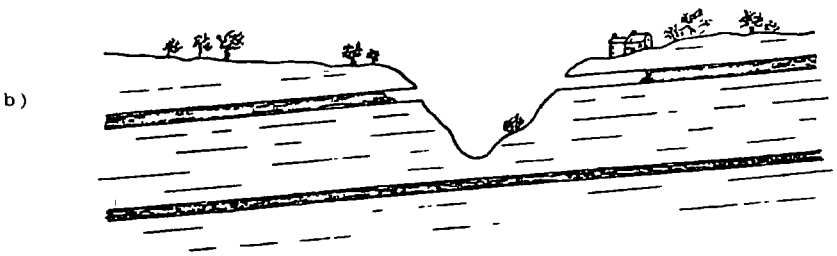

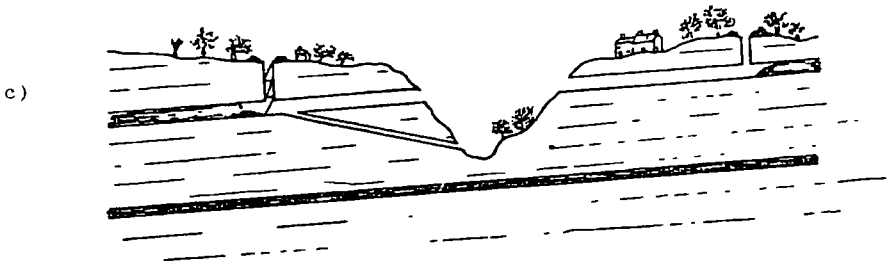

Early methods of mineral working

a) The "Bell pit" method of mineral working.

b) Outcrop working in steep sided valley.

c) Working of coal by the "Pit and Adit" system. Adits were driven into the seam with outlets (or soughs) at a lower level than the workings themselves to allow any accumulation of water to escape.

Figure 1 2 Early Mining Methods

2. The period between the 14th Century and the mid 17th Century when the majority of the coal was worked in ground drainable by soughs. This is the so called 'pit and adit' era (Fig. 1.2).

3. A period from about the beginning of the 17th Century through to the early 18th Century when the mines developed below the level of free drainage and simple pumps were required to keep the pits dry. This period saw the main diversification and development in the working methods.

4. A period from the early 18th Century through to the 19th Century which was characterised by the development of steam drainage. During this period most of the drainage problems were solved and 'tubbing' of watery strata during shaft sinking operations was developed. These advances laid the foundations for the development in the 19th Century of the deep winnings in the concealed coalfields.

5. A period from the early 19th Century onwards covering the development of the safety lamp. This invention largely made pillar robbing, or working the 'broken', feasible and many old mines were reworked from this time onwards.

While any division, whether on the basis of technology, drainage, or demand is quite arbitrary, the concepts are never the less valuable. The development of a coal mine in an area ultimately depended on the technology available and the demand for the product. Engineering geologists today are interested in whether these criteria were satisfied at a given date, in a given location. That is, was it profitable to sink a coal mine at point X at that time. If it was then how deep and how extensive was it likely to be. Having ascertained the likely depth and age relationship for an area, some assessment can be made of the mode of working employed and hence the likely geotechnical problems that exist in the area.

Some of these questions can, in part, be answered by integrating into the previous concepts of technology and demand a third concept of transport. Coal is a bulk commodity and transport has always been the key to its development.

Transport history within Britain can be conveniently divided into three periods :-

1. The period prior to about 1760 when the only transport available was navigable rivers, sea transport, roads and in some cases tramways.

2. The period from about 1760 to 1815 which was dominated by the development of canals.

3. The period post 1830 during which railways were developed. Some of the rapid increase in demand for 'steam coals' (development of the S. Wales coalfield) was in response to the development of steam engines.

1.3 ECONOMIC DIVISIONS OF THE COALFIELDS.

On the basis of transport it is thus possible to sub-divide each of the coalfields into sea sale and land sale districts. From about 1760 a third division, that of industry sale can also be included.

During the industrial revolution the main demand for coal came from the household market. Prior to the development of the canals, the sea sale districts of a coalfield, or the parts of a coalfield with a navigable river, developed rapidly unlike the land sale districts which had a virtually static and largely seasonal demand.

Most roads during the 17th and 18th Centuries were in a deplorable condition and this restricted inland coal sales to within a maximum distance of about 10 miles of the pit head. Neff (1932) estimates that the cost of coal almost doubled for every 2 miles from the pit head, and in 1675 it was said that carrying coal 300 miles by sea was ordinarily no more expensive than carrying it 15-20 miles by land. In the case of the Newcastle-London trade route the economic cut-off was 3-4 miles inland from the River Tyne.

This relative cheapness of sea transport was not challenged until the development of the canals and railways. These inventions brought to the land sale districts all the advantages and opportunities such as wider distribution

that had hitherto only been enjoyed by the sea sale districts.

In terms of mine development, the export potential of sea sale districts meant that the mining in these regions developed deeper and faster than there land sale equivalents. At this time sea sale areas were technologically the most advanced (eg. Newcastle and Cumberland in late 18th Century), and were the first to systemise their working techniques. Such areas quickly abandoned the wasteful methods of mining such as irregular shaped pillars, random coal exploitation, stacking of small coal underground and so forth (slack was used for salt production in sea sale districts, cf. the stacking of slack in the Midlands). Furthermore, the relatively large size of sea sale collieries meant that the owners were correspondingly more wealthy and thus had more finance available for investment in the development of the new mining techniques. It is interesting to note that the collieries in the Tyne sea sale district (which were probably the richest) were the first to adopt panel work as well as pillar robbing or 'working the broken' in the 1830's. These areas were also the first to adopt power winding in order to maximise coal production from a single shaft. It was also sea sale districts that developed and first used safety lamps.

1.3.1. SEA SALE DISTRICTS.

Prior to the development of canals and railways, the output of a sea sale colliery would have been about 4-6 times that of a land sale colliery. At the beginning of the 18th Century three sea sale collieries in the Broxley district of the Bristol and Somerset coalfield each produced upwards of 30,000 tons/year. At the same time 34 collieries in the Durham sea sale district were each providing somewhere in the region of 55,000 tons/year (Neff, 1932).

1.3.2. LAND SALE DISTRICTS.

Although the sea sale districts were the deepest and best equiped, any assumption that the majority of the coal produced came from these districts would be entirely false. Figure 1.3 shows the percentage output of coal for each district.

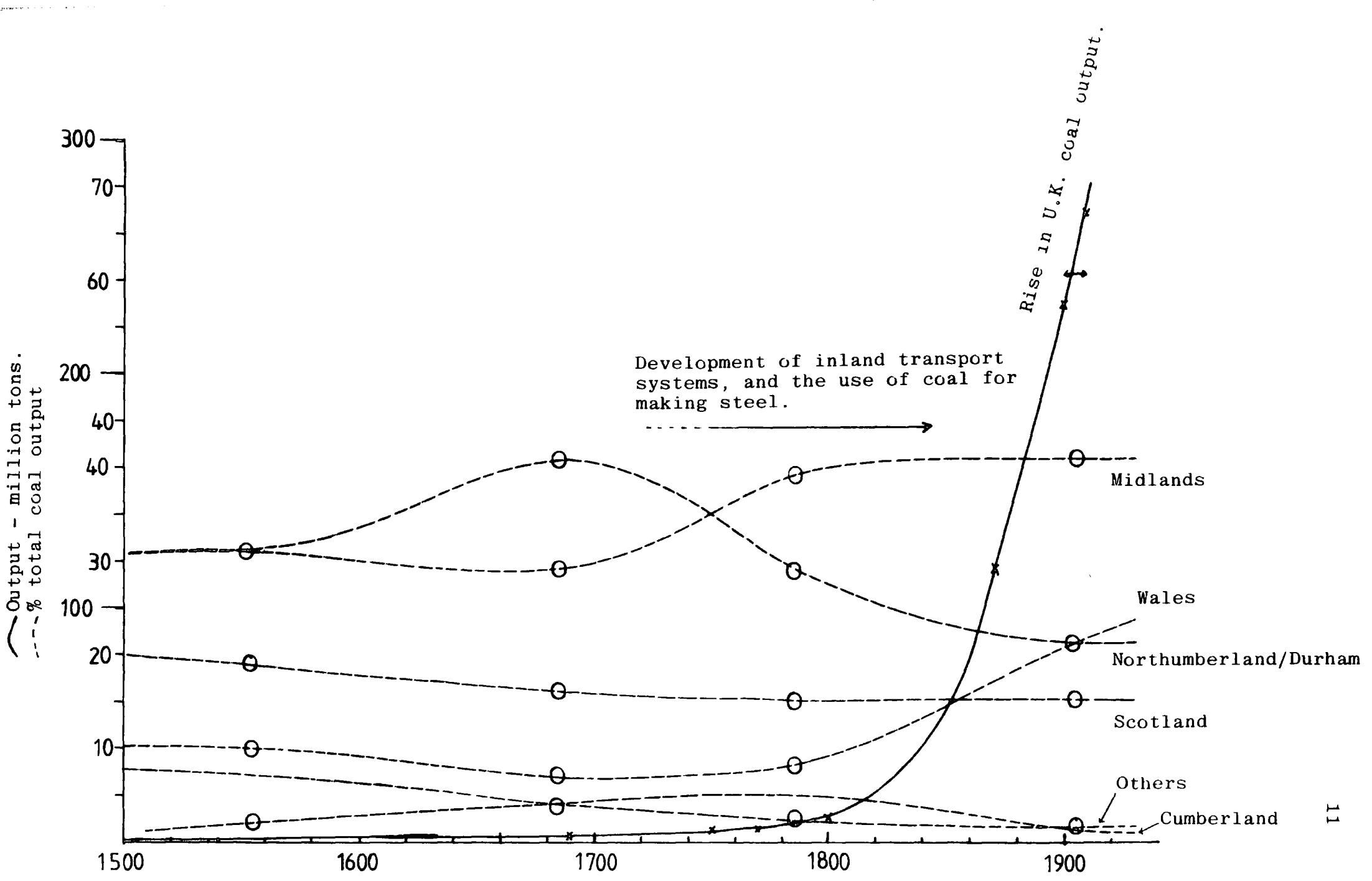

Figure 1.3 Coalfield output expressed as a percentage of total output.

The difference between the predominately sea sale and the land sale districts is that in the latter there were a greater number of collieries each supplying a small local demand. This led to piecemeal and often wasteful exploitation. At the beginning of the 18th Century the annual output of the average land sale colliery has been estimated to be between 2,000 and 5,000 tons per annum. At the beginning of the 19th Century, before the arrival of the railways, the output of the land sale Durham collieries was about 5,600 ton/year per colliery. This is one tenth of the output from an equivalent sea sale colliery at this time.

The small size of the land sale collieries meant that investment was also less. This restricted the operation to the near surface because of the large cost of pumping and winding. Such features changed dramatically with the arrival of canal and railway transport, and many operations within reasonable distance of such facilities exploded into life in response to the opportunity these afforded (Smailes, 1935).

1.3.3. INDUSTRY SALE DISTRICTS.

The development of industry sale districts has already been mentioned in connection with land sale districts. With the development of the canal system, the coalfields of the Midlands were opened up to a whole new market. Previous to this time coal had been confined largely to domestic use, but with the achievement of Dud Dudley in 1707 in smelting iron with coal (a process not widely implemented until 1750), the coal industry was set for rapid growth. Prior to this time 50% of the nations' iron had been imported from Sweden.

To summarise, sea sale collieries can generally be said to have been deeper, better worked and to have had fewer shafts per colliery than their land sale counterparts. With the development of land based transport systems and the new industrial processes, sea sale collieries declined relative to land sale collieries. This was because the former had already exploited the rich surface seams and were faced with more expensive sinkings to deeper seams. These

financial pressures led, in the sea sale districts, to the development of pillar robbing and the introduction of retreat mining systems (working the broken).

1.4. SHAFT DEPTHS AND MINING METHODS.

Figure 1.1 shows both the increase in natural coal production as well as the increase in depth for the Northumberland and Durham coalfield. It follows from the previous discussion that the other coalfields will have very different depth to age relationships. To obtain some idea of these relationships a systematic study was undertaken of all the available coal mining literature. This included a number of primary sources (eg. Contemporaneous descriptions of workings, etc.) as well as a large number of 19th Century secondary sources too numerous to mention (over 40).

These works were searched for references to coal mine or shaft depths. Where this information was found it was recorded, together with the location of the coal mine and the date of the original observation. This information has been summarised in Figures 1.4a-d and these Figures probably represent the maximum depth of coal workings in the coalfields at any given time. It should be emphasised however that the authors of the primary sources (from which the information was originally extracted) usually only recorded the 'exceptional' mine. At that time an exceptional mine was one that was unusually deep or had particular technological problems. The information in Figures 1.4a-d should therefore, be used only as an indicator of the likely maximum depth that was attainable in the district at the time.

Coal mining developed in response to economic demands and because the requirements and conditions in the different coalfields varied (ie. geological structures, seam thickness, roof strength, floor strength, etc.) it is not surprising that the methods of working diversified. By the beginning of the 18th Century local methods of working had developed and become well established even entrenched (Dunn, 1852). In the following centuries attempts to introduce 'new methods' were often fiercely resisted by the local miners. It was only at about the turn of the 19th Century that local systems and methods of working

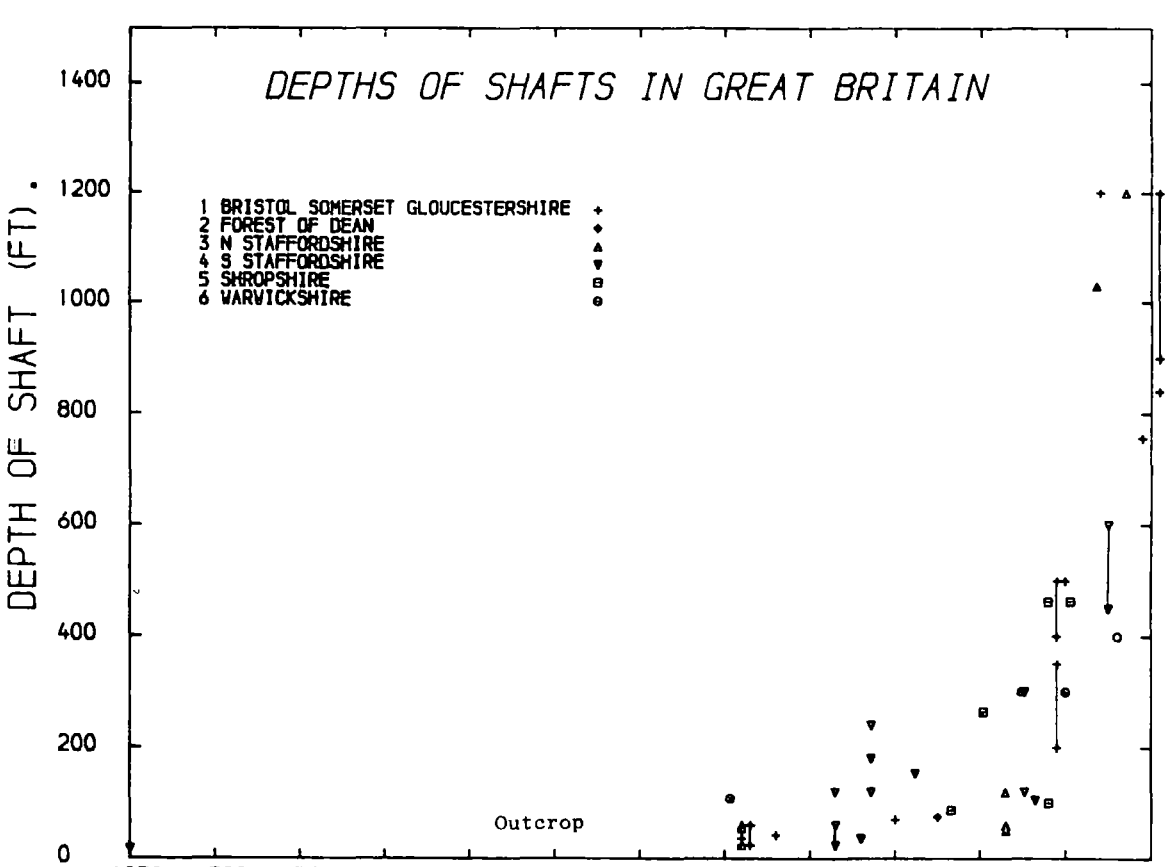

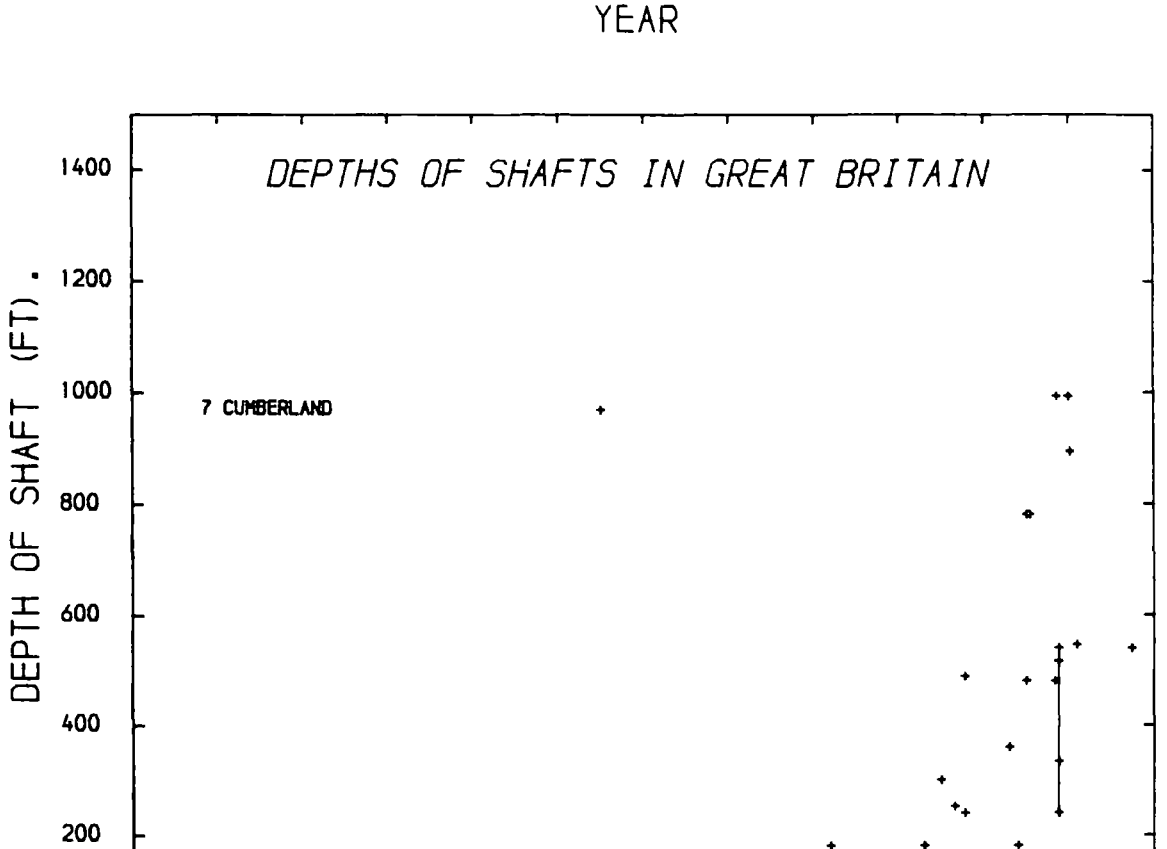

Figure 1.4a Age - depth relationship for the major coalfields

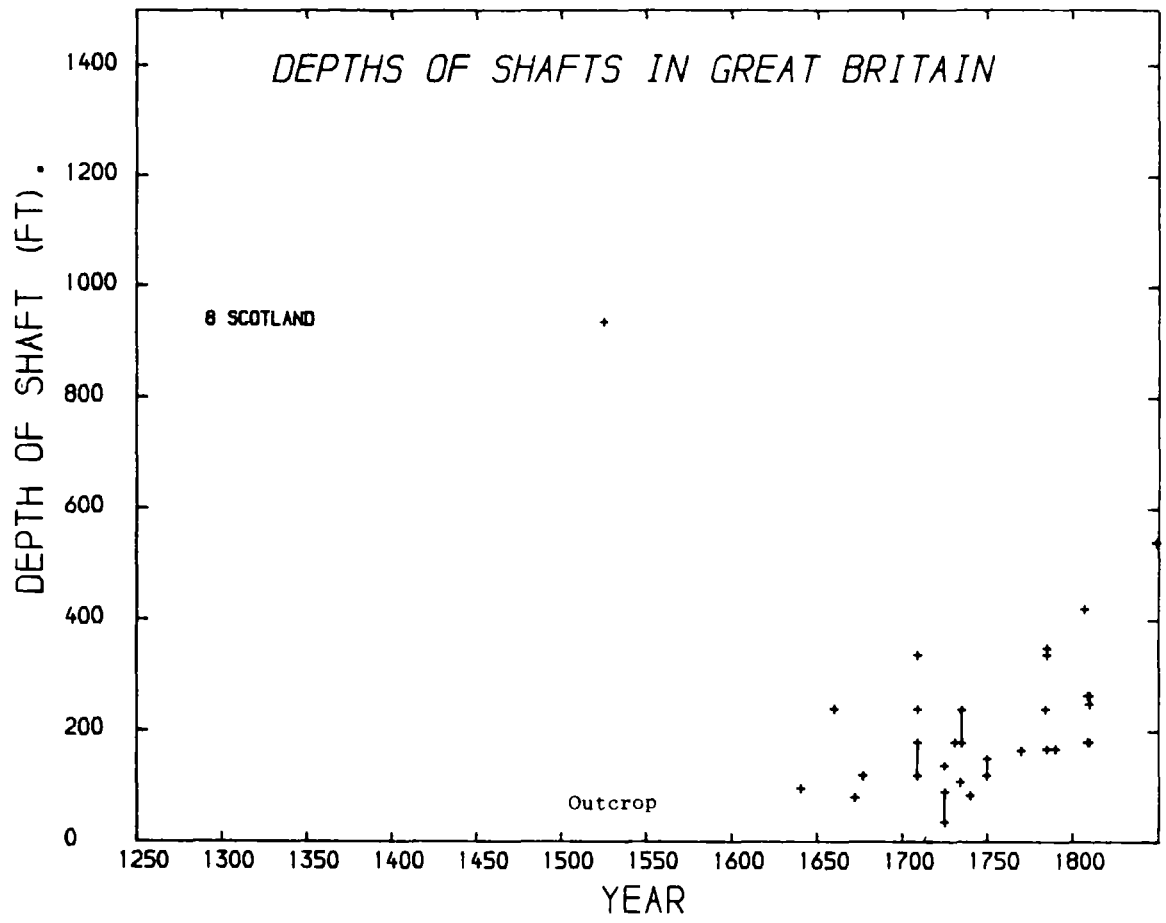

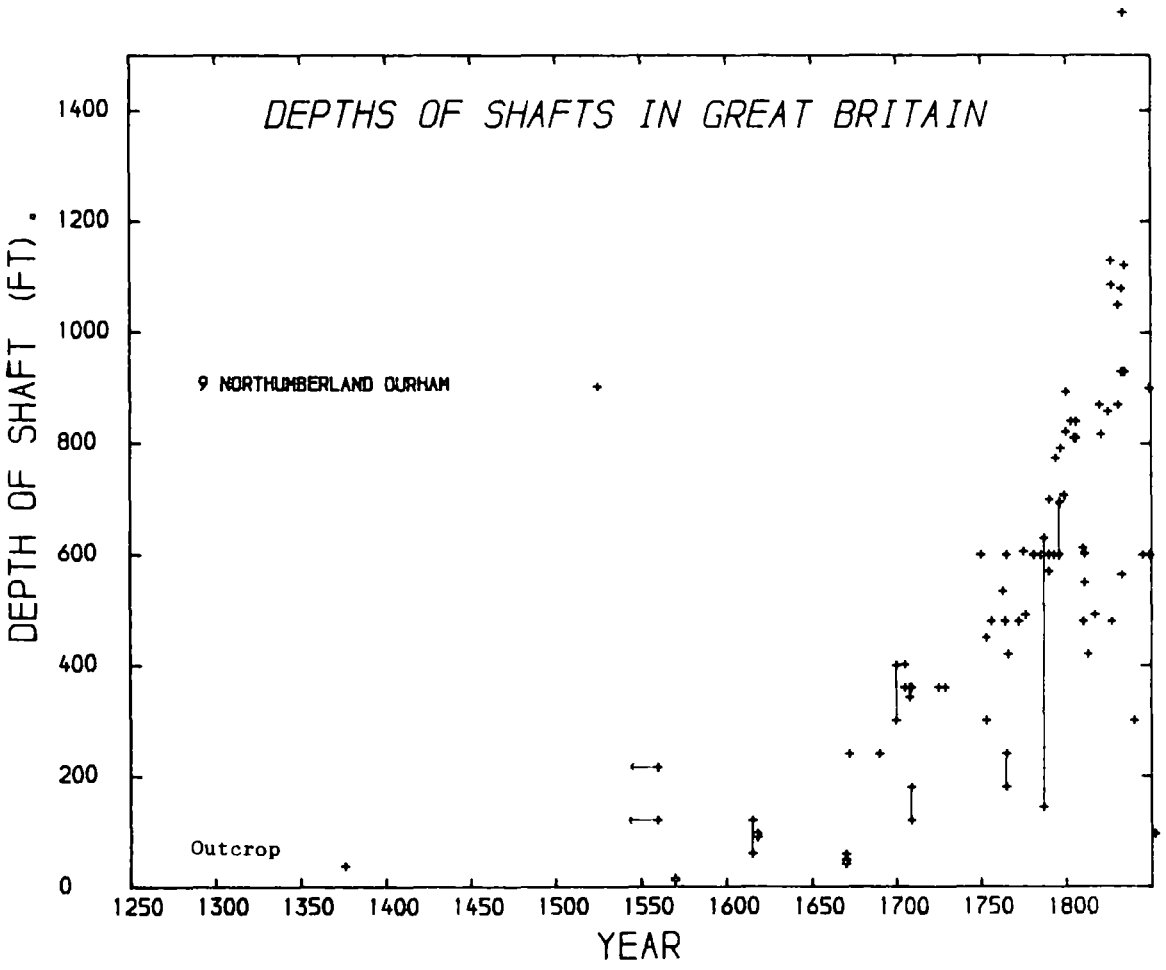

Figure 1.4b Age - depth relationship for the major coalfields

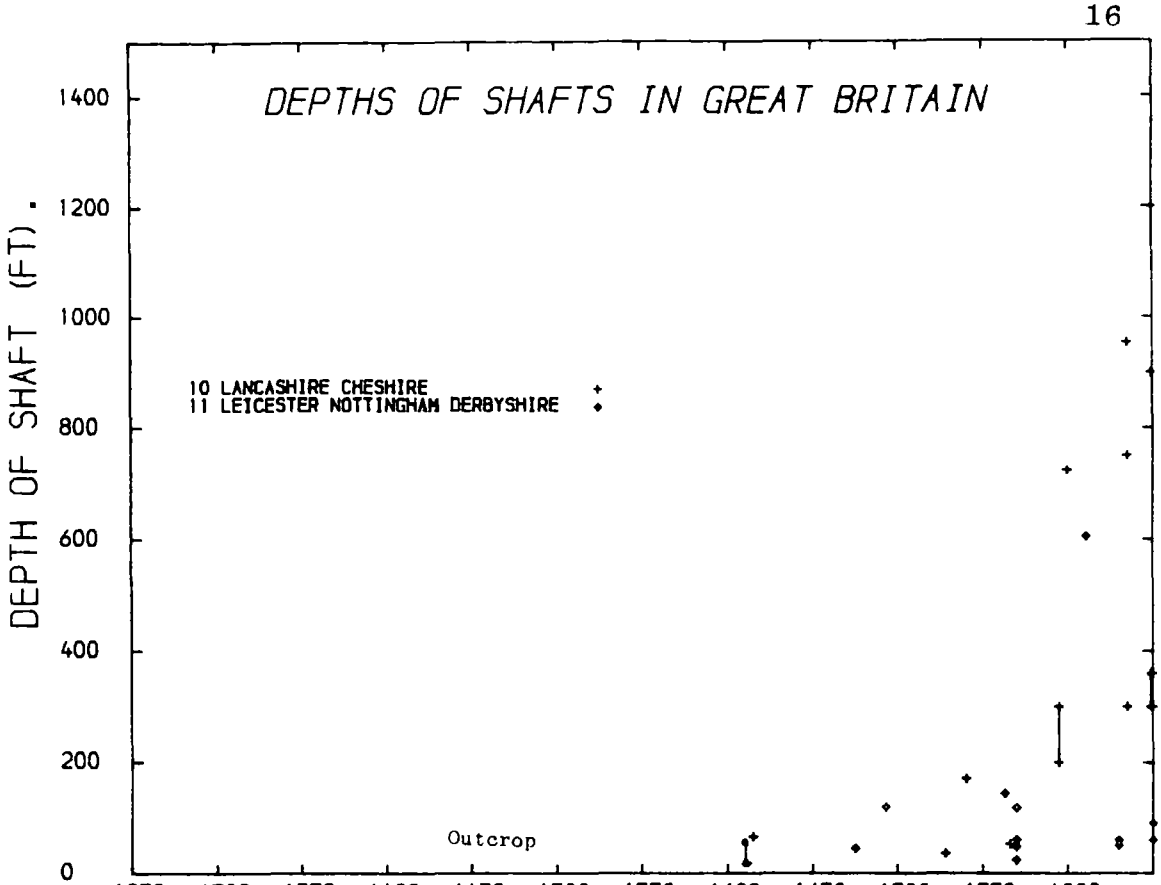

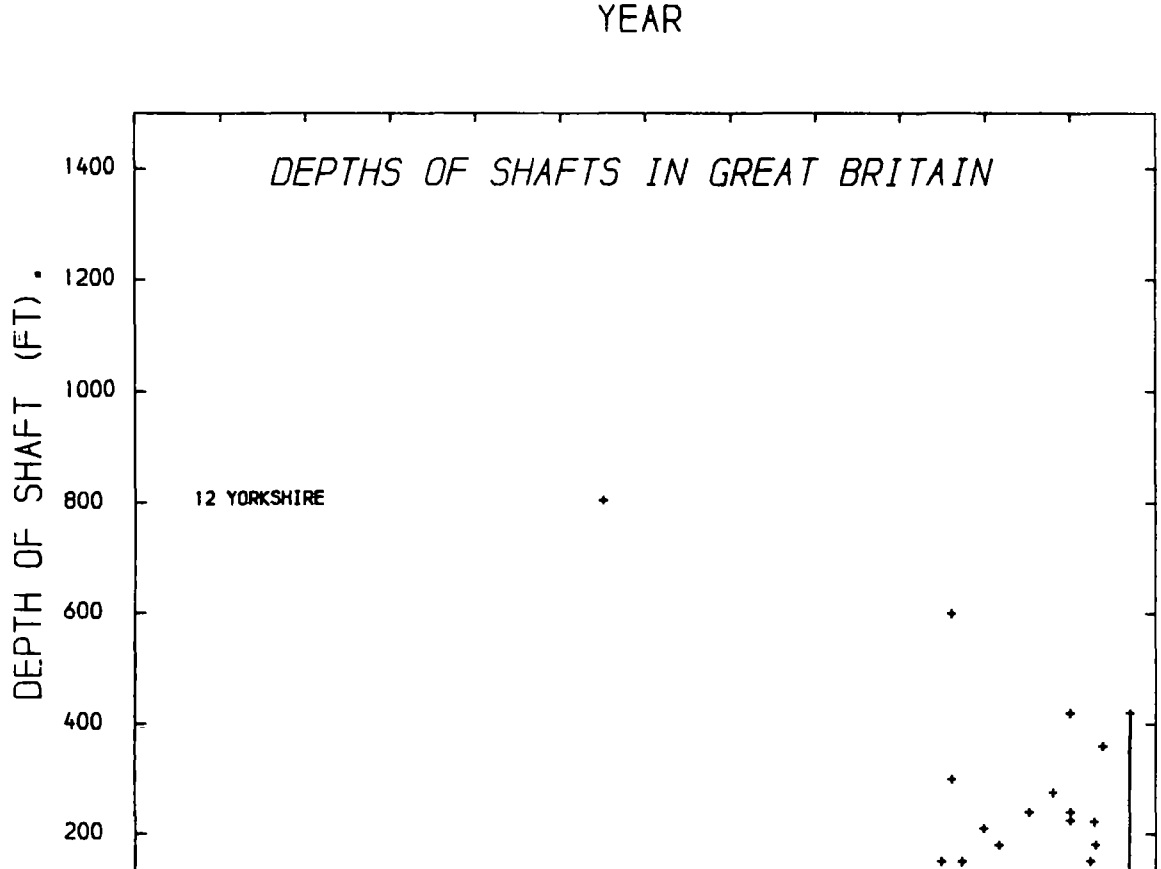

Figure 1 4c Age - depth relationship for the major coalfields

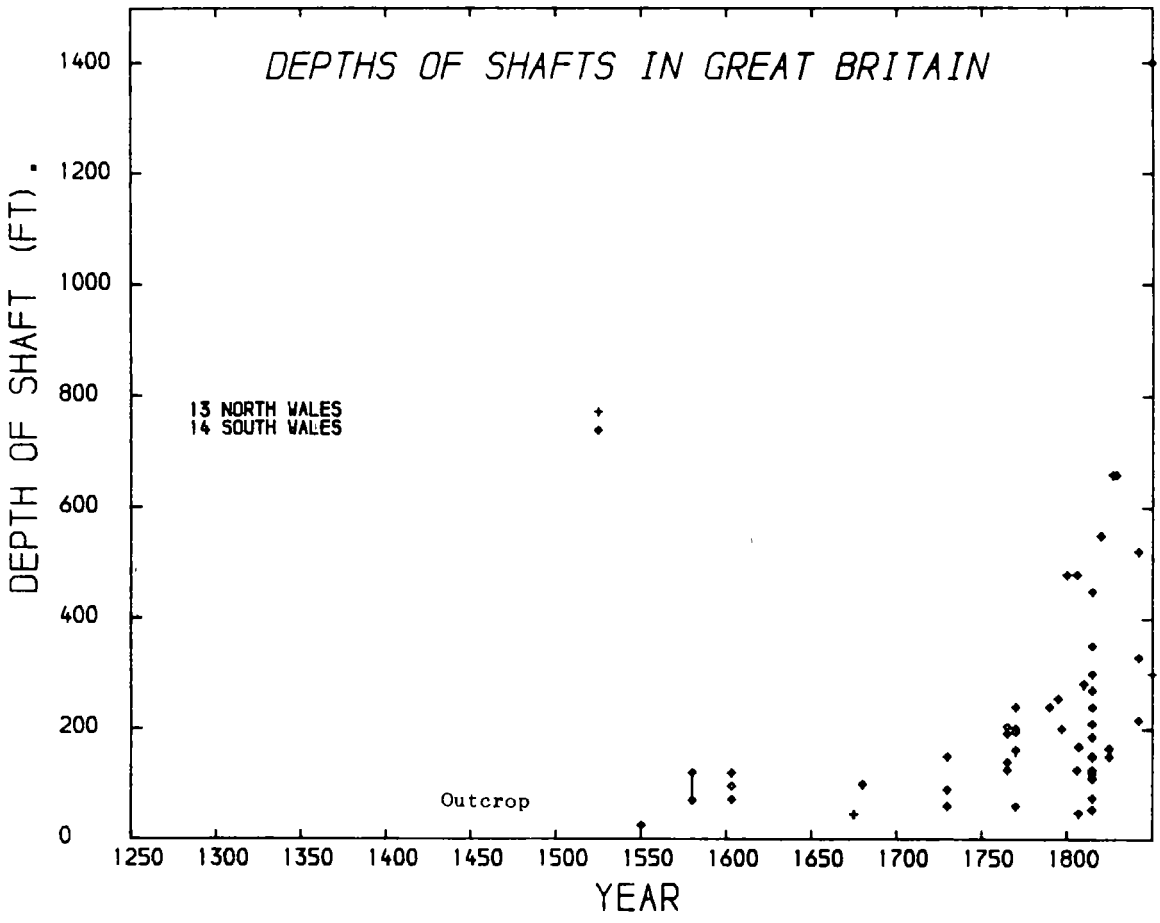

Figure 1 4d Age - depth relationship for the major coalfields

started to break down. In the last Century the diversification has been dramatically reduced primarily because of increased mechanisation and the relatively uniform cost of distribution. This has brought about the virtual elimination of pillar and stall technology from British mines and the almost universal use of longwall techniques.

Galloway (1835) summarised the diversifications in working methods and recognised two principle methods of working : pillar and stall and longwall. At a slightly later date a third system , intermediate between the first two, developed which was sufficiently different for Galloway (1835) to assign it its own category. Appropriately he refered to this system as the "intermediate system".

Probably the greatest diversifications exist within what may be termed the pillar and stall method of mining. Within this group regional patterns of working emerged and each variant was given its own name, for example 'Stoop and room' (Scotland), 'Bord and pillar' (North east), 'Post and stall' (S. Wales), 'Post and bank' (Yorkshire). Some of the systems are illustrated in Figure 1.5.

The intermediate system is perhaps the only one that needs explanation. In this system the seam was divided up by roadways into large pillars or panels. Unlike the pillar and stall technique, which created small pillars, the main coal production from the intermediate system came from the working (by longwall methods) of the centre of the large pillars. By this method virtually the complete pillar was removed except for narrow supporting ribs which were left to support the passages (Fig 1.5).

The regional diversification of the mining techniques is further complicated by the adoption of retreat mining. In some areas the mine was first developed to its boundaries at which point the coal was then worked in a direction towards (outbye) rather than away from the shaft bottom.

Table 1.2 and Figure 1.6 summarise the methods of working adopted. The information implies that the greatest problems from old workings will be in those areas traditionally worked by pillar and stall techniques. In contrast

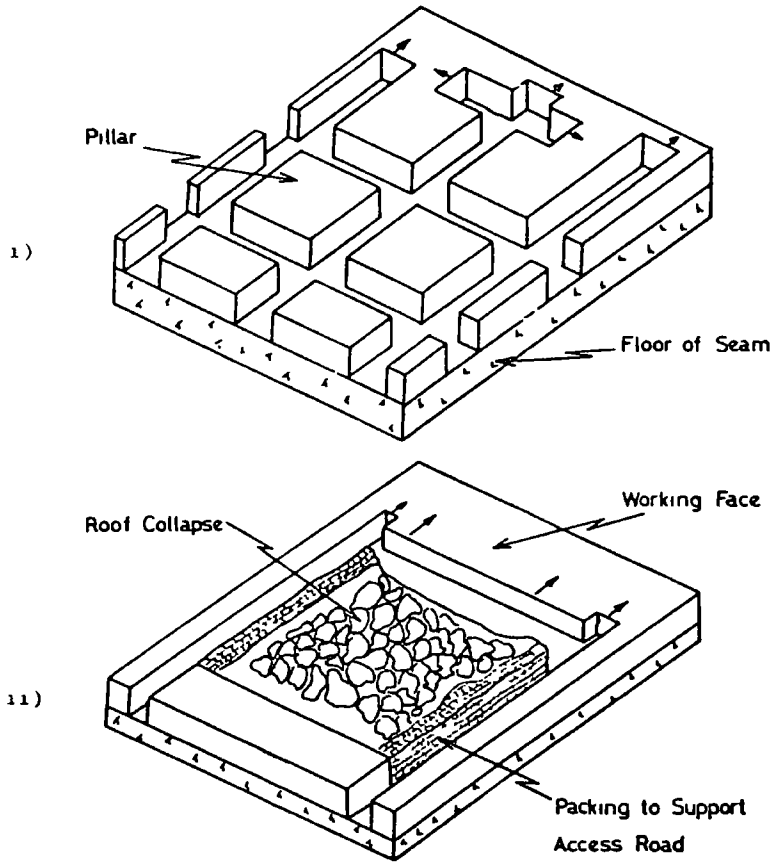

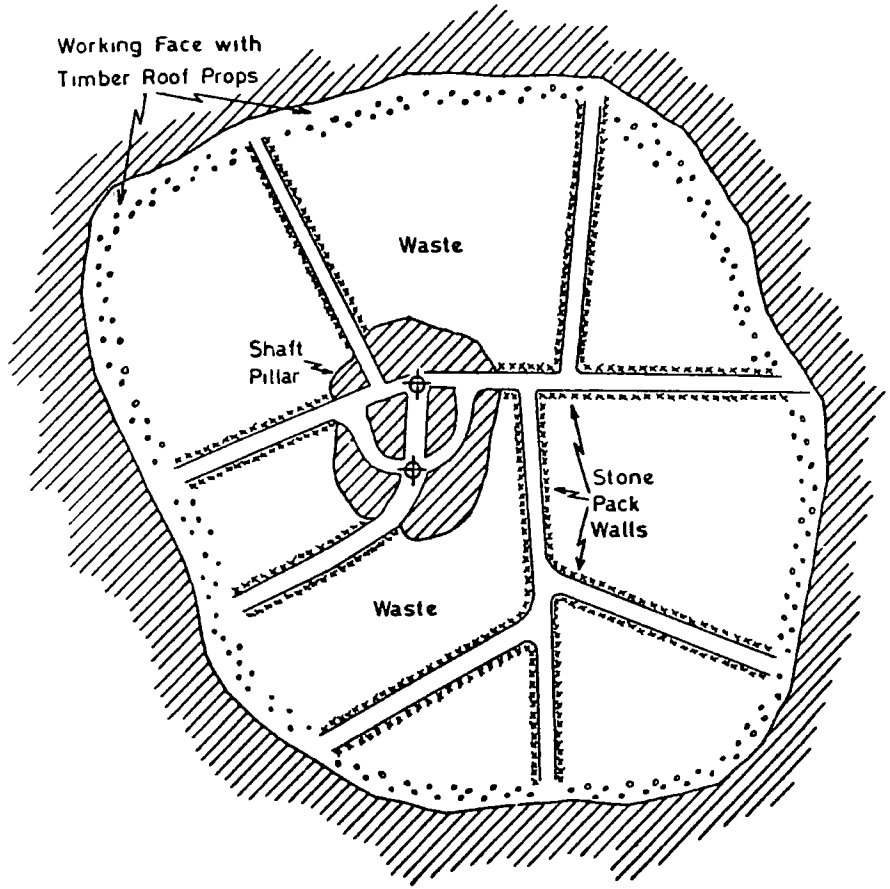

FIGURE 1.5 a - b EARLY METHODS OF MINE WORKING.

a) Diagrammatic layouts of mining methods

i) Room-and-Pillar workings

ii) Longwall workings Arrows indicate direction of advance of faces.

b) Early longwall workings. In this 19th Century longwall system, faces were driven out from a pair of shafts protected from subsidence by a coal pillar. The resulting face was roughly circular. The need to keep open gates through the wastes meant the system was self limiting and not suited to mechanised methods

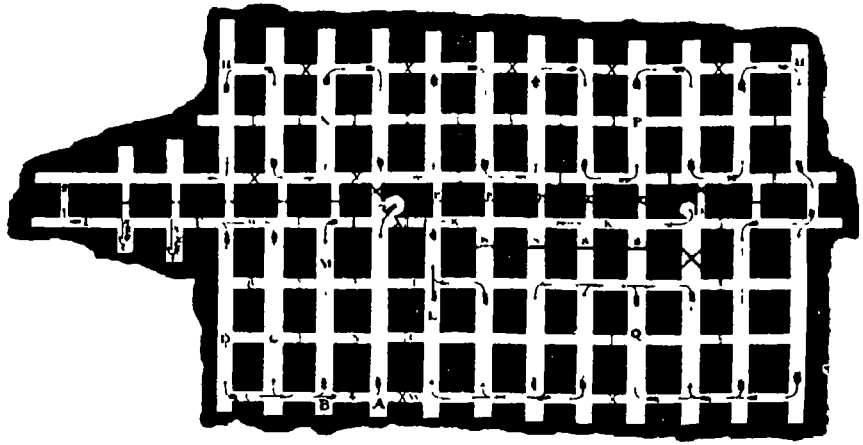

f. Typical pillar layout in a late 18th. C. mine in the Northumberland/ Durham coalfield. Arrows indicate ventilation flow. Note shaft positions. (after Galloway, 1835).

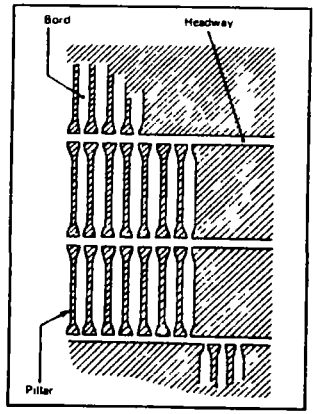

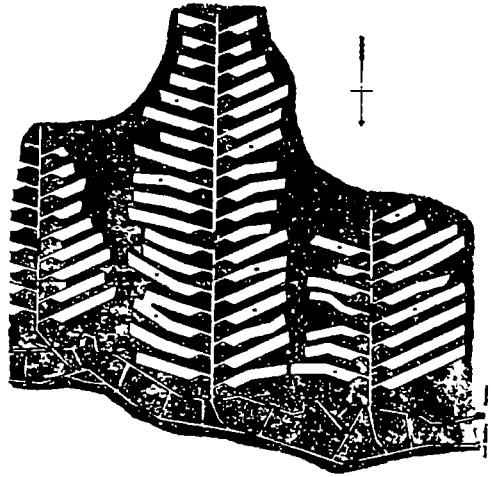

g. Bord and pillar working - Derwent main, Newcastle. Late 17th. C. Note necking of bords to increase roof stability at the intersections (after Galloway, 1835).

h. Post and stall workings in a dipping seam - South Wales. 17th. C. (after Galloway, 1835).

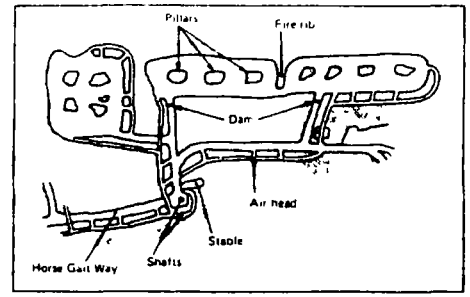

c. Square work - South Staffordshire, early 18th. C. This method of working was developed to work the Staffordshire thick seam which was susceptible to spontaneous combustion. (After Galloway, 1835)

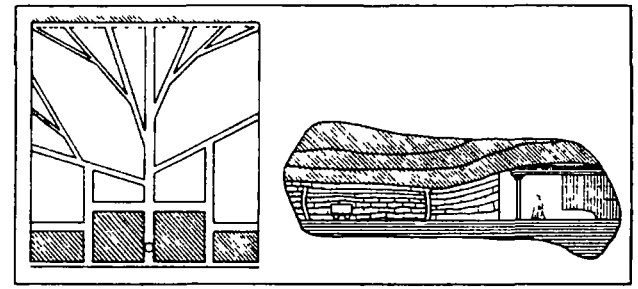

d. The longwall method introduced in Shropshire in the late 17th. C. (After Galloway, 1835).

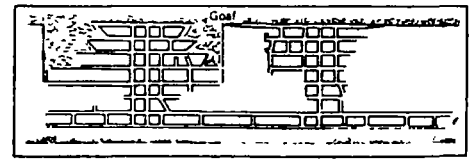

e. Room and pillar working in very steeply dipping seams - Scotland, Lancashire, Staffordshire and Somerset. (After Hughes, 1904).

FIGURE 1 5 c - h EARLY METHODS OF MINE WORKING

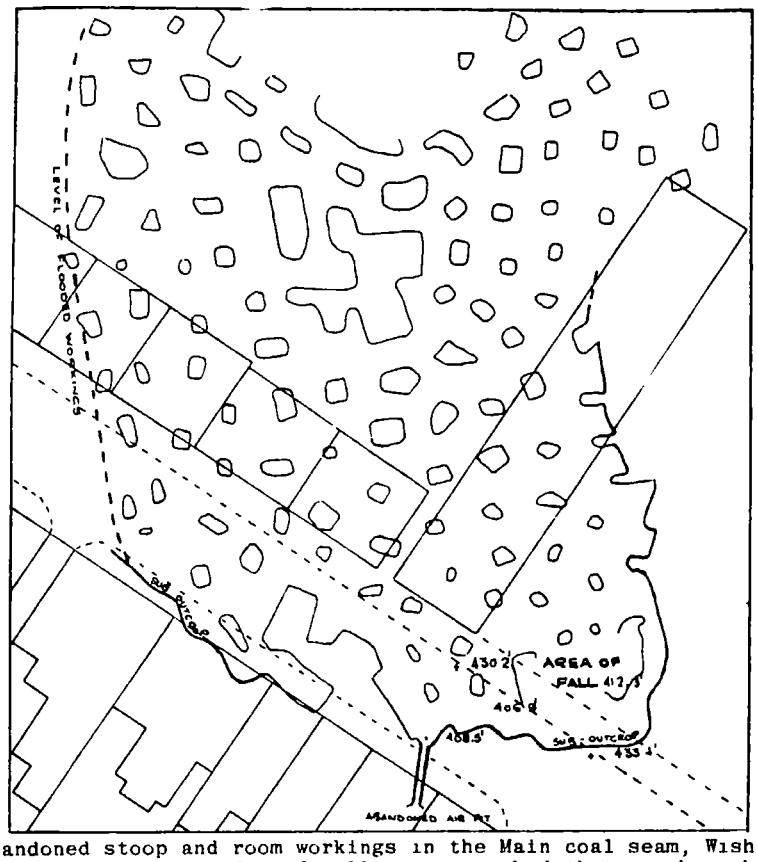

i. Abandoned stoop and room workings in the Main coal seam, Wishaw Scotland. An area of roof collapse is marked that was brought about by the vibrations of an earth moving machine. (After Maxwell, 1971).

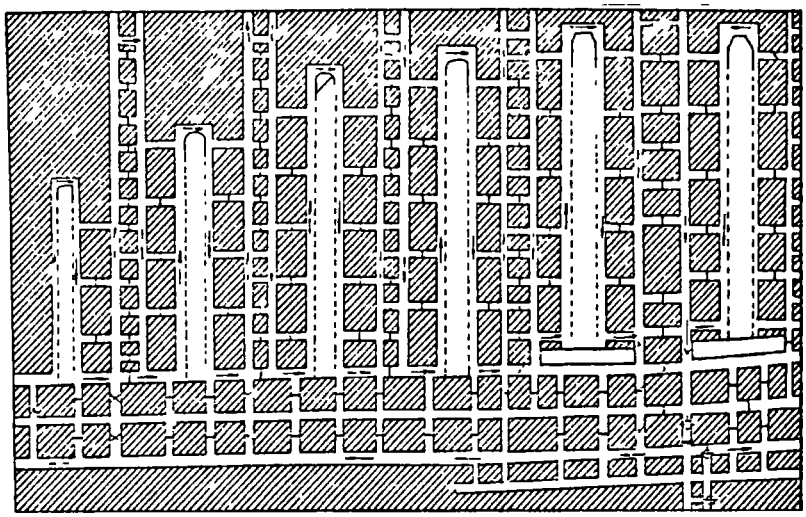

j. South levels, Lund-hill mine. 'Intermediate' system of working typical of Yorkshire early 19th. C. Arrows show direction of ventilation. (After Hall, 1977).

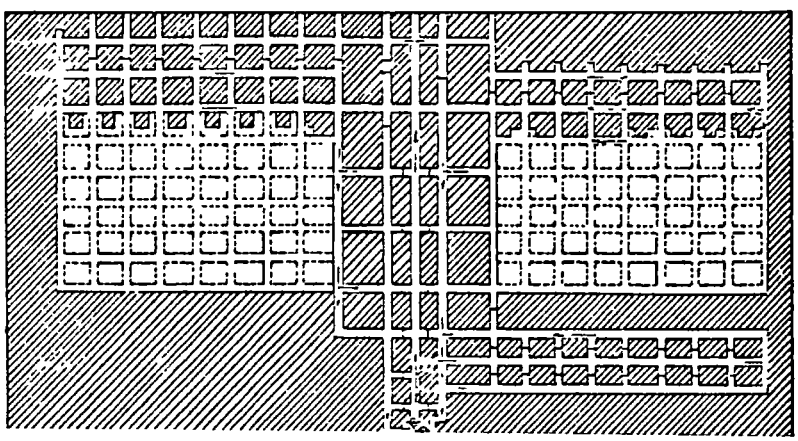

k. Modified pillar workings. This method, widely adopted in the north of England in the late 19th. C., employed teams of miners driving the headings (working the whole), whilst others followed clearing the pillars created (working the broken).

FIGURE 1.5 i - k EARLY METHODS OF MINE WORKING

Method of Working

Pillar and Stall	Intermediate	Longwall
Northumberland	E. Yorkshire	Shropshire
Durham	Derbyshire	N. Staffs
Scotland	Nottinghamshire	S. Staffs
Cumberland	Leicestershire	Warwickshire
Lancashire	N. Staffs	Somerset
Cheshire	N. Wales	Forest of Dean
S. Wales		Scremerston district (Northumberland)

Direction of working.

Those coalfields operating retreat mining.

Central parts of England
N. Staffordshire
S. Staffordshire

Parts of the following:-

Warwickshire
Shropshire
Lancashire
Yorkshire
Derbyshire
S. Wales

(After Galloway, 1835)

Table 1.2 Methods of working adopted by the coalfields of Britain.

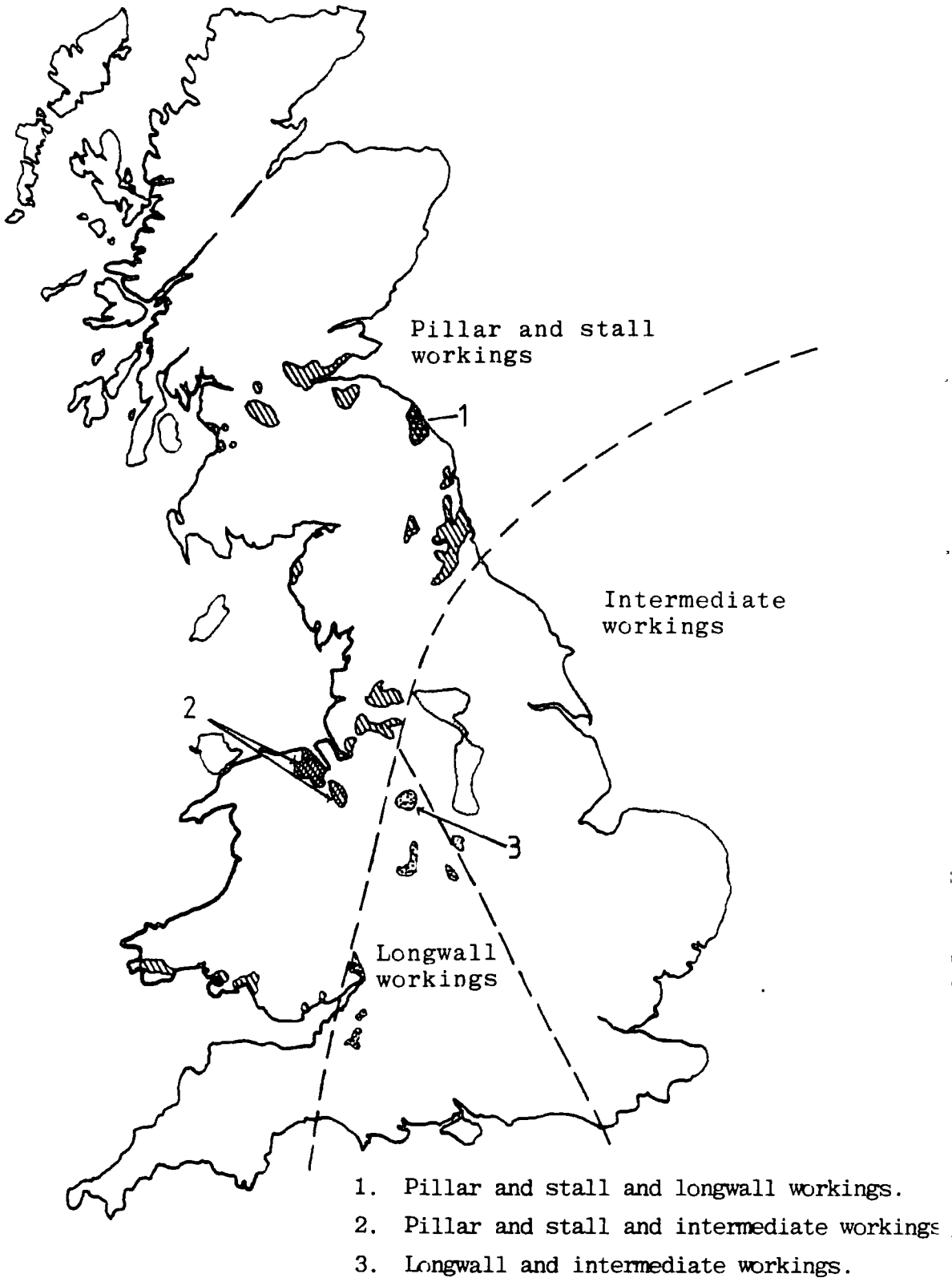

Figure 1.6 Distribution of exposed coalfields in the U.K. and adopted methods of mining.

those coalfields that have always used longwall methods will cause the least problems, as the mines in the areas will have completely collapsed long ago. Plate 6 shows a typical early 18th Century (Leicestershire) Midlands longwall face. The face was back-stowed with slack and partings as the workings progressed. In such a case the only potential source of danger are 'open' roadways at the edge of the pillars. The waste in this case was very well consolidated and stable.

1.4.1. MINE LAYOUT.

Prior to the late 19th Century the mines were all worked by hand, and therefore in the absence of other factors, such as a steep dip, the layout of the mine was usually determined by the cleat direction in the coal. In Britain the major cleat direction is approximately NNW-SSE, but local variations from this direction are common. A coal face advancing at right angles to the cleat direction was generally easier to get than a coal face running parallel to the cleat. Where the coal was worked at right angles to the cleat it would come down in long slabby pieces especially if the weight of the roof strata was 'thrown on to the face'. A working in this orientation was known as 'the face' or 'bord'. A coal face advancing parallel to the cleat was said to be on end or headways to the coal. Faces in this direction produced cube shaped coal and were much harder to work. However, in there favour they generally offered better roof conditions. A face in a direction midway between the bord and end was referred to as being 'half and half' or 'crosscut'. Early mechanised coal faces were often on end or at a few degrees from it.

The best roof conditions were usually encountered in the headings. This was because the orientation of the cleat in the pillars made them 'soft' at the edges. Headings were thus generally used for transport and access while the main coal production came from the bord or face workings (eg. Holland, 1841)

Workings parallel to the cleat (bordways workings) are therefore usually wider than workings at right angles to the cleat (headings). This should be borne in mind in the following sections. Working in crosscut was also apparently avoided

where ever possible.

In other coalfields however, notably S. Wales and the Edge district in Scotland crosscut working was carried out, but this was due to the highly inclined nature of the seams. Taylor (1983) has also reported instances of crosscut workings in Yorkshire, but this was apparently done to overcome stability problems arising from well developed jointing in the massive sandstone roof.

In steeply dipping seams headings were frequently driven on full dip with the bord driven on or close to the strike of the coal seam. By this method the working places were made as near horizontal as possible. An extreme version of this practice is illustrated by the workings in the Edge district in Scotland (Figure 1.5). Here the seams commonly dip at angles in excess of 70 degrees and in the past coal was won by overhand stoping techniques.

The underground layout of a modern mechanised longwall mine is generally controlled by the frequency and orientation of the faults that occur in the area. In the past the structural geology of a colliery was of less importance because hand mining was much more flexible. Small faults were usually accommodated in the pillar layout if or when they were encountered. However, the more major faults did have a profound effect on the development and size of the early mines. In Lancashire for example, faulting divides the coalfield into a number of fairly narrow belts. In such situations the size and shape of the collieries were often controlled by such boundary faults.

The throw of a fault did not necessarily have to be very great to promote a 'parallel or ribbon development'. From an early date faults were recognised as potential 'feeders' for water and so were treated with caution (economics of pumping).

In the previous section an attempt has been made to draw the readers attention to the complexity of the development of the coalfields in Britain. The numerous factors discussed obviously affect the magnitude and nature of the geotechnical problems that are faced today. The same factors also affect the quality and value of the data that can be gathered in the field. Each area underlain by old

mine workings will face site specific problems, and therefore the analysis and comments presented in the following sections can only ever be summary observations on what is a very complicated geotechnical problem.

1.5. COLLAPSE MECHANISMS.

Many theories have been proposed to explain the general effects of stress re-distribution that occur around a hole in rock or soil. All however, recognise the fundamental properties of the system. These are: that when a tunnel is driven in soil or rock, the pressure which develops on the roof supports is much less that the geostatic load due to the weight of the rock above, while the force at the abutments of the opening increases in proportion. Therefore, at some point above the roof, the geostatic load has been shed to the surrounding material. The load is said to have arched over the cavity. The term arching does not necessarily signify the shape of the opening, but rather refers to the mechanism of load transfer (Terzaghi, 1946).

If most of the overburden load is shed to the abutments, there must be some theoretical surface connecting the two abutments which is subject to small or zero forces. The weight of the rock above this plane is shed to the abutments, while the weight of rock below this imaginary plane equals the load acting on the supports. The area of roof below this imaginary plane has been referred to by a number of different names including the suspended zone (Trollope, 1966), the destressed zone (Isaacson, 1962, Adler et al., 1968, Peng, 1978), the arch core (Denkhaus, 1964), the Trompeter zone (Szechy, 1970), the dropping wedge (Szechy, 1970), the primary movement zone (Wiggil, 1963) and so forth. They are all synonymous and more or less self-explanatory.

The material within the suspended zone will drop out unless it is supported by artificial propping, or it supports itself through some self-supporting mechanism. In the situation of old coal-mine workings, where artificial propping has either been removed, or is completely rotted and largely ineffectual, the efficiency of the self-supporting mechanism can be considered as being inversely proportional to the likelihood of collapse.

If the self-supporting mechanisms within the immediate mine roof are insufficient to maintain stability, the roof will collapse creating an irregular (overbreak) cavity above the opening. This cavity despite initial stability, will eventually work its way upward, until a final equilibrium is established where the disruptive forces acting on the roof are balanced by the forces generated by the self-supporting mechanism (Hall, 1910). The point at which equilibrium is established is referred to by Terzaghi (1946) as the maximum height of overbreak, and the load that such a mass would impose on a roof support is referred to as the secondary rock pressure (Fig 7.6).

So far, the remarks have been concerned with collapse in rock or cohesive soil where the material has some ability to corbel over the void. In cohesionless material the ability to corbel is reduced. However, the same effect observed in cohesive soil or rock, namely that the weight supported by the roof of the opening is considerably less than the overburden weight, is still observed. To account for this Terzaghi (1946) proposed the concept of a 'ground arch', where the weight of the overlying material was proportioned out and re-distributed to the abutments (Fig 7.13). The fundamental difference between the ground arch or 'earth pressure', and the height of the destressed zone and 'secondary rock pressure' (Terzaghi, op.cit.) lies in the mechanism of arching, and thus in the predicted height of collapse. With secondary rock pressure, only the rock in the destressed zone is liable to collapse, and its collapse does not affect the surrounding material. In cohesionless material however, the presence of the material within the ground arch is vital to the stress redistribution mechanism. Indeed, the stress re-distribution will only occur if the material is restrained from movement. If the support is withdrawn, the material would flow into the void until the void was completely filled. In these circumstances, the boundary between the stable and unstable material would be defined by two failure planes extending upwards at an angle of $45+\phi/2$ to the horizontal.

The two theories thus predict very different outcomes for a collapsing mine roof. Rock pressure theories predict that a peaked arch will develop above the

mine opening, such that the resulting vault is compatible with both the existing gravitational and regional stresses, and the properties of the strata (Jennings, 1966). Earth pressure theories, on the other hand, predict that the mine opening will fill with roof debris and no stable arch will develop.

The arches referred to later in Chapters 3 and 9 are thus seen to be arches in the rock pressure or mining sense, and not arches in the ground engineering sense. In the majority of collapsing 'Pillar and Stall' mine workings, the roof corbels over the void, and forms a quasi-stable arch. Such old workings are thus behaving according to rock pressure theory.

1.6. METHODS OF ANALYSIS.

The previous section shows that in deciding whether or not an old working will be stable it is necessary to consider:-

1. The efficiency of the self-supporting mechanism within the suspended zone.

2. The development of the main arch and its stability.

The self-supporting capabilities of the material within the suspended zone are important because if the material is stable, further analysis to predict the size and mechanism of the collapse is unnecessary. However, if the material cannot support itself, and drops out, the second problem, that is the height of the collapse associated with the suspended zone, must be considered.

The two problems require different methods of analysis. The stability of the suspended zone relies on self-generated support. Coal and ironstone are stratified minerals, and the rocks in which they occur are sometimes split by horizontal discontinuities to form rock beams. Providing that major vertical discontinuities are absent form the roof of the working, these beams can be analysed using classic beam theory (see Chapter 4). Beam theory however, is inappropriate where the roof of the working is cut by well-defined discontinuities. In these circumstances, Voussoir arch analysis (Chapter 5), or a mechanistic model (Chapter 6) may be used. Alternatively, if the material is

very cohesive, one of the limit equilibrium theories may be more suitable. These equate the cohesion (shear strength component) mobilised on the failure planes with the disruptive forces acting to cause failure.

When one of the above analysis, or common sense, suggests that the material will be unable to support itself, the problem resolves itself to the height of the suspended zone, and the stability of any arch that develops. Such a problem is best dealt with by either one of the statistical of observational relationships discussed in Chapter 3, or by one of the numerous dome ar arching theories that are reviewed in Chapter 7.

In many situations an investigator will be unsure whether or not an arch, in the mechanical or rock pressure sense, will develop. Alternatively, there may be insufficient information available to use one of the other more sophisticated techniques. In such cases Bulking theory (Chapter 8) can be utilised. Bulking theory makes the fewest assumptions about the material properties of the rock,and the mechanism of collapse. Thus it can be used to predict the ultimate height to which a void could migrate.

The quantity and quality of the input data for the theories outlined, is reflected by the confidence that can be placed in the analysis. Beam or Voussoir theory demand the most detailed input and correspondingly provide a guide to the mimimum height of collapse that could be expected. On the other hand, Bulking theory demands the least input, but predicts the maximum height for a collapse.

1.7. THE EFFECT OF DISCONTINUITIES.

All rock masses are cut, to a varying degree, by discontinuities. The discontinuities can be on a small scale, represented by mere hair-line cracks in the rock mass, or can be of major vertical extent, when they are termed joints. In the horizontal plane sedimentary rock masses are divided by bedding into loosely bonded mechanical units.

John (1962) summarised the effect that discontinuities play in the role of rock

mechanics.

"For most engineering problems, the technical properties of a rock mass depend far more on the system of geological separations within the mass than on the strength of the rock material itself".

Thus, it is logical to propose that the mode of failure of an old working will depend more on the system of discontinuities, than on the strength of the rock mass.

The pattern of discontinuities in the rock mass is three-dimensional and tends to break the rock mass into discrete blocks which are loosely bonded to one another by interlocking, and small cohesive forces. The efficiency and strength of these bonds is very important to the mechanical behaviour of the rock mass and will be returned to later, in Chapter 6. For the moment however, the blocks will be considered as discrete, cohesionless and free to move.

The spacing and vertical extent of the discontinuities and the size of the opening in the rock mass effect the mechanism of collapse. Consider an infinitesimally narrow opening in a normally bedded and jointed rock mass. With such a small opening there is a high chance that a rock block, formed by the intersection of the three sets of discontinuities, will cover and bridge the narrow opening. However, if the span of the working is increased, first one then progressively more and more vertical intersections, and hence blocks, will intersect the roof of the working. Unlike the initial situation, where the blocks bridged the opening, the blocks in this case will be unsupported and may fall out. These unsupported blocks form the base of the suspended or destressed zone. If the width of the working is further increased, the ratio between the span of the opening and the length of the blocks increases proportionally, until a point is reached when the size of one block is insignificantly small in comparison to the size of the working.

The response of the material that forms the roof of this theoretical working varies depending on the size of the opening. At one extreme, the material can act like a beam and span the void whereas, at the other extreme, the rock mass

more closely resembles a cohesionless soil. Thus, there is a scale effect. This effect can be removed by taking the average size of the blocks forming the roof of the working and dividing the value by the span of the working. By taking this normalised ratio, similar modes of collapse will group together irrespective of the actual sizes of the opening or the discontinuity spacing (Fig 1.7).

Once a mode of failure has been recognised and classified, it is possible to apply, or develop, a suitable analysis technique to solve the problem. This theme of classifying the old working, isolating the important element, and analysing for its failure unifies the following chapters. Each failure mode is considered in turn, and assessed for its value in predicting the collapse of old workings.

1.8. CLASSIFICATION OF COLLAPSE STRUCTURES.

The modes of collapse of old workings are extremely complex, and are governed by dozens of variables, many of which are not measurable. However, from field observations made during this project, only a few appear to exert a major influence. The remaining variables are best considered as modifiying the effects of the main variables.

The variables that are considered as having a controlling effect on the mechanism of collapse are:-

1. Effective bed thickness
2. Faulting and Jointing
3. Effective unit length

1.8.1. EFFECTIVE BED THICKNESS (EBT).

The roof rocks associated with stratified minerals are usually well-bedded and often exhibit a tendency to split or delaminate along well-defined bedding planes. Wardell and Wood (1965) noted that a conventional lithological log of

the strata, does not necessarily provide a good guide to the mechanical thickness of the rock unit. In some conditions a seemingly massive rock will split into numerous thin plates, while in other situations, a thick lithological unit will be devoid of any planes of separation. For this reason, the present investigator prefers to use the term ' Effective bed thickness ', when considering the mechanical thickness of the blocks making up the roof strata.

1.8.2. FAULTING AND JOINTING.

Where these are well developed, they are so disruptive to the roof of an old working that, in controlling collapse, they may be considered to override all other variables. Mechanisms for joint controlled collapse have been suggested by some authors (see Price, et al., 1969). Such failures can result in spectacular collapses extending high above the roof. Field observations suggest that above old coal workings such 'chimney caves' are unusual, which is fortunate as there is no reliable method that can be used to predict their maximum vertical extent. The vertical extent of the collapse depends on the vertical continuity of the joint. In most cases this is usually not very great, so the joint element of the collapse terminates at some point above the coal seam (Plate 6). From the examples seen in the field, the main danger of these chimney caves would appear to be that they move the 'normal collapse structure' to a point well above that which would be expected. In consequence, any calculations of collapse height based on 'a normal situation' become irrelevant.

1.8.3. EFFECTIVE UNIT LENGTH (EUL).

Jointing is a well known macro-feature of a rock mass. However, there are numerous other, smaller scale, vertical discontinuities in the near-surface rocks, which were probably caused by the effects of rebound or stress relief (Nichols, 1980). Although the joints form obvious planes of separation, their effect is usually absorbed by these, more numerous, hair-line cracks and fissures. It has been observed that these cracks and fissures can have a far greater effect than jointing on the ultimate size of the blocks that form the

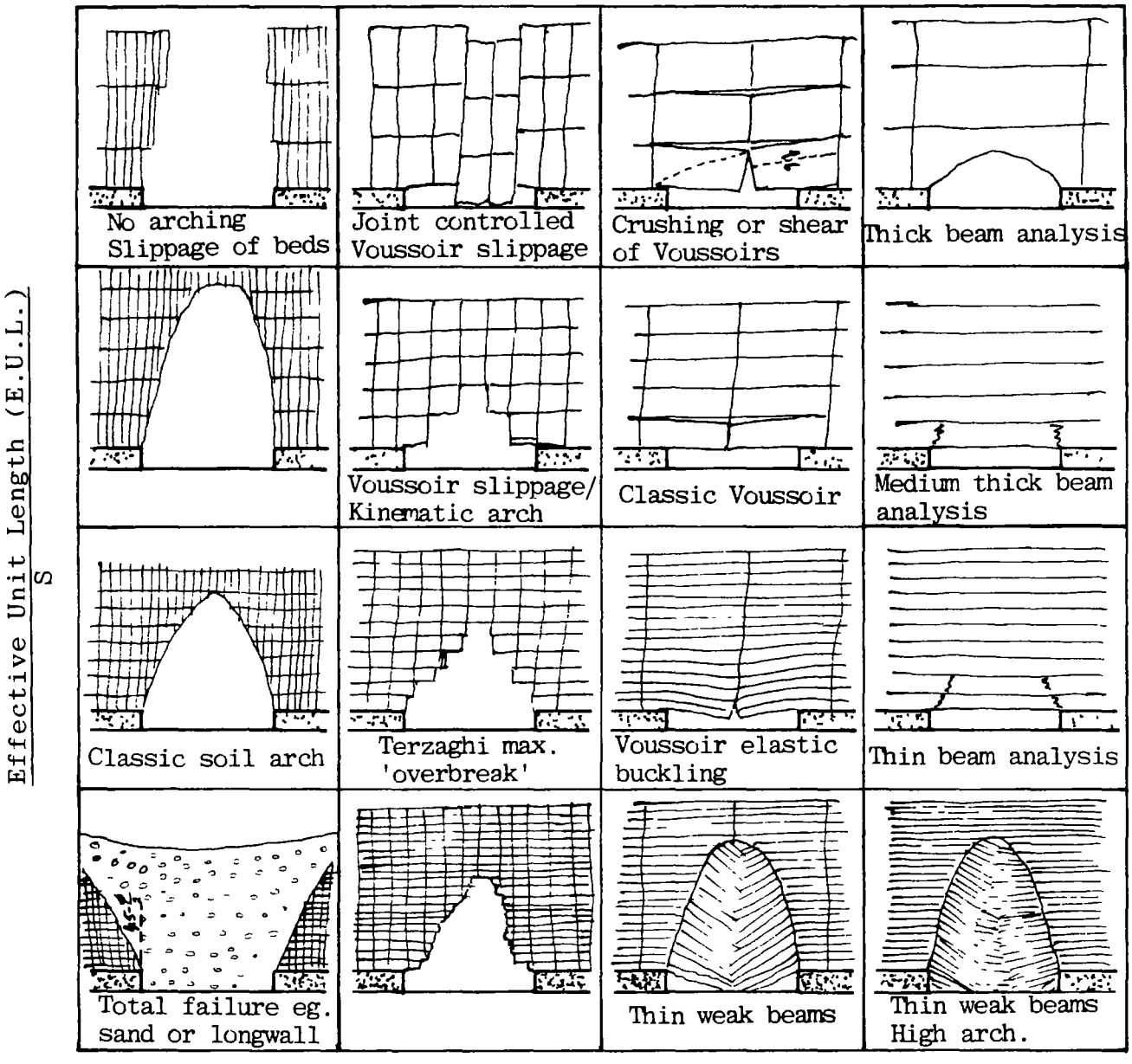

Where S = Span width

Figure 1.7 Classification of old workings.

roof of a working. This is especially the case in siltstones and other argillaceous rocks, where joint systems are generally less well defined, and random tight fissures of limited areal extent are common (See Price et al., 1969). For the purpose of the present investigation, the average distance between such discontinuities will be referred to as the 'effective unit length' (EUL), and all jointing effects are assumed to be incorporated within this variable.

A relationship between the effective bed thickness and the effective unit length has been found and is discussed in detail in Chapter 6.

1.9. CLASSIFICATION SYSTEM.

Old workings vary considerably in size, but when the ratio of the effective bed thickness to the span of the working is taken, the effect of size ceases to be of such importance, and similar failure modes group together. While this grouping may be of value, it is itself modified by the effect of the third variable discussed above, the effective unit length. However, by using these two variables together, it becomes possible to qualitatively classify old workings. The suggested classification is shown in Figure 1.7.

Depth can have a considerable effect on the development of arching (see Getzler, 1970). However, old workings which affect surface structures are usually at a sufficient depth, in comparison to their width, for the effect of depth on the development of arching to be ignored. The proposed classification assumes that the workings are at a sufficient depth for arching to develop (see Plate 6, for an example of where this is not the case).

To obtain the maximum benefit from the classification, it is best not to consider the axis notations (ie. EBT/S and EUL/S) in too rigid terms. For instance, the EBT/S ratio is best considered, not as the actual thickness of any split horizon, but more the tendency for that horizon to split into units of approximately the specified thickness. Such a tendency is controlled by the tenacity of one lamination for another, which in turn is a combination of the

shear, tensile and cohesive strength associated with the contact. Thus, the increase in the EBT/S ratio can also be interpreted as an increase in the apparent cohesive strength between the laminae, or an increase in the rock's tendency to act like a beam.

Similarly the EUL/S ratio is loosely defined as the tendency of a bed to break into smaller lengths, rather than the actual lengths of the unit pieces.

The EUL of a rock is governed by many factors including jointing, the tensile strength, or modulus of rupture of the rock, and the Young's modulus. An increase in the EUL/S ratio can be interpreted as an increase in the tensile strength of the rock, or perhaps a decrease in its Young's modulus (the rock becomes more flexible therefore less brittle).

It is worthwhile developing the concept of the EUL one stage further. At the edge of an old working, the beds can be considered as cantilever beams. The maximum bending moment and shear stress in a cantilever beam occur at the abutment, and both decrease linearly to zero at its free end. (see Chapter 4). If the rocks on the side of an old working failed according to cantilever beam theory, the edge of the working would be almost vertical. (see also Chapter 4 for a calculation of the maximum cantilever span based on the tensile strength of the rock). Instead, observations suggest that the collapse structure above an old working is stepped, like an inverted staircase (Jones and Davies, 1929, Fig 6.1). Therefore, it follows that the cantilevers are not breaking at the point of maximum stress, but are possibly failing when the outer fibre tensile stress exceeds the strength of some discontinuity within the beam (for thin beams shear stresses are not important, Chapter 4).

An analogy can be drawn with the concept of suitably orientated Griffiths cracks in rock mechanics (Farmer 1968). It is suggested that a rock with a low EUL has a high number of suitably orientated imperfections per unit length and therefore, breaks nearer to the point of maximum stress. On the other hand, a rock with a high EUL has relatively fewer imperfections per unit length and so, on a probability basis, is more likely to break at a greater distance from the

point of maximum stress. Implicit in this hypothesis, is that the rock seldom fails by pure tensile failure, but usually fails along a previously formed discontinuity. Considering the results that can be obtained from beam theory, for the critical length of a cantilever, this may not be too far from reality (Chapter 4).

1.9.1. PRACTICAL USE OF THE CLASSIFICATION.

It is appreciated that the terms used for the axis notation are rather nebulous. However, the terms are still quite definable. The importance of the classification system lies in expressing the relationship between the failure types, and the effect that a change in one of the variables may have on the mode of failure, and hence method of analysis.

Consider the following hypothetical example in which the roof of the old working is heavily fragmented both vertically and horizontally. If the span of the working is sufficiently large, the EBT/S and EUL/S ratios would classify the old working in the bottom left hand corner of Figure 1.7. Under these circumstances it would be expected that the working would completely collapse, in a similar fashion to an opening in dry sand. Such a situation could satisfactorily be analysed using conventional soil mechanics (plane of failure = $45+\phi/2$ to horizontal), or by the use of longwall subsidence techniques (NCB. 1975). However, if the span of the working was reduced, the overall stability of the system would increase. Within the classification a decrease in span affects both axis ratios equally. Thus, the position in Figure 1.7 shifts diagonally towards the top right hand corner away from the origin and towards a failure characterised by a high vaulted arch. Such a problem could be analysed by arching theory (Chapter 7), or using a statistical approach (Chapter 3). The working becomes progressively more and more stable as the width of the working decreases and hence the axis ratios increase. At a critical point (Chapter 6) the suspended zone will become stable from which point Voussoir beam analysis may be appropriate (Chapter 5). Ultimately pure beam theory (Chapter 4) will be sufficient to analyse the situation.

1.9.2. MODIFYING VARIABLES.

The balance between stability and instability in the roof of an old working is so fine, that the effects of changes in variables such as the Young's modulus, shear strength, tensile strength, density, moisture content etc., cannot be ignored. However, these variables are so inter-related that they can be considered under general headings.

a. MOISTURE CONTENT. Increasing the moisture content in the environment around an old working is likely to reduce the strength of the rock, this will effect both the EBT and EUL. The relative reduction in each of the ratios, will ultimately depend on the rock type, and its induration. A rapid increase in the moisture content might effect the EUL ratio more than the EBT ratio by rapidly reducing the vertical shear strength. Such a relative change would shift the mode of failure vertically downwards, and towards the X-axis. On the other hand, a slow change in the moisture content may have a similar effect on both the ratios, in which case the mode of failure would shift diagonally towards the origin.

b. WEATHERING AND TIME. These have much the same effect as a slow increase in the moisture content. The weathering process will propagate fastest along the discontinuities, and make delamination and vertical fissuring more likely (Aughenbaugh, 1981)

c. ENVIRONMENTAL STRESS CHANGES. These can be of two origins:-

1. Pillar Failure. This acts to increase the span of the working, in which case the failure mode moves diagonally towards the origin.

2. Ground strains. These can either increase the EUL, (decrease in shear strength due to decreased horizontal force), or decrease the EUL ratio depending on the sign of the strain.

1.9.3. INTERACTION OF FAILURE MODES.

Should the nature of the rock change, the development of one failure mode will not necessarily preclude the development of another mode of failure. An obvious example of such a situation would be where a reasonably thin roof rock was overlain by gravel or soil. A normal arch would probably develop within the rock, but its apex might break through the junction between the rock and the gravel. In such a situation, the gravel might flow into the working resulting in a 'soil type failure' and subsidence on the surface. Figure 1.8 (adapted from Wiggil, 1963) shows such a situation. More frequently however, the situation is reversed, and an old working bridges (Chapter 3, Plate 5).

1.10. CONCLUSIONS.

The proposed classification contains many elements common to other classification systems. It probably bears the closest resemblance to the 'sequence of load transfer' for a mine roof proposed by Adler and Sun (1968), and Adler (1973). These authors charted the effect of increasing span on the response mechanism within the mine roof and proposed four stages of load transfer or collapse development. Their four sequences closely follow the diagonal of the proposed classification system. Adler (op. cit.) thus acknowledged the importance of the roof span on the mode of failure of a mine roof. However, his sequence assumes that the relative thickness and length of the blocks remained constant for all working widths.

In contrast, Terzaghi (1946) proposed a classification of roof loads which took account of the spacing of the discontinuities, and the size of prospective roof blocks. In recent years, this type of system has developed rapidly into the sophisticated rock mass classification systems proposed by authors such as Barton, Lien and Lunde (1974), and Bieniawski (1979, 1981), (See review by Hoek and Brown, 1980). These classification systems recognise the dominant effect that jointing and discontinuities play on the stability of an underground opening, and use various 'indexes' to quantify the effects on stability of variations in a number of variables. The systems however, do not consider the potential height of collapse for an excavation, but concentrate on predicting

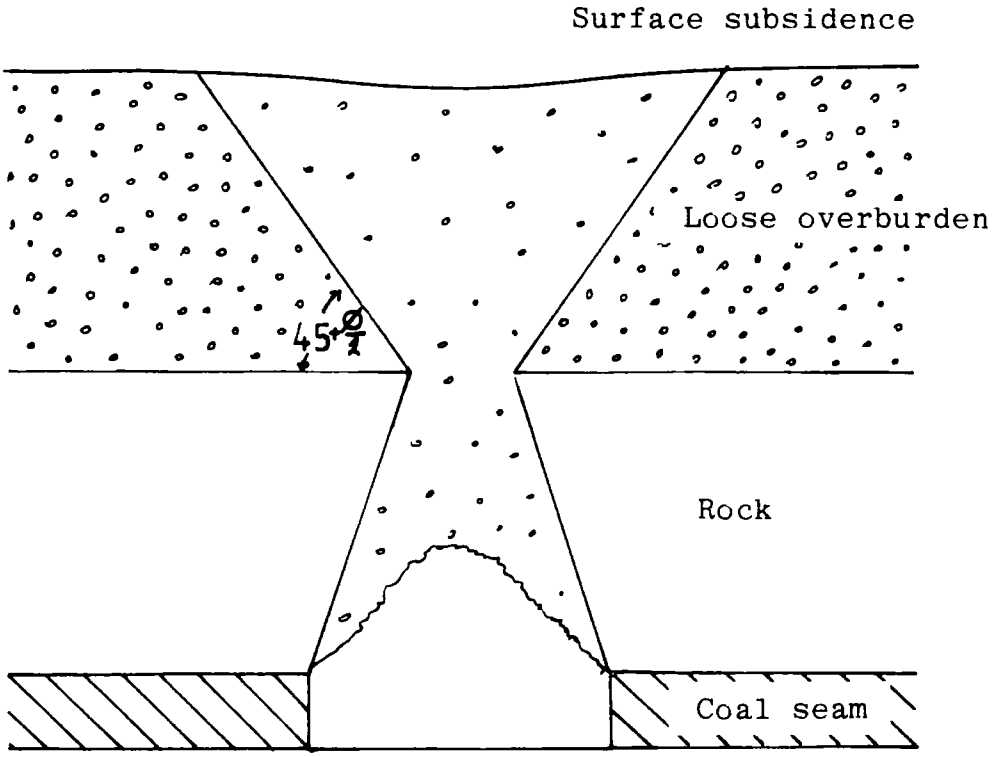

Figure 1.8 Interrelationship between an arch and loose overburden material (after Wiggil, 1963).

the initial stability and the support requirements for the excavation.

Finally, Protodyakonov (Szechy, 1970) recognised the inter-relationship between rock strength, discontinuity spacing and height of arch, and incorporated these variables into his arching theory (Chapter 7).

At the moment the proposed classification system described in the previous sections, is purely conceptual, but in the future, it would seem possible to develop and extend the scheme to incorporate the quantitative elements common to the other classification systems mentioned above. However, as noted in Chapter 6, more attention will need to be placed on the effective bed thickness and the effective unit length, rather than bedding and jointing.

1.11. SUMMARY.

The development of the coalfields has been shown to be extremely complicated but essentially controlled by economic factors. There was little contact between the coalfields, and therefore a combination of economic pressures and variation in the structural geology of the coalfields lead to regional diversification in working techniques. This diversification developed at an early date, but by the late 18th. or early 19th Century the country could broadly be divided into three regions. Within a region each coalfield operated a slightly different variant on the regional mining method.

This rich diversity of mining methods complicates the present day geotechnical problems associated with old mine workings. However, provided that the complexity of the problem and the relative simplicity of the solutions presented in the forthcoming chapters is not forgotten, it is possible, and valid, to consider old workings in a simpler and more stylized form.

The mode of failure of an old working is considered to depend more on the system of geological separations within the rock mass, than on the strength of the rock material itself. A conceptual classification of old workings based on this approach is proposed. Within this classification, a distinction is drawn between earth pressure theories, which predict that no stable arch will develop

above an unsupported old working, and rock pressure theories which predict the development of a stable arch and a suspended or destressed zone.

The stability of on old working can be considered from two fronts. The first considers the development and stability of the main load-bearing arch. The second, considers the stability of the material within the suspended zone.

The most appropriate method of analysis is related to the ratio between the relative size of the opening and the blocks created by the intersections of the discontinuities. The classification is suggested as an aid to choosing an appropriate analysis technique.

In the following Chapters, the results are presented of field measurements, made by the present writer, on old working collapse structures. Following this, the various methods of analysing the collapse of an old working are considered in detail. The order in which the analysis techniques are presented progresses from beam theory, through Voussoir arch analysis and mechanistic models, to arch or dome theories. Finally, Bulking theory is considered. In terms of the suggested classification, the methods of analysis are seen to progress from low to high EBT/S and EUL/S ratios.

CHAPTER 2

FIELD INVESTIGATION OF OLD WORKINGS.

2.1. INTRODUCTION.

Until the early 1970's, investigations into the collapse of old shallow mine workings were virtually restricted to surface studies. Such studies attempted to define a safe depth to old workings by trying to relate the incidence of crown holes to the depth of the worked seam. This approach proved rather inadequate as no assessment of the degree of underground collapse was possible, and the effect that discontinuities and different rock types had on the collapse mechanism could only be speculated upon. Underground observations had, over the centuries, given some idea of the shape of failure zones as well as the ideas of bridging of failure arches by competent rocks (eg. Callon, 1874, Fayol, 1885, Jones and Davies, 1929). However, such underground observations of old workings were both dangerous and in many cases impossible in areas of large-scale collapse.

The high walls of opencast coal sites offer a unique opportunity to study old workings and collapse structures in section rather than in plan view. To the writer's knowledge, Walton and Taylor were the first to systematically record the dimensions of collapse structures above old workings, although illustrative photographs of migrating voids in opencast sites had been published previously (Wardell and Wood, 1965). These early measurements by Walton and Taylor were made at a number of opencast sites, and 41 such measurements from Pethburn opencast site, Co. Durham, were published in Walton and Taylor (1977). The height measurements were estimated by eye with the aid of a staff placed against the collapse structures for scale. The measured width of the working and the height of collapse were the only measurements recorded, and only a few oblique photographs were taken.

Challinor (1976) visited a number of opencast sites in the North East and recorded collapse structure above 47 old workings. This M.Sc. project acted as a feasibility study and dummy run for the present writer's investigations.

Challinor recorded the collapse structures by both field measurements and with orthogonal photographs, but like Walton and Taylor (op cit.) the only measurements made were the height of collapse and the span or width.

The present study refined the techniques of recording old workings in high walls of opencast sites and between 1977 and 1981 one hundred and thirty seven (137) old workings and collapse structures were recorded and measured. In addition to these, sufficient additional information was found to be available for 14 of Challinor's old working records to warrant their inclusion in the data base.

2.2. FIELD LOCATIONS.

Opencast coal-mining in Britain is controlled by the NCB Opencast Executive. The Executive both plans and licences the operation of nearly all opencast coal sites with a production of over 50,000 tonnes. Private companies can operate opencast sites under licence from the Opencast Executive, provided that their total tonnage is estimated to be less than 50,000 tonnes.(At the time of the fieldwork this figure was 25,000 tonnes). In exceptional circumstances larger opencast sites may be licenced by the NCB if there are additional motives for their development, such as large-scale land reclamation and restoration. Telford new town is an excellent example of this sort, in that a large part of the new town is built on reclaimed land. Finally, some quarries are allowed to produce coal as a by-product, as for example, fireclay quarries and brickpits.

Initially, the present study was restricted to NCB opencast sites, but was soon extended to cover both private sites and those licenced to County Councils as part of reclamation work. It proved necessary to visit over 35 NCB and private opencast sites, as well as a number of fireclay quarries, to establish whether or not there were suitably preserved old workings exposed in the cuts.

Of the many sites visited the following provided suitably well exposed old workings (Table 2.1).

TABLE 2.1. SITES VISITED WITH SUITABLE EXPOSURE OF OLD WORKINGS.

Country	County	Opencast Site	Grid Ref.	Supervisor
Scotland	Ayrshire	Benbain	NS 520 080	NCB
	Lothian	Blindwells	NT 395 752	NCB
England	Northumberland	Acclington	NV 230 070	NCB
		St. Andrews *	NZ 053 551	NCB
	Durham	Cowsley *	NZ 145 420	NCB
		Esh Winning *	NZ 195 429	NCB
		Ibbetsons	NZ 195 485	NCB
		Pit House	NZ 214 404	Durham C.C.
		Tanners Hall	NZ 176 375	NCB
		Tow Law	NZ 122 393	Private
		West Brandon	NZ 399 196	NCB
	Cumberland	Low Close	NY 075 350	NCB
	W. Yorkshire	St. Aidens	SE 368 275	NCB
	Derbyshire	Morrels	SK 382 472	NCB
		Park Meadow	SK 403 472	NCB
	Leicestershire	Coalfield Farm	SK 439 311	NCB
Wales	W. Glamorgan	Maesgwyn	SN 890 090	NCB
		Maes y Marchog	SN 870 070	NCB

* Sites investigated by Challinor (1976).

In addition to the opencast coal sites, a number of old ironstone mines were investigated, primarily because of the excellent survey and 'potential hazard plans' that were preserved by the British Steel Corporation's Survey Department at Ibstock. Two sites were selected:

Finedon	G.R.	SP 922 717
Holwell	G.R.	SK 741 236

Lastly, a number of old lead mines were investigated where such mines were accessible, and had either shale or sandstone roofs for part of their extent. As expected, very little could be gained by viewing collapse structures from underground.

2.3. DEVELOPMENT AND OPERATION OF AN OPENCAST SITE.

Old workings are very much a part of opencast operations, and as the recording of old workings in the high walls of opencast sites is entirely dependent on one phase in these operations it is worthwhile to briefly consider the development

and operation of a typical opencast site as let by the NCB Opencast Executive.

2.3.1. DEVELOPMENT.

The aim of an opencast coal site, apart from the special cases already dealt with, is to produce the maximum amount of high grade coal at a steady tonnage, for the minimum cost, and with the maximum safety. To achieve these aims detailed investigations and planning are carried out prior to any development work.

The NCB Opencast Executive are responsible for locating potential opencast sites and producing a detailed geological and production plan for the site. This necessitates an extensive drilling programme to locate and map the various coal seams, and to locate and prove any areas of previously worked coal. On the basis of these geological investigations the Opencast Executive provide a detailed working plan which includes forecasts for potential recoverable tonnages of coal per seam and sub-area of the site.

After the Opencast Executive have had the plans approved by the local planning authorities, which usually means a public enquiry, the results of the investigations and forecasts are offered to a number of private contractors who are invited to submit tenders on the basis of a price per tonne of coal produced. Once the tender from a contractor has been accepted, and development of the site has begun, the Opencast Executive have little control on the day to day operation of the site. Their role is primarily one of monitoring the production and independently assessing the volume (and tonnage) of coal produced. This leaves the contractor free to operate the site, within the constraints of the planning consent, in a manner likely to be most cost effective. This is usually, broadly in line with the plan suggested by the Opencast Executive. During the life of the opencast site, the Opencast Executive offer a free consultancy service to the contractor. This service is largely for technical problems that may arise in such areas as coal preparation and geotechnology.

The normal day to day NCB supervision of the site is restricted to a Resident Engineer, and one or two Opencast Executive surveyors. It was through these Officials with Regional NCB approval that access to the sites was sought and obtained.

2.3.2. OPERATION.

During the initial planning stage, the site is divided into a number of cuts, which are phased to produce coal of a certain quality and quantity. Evenness of production is important as stockpiles are wasteful in terms of handling costs. The initial cuts are commonly opened by dragline excavators. These are used to remove the overburden above the coal seams with or without assistance from ripping or blasting. After the initial cut the high wall, or quarry face, is extended by a dragline excavator. This operates by digging and casting the fresh material back into the old cut. A characteristic profile emerges of a fresh quarry face, or high wall, followed by the 'coaling cut', behind which, is the cast pile or low wall (Fig. 2.1).

The operation of the dragline excavator is usually too coarse to prepare the top of the coal seam adequately for coaling. Therefore, further stripping is usually necessary. Bucket excavators, scrapers and even wheelbarrows, brushes and shovels (in areas of old workings) may all be used during this operation, which is aimed at reducing the ash content of the coal to a minimum.

Coaling takes place once an area of coal has been prepared, and involves digging the coal from the seam with a bucket excavator and dumping it straight into trucks to be taken to the power station or relevant destination. This usually involves a number of trucks, contracted from outside companies, which run in relay to the destination and then return for more coal. Hold-ups in the cut at this phase in the operations are avoided, since trucks standing idle represent wasted money to the site contractors. Once the cut has been coaled the next phase of the operations is started. This may be starting the next cut, or the deepening of it to get to a lower seam.

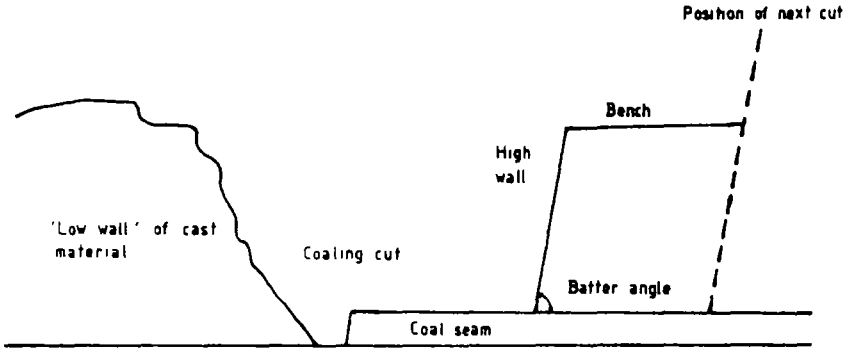

Figure 2.1 Nomenclature and typical cross section through an opencast coalface.

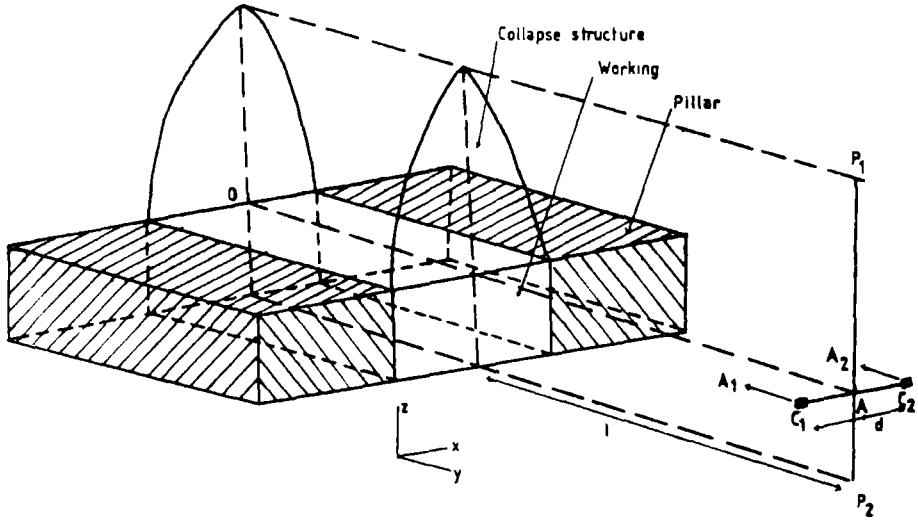

C_1 & C_2	Camera positions - parallel to roadway axis in y-z plane
P_1 & P_2	Plane projected through the mid-line of the roadway
A_1 & C_1	Photographic axes
A_2 & C_2	
d	Camera base (controls stereographic effect)
l	Camera to object distance (controls scale and stereophotographic effect)
x,y,z	Notational axes
O - A	Roadway axis

Figure 2.2 Stereo-photography and old workings - nomenclature.

At some stage in the coaling process, usually during a morning, the NCB surveyors move in to survey the cut. One of their jobs is to provide an independent estimate of the tonnage of coal extracted, and keep a record of daily or weekly progress.

2.3.3. LOCAL VARIATIONS.

The optimum time for recording old workings on an opencast site is just after coaling and prior to any cleaning or development work. At this phase in the operations the coal has been removed, and a full section through the coal seam, old working and any collapse structure can be seen. As will be appreciated, this is also one of the busiest times in the cut, and any interruptions to the work must be kept to a minimum.

The method of working an opencast site is entirely in the hands of the contractors, so there are many local variations in working practice. Unfortunately areas of old workings seem to be one of the areas in operations most prone to local variations, and these can significantly effect the quality or even the possibility of making any measurements.

a. EXPOSURE. Two systems of coaling seem to be in operation in areas of old workings. The most common method is for remnant coal pillars to be extracted one by one as each becomes available. The alternative, less common method, is for all the old workings in a cut to be cleaned and prepared for one single coaling operation during which the remnant pillars are removed in one operation (Plate 4). For recording purposes the latter method is preferable, because with the former method of individual pillar removal, photography and access to the old workings is severely restricted by the surrounding working plant. In addition, the time taken to coal and prepare the next old working is usually greater than that available for one site visit. However, three or four cuts were visited, during the fieldwork, where the old workings in the cut had been completely cleaned prior to coaling. These cuts generally offered free access to numerous old workings, and spectacular views of the old mining systems when viewed from the high wall (Plate 1).

b. PARTINGS. The aim of a site is to maximise both coal production and safety thus, the batter angles of the high wall are usually made as steep as possible. Old workings can however, affect the stability of the high wall (Walton and Taylor, 1977, Walton and Atkinson, 1978). Therefore, on some sites once a cut has been coaled, the coal partings and any loose material produced from grading the access roads will be stowed into and against the exposed old workings. This helps to stabilise the high wall as well as removing mine waste from haulage routes used by site traffic. It will be appreciated that under this system, old workings can become obscured at an alarming speed, and can even be obliterated altogether.

c. EXCAVATION RATE. The speed of operations on an opencast site varies from one of frantic activity to a dead halt. Some old workings in cuts remain visible for months, while others disappear in minutes. Timing arrivals at a site was probably one of the hardest features of the fieldwork.

d. SPLIT SITE OFFICIALS. Although the writer possessed letters of introduction and permission to visit and record old workings on opencast sites, individual site access for every visit had to be authorised by the local NCB Site Agent. Some small sites especially those in Co. Durham, were worked on a time share basis with the site agents and surveyors moving between as many as three separate sites. This obviously imposed access restrictions to such sites.

2.4. SITE PROCEDURES.

At the beginning of the project, the original idea had been to record all old workings exposed in the high walls of opencast sites wherever and whenever they occurred across the country. On each site, the aim was to follow through the old workings as they appeared in successive cuts. In this way it was hoped to build up a three-dimensional pattern of collapse for every site in the country. Site experience however, proved that this aim was too ambitious, and practically unfeasible.

2.4.1. NOTIFICATION.

After an initial introductory visit to a site, the University's telephone number and the writer's extension were left with the Site Agent with a request to contact the University whenever further old workings were exposed on his site. Of the numerous agents with whom a phone number was left, only two ever phoned to report old workings. Of these, in fact only one telephoned regularly. There were a number of very good and obvious reasons why this happened.

One of the difficulties encountered was the misunderstanding of the definitions of an old working. To most site officials, old workings are thought of as areas of broken coal exposed in the bottom of the cut just prior to coaling, not as roadways seen in section in the high wall after coaling. On several occasions, visits were made to sites which apparently had excellent old workings exposed in the high wall only to find that coaling had not yet taken place, and the widths of the workings could not be evaluated.

The method of notification that evolved however, proved to be quite successful and seemed to be greatly preferred by site agents. This was to ring at fairly frequent intervals and if the site had old workings exposed, to arrange an approximate time for a visit. This meant that several sites could be assessed and visited together over a period of a few days, which better justified the cost of travel. Such informed visits were accepted by Site Agents and there was no occasion when access was refused; even random visits without prior notification were treated cordially.

Following particular workings through successive cuts proved to be very difficult. The main problem was that the width of a cut was far greater than the size of the pillars and roadways. It was therefore, pure chance whether or not the next cut would expose the correct section through the pillar. The problem was further complicated by the time involved between the cuts, this varied but at times was much as 18 months. These problems, and the size of the time window for recording the workings, conspired to make the attainment of a three-dimensional picture of collapse almost impossible. A similar concept has

been applied successfully to the sedimentology of the Coal Measures (Fielding, 1982), but the scale effect is less pronounced and the time window for recording geological information is much larger.

2.4.2. SITE ACCESS.

Access and supervision while on site varied. Permission was always sought, and obtained, from the NCB Resident Engineer before going on site. This was for both courtesy and safety reasons. The supervision offered varied, depending on the working situation within the cut, and on how well-known the writer was at the site. Usually transport was offered to the various cuts and the official waited while the relevant measurements were made.

2.4.3. SITE OBJECTIVES.

The objectives on site were to record each old working by a method that was :-

Quick
Accurate
Efficient
Safe

The speed was necessary for two reasons. Firstly, the fieldwork had to be fitted in with coaling or dragline operations, often only a few seconds were available between coal trucks or close passes by the dragline. The second reason was to reduce to a minimum the time that the supervisor had to wait. It was considered that if a site visit could be carried out in less than an hour future visits would not be viewed as too disruptive, and so access would not be withheld.

Any method chosen had to be efficient because the chances of finding the old working exposed on a future visit were very limited.

Two methods were evaluated:-

a. DIRECT MEASUREMENT. This was found to be slow, unsafe and inaccurate. Old working collapse-structures are far too large to be accurately measured by a

single person, and measuring something above a height of approximately 2 metres is prone to error. The method also involves a lot of time standing in front of the face, there is therefore, a constant danger from small toppling failures. Wandering around beneath the high wall does not impress NCB personnel and is counter-productive to gaining site access. The method is also slow, and apart from the 'thinking' time, and the time involved in measuring the structure, there is a considerable amount of other information to be recorded.

b. PHOTOGRAPHS. Whilst this method overcomes many of the problems dealt with above, it is impossible from a simple photograph to assess parallax errors. The face of a high wall is seldom vertical and old workings seldom run at right angles through the high wall. These reservations can be overcome by using stereo-photography. Stereo-photographs are fast, safe, accurate, and require only one person. In addition they offer the ability to study the collapse structure in detail at leisure. In consequence, only a cursory amount of time is needed on site to record direct information, this releases time that can be used for obtaining other information from the site personnel, or for making strength estimates. In fact 'on site' strength testing was dropped after about 9 months; once again, because of the time factor.

2.5. STEREO-PHOTOGRAPHY AND OLD WORKINGS.

2.5.1. SOURCES OF PARALLAX ERROR.

One of the major problems and sources of errors in the use of stereo-photography for recording old workings, is deciding on the positions from which to take the photographs. Old workings are seldom orthogonal to the face of the high wall and the visual condition of the working and collapse structure is often so poor that it is sometimes extremely difficult to decide in the field even where the old working is, let alone in which direction the roadway runs. The orientation of the roadway to the photograph ultimately dictates the accuracy of any photogrammetric measurements, and for this reason great care has to be taken to locate the correct position from which to take the photographs.

The correct location for the midpoint between the stereo-photographs lies somewhere along a plane projected through the mid-line of the roadway and at a height approximately equal to, or slightly greater than the roof of the working. (Fig. 2.2). To obtain a stereo-photographic pair, one photograph is taken from either side, and equidistant, from the roadway mid-line. The axis of the camera must be parallel to the roadway axis in the y-z plane. If the photographic axes converge, or diverge, the stereographic effect is reduced and may be lost.

The ability to identify a roadway axis in the field develops with practice. Numerous characteristics such as, the relative shape of the two sides of the failure arch, traces of pillar lines in the floor of the cut, the matching of shadows and the centering of 'vanishing points' within the old workings, in addition to numerous other criteria, can all be combined to obtain a fair estimate of the line of the roadway axis.

To make accurate and reliable measurements from the stereo-photographs some method of scaling the prints is necessary. The simplest form of scaling a photograph is to incorporate into it some measure of distance, and the most convenient and visually readable device is a survey staff. The positioning of the survey staff against the collapse structure is probably even more important than locating the roadway axis. Severe parallax errors can be created by a poor choice of staff location.

There are four sources of gross parallax error which can affect the ultimate accuracy of the photogrammetric measurements: They are illustrated in Figures 2.3 to 2.7 and are discussed below.

a. ORIENTATION OF THE AXIS OF THE PHOTOGRAPH RELATIVE TO THE ROADWAY AXIS. Parallax errors can occur both in the horizontal and vertical planes. Figure 2.3 represents the effect of parallax errors in the horizontal plane. The shapes of the arches A and C are distorted which makes the widths of the workings appear narrower than the undistorted arch B, whose axis is in line with the diagram. Similar distortions can occur in the vertical plane. In Figure 2.4, for instance, the view of the observer is above the axis and foreshortening

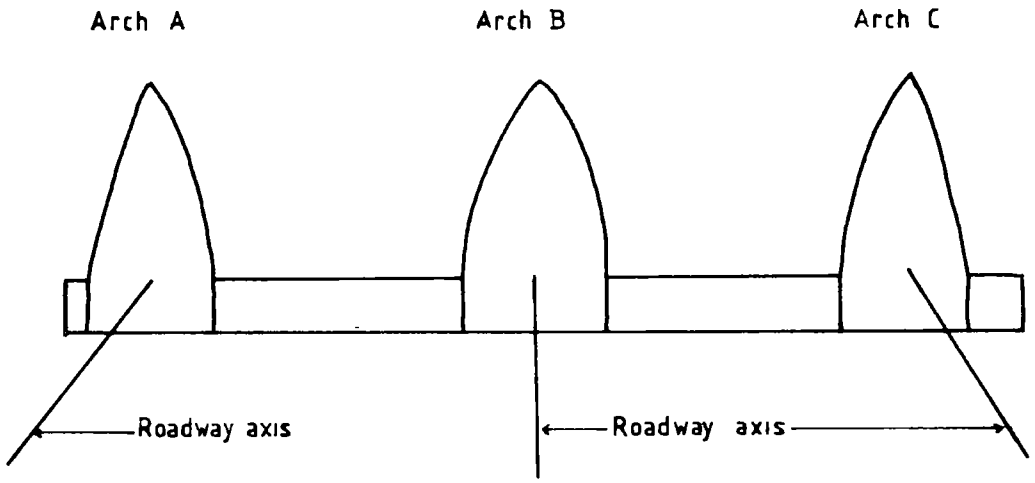

Figure 2.3 Perspective view of high wall showing foreshortening and distortion effects in arch sections.

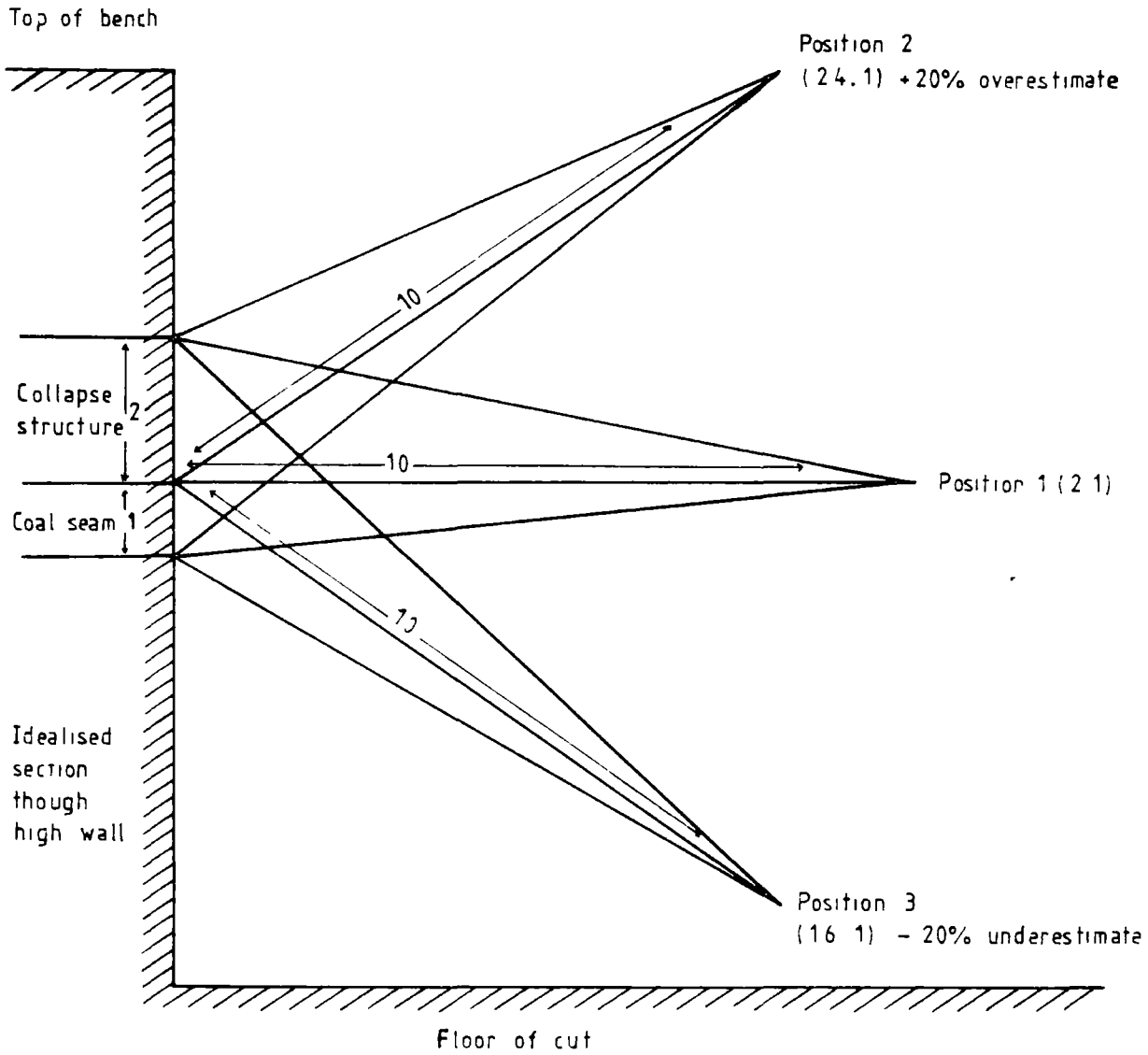

Position 1 = On axis of old working. Records correct ratio of collapse height to seam thickness

Position 2 = As seen from above old working. Overestimates ratio of collapse height to seam thickness by about 20%.

Position 3 = As seen from below old working. Underestimates ratio of collapse height to seam thickness by about 20%.

Figure 2.4 Foreshortening and overestimation of heigh due to parallax errors.

in the region of the coal seam would, in this instance, lead to a 20% overestimation of the arch height.

b. INCLINATION AND DISTANCE OF THE STAFF FROM THE HIGH WALL. The effect in plan view, that a section angle can have on the accuracy of the measurements is shown in Figure 2.5. Position A is the correct staff location, but 'loose' high walls and large high wall batter angles sometimes make staff placement a problem. It is however, perfectly acceptable to use the staff horizontally so long as the staff (as in the vertical situation) is in the immediate vicinity of the arch structure, preferably crossing it, and at right-angles to the roadway axis.

c. ORIENTATION OF THE CUT TO THE ROADWAY AXIS. Figure 2.6 shows in plan view the effect that a section angle can have on the accuracy of the measurement of width. In these situations the location of the true roadway axis is essential.

d. BATTER ANGLE. This is probably one of the greatest of the difficulties. In severe cases where the batter angles are very large, accurate photogrammetric measurements may be impossible (Fig. 2.7).

While the problems have all been discussed singly, they often occur together. If any confidence is to be had in the final measurements, the use of stereo-photography in these circumstances is absolutely essential. With single photographs there can be no appreciation of any potential parallax errors. Stereo-photographs however, provide not only an appreciation of the parallax errors involved, but the differential parallax between the photographs can be used to estimate the true measurements. This can be done by projecting by eye the relevant perspective lines towards and through the staff.

One further problem that must be appreciated while photographing and recording old workings is the structures position within the overall mine layout. Old workings exposed in the high wall are usually considered as roadway sections (eg. Figs. 2.2 to 2.7). However, it is feasible that the high wall may show just one edge of an intersection collapse structure (Fig 2.8). Field experience and careful examination of the stereo-photographs are usually sufficient to

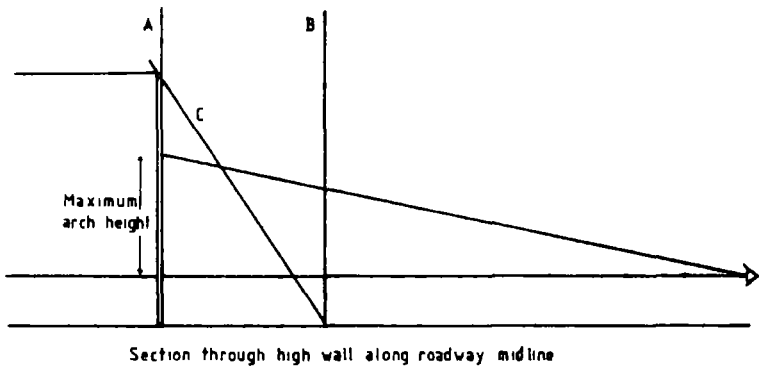

Staff A records correct height of collapse
Staff B records 71% of the correct height
Staff C records 107% of the correct height

Figure 2 5 Section through high wall and effect of staff position and inclination on the accurate measurement of arch collapse height

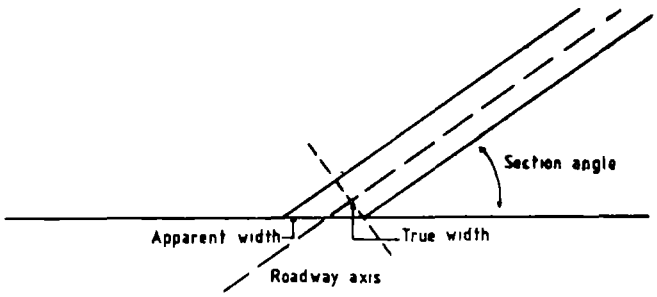

Figure 2.6 Plan view of roadway and the effect of section angle on the estimation of width.

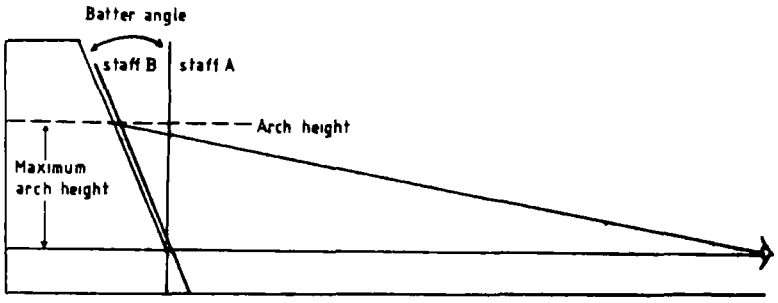

Staff A measures 87.5% of correct arch height
Staff B measures 107.5% of correct arch height

Figure 2.7 Section through old working and the effect of batter angle on accurate measurements of collapse heights.

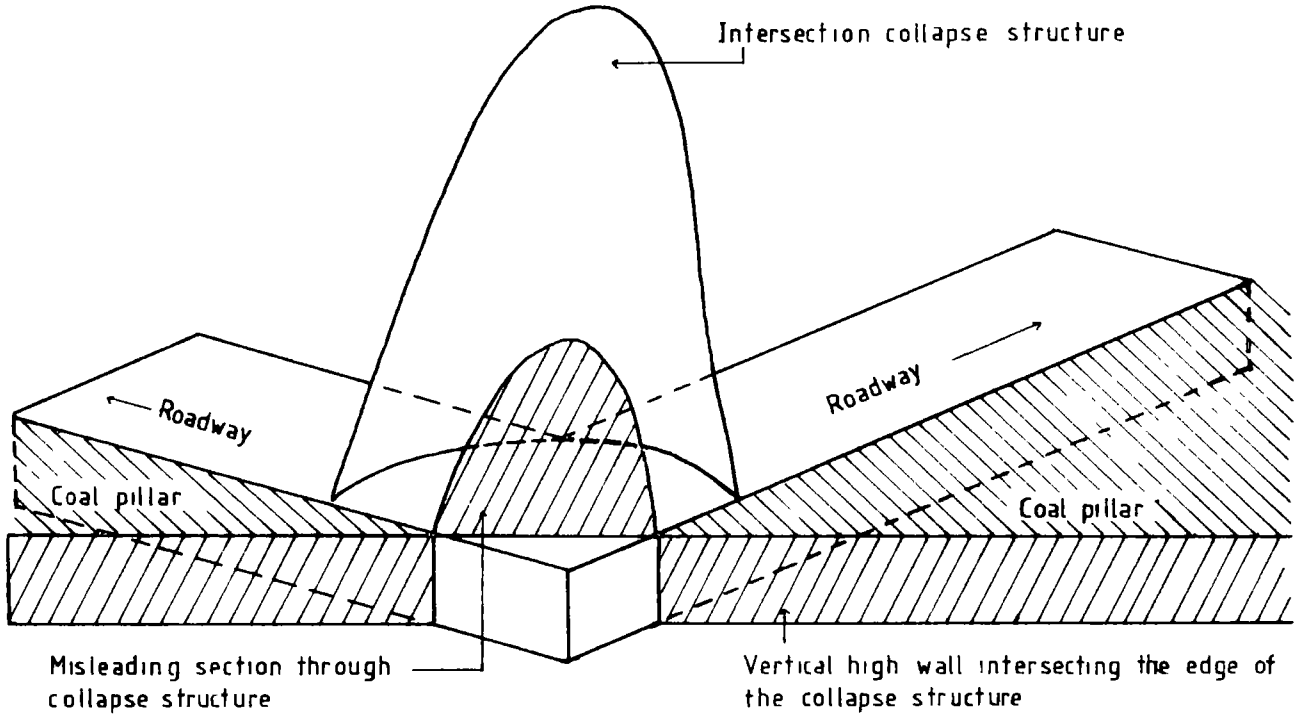

Figure 2.8 Effect of intersection orientation on the measurement of the collapse geometry.

distinguish between a simple roadway and the more complex intersection collapse structures. This problem will be returned to later in the text (Chapters 8 and 10).

2.5.2. SCALE AND VERTICAL EXAGGERATION.

a. SCALE. Assuming that the foregoing criteria are satisfied (i.e. that the photographs are taken at an equal height and in a plane at right angles and parallel to the roadway axis), an investigator has only two remaining controls on the location of the two photographs. These are the distance at which the photograph is taken from the rock face (l) and the distance between the two camera positions, the camera base, (d), see Figure 2.2. The former distance (l) controls the scale of the negative, while the latter distance (d) controls the vertical exaggeration of the photographs. The scale of the negative is given by f/l where f is the focal length of the camera. In aerial photography, contact prints are usually used for interpretation, therefore any photogrammetric formulae for the negatives hold true for the positive prints. In this case However, enlarged positives were printed and thus the scale of the print is not the same as the scale of the negative.

While it is perfectly possible to calculate the appropriate new scales from 'apparent focal lengths' and distances, it is much more convenient to incorporate a scale, such as a survey staff, within the photograph. By doing this, the distance to the rock face and the camera base need never be known and becomes almost irrelevant. For purposes of record however, the typical scales for the negatives were of the order of 1:200, while the prints had a scale of about 1:30.

b. VERTICAL EXAGGERATION. The human brain perceives depth using the eyes to measure differential parallax. The minimum variation in the angle of differential parallax that the human eye can detect is of the order of about 30 seconds of an arc (Allum, 1966). This is about equivalent to a distance of 427m. Beyond this distance there can be no appreciation of depth unless the eyebase is artificially increased (as for example by the use of a pair of

binoculars). All the high walls photographed, lay well within this distance and hence, a camera base equivalent to that of the human eye (65.4mm.) could have been chosen. However, vertical exaggeration enhances the texture of the rock and greatly aids interpretation of the assessment of parallax error. Thus, a camera base greater than that of the human eye is advantageous.

The camera base not only controls the vertical exaggeration of the stereo-image, but also controls the area of overlap between the photographs. For aerial photographic purposes, overlap is of more importance than vertical exaggeration and an overlap of about 60% between adjacent photographs is usually chosen (Allum, 1966). In our situation, the camera to object distance, and the focal length of the lens are in a completely different ratio to their aerial counterparts. Therefore, a camera base equivalent to a 60% overlap would provide a vertical exaggeration too great for the brain to accommodate easily.

In practice a camera base of about 0.8m, for a camera to rockface distance of 10m, was found to be very satisfactory. For a standard-size print, viewed through a normal mirror stereoscope, this provided a depth perception approximately equivalent to viewing the rock face from a distance of 0.8m. However, because the scale of the image can be varied independently of the vertical exaggeration (by varying the degree of magnification provided by the stereoscope), the apparent distance that the rock face can be viewed from, while maintaining the depth perception equivalent to 0.8m, varies from several metres to less than one metre.

It is for these reasons that the general quality and quantity of information retrievable from stereo-photographs is far greater than that obtainable from a single photograph. Indeed, in many cases, especially where the collapse structures are beyond easy reach, the information obtainable from stereo-photographs can be superior to field measurements, and is certainly obtained at far less risk.

The detailed mathematical relationships between vertical exaggeration, scale and viewing distance can all be obtained from any good photogrammetry text.

However, a warning is given that none of the relationships should be used unless an investigator is fully aware of the implications that arise from enlarging the negatives and thereby altering the apparent focal length of the camera lens.

2.5.3. PHOTOGRAPHIC TECHNIQUES.

a. EQUIPMENT. Although special stereoscopic cameras are available (Ross-Brown and Atkinson, 1972), their prohibitive cost and large-size made their use impractical. For this reason a good quality 35mm SLR Camera (Yashica TL Electro X , 50mm F1.4 lens) was used throughout the project.

A 35mm black and white negative format was used because of the easy availability and cost of the film and processing. A 125 ASA film was found to be adequate for summer use, but 400 ASA occasionally uprated to 800 or even 1200 ASA was generally needed during winter site visits. However, 125 ASA film was always used in preference, as the grain of the film was less obtrusive when the prints were viewed at a high magnification. The films were developed and printed onto 'hard' paper, to a size approximately equal to half plate (8in x 6in), and pairs of stereo-negatives were printed under identical conditions.

b. HIGHLIGHTING. The majority of the rocks encountered during the site visits were some shade of grey, and in the initial stages of the project it was thought that there may be problems in interpreting lithological boundaries from the simple black and white photographs. Unfortunately, there are no filters that can be used to help differentiate between different shades of grey. However, careful control of the film developing and printing can 'stretch or compress' the grey scale in the final photograph, thereby increasing the detail and definition within these colours. Unfortunately, these processing controls were not routinely available within the Department.

The problems were overcome in the field by the use of white cellulose spray paint. With the aerosol paint, features of interest could quickly and easily be highlighted, and the practice became a routine field procedure. The usual features highlighted included the top corners of the coal pillars, structural

details of the collapse, geological marker horizons and all relevant stratigraphic boundaries, coal leaves and partings. The white paint proved extremely effective and greatly aided the speed and accuracy of the interpretation. It also served a secondary function of preventing the re-recording of the same working on a subsequent site visit. The effect of highlighting can be seen in many of the photos included in the thesis (eg. Plates 3, 5 and 8).

2.5.4. ACCURACY.

The potential accuracy obtainable from photogrammetric methods is extremely high, but the choice of camera and field procedures obviously limits this potential accuracy (Wickens and Barton, 1971, Ross-Brown and Atkinson, 1972). In any event the quality of the final measurements is only as good as the sum of the accuracy of the component parts. As no quantitative measurements of depth were to be made from the photographs, it was decided not to worry about whether the axes of the two photographs were truly parallel. (This should be borne in mind by anyone attempting to re-interpret any of the photographs). This simplification does not affect the accuracy of the spatial measurements, which is controlled by the parallax errors discussed above, the quality of the photographic equipment, and the accuracy achieved during the final measurements.

During interpretation under high magnification it was usually possible, to measure detail from the prints to within + or - 0.25mm. This is equivalent to a ground distance of about 3.5mm. In practice however, the parallax errors discussed above are the major source of error and must be taken into account to obtain a true assessment of accuracy. Experience has shown that accuracies of the order of + or - 25mm are quite feasible from a good set of orthogonal photographs. However, for poor quality photographs the accuracy can drop quite markedly, and with the very worst of the photographs, the accuracy may be as bad as + or - 20%.

The accuracy of the method described above was tested at the initiation of the project. A number of old workings were carefully measured on site, and the

resulting values were compared against measurements made from the photographs. In all cases the field measurements lay within 4.0% of the photogrammetric measurements.

2.6. LABORATORY TESTING.

Laboratory testing was carried out on selected rock samples from the opencast sites. The tests carried out included assessments of strength, moisture content and mineralogical composition.

2.6.1. STRENGTH TESTING.

Strength testing using a point load test was routine for rock from the roofs of the old workings. The 'Brook irregular lump method' of testing and interpretation (Brook, 1977, 1980) was used throughout the project and was found to be satisfactory. From experience it was found that between 15 to 20 samples of different sizes were needed to provide a good assessment of the rock strength. Sandstones and siltstones proved to be the easiest and most consistent of the materials tested, while mudstone often gave poor results with the data showing considerable scatter. The difference in behaviour between the rock types was entirely due to the way the material broke under the conical platens. The sandstone and siltstones nearly always broke cleanly between the points of the platens, while the mudstones tended to break conchoidally and through plant or other fossil remains.

In the early stages of the fieldwork all strength testing was done on site, but it was felt that the time spent in testing the rock was starting to prejudice site access. Representative material was therefore collected, during the site visit, and tested later in the laboratory. At the time of the site visits, the enormous effect that a small change in moisture content would produce on the measured rock strength was not fully appreciated by the writer. (see Denby et al., 1982) During field testing the moisture content of the rocks varied depending on the time of year and weather conditions at that time. Unfortunately, this limits the value of the strength results, and has precluded

any detailed study of the results in Chapter 3.

2.6.2. MINERALOGICAL/CHEMICAL ANALYSIS.

Mineralogical/chemical analysis was carried out on samples of mudstones and siltstones using both XRF and XRD. X-Ray diffraction was carried out on most of the rock types tested for strength, and the proportion of the various minerals in the sample were evaluated using a 10% Boehemite internal standard. A description of the technique employed and a copy of the calibration curves will be found in Smith (1976).

2.7. DATA COLLATION.

2.7.1. PHOTO-INTERPRETATION.

Many of the items of information required from the interpretation of the stereo-photography contained strong subjective elements. Even what appeared to be straightforward measurements, such as the width of an old working, often required some interpretation because of parallax errors. It was therefore, felt that interpretational bias could be introduced into the data if the photographs were interpreted piecemeal. For this reason no photograph was interpreted until a large number of case histories had been accumulated.

The interpretation was concentrated into two sessions each lasting about two to three weeks. The first session, after the first year of fieldwork, interpreted to about eighty of the old workings, while the interpretation of the remaining case histories was delayed until all the fieldwork had been completed. By this means it is hoped that at least some of the potential subjective errors have been eliminated. Needless to say, continuity between the two interpretation sessions was maintained by, in the second session, re-interpreting a number of the earlier cases.

Each photograph was interpreted at least twice using a standard mirror stereoscope with an optional x3 binocular attachment. As discussed previously, no differential parallax measurements for the assessment of depth were made.

The procedure for each stereo-pair was identical. All quantitative measurements were taken during the first interpretation. These included information such as the height of the collapse, the width of the working and so forth. These values were noted on a data sheet, and were subsequently individually scaled to true measurements using the scaling information contained within the prints. At this point various pertinent ratios, such as the height of collapse to span (width), were also calculated.

All the qualitative information was gathered from the second interpretation and included such data as the visual condition of the old working, and so forth. It also provided an opportunity to review all the information known about the old working. This information synthesis brought together, not only the data from the first two interpretation sessions, but also laboratory data, additional field observations, and historical and site details. All this information was then coded onto a single data sheet, ready for further encoding in preparation for the computer analyses (see Appendix 1).

2.7.2. CHOICE OF VARIABLES.

The aim of the project was to look for any statistical relationship between the old workings and their degree of collapse. Forty seven variables were chosen to characterise the workings. These variables fell into five well-defined groups:

1. Administrative details such as the site location, photographic reference numbers, strength assessment numbers, etc.

2. Quantitative measurements, including the width of working, height of collapse, depth of working, etc., and a number of characterising ratios.

3. Geological and structural data such as rock descriptions, jointing frequency, etc.

4. Qualitative measurements, as for example the visual condition of the

workings or their degree of collapse.

5. Historical data: mainly information on the age of the workings and their condition at the time of abandonment (stowed,propped etc.).

In practice the collapse of an old working is often incomplete and may have been checked by a strong rock in the roof sequence (bridging). To accommodate such situations of partial collapse, a further 13 variables were added. This brought the total number of potentially recordable variables for each old working up to sixty (see Table 2.2 and Appendix 1).

Inevitably, in every data base there will be cases which have not been recorded. To avoid any possible errors, or confusion, that may result during a subsequent analysis, it is essential that these cases can be distinguished from the bulk of the data. Therefore, throughout the data set, missing values have been represented as zero. The statistical program used for the analysis was instructed to recognise this fact, and where true values of zero were present they have been assigned the smallest nominal positive value possible for the variable.

It will be appreciated that in many instances the material that bridges the span is identical to the main rock type. To differentiate these situations from those where the bridge was of a different rock type, each of the thirteen variables had a repeat option. This value was chosen as 9, 99, or 9999.

A summary of the variables, their codes, units, statistical characteristics, column position in the data set, and the permitted missing data and repeat codes will be found in Table 2.2. In the remainder of this section, the variables, whose definitions are perhaps not obvious, are discussed further. A list of the remaining codes and scales, adopted for the coding, will be found along with a listing of the data in Appendix 1.

2.7.3. DEFINITION OF VARIABLES.

a. GEOTECHNICAL DATA. The codings for all the geotechnical variables are based

DATA VARIABLES USED IN PROGRAM

FIRST READ (CARD 1)

PARAMETER	VARIABLE NAME	UNITS	DATA TYPE	NO. COL	CODES UN	CODES R
FIELDWORK DATE	J1	YRS	I	5		
LOCATION (OPENCAST SITE)	J2			6		
PHOTO REFERENCE NUMBER	J3			2		
STRENGTH REFERENCE NUMBER	R4					
APPROX. AGE OF WORKING	J5	YRS	I	4	Y	
VISUAL CONDITION	J6		O	1	Y	
DEPTH BENEATH THE SURFACE	R7	M	R	3	Y	
SEAM NAME	J8			2	Y	
SEAM THICKNESS	R9	M	R	3	Y	
SEAM CONDITION	J10		O	1	Y	
MAIN ROCK TYPE	J11			2	Y	
COLOUR (HUE,SHADE,COLOUR)	J12,JJ12,JJJ12			3*1	Y	
GRAIN SIZE	J13		I	1	Y	
BED THICKNESS	JJ13		I	1	Y	
MINERALOGY	J14,K,L,M,N,O			6*1	Y	
QUARTZ TO CLAY RATIO	R15		I	2	Y	
MOISTURE CONTENT %	J16	%	R	2	Y	
ROCK STRENGTH (UCS)	R17	MN/M2	R	3	Y	
STRENGTH METHOD OF ASSESMENT	J18			1	Y	
DEGREE OF WEATHERING	J19		O	1	Y	
EFFECTIVE BED THICKNESS	R20	CM	R	3	Y	
JOINT FREQUENCY	J21		I	1	Y	
J.CONDITION (OPEN,INFILL)	J22,JJ22		O	1+1	Y	
VERTICAL EXTENT J23			I	1	Y	
BRIDGE ROCK TYPE	J24			2	Y	Y
BRIDGE ROCK COLOUR	J25,JJ25,JJJ25			3*1	Y	Y
GRAIN SIZE	J26		I	1	Y	Y
BED THICKNESS	JJ26		I	1	Y	Y
BRIDGE ROCK STRENGTH	R27	MN/M2	R	3	Y	Y
DEGREE OF WEATHERING	J28		O	1	Y	Y
EFFECTIVE BED THICKNESS	R29	CM	R	4	Y	Y
BRIDGE WIDTH	R30	M	R	4	Y	
BRIDGE THICKNESS	R31	CM	R	4	Y	Y=R29
JOINT FREQUENCY	J32		I	1	Y	Y
J.CONDITION (OPEN,INFILL)	J33,JJ33		O	1+1	Y	Y
ARCH HEIGHT (MIGRATED)	R34	M	R	4	Y	
THEORETICAL ARCH HEIGHT	R35	M	R	4	Y	
ANGLE DEGREES FROM HORIZ.	J36	DEGR.	R	2	Y	
WIDTH OF OLD WORKING	R37	M	R	4	Y	
HEIGHT(COLLAP):WIDTH RATIO	R38	M	R	4	Y	
DEGREE OF BRIDGING OF ARCH	J39		O	1	Y	
TYPE OF O.W. INFILL	J40		O	1	Y	
FLOODING IN OLD WORKINGS	J41		O	1	Y	
DEGREE OF COLLAPSE	J42		I	1	Y	
PERCENTAGE COLLAPSE	J43	%	R	2	Y	
ADDITIONAL COMMENTS CARD	J44			3		
THICKNESS OF PILLAR	J45	M	R	2	Y	
PERCENTAGE EXTRACTION	J46	%	R	2	Y	
SPAN WIDTH : SEAM THICKNESS	R47	M	M	4	Y	

Table 2.2 Variables recorded during interpretation

on the Report by the Geological Society Engineering Group Working Party on the description of rock masses for engineering purposes (Anon, 1977).

b. QUANTITATIVE MEASUREMENTS. The definitions for the various distances measured from the stereo-photographs are shown in Figure 2.9. In practice the height of collapse was sometimes difficult to assess. This was due to areas of obviously very unstable rock 'hung up' in the roof (see Trollope's (1966) 'suspended zone' model and Fig. 6.1). The definition was therefore modified, and the maximum height of collapse, was taken as the position in the arch where the rock showed no sign of imminent collapse.

c. THEORETICAL MAXIMUM HEIGHT OF COLLAPSE. The concept of a theoretical maximum height of collapse was introduced to remove the distortive effect that bridging could cause in a statistical analysis. Field observations, from sites with uniform roof lithologies, had suggested that the height of collapse was related to both the rock type and its 'intactness'. However, single lithology roof rocks are uncommon, and while, for an individual case, the presence in the main roof of a strong rock capable of bridging the void is very important, it provides little information when looking at the collapse potential for a single specific rock type. If the bridging effect is not removed a statistical analysis on the height of collapse for a given rock type would, in fact, record the average height above the old working at which a strong rock will occur.

To overcome this, the theoretical maximum height of collapse, (Fig. 2.9) was introduced, and is predicted by projecting the closure rates for the arch through the bridging rock to an imaginary apex high in the roof. This apex, assuming the closure rate remains constant, would thus represent the probable final limit of collapse for the arch if the bridging rock had been absent.

There are a number of theoretical objections to such a maximum height of collapse, these are:-

1. The projection of the existing arch line may be fair but only if the working has almost completely collapsed. For workings which have hardly collapsed, a small variation in the arch closure will make a great difference to the

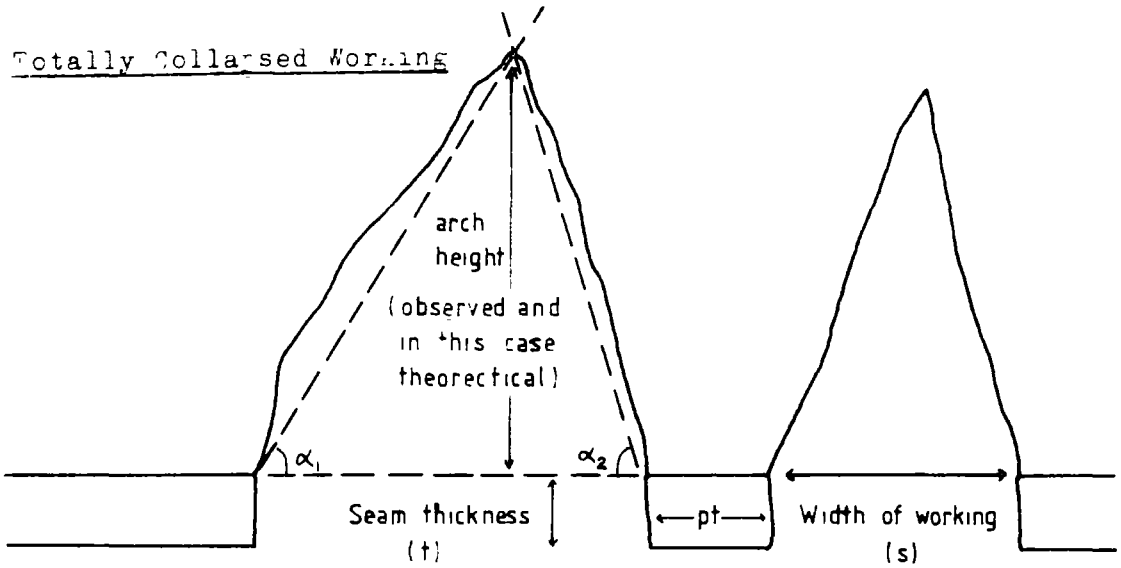

TMH = Theoretical maximum height of collapse
h = Collapse height
S = Width of working
w = Bridge width
t = Seam thickness (worked)
= Angle to apex of theoretical collapse
pt = Pillar thickness

Angle of collapse $\alpha = \frac{\alpha_1 + \alpha_2}{2}$

Partially Collapsed Working

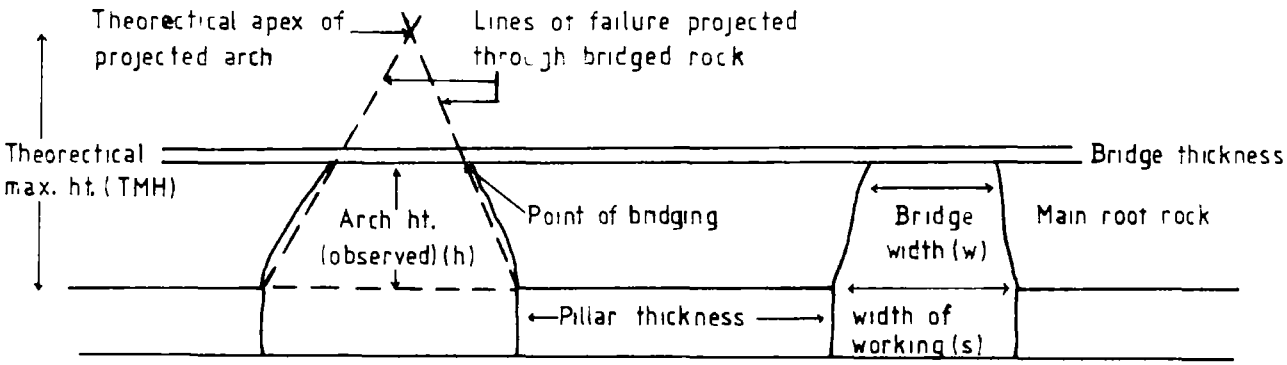

Span width : seam thickness = $\frac{S}{t}$

Collapse height : span width ratio = $\frac{TMH}{S}$

$$\%\text{collapse} = \frac{h}{TMH} \times 100$$

$$TMH = \frac{\tan \alpha \times S}{2}$$

$$\alpha = \tan^{-1}\left(\frac{2h}{S - w}\right)$$

Figure 2.9 Definitions of measurements made on photographs of old workings.

calculated theoretical maximum height.

2. The rate of closure is calculated as the average angle for the two half arches between the roofline and the initial point of bridging. These assumptions make no accommodation for the shape of the failure arches, or the possibility that the rate of closure increases as the apex is approached.

The first objection, while not overcome, is at least assessed by calculating the percentage collapse.

$$\text{Percentage collapse} = \frac{\text{Observed height}}{\text{Theoretical collapse height}} \times 100$$

The accuracy of the theoretical maximum height of collapse will increase as the percentage collapse increases.

There is no answer to the second objection. Some assumption has to be made on the shape of the failure surface, and the choice of a linear fit does at least predict the maximum collapse height and could be proportionally reduced to accommodate a particular shape as required (see Chapter 9).

On balance the advantages of predicting a theoretical maximum height of collapse outweigh the disadvantages.

The height to width ratio is calculated from the theoretical maximum height of collapse for similar reasons to those explained above. There is no other way of making the ratio directly comparable between different arch widths and rock types without first removing the problems of bridging. The adoption of a 'theoretical collapse height' does not ignore the basic data. General (true) height of collapse statistics may be found in Table 3.1.

2.7.4. PROGRAM 'VALIDAT'.

Raw data, in the form of numbers and codes, is hard to assimilate and difficult to check. The program VALIDAT (Appendix 1) was written to decode the raw data and provide a hard copy, written summary, of the data for each old working.

Table 2.3 is a typical example of the output that can be obtained by running the data (also in Appendix 1) through the program.

Also included in Appendix 1 is a listing of the program DATAMEDDLER. This program reorganises the raw data, changing the repeat codings to their appropriate main rock values.

2.8. SUMMARY.

Opencast sites have proved to offer a unique opportunity to study collapsed old workings in section. It has been found that accurate measurements of the dimensions of the collapse structures can be quickly and efficiently obtained by using stereo-photographic techniques. The main advantage of this technique is its speed, accuracy and safety. However the advantages can only be capitalised upon provided that the parallax errors associated with the technique are minimised. To a large extent the worst of the parallax errors can be eliminated, on site, by the careful choice of photographic location and the identification of roadway axis or the mid-line. At the interpretation stage of the fieldwork, the subjective elements in the photographic interpretation were minimised by concentrating the data-synthesis into just two concentrated periods. Sixty (60) variables were chosen to characterise each old working, and subsequently the data were coded onto computer both for convenience and in preparation for statistical analysis.

In all, 151 old workings have been recorded from 18 opencast sites spread across Scotland, England and Wales.

FIELDWORK DATE.	310778
OPENCAST SITE.	LOW CLOSE
PHOTO REFERENCE NUMBER.	1239
STRENGTH REFERENCE NUMBER.	26.00
APPROX. AGE OF WORKING.	1880
VISUAL CONDITION.	POOR
APPROX. DEPTH OLD WORKINGS.	6.00
SEAM NAME.	METAL
SEAM THICKNESS.(M).	1.00
SEAM CONDITION.	SLIGHT CLEAT
MAIN ROCK TYPE.	SHALEY MUDSTONE
MAIN ROCK COLOUR.	DARK GREYISH BLACK
GRAIN SIZE.	V.FINE
BED THICKNESS.	THINLY LAMINATED 2 -6 MM
MINERALS IN ORDER OF ABUNDANCE.	
KAOLINITE QUARTZ	ILLITE SIDERITE
QUARTZ TO CLAY RATIO.	0.3 CARBON + OTHERS
MOISTURE CONTENT PER CENT.	UNKNOWN
ROCK STRENGTH MN/SQ.M.	42.00
STRENGTH METHOD OF ASSESMENT.	POINT LOAD
DEGREE OF WEATHERING.	SLIGHTLY
EFFECTIVE BED THICKNESS.(CM).	6.00
JOINT FREQUENCY.	WIDE
JOINT CONDITION.	CLOSED NO INFILL
JOINT VERTICAL EXTENT.	0-0.5M
BRIDGE ROCK TYPE.	AS ABOVE SHALEY MUDSTONE
BRIDGE ROCK COLOUR.	AS ABOVE DARK GREYISH BLACK
GRAIN SIZE.	AS ABOVE V.FINE
BED THICKNESS.	AS ABOVE THINLY LAMINATED 2 -6 MM
BRIDGE ROCK STRENGTH MN/SQ.M.	AS ABOVE 42.00
DEGREE OF WEATHERING.	AS ABOVE SLIGHTLY
EFFECTIVE BED THICKNESS.	AS ABOVE 6.00
WIDTH OF BRIDGED SPAN.(M).	0.01
THICKNESS OF BRIDGE.	AS E.B.T. ABOVE.
JOINT FREQUENCY.	AS ABOVE WIDE
JOINT CONDITION.	AS ABOVE CLOSED NO INFILL
ARCH HEIGHT. (M) (MIGRATED).	1.22
THEORETICAL ARCH HEIGHT.(M).	0.22
ANGLE,DEGREES FROM HORIZONTAL	12
WIDTH OF OLD WORKING.(M).	2.04
HEIGHT : WIDTH RATIO.	UNKNOWN
DEGREE OF BRIDGING OF ARCH.	COMPLETE
TYPE OF O.W. INFILL.	NO STACKING
FLOODING IN OLD WORKINGS.	TOTAL
DEGREE OF COLLAPSE.	SUPERFICIAL 10-30%
PERCENTAGE COLLAPSE.	1
ADDITIONAL COMMENTS CARD.	24
THICKNESS OF PILLAR (METERS)	UNKNOWN.
PERCENTAGE EXTRACTION.	50
SPAN WIDTH : SEAM THICKNESS.	2.04
RATIO OF E.B.T. TO O.W. WIDTH	33(MAIN ROCK)
RATIO OF E.B.T. TO O.W. WIDTH	33(BRIDGE ROCK)

Table 2.3 Typical output from the program VALIDAT

C H A P T E R 3

DATA ANALYSIS AND INTERPRETATION

3.1. INTRODUCTION

The database described in the Chapter 2 contains in the region of 10,000 pieces of data. This is small in terms of databases and was therefore, easily accommodated within the Michigan Interactive Data Analysis System (MIDAS, 1976).

The analyses of the data base broke down conveniently into three stages. These were:-

1. Data verification.
2. Summary statistics and intra-variable variation.
3. Variable inter-relationships.

The first of these, data verification, was important as it was the last time that any mistakes in the raw data were likely to be spotted before they would distort the statistics. Inevitably within 10,000 pieces of information there will be the occasional wild data point, and these can often be detected by examining the minimum and maximum recorded values, and comparing them with the spread of the remaining data. The summary statistics and inter-relationships of the variables form the bulk of the analysis and are dealt with below.

3.2. SUMMARY STATISTICS

Summary statistics include any method by which the data can be characterised, such as histograms, frequency distributions, means, standard deviations, medians, percentiles and so forth. The most common summary statistic in general use is the mean and standard deviation, but this statistic assumes that the variable has a 'normal distribution'. Many of the analytical variables, as for example depth, width, and height, do not have a normal but a skewed distribution. In addition, variables of a 'categorical nature', that is variables which consist of groupings, as for example joint frequency (6 levels), or bed thickness (7 levels) (see Appendix 1), cannot be summarised in such a

way. To overcome these problems, the majority of the data have been summarised by histograms. These offer more information for skewed analytical data than could be obtained from medians and percentiles, and are one of the few ways of summarising categorical data. However, a summary Table for means, standard deviations and medians is presented in Table 3.1, but caution should be exercised in using mean values.

The variables dealt with in this Chapter fall naturally into two groupings. First, there are the variables which reflect some aspect of the condition, location, age and so forth of the workings. These comprise a set of information which describe the average conditions of an old working. The second group contains the variables which bear directly on the individual collapse. These include such things as the width of working, and the height of collapse.

3.2.1. GENERAL OBSERVATIONS ON OLD WORKINGS

The visual condition of the workings (Fig 3.1), reflects both the quality of the exposure of the old working, as well as the quality of the photographs. This variable is thus, indirectly, a measure of the accuracy of the measurements. (See Chapter 2.5.4). An excellent old working is one where a full section through the seam and collapse structure was seen, and where there has been no need to make any judgement about the width of working, seam height and so forth. On the other hand, a poor old working is one that was poorly exposed and where some assumption has had to be made during the interpretation about either or both the width of working, and seam thickness. It is satisfying to note that two thirds of the data represent well exposed, well photographed examples of old workings. However, it should be remembered that very poorly exposed old workings were ignored at the time of the field work and so are not recorded. Therefore, this high proportion of well exposed old workings is not a reflection of the overall proportion that were found on site.

The abandonment dates, for the mines represented by the workings, vary between about 1700 and 1956, with no single period showing any dominance.

Variable	Units	n	Min.	Max.	Mean	Std.Dev.	Skewness	Kurtosis	Median	Percentiles 2.5	Percentiles 97.5
Depth	m	111	1.30	75.0	12.73	8.82	3.83	21.81	10.00	4.70	40.0
Seam thickness	m	151	0.60	2.50	1.14	0.292	1.52	5.14	1.10	0.60	1.90
Strength	MN/m^2	133	6.0	56.0	25.54	10.09	0.61	0.75	26.0	7.60	50.0
Effective bed thickness	mm	148	10.0	170.0	61.60	33.80	0.74	0.44	58.00	15.00	58.0
Bridge effective bed thick.	mm	150	5.0	1000.0	134.10	177.40	2.95	9.24	70.00	15.00	900.0
Bridge width	m	140	0.01	10.56	0.98	1.32	4.27	24.91	0.73	0.01	3.37
Bridge thickness	mm	150	2.5	1000.0	150.90	211.30	2.67	6.96	70.00	0.60	1000.0
Arch height	m	145	0.01	13.60	2.15	2.20	2.46	8.19	1.50	0.05	7.70
Theoretical height	m	139	0.01	24.00	3.47	3.38	3.28	14.43	2.45	0.10	11.00
Angle α	^{o}	146	1.00	90.0	62.10	16.31	-2.04	4.64	66.0	6.00	82.00
Working width	m	147	0.8	18.0	2.78	2.20	3.93	20.29	2.10	1.0	8.73
Height to width ratio	-	134	0.06	4.9	1.27	0.703	2.01	6.31	1.15	0.31	3.24
% Collapse	%	136	1.00	99.0	63.24	28.94	-0.286	-1.003	62.00	1.00	99.0
Pillar thickness	m	97	1.00	30.00	6.72	5.38	1.94	4.69	5.0	2.00	25.0
Collapse ht/seam thickness	-	147	0.58	10.10	2.38	1.39	2.20	7.25	2.06	0.88	6.93
Width normalised	-	139	0	99.91	63.04	29.52	-0.229	-1.012	62.20	0	99.81
Height normalised	-	145	1.09	436.5	145.4	90.08	0.642	-0.058	126.53	10.87	319.77
Angle $>25^o$	^{o}	139	25.00	90.0	64.85	10.82	-1.185	2.311	67.0	36.00	82.00
Observed ht:width ratio	-	145	0.055	2.18	0.727	0.450	0.642	-0.058	0.63	0.055	1.60
Aspect ratio width/seam thick	-	147	0.667	10.14	2.41	1.41	2.170	6.814	2.06	0.938	6.94
Bridge width/thickness ratio	-	135	0.029	800.0	13.4[+]	20.5	3.186	12.28	6.06	0.077	78.62

A normal distribution has a skewness and a kurtosis value of 0. (See Snedecor and Cochran (1980) for tables of significance.)

[+]4 values greater than 123 removed before calculation of mean, median and percentiles.

TABLE 3.1

SUMMARY STATISTICS FOR OLD WORKINGS

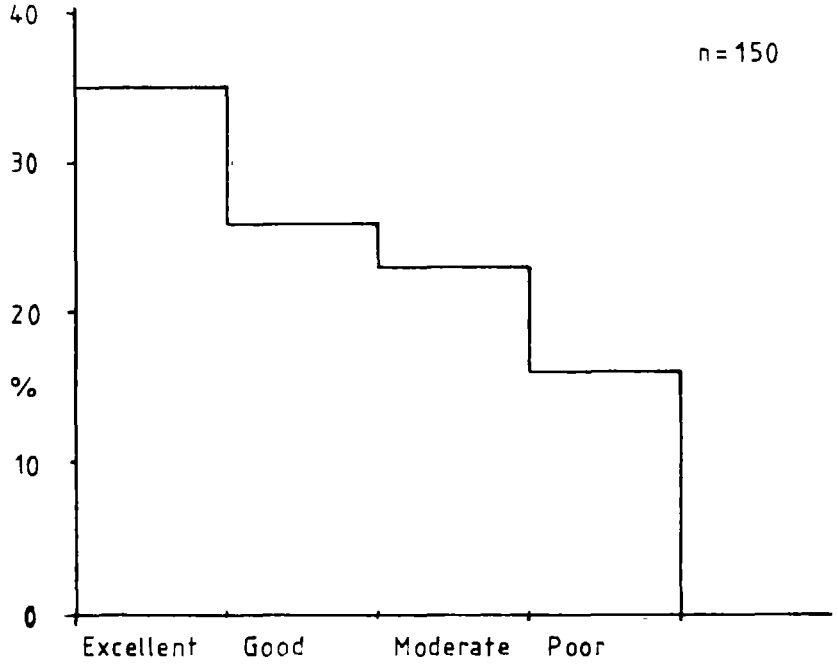

Figure 3.1 Visual condition of old workings.

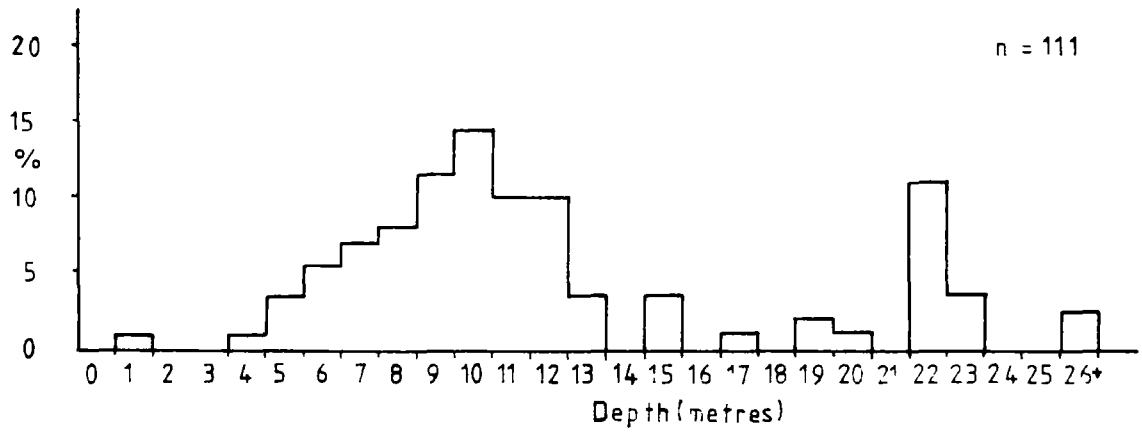

Figure 3.2 Depth of old workings from surface.

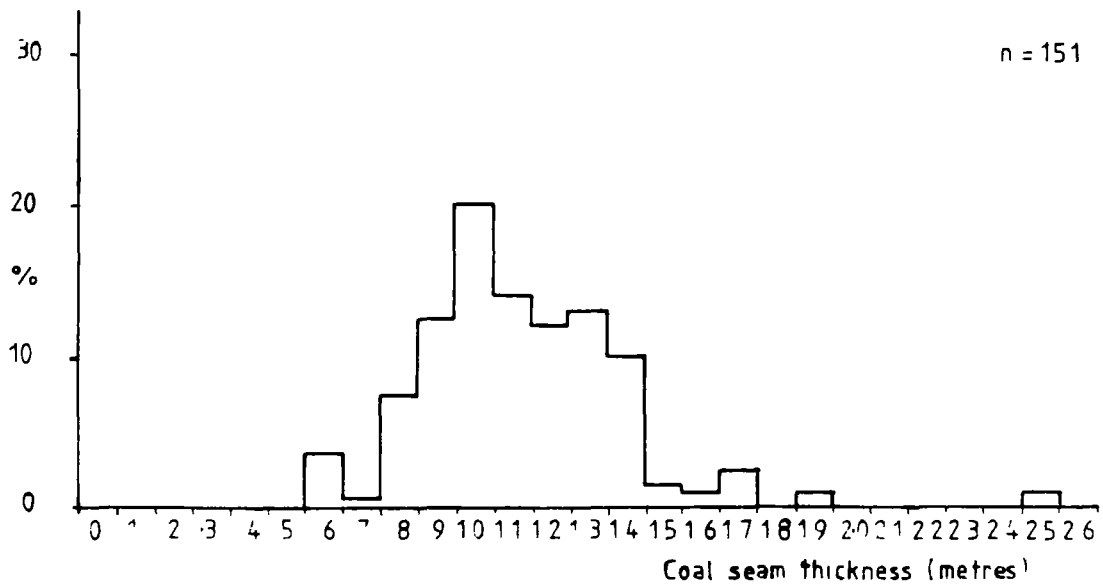

Figure 3.3 Coal seam thickness.

The depths from the surface to the roofs of the old workings, vary between a minimum depth of about 1m and a maximum depth of 75m (Fig 3.2). The higher values reflect the deeper opencast sites of South Wales, where the sites work the more valuable anthracite seams. However, the majority of the data are concentrated between 4m and 24m, and have a median depth of only 10m. Thus, the observations, and any deductions drawn from the data in the remainder of this Chapter, must be thought of as typical of only very shallow mine workings.

The coal seams investigated during the study varied in thickness from 0.6m to 2.5m (Fig 3.3) and had a mean thickness of 1.14m (median 1.10m, Table 3.1). The distribution of the data is slightly skewed towards the thinner seams and is more peaked than normal.

The rocks overlying the old workings were, as would be expected, dominated by mudrocks (Fig 3.4) . About three quarters of the workings were roofed by some type of mudrock with mudstones (31%) the most common. The majority of the roof rocks (79%) appeared to be fresh and showed no sign of weathering. This is a little surprising considering the average depth of the workings. The average strength of the roof rock (Fig 3.5) reflects the distribution of rock types and had a median value of 26 MN/m2 (Table 3.1). There were problems standardising moisture contents, and therefore, a detailed analysis of any variation in strength is inappropriate.

The variable referred to as 'effective bed thickness' was determined subjectively after an examination of the thickness of the rock fragments comprising the arch fill. A lithological horizon may appear to be massive, when seen intact in the high wall, but can often disintegrate along hairline cracks when it forms the roof of an old working. This is discussed in more depth in Chapter 6. The mean effective bed thickness was found to be 61.6mm (median 51.8mm, Table 3.1 Fig 3.6), but this is not a good representation of the data even though the statistics suggest that the distribution is fairly normal. Study of the histogram of the effective bed thickness (Fig 3.6) shows that the majority of the typical rock fragments, comprising an arch core, vary in thickness between 30mm and 70mm. This distribution of the actual thickness of

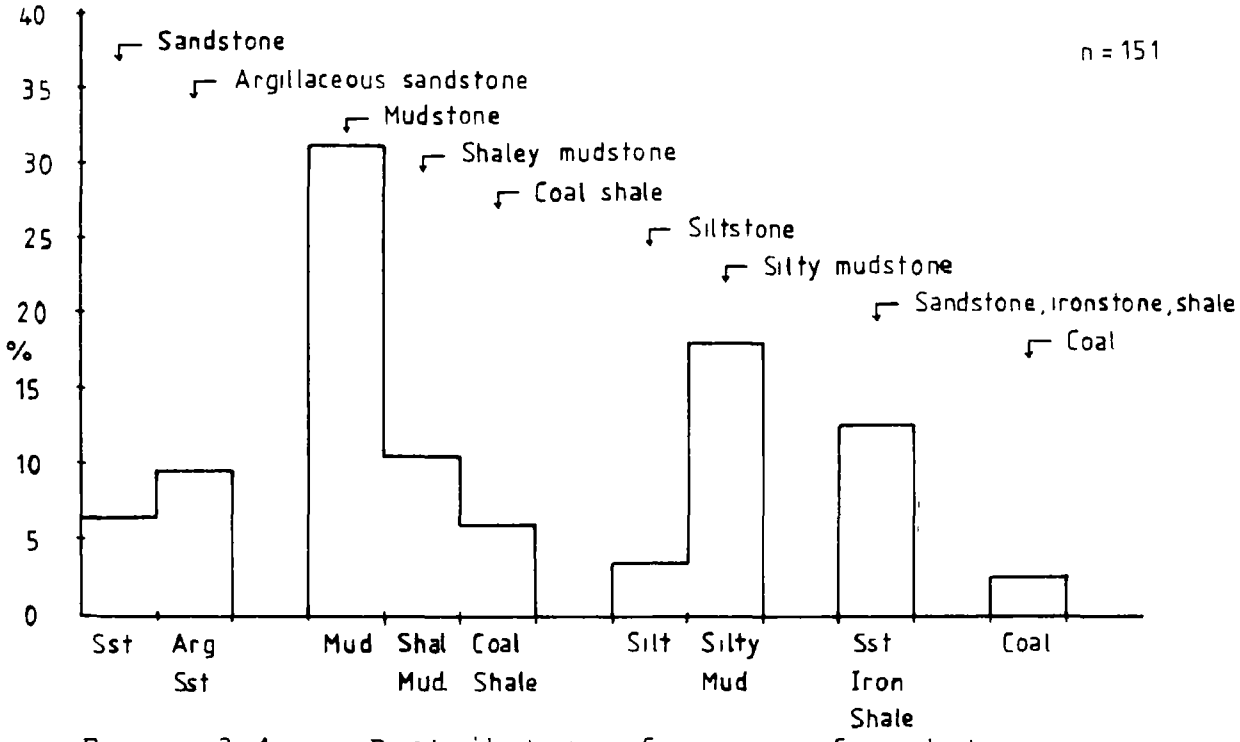

Figure 3.4 Distribution of main roof rock types.

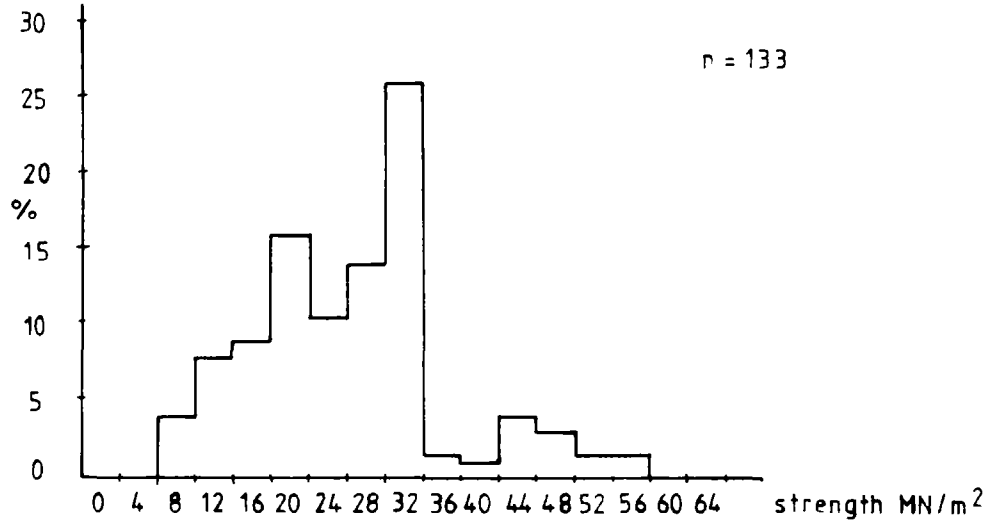

Figure 3.5 Average strength of roof rocks.

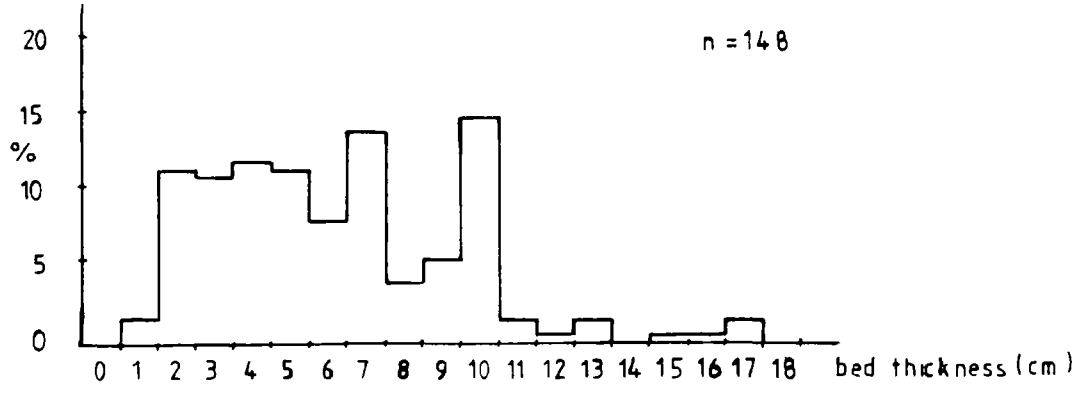

Figure 3.6 Effective bed thickness (main roof rock)

the average core fragments contrasts with the distribution of the bed thickness (Fig 3.7). The average bed thickness seemed to be fairly evenly distributed between thinly laminated and medium thick rock units (6mm to 0.2m).

Little information of value was obtained from the joint data. The joints are typically between 0.2 and 0.6m apart (wide Fig 3.8), with no infilling and of variable vertical extent. Figure 3.9 shows the distribution for the vertical extent of the major joints.

The majority of the workings (76%) showed no evidence of flooding (Fig 3.10), and had been abandoned without any major stowage (Fig 3.11). In fact only about 18% of the workings showed any sign of stowage, and this figure includes about 3.5% of workings which had been completely stowed. In situations of partial stowage it was common to see the roadway stowed on one side only so that access, and presumably ventilation, was maintained to other areas of the mine.

3.2.2. DIMENSIONS OF OLD WORKINGS AND COLLAPSE STRUCTURES.

The main interest of the present study was the state of collapse of the individual old workings. The state of collapse can be recorded by numerous different methods, some of which have already been described in Chapter 2.7.3. While much of the information is duplicated by the different recording techniques, each method is sufficiently different to be of value.

a. DEGREE AND CONDITION OF COLLAPSE STRUCTURES

The typical condition for an old working is one of semi-collapse. This is well demonstrated in Figure 3.12, where an assessment of the degree of collapse shows that about 80% of all the workings were in a state of major collapse. Of the 20% that showed only superficial collapse, only 3.5% were completely open and stable.

The percentage collapse (Fig 3.13, Table 3.1) supports the observations made above, but provides a more detailed breakdown of the data. It should be remembered however, that the methods of assessment for the degree of collapse

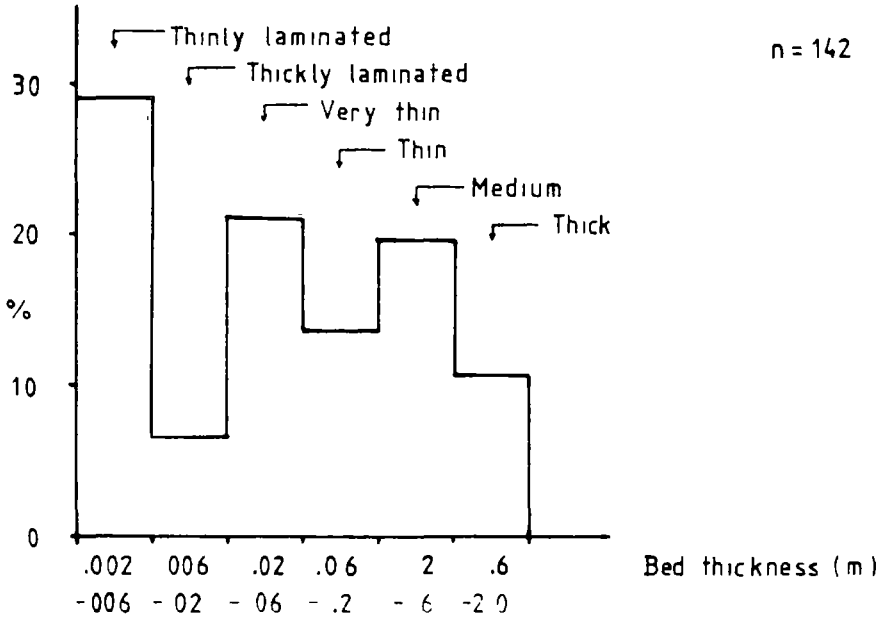

Figure 3.7 Distribution of bed thicknesses.

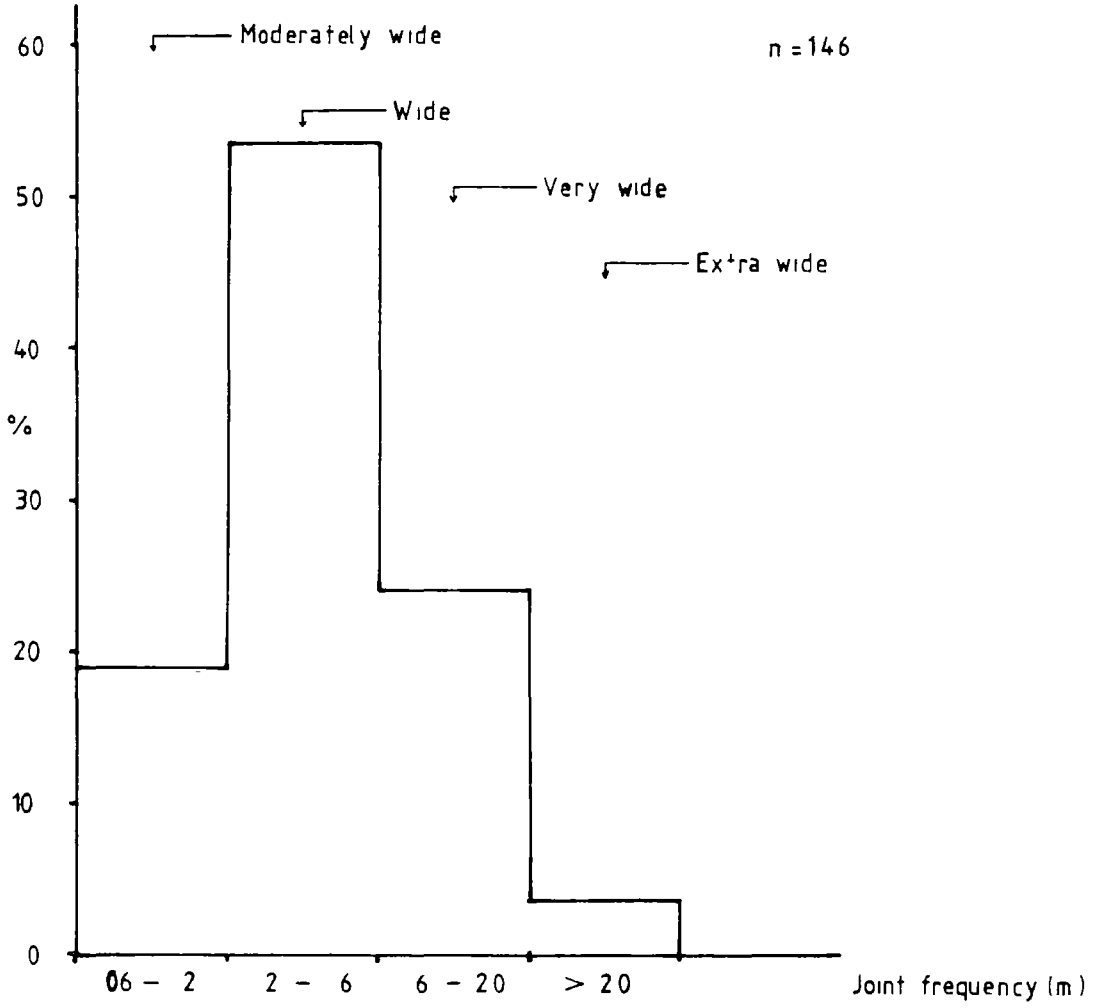

Figure 3.8 Distribution of joint frequency (main roof).

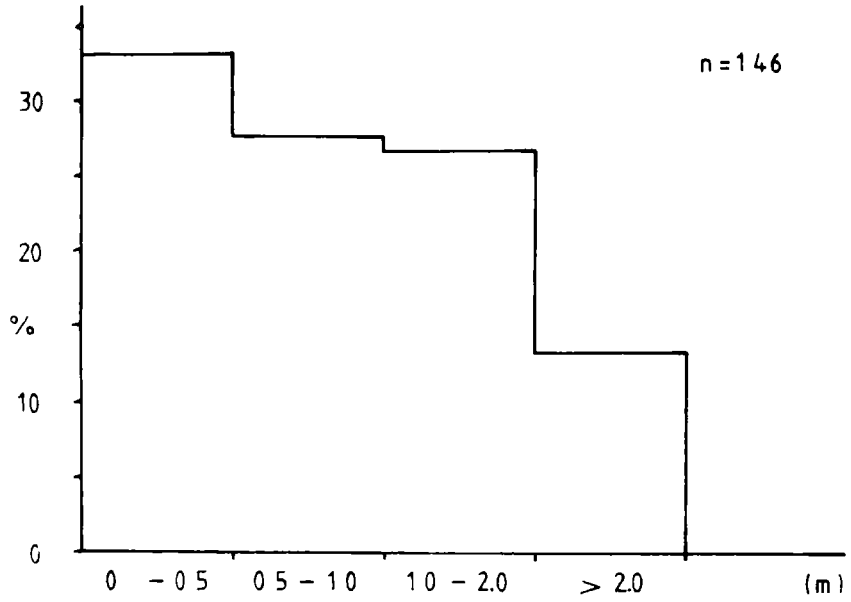

Figure 3.9 Distribution of joint vertical extent (main roof).

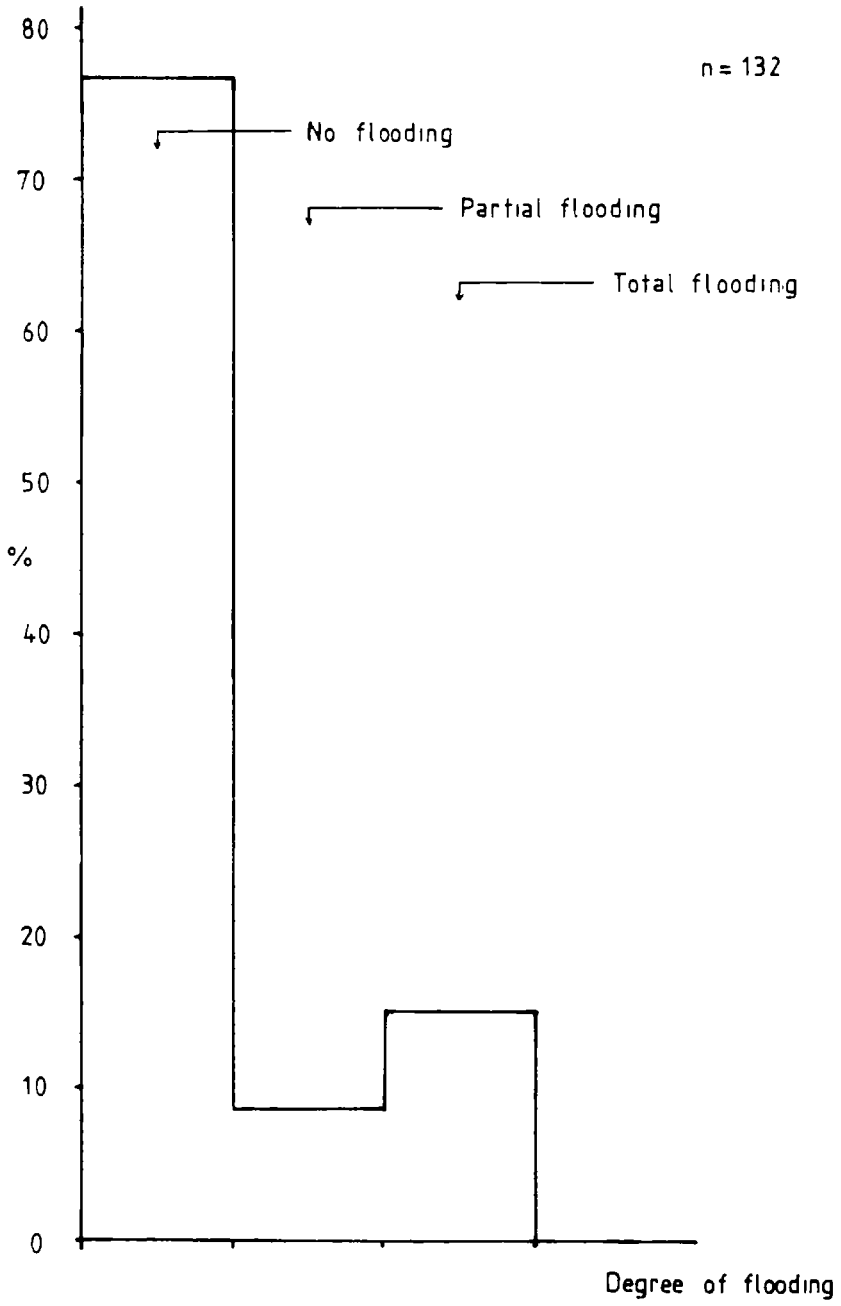

Figure 3.10 Flooding of old workings.

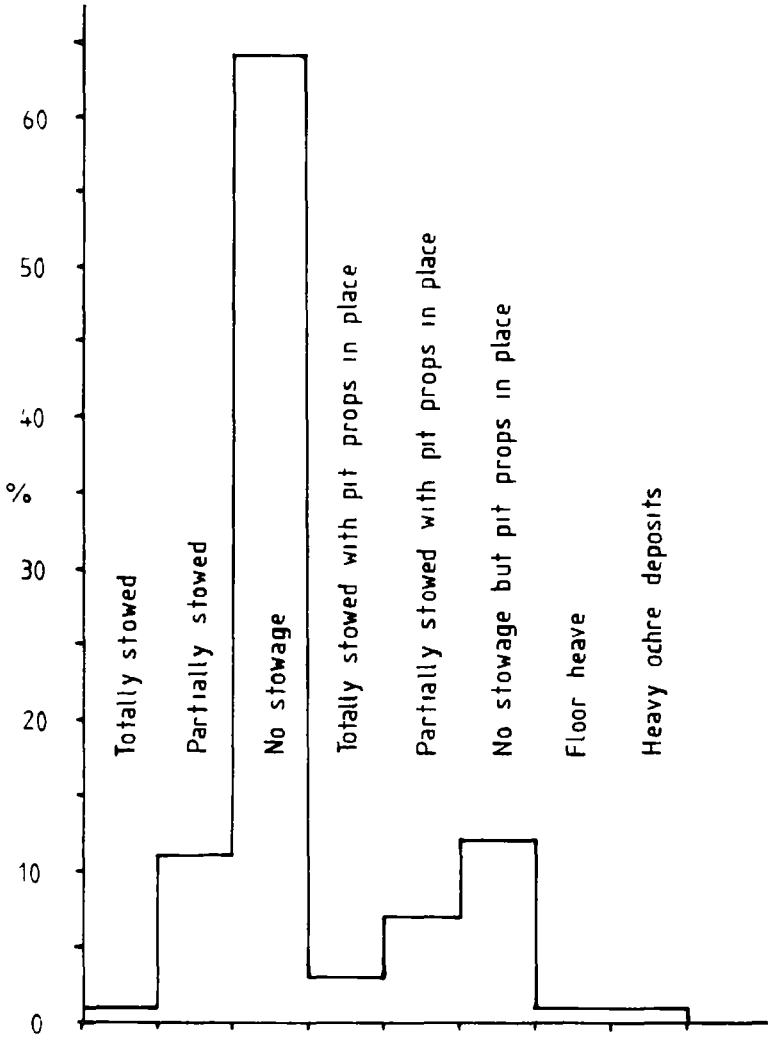

Figure 3.11 Type of old working infill (at time of abandonment).

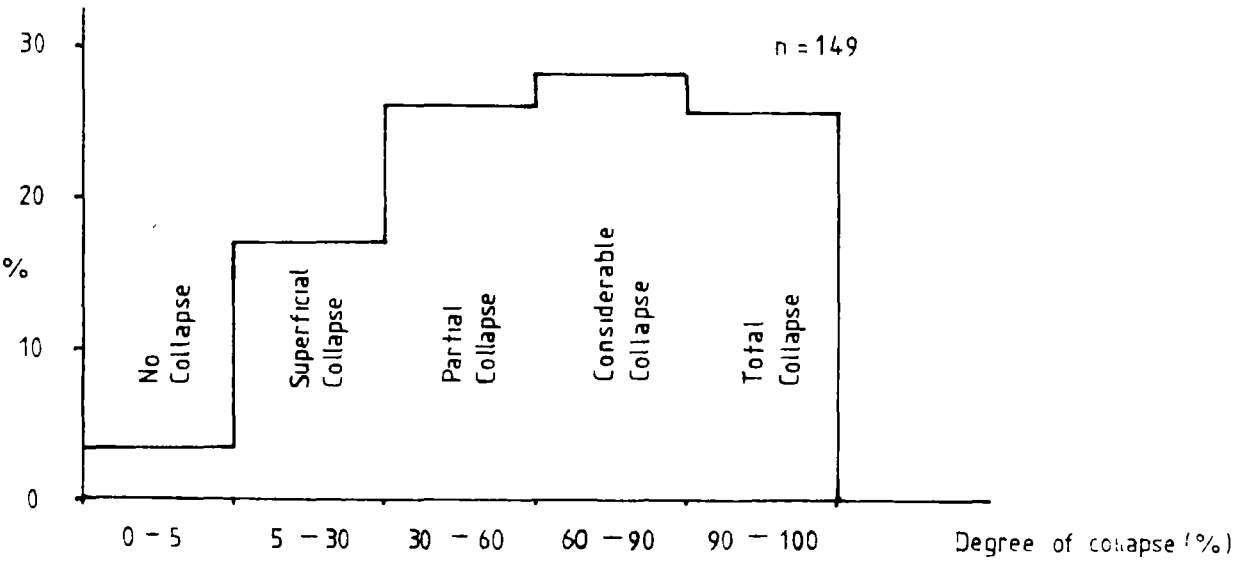

Figure 3.12 Degree of collapse (visual assessment).

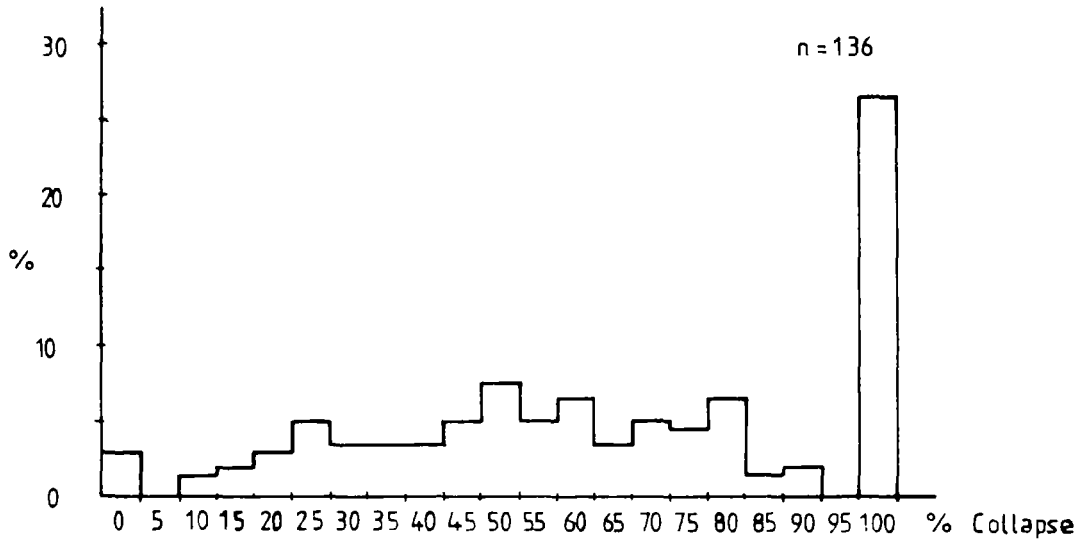

Figure 3.13 Percentage collapse of old workings.

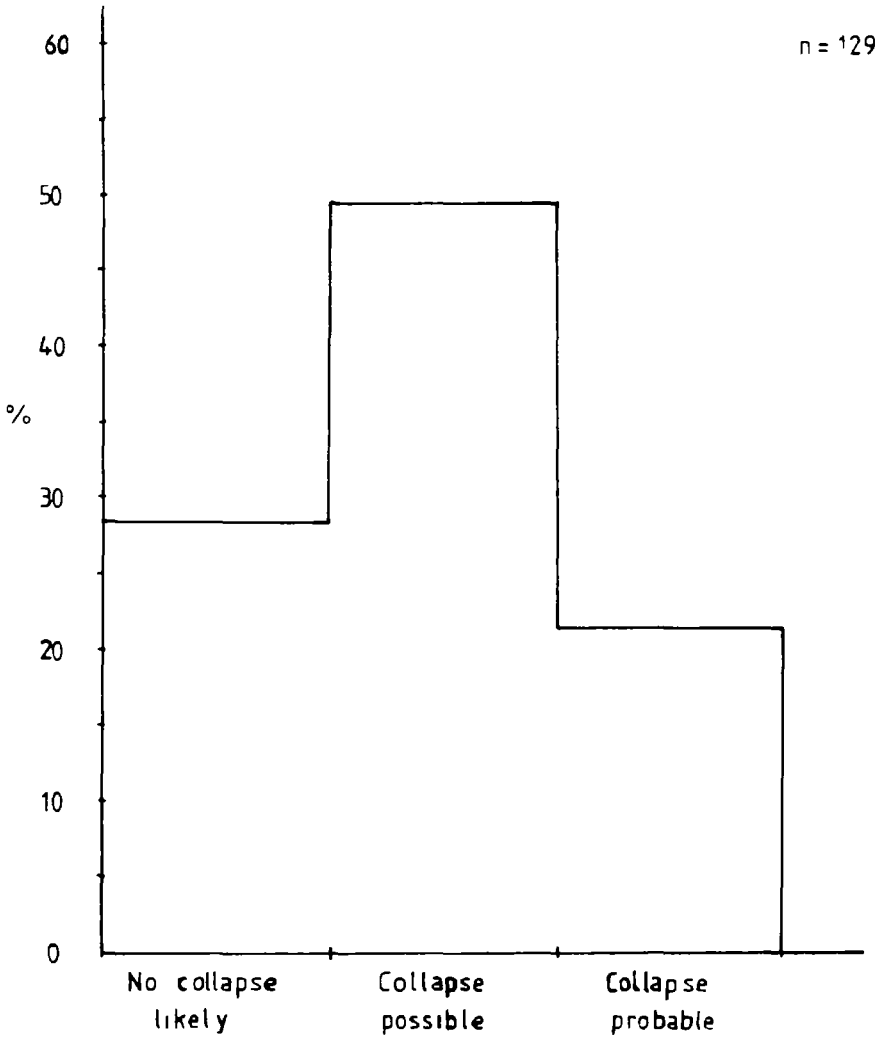

Figure 3.14 Effectiveness of rock bridging.

and the percentage collapse are based on the observed height of collapse compared to the theoretical height of collapse. Because the theoretical maximum height of collapse does not take the curvature of the arch into account, the maximum height is exaggerated and so the assessment of the state of collapse is underestimated. These assessments of the degree and percentage of collapse will therefore be on the conservative side. Referring to Figure 3.13 it can be seen that about 25% to 30% of all the old workings had completely collapsed, forming a well-defined arch extending into the roof. Of the remaining 60% or so, most showed a significant degree of collapse. A comparison between the two methods reveals an apparent discrepancy between the numbers of old workings showing no collapse at all. The difference of 0.6% is not important and just reflects the number of workings for which an accurate assessment could not be obtained for the more precise percentage collapse.

The previous variables considered the amount of collapse that had occurred and were not concerned with the possibility of any further collapse. Figure 3.14 is a subjective assessment of the void arresting potential of the rock unit above. It suggests that about 30% of the workings had reached equilibrium and were stable unless the roofs were subjected to some violently disturbing action. About 21% of the workings were unstable and in a state of imminent collapse. With these it was considered to be only a matter of time before further major collapse occurred. However, a large proportion of the arches viewed (50%) had reached an uneasy equilibrium. It is this and the unstable group that would be affected by external variables such as vibration, changing moisture content, heavy surface loading and so forth. This should be kept in mind when considering or using the average observed height of collapse, and is one reason why the theoretical maximum height of collapse is a more reliable estimate than the observed height of collapse for predicting the limit of collapse. It will be appreciated that, for predictive purposes, there is little point in quoting an average observed height of collapse if it has to be qualified by saying that there is a 70% chance that the void will migrate higher if disturbed.

The average width of the roadways, measured at roof height, are shown in Figure

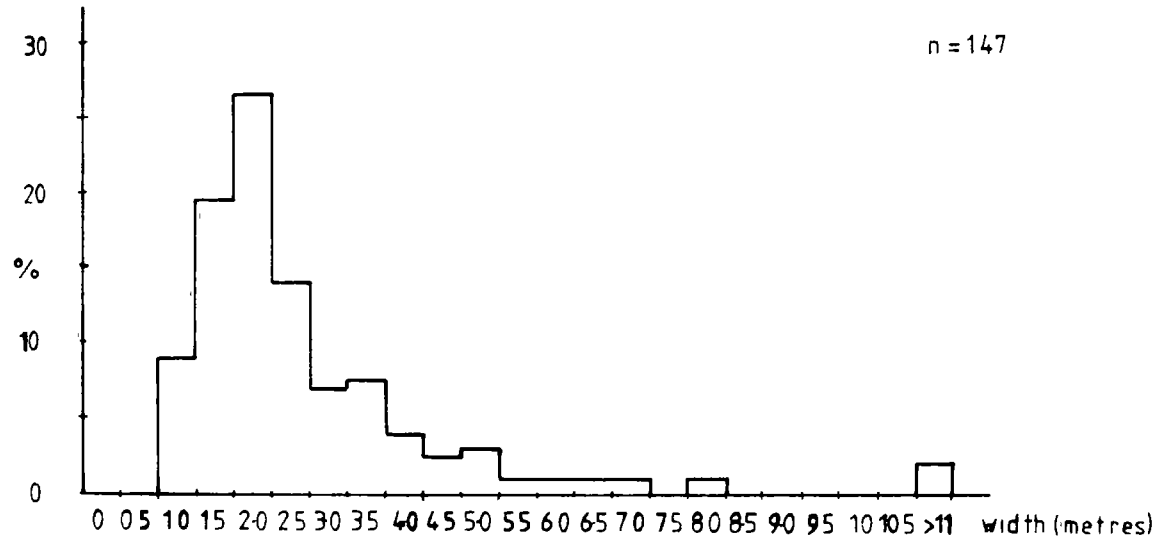

Figure 3.15 Width of old workings.

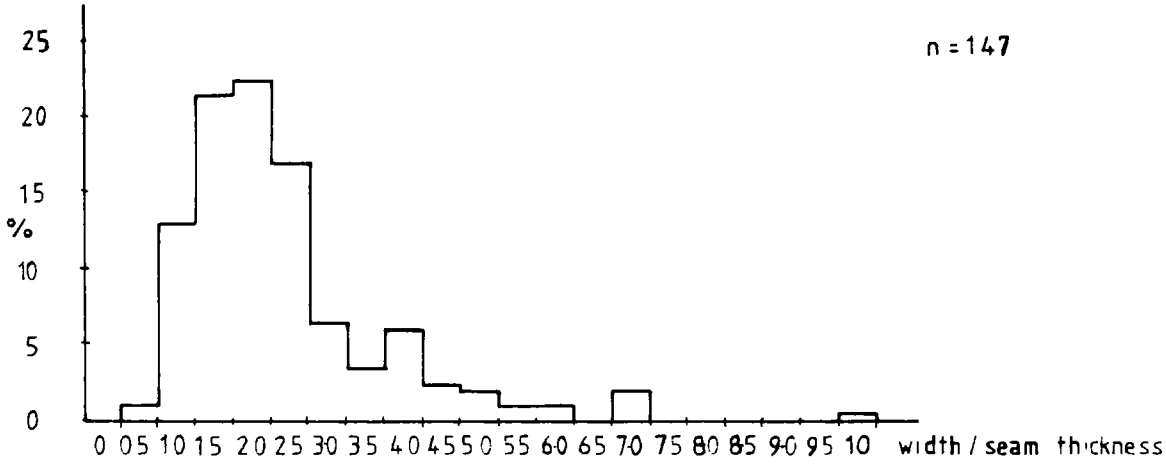

Figure 3.16 Aspect ratio of old workings.

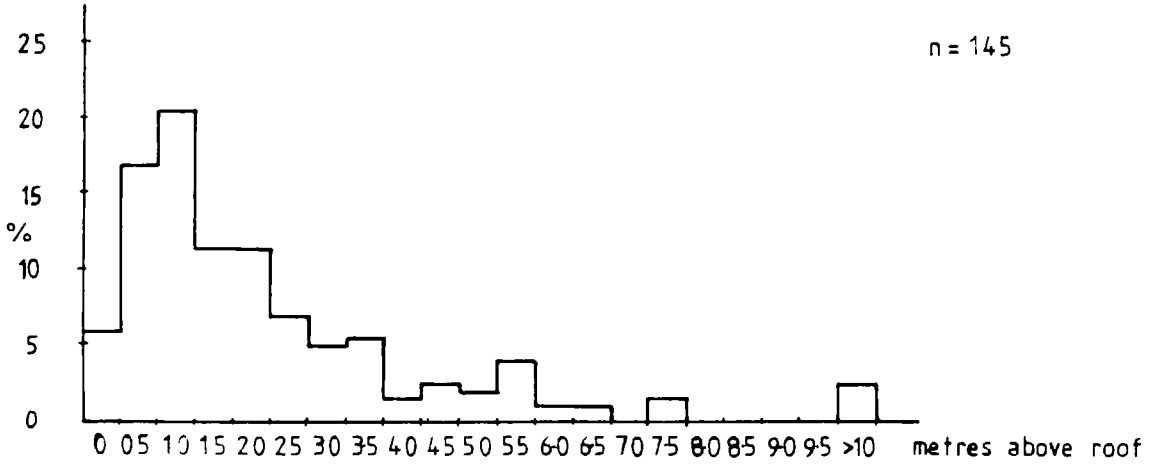

Figure 3.17 Observed collapse height of old workings.

3.15. The median width is just over 2m (Table 3.1), but this value should not be taken too literally because, as explained in Chapter 1, many roadways were driven wider in the direction of the cleat than in the direction against the cleat. This minor variation has been lost in the statistics. The reasons for variable width roadways have been discussed in more depth in Chapter 1. From Figure 3.5, the bulk of the data is observed to lie between 1 and 5m. This confirms the observations of Wardell and Wood (1965) who suggested that old workings were rarely less than 2m or greater than 5m in width.

The ratio between the width of the working and the thickness of the coal seam provides data on aspect ratios for an old working. The distribution is seen to be fairly normal (Fig 3.16), and has a median value of 2.06 (Table 3.1). Thus, an 'average' old working is twice as wide as the thickness of the worked coal.

The observed height of the collapsed arch and the theoretical collapse height are shown in Figures 3.17 and 3.18. Used on their own and divorced from the width of working (which is one of the major controls on the height of collapse) they are of little value. However, a comparison between the two histograms shows the effect of projecting the observed height of collapse through to a theoretical collapse height.

b. COLLAPSE RATIOS AND METHODS OF QUANTIFYING THE HEIGHT OF COLLAPSE

The ratios of collapse height to working width are of greater value (Figs 3.19 and 3.20, Table 3.1). Figure 3.19 represents the observed collapse height to width ratios for the old workings. However, it should be remembered that while these ratios reflect the condition at the time of observation, about 70% of the workings are likely to collapse further if disturbed. The choice of using the theoretical maximum height of collapse divided by the width overcomes this problem (Fig 3.20), but will conversely overestimate the probability of collapse. For predictive purposes however, one must still recommend these values.

The ratio of theoretical height of collapse to width appears to be distributed

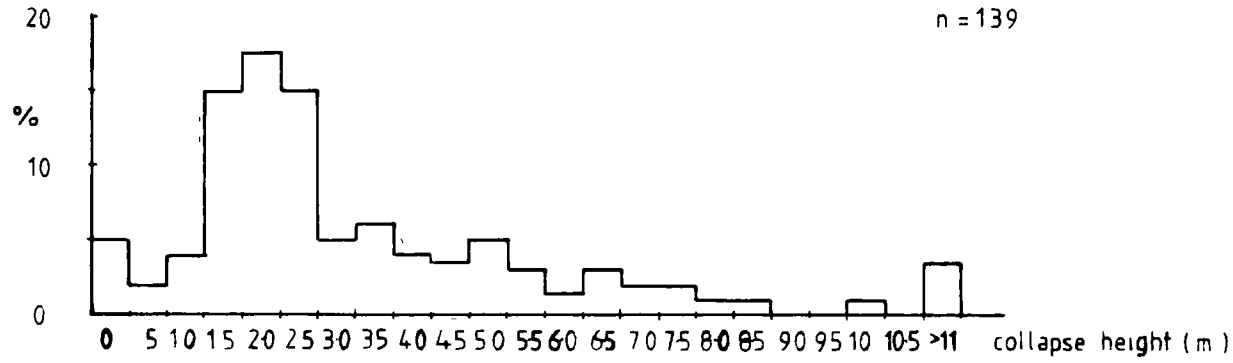

Figure 3.18 Theoretical collapse height of old workings.

Figure 3.19 Ratio of observed collapse height/working width.

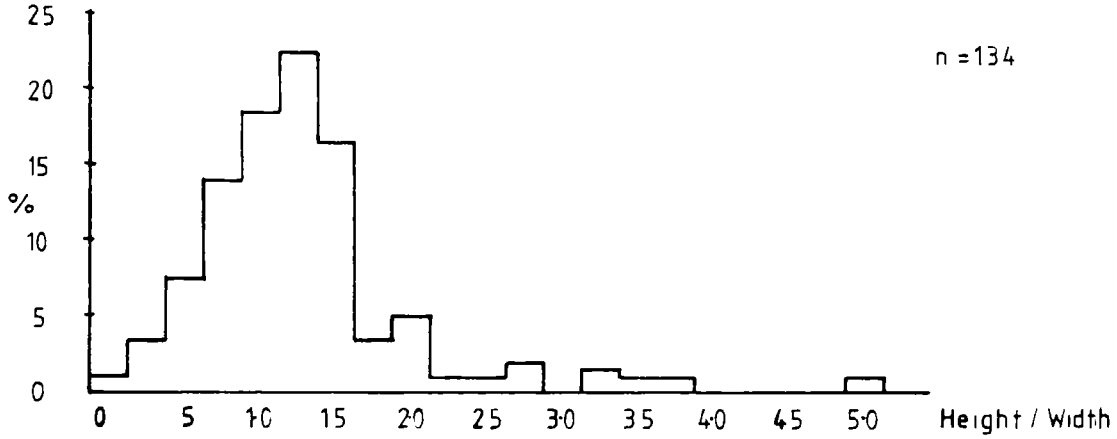

Figure 3.20 Ratio of theoretical collapse height/working width.

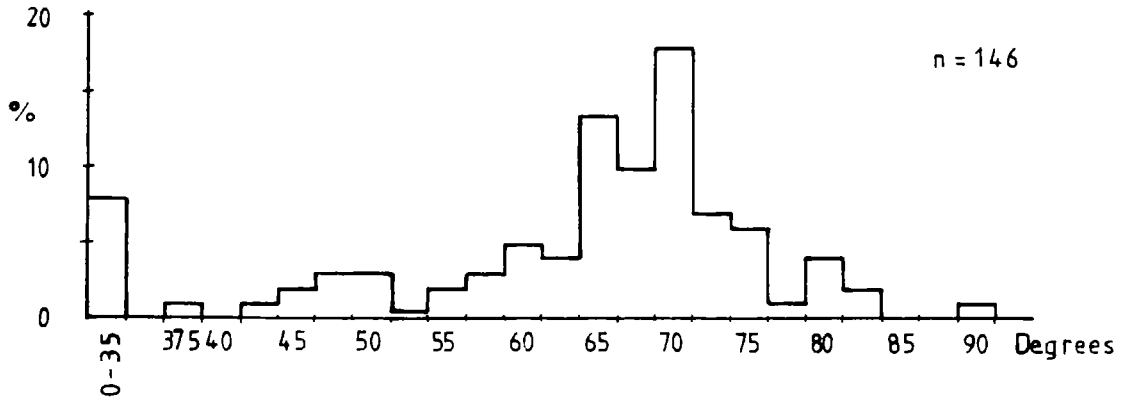

Figure 3.21 Angle alpha (angle to apex of arch).

almost 'normally'. However, appropriate statistical tests (Table 3.1) show that the data are slightly skewed towards the higher ratios. This may be because there can be no ratios less than zero, whereas at the other end, theoretically at least, the ratios can approach infinity. The skew is reflected in the difference between the mean ratio at 1.27 and the median ratio at 1.15. The data and also slightly more peaked than a normal distribution.

It is tempting to ignore the median and use the statistics of a normal distribution to predict likely collapse frequencies from the height to width ratios. If this were done, the data suggests that the use of the mean and standard deviation would overestimate rather than underestimate the collapse frequency for the high height to width ratios.

The alternative method of predicting the likely height of a collapse would be to use the alpha angle, that is, the included angle between the arch apex and the horizontal (Fig 3.21). This variable also approximates to a normal distribution except that the data are slightly skewed towards the higher angles and like the height to width ratio is slightly more peaked than 'normal' (Fig 3.21, Table 3.1). The skew is reflected in the difference between the mean angle of 62.1 degrees and the median angle of 66 degrees. The apparent marked difference between these two values is due to the effect on the data of the stable openings. Stable openings obviously have a very low angle, and these low values are pulling down the mean statistics thus giving a false impression of the true average collapse angle. To overcome this bias, the data were reworked omitting the few cases where the failure angles fell below 25 degrees. This effectively removed the stable workings and hence the bias from the analysis.

With the aid of this correction, the mean average angle increased to 65.4 degrees while the median angle increased only slightly to 67 degrees (Table 3.1). The shape statistics also improved, with the distribution approximating more closely to a normal distribution. These angles can be translated into equivalent height to width ratios by taking half the tangent of the angle. For the situation discussed above the average angles, and equivalent height to width ratios, are shown in Table 3.2. Also included in the Table are the calculated

Method of Assessment	n	Mean or median value angle α^{o}	Equivalent ht:width ratio 0.5 tanα	Equivalent ϕ where $\alpha = 90-\phi$*
Mean angle all data	146	62.1	0.944	27.9^{o}
Median angle all data	146	66.0	1.12	24^{o}
Mean angle (over 25^{o})	137	65.4	1.09	24.5^{o}
Median angle (over 25^{o})	137	67.0	1.18	23^{o}

*See Table 7.3 for source of relationship.

TABLE 3.2

TYPICAL ARCH ANGLES (ALPHA)

angles of internal friction for the rock. These values were calculated on the assumption that the arch failed in shear, where the failure surface (represented by the angle alpha) had an angle of arctan(S/2h) where S=span, h=theoretical collapse height (Protodyakonov, Bierbaumer, see Szechy, 1970, Chapter 7).

An alternative method to examine the relationship between the height of collapse and the width of the workings is to look at the normalised variables. These are referred to as the normalised width and the normalised height and are used more extensively at a later stage in the analyses. The definition and relationships between these variables is shown in Figure 3.22. The average distance along the x-axis from the abutment to a point perpendicularly below the point of bridging is given by:-

$$d = \frac{S - B}{2}$$

where S = width of working
B = width of rock bridge
h = height of collapse

If this value is divided by half the width of the working and multiplied by 100, a completely collapsed arch would have a normalised width of 100 while a completely stable roof would have a normalised width of zero. Values in between represent the percentage of arch closure.

$$dn = \frac{S - B}{S} \times 100$$

The collapse height can similarly be normalised. Thus:-

$$hn = \frac{h}{S} \times 100$$

The normalised height (Fig 3.23) gives the observed height of collapse in terms of half the width of working, that is, half of this value would be equivalent to the height to width ratio discussed above (Fig 3.20).

Of the two variables the normalised width is of more interest at this stage because it can be thought of as a measure of the degree of closure. This variable is therefore, an alternative method of looking at the degree to which an old working has collapsed. The variable should reflect the same trends as

Figure 3.22 Nomenclature and method for normalising height and width of collapse.

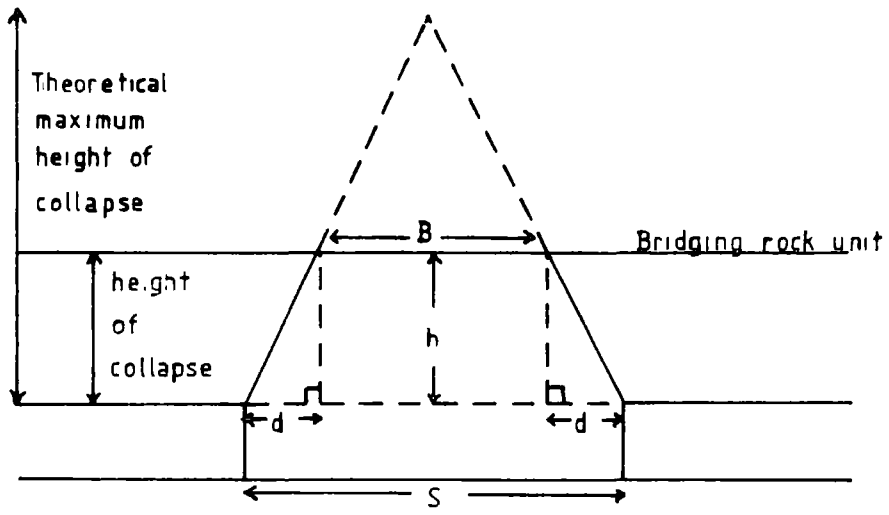

B = bridge width
S = width of working
h = height of collapse observed
d = distance from abutment to perpendicular from point of bridging

$$d = \frac{S - B}{2}$$

Normalised collapse values with respect to a half arch.

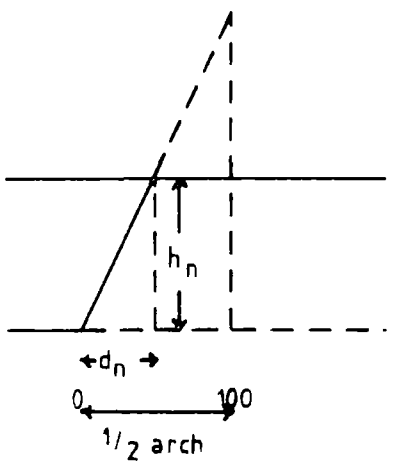

$$d_n = \frac{S - B}{S} \times 100$$

$$h_n = \frac{h}{S} \times 100$$

d_n = normalised width
h_n = normalised height

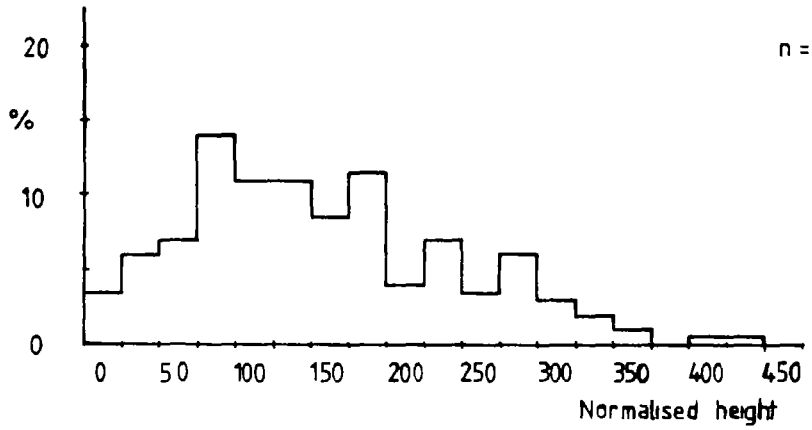

Figure 3.23 Normalised observed height of collapse.

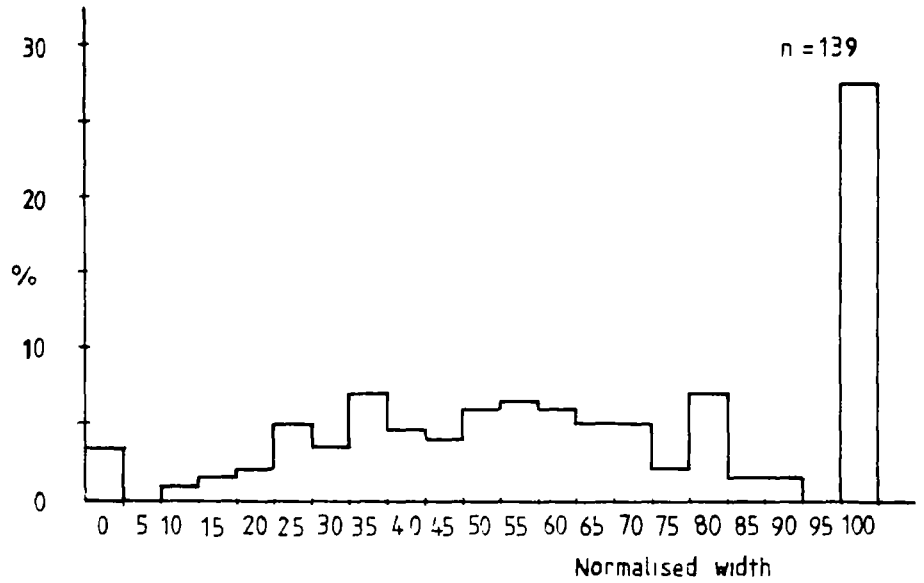

Figure 3.24 Normalised width of collapse.

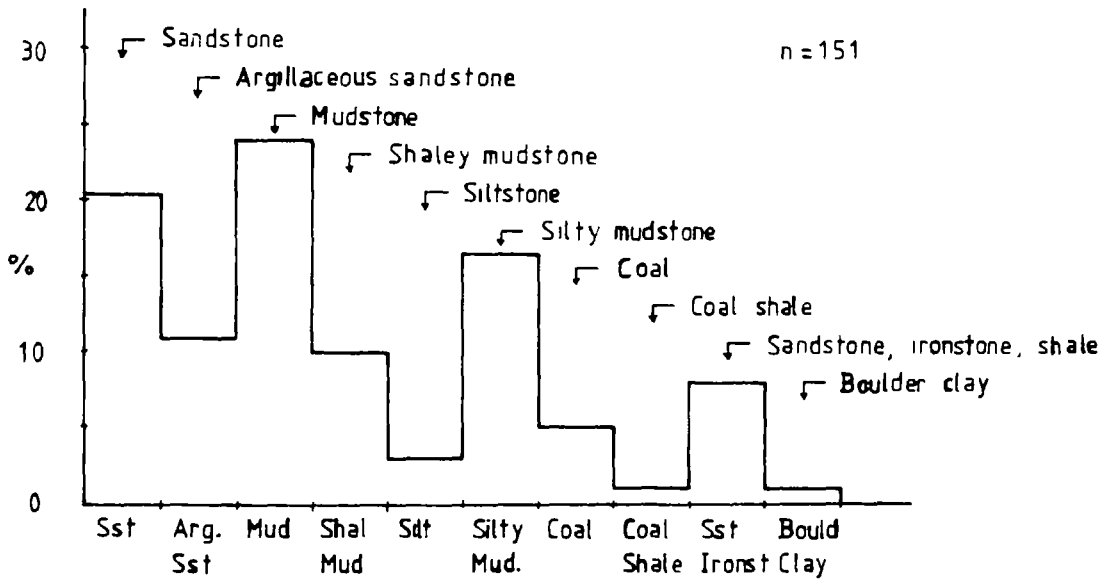

Figure 3.25 Distribution of bridge rock types.

those observed for the percentage collapse (Fig 3.13). However, it will differ from the percentage collapse because, unlike the latter variable, no assumptions have been made about the shape of the failure surface. Thus, the normalised width represents more accurately the general collapse condition of the average old working.

The histogram of this variable (Fig 3.24) shows that about 27% of the workings have completely collapsed; but if these are ignored for the moment, the remaining workings are seen to vary 'normally' between partially collapsed and totally collapsed. It will be observed that the central point of this distribution, which represents the average old workings, has a normalised width of about 50%. This implies that, for a typical old working, the width of the arch at the point of bridging has been reduced to 50% of the initial width of working. Hence we can justifiably refer to old workings as being in a state of semi-collapse.

3.2.3 BRIDGING EFFECTS

The foregoing data on the amount of the collapse, suggest that bridging is an important void arresting mechanism. The distribution of the rock types, forming the rock bridges, are shown in Figure 3.25. Field observations have shown that a sandstone horizon will usually arrest a void, especially if it is located some distance above the immediate roof. However, not every roof rock sequence contained a competent sandstone horizon. Thus, the increase in the dominance of the sandstones over other rock types from about 16% in the immediate roof (Fig. 3.4) to 31% in the case of rock bridges definitely underestimates the importance of sandstones in arresting a migrating void.

The effective bed thickness of the bridge rock (Fig 3.26) shows the average thickness of the fragmented units which bridged the void. The spread of the data for this variable is much greater than for the effective bed thickness of the main roof strata (Fig 3.6). However, somewhat surprisingly the bulk of the distribution still lies between about 30mm and 70mm. This suggests that, apart

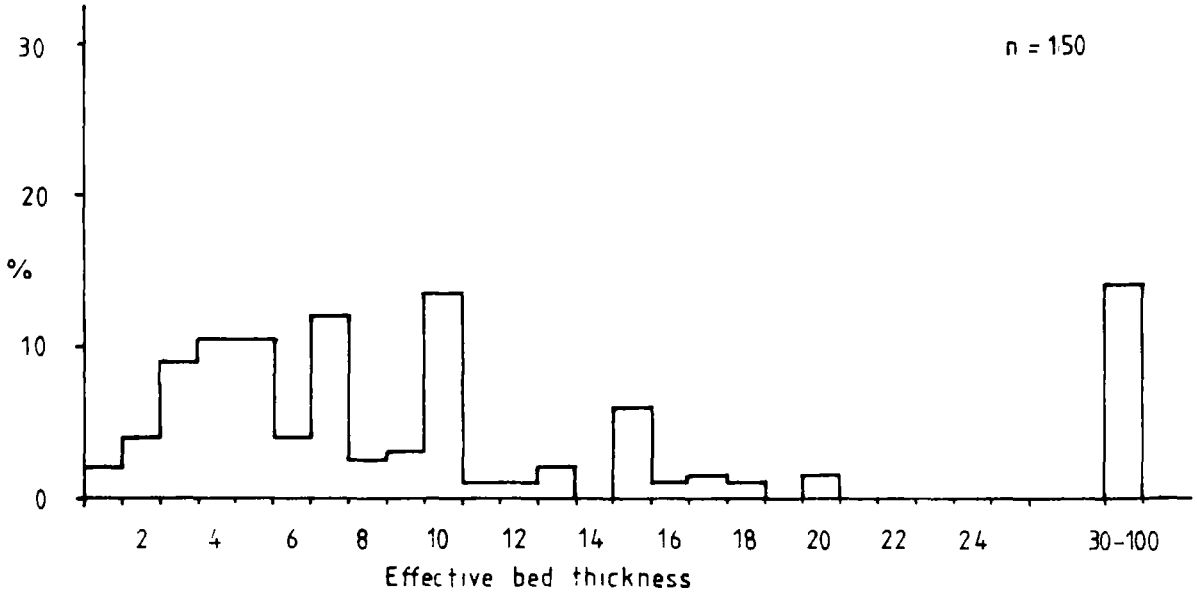

Figure 3.26 Effective bed thickness: bridge rock.

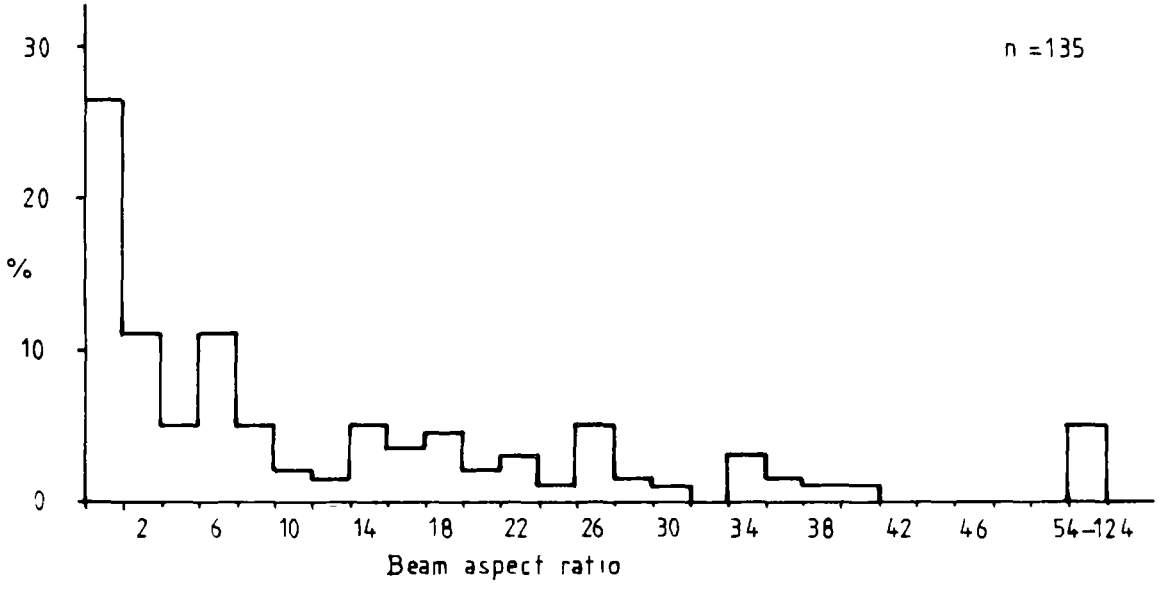

Figure 3.27 Ratio of bridge width/bridge thickness.

from the case of sandstones, most of the voids are bridged when the span of the void decreases to an acceptable level, not when a more competent roof rock was encountered.

This theme was investigated further. Both the thickness of the bridging unit and the span of the bridged space were recorded, and a histogram of the ratio between bridge width / bridge thickness (Fig 3.27) shows that the median ratio is about 6.5 : 1 (Table 3.1). To put this another way, the average beam that bridges the void has a span 6.5 times greater than its thickness. This ratio would be expected to vary with different rock types and of the four rock groups chosen, interbedded sandstones, ironstones and shales had the lowest bridge beam aspect ratio (median = 1.43 Table 3.3), followed by sandstone (median = 5.54) then siltstones (median = 6.46) and finally mudstones (median = 12.00). Thus, mudstones form the longest and thinnest beams while the interbedded sandstones are, relatively speaking, the shortest and thickest. This variation, reflected by the different values for the different rock types, conveniently introduces the whole problem of intra-variable variation.

3.3. INTRA-VARIABLE VARIATION

3.3.1. INTRODUCTION

The statistics presented above assume that the relationships and values summarised are independent of the effects of other variables. Such an assumption is obviously a little naive, but when data is limited it is necessary to establish its broad characteristics. The data base was designed primarily to study variations in the collapse height of old workings, and after an exhaustive study it was found that the majority of inter-relationships could generally be explained by variations in either or both the width of working, and the type of rock forming the roof of the old working. These variables can thus be considered as the key variables, with the variation in rock type responsible for the main intra-variable variation.

There was insufficient data to look for intra-variable variation for each of the

Rock Group	Variable	Units	No. of samples	Minimum	Maximum	Mean	Std. Dev.	Skewness	Kurtosis	Median	Percentiles 0.025	Percentiles 0.0975
	% Collapse	%	19	26.0	99.0	74.53	25.68	-0.431	-1.294	80.0		
	Working width (S)	m	19	1.53	14.20	4.31	2.59	3.07	9.55	3.73		
	Observed collapse height	m	19	1.74	7.70	4.25	1.75	0.051	-1.04	4.55	As Minimum	As Maximum
	Theoretical collapse ht.	m	19	3.80	20.60	6.13	3.67	3.46	11.26	5.07		
1	Theoretical ht:S ratio	-	19	1.06	3.16	1.50	0.48	2.37	5.64	1.42		
	Angle ∝	°	19	65.0	81.0	70.58	4.02	1.01	0.66	71.0		
	Width:normalised	-	19	25.63	99.84	73.94	26.69	-0.35	-1.44	79.7		
	Bridge width/thickness	-	19	0.028	30.17	3.94	7.097	2.858	8.03	1.43		
	Seam thickness	m	19*	0.90	1.70	1.21	0.264	0.013	-1.406	1.4		
	% Collapse	%	22	1.00	99.00	68.32	31.95	-0.57	-1.04	76.0		
	Working width (S)	m	24	1.47	11.10	3.62	2.39	1.66	2.29	2.81		
	Observed collapse height	m	24	0.01	9.85	2.35	1.93	2.53	7.68	2.13	As Minimum	As Maximum
	Theoretical collapse ht.	m	24	0.01	10.78	3.49	2.73	1.55	1.44	2.53		
2	Theoretical ht.S ratio	-	23	0.37	2.54	1.056	0.46	1.35	3.02	1.01		
	Angle ∝	°	24	1.00	79.00	57.42	17.23	-1.79	3.20	61.0		
	Width:normalised	-	23	0	99.91	74.10	30.84	-0.86	-0.47	82.1		
	Bridge width/thickness	-	23	0.059	78.62	12.77	18.81	2.034	4.46	5.54		
	Seam thickness	m	24*	0.90	1.60	1.20	0.162	-0.063	0.200	1.20		
	% Collapse	%	30	1	99.0	65.5	31.77	-0.39	-1.18	67.0		
	Working width (S)	m	30	1.3	4.94	2.39	0.98	1.63	1.81	2.09		
	Observed collapse height	m	30	0.13	7.67	2.19	1.69	1.46	2.17	1.84		
	Theoretical collapse ht.	m	30	0.13	11.0	3.44	2.44	1.28	1.26	2.59	As Minimum	As Maximum
3	Theoretical ht:S ratio	-	30	0.06	4.90	1.48	1.05	1.69	2.58	1.14		
	Angle ∝	°	32	7.0	82.0	65.0	14.42	-2.09	6.25	67.0		
	Width:normalised	-	30	0	99.8	66.07	31.7	-0.39	-1.11	67.4		
	Bridge width/thickness	-	29	0.083	96.67	12.80	20.82	2.66	7.47	6.46		
	Seam thickness	m	32*	0.60	1.90	1.10	0.313	0.33	-0.019	1.10		
	% Collapse	%	63	1.00	99.0	56.98	26.13	-0.20	-0.65	58.0	1.0	99.0
	Working width (S)	m	71	0.80	18.0	2.27	2.18	5.77	37.47	1.93	0.92	8.73
	Observed collapse height	m	69	0.01	13.6	1.56	2.29	3.98	17.33	1.00	0.05	12.8
	Theoretical collapse ht.	m	69	0.05	24.0	2.75	3.58	4.40	21.28	2.00	0.01	17.1
4	Theoretical ht:S ratio	-	61	0.23	3.57	1.20	0.59	1.31	3.21	1.14	0.24	2.75
	Angle ∝	°	67	1.0	90.0	60.82	16.86	-1.79	3.39	65.0	6.0	82.0
	Width:normalised	-	65	0	99.7	54.55	26.42	-0.042	-0.604	54.6	0.0	99.62
	Bridge width/thickness	-	62	0.167	123.3	17.16	23.08	3.214	11.52	12.00	0.2	119.4
	Seam thickness	m	72*	0.60	2.50	1.113	0.324	2.434	7.756	0.70	1.0	2.50

*Number of samples not number of coal seams.

Rock Groups: 1=Interbedded sandstone, ironstone and slate. 2=Sandstone. 3=Siltstone. 4=Mudstone.

TABLE 3.3

VARIATION WITHIN COLLAPSE VARIABLE DUE TO ROCK TYPE

9 recorded rock types. consequently the approach used was to aggregate rock types into groups of similar lithologies. The groups chosen were:- Sandstones, siltstones, mudstones, and interbedded sandstones ironstones and shales. The sandstone group comprised sandstone and argillaceous sandstone, while the siltstone group included siltstone and silty mudstones. The mudstone group in addition to mudstones, included shales and coaly shales. The interbedded group was the only poly-lithological rock group considered, and was comprised of interbedded ironstones and shales, and interbedded sandstones and shales.

The variables which characterise the degree of collapse, and the collapse potential of an old working, were re-examined for each of the four rock groups. Non-parametric statistics (Kruskall Wallis and Median tests, MIDAS, 1976) were used to decide whether the observed differences within the variables were statistically significant and related to the rock groupings. These statistics test the null hypothesis 'that the distribution of the specified variable is the same for each of the rock groups', against the alternative hypothesis, 'that the distribution of the specified variable is different for at least one of the specified rock groups'.

The Kruskall Wallis test is a statistically more powerful measure of equality, than the median test, but it assumes that the data have been drawn from a continuous underlying population with no, or few, "tied values". Where there are tied values, that is, identical values for more than one case, or where the data is discrete, the test is compromised and more weight should be attached to the less powerful Median test. A summary of the tested variables and groupings, and their significance can be found in Table 3.4. Where relevant, the levels of significance are quoted in the following format (0.0000,0.0000). The former statistic refers to the Kruskall Wallis test while the latter statistic refers to the Median test. In both cases a low value implies a high level of significance.

Detailed study of the intra-variable variation, for the rock groups discussed above, revealed an interesting set of inter-relationships. It is quite possible that most of the variables, that describe the collapse potential of an old

Variable	Variation present between rock groups	Rock Grouping tested	Level of Significance Kruskall Wallis	median	Comments
Width of working (S)	Yes	SS, Silt, Mud	0.0005*	0.0146	
Observed height of collapse	Yes	SS, Silt, Mud	0.0006	0.0000	
Theoretical height of collapse	Yes	SS, Silt, Mud	0.0165	0.0156	
Seam thickness	Yes	SS, Silt, Mud	0.0277	0.0158	
Theoretical collapse ht:S ratio	No	SS, Silt, Mud	0.3050	0.7648	
Angle Alph, (Apex angle)	No	SS, Silt, Mud	0.0920	0.1961	
% Collapse	No	SS, Silt, Mud	0.1929	0.2043	(Tied values)
Width x	No	SS, Silt, Mud	0.0055	0.0529	(Tied values)
Width of working (S)	Yes	SS, Silt, Mud, Int.	0.0000	0.0000	
Observed height of collapse	Yes	SS, Silt, Mud, Int.	0.0000	0.0000	
Theoretical height of collapse	Yes	SS, Silt, Mud, Int.	0.0000	0.0000	
Bridge w:bridge thickness ratio	Yes	SS, Silt, Mud, Int.	0.0002	0.0192	
Seam thickness	Yes	SS, Silt, Mud, Int.	0.0403	0.0330	
Theoretical collapse ht:S ratio	Yes	(SS, Silt, Mud)-Int.	0.0059	0.0037	
Angle Alph, (Apex angle)	Yes	(SS, Silt, Mud)-Int.	0.0015	0.0002	
% Collapse	No	(SS, Silt, Med)-Int.	0.0334	0.4592	(Tied values)
Width x	No	(SS, Silt, Med)-Int.	0.0370	0.4810	(Tied values)

*Level of significant = 0.0005 = 0.05%

The hypothesis that the distribution of working widths are the same for the three rock types is rejected at the 0.05% level of significance i.e. the widths are different at 99.95% level of significance.

TABLE 3.4

LEVELS OF SIGNIFICANCE FOR VARIABLES GROUPED BY ROCK TYPE

working, are affected to some degree by the type of rock involved. However, because of the limited amount of data available for analysis only the grossest of the variations are likely to be shown to be different statistically. The summary statistics, by rock group, for all the variables mentioned in the following Section, will be found in Table 3.3.

The nature of the roof rock was found to affect the value for some variables. During the analysis it was found that the poly-lithologic rock group seemed to behave in a different manner to the three remaining mono-lithological rock groups. The trends and relationships found for the mono-lithological rock groupings are discussed below, while the variation in the interbedded rock group will be considered when the variation in the mono-lithologic rock groups have been established.

3.3.2. INTRA-VARIABLE VARIATION IN MONO-LITHOLOGIC ROCK GROUPS.

The width of the old working was found to vary depending on the rock type that constituted the immediate roof. The widest workings were driven in coal seams where sandstones formed the main roof, while the narrowest workings had mudstone roofs. The siltstone rock group formed an intermediate group between the wide sandstone, and the more narrow mudstone roofed workings (Tables 3.3 and 3.4).

The observed trend for the width of the workings was reflected by the height to which the workings collapsed. Both the observed height of collapse and the theoretical height of collapse varied between the different rock groups. Old workings roofed by sandstone collapsed higher than the siltstone or mudstone roofed workings. The observation that both the working width and the height of collapse vary in the same direction for the different rock groups suggests that these variables are strongly related. This is therefore, in keeping with previous observations on the inter-relationship between working width and collapse height (Walton and Taylor, 1977) and is discussed in more detail in Chapter 3.4.3.

No statistically significant variation between the different rock groupings for either the observed height to width ratio or the theoretical height to width ratio were found. Such an observation suggests that the height to which an old working will collapse is, for a given working width, independent of the rock type. This observation was confirmed by the analysis on the angle of the failure surface. Once again, no statistically significant variation was found between the three different mono-lithologic rock groups for the average collapse angle. This angle is refered to elsewhere in the text as angle alpha (Chapter 9.3.3).

The direction of variation between the three rock groups, for both the angle alpha and the two collapse height to width ratios, was found to be different from the variation noted for the width and height of collapse. The rock groups were, in order of increasing angle and ratio, sandstone, mudstone and siltstone.

It will be recalled that the percentage collapse and the variable referred to earlier as the normalised width, are two semi-independent assessments of the degree of collapse of an old working. No statistically significant variation was found in either of these two variables for the three mono-lithologic rock groups investigated. This suggests, somewhat surprisingly, that the degree to which an old working has collapsed is independent of the roof rock and thus, this data refutes the commonly held belief that old workings roofed with sandstones are more stable than old workings roofed by mudstone Wardell and Wood (1965). The variation there is in the percentage collapse and normalised width (Table 3.3) more closely reflects the observed trend for the angle alpha and the height to width ratios than it does the trend shown by the height of collapse or the width of working.

The overall pattern that emerges, for the three mono-lithologic rock groups, suggests that while the width of working and height of collapse do vary for the different rock groups, the angle of the failure surface, the two expressions for collapse height to width ratios, and the percentage collapse do not vary. These observations suggest that the 'old miners' altered the width of the working to suit the roof conditions, and thus attempted to optimise the support

requirements for the working. In other words, it is suggested that the working was driven to maintain an average factor of safety of one with the miners relying on the roof support to provide the additional safety factor. If this were the case it would explain why there is no statistically significant difference in the degree of collapse between the three different rock groups. The variation in the working width is thus offset by the different mechanical characteristics of the roof rock.

The fact that the angles and ratios of collapse do not vary for the different rock types is useful because it considerably simplifies the use of these relationships for practical predictive purposes.

3.3.3. INTRA-VARIABLE VARIATION FOR THE POLY-LITHOLOGIC ROCK GROUPS.

The rock group comprising the interbedded rocks did not follow the trends observed for the mono-lithological rock groups. Old workings overlain by interbedded rocks were found, on average, to be wider and to have collapsed higher than workings with mono-lithologic roof rocks. Of more significance however, was the observation that the collapse structures in the poly-lithologic rock group had significantly greater collapse height to width ratios, and steeper failure surface angles, than the other rock groups, within which no statistically significant variation was found (Tables 3.3 and 3.4). While the equivalent height (ie. the h:S ratio) of a collapse was greater for the interbedded rock group, the degree of collapse did not differ significantly. There was no statistically significant variation (Tables 3.3 and 3.4) for either the percentage collapse or the normalised width. Therefore, no rock type has been found to alter the amount that an old working has collapsed.

On reflection, the observation that voids migrate higher in interbedded as opposed to mono-lithological rock groups is probably not very surprising. Coastal cliff faces composed on interbedded rocks are, as a general observation, usually more unstable than cliffs composed of only one rock type. The reason for the decreased stability shown by such interbedded rocks must be due to the rapid alternation between competent and incompetent layers. This perhaps,

destroys the structural coherence of the rock unit, and enhances the effects of delamination, bed separation and fracture.

Finally, one surprising variation was discovered within the data base. The thickness of the coal seam was found to vary depending on the type of rock that formed the roof. Mudstones were found to overlie the thinner coal seams while sandstones overlay the thicker coal seams. The level of significance (Tables 3.3 and 3.4) indicated that the relationship was only possibly significant, and it is difficult to think of a convincing set of geological reasons to explain this observed variation. It is quite possible, considering the small number of opencast sites, and hence coal seams involved, that the trend is a purely chance relationship. Variation was also found within the different rock groups for the ratio between the width of the working and the thickness of the coal seam (aspect ratio). Both of these variations are probably related, and their effect will be considered further in Chapter 3.4.4.

One or two other variables were found to cause intra-variable variation. Of these the joint spacing and vertical extent of the joints were found to effect the width of working and height of collapse. Wide or moderately wide jointing, and large vertical extents were found to be related to wide and high arches. This is obviously a reflection of rock type and is not considered further. (ie. weak rocks cannot store strain energy and are therefore more closely jointed than strong rocks. eg. Ladeira and Price, 1981). None of the other 'collapse variables' discussed above were found to vary with jointing.

3.4. VARIABLE INTER-RELATIONSHIP

3.4.1. INTRODUCTION

The data base was systematically searched for inter-relationships between the variables recorded during the field and laboratory study. Numerous correlation matrices and scatter plots were generated but, with the exception of the few relationships discussed below, the overall impression was one of almost total lack of association. In fact, the value and interest of the operation lay not

in the variables that were related, but rather in the variables that were not related. The following section deals with the most important of these relationships or non-relationships. It can safely be assumed that if a particular pair of variables have not been mentioned, there was no meaningful or statistically significant correlation between them.

The inter-relationships can be divided into two groups. The first group reflects the general inter-relationship between an old working and its environment, while the second group includes any relationship which affects the amount or degree of collapse of an old working.

3.4.2. GENERAL INTER-RELATIONSHIPS

No meaningful or statistically significant inter-relationships were found between the approximate age of abandonment of the mine and any of the descriptive variables. Probably one of the most interesting of all of these non-relationships is the poor correlation between the age of working and the depth of the coal seam. A relationship between these two variables has already been established in Chapter 1. However, when it is considered that the median depth of the workings seen in the field was only about 10m, it is not very surprising that a relationship fails to emerge. Early mining technology was perfectly capable of dealing with such shallow depths and therefore, age does not enter into the question. A similar reason is probably sufficient to explain the non-relationship between the thickness of the seam and the age of the workings. Shallow coal seams were always in demand provided that the seams were reasonably thick.

No relationship was found between the degree of flooding and the depth of the working, or between the width of the coal pillar and depth.

3.4.3. COLLAPSE INTER-RELATIONSHIPS

a. INTER-RELATIONSHIPS BETWEEN WIDTH OF WORKING AND HEIGHT OF COLLAPSE.

The width of working has been shown by previous authors to affect the observed

height of collapse of an old working (Walton and Taylor, 1977). The relationship between the two variables for the Coal Measures rocks investigated is shown in Figure 3.28. A few of the problems encountered when trying to quantify such a relationship have already been commented upon, and the theoretical height of collapse was shown to overcome some of these objections. The relationship between the theoretical height of collapse and the width of working is shown in Figure 3.29. The main problem lies with characterising the data so that it can be used for predictive purposes in practical situations. The major value of such information does not lie in predicting the average height of collapse. This central tendency value, by its very definition, assumes that the height of 50% of the arches will exceed this value. For predictive purposes, it is desirable to predict a height of collapse for a given width of working, such that the vast majority of the variation is included. There are a variety of statistical techniques by which such an assessment can be made. These include standard deviations, standard errors and percentiles. The following Section will explore these methods and will examine which statistical technique is most suitable for characterising the collapse height and span width data.

A least squares regression analysis is probably the most obvious method by which to characterise the relationship between the theoretical collapse height and width of the working (Fig 3.30). For the data in question, such an analysis produced the following relationship:-

Theoretical height of collapse = 1.266 x width - 0.108

Standard error = 1.834

A t-test on the significance of the intercept value indicated that there was no evidence to suggest other than the intercept was equal to zero. As this is theoretically justifiable, the regression analysis was recalculated under the assumption that the intercept was zero. The new regression equation obtained was:-

Theoretical height of collapse = 1.242 x width

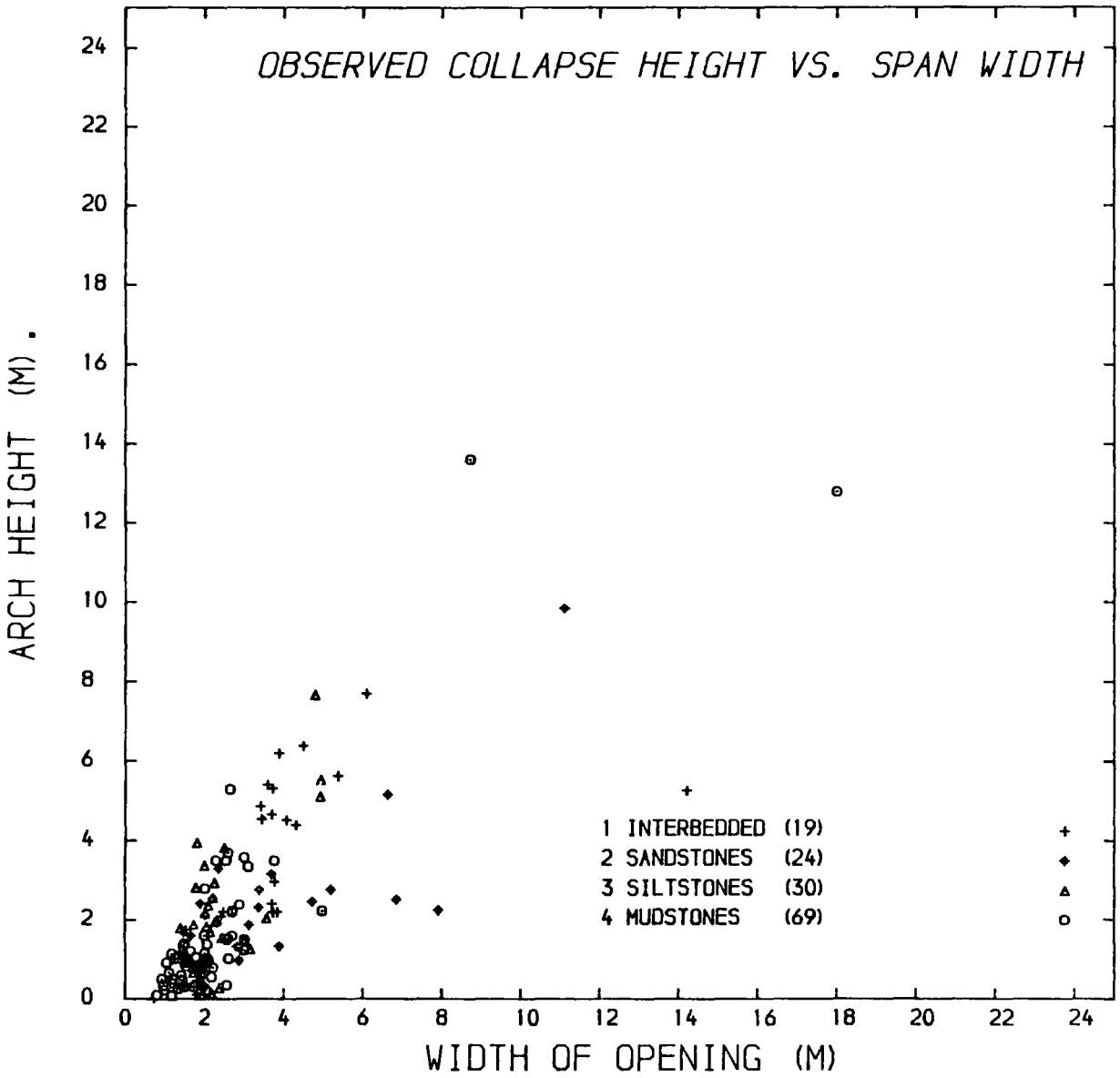

Figure 3.28 Variation in observed height of collapse with width of working.

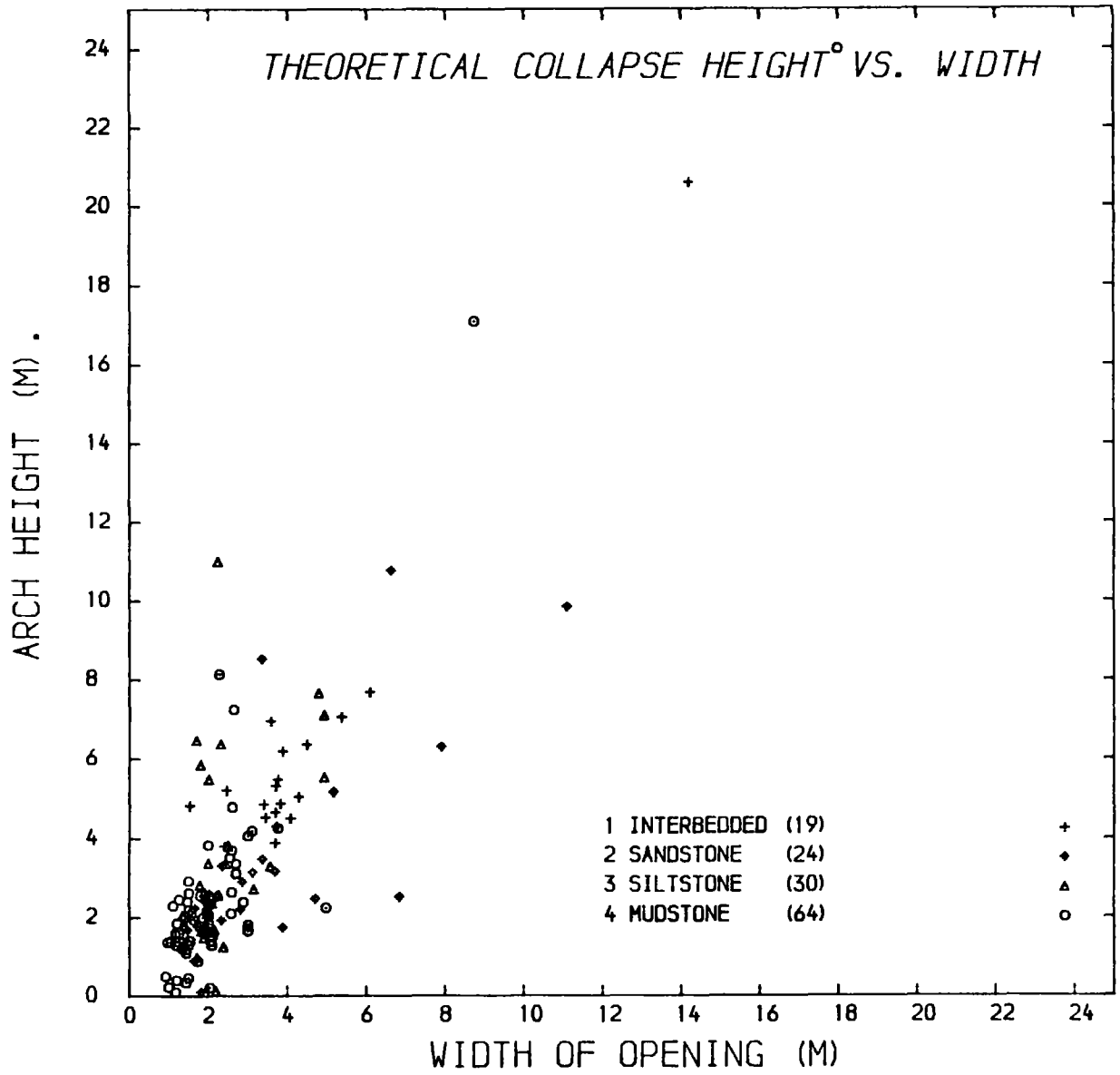

Figure 3.29 Variation in theoretical height of collapse with width of working.

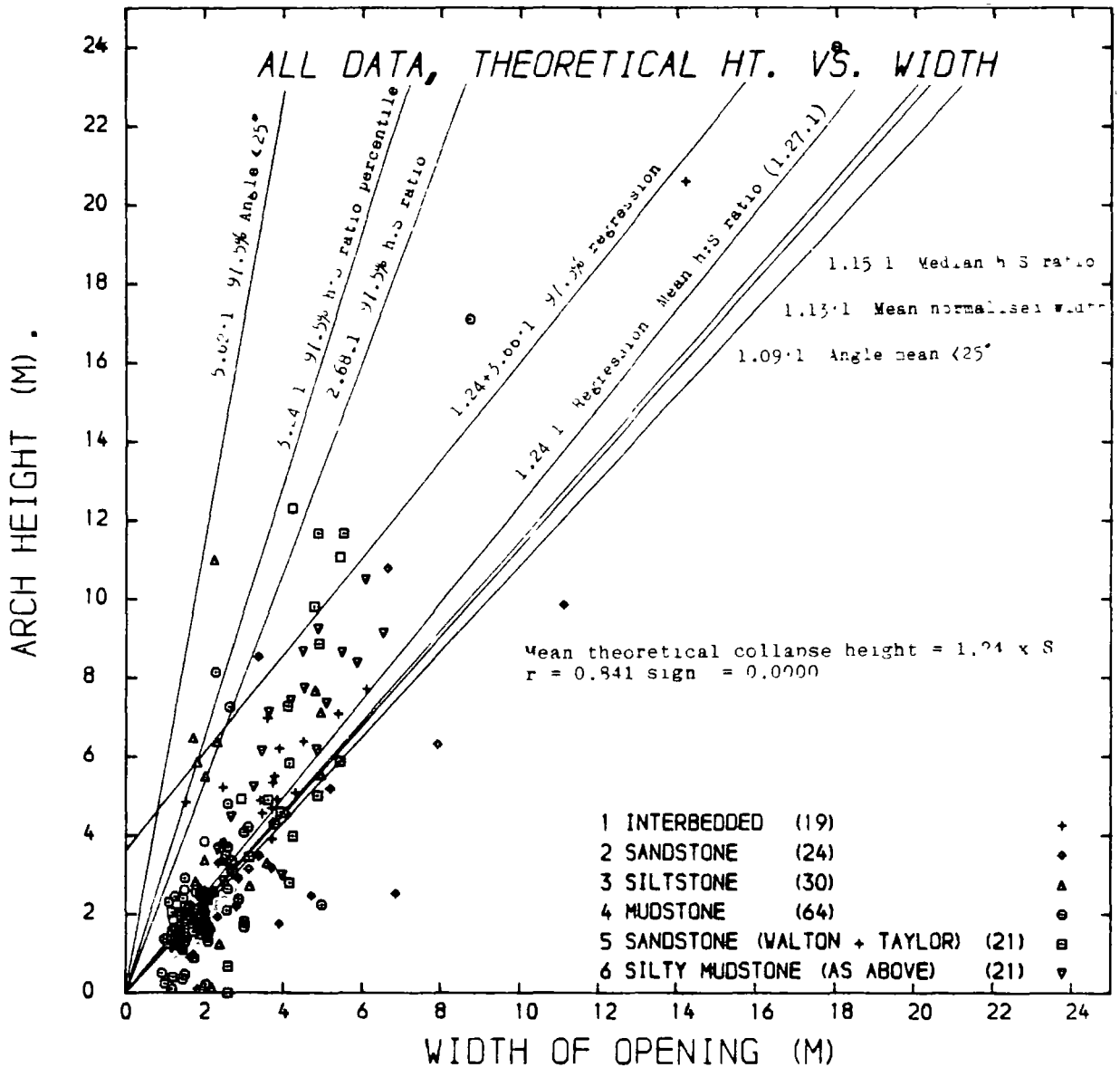

FIGURE 3 30 CHARACTERISATION OF VARIATION IN THEORETICAL HEIGHT OF COLLAPSE AND WIDTH

Standard error = 1.829

This relationship has been plotted in Figure 3.30

Also plotted in this Figure is the line corresponding to twice the standard error of the regression. If the statistics of the regression equation were satisfactory, about 97.5% of the data should fall below this line. This is clearly not the case. However, the whole validity of the regression equation is called into doubt without even looking at the relationship. It was shown earlier that both the variables involved had a skewed distribution, and were not distributed normally. The regression analysis assumes firstly, that both the variables are normally distributed and secondly, that any residual variation from the mean line is independent of value of the dependent variable. This second assumption clearly does not apply as the spread of the data fans out from the origin (Fig 3.30). Thus for these variables the theoretical validity of the regression analysis and the equation it produces is extremely doubtful.

However, the problem remains in how to characterise the data. The height to width ratio has been discussed earlier as being of potential use for predictive purposes. This ratio can be plotted on the raw data, from which it was indirectly obtained. The mean height to width ratio falls very close to the regression line. This is to be expected because of the statistical assumptions that lie behind the calculation, for the ratio, of the mean and standard deviation. The test of the value of the ratio lies with the position of the line corresponding to twice the upper standard deviation of the mean height to width ratio. The equation for this line, which corresponds to about 97.5% of the data, has a coefficient of 2.68 (2 x 0.703 + 1.27) and has been plotted on Figure 3.30. It will be seen to more accurately reflect the spread of the data than the twice the standard error line obtained from the regression equation.

The angle of the failure surface, angle alpha, has also been discussed as a possible candidate for predictive use. It will be recalled that when the values were adjusted to remove the exaggerated effects of the stable old workings, the data was found to approximate to a normal distribution. The mean angle of 65.4

degrees (sd=9.76) is equivalent to a height to width ratio of 1.09. This line has also been constructed on Figure 3.30. Also included on this Figure is the line corresponding to about 97.5% of the data. The equation for this line is found by taking half the tangent of the upper second standard deviation of the angle (65.4 + (2 x 9.76) degrees). The equation of the line is:-

Collapse Height = 5.62 x Width of working

The value is seen to be a little extreme and to exaggerate the danger of collapse.

The mean height to width ratio and the mean angle, as well as the 97.5% percentiles for these variables, have also been plotted on Figure 3.30.

This summary of possible methods with which to characterise the relationship between the theoretical height of collapse and the width of working has shown that, for the average or median collapse ratio, there is little difference between any of the methods. However, for predictive purposes, and when using a particular confidence interval, the value of the regression equation is seriously in doubt. Of the remaining methods, either the mean height to width ratio or the mean angle may be used. The former ratio will underestimate the maximum height of collapse, while the latter angle will overestimate the collapse height. On balance and considering the assumptions made initially to derive the theoretical height, the height to width ratio is probably the most appropriate value to use.

The relationship derived above, for the 'maximum' theoretical height to width ratio, has been over-plotted on the relationship between the observed height of collapse and the width of working (Fig 3.31). The relationship is seen to easily enclose all the observed collapse height data, and is thus, possibly a little conservative. A relationship of height = 1.63 x width is possibly more appropriate for this data. However, because 70% or the workings have not completely collapsed it would be unwise to use it for predictive purposes.

b. COMPARISON OF COLLAPSE RATIOS WITH PREVIOUS STUDIES.

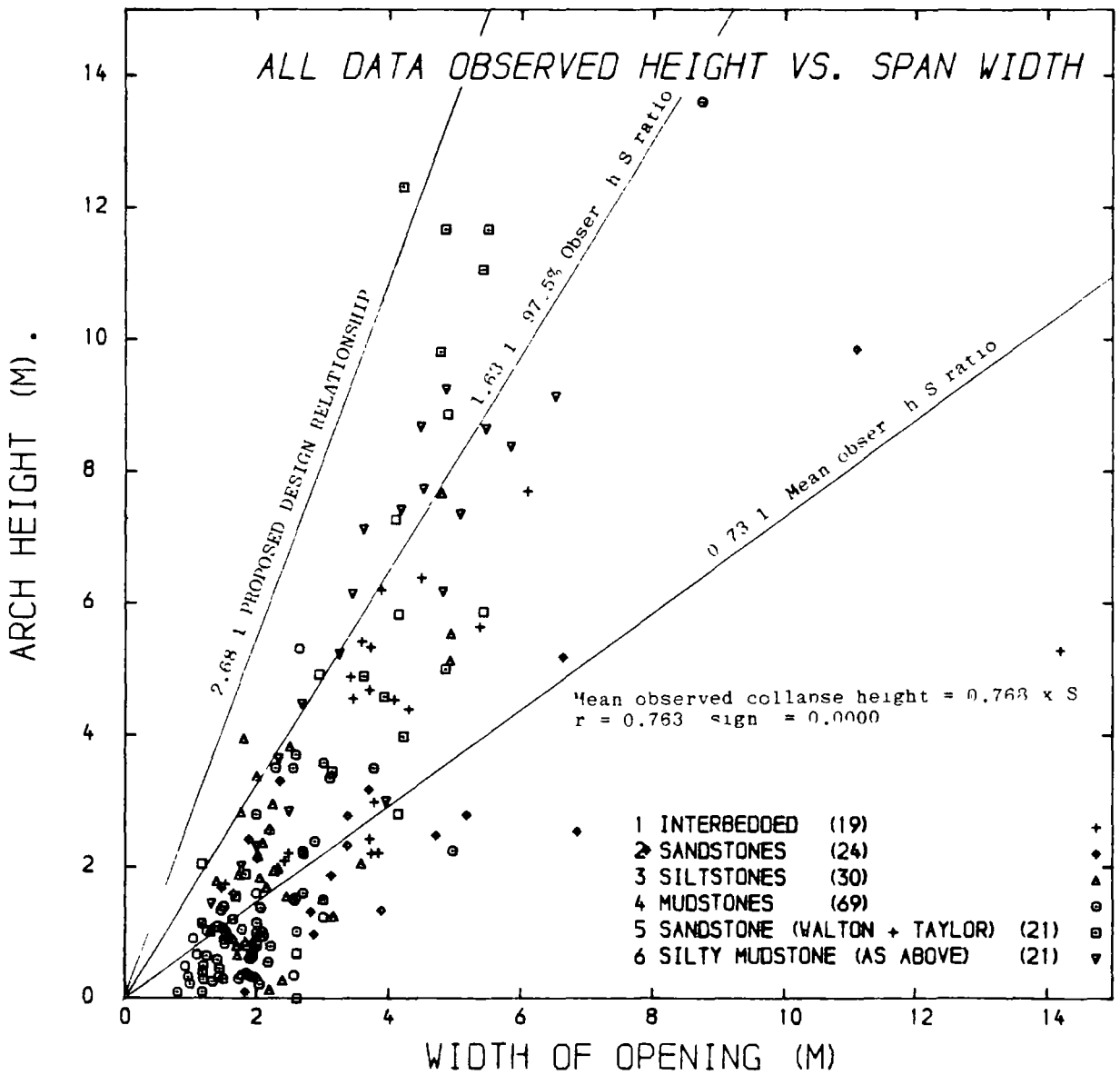

FIGURE 3 31 CHARACTERISATION OF VARIATION IN OBSERVED HEIGHT OF COLLAPSE AND WIDTH

The collapse height and span width obtained during the present study were compared with similar data gathered by Walton and Taylor (1977) from the Pethburn opencast site. These authors measured the height and width of 42 collapse structures in two rock types, a sandstone and a silty mudstone (Fig 3.32). Photographs of these workings (Walton, 1983) showed that the arches were generally well developed and in an advanced state of collapse. Height to width ratios were calculated for the data and a number of non-parametric analysis of variance tests were carried out to compare the ratios derived from Walton and Taylor (op.cit), with the observed height to width ratio and the theoretical height to width ratios that have been discussed so far.

The analyses showed that there was a significant difference between the observed height to width ratio, and the height to width ratio calculated from the Walton and Taylor data. However, there was little difference between the theoretical height to width ratio and the Walton and Taylor data. From this it is inferred that the collapses observed on the Pethburn opencast site were exceptional only in that the arch development was significantly greater than usually found on other opencast sites. The median collapse ratio of the Walton and Taylor data is in line with the theoretical maximum height of collapse calculated from the data base. It will be recalled that the theoretical maximum height of collapse was specifically designed to overcome and remove the bias caused by workings that had failed to collapse completely. The similarity between the well-developed Pethburn arches and the theoretical height of collapse justifies the calculation of this variable.

Finally, the recommended design relationship (Height = 2.69 x width) has been superimposed on the Walton and Taylor data (Fig. 3.32). The relationship encloses all but one of the observed data points. The data point not enclosed has a height to width ratio on 2.92.

The value derived above for the height to width ratio, has been shown to just enclose 180 out of 181 collapse structures from many different locations. Therefore, the relationship is suggested as suitable for predicting the likely

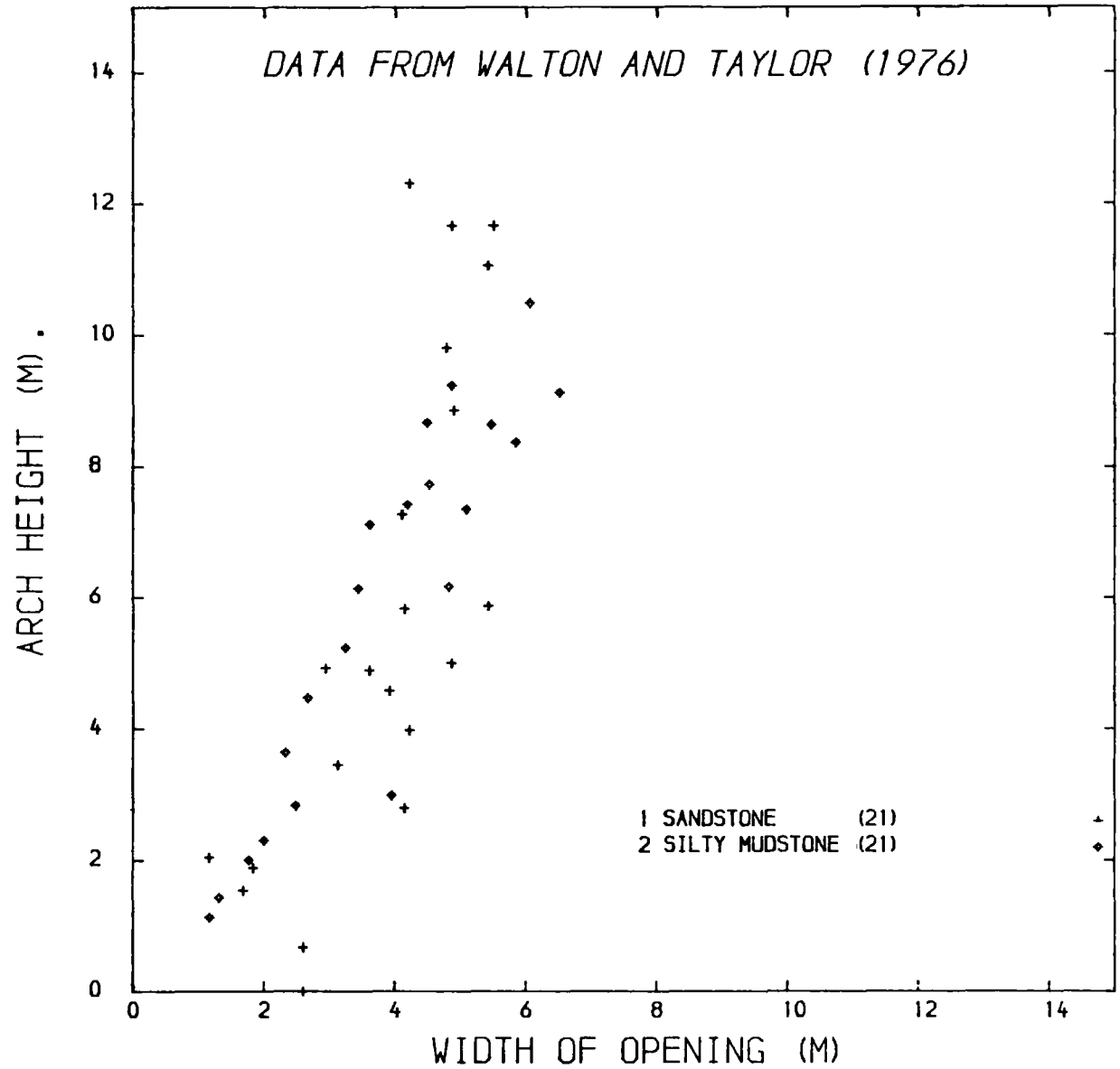

Figure 3.32 Variation in height of collapse with width for Pethburn O.C. Site.

maximum height of collapse for an old working in typical Coal Measures rocks. By adopting such a value one is designing by failure probabilities, not by a factor of safety. A relationship of (Ht. = 2.69 x width), which encloses 97.7% of the theoretical collapse height data, predicts that out of 100 collapses that completely develop to their full potential, only about 2 would be expected to migrate beyond the predicted height. The important phrase in the last sentence was, 'developed to their full potential'. It has been shown that only a few workings do collapse completely. Thus, the actual probability of a collapse exceeding the predicted height is much lower.

If the distribution of the 'observed height of collapse to width' ratio is taken as being normally distributed, the relationship (Height = 2.69 x width) is approximately equal to a collapse probability of 0.003%, or 1 in 33,333. The assumptions made, concerning the distributions of both variables, make accurate probability assessments unreliable. However, it is sufficient to say that the suggested relationship is the maximum height to which a failure could reasonably be expected to migrate without external interference (such as heavy additional loading). If a void migrates beyond this value the control will probably not be one of arching, but possibly a cohesion-less type failure or a joint controlled collapse (Chapter 10).

3.4.4. OTHER STATISTICAL INTER-RELATIONSHIPS

No other meaningful or statistically significant relationships were found between the width of working and any other measured variable. Surprisingly, there was no evidence to suggest that narrow workings were more stable, or had collapsed to a lesser degree than wide workings. Likewise there was no evidence that the width of the bridging rock unit varied with the width of the working. The width of working has been established as being strongly related to the observed collapse height and theoretical collapse height. It is therefore, not surprising that no relationship was found between these variables and the bulk of the data.

There was very slight evidence to suggest that the effective bed thickness was

related to the theoretical height of collapse (r =0.22 sign =0.0084). This relationship is assumed to be indirectly related to the effect of the rock type on the height of collapse, a relationship which has already been noted.

No relationship was found between the depth of the workings and either the collapse ratios or the angle alpha. This suggests that plastic failure of the roof rocks need not be considered as a failure mechanism, and confirms the initial field observations that plastic failure was rare.

Probably one of the more interesting observations to emerge from the analysis is the poor relationship between the height of collapse and any of the normally recorded standard geotechnical parameters, such as jointing and bed thickness. It will be remembered that these values were recorded using the categories suggested by the Engineering Geology Working Party on Rock Mass Classification (Anon, 1977). Similar classifications have been used in rock mass studies by numerous authors (Bieniawski, 1979, 1981) for predicting stability and stand-up times. The poor correlation between such categorical groupings and the collapse parameters suggests that, for old coal mine workings, the groupings are too coarse to be of any real value in predicting stability. The correlation further suggests that the collapse of an old working is not necessarily controlled by the macro-structure of the rock but possibly by its micro-structure. A concept that has received little attention in the literature.

b. SEAM THICKNESS.

In the past, several investigators have advocated the use of relationships based solely on the thickness of the coal seam for predicting the height of collapse of an old working (Price et al., 1969, Taylor, 1975, Thorburn and Reid, 1977, Piggott and Eynon, 1977, Higginbottom, 1984). These relationships have been justified using simple formulae based on bulking theory. The popularity of this type of approach is based on the fact that seam thickness is commonly the only parameter which is known at the 'desk study' stage of a site investigation. The whole question of bulking is examined in considerably greater depth in Chapter 8, where a comprehensive review of the appropriate recommended design formulae

will be found. At this stage of the research, the object was to examine the data to establish whether a relationship between collapse height, or theoretical collapse height, and the thickness of a coal seam could be found. Scattergrams of these variables are presented in Figures 3.33 and 3.34.

The majority of the data suggest that the two variables are not related, but there is some evidence that a confining envelope can be applied to the data. This envelope is of the form:-

Observed height of collapse = 6.5 x seam thickness (Fig. 3.33)

For the theoretical height of collapse (Fig 3.34), this ratio has to be increased to:-

Theoretical height of collapse = 9.8 x seam thickness

The coefficient for the observed height of collapse is not greatly different from (Ht.= 8t) proposed by Taylor (1975), or (Ht.=7t) Walton and Taylor (1977), for predicting the height of the average collapse. likewise, the value of 10, recommended by Piggott and Eynon (1977) as the maximum height that a collapse would occur, is very similar to the coefficient obtained for the theoretical height of collapse. At first sight these coefficients would seem to endorse the relationships suggested by these authors. However, very few of the old workings used in the analysis had in fact completely bulked, and the present investigations, detailed in Chapter 8, show that the theory on which these simple bulking relationships were based is very suspect. However, the facts do suggest a relationship between the seam thickness and collapse height. Therefore, some factor, other than bulking, was sought to explain the relationship.

In Chapter 3.3.2 the relationship between the seam thickness and the type of rock forming the immediate roof was discussed. It was also shown that the working width varied depending on the roof rock. It is therefore, not surprising that some evidence of a relationship between the width of working and the seam thickness was found (Fig 3.35). Although the majority of the data in

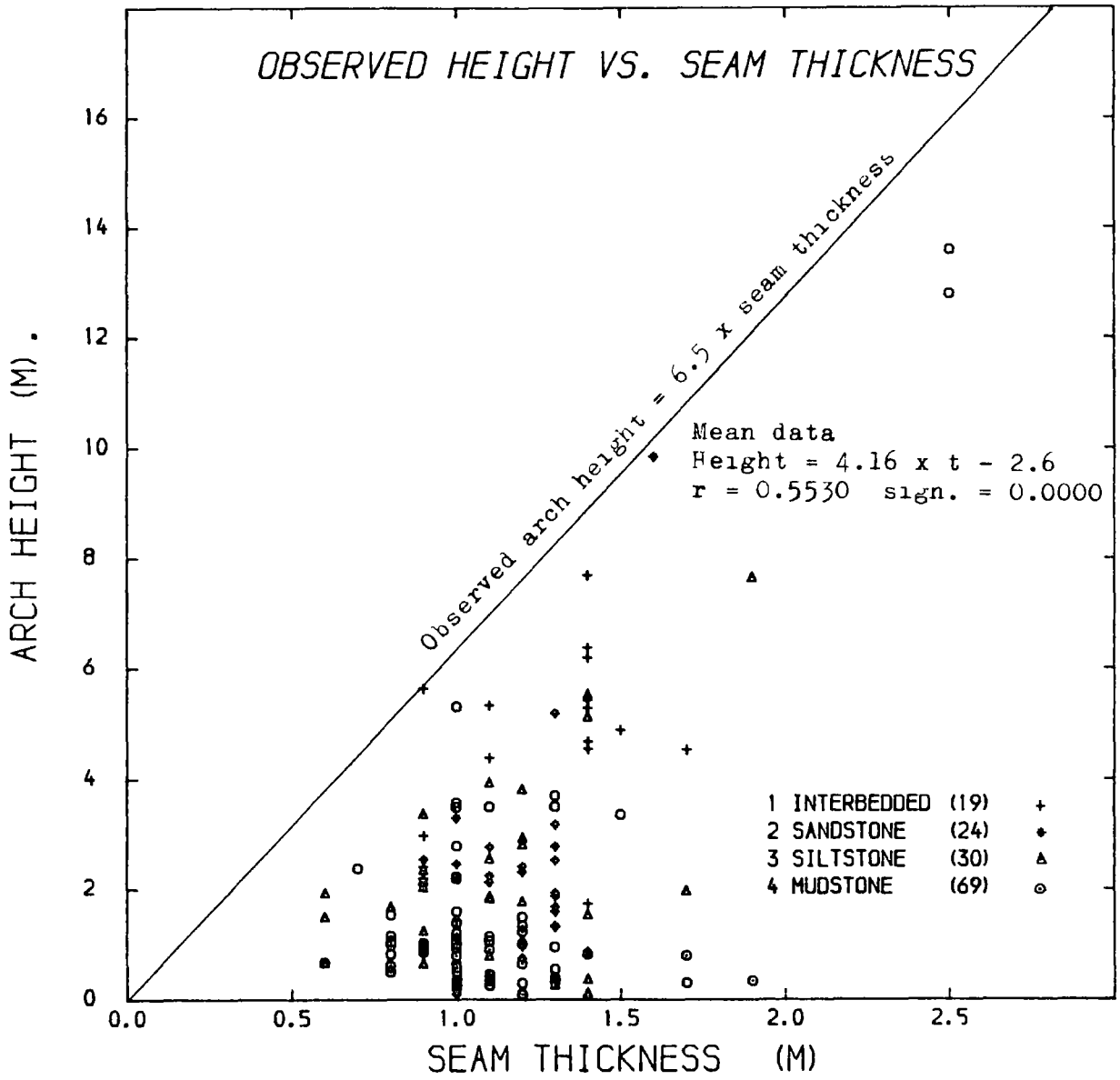

Figure 3.33 Variation in observed collapse height with thickness of coal seam.

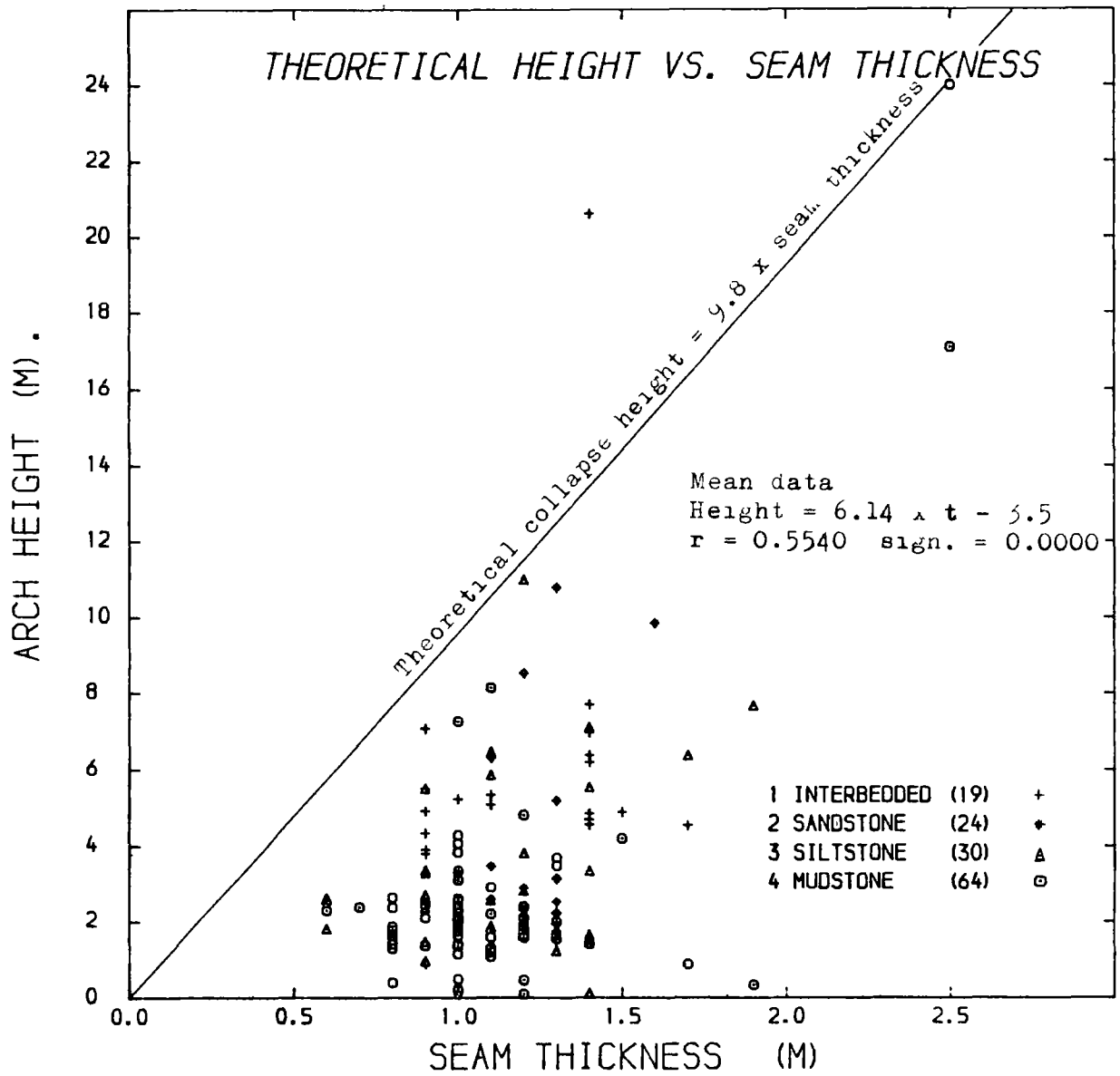

Figure 3.34 Variation in theoretical height of collapse with thickness of coal seam.

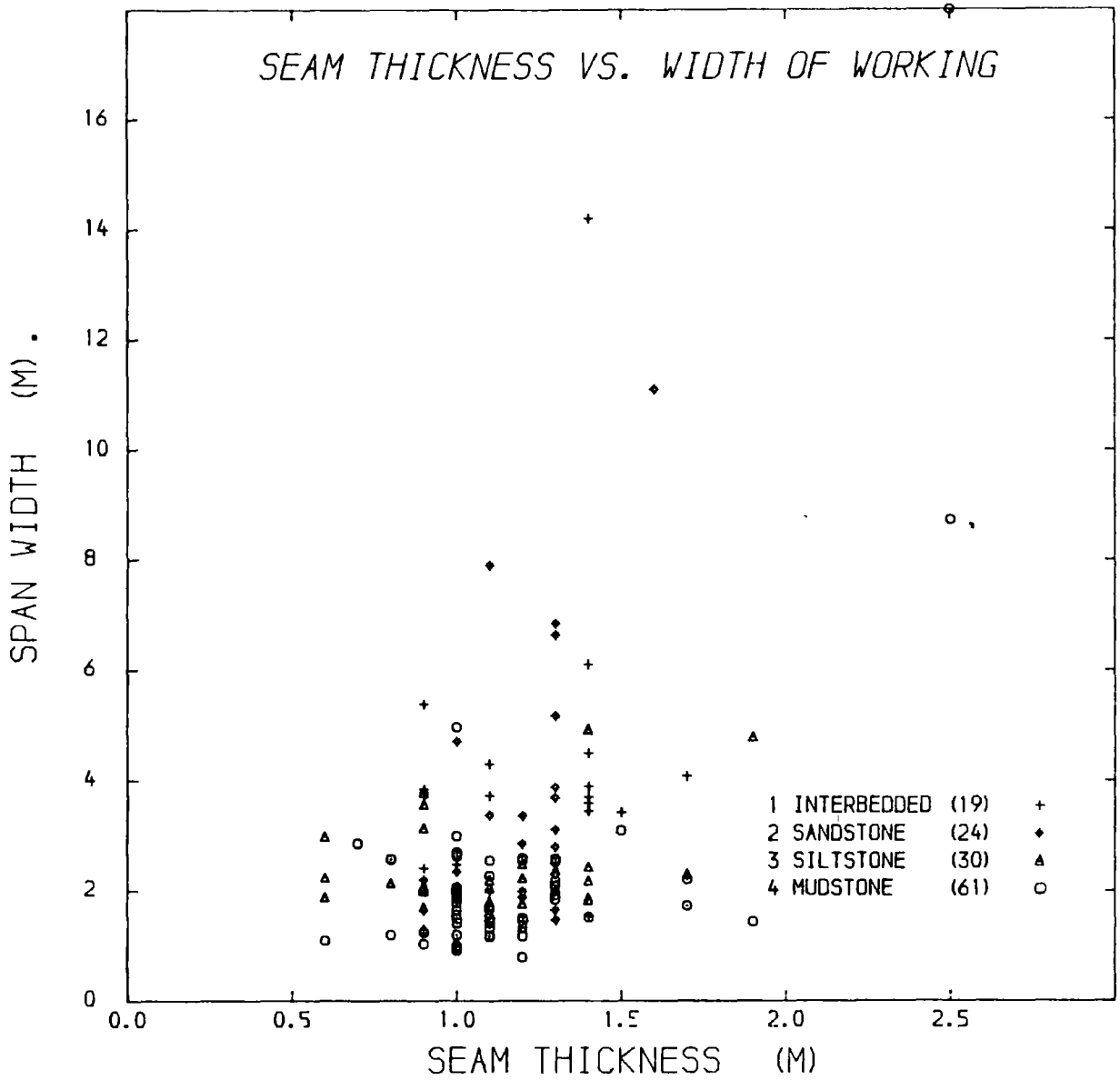

Figure 3.35 Variation in width of working with seam thickness.

this relationship suggests that the width of the working is not related to the seam thickness, an envelope can be applied that encloses the data. This is theoretically justifiable and was done for the relationship between seam thickness and collapse height. It is observable that thick seams have been worked with wider headings than thinner seams, and it is tentatively suggested that this observation is possibly a reflection on the working practice. One explanation could be that perhaps thinner seams were worked with narrower headings to improve roof conditions. It would be more cost effective to supply large quantities of roof support in thicker seams than in thinner seams. Alternatively, the relationship between working width and seam thickness could be related to the variation in seam thickness and rock type noted in Chapter 3.3.3. This is an area where no obvious explanation is forthcoming.

Whether or not one of the explanations for the variation in working width with seam height is accepted, there is as much evidence in the data base to suggest that the width of working varies with the seam thickness, as there is that the collapse height varies with the seam thickness. In view of the proven relationship between span width and collapse height, it is suggested that the relationships between collapse height and seam thickness is based on a common variation with the width of working. Therefore, it is not related to bulking as suggested by traditional theory.

This link between the seam thickness and the collapse height can be explored further. The aspect ratio of the workings, that is the ratio between the width and height of the opening, has been shown to have a median value of 2.06. Thus, for a coal seam one unit thick, the width of the working would be expected to be about 2 units. The likely maximum collapse height to width ratio of 2.68 proposed above, suggests that a working with a span of 1 unit would collapse to a height of 2.68 units. Therefore, the product between these two ratios reflects the expected maximum height of collapse for an average seam thickness, that is:-

$$2.06 \times 2.68 = 5.83$$

Therefore, it is quite possible to arrive at a relationship between the seam

thickness and the collapse height that is similar to the relationships suggested by previous authors for bulking, and similar to the values shown above (Fig 3.33 and 3.34) which act as envelopes on the relationship between seam thickness and collapse height. The fundamental difference is that the relationship just derived predicts the height of collapse by first predicting the width of working from the seam thickness. This link between the seam thickness and the working width, and the working width and the collapse height of an old working is considered to be the principle explanation for the observed relationship between seam thickness and the collapse height of an old working. This relationship is completely independent of bulking yet produces similar values to the so-called bulking relationships proposed by numerous authors.

The main argument in favour of using the seam thickness to predict the height to which a void will migrate is that in many situations the investigator will have no accurate idea of the width of the working, but will have some idea of the thickness of the coal seam. While the bulking coefficients, proposed by the authors mentioned above have not been proved to be wrong,and do appear to be more or less correct, the validity of the theory on which the relationships are based, is very questionable. It is considered that a false sense of security is created by using one of these relationships between the seam height and the height of the collapse. When such a relationship is used the investigator is unwittingly assuming a width of working from the height of coal seam, and from the assumed working width will then be predicting the likely height of collapse. Thus, by using such a relationship, the investigator is unknowingly assuming a width for the working which was the very thing that he felt he had insufficient information to assume in the first instance. At least, when the width of working is assumed and used to predict the height of collapse the investigator is aware, and can control, the sources of error.

c. DEGREE OF COLLAPSE

The degree of collapse and the age of the working were investigated to see whether there was a correlation between the variables. Apart from the very

recent old workings, that is those workings that are less than about thirty or forty years old, there was no increase in the degree of collapse with increasing age. It is thought that the very recent workings are slightly more stable because, in many instances, the wooden pit props are still in place and are providing some support for the roof.

No other relationships between either the percentage collapse or the normalised width and any of the variables discussed above could be found. Therefore, it must be concluded that the degree to which an old working has collapsed cannot be predicted, with any degree of reliability, by any measured variable. This observation provides further justification for recommending the use of relationships based on the theoretical collapse height rather than the observed height of collapse.

d. SHAPE OF THE FAILURE SURFACE

The normalised height and the normalised width are two variables that were calculated and used in the first section concerned with descriptive statistics (Chapter 3.2.2). These variables are a measure of the degree of natural closure that has occurred in the arch at the point at which the void was bridged. The data were normalised to provide a uniform scale and every old working that has been bridged provides one point on the graph which is equivalent to the degree of closure at the height in the arch at which the void was bridged. The variation in the degree of collapse means that there is a good spread of data points for these variables (Fig 3.36). If the profile of the typical arch changed with increasing collapse, the variation would show on the plot of the normalised variables.

From a scattergram of the variables (Fig 3.36), it is evident that the variation in the data is greater than any possible underlying effect of curvature. Therefore, in the absence of better data, it must be concluded that the average shape of an arch has not been proved to be curved and that a linear failure surface is appropriate to characterise most arches. Such an analysis obviously makes no concessions for the effects of any other variables and must be

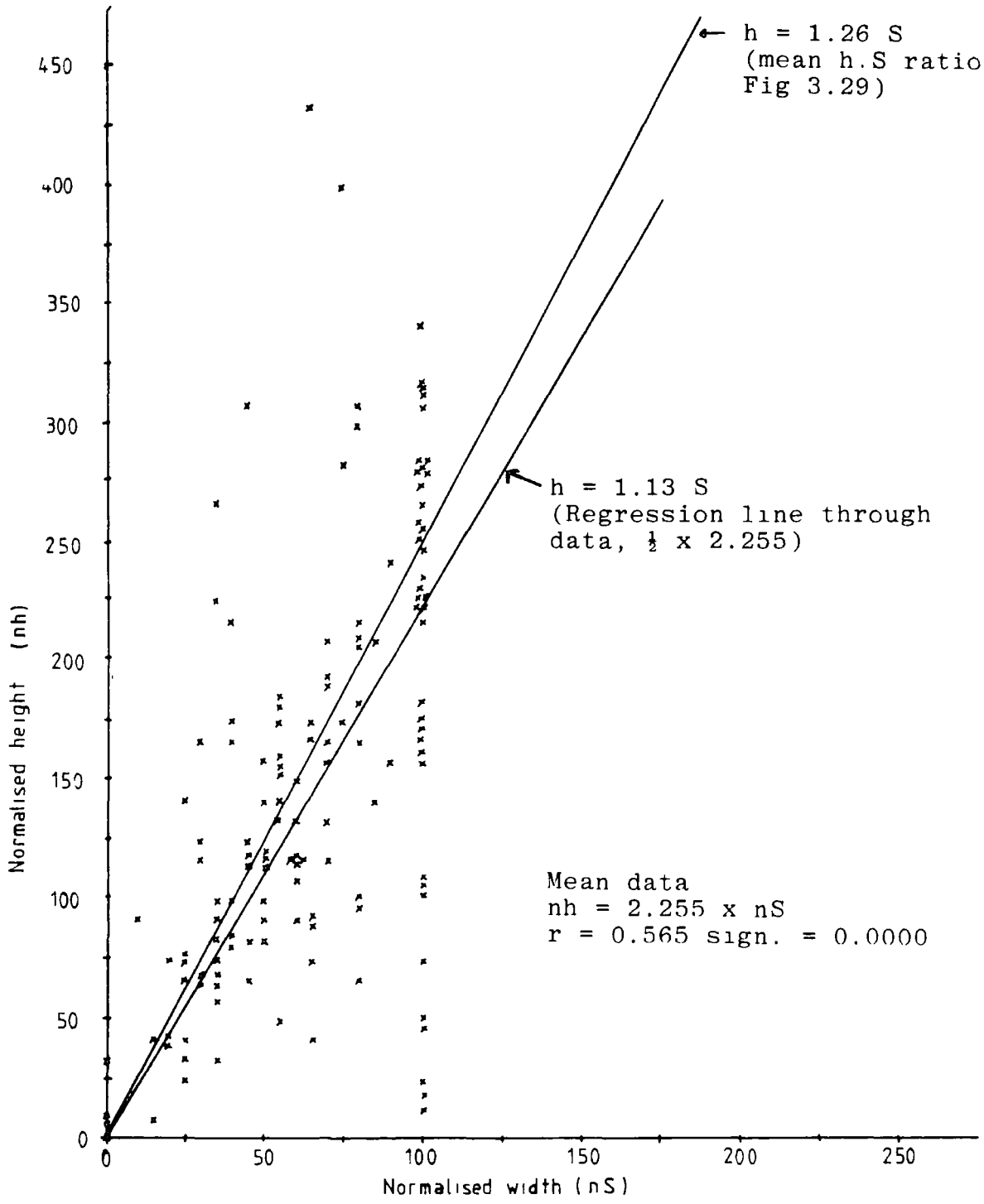

Figure 3.36 Variation between normalised, collapse height and width.

considered to be very general. The question of the shape of an old working is returned to in Chapter 9.

A regression line constructed through the data gives an average collapse height for the arch of 1.13 times the span of the working. This line has been constructed on Figure 3.36. Also shown is the mean theoretical collapse height to width ratio for all the data.

3.5. SUMMARY

Field observations and analysis of measurements have shown that the average old coal-mine working is in a state of semi-collapse, and that the main void arresting mechanism within the system is bridging. This occurs either when a thick competent bed is encountered, or when the span of the arch has been reduced, by corbelling, to a bridgeable width.

The height of collapse of the working has been found to be proportional to the width of the working, while the width of the working has been found to be related to both the type of roof rock and the thickness of the coal seam.

The ratio of the theoretical collapse height divided by the span of the working has been found to be satisfactory for characterising the relationship between the two variables. Although the ratio is not distributed normally, the distribution is sufficiently close to warrant the use of the mean and standard deviation for predictive purposes. A relationship of (Collapse height = 2.68 S), where S is the span of the working, is suggested as a possible relationship for predicting the maximum likely height of collapse for arching failures. This relationship was found adequate to encompass 180 out of 181 observed collapse structures.

The so-called bulking relationships for predicting the height of collapse from the seam thickness (Price et al., 1969, Taylor, 1975, Walton and Taylor, 1977, Piggott and Eynon, 1977, Higginbottom, 1984) are suggested as being theoretically incorrect but, inspite of this, fairly reliable. Similar values have readily been obtained from the inter-relationship between seam thickness,

working width and collapse height. The disadvantage with bulking relationships is that they obscure the sources of error. This can, in use, lead to a false sense of security therefore, for practical purposes, such relationships require intelligent application.

The degree to which an old working has collapsed appears to be independent of any recorded variable, and there is no evidence to suggest that very old workings have collapsed more than recent workings. In general, the height and the degree to which an old working has collapsed do not appear to be controlled by the macro-structure, such as jointing, of the overlying rock. The recommended techniques for recording such macro-structures seem to be too coarse to be of any but very generalised value in predicting collapse. Therefore, it is considered that geomechanical classification systems are unlikely to be of much value for predicting the height of collapse in the highly specialised field of old coal-mine collapse.

CHAPTER 4

BEAM THEORY

4.1. INTRODUCTION.

Coal is a stratified deposit, and the rock forming the immediate roof is also often well stratified. In such a situation it is possible to consider the immediate roof of an opening as a series of beams (Plates 3 and 8). Halbaum (1905) was the first to utilise this approach to mining subsidence, and although his emphasis was on the prediction of collapse above longwall faces, it was recognised that this method had potential for smaller scale collapse features (Briggs, 1929).

A number of assumptions have to be made about the properties of the mine roof in order to be able to theoretically justify the use of beam theory. These assumptions are:-

a. That the beam is made of a homogeneous, isotropic and linearly elastic material.

b. The beam is straight and has a uniform cross-sectional area along the axis of the beam.

c. All loads and reactions are perpendicular to the axis of the beam and lie in the same plane, which is a longitudinal plane of symmetry.

d. The beam span is at least twice the beam thickness.

e. The length of the beam is at least twice the beam span.

Rock beams are body-loaded structures, but this has been shown to be adequately approximated by a uniformly loaded beam, where the load is equal to the rock density multiplied by the thickness of the beam. (Caudel and Clark, 1955, Obert et al., 1960).

4.2. BEAM THEORY.

An elementary mechanics or materials text recognises three types of beams:- cantilever, simple and clamped.

4.2.1. CANTILEVER BEAM.

Table 4.1 shows the important relationships for a cantilever beam. The maximum tensile and shear stress occur at the abutment so it would be expected that a beam would fail at this point. Halbaum (1905) considered a longwall face in terms of a cantilever beam, but on a smaller scale the beds forming the side of an arch can all be considered as small cantilever beams. Using this analogy it is possible to calculate the critical length for a cantilever beam for different values of tensile strength and beam thickness. Figure 4.1 has been plotted using the relationships in Table 4.1, and shows the critical lengths for typical strength mudrocks.

The 'median effective' bed thickness was observed to be about 0.058m (Table 3.1). From Figure 4.1, which assumes a density of 2.5Mg/m2, the critical length for a cantilever beam, with a tensile strength of between 2 and 4MN/m2, is between 1.15 and 1.65m. Site observations (Plate 5) suggest that mudrock beams of this length are unlikely. Therefore, it must be concluded that, either the edges of old workings are not acting as cantilever beams, or more likely, the strength of the mudrocks in tension is considerably less than that indicated from Point Load Tests (Appendix 1).

4.2.2. SIMPLE BEAM.

Table 4.2 shows the important relationships for a simple supported beam. Adler et al. (1968) suggested that at shallow depths, the immediate roof of an opening could be considered as a series of simply supported beams. The maximum bending moment for a simple beam occurs at its midspan. Therefore, the maximum tensile stress occurs at the bottom edge of the midspan, while the maximum compressive stress occurs at the top edge. Rock is much weaker in tension than

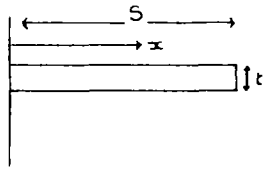

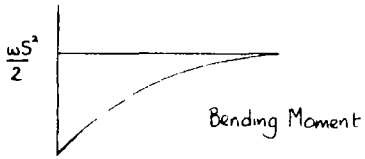

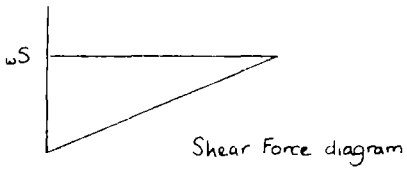

	At x	At maximum	Maximum at Location
Bending Moment	$BM_x = \frac{\omega(S-x)^2}{2}$	$BM = \frac{\omega S^2}{2}$	abutment
Shear force	$SF_x = \omega(S-x)$	$SF = \omega S$	abutment
Deflection	$\delta x = \frac{\omega}{2EI}\left(\frac{S^2x^2}{2} - \frac{Sx^3}{3} + \frac{x^4}{12}\right)$	$\delta = \frac{\omega S^4}{8EI}$	at end
Tensile Stress	$T_x = \frac{3\omega(S-x)^2}{t^2}$	$T = \frac{3\omega S^2}{t^2}$	
Maximum Length	$S = \sqrt{\frac{Tt^2}{3\omega}}$ $\sqrt{\frac{Tt}{3p}}$		

Where -

ω = wt per unit length

S = cantilever length

x = distance from abutment

p = density

t = thickness

T = tensile stress / strength

I = Moment of Inertia of beam section

E = Young's Modulus

$\omega = pt$

$I = \frac{bt^3}{12}$ (Assuming b = unit depth)

TABLE 4.1 RELATIONSHIP FOR CANTILEVER BEAM UNDER UNIFORM LOADING

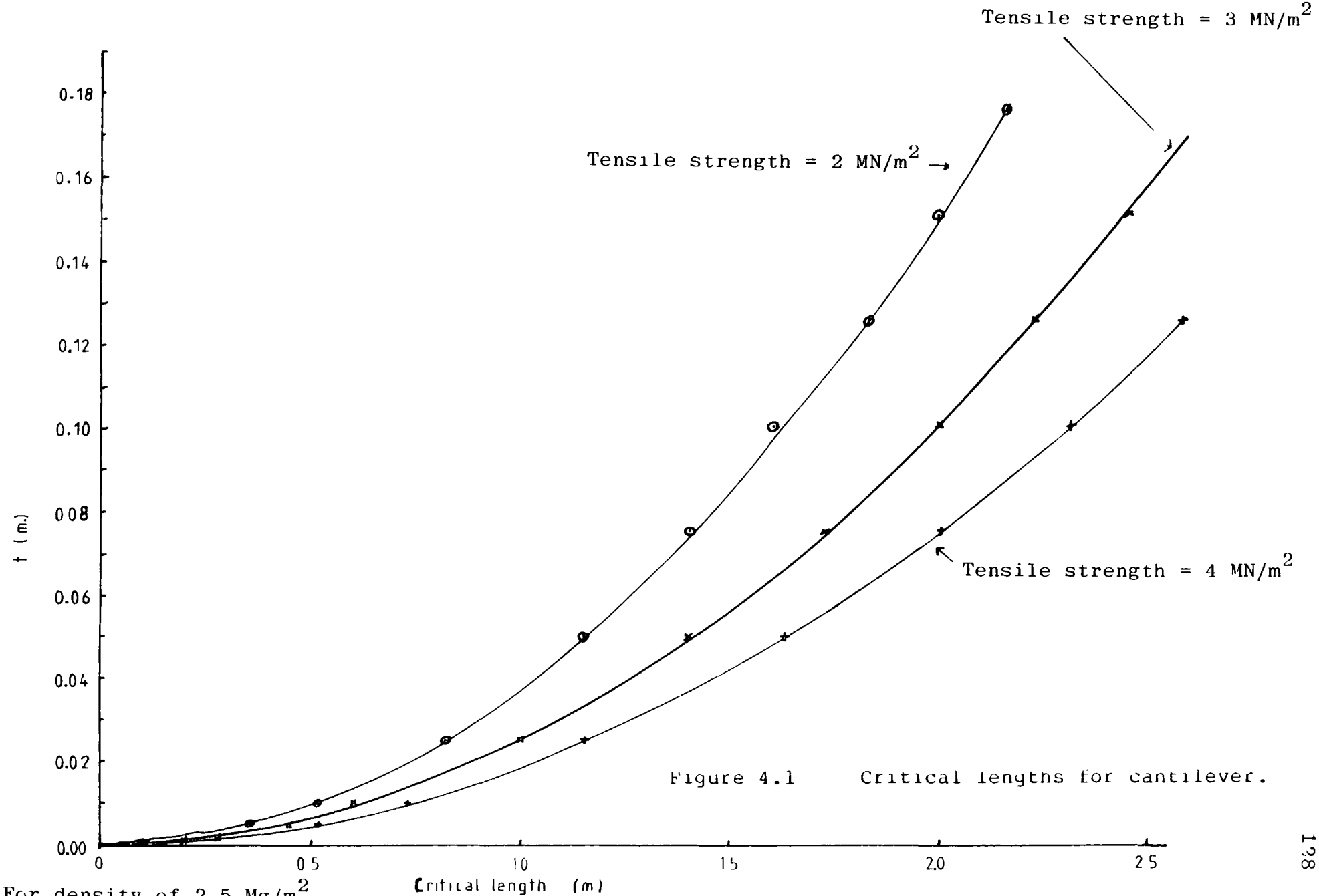

Figure 4.1 Critical lengths for cantilever.

For density of 2.5 Mg/m^2

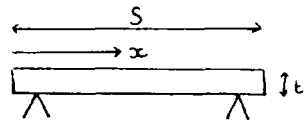

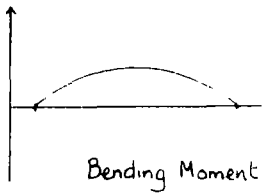

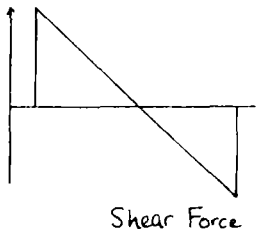

	At x	At maximum	Maximum at Location
Bending Moment	$BM_x = \frac{\omega}{2}(Sx - x^2)$	$BM = \frac{\omega S^2}{8}$	centre
Shear force	$SF_x = \omega\left(\frac{S}{2} - x\right)$	$SF = \frac{\omega S}{2}$	abutments
Deflection	$\delta_x = \frac{\omega x}{24EI}(S^3 - 2Sx^2 - x^3)$	$\delta = \frac{5\omega S^4}{384EI}$	centre
Tensile Stress		$T = \frac{3\omega S^2}{4t^2}$	centre
Maximum Length (tensile)		$S = \sqrt{\frac{4Tt^2}{3\omega}}$	
Shear Stress		$\tau = \frac{3\omega S}{4t}$	abutments

$\omega = pt$

$I = \frac{bt^3}{12}$ (Assuming b = unit depth)

(nb see Table 4.1 for explanation of other terms)

TABLE 4.2 RELATIONSHIP FOR SIMPLY SUPPORTED BEAM UNDER UNIFORM LOADING

compression and so failure, of the top edge, under compression can usually be ruled out. Simple beams usually fail in tension at the midspan of the bottom edge.

The shear stresses generated at the beam abutment, are usually ignored provided that the beam span is large compared to its thickness. From the equations for the maximum tensile and shear stress (Table 4.2), the critical ratio for a simply supported beam can be shown to be :-

$$\frac{\text{Maximum tensile stress}}{\text{Maximum shear stress}} = \frac{S}{t} \qquad \ldots\ldots\ldots\ldots\ldots\ldots \text{Eq 4.1}$$

Thus, for beams that are long compared to their thickness, and for the usual situation where rock is weaker in tension than shear, the effect of shear stress can be neglected with little error.

4.2.3. CLAMPED BEAM.

Table 4.3 gives the important relationships for a uniformly loaded clamped or encaster beam. Merril (1954), Isaacson (1962), Wardell and Wood (1965), Wardell and Eynon (1968), Adler et al. (1968), Wright (1973), Hoek and Brown (1980), and indeed most authors recommend the use of the clamped beam formulas in a stability analysis of an opening.

The maximum deflection for a clamped beam, as for a simple beam, occurs at the midspan. However, the maximum shear stress and maximum bending moments occur at the abutments. Indeed, at the centre of the beam the tensile stress is one half (0.5) the maximum value at the abutments. A comparison between the maximum bending moments for simple and clamped beams (Tables 4.2 and 4.3), will show that the maximum bending moment for an encaster beam is two thirds (2/3) of the value quoted for the simply supported beam. In addition, the point of maximum bending moment has shifted from the midspan to the abutments. Therefore, a clamped beam is substantially stronger than a simply supported beam, but perhaps of greater interest, clamped beam theory predicts tensile failure at the abutments rather than at the midspan. Thus, clamped beam theory will predict a

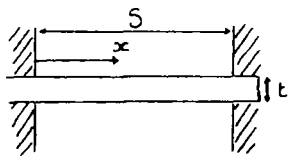

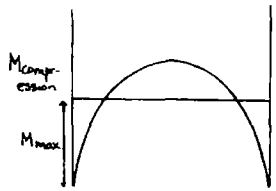

Bending Moment

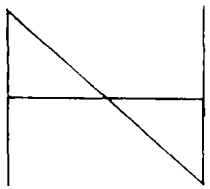

Shear Force

	At x	At maximum	Maximum at Location
Bending Moment	$BMx = \frac{\omega}{12}(6Sx - S^2 - 6x^2)$	$BM = \frac{\omega S^2}{12}$	abutments
Shear force	$SFx = \frac{\omega S}{2}\left(1 - \frac{2x}{S}\right)$	$SF = \frac{\omega S}{2}$	abutments
Deflection	$\delta x = \frac{\omega x^2}{24EI}(S-x)^2$	$\delta = \frac{\omega S^4}{384EI}$	centre
Tensile Stress		$T = \frac{\omega S^2}{2t^2}$	abutments
Maximum Length (tensile)		$S = \sqrt{\frac{2Tt^2}{\omega}}$	
Maximum Length (shear)		$S = \frac{4T\tau}{3\omega}$	
Shear Stress		$\tau_{max} = \frac{3\omega S}{4t}$	abutments

$\omega = pt$

$I = \frac{bt^3}{12}$ (Assuming b = unit depth)

(nb see Table 4.1 for explanation of other terms)

TABLE 4.3 RELATIONSHIP FOR CLAMPED BEAM UNDER UNIFORM LOADING

stronger and more stable roof to an old working than simple beam theory.

In common with simply supported beams, failure of clamped beams in compression or shear are usually ignored, provided that the span of the beam is large compared to its thickness. The critical ratio can be shown to be (Merril, 1954), (Table 4.3) :-

$$\frac{\text{Maximum tensile stress}}{\text{Maximum shear stress}} = \frac{2S}{3t} \qquad \text{.....Eq 4.2}$$

This ratio is lower than that for the simply supported beam, therefore the aspect ratio of the beam is more important.

4.2.4. ELASTIC ABUTMENTS.

Until now, the beam or roof has been considered as resting on rigid abutments. This is an obvious over-simplification which goes some way to explaining why the results obtained from simple beam theory do not tally with measurements and observations made below ground (Merril, 1957, Hofer and Menzel, 1964). It is therefore pertinent to consider the effect of introducing elastic abutments into the problem.

Some control over the moments, and hence tensile stresses in a beam, can be achieved by varying the stiffness of the supporting pillars. The moment in a beam is directly proportional to its curvature thus, anything done to reduce the curvature, such as making the supports elastic will reduce the moment at that point. A clamped beam supported by rigid pillars has the maximum bending moment at the abutments. As the abutments soften, the curvature of the beam, and hence the bending moments, reduce. The position of the maximum bending moment is gradually transferred towards the centre of the beam until, with very soft abutments the situation approximates to a simply supported beam. Tables 4.4 and 4.5 summarise two methods of calculating the bending moments associated with elastic abutments for thin single layer roofs. Table 4.6 shows the effect of varying the rigidity of the abutment on the position and value of the bending moments.

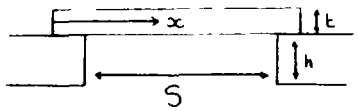

Bending Moment at x $\quad BMx = -\frac{\rho x^2}{2} + \frac{\rho S}{2}\left(x + \frac{1}{\alpha} - \alpha\beta\right)$

Deflection at x $\quad \delta x = \frac{P}{Cu}\left[\alpha^4 x\left(\frac{x^3}{6} - \frac{x^2 S}{3} - \frac{Sx}{\alpha} - \frac{1}{\alpha^2}\right) + S\alpha^3\beta(1+\alpha x)^2 + 1\right]$

Where -

$P = tp$

$Cu = \frac{En}{h(1-Vu^2)}$

$I = \frac{t^3}{12}$

$k = \frac{EI}{1-V^2}$

$\alpha = \left(\frac{Cu}{4k}\right)^{1/4}$

$\beta = \frac{\left(\frac{S^2}{6} + \frac{S}{\alpha} + \frac{1}{\alpha^2}\right)}{(\alpha S + 2)}$

M = Maximum Bending Moment

I = Moment of Inertia of beam

Cu = Modulus of Foundation

S = Span width

t = beam thickness

h = abutment thickness

En = Young's Modulus for abutment

E = Young's Modulus for beam

Vu = Poisson's ratio for abutment

V = Poisson's ratio for beam

ρ = beam density

TABLE 4.4 RELATIONSHIP FOR CLAMPED BEAM UNDER UNIFORM LOADING SUPPORTED BY ELASTIC ABUTMENTS (after Stephansson, 1971)

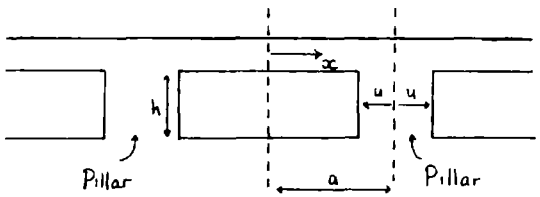

Where -

a = half the centre to centre distances between pillars

u = half the width of the pillar

h = effective height of pillar (seam thickness)

$$BM_{abutment} = \frac{\alpha\,(AB+CD)}{(a-u)\alpha\,(AB+CD)+\sinh^2\alpha u+\sin^2\alpha u} \times \left[\frac{V_o\,(AB-CD)}{2\alpha^2\,(AB+CD)} - \frac{q}{3}(a-u)^3\right]$$

then Moment at x = $BM_x = \frac{q}{2}(a-u+x)(a-u-x) + BM_{abutment}$

$A = \sinh\alpha u$ (hyperbolic sine)

$B = \cosh\alpha u$ (hyperbolic cosine)

$C = \sin\alpha u$

$D = \cos\alpha u$

$V_o = (a-u)q$

$\alpha = \left(\frac{3E_p}{hEbt^3}\right)^{1/4}$ [assumes ν is the same for both abutment and beam. After simplification identical to α of Stephannson]

q = pt

E = Young's Modulus of beam/pillar (subscript denotes which)

t = beam thickness

b = beam depth (usually taken as 1)

TABLE 4 5 RELATIONSHIP FOR CLAMPED BEAM UNDER UNIFORM LOADING SUPPORTED BY ELASTIC ABUTMENTS (after Wright, 1973)

E	*Bending moment (M kg cm)* $x = -l$	$x = -3l/4$	$x = -l/2$	$x = -l/4$	$x = 0$	$x = l/8$	$x = l/4$	$x = 3l/8$	$x = l/2$
$1\ 10^6$	$-0\ 78\ 10^2$	$0\ 11\ 10^4$	$0\ 19\ 10^4$	$-0\ 24\ 10^3$	$-0\ 46\ 10^2$	$0\ 12\ 10^4$	$0\ 35\ 10^3$	$0\ 56\ 10^3$	$0\ 6\_\ 10^2$
$5\ 10^5$	$-0\ 74\ 10^-$	$0\ 13\ 10^3$	$0\ 25\ 10^4$	$-0\ 14\ 10^3$	$-0\ 51\ 10^2$	$-0\ 32\ 10^4$	$0\ 31\ 10^2$	$0\ 51\ 10^3$	$0\ 5\_\ 10^2$
$2\ 10^5$	$0\ 39\ 10^4$	$-0\ 10\ 10^3$	$0\ 10\ 10^4$	$-0\ 35\ 10^4$	$-0\ 56\ 10^2$	$-0\ 80\ 10^4$	$0\ 26\ 10^2$	$0\ 46\ 10^3$	$0\ 5\_\ 10$
$1\ 10^5$	$0\ 14\ 10^4$	$-0\ 15\ 10^2$	$0\ 95\ 10^2$	$0\ 11\ 10^4$	$-0\ 58\ 10^5$	$-0\ 10\ 10^3$	$0\ 23\ 10^3$	$0\ 43\ 10^3$	$0\ 50\ 10^2$
$5\ 10^4$	$-0\ 19\ 10^6$	$0\ 49\ 10^4$	$-0\ 11\ 10^3$	$0\ 27\ 10^4$	$-0\ 61\ 10^5$	$-0\ 13\ 10^5$	$0\ 20\ 10^3$	$0\ 41\ 10^3$	$0\ 48\ 10^2$
$1\ 10^4$	$-0\ 30\ 10^3$	$-0\ 12\ 10^4$	$0\ 50\ 10^4$	$0\ 52\ 10^3$	$-0\ 65\ 10^5$	$-0\ 17\ 10^5$	$0\ 16\ 10^3$	$0\ 37\ 10^3$	$0\ 44\ 10^2$

E	*Deflection (y cm)*								
$5\ 10^7$	0 00	0 00	0 00	0 00	0 00	0 00	0 01	0 01	0 01
$1\ 10^7$	0 00	0 00	0 00	0 00	0 01	0 01	0 01	0 01	0 01
$5\ 10^6$	0 00	0 00	0 00	0 00	0 01	0 01	0 02	0 02	0 02
$1\ 10^6$	0 00	0 00	0 00	0 00	0 01	0 03	0 04	0 05	0 06
$5\ 10^5$	0 00	0 00	0 00	−0 00	0 02	0 04	0 07	0 09	0 09
$1\ 10^5$	0 00	0 00	0 00	−0 00	0 03	0 13	0 23	0 31	0 34
$5\ 10^4$	0 00	0 00	0 00	−0 00	0 04	0 21	0 41	0 56	0 62

E	*Outer fibre stress for lower surface (kg/cm²)* $x = 0$	$x = l/2$
$1\ 10^6$	−12	17
$5\ 10^5$	−14	16
$2\ 10^5$	−15	14
$1\ 10^5$	−16	14
$5\ 10^4$	−16	13
$1\ 10^4$	−17	12

E	*Deflection excluding abutment deformation* $\frac{p}{k_0}$ *(cm)* $x = 0$	$x = l/2$
$1\ 10^6$	0 01	0 05
$5\ 10^5$	0 02	0 09
$2\ 10^5$	0 02	0 19
$1\ 10^5$	0 03	0 34
$5\ 10^4$	0 04	0 62
$1\ 10^4$	0 09	2 59

[1] Constant values $l = 1{,}500$ cm, $H = 150$ cm, $E_u = 500{,}000$ kg/cm², $h = 1\ 500$ cm, $\rho = 2\ 6$ g/cm³, $\nu_u = \nu_L = 0\ 2$

Table 4.6 The effect of varying the rigidity of the abutment on the position and value of the bending moments (after Stephansson, 1971)

4.3. CLASSIFICATION OF SINGLE OPENINGS.

From the assumption that the immediate roof of an opening behaves as a gravity loaded beam resting on elastic abutments, Stephansson (1971) classified openings according to the number, thickness and flexural rigidity of the beams that formed the roof. A slightly modified version of his classification is shown in Figure 4.2.

4.3.1. SINGLE LAYER ROOFS.

Single layer roofs can be divided into 3 groups depending on the ratio between the span length and the thickness of the beam.

a. THIN LAYER ROOFS. (length : thickness ratio > 5). In thin layer roofs, the deformations due to shear stress can be disregarded. Consequently any cross-section of the roof layer remains plane during bending, and the stress in any fibre perpendicular to the cross-section is proportional to its distance from the neutral axis.

b. MEDIUM THICK ROOFS. (length : thickness ratio between 5 and 2). In this interval the influence of shear stresses can no longer be ignored and the deformation curve may be regarded as the sum of the curvature due to the bending moment and that due to the shear. The inclusion of shear increases the deflection and thus the tensile stress.

c. THICK LAYER ROOFS. (length : thickness ratio < 2). For thick layer roofs the influence of shear stress is proportionally greater, and the inclusion of shear stresses means that the stresses are no longer symmetrical about the mid-section of the beam. This asymmetry leads to a downward movement of the neutral axis towards the bottom part of the beam. For very thick roofs, the roofs will fail by shear before failing by tension. Such a problem is best approximated by the theory of openings in an infinite elastic media (eg. finite element analysis).

Single layer roof

1. Thin roof

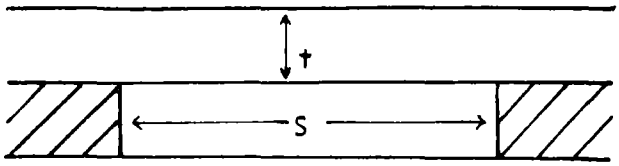

$t < \frac{S}{5}$ Ignore effect of shear stress

2. Medium thick roof

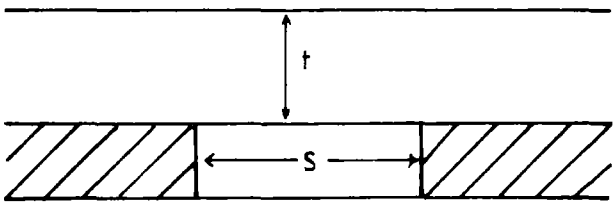

$\frac{S}{2} > t > \frac{S}{5}$ Inclusive shear stress in the layer

3. Thick roof

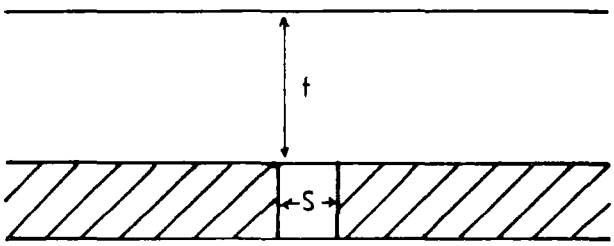

$t > \frac{S}{2}$ Too thick for beam analysis

Double layer roof

4.

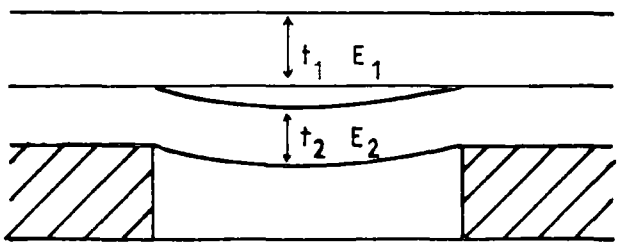

$E_1I_1 > E_2I_2$

Detaching of beds

5.

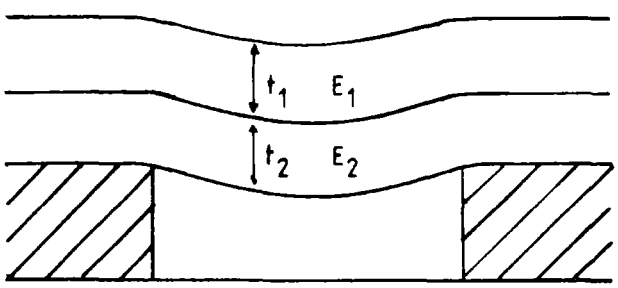

$E_1I_1 < E_2I_2$

Beds act as one beam

Figure 4.2 Classification of single openings.

4.3.2. DOUBLE LAYER ROOFS.

When the immediate roof of a mine consists of 2 rock units, there are three situations that have to be considered. The flexural rigidity of a beam is given by:-

$$E \times I = E \times \frac{S \times t^3}{12} \qquad \text{.....Eq 4.3}$$

where:- I = Moment of inertia of the beam
E = Young's modulus
S = span of beam
t = thickness of beam

From equation 4.3 it will be noticed that the thickness of the section has a major influence on the rigidity of the beam, thus thin beams are more flexible than thick beams.

When the uppermost beam has a higher flexural rigidity than the lower member, (assuming frictionless contacts), the lower layer will deflect more that the upper layer and the two members will separate. This separation may produce a cavity between the beams and such a cavity is sometimes referred to as a Weber cavity (Denkhaus, 1964).

When the uppermost beam has a lower flexural rigidity than the lower beam, the upper beam will try to deflect more than the lower beam, and in doing so will act as a surcharge load on the lower beam. This load on the lower beam can be calculated from the following equation:-

$$Wi = E \times I \times \frac{\sum_{i=1}^{n} (Y \times t)i}{\sum_{i=1}^{n} (E \times I)} \qquad \text{.....Eq 4.4}$$

For example in the case of a two layer situation:-

$$W = \frac{E1 \times t1^3 \times (Y1 \times t1 + Y2 \times t2)}{(E1 \times t1^3 + E2 \times t2^3)} \quad \text{.....Eq 4.5}$$

where n = number of beds comprising the immediate roof
Yi = unit weight of beam i
ti = thickness of beam i
Ei = Young's modulus of bed i
Ii = moment of inertia of bed i

In the above equation the values of 1 and 2 refer to the bottom and top beds respectfully.

If the density and Young's modulus are the same for both members, the maximum load W occurs when the upper layer is a half (0.5) the thickness of the lower layer. Under this condition the lower member must support a 33.3% increase in load per unit length.

A similar situation occurs for a three member beam. As above, the maximum additional loading occurs when the upper 2 members are of equal thickness and about a half (0.5) as thick as the lowest member. Under these conditions the lowest member will have to support an extra 63% increase in load per unit length. (Merril, 1954).

The relationship is conservative as it tends to overestimate the load W, since it neglects the resistance to bending provided by frictional resistance between the bedding planes. For the same reason it progressively loses validity as the total thickness of the immediate roof exceeds the span of the opening. The same limitations exist for the thickness of the individual beds, as outlined in the section on single beam; thin, medium and thick layer roofs (Chapter 4.3.1.).

4.3.3. DIPPING BEDS.

It has been assumed so far that the beams are horizontal and subjected to no horizontal forces. In certain circumstances this may be to much of a simplification. For the situation where an opening has been driven along the strike of a seam, the value for the unit load, W, is modified by the cosine of the angle of dip:-

W inclined = W horizontal x cosine θ

where angle θ is the angle of dip.

In reality the influence of the angle of dip is generally ignored for beds dipping less than 10 to 15 degrees. A correction for a dip of even 20 degrees will only reduce the unit load by 6% (Wright, 1973).

4.3.4. HORIZONTAL IN-SITU STRESSES.

Horizontal in-situ stresses are generally present in underground workings and their effect is crucial to the stability of the immediate roof of an opening. The stresses may well vary with time, and may be drastically modified by other mining operations in the area, especially where underlying coal seams are being worked.

Roof beams subjected to axial loading behave as beam columns. In a beam column, the axial load increases the moment in the beam by the so-called 'secondary bending effect' (Wright, 1973). Moments can become very large for slender beams under high axial loading and produce elastic buckling of the beam. The moments at the abutments and midspan, for both clamped and simply supported beams, are given in Table 4.7. Note that the expressions on the right hand side of the equation, the secondary bending effect, act as multipliers to the standard equation (Tables 4.2 and 4.3).

The maximum tensile or compressive stress in the beam column is the sum of the stresses due to the axial load P or the unit load p, and the stresses due to bending. These are:-

$\sigma_{tot} = P + \sigma_{bending}$

In practice the addition of p to the bending stress increases the compressive stress in the beam and reduces the tensile stress. Therefore, a column beam under a horizontal stress has a much higher factor of safety against tensile failure than a beam with no axial load.

Simple

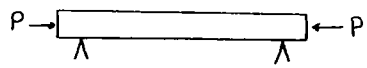

Clamped

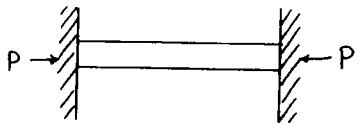

$$BM_{max} = \frac{wS^2}{8}\left[\frac{2\,(1-\cos V)}{V^2\cos V}\right] \qquad \sigma_{bend}\left(\begin{matrix}\text{Tensile/compressive}\\ \text{stress}\end{matrix}\right) = \frac{3wS^2}{4t^2}\left[\frac{2\,(1-\cos V)}{V^2\cos V}\right]$$

$$BM_{abutment} = -\frac{wS^2}{12}\left[\frac{3(\tan V - V)}{V^2\tan V}\right] \qquad \sigma_{bend}\left(\begin{matrix}\text{Tensile/compressive}\\ \text{stress}\end{matrix}\right) = \frac{wS^2}{2t^2}\left[\frac{3(\tan V - V)}{V^2\tan V}\right]$$

$$BM_{centre} = \frac{wS}{24}\left[\frac{6(V-\sin V)}{V^2\sin V}\right] \qquad \sigma_{bend}\left(\begin{matrix}\text{Tensile/compressive}\\ \text{stress}\end{matrix}\right) = \frac{wS^2}{4t^2}\left[\frac{6(V-\sin V)}{V^2\sin V}\right]$$

Where $V = \frac{180\,S}{\pi}\sqrt{\frac{3P}{Et^3}}$

P = total axial load on a beam of unit length

p = axial load per unit thickness of beam

w = weight per unit length of beam

E = Young's Modulus

t = thickness

For both cases axial stress due to the axial load P or unit load p are additive to the axial stress produced by the bending moments

Thus $\sigma_{total} = p + \sigma_{bending}$

TABLE 4.7 RELATIONSHIP FOR CLAMPED AND SIMPLY SUPPORTED BEAM COLUMNS (after Wright, 1973)

4.4. FACTOR OF SAFETY USED IN BEAM THEORY.

In the study of the collapse of old workings, the term 'factor of safety' is not really very descriptive, and it would be better to refer to the concept as a measure of confidence in the validity of the analysis technique. Merril (1954) in the construction of an experimental underground room in oil shale, determined from clamped beam theory (Fig. 4.3), that the maximum theoretical span for the room, which had an 8 ft. (2.44m) thick roof, should be about 200 ft. (61m). In reality, the roof showed signs of collapse at a span width of only 80 ft. (24.4m). A factor of safety of 8 applied to the relationship would have predicted the maximum theoretical roof span to be 72 ft. (21.9m). This value of 8 is widely recommended as an initial design factor of safety for openings required to stand for a long time (Merril, 1954). A factor of safety of 4 has been suggested by Wright (1973) as suitable for temporary access roads or in situations where there is a good understanding of roof conditions.

4.5. PLATE THEORY.

The application of beam theory to the immediate roof of a mine is only valid so long as the roof acts like a beam. Where the length of the excavation, normal to the span of the section considered, is small the strata can no longer be approximated to a beam and analysed in two dimensions, but must be analysed in three-dimensions using the theory of flat plates (Table 4.8).

Plate theory is very complex and yet like beam theory two types of support are recognised. These are simply supported plates and clamped plates. Similar restrictions and arguments as outlined for simple and clamped beams apply to their equivalent plate situations.

The maximum bending moment is greatest for simply supported plates, and occurs at the centre of the plate. For clamped plates the maximum bending moment occurs at the edges. For plates that are rectangular rather than square, the maximum bending moment, and therefore stress, occurs at the mid-point of the longest side of the rectangle (Table 4.8, Isaacson, 1962).

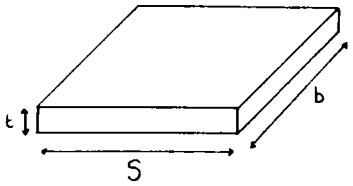

Conditions

$\frac{S}{b} < 2$ = Plate analysis

$\frac{S}{b} > 2$ = Beam analysis

When $\frac{b}{a}$ = 2 or greater, plate and beam calculations are within 1% for max stress 12% for deflection

$$\delta_{max} = \frac{C \rho a^4}{E t^2}$$ at centre of plate

$$\Upsilon_{max} = \frac{6 B \rho a^2}{t}$$ middle of larger side of plate failure (as beam) at edges

$$\text{Max span} = a = \sqrt{\frac{\Upsilon t}{6 \rho B}}$$

$$t = \sqrt{\frac{\rho}{E(D_2 - D_1)}\left(C_2 a_2^4 - C_1 a_1^4\right)}$$

Alternative equation for deflection

$$\delta_{max} = \frac{\omega (1 - \sigma^2)(2a^2 - x^2)^2 \times (2b^4 - y^2)^2}{2 E t^3 (2a^4 + 2b^4)}$$

b/a	B	C
10	00513	0 0138
11	00581	0 0164
12	00639	0 0188
13	00687	0 0209
14	00726	0 0226
15	00757	0 0240
16	00780	0 0251
17	00799	0 0260
18	00812	00267
19	00822	0 0272
20	00829	00277

Where

δ_{max} = maximum deflection

Υ_{max} = maximum tensile stress

a = shorter of two horizontal dimensions

b = longer of two horizontal dimensions

E = Young's Modulus

ω = Load per unit area

C = constant - depends on ratio of b/a and Poisson's ratio

B = constant - depends on ratio of b/a and Poisson's ratio

ρ = density

t = thickness

x, y = distances measured from origin at centre of plate

TABLE 4 8 RELATIONSHIP FOR CLAMPED PLATES UNDLR UNIFORM LOADING
(after Wright, 1973, Isaacson, 1962)

With an increase in the length of a clamped plate, values for the maximum stress and deflection approach those obtained for clamped beams. At a length to span ratio of 2, the variation in the maximum stress calculated by the two different formulae, differ by approximately 1%. The difference between the two predicted deflections is about 12% (Merril, 1954).

It must be remembered that plate theory only applies when the immediate roof of the mine is clamped along all its edges. If the roof is cut by a number of joints then the use of plate theory would be incorrect, and beam theory would be more appropriate.

4.5.1. STRESSES AT INTERSECTIONS.

Plate theory is potentially of most value in predicting the stresses, and hence stability at intersections, where the roof is supported at its four corners. However, plate theory assumes that an entry is completely surrounded, and resting on an abutment. This is obviously not the case at intersections and is, incidentally, also an impossible situation in a mine.

Wright (1973) provides a solution to the problem of calculating the stresses at intersections. The method assumes that the mine was laid out on a regular pattern and that all the roadways meet at right angles to one another. The solution is approximate, but considering the probable quality of the input data, Wright (1973) considers that the analysis can prove useful. The detailed equations and relationships are summarised in Table 4.9.

The technique assumes that the mine area is pillared, either on a regular grid pattern, or on a staggered pattern (see Table 4.9). For a given pillar pattern, influence functions can be read from the nomograms (also presented in the Table). These act as multipliers to the basic maximum bending moment relationships for the situation of a uniformly loaded clamped beam already met in Chapter 4.2.3, (Table 4.3).

There are three influence functions:-

Regular Pillar

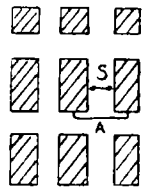

Staggered Pillar

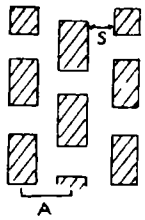

Where -

V = Poisson's ratio of roof slab in axial (horizontal) direction

E = Young's Modulus, subscript denotes pillar (vertical direction) or slab (horizontal direction)

A = Centre to centre distance between pillars

h = Height of pillar

t = Thickness of roof slab

Max = Maximum absolute value (-ve or +ve)

$$M_{centre} = \frac{\omega S^2}{24} \qquad M_{abut} = \frac{\omega S^2}{12}$$

$$\text{Pillar factor } C = \frac{3}{4}(1-V^2)\left(\frac{E_p}{E_s}\right)\left(\frac{A^4}{ht^3}\right)$$

For both maximum negative and positive moments calculated

MF1 ± = see Factor 1

MF2 ± = see Factor 2

MF3 ± = see Factor 3

Max neg = $M_{abut} \times MF1 \times MF2 \times MF3$

Max centre = $M_{centre} \times MF1 \times MF2 \times MF3$

$$\sigma_{\text{tensile/comp}} = \pm \frac{6\,Max}{t^2} \quad \text{(Within } \pm 20\%\text{)}$$

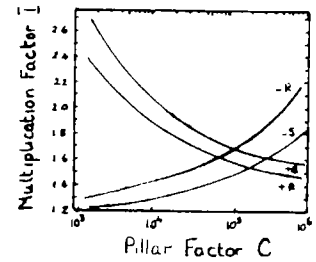

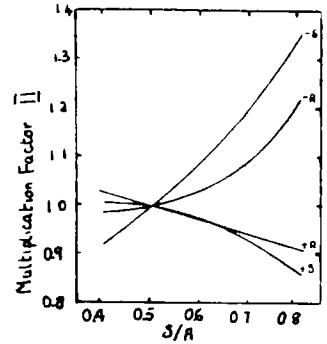

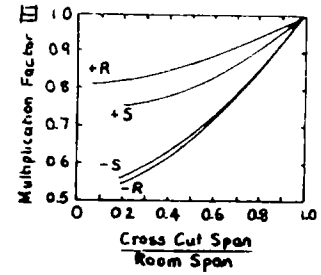

+R = Max pos moment, regular pattern
-R = Max neg moment, regular pattern
+S = Max pos moment, staggered pattern
-S = Max neg moment, staggered pattern

TABLE 4 9 CALCULATION OF STRESSES AT INTERSECTIONS IN A MINE LAYOUT (after Wright, 1973)

a. INFLUENCE FUNCTION 1. Relates the pillar factor C, which is a measure of the stiffness and rigidity of the roof and pillar, to the size of the moments produced in the beam. The effects are similar to those discussed previously with reference to elastic abutments, that is, the maximum negative bending moment increases as the pillars become thicker, and decreases as the immediate roof beam becomes thicker. Therefore, roof conditions will deteriorate as the roof becomes thinner, and will improve as the pillars become smaller and more compressible.

b. INFLUENCE FUNCTION 2. Relates the maximum negative bending moment to the relative sizes of the opening and the pillars. The negative bending moment increases as the span increases. In other words, roof conditions deteriorate with increasing span.

c. INFLUENCE FUNCTION 3. Relates the relative size of the rooms and crosscuts to the maximum bending moments. The bending moments decrease as the crosscuts decrease in width.

EXAMPLE - BURNHOPE COLLIERY.

The potential stability of the immediate roof of the old Burnhope colliery has been analysed as an example of the use of the intersection stability relationship presented above. The calculations are laid out in Table 4.10.

The colliery was almost completely removed during opencast mining operations in 1978. The writer has a full set of data relating to the roof conditions above the workings in the 5/4 seam. The old workings plan showed that a conventional 'Newcastle' system of pillar working had been adopted , but the plan did not show that the top leaf of the 5/4 seam had been re-worked prior to closure (see Plate 1). During this second working, the top leaf of the coal was removed from the pillar to a depth of about 0.6m. This robbing almost doubled the effective span of the working.

Two calculations were attempted, the first was to estimate the stress and stability of the roof after the initial working, and prior to the removal of the

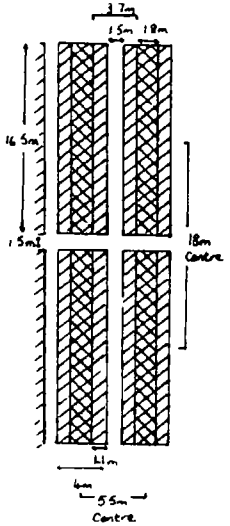

Example Burnhope Colliery

Sandstone roof 0.3m thick
2m weak shale roof overlying baam
$E_{initial\ roof}$ = 6000 MN/m²
$E_{shale\ roof}$ = 4000 MN/m²
$E_{coal\ pillar}$ = 3000 MN/m²
ν roof = 0.2
density of rock = 2.6 Mg/m³
Coal thickness h = 1.3m
Top leaf of coal = 0.6m
Bottom leaf of coal = 0.6m

1 Calculation of roof load ω (Eq 45)

$$\omega = \frac{E_1 t_1^3 \times (\gamma_1 t_1 + \gamma_2 t_2)}{(E_1 t_1^3 + E_2 t_2^3)}$$

$$= \frac{6000 \times 0.3^3 \times (0.026 \times 0.3 + 0.026 \times 2)}{6000 \times 0.3^3 + 4000 \times 0.3^3}$$

$$= 0.03588 \quad \text{MN (load per unit length)}$$

2 Calculation of max bending moments at centre and abutments for the initial mining situation of 15m headings

$$M_{centre\ (+ve)} = \frac{\omega S^2}{24} \qquad M_{abut\ (-ve)} = \frac{\omega S^2}{12}$$

$$= \frac{0.03588 \times 15^2}{24} \qquad = \frac{0.03588 \times 15^2}{12}$$

$$= 0.003364 \ \text{MN/m run} \qquad = 0.006728 \ \text{MN/m run}$$

3 Calculation of Pillar Factor C

$$C = \frac{3}{4}(1-\nu^2)\frac{E_p}{E_s}\left(\frac{A^4}{ht^3}\right)$$

$$= \frac{3}{4}(1-0.2^2)\frac{3000}{6000}\left(\frac{5.5^4}{1.3 \times 0.3^3}\right)$$

$$= 9385.27$$

4a Estimation of Multiplication Factor I from graph (Table 4.9)
(The pillaring system is regular therefore use R+ve and R-ve)

R +ve = 1.93 R -ve = 1.42

5a Estimation of Multiplication Factor II from graph (Table 4.9)
S/A = 15/5.5 = 0.273

R +ve = 1.06 R -ve = 0.97

6a Estimation of Multiplication Factor III from graph (Table 4.9)

$$\frac{x\ cut}{room\ span} = \frac{1.5}{1.5} = 1 \qquad MF\ III = 1$$

7a Calculation of maximum +ve and -ve bending moments in plate

Max mum +ve moment = $M_{cent} \times MF\ I \times MF\ II \times MF\ III$
= 0.003364 × 1.93 × 1.06 × 1
= 0.00688207

Maximum -ve moment = $M_{cent} \times MF\ I \times MF\ II \times MF\ III$
× 0.006728 × 1.42 × 0.97 × 1
= 0.009266

8a The maximum moment is -ve, thus the maximum tensile stress is -

$$\sigma_{tens} = \frac{6\ max\ -ve}{t^2} = \frac{6 \times 0.009266}{0.3^2}$$

$$= 0.6177 \ \text{MN/m}^2$$

9a The tensile strength of the rock is 5.0 MN/m²

$$\text{Factor of safety (FS)} = \frac{5.0}{0.6177} = 8.094$$

2b Calculation of maximum bending moments at centre and abutments for a 'robbed' situation where bords are 3.7m wide

$$M_{cent\ (+ve)} = \frac{0.03588 \times 3.7^2}{24} \qquad M_{abut\ (-ve)} = \frac{0.03588 \times 3.7^2}{12}$$

$$= 0.02047 \ \text{MN/m run} \qquad = 0.04093 \ \text{MN/m run}$$

3b Pillar Factor C

$$C = \frac{3}{4}(1-\nu^2)\frac{E_p}{E_s}\left(\frac{A^4}{ht^3}\right) = \frac{3}{4}(1-0.2^2)\frac{3000}{6000}\left(\frac{5.5^4}{1.3 \times 0.3^3}\right)$$

$$= 9355.27$$

4b Multiplication Factor I

R +ve = 1.93 R -ve = 1.42

5b Multiplication Factor II $\frac{S}{A} = \frac{3.7}{5.5} = 0.673$

R +ve = 0.94 R -ve = 1.07

6b Multiplication Factor III

$$\frac{x\ cut}{room\ span} = \frac{1.5}{3.7} = 0.405$$

R +ve = 0.85
R -ve = 0.63

7b Calculation of maximum +ve and -ve bending moments in plate

Max +ve moment = $M_{cent} \times MF\ I \times MF\ II \times MF\ III$
= 0.02047 × 1.93 × 0.94 × 0.85
= 0.03157

Max -ve moment = $M_{abut} \times MF\ I \times MF\ II \times MF\ III$
= 0.04093 × 1.42 × 1.07 × 0.63
= 0.039179

8b The greatest moment is -ve thus the maximum tensile stress is -

$$\sigma_{tens} = \frac{6\ max\ -ve}{t^2} = \frac{6 \times 0.039179}{0.3^2}$$

$$= 2.6119$$

8c The tensile strength of the rock is 5.0 MN/m²

$$FS = \frac{5.0}{2.6119} = 1.91 \quad \text{of original working width (FS)}$$

TABLE 4.10 CALCULATION OF THE POTENTIAL STABILITY OF THE IMMEDIATE ROOF OF THE BURNHOPE COLLIERY

top leaf, while the second was to estimate the stresses and stability after the second working, when the span of the working had increased. In the field, there was no evidence of extensive propping of the roof for the 'first working'. However, during the second working, sprogs had been extensively used between the top of the first leaf and the roof rock, in the robbed area of the pillar.

In the area considered, the geology of the immediate roof was simple. The roof was composed of a strong 0.3m thick bed of sandstone and Point Load Tests suggested that the compressive strength was of the order of 65 MN/m2. This would mean that the tensile strength would be approximately 5.0 MN/m2. The sandstone roof is overlain by thinly bedded siltstones.

The situation is a type D2 situation (Table 4.9) and the equation 4.5 indicates that a proportion of the weight of the siltstone would be borne by the sandstone roof. After calculating the weight per unit length, the maximum positive and negative bending moments are calculated using the theory of a clamped beam. Values for the Young's modulus and Poisson's ratio were not determined for the roof rocks, but appropriate values were obtained from the literature. From these and the measured dimensions of the pillars, rooms and crosscuts, the pillar function and influence function were calculated. Finally the total bending moment was evaluated and the maximum stress calculated.

The results are quite interesting and suggest that, prior to the pillar robbing, the roof was quite stable. However, the effect of the pillar robbing was to considerably reduce the factor of safety for the roof. In the field, the roof was observed to have collapsed in every room and crosscut examined, but had only partially collapsed in a heading which had been left 'whole', ie. in an area of the mine not robbed.

4.6. SUMMARY.

Quite stringent assumptions have to be made in order to use beam or plate theory, and it is extremely doubtful whether, in the case of old coal mines, these assumptions are met. Very few cases were seen where the roof of an old

working in coal was free from discontinuities. However, the study of beam theory is of value because it does provide a very good introduction to, and understanding of, some of the mechanisms that may be operating in a collapsing working. Specifically, it can be used to check whether in fact the sides of arches do behave and fail as cantilevers.

The main use for beam theory is limited to situations where the roof of the working is very competent. Although such situations appear to be rare in Coal Measure rocks, they are more common in other types of workings such as limestone and ironstone. In such a situation they could be particularly useful where only a thin beam separates incompetent rock or soil from the workings. Here, the question of the stability of the roof beam is the key to predicting collapse.

Conspicuous by its absence, in the foregoing text, is any mention of computer modelling. All the conditions and situations detailed above are ideal for analysis using finite element or finite difference techniques. An analysis using one of these techniques would undoubtedly be more accurate, and more flexible than the relationships presented above. At the start of the project, some finite element analyses were performed on typical old working geometries (Fig 4.3). However, it soon became apparent that some work had already been done in this field, (Stephansson, 1971, Barker and Hatt, 1973, Langland, 1978) and that anyway, the vast majority of old workings could not fulfil the stringent conditions assumed by such analyses, even if all the input parameters could be accurately obtained. For the smaller scale problems dealt with above, there is little point in running a highly sophisticated and accurate finite element program when, at the end of the day, a factor of safety of eight is applied to the result. This is especially true when a simple analysis can be carried out quickly with just the aid of a calculator. Barker and Hatt (1973) compared and found good agreement between, predicted values for the factor of safety of a mine roof obtained by a finite element analysis, and those obtained from the simple beam theory presented above.

One valid argument against the use of beam theories for analysing old workings is that they imply the roof of a working will collapse if the beam fails in

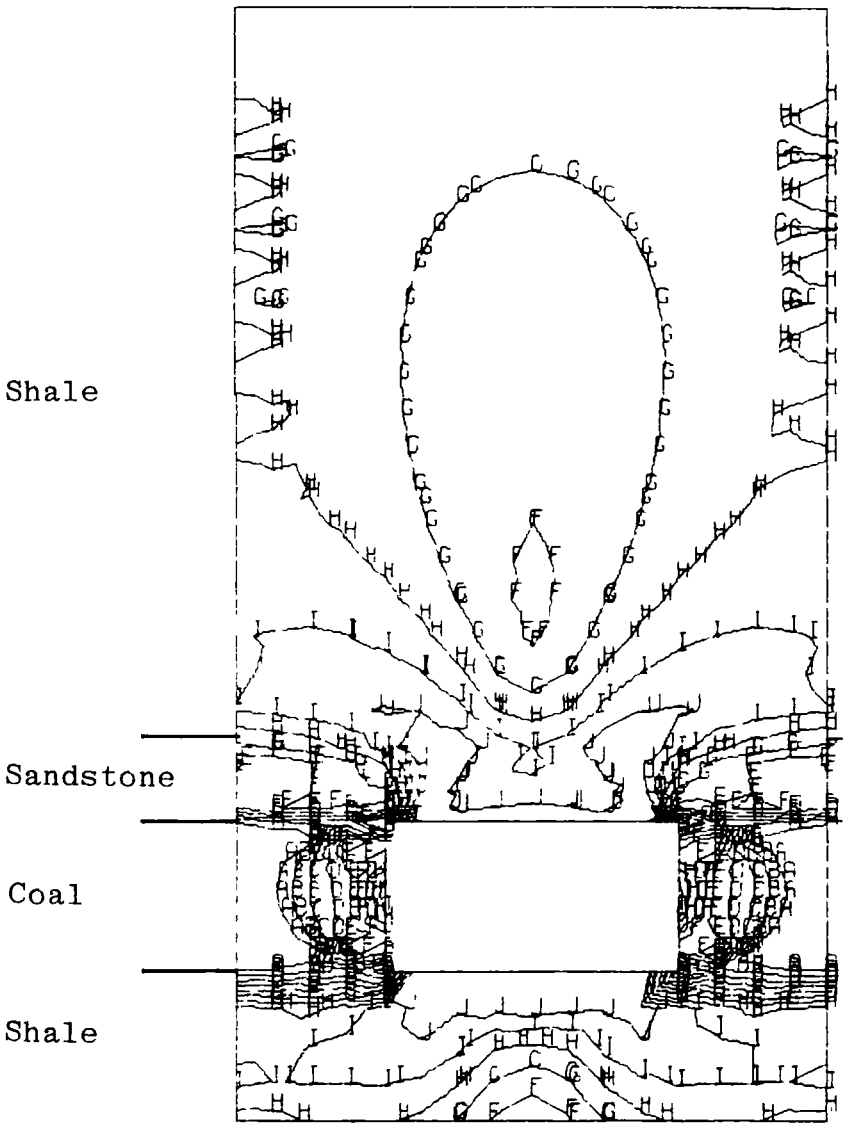

Rock	$\overset{*}{E}$ (MN/m^2)	(Mg/m^3)
Shale	200	2.65
Sandstone	400	2.60
Coal	150	1.36

* Typical E values ÷ 10

Figure 4.3 Stress distribution around a typical old working - finite element analysis

tension (See Wardell and Wood, 1965, as an example) . This is not necessarily the case; the stability of the cracked beam will depend on the inter-relationship of a number of factors. The solution of these factors opens up a completely new field of investigation based on the properties of a cracked or Voussoir beam. This subject is dealt with in the next Chapter.

CHAPTER 5

VOUSSOIR BEAM THEORY

5.1. INTRODUCTION

In the analysis of beams and plates (Chapter 4), it was assumed that the immediate roof of the opening was not cracked and could transmit tensile stresses. For a clamped beam, the theories predict that tensile failure, or cracking, will occur in the immediate roof above, or in the vicinity of the abutments. Once cracked, the roof will act as a simply supported beam and thus might crack once more at the mid span. In the context of simple beam theory, the beam has failed. However, the presence of vertical cracks in the roof does not necessarily mean that the roof will collapse (Plates 3 and 5).

The fact that a cracked beam restrained at its ends could stand safely without artificial support was first demonstrated with the aid of models by Bucky (1934). Later, Evans (1941), attempted an analytical solution of the problem and to describe the structures coined the term 'Voussoir beam', after the well-known masonry arches. Other investigators Wright (1972, 1973), Thorburn and Reid (1977), Potts et al. (1979), have used the terms linear arches or flat arches to describe such pseudo-beams, and the general analysis technique is now usually referred to as linear arch analysis (Wright, 1973).

The stability of a Voussoir beam relies on the presence of lateral forces to hold together the individual blocks which together comprise the roof beam. Such forces can be self-generated by the immediate roof. Take for example a simple situation of a roof cracked at the abutments and at the midspan. The composite beam will deflect downward due to slight rotation of the blocks about the abutment contacts. This generates thrust at the top of the blocks midspan, and at the bottom of the blocks at the abutments. Evans (1941) suggests that irrespective of how many blocks constitute the composite beam, the thrust will be transmitted between the edges of the blocks by a parabolic-shaped compression arch (Fig. 5.1) The thrust, stress and deflection of the Voussoir beam will be proportional to both the body weight of the beam, as well as any surcharge load

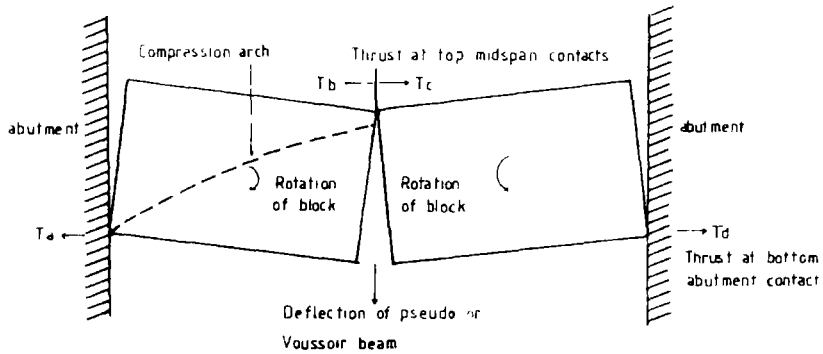

Thrust = Ta = Tb = Tc = Td

echanics of a Voussoir arch

Theoretical load transfer in a Voussoir beam

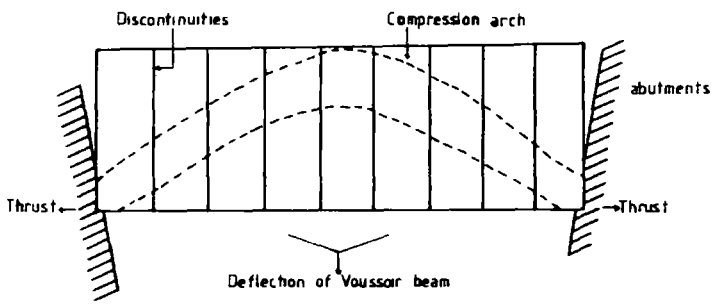

Figure 5.1 Mechanism of a Voussoir beam.

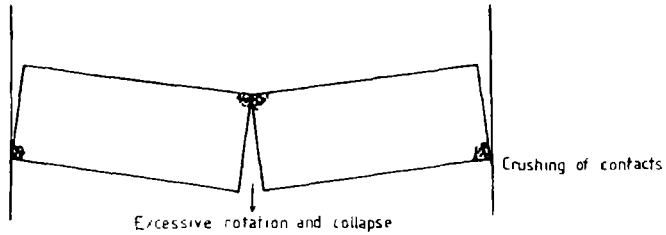

rushing

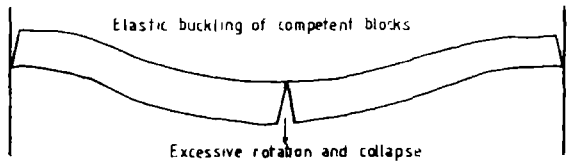

lastic buckling

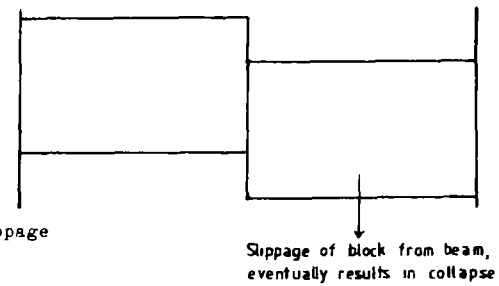

lippage

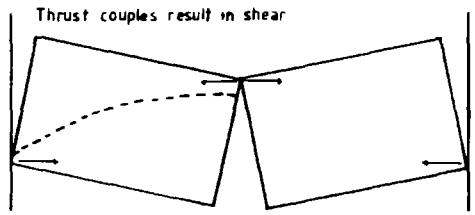

hear

Figure 5.2 Modes of failure for a Voussoir beam.

due to collapsed thinner layers that may load the beam from above.

5.2. MODE OF FAILURE OF VOUSSOIR BEAMS

5.2.1 INTRODUCTION

Four modes of failure for Voussoir beams have been recognised (Fig 5.2). These are:-

a. CRUSHING. If the interblock forces are sufficiently high crushing will occur at the block contacts. Crushing allows the beam to deflect, which in turn increases the forces acting on the contacts. If the contacts completely crush out, total collapse of the beam may occur and will be due to excessive rotation.

b. ELASTIC BUCKLING. If the blocks are long and thin, the pseudo-beam may be in-sufficiently rigid to resist deformation. In this case the blocks buckle, and collapse occurs due to excessive rotation of the beam.

c. SLIPPAGE. This can be due to one of two reasons. Either the coefficient of friction at the contacts or the lateral forces generated by rotation may be insufficient to prevent slippage of one or more blocks from the pseudo-beam. Complete collapse will occur when one of the component blocks slips out.

d. SHEAR FAILURE. may occur in through one of the blocks in the beam as a result of the thrust exerted at its contacts. The shear plane can either develop diagonally between the contacts and hence through the block, or along the bedding plane and parallel to the roof of the opening.

The mode of failure is controlled by the dimensions, and material properties of the blocks which make up the Voussoir beam. Failure can be by one, or any combination of the failure modes described above. In order to gauge the overall stability of the beam, it is necessary to assess, in turn, the factor of safety for each mode of failure.

In the remainder of this rather long chapter, sections have been devoted to each of the above modes of failure. However, to begin with, the basic equations are

developed to investigate the fundamental relationships between the contributions of the various authors.

In dealing with the modes of failure, greater space has been allocated to the first two failure mechanisms, namely crushing and elastic buckling. This is because it is in the analysis of these failure modes that the most contentious assumptions have and are made. In addition, recent work (Beer and Meek, 1982) has developed these areas to accommodate the analysis of 3-D Voussoir plates and dipping roof beams.

5.2.2. INITIAL ASSUMPTIONS

Many of the assumptions implicit in linear arch analysis are the same as those required for simple (ie continuous) beam theory. Some of the assumptions can be relaxed or accommodated at a later stage in the analysis and, where important, these are discussed in the relevant section. The basic assumptions used in linear arch analysis are:-

1. That the material comprising the roof and abutments is perfectly homogeneous, isotropic and linearly elastic.

2. The ground above the immediate roof is completely destressed in a direction normal to bedding

3. The rock mass has parted along smooth and frictionless bedding planes to form a series of beams or plates

4. The beam or plate consists of a tension-less type material, and the distribution of compressive stresses at the centre and abutment contacts is linear.

5. The beam or plate is still continuous with the adjacent strata, and no appreciable vertical displacement of the ends has occurred.

6. Any elastic strain of the abutments, under horizontal compressive stress, is negligible (ie. the abutments are rigid).

5.2.3 DERIVATION OF THE PRINCIPAL EQUATION.

The assessment of the stability of a mine roof by linear arch analysis was first attempted by Evans in 1941. He formulated the equations on which most of the later analysis are based. For the Voussoir beam to be statically determinant it is necessary to make some assumption concerning the length of contact over which the thrust operates at the abutment and midspan. From this, the moment or lever arm can be calculated, and it is this which is essential to the analysis. Evans (1941) assumed a length of contact between the blocks equivalent to half the block thickness (n = 0.5) The expression for the bending moment due to the weight of the beam is given by Evans (1941) (Fig 5.3) as:-

$$\frac{1}{8} w S^2 t$$

or

$$\frac{Q S}{8}$$

where:-
w= unit wt. of beam plus any surcharge
S= span of beam
t= thickness of beam
Q= wSt = wt of beam

Evans (1941) suggested that the overall moment of resistance of the beam M, had three components:-

$$M = M1 + M2 + M3$$

where M1= small moment due to simple bending of the beam

$$M1 = T \times \frac{nt}{6} \qquad (T = \text{thrust})$$

M2= larger moment induced by the thrust acting over the initial moment arm Z where:-

$$Z = t\left(1 - \frac{2n}{3}\right)$$

Thus:-

$$M2 = T \times Z$$

$$= T \times t\left(1 - \frac{2n}{3}\right)$$

M3 is a small moment induced at each end of the beam because the centre of thrust does not coincide with the centre of the area under compression

$$M3 = T \times \frac{nt}{6}$$

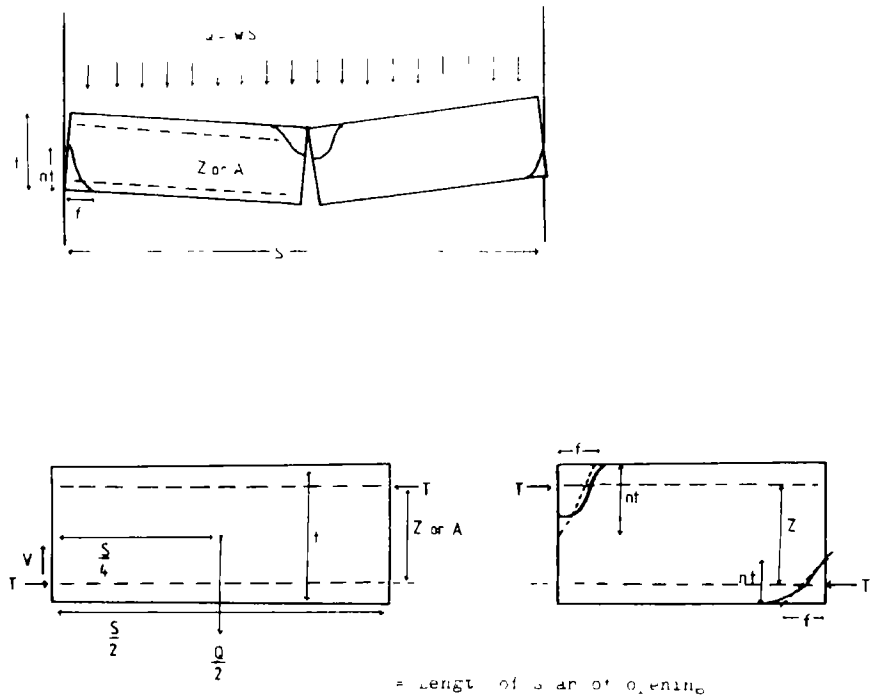

= Length of a bar of opening

t = Thickness of block

T = Thrust acting on block

nt = Area of block over which thrust is acting

Q = Total weight of unstable blocks

ρ = density of block

g = Acceleration due to gravity

f = Maximum compressive stress

—— = Actual stress distribution

---- = Assumed stress distribution

z = Moment arm between thrust centroids

Figure 5.3 Nomenclature of the Voussoir beam.

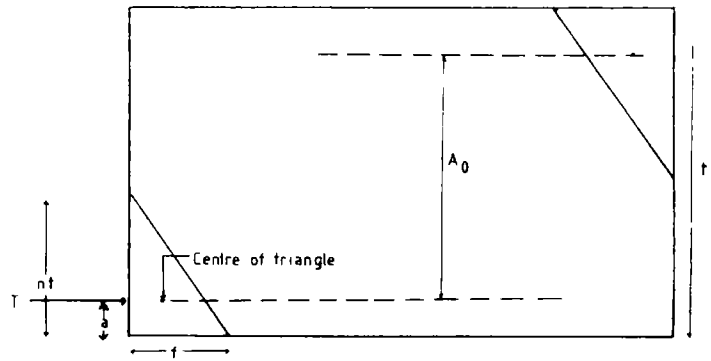

f = Horizontal compressive stress

nt = Fraction of beam thickness under horizontal compressive stress

a = I/3 nt Distance from beam surface at which Thrust operates

Figure 5.4 The relationship between thrust and stress in a Voussoir beam.

Thus:-

$$M = M1 + M2 + M3$$

$$= T\left(t\left(1 - \frac{2n}{3} \right) + 2\left(\frac{nt}{6} \right) \right)$$

$$= T \times t\left(1 - \frac{n}{3} \right)$$

$$= T \times R$$

where:-

$$R = t\left(1 - \frac{n}{3} \right) \quad \text{.....(Eq 5.1)}$$

= theoretical moment or lever arm

Thus, equating the bending moment to the total moment of resistance gives:-

$$\frac{Q\,S}{8} = T\,R \quad \text{.....(Eq 5.2)}$$

This is the fundamental equation for the stability of the Voussoir beam, and is repeatedly referred back to throughout the forthcoming analysis.

By simple rearrangement of this equation the thrust T in the system can be obtained.

$$T = \frac{Q\,S}{8\,R}$$

If the thrust can be found so to can:

a) The stress at the contacts. If the stress exceeds the strength of the material, crushing will take place.

b) The frictional resistance against slippage of the blocks

c) The resistance to shear. The thrust acts as a couple, therefore the shear stresses can be calculated.

Thus, the basic equation can be used to solve three of four modes of failure for a Voussoir beam, and is used as the basis for the fourth, the analysis of elastic buckling.

5.2.4 THEORETICAL PROBLEMS WITH THE ANALYSIS

a. INTRODUCTION OF VARIABLE MOMENT ARMS

While simple in concept, the theory is not quite as straight forward as initially presented. Evans (1941) recognised that at the contacts with the abutments and neighbouring blocks, the internal stress distribution for a block would be complex. However, he (and all later investigators), assumed that the shape of the distribution could be approximated to a triangle. Both Wright and Mirza (1963), and Wright (1972), using photoelastic and finite element techniques respectively, showed that this assumption was in fact fair (see Figs. 5.5 & 5.6)

However, these investigations also showed that the length of contact, or the area of the block over which the thrust operated, was considerably less than the half the block thickness (n= 0.5) that Evans (1941) had taken as being a reasonable contact area. These authors thus proved that the contact length was much less, and so the maximum stress at the contact was correspondingly much greater than hitherto assumed. Furthermore, they showed that the length of contact was dependent on the aspect ratio of the blocks. It has already been shown that the contact length affects the 'effective moment or lever arm' of the system (Chapter 5.2.3), therefore without a realistic value for n, analysis of the Voussoir beam, theoretically at least, is once more insoluble.

Wright (1972, 1973) overcame this problem by using a series of physical tests and finite element runs to determine the relationship between the contact length and aspect ratio for a series of beams. He fitted an empirical equation to these data, thus side-stepping the theory and directly relating the moment arm to the span to thickness ratio of the beam being analysed. He called this theoretically derived moment arm A, so that it was not confused with the equivalent moment arm R derived theoretically by Evans (1941).

Potts et al. (1979) in a similar analysis also overcame the problem by deriving empirical equations to fit experimental data. However, Beer and Meek (1982) in an analysis very similar to that of Evans (1941) states: 'The value of n is

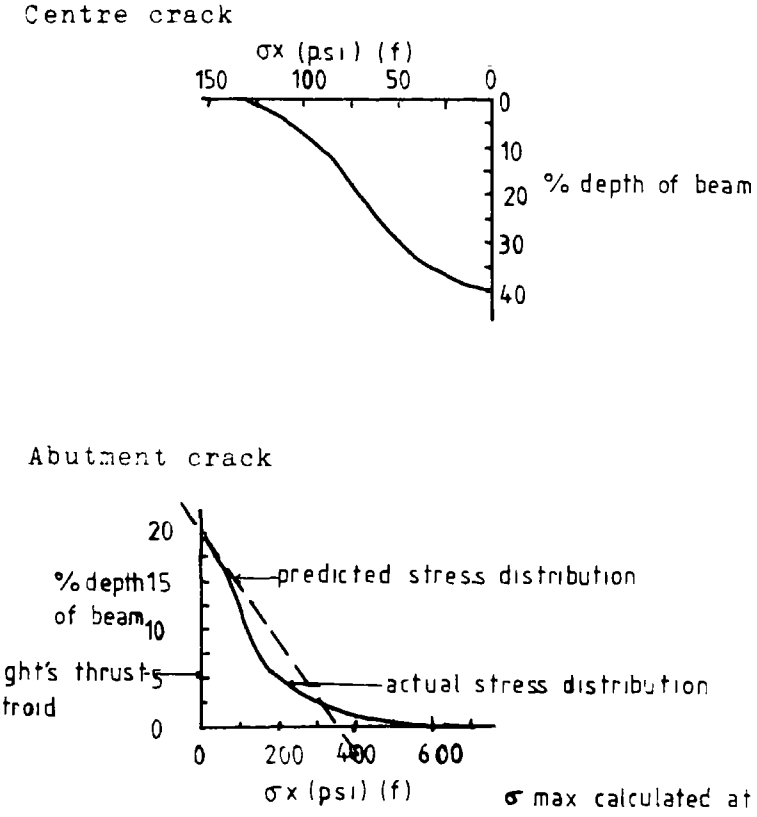

Figure 5.5 Distribution of horizontal compressive stress on centre and abutment cracks for a span: thickness ratio of 4.

Q = 22.975 E = 1 x 10^6 p.s.i.

Potts range was fro' 4-24, position varied with s:t ratio. Centroid of t icker beams nearer bear centre. As bear failed centroid osition migrated towards centre. Thrust centroid at abutment between 6-18, beam depth.

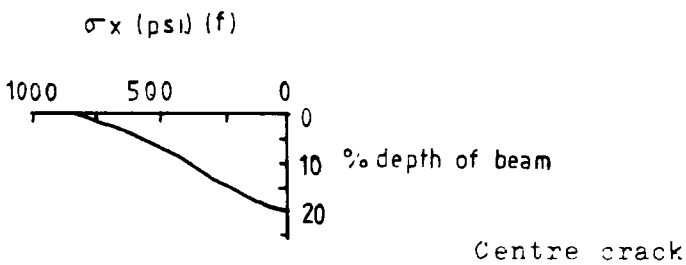

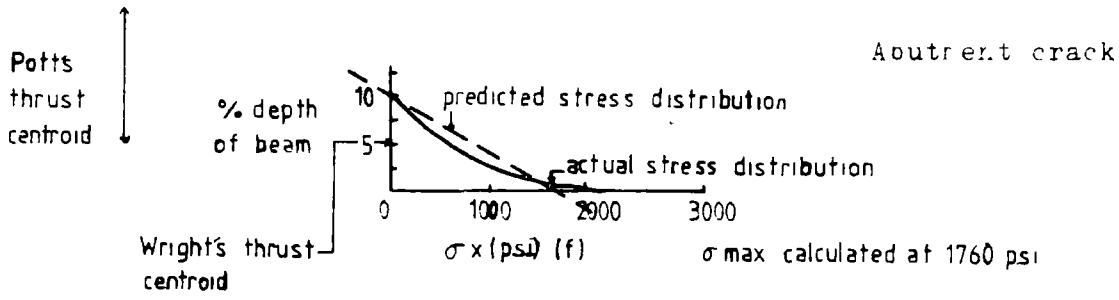

Figure 5.6 Distribution of horizontal compressive stress on centre and abutment cracks for a span: thickness ratio of 24.

Q = 47.172 E = 1 x 10^6 p.s.i.

determined in an iterative way within the computer program and it is not necessary to assume a contact length a priory'. Unfortunately he makes no comment on how 'n' is derived, or what parameter is used to define it. In addition he simplified the relationship for the moment of resistance and omitted the M1 and M3 components included by Evans (1941) (Chapter 5.2.3). Thus for the analysis of Beer and Meek (1982):-

$$R \simeq Z = t\left(1 - \frac{2n}{3}\right)$$

To summarise the situation therefore:-

R = moment of resistance (Evans, 1941)

Z = height of moment arm ($Z \simeq R$ according to Beer and Meek, 1982)

A = height of moment arm ($A = Z \simeq R$ according to Wright, 1972)

(cf. Evans, 1941, Eq. 5.1 Chapter 5.3.1(d))

In addition to the problem of the length of the moment arm, Wright (1972) also made a number of pertinent observations. He noted that while the total moment is readily calculated, other critical parameters such as the location of the centre of the moment arm and the shape of the horizontal stress distribution within the block cannot be theoretically obtained. Furthermore, as the load Q increases and the centre of the beam rotates down, the moment arm A or Z can be expected to decrease and to cause the thrust T to increase more rapidly than the increase in load. He concluded that:-

'An analytical solution to the forces and stresses acting in a cracked beam was attempted but could not be solved without prior simplifying assumptions which, it was felt, were more apt to be wrong than right'.

As a result of his detailed investigations Wright (1972) fitted empirical equations to all the data he had gathered and thus presented a comprehensive suite of equations that could be used, with some confidence, for the analysis of Voussoir beams.

Beer and Meek (1982) recognised that the original theory of Evans (1941) was fundamentally sound, but that some of the initial assumptions were wrong. He ignored the comments made by Wright (1972) and developed the original theory of Evans (1941) to accommodate dipping beds. In addition he extended the analysis into three dimensions and the analysis of slabs and plates by using the concept of yield lines from structural concrete design.

What we have, therefore are three techniques for the analysis of a Voussoir beam:-

1. The theoretical approach of Evans (1941) and Beer and Meek (1982), which, though fundamentally sound, gives the wrong answers because a number of the assumptions made are incorrect.

2. The empirical approach of Wright (1972, 1973) which, although lean on theory, gives the correct results.

3. A second empirical approach by Potts et al. (1979) which is specific to coal measure rocks ('Minestone' of Potts et al., 1979) and has less of a theoretical basis than the analysis of Wright.

In the remaining sections of this chapter the present writer has attempted to unify all three approaches by using the empirical relationships, derived from the laboratory tests of Wright (1972) and Potts et al. (1979) to correct the assumptions which are the source of the inaccuracies in the theoretical approach of Evans (1941) and Beer and Meek (1982). By doing this it is hoped that one can have more confidence when extending the theoretical analysis to deal with the dipping beds and three-dimensional problems of Beer and Meek (1982).

b. INTRODUCTION OF ELASTIC DEFORMATION

Up to this point Voussoir beam analysis has only been considered from the viewpoint of rigid block mechanics. The thrust generated in the system is directly proportional to the rotation of the blocks. This deflection has two sources:

1). Inelastic deformation - resulting from the absorption by the system of the space between blocks in the beam or abutment; abutment yield (inelastic).

2). Elastic deformation - due to the deformation of the blocks or abutment ; abutment yield (elastic)

Elastic deformation shortens the span of the Voussoir arch, thus increasing the thrust. Therefore, an idea of the stress distribution within the beam is needed to make an assessment of the effect of elastic shortening on the arch.

5.2.5 SUMMARY

In summary, to reconcile empirical and theoretical approaches to the problem, it is necessary to identify those areas in the theory where incorrect assumptions have been made. These areas are:-

(a) The shape of the stress distribution within the blocks at the contacts.
(b) The position of the thrust centroids at the contacts.
(c) The location of the centre of the moment arm.
(d) The length of the moment arm (and indirectly the value of n).
(e) The distribution of stress within the beam.

These are dealt with later in the Chapter, but as the solution to these problems is heavily dependent on the original work of Evans (1941), Beer and Meek (1982), and Wright (1972, 1973), it would seem appropriate first to briefly outline the similarities and differences in their approach to the analysis.

5.3 ANALYSIS FOR CRUSHING AND ELASTIC BUCKLING - TWO DIMENSIONAL ANALYSIS

In the following Sections Voussoir beams are treated as two dimensional problems. The third dimension of the beam, depth, is assumed to be of unit length, and to play no part in the stability of the system. In practical terms, this is not as restrictive an assumption as may at first sight appear and many mine roofs can be successfully analysed using two dimensional theory.

Throughout the remainder of this Chapter only the simplest form of a Voussoir

beam is considered. This is because Wright (1972) found, from his experiments on models, that the worst configuration was when the beam was cracked in only three places; at the two abutments and at midspan. This observation was confirmed by some results from finite element analyses in which he compared a simple 3 crack Voussoir beam with a Voussoir beam cracked in 21 places. The results showed that even though the thrust in the multi-cracked beam was 8% higher, the deflection 12% higher and the moment arm 7% shorter, the area of abutment contact was almost 55% larger than for a simple Voussoir model. The much larger area of contact exhibited by the multi-cracked beam, means that the stresses at the abutment contact are considerably lower than for an equivalent 3 crack Voussoir beam and hence the probability of failure by crushing or elastic buckling is greatest for a simple 3 crack Voussoir beam.

5.3.1. THE ANALYSIS TECHNIQUE

a. INTRODUCTION

In outline the calculation sequences for the two main analysis techniques (ie those of Evans and Wright) are very similar. However, there is a difference in approach. The calculation sequence of Evans (1941) and Beer and Meek (1982) are worked from the start in terms of stress whereas Wright (1972, 1973) operates in terms of thrust, and only calculates stresses at the end of the calculation sequence. A comparison of the calculation sequences is presented in Table 5.1, and the analysis techniques are presented in greater detail later in the Chapter.

b THE RELATIONSHIP BETWEEN THRUST AND STRESS IN A VOUSSOIR BEAM

The thrust can be considered to act through the centre of gravity of the area of maximum stress. Thus, assuming a triangular stress distribution the thrust will act through a point 1/3 of the distance from the edge of the beam (Fig 5.4)

The basic equation relating thrust to stress for this situation is:-

(see Fig. 5.4)

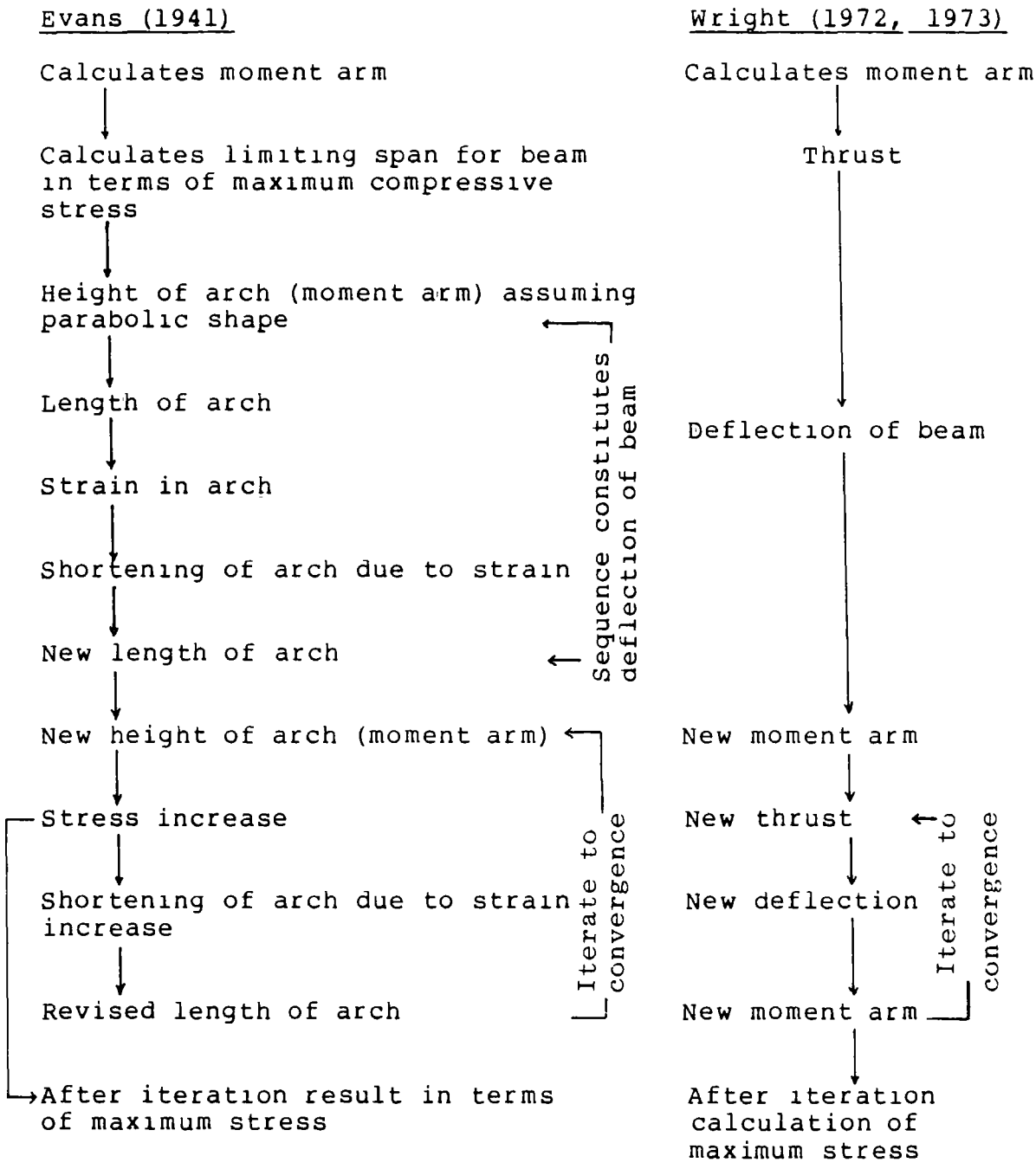

TABLE 5.1

COMPARISON OF ANALYSIS TECHNIQUES PRESENTED BY EVANS (1941) and WRIGHT (1972, 1973)

$$T = \frac{f\ n\ t}{2}$$

where:-
f = horizontal compressive stress
n x t = fraction of beam thickness (t) under horizontal compressive stress
a = 1/3 n x t distance from beam surface at which thrust operates

Re-arranging this equation gives:-

$$f = \frac{2\ T}{n\ t}$$ (Evans, 1941 and Beer and Meek, 1982)

$$f = \frac{2\ T}{3\ a}$$ (Wright, 1972)

$$f \simeq \frac{2\ T}{t - A}$$ (Wright, 1973)

A = height of moment arm

Each of these equations relating thrust to stress have been used in previous analysis as indicated.

c. ANALYSIS TECHNIQUE OF EVANS (1941)

A detailed derivation of the analysis technique of Evans (1941) is beyond the scope of this chapter. As a result the calculation sequence , as applied to a practical problem, is detailed below (see Appendix 2 for example). The reader is directed to the original paper for further explanation of the derivation of any of the equations used.

Maximum bending moment

$$\frac{w\ S^2\ t}{8}$$

where:-
w = unit weight of beam + surcharge
S = span of beam
p = density of beam
g = acceleration due to gravity
t = thickness of block
T = thrust = (f/2) x nt
f = maximum stress
n t = depth of section under horizontal compression
R = 'effective moment arm'=t(1 - n/3)
Subscripts 0,1,2 etc. refer to cycle in iteration sequence.

Maximum moment of resistance

$$M = T \times R$$

$$= f\ t \left(\frac{2}{2} - \frac{n}{6} - \frac{n^2}{2} \right)$$

$$= 5/24\ f\ t^2$$ (when n = 0.5 (used by Evans))

Equating bending moments due to the weight of the beam to the moment of resistance:-

$$\frac{w S^2 t}{8} = f t^2 \left(\frac{n}{2} - \frac{n^2}{6} \right)$$

(This is the basic equation Eq 5.2 but in terms of stress not thrust)

Thus the initial span length of the beam (S) is:-

$$S = \left(\frac{8 f t^2 (n/2 - n^2/6)}{w} \right)^{1/2}$$

Under the assumption that the weight of the structure is supported through the development of a parabola-shaped arch within the blocks (Fig. 5.1), then the Initial height of arch (Z) or the 'distance between the thrust centroids' is:-

$$Z = \left(1 - \frac{2n}{3} \right) \times t$$

Thus the initial length of arch (L) is:-

$$L = S + \frac{8 Z^2}{3 S}$$

The mean strain within the beam is:-

$$\frac{11 f}{24 E}$$

Therefore the total linear strain (X) is:-

X = length of arch x mean strain

$$= \left(S + \frac{8 Z^2}{3 S} \right) \frac{11 f}{24 E} \quad \ldots\ldots\ldots\ldots\ldots\ldots\ldots\ldots\ldots\ldots \text{(Eq. 5.3)}$$

Thus the revised length of arch (due to strain shortening) is (Ll = L - X)

$$Ll = S + \frac{8 Z^2}{3 S} - \left(S + \frac{8 Z^2}{3 S} \right) \frac{11 f}{24 E}$$

And the revised height of arch (because the length has changed, Z1) is :-

$$Z1 = \left(\frac{3\,S}{8} (L1 - S) \right)^{1/2}$$

If Z1 is approximately the same as Z, then the blocks are effectively rigid and the analysis is complete. However, if $Z1 \neq Z$, the increased rotation of the blocks will increase the thrust which will increase the elastic strain. Therefore, the procedure is restarted using the new parameters and iterated in this fashion until convergence is obtained.

Hence, when $Z1 \neq Z$, the stress increase at the contacts (f1) is:-

$$f1 = \frac{Z}{Z1}$$

The revised total linear strain within the beam (X1) is:-

$$X1 = X \times f1$$

$$= L \frac{11f \times f1}{24\,E}$$

The second revised length of the arch (L2) is:-

$$L2 = l - X1$$

and the second revised height of the arch (or moment arm, Z2) is:-

$$Z2 = \left(\frac{3\,S}{8} (L2 - S) \right)^{1/2}$$

If $Z2 \neq Z1$ iteration continues, thus the stress increase at the abutments is:-

$$f2 = Z1 / Z2$$

$$X2 = X \times f2$$

$$L3 = L - X2$$

$$Z3 = \left(\frac{3\,S}{8} (L3 - S) \right)^{1/2}$$

- and so on - to convergence (usually within 2-3 cycles)

d. ANALYSIS TECHNIQUE OF BEER AND MEEK (1982)

The analysis technique of Beer and Meek (1982) is very similar to that of Evans (1941) outlined above. It does however, differ in three respects.

(a). The most important difference is that unlike Evans (1941), Beer and Meek (1982) do not assume a contact length between the block and the abutment in the calculation, but leave the term n as a variable. Unfortunately they do not define the term n in their paper, but state that it is arrived at iteratively within a computer program. However, no clue is given as to how this is achieved, and it is questioned whether it can be derived 'iteratively'.

(b) Secondly, in their derivation of the moment of resistance they omit the effects of the M1 and M3 components. This leaves the main component of the moment of resistance (M2) as:-

$$M2 = t\left(1 - \frac{2n}{3}\right)$$

This is in fact the height between the thrust centroids which in the Evans (1941) solution was separately defined as Z (Chapter 5.2.3).

This simplification has also been made by Wright (1972, 1973) and does in fact simplify the calculations considerably. An attempt was made by the present writer to incorporate the M1 and M3 components of the moment of resistance into the analysis but it was found that the problems created were much greater than the problems solved, and the attempt was abandoned.

(c). The third difference lies in the number of iterations that the sequence can progress through. The analysis of Beer and Meek (1982) allows for only a single iteration. In other words there is no successive correction of the thrust due to elastic shortening in the beam after the initial correction. In the examples tried by the present author using the original equations of Evans (1941), this limitation would appear to make only a marginal difference. The exception would be in the analysis of very elastic beams, and further comment will be made on this topic later (Chapter 5.3.2 e).

e. ANALYSIS TECHNIQUE OF WRIGHT

In his two papers Wright (1972, 1973) presents what at first sight appears to be two sets of equations for the analysis of Voussoir beams. In fact there are only minor differences, with the 1973 paper being a simplified version of the 1972 analysis. In the 1972 paper the equations were normalised with respect to the thickness and Young's modules of the beam. In addition, terms were included to analyse for an initial axial force or ground pressure. To facilitate comparison with the theoretical approach of Evans (1941) and Beer and Meek (1982), the equations have been simplified by removing the term for axial force, and are presented as unique solutions rather than in the original normalised version used by Wright (1972). Differences between the 1972 and 1973 analysis techniques are discussed later in Chapter 5.3.2 d, as are the extensions of the equations to include axial pressures (Chapter 5.3.3 c).

THE CALCULATION SEQUENCE OF WRIGHT (1972)

CALCULATION OF MOMENT ARM

$$Ao = 0.72 \left(\frac{S}{t}\right)^{0.08} \times t$$

where:-

S = span of beam
t = thickness of beam
A = length of moment arm
T = thrust
Q = wt. of beam plus any surcharge
p = density
g = acceleration due gravity
E = Young's modulus
Subscripts 0,1,2 etc. refer to iteration number.

CALCULATION OF THRUST

$$To = \frac{Q\ S}{8\ Ao} \quad \text{(as Eq 5.2)}$$

DEFLECTION OF THE BEAM

$$do = \frac{1.2\ Ao\ S^{1.78}\ T}{t^{2.78}\ E}$$

NEW HEIGHT OF MOMENT ARM (recalculated because of beam deflection)

$$A1 = Ao - do$$

NEW THRUST (because moment arm changed)

$$T1 = \frac{Q\ S}{8\ A1}$$

NEW DEFLECTION (because thrust changed)

$$dl = \frac{1.2\ Ao\ S^{1.78}\ T1}{t^{2.78}\ E}$$

If 'dl' is not approximately equal to 'do', then the iteration continues thus:-

NEW HEIGHT OF MOMENT ARM

$$A2 = Ao - dl$$

NEW THRUST

$$T2 = \frac{Q\ S}{8\ A2}$$

NEW DEFLECTION

$$d2 = \frac{1.2\ Ao\ S^{1.78}\ T2}{t^{2.78}\ E}$$

The iteration is continued until the desired convergence is obtained (n.th iteration). The position of the thrust centroid at the abutment contact is then determined from:

$$a = 0.294\ (t-An)$$

The maximum stress at the abutment contact (σ max) can be calculated:-

$$\sigma \text{ max} = \frac{2\ T}{3\ a}$$

f. SUMMARY

To aid comparison and comprehension of the analytical techniques outlined above, an example is given in Appendix 2 which has been solved by the equations of both Evans (1941) and Wright (1972).

5.3.2. SOLUTION OF PROBLEMS

A comparison of the results produced by the different analysis techniques (Appendix 2) shows the extent of the error in the theoretical solution of Evans (1941). Wright claims that his 1972 analysis can calculate the thrust to within 3%, the deflection of the beam to within 18% and the stress to within 30%. The stress calculated by the Evans solution is less than a quarter of that predicted by Wright.

It has already been suggested that some of this error can be attributed to the assumptions that both Evans (1941), and to a certain extent Beer and Meek (1982) have had to make in their analysis. The problem areas were outlined previously (Chapter 5.2.5), but are repeated here for convenience. They are:-

a) the shape of the stress distribution of the contacts.
b) the position of the thrust centroid
c) The position of the centre of the moment arm
d) The length of the moment arm
e) The stress distribution within the blocks.

In the following section each of these problem areas are dealt with in turn.

a) THE SHAPE OF THE STRESS DISTRIBUTION AT THE CONTACTS

Figures 5.5 & 5.6 (after Wright, 1972) show the typical distribution of the horizontal compressive stress (σX), within a beam cracked vertically in the centre and at the two abutments. Wright showed that the shape of the stress distribution at the abutment and centre contacts was not triangular but nearly approximated a triangular shape, particularly in beams with a high span to depth ratio (See Fig. 5.5 & 5.6). Both the shape and the values predicted by the relationship of Wright (1972) can be seen to approximate reasonably well to the theoretically obtained values.

b) THE POSITION OF THE THRUST CENTROID

The thrust acts through the centre of the stressed area. Hence, under the assumption of a triangular stress distribution, the position of the thrust

centroid will be one third of the contact distance from the edge of the beam. The position of the thrust centroid as calculated by Wright is shown in Figures 5.5 and 5.6.

Measurements by Potts et al. (1979) on physical models with a span to thickness ratio (s:t) ranging from 4 to 24, showed that for a given s:t ratio, the position of the abutment thrust centroid remained remarkably constant until just before failure. As failure approached, the position of the thrust centroid tended to move towards the centre of the beam. Results from the tests suggested that the actual position of the abutment thrust centroid varied with the s:t ratio of the beam, ranging from 6 to 17% of the beam depth from the loaded edge. They noted that, in general, the thicker beams had the thrust centroid further into the depth of the beam than with thinner beams.

These observations are predicted by Wright's (1972) equations, but the position of the thrust centroid (Figs. 5.5 and 5.6), calculated using his equations, lies towards the lower bound of the range observed by Potts et al. (1979). This suggests that the stresses predicted by Wright for the abutment crack will be slightly higher than those observed by the other authors.

c) THE POSITION OF THE CENTRE OF THE MOMENT ARM

Wright (1972) showed that for a simple Voussoir beam, the stresses at the abutment contact were always higher than at the centre contact. This observation was made during both the finite element and physical modelling. However, in contrast, Potts et al. (1979) found that the stresses were highest at the centre crack, and that failure always took place by crushing at this point.

The apparent contradictory evidence could be explained by the method of loading used by the two research groups. Wright (1972) used 'body loading' to generate the stress distributions for his finite element analysis (The loading system that would occur in a natural environment). For his physical modelling however, he loaded the beams from above using a distributed load. Potts et al. (1979) on the other hand, devised a new loading system for their model experiments. They used a pressurised oil-filled tube which was in constant contact with the beam,

to load the beam from below thus bending the beam upwards against gravity. This loading system has the disadvantage in that as the tube expands it will try to force the entire beam vertically upwards.

Which ever loading system is considered the most natural, both investigators noted that the stresses are greater at one contact than at the other. However, by definition the thrust must be the same for each contact, thus the area of the two contacts must be different. Hence, the position of the centre of the moment arm (ie. the midpoint of the distance between the thrust centroids) will not coincide with the centre of the beam. Both Evans (1941) and Beer and Meek (1982) failed to recognise this, and their analyses assume that the centre of the moment arm does coincide with the centre of the beam.

Wright found from his experiments that the position of the thrust centroid (a) at the abutment could be approximated by:-

$$a = 0.294\ (t-A)$$

t = thickness
A = length of moment arm.

Using this relationship, and under the assumption of a triangular stress distribution at the contacts, the area of contact represented by C (Fig. 5.7) can be derived for the respective contacts as follows: (Subscripts a and c refer to abutment and centre contacts respectively).

$$Ca = 3 \times 0.294\ (t-A) = 0.882\ (t-A)$$

$$Cc = 3 \times 0.706\ (t-A) - 2.118\ (t-A)$$

Thus, the ratio of the area of contact at the abutment to the area of contact at the centre crack is equal to:-

$$\frac{Cc}{Ca} = 1 : 2.40136$$

This suggests that the area of the centre contact is just over 2.4 times that of the abutment contact area. In making this calculation it is not necessary to know the position of the centre of the moment arm, only that the area of

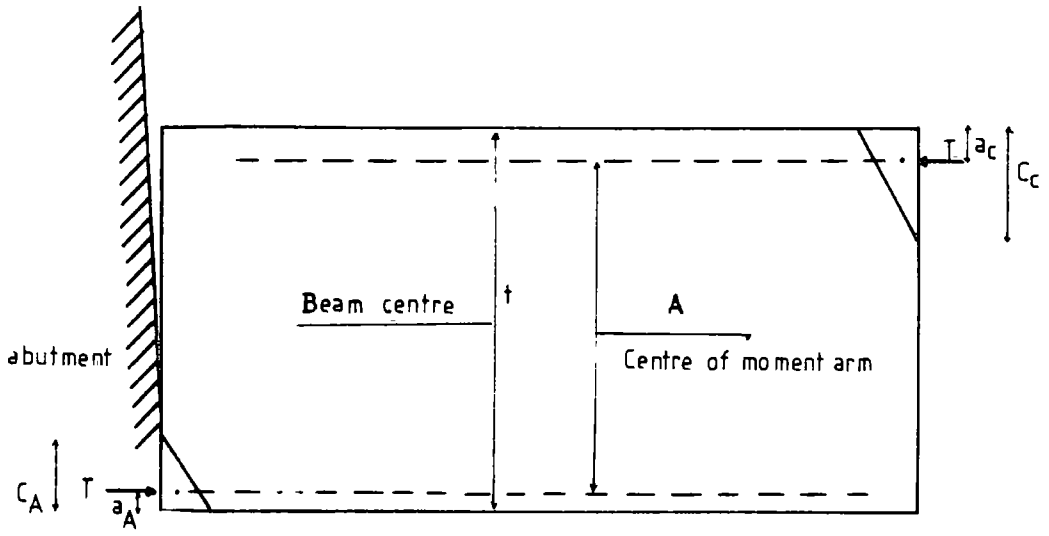

$$a_A = 0.294\ (t - A)$$

$$a_c = 1 - 0.294\ (t - A)$$

$$= 0.706\ (t - A)$$

Figure 5.7 The position of the centre of the Moment arm 'A'.

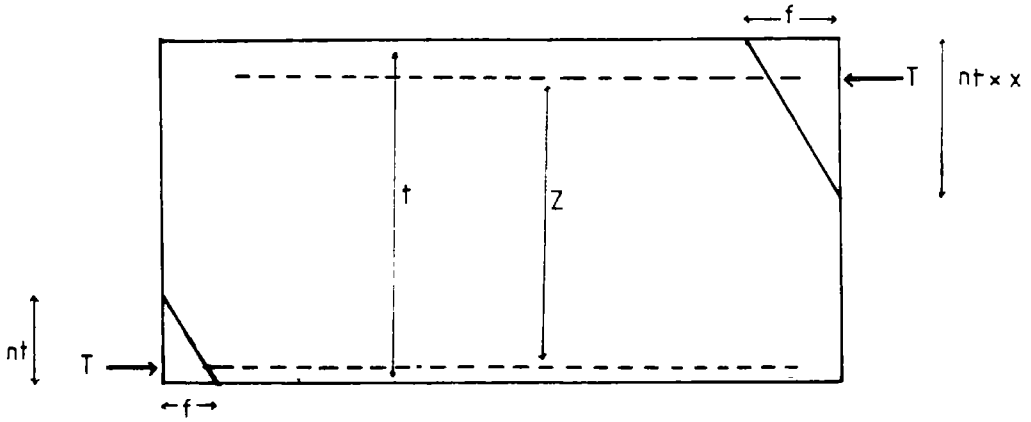

$$Z = t - \left(\frac{1}{3} nt + \left(\frac{1}{3} nt \times X \right) \right)$$

Figure 5.8 Revised nomenclature for a Voussoir beam.

contacts are different, and that the asymmetry, or Y as it shall be termed, has a value of 2.4

d) LENGTH OF THE MOMENT ARM.

Evans (1941) assumed that there was no asymmetry in the stress distribution and defined the area of contact at both abutment and centre cracks to be equal to n x beam thickness, where n = 0.5. If however, the distance between the thrust centroids or moment arm (height of arch) is redefined to include the Y term to account for asymmetry (compare Fig 5.8 with Fig 5.3), the following equation is obtained:

$$Z = t - \left(\frac{1}{3} n t + \left(\frac{1}{3} n t Y \right) \right)$$

substituting the values for Y obtained above into this relationship gives:-

$$Z = t-(1/3\ nt + (1/3nt \times 2.40136))$$
$$Z = t-(1.133787\ nt)$$
$$= t\ (1-1.133787n) \quad \text{.....(Eq 5.4)}$$

Wright (1972) found that (empirically) A had the following value:-

$$A = 0.72 \left(\frac{s}{t} \right)^{0.08} t$$

Since it has been shown that A = Z (Chapter 5.2.4) then equating these values gives:-

$$0.72 \left(\frac{s}{t} \right)^{0.08} t = t - 1.133787\ n\ t$$

Therefore:-

$$n = \frac{t - 0.72\ (s/t)^{0.08}\ t}{1.133787\ t}$$

or $$n = 0.882 - 0.63504\ (s/t)^{0.08} \quad \text{.....(Eq 5.5)}$$

Thus the term (n), which was previously given a nominal value of 0.5 by Evans (1941), has now been assigned an empirical value derived from the tests made by Wright (1972). This value will vary depending on the aspect ratio of the beam. To illustrate the difference between the values predicted by the different authors for the length of the moment arm A or Z, a beam with a span to thickness ratio of 12. (ie t = 1, s = 12) is considered. The difference between the

original relationship of Evans (1941), and the equation of Wright (1972) who it should be remembered, claims to predict the moment arm to within 3% is significant. Thus:-

EVANS (1941) predicts:-

$$Z = t\left(1 - \frac{2n}{3}\right)$$

$$= t \times 2/3$$
$$= 0.667 \text{ units}$$

while Wright (1972) predicts

$$A = 0.72 \left(\frac{s}{t}\right)^{0.08} t$$

= 0.878 Units - a difference of 24% between the two approaches.

If the newly derived relationships discussed above are used for the same beam example then:-

$$n = 0.882 - 0.63504 \left(\frac{s}{t}\right)^{0.08} \qquad \text{(see Eq 5.5)}$$

Thus substituting the appropriate values into the above equation gives an empirically derived value for n of:-

$$n = 0.1073$$

Using the relationship derived above Eq 5.4 , the length of the moment arm or arch height (taking asymmetry into account) is:-

$$Z = t(1 - 1.133787\ n)$$

substituting in the value for n obtained above gives:-

$$Z = 0.878$$

Thus, the same length of moment arm is obtained by this technique as was obtained using the equations of Wright (1972) These new relationships, derived by the present writer, can thus be used to predict both the moment arm and also the stress, at the abutment contact, to the same level of accuracy as obtained by Wright (1972). The advantage these new relationships offer is that the empirical accuracy levels can now be obtained within the theoretical analysis of Evans (1941) and Beer and Meek (1982).

1. THE CHOICE OF EQUATIONS FOR DETERMINING THE LENGTH OF THE MOMENT ARM A.

Before leaving the question of calculating the length of the moment arm, it is germane to consider an alternative relationship for A given by Wright (1973). In his original, and most detailed paper, Wright (1972) quotes the following relationship for A:-

$$A = 0.72 \left(\frac{S}{t}\right)^{0.08} t \quad \ldots\ldots\ldots \quad (1972)$$

In the 1973 paper A has a different value namely:-

$$A = 0.91\, t - \frac{0.44\, t^2}{S}$$

Table 5.2 shows values for A calculated using both of the expressions proposed by Wright. The results suggest that there is little difference between the two equations. However, Table 5.3 shows values for n recalculated from the two A equations. This relationship is plotted in Figure 5.9. The data shows that over a range of s:t ratios from 4 to 12 there is little to choose between the two equations. However, at the lower s:t ranges, the 1972 relationship fits the data better than the 1973 relationship, while beyond a s:t ratio of about 15, the 1973 relationship provides a better approximation. On balance therefore, the 1972 formulation would appear to be the most useful equation.

The change in the area of contact with the s:t ratio is clearly displayed by Figure 5.9. It will be remembered that the thrust centroid is located at 1/3 n and that Potts et.al. (1979) noted that the thrust centroid for thicker beams, (ie beams with a lower s:t ratio), had the thrust centroid closer to the beam centre. That is the 1/3 n value was larger. This trend can be seen in the graph (Fig 5.9).

It is also of interest to note that the calculated n values are a long way from the value of 0.5 used by Evans (1941) in his analysis.

e) STRESS DISTRIBUTION WITHIN THE BLOCKS

At this point it is necessary to return to the theoretical treatment of Evans

$\frac{S}{t}$	A_{72}	A_{73}
1	0.72	0.47
2	0.76	0.69
3	0.78	0.76
4	0.80	0.80
5	0.82	0.82
6	0.83	0.84
7	0.84	0.85
8	0.85	0.86
9	0.86	0.86
10	0.87	0.87
11	0.87	0.87
12	0.88	0.87
15	0.89	0.88
20	0.92	0.89

TABLE 5.2

VARIATION IN 'A' VALUES FOR DIFFERENT SPAN:THICKNESS RATIOS

$\frac{S}{t}$	1972 Equation A	1973 Equation B
1	0.247	0.467
2	0.211	0.273
3	0.188	0.209
4	0.172	0.176
5	0.160	0.157
6	0.149	0.144
7	0.140	0.134
8	0.132	0.128
9	0.125	0.123
10	0.119	0.118
11	0.113	0.115
12	0.107	0.111
15	0.093	0.105
20	0.075	0.099

Equation A = $n = 0.882 - 0.63504 \left(\frac{S}{t}\right)^{0.008}$

Equation B = $n = 0.07938 + 0.38808 \left(\frac{1}{S/t}\right)$

TABLE 5.3

VARIATION IN 'n' VALUES PREDICTED BY EQUATIONS OF WRIGHT

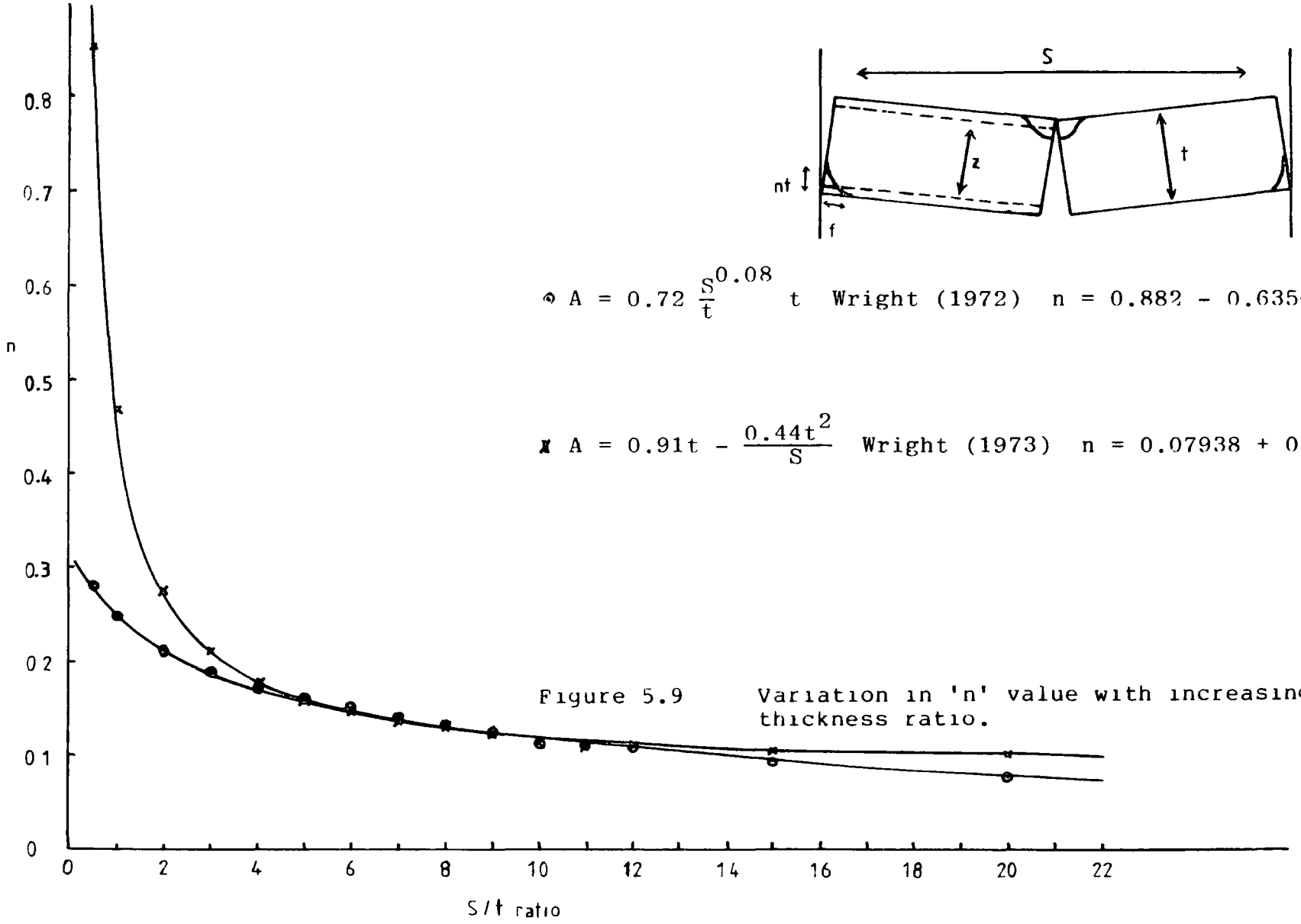

○ $A = 0.72 \left(\frac{S}{t}\right)^{0.08} t$ Wright (1972) $n = 0.882 - 0.63504 \left(\frac{S}{t}\right)^{0.08}$

✖ $A = 0.91t - \frac{0.44t^2}{S}$ Wright (1973) $n = 0.07938 + 0.38808 \frac{1}{S/t}$

Figure 5.9 Variation in 'n' value with increasing span: thickness ratio.

(1941) and Beer and Meek (1982). Both give equations for the total linear strain (X) in the system as:

$$X = S \frac{11\ f}{24\ E}$$

Where;- S = span length
f = compressive stress
E = Young's modulus

Evans (1941) considered that the average stress across the length of the arch would be equal to about half the maximum compressive stress, ie 11/24 f. However, in the calculation sequence, the much higher stress levels predicted by the new equations means that the shortening due to strain increases proportionally. This in turn increases the thrust which results once more in an increase in the strain. In a short time, the iteration sequence within the analysis of Wright (1973) and Beer and Meek (1982) becomes numerically unstable and the results given by the theoretical solutions begin to diverge rapidly from the empirical solutions of Wright. In physical terms, the blocks in the theoretical solution of Evans (1941) and Beer and Meek (1982) are failing by elastic buckling, while the blocks of the empirical solution of Wright are reaching equilibrium.

This could be the reason why Beer and Meek (1982) restricted their analysis to a single iteration cycle. By reducing the value for n but keeping the average stress the same, the threshold for elastic buckling is depressed. In these circumstances eliminating the iteration cycle will crudely remove the instability problem however, it does not cure the source of the problem. Unfortunately, it is impossible to make a definitive judgement on this matter, without some measure of the n values used by Beer and Meek (1982).

Figure 5.10. shows the distribution of compressive stress in a cracked beam with a s:t ratio of 12. The 1972 equation of Wright predicts a maximum compressive stress at the abutment contact of 1252 psi (8.63 MN/m2). 11/24 's of this value is 574 psi (3.95 MN/m2), but a study of the stress distribution in Figure 5.10 shows that as an average value this is obviously far too high. Measurements from the stress distribution across the length of the arch (Fig. 5.10) gave an average stress level of about 134.7 psi (0.928 MN/m2). As no

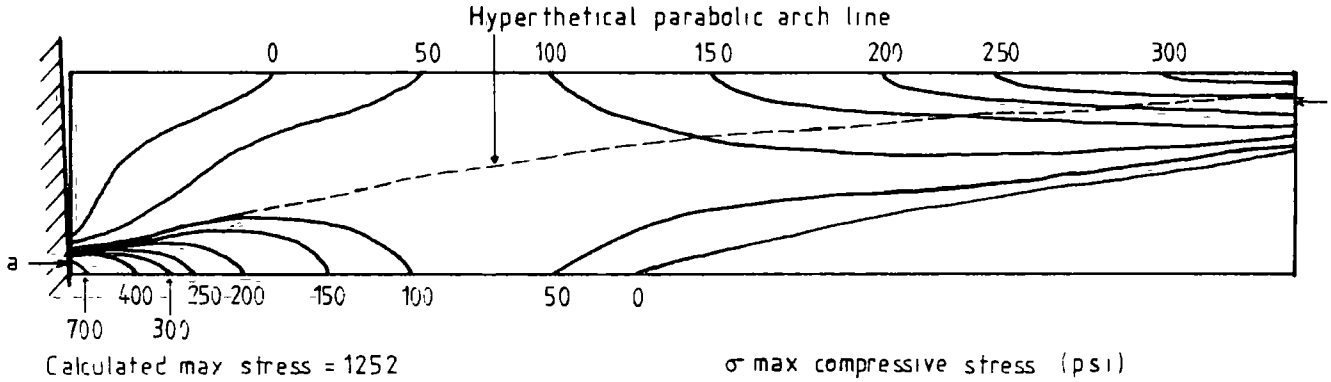

Contours of equal maximum compressive stress in a cracked beam with a b:t ratio of 12, and with $\nu = 4.92 \cdot 5_{psi}$ E = 1 x 10^{-6} psi. Note areas of no compressive stress at the bottom right and top left corners of the beam.

Average stress along parabolic arch line = 154.8 psi.

Figure 5.10 Stress distribution within one element of a Voussoir beam (after Wright 1972).

contour values over 700 psi (4.826 MN/m2) were plotted on the original diagram, this will be an underestimate of the true value.

The difference between 574 PSI and 135 PSI (3.95, 0.928 MN/m2), for the average stress across the beam, is too great a difference to ignore, and thus the average stress of 11/24 the maximum compressive stress proposed by Evans (1941) is obviously incorrect.

It will be recalled that Wright (1972) found that the empirical equation for the deflection of the beam was:-

$$d = \frac{1.2\,A\,S^{1.78}\,T}{t^{2.78}\,E}$$

This was found to fit the data to within 18%. Buried within this equation is the average stress distribution along the arch for a beam. By suitable rearrangement of the equation of Evans (1941), the revised height of the arch or the revised moment arm Z, (ie. the length of the moment arm after the first iteration) is:-

$$Z = \left(\frac{3S}{8} \left(\frac{8Z^2}{3S} - \left(S + \frac{8Z^2}{3S} \right) \times \frac{11 \times 2T}{24\,E\,n\,t} \right) \right)^{1/2}$$

If k is substituted in the equation for the average compressive stress term (11/24), then the equation may be written as follows:-

$$Z = \left(Z^2 - \frac{3S\,T\,k}{4\,E\,n\,t} + \frac{2Z^2\,k\,T}{E\,n\,t} \right)^{1/2}$$

According to Wright (1972) however, the revised height of the arch or revised moment arm Al is:-

$$Al = Ao - d \qquad d = \text{deflection of beam}$$

$$= Ao - \frac{1.2\,Ao\,S^{1.78}\,T}{t^{2.278}\,E}$$

Thus equating the relationships of Wright (1972) and Evans (1941) (Al = Z1) we obtain:-

$$Ao - \frac{1.2\,Ao\,S^{1.78}\,T^{2}}{t^{2.78}\,E} = \left(Z^{2} - \frac{3\,S^{2}\,T^{2}\,k}{4\,E\,n\,t} + \frac{2\,Z^{2}\,k\,T^{2}}{E\,n\,T^{2}}\right)^{1/2}$$

and solving for k one obtains:

$$k = \frac{4\,E\,n\,t\,(M^{2} - Z^{2})}{T^{2}\,(8\,Z^{2} - 3\,S^{2})}$$

where:-

$$M = \left(Ao - \frac{1.2\,Ao\,S^{1.78}\,T^{2}}{t^{2.78}\,E}\right)$$

k= expression for average stress distribution along arch line in a Voussoir beam.
M is infact equivalent to the last iteration for A (the new height of the moment arm, see Appendix 2)

The average stress distribution coefficient k can now be related to the span to thickness ratio of the beam in question. Once more the empirical relationships of Wright (1972) have been used to correct the errors in the original theory of Evans (1941).

As a check, the solution is applied to the problem in hand Appendix 2. It has already been shown from the analysis of Wright (1972) that;-

T2 = 847.062 psi (5.84 MN/m2)
A3 = M = 10.46558 inches (0.2658m)

L = 144 inches (3.675m)
t = 12 inches (0.3048m)
E = 1 x 10 psi (6895 MN/m2)
Q = 492.5 lb. (223.4 Kg)

Using the requisite equations: (Eq 5.5 and Eq 5.4 respectively)

$$n = 0.882 - 0.63504\left(\frac{S}{t}\right)^{0.08}$$

$$= 0.107296$$

$$Z = t - (1.133787nt)$$
$$= 10.54018501$$

$$k = \frac{4Ent\,(M^{2} - Z^{2})}{T^{2}\,(8Z^{2} - 3S^{2})}$$

$$= 0.1554$$
$$K = 1/6.44$$

The measured value for k from Figure 5.10 is;-

$$k \text{ measured} = \frac{\text{Average compressive stress (measured)}}{\text{Max. compressive stress (calculated)}}$$

$$k \text{ measured} = \frac{134.8}{1252}$$

$$= 0.10767$$

Thus:-

$$k \text{ measured} = \frac{1}{9.29}$$

This value is sufficiently close to the calculated value (1/6.5) to confirm the accuracy of the equations. As pointed out above, the measured value for the average compressive stress will be an underestimate because no contour values above 700 p.s.i. were evaluated.

Using the relationship derived above various values of k have been calculated for a range of S:t ratios. Table 5.4 shows the relationship between the aspect ratio and K.

TABLE 5.4. APPROXIMATE CHANGE IN AVERAGE STRESS LEVELS (k) WITH INCREASING S:t ASPECT RATIO.

S:t ratio	1/k
2:1	1.4689
4:1	3.3886
6:1	4.7336
12:1	6.5290

This relationship is plotted in Figure 5.11 and shows the change in average beam stress with increasing S:t ratios.

i. TRANSITION ZONE BETWEEN SHEAR AND CRUSHING OR ELASTIC BUCKLING.

From their model studies Potts et al. (1979) made the observation that a

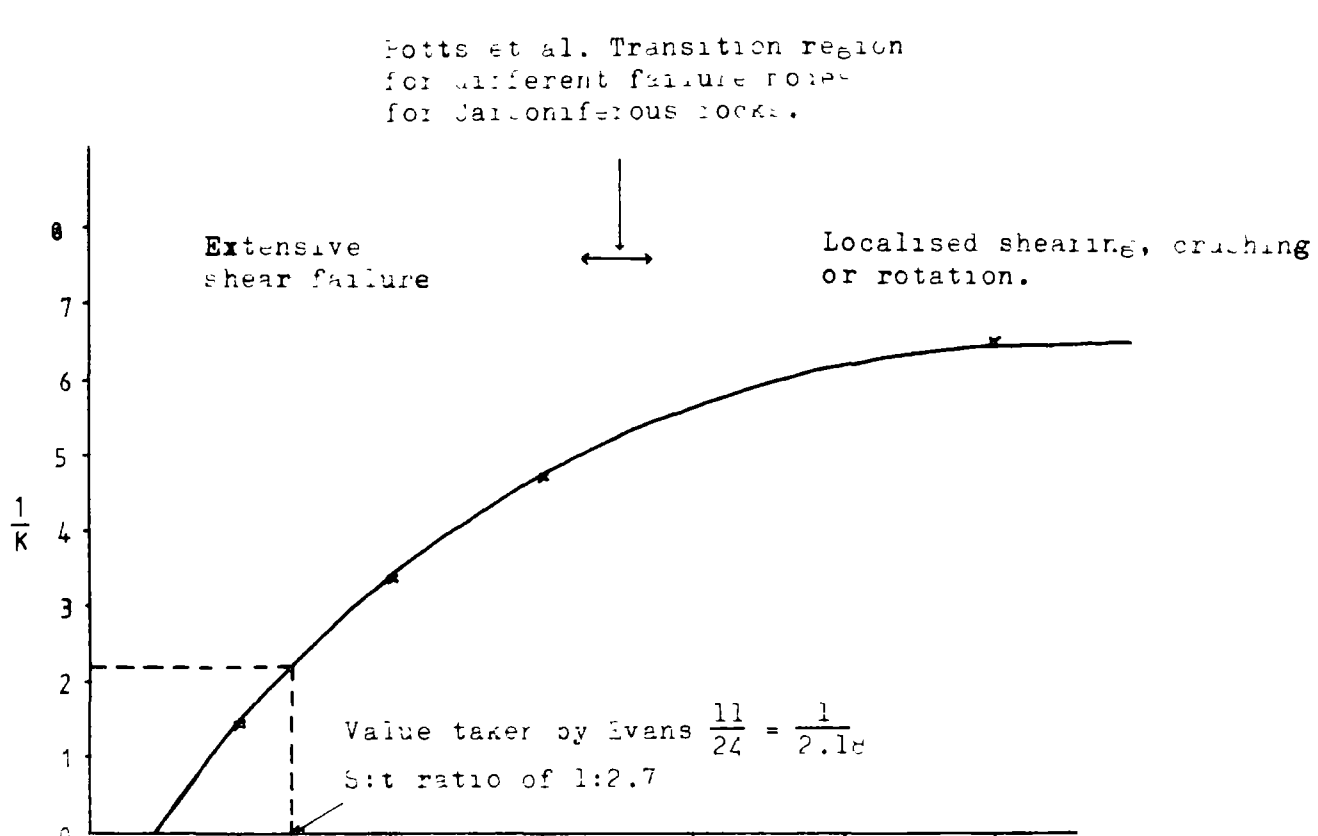

Figure 5.11 Distribution of average stress in a beam as a function of the maximum compressive stress at the abutment contact for different span: thickness ratios.

thicker beam is under a much higher average stress than a thinner beam. They concluded that beams with low s:t ratios were more likely to fail in shear than by crushing of the contacts and defined a transition zone between shear and crushing for Carboniferous mine roof rocks ('minestone' of Potts et al., 1979) at a S:t ratio of between 6.5 to 7.5. They suggested that beams thicker than these values generally failed by shear whereas, thinner beams (ie beams with a higher S:t ratio) failed by either crushing or elastic buckling.

Obviously the transition zone depends on the ratio of the horizontal shear strength to the uniaxial compressive strength. For example the transition zone for a homogeneous sandstone would be expected to be depressed towards a smaller S:t ratio; ie, thicker sandstone beams would resist shear better than say siltstone beams. However, a well-bedded shale would have the transition zone displaced towards the larger S:t ratios.

Qualitatively the k value used by the present writer is a useful parameter for defining the transition point between shear and crushing. However, quantitatively anisotropy in the shear and compressive strength of the rock complicate the problem, and as the degree of anisotropy increases the analysis progressively looses validity. This is because the average stress distribution equation used to derive k assumes that the material is homogeneous and isotropic.

ii. TRANSITION ZONE BETWEEN SHEAR OR CRUSHING AND ELASTIC BUCKLING

Wright (1972) found from his experiments that the onset of elastic buckling occurred when the measured deflection[6] of the beam was approximately equal to between 16% to 19% of the beam thickness. He therefore, suggested that the danger point would occur at a deflection value of 14% of the beam thickness. Thus, when the δ:t ratio is greater than about 0.14 the beam will probably fail by elastic buckling. In these circumstances the thrust equation will progressively loose validity. With δ:t values less than about 0.14 the beam will be stable or if it does fail will fail by either shear or crushing of the contacts.

5.3.3 FURTHER DEVELOPMENT OF VOUSSOIR BEAM THEORY

a. ELASTIC STRAIN IN THE ABUTMENTS

Until now, the abutments of the Voussoir beam have been considered to be rigid. Evans (1941) suggested a method by which elastic deformation in the abutments could be included into the analysis. He assumed that the stresses in the abutments produced, from the thrust of the Voussoirs, reduced to zero at a distance into the abutment equal to the beam span. He suggested that the average stress in the abutment rocks was equal to 1/8 the maximum calculated contact stress and observed that by using this simplification it was possible to calculate the total elastic strain, or yield, of the abutment. The value for E chosen for the abutment rock will however, not be the same as that used for the beam material. For the abutments it is assumed that the material is constrained in a direction at right angles to the applied thrust and in this situation the E value equals:- (Morley, 1953).

$$Er = Ef \frac{m\,(m-1)}{(m-2)\,(m+1)}$$

where:-

v = Poisson's ratio
m = Poisson's number
Ef = E(free conditions)
Er = E(restrained)

Assuming a value for m equal to 4 ie v = 0.25

$$Er = 1.2\,Ef$$

As

$$E = \frac{\text{stress}}{\text{strain}}$$

The strain in the system is:-

$$\text{strain (e)} = \frac{f}{8 \times 1.2\,E}$$

The total yield in the abutments (remembering that there are two) is therefore given by:-

$$X = e \times S$$

$$= \frac{f \times S}{4.8\,E}$$

In its effect on the arch, this yield may be treated as an additional strain in

the length of the arch, and thus can be added to the X value previously obtained for the elastic shortening of the beam (Eq 5.3).

i. CAUTIONARY NOTE

Extreme care should be taken if abutment deformation is used in the analysis, as the relationship is heavily dependent on the 'average' stress in the abutment rocks. Further work should be done to assess the validity of the 1/8 f assumption made by Evans (1941).

b. EFFECT OF GROUND STRAINS DUE TO LONGWALL WORKING ON A VOUSSOIR BEAM

i. INTRODUCTION

There are many documented cases of old workings collapsing as a result of the extraction of a deep underlying coal seam by longwall methods. Voussoir beams are particularly susceptible to horizontal ground strains, and it should be possible to assess the effect that a subsidence trough might have on a Voussoir beam.

The horizontal ground strains, due to longwall working vary depending on the position of the longwall workings in relation to the surface or horizon of old workings. A typical subsidence wave resulting from the advance of a panel, consists initially of a zone of extension which reaches a peak value when the panel is beneath the structure. This zone is followed by a zone of compression as the panel passes beyond the structure. The general value of the ground strains are predictable, and are related to both the size of the panel as well as the thickness and depth of the worked seam NCB (1975). Subsidence strains are generally expressed in terms of a change in length of a piece of ground. Usually this is presented as millimetres of shortening, or extension, per metre of ground or structure.

ii. EFFECT OF EXTENSION

A Voussoir beam will be effected by a subsidence wave in one of two ways.

Firstly as the zone of extension approaches, the distance between the abutments will increase and, as a result, the beam will deflect more. This deflection may lead to an increase in thrust which in turn may be sufficient to promote failure in one of the ways described elsewhere (Chapter 5.2.1).

This effect can be analysed in the Modified Evans solution by treating the ground strain as a additional shortening of the arch length. If the value for E+ (positive extension) is added to the value for the elastic shortening in the beam (X) (Eq 5.3), the increase in thrust, and hence the effect on the stability of the beam, can be found.

iii. EFFECT OF COMPRESSION

When a longwall panel passes beneath a Voussoir beam, the ground strains will reverse and become compressive. The effect of compression on a Voussoir will be to further increase the thrust at the contacts. This is because the beam will be unable to deflect back (ie. upwards) into its initial position to counteract the shortening of the distance between the abutments.

The quantitative effect of this is more difficult to predict, but may be approximated by:-

$$\text{Increase in stress} = \frac{E}{\text{strain}}$$

This increase in stress will need to be added to the appropriate value for the stress at the contact. It may promote failure by crushing, elastic buckling or block shear.

iv. STRAIN CONCENTRATION

A Voussoir beam has been shown to be particularly susceptible to the effects of a subsidence wave. The analysis assumes that the ground strain experienced by the structure will be proportional to its length. However, in reality it is quite possible that a much larger proportion of the ground strain will be absorbed by a Voussoir beam. In an area of pillar and stall workings, the

ground strain for the opening plus the ground strain appropriate to the thickness of the pillar may well have to be accommodated by the Voussoir. It is even feasible that the strain for an entire area may be absorbed by one or two suitably located old workings. The effect of such strain concentrations are difficult to anticipate. Thus caution should be employed when using the relationships derived above.

c. INCLUSION OF AXIAL FORCES INTO VOUSSOIR BEAM ANALYSIS

Until now, only the simplified versions of the empirical equations derived by Wright (1972, 1973), have been used in the analysis. However, he also included in his original equations terms to account for any axial or horizontal forces that may be present in the ground prior to collapse.

The full version of his equations are presented below. These can be used to analyse Voussoir beams also subjected to axial loads.

$$Tp = \frac{Pt}{4A} + \left(\frac{P^2 (8A^2 - 4At + t^2)}{8A^2} + \frac{QS(QS - 4Pt)}{64A^2} \right)^{1/2}$$

The equation for the deflection (d) of a beam under axial load is:-

$$d = \frac{PS^2}{16t^2 E} + \frac{1.78}{2.78} \frac{1.2AS}{t E} \left(T^2 + P^2 - 2TP \frac{0.23P^2 S^{0.22} t^{0.78}}{A} + \frac{0.23PT^2 S^{0.22} t^{0.78}}{A} \right)^{1/2}$$

Where:- t = thickness of beam
T = horizontal thrust per unit width
Q = total weight of beam per unit width
P = initial or prior axial force on beam per unit width
E = Young's Modulus
A = Length of lever arm
S = Span of beam

These equations are only valid for an axially loaded beam in which the transverse load Q, is sufficiently large to maintain the cracks open. In this situation T will be greater than P. However, if the transverse load Q is not sufficiently great, the Voussoirs will be clamped together by the horizontal

force P and the beam will behave as a beam column. The formulae given for 'simple beams' under axial load (Chapter 4) can be used to test whether the vertical load (Q) is sufficient to open the tensile fractures and cracks. If the load is sufficient then the use of the above equations is valid.

Care should be exercised in using these equations in very high axial stress situations, as Wright (1973) only guarantees their accuracy for low stress environments.

5.3.4 Summary

Using the empirical corrections to the theory that have been evolved in the foregoing sections, it is now possible to use the analytical technique of Evans (1941) to derive the maximum stress in a Voussoir beam to the same degree of accuracy as that predicted by Wright (1972). It is pertinent to recall at this point the reason for correcting the theoretical approach.

Until now, the methods have been limited to the analysis of two-dimensional Voussoir beams, that is beams that are infinitely long compared to their span. Beer and Meek (1982) using the concept of yield lines from structural reinforced concrete design, extended the theoretical approach to cover the solution of Voussoir beams in three-dimensions. The present writer has drawn attention to and suggested corrections to a number of errors overlooked by both Evans (1941) and Beer and Meek (1982) in the theory for the two-dimensional case. The analysis is therefore, now in a position where it can be extended into three-dimensions with greater confidence than previously possible. This opens up the possibility of analysing Voussoir beams of finite length. Furthermore, it is now a simple step to a accommodate into both two and three dimensions the effects of dipping rather than purely horizontal strata.

5.4. ANALYSIS FOR CRUSHING AND ELASTIC BUCKLING - THREE-DIMENSIONAL ANALYSIS

5.4.1. SQUARE PLATES

The extension of Voussoir beam analysis into three dimensions involves the

modification of the two-dimensional relationships to cater for the extra dimension of length. The basic equations are very similar. Throughout the forthcoming analysis of Voussoir plates, it is assumed that tension cracks will have developed in the positions shown in Figure 5.12. Under these assumptions the relationship for moment equilibrium, which is the basic equation of the Voussoir analysis, is given by Beer and Meek(1982) as:-

$$\frac{w S t^2}{4} \times \frac{1}{6} = T \times Z$$

where:- T = thrust = $\frac{f n t}{2}$

Q = weight of beam = $p S g t$

w = unit wt. of beam

t = beam thickness

S = beam span

p = density

g = acceleration (gravity)

f = max. compressive stress

Z = height of moment arm

By rearranging the equation:-

$$\frac{Q S}{8} \times \frac{1}{3} = T Z \qquad \text{.....(Eq 5.6)}$$

A comparison between this equation (5.6) and the equivalent equation for the two-dimensional solution (Eq 5.1), will show that the left hand side of the 3-D equation is one third of the value derived for the two-dimensional solution. Further derivation of the design formulae is identical to the original theory of Evans (1941) except where the change in length of the arch is computed. At this point the analysis must take into account the fact that the stress is biaxial instead of uniaxial.

For 3-D analysis
the elastic shortening is given by:-

where, v = Poisson's ratio and the other terms are as before.

$$X = k \frac{S}{E} S (1-v) \qquad \text{.....(Eq 5.7)}$$

5.4.2. RECTANGULAR PLATES

The theory for rectangular plates is slightly more complex than that presented for square plates. This is mainly due to the problems associated with the positioning of the cracks. The analysis starts with the calculation of the pattern of yield lines (ie tensile failures) in the plate. Distance X (Fig

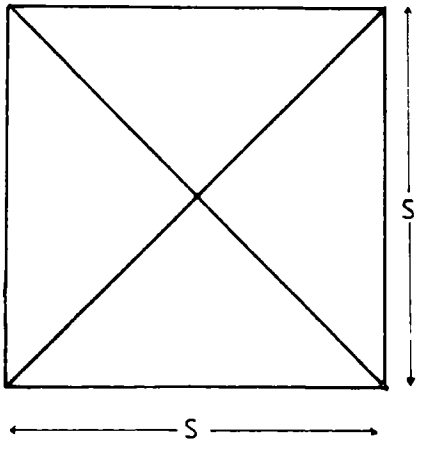

Figure 5.12 Assumed yield lines for square panel.

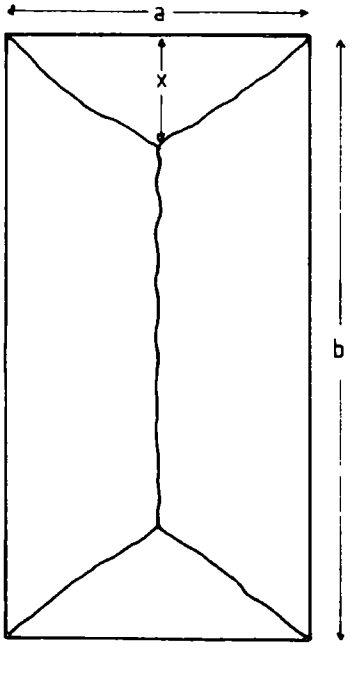

Figure 5.13 Assumed yield lines for a rectangular panel.

5.13) is of particular importance in this respect, and is given by Beer and Meek (1982) as:-

$$X = \frac{a}{2}\left(\left(R^2 + 3\right)^{1/2} - R\right)$$

where, R = a/b. ie the ratio of short span to long span.

Once the value for X has been found, the expression for the basic equation for a trapezoidal panel becomes, (Beer and Meek, 1982):-

$$w\,t\,a^2\left(\frac{1}{8} - \frac{1}{6}\frac{X}{a}R\right) = T\,Z \qquad \text{(cf. 2-D equation 5.1)}$$

As before, the remaining equations are derived in a similar way to those of the 2-D situation except that the equation for elastic shortening is now modified by the aspect ratio of the plate (R), Thus:-

$$X = K\left(\frac{f}{E}L(1-VR)\right) \qquad \text{.....(Eq 5.8)}$$

When the plate is square, that is when K = 1, the above equation reduces to the one given previously (Eq. 5.3).

Further investigation of the equation for a trapezoidal panel leads to an estimate of how long the panel needs to be for the solution to reduce to that of a two dimensional Voussoir beam.

For a three-dimensional rectangular plate the modifying function (call it y) is:-

$$y = \frac{1}{8} - \frac{1}{6}\frac{X}{a}R$$

expanding this, gives:-

$$y = \frac{1}{8} - \left[\frac{a\left(\left(\left(\frac{a}{b}\right)^2 + 3\right)^{1/2} - \frac{a}{b}\right)}{12b}\right]$$

A series of values for y can be produced by substituting different values for the length and span of the plate into the equation for y (Table 5.5).

TABLE 5.5 The effect of a third dimension on the Voussoir equation.

Roadway width a	Roadway length b	Roadway aspect ratio x	Modifying function y	reciprocal of y
1	1	0.5	0.04166	1/24
1	2	0.65	0.07083	1/14
1	3	0.715	0.08527	1/11.7
1	4	0.75	0.09375	1/10.66
1	5	0.772	0.09926	1/10.07
1	10	0.817	0.11138	1/8.978
1	20	0.841	0.11799	1/8.475

It will be recalled that the equivalent reciprocal value for a two-dimensional Voussoir beam is 1/8 (Eq 5.2). In Table 5.5 therefore, when the reciprocal y value approximates to 1/8, that is when the roadway is very long, the stresses will approximate to a 2-D beam situation. But as the roadway shortens the stresses decrease steadily until the minimum stress is reached which is the situation for the square plate. Here the stresses are 1/3 of those for a 2-D Voussoir beam. In practice it would appear that beams more than about 20 times as long as their span are best approximated by two-dimensional Voussoir beam theory.

5.4.3. PRACTICAL IMPLICATIONS OF THE THREE-DIMENSIONAL ANALYSIS

It should be borne in mind that 3-dimensional solutions are only required when the plate is clamped on all four sides. For a situation where the mine roof is cut by strong joints, the plate is broken up into smaller slabs as illustrated in Figure 5.14. In this case the analysis of the section a and b would need to be based on 2-D Voussoir beam theory and not slab theory.

5.4.4. FURTHER EXPANSION OF THE EQUATIONS TO ACCOMMODATE DIPPING ROOFS.

The load (Q) that is supported by the Voussoir arch is a function of gravity (See Fig 5.15). Thus, as the dip of a beam increases, the load (Q) is modified by the cosine of the angle of dip. For a bed dipping at an angle alpha (α) the

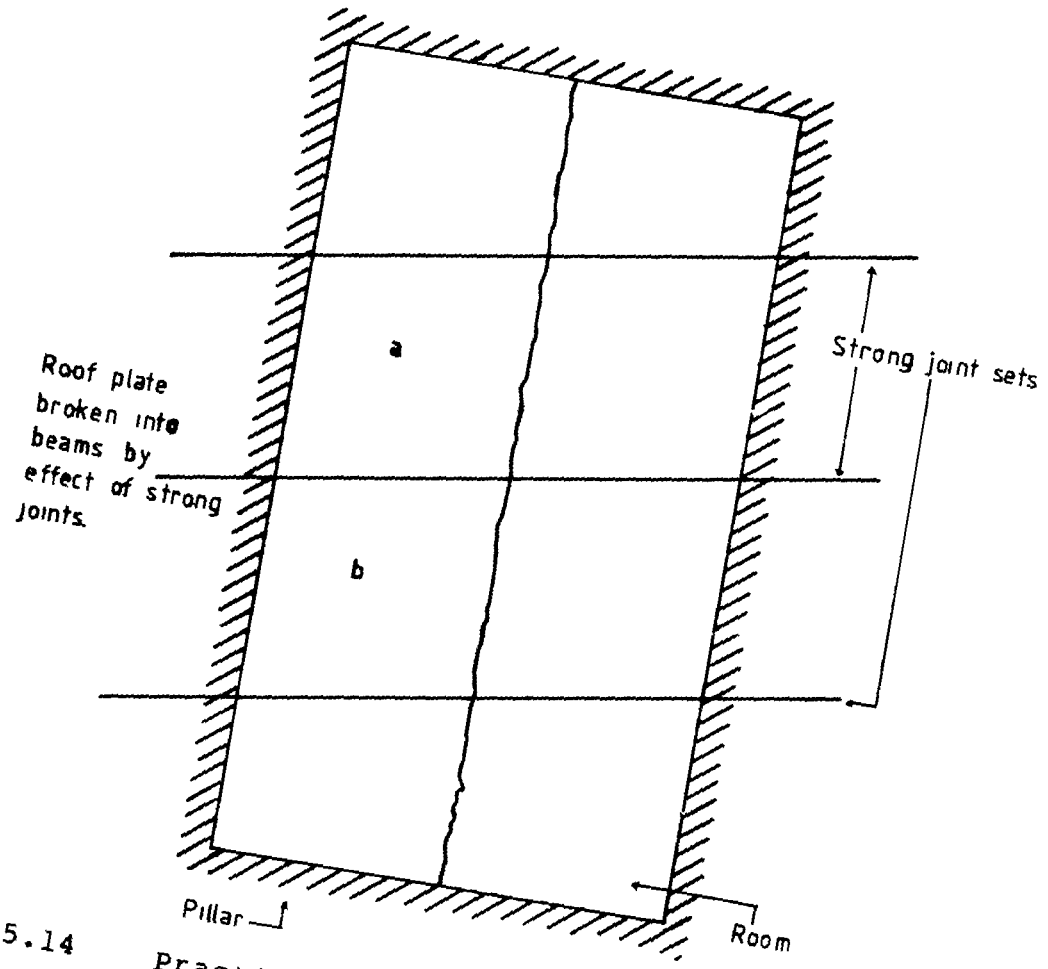

Figure 5.14 Practical restrictions of 3-D Voussoir plate analysis.

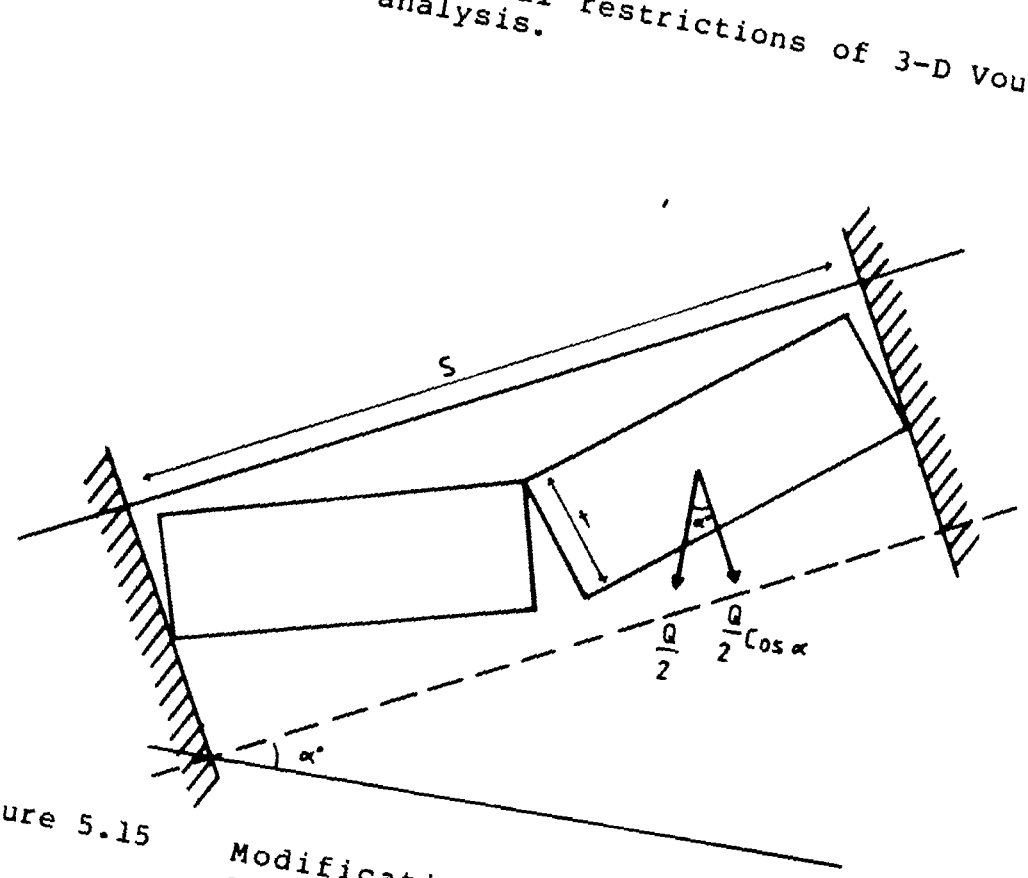

Figure 5.15 Modification of Voussoir beam theory to accommodate dipping beds.

modified load is given by:-

$$Q = Q \cos(\text{alpha})$$

Thus to accommodate a dipping bed all that is required is the substitution of Q cos(alpha) in place of Q in any of the foregoing equations.

5.5. SUMMARY OF ANALYSIS TECHNIQUES AVAILABLE FOR 2-D AND 3-D VOUSSOIR BEAMS.

Three analysis methods are now available for the analysis of Voussoir beam for failure by crushing or elastic buckling. Table 5.6 has been constructed to assist in the choice between the different analysis methods.

Table 5.6 Choice of analysis techniques for the analysis of Voussoir beams.

PROBLEM	ANALYSIS TECHNIQUES MODIFIED* EVANS	MODIFIED* BEER	WRIGHT
No Lateral Pressure	2	3	1
Lateral Pressure	X	X	1
Dipping Beds	1	1	1
2-D Solution	2	X	1
3-D Solution	X	1	X

Solution valid for:- (Numbers in order of preface).---------->

See notes on validity in relevant sections.
* Modified by present writer.

The table can be read in the following manner. Suppose a 2-d solution for a situation with no lateral pressure is required. Look up the 2-D solution and follow the row across to find the lowest column score. Follow the column up or down to see if the technique is valid for no lateral pressure. In this case, the preferred analysis technique is by Wright (1972) with as second choice the modified Evans. The modified Beer et al. solution is in this instance unsuitable. It can be seen that for certain requirements (e.g. 3-D solution with lateral pressure) the problem at present may be insoluble.

All aspects of Voussoir beam failure by crushing or elastic buckling have now been covered. However, there still remain two failure modes that have not

received much attention. These are failure by sliding and failure by shear. These modes of failure are dealt with in the remainder of this Chapter.

5.6. ANALYSIS OF VOUSSOIR BEAMS FOR FAILURE BY SLIPPAGE.

If there is insufficient horizontal force acting across the joints and fracture surfaces of a mine roof, the roof may fail by individual blocks slipping out of the roof. Within this category two modes of failure are commonly encountered, monolithic failure and Voussoir slippage. These are shown in Figure 5.16.

5.6.1. MONOLITHIC FAILURE.

This failure mechanism does not strictly belong with the previous sections on Voussoir beams because it contains no element of block rotation or arching. However, the analysis is included here because it is relevant to Voussoir arch failure.

In monolithic failure a section of the mine roof simply falls out due to insufficient horizontal pressure. This mode of failure, which has also been referred to as a joint controlled collapse Price et al. (1969), and 'Extended void migration', Challinor (1976), can affect large parts of a potential roof. Monolithic failure can move the zone of true arching into strata well above the normal expected limit. An interesting case history, where this is suggested to have happened, is given by Henry (1975), and involves a collapse above an old pillar and stall oil shale mine in Scotland.

The horizontal thrust required for stability is found from the relationship:-

$$H = \frac{Q}{2} \cot \phi$$

where:- Q = weight of beam
H = required thrust
ϕ = angle of friction.

for limiting stability (ie for a factor of safety of 1)

$$\frac{Q}{2} = H \tan \phi \quad \ldots\ldots\ldots\ldots\ldots\ldots\ldots\ldots\ldots\ldots\ldots\ldots\ldots\ldots \text{(Eq 5.9)}$$

onolithic failure.

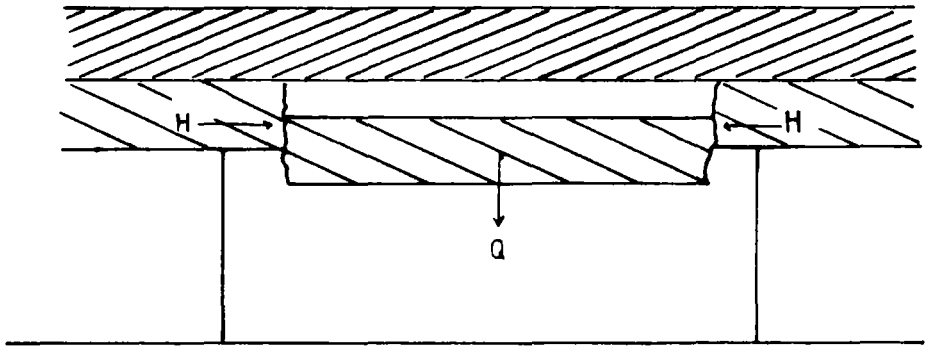

Voussoir failure.

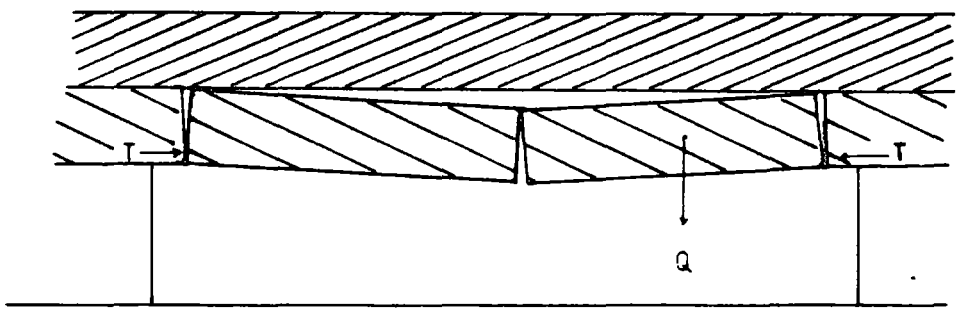

Figure 5.16 Failure of Voussoir beams by slippage.

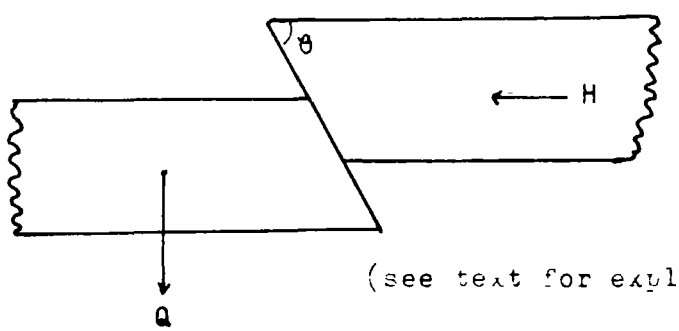

(see text for explanation of symbols)

Figure 5.17 Force relationship for dipping joint sets.

The factor of safety for a given situation (FS) is :-

$$FS = \frac{\text{resisting force}}{\text{driving force}}$$

$$= \frac{H\tan\phi}{Q/2}$$

Thus:-

$$FS = \frac{2H\tan\phi}{Q}$$

This relationship can be generalised and expanded to accommodate cracks in the roof that are not vertical and which exhibit an apparent or true cohesion Wright (1973).

For a mine roof cut by dipping joints and cracks the most critical discontinuity is the one nearest to and dipping towards the abutment. A simple method to analysis for possible sliding along this surface is to resolve the resultant axial force (H) and the shear force (V) into components normal and parallel to the crack surface. The component parallel to the surface is the driving force tending to cause sliding. This is resisted by an opposite force that can have a maximum value equal to the normal component multiplied by the coefficient of friction of the crack surface, plus any apparent cohesion (Fig. 5.17).

Thus:-

$$\text{Driving force} = H\cos\theta + \frac{Q}{2}\sin\theta$$

$$\text{Resisting force} = \left(H\sin\theta - \frac{Q}{2}\cos\theta \right) u + C\,A$$

where:- Q = weight of block
0 = angle of crack
H = thrust
C = apparent cohesion
A = Area over which cohesion is acting

Equating these relationships gives the factor of safety for a monolithic roof:-

$$FS = \frac{\left(H\sin\theta - Q/2\cos\theta \right) u + C\,A}{H\cos\theta + Q/2\sin\theta} \quad \ldots\ldots\ldots\ldots\ldots\ldots \text{(Eq 5.10)}$$

5.6.2 VOUSSOIR SLIPPAGE

Failure of a Voussoir beam can occur if the thrust generated by the rotation of the blocks is insufficient to prevent the slippage of one of the blocks from the system. The general equation for a linear arch, or Voussoir beam, was introduced in Chapter 5.2.3 (Eq 5.2):-

$$\frac{Q\,S}{8} = T\,Z$$

where:- Q = weight of roof + any surcharge
S = Span
Z = Moment arm

Rearranging this equation gives the thrust (T) produced from simple rotation:-

$$T = \frac{QS}{8Z}$$

But for limiting stability it has already been shown (Eq 5.9) that:-

$$\frac{Q}{2} = H\tan\phi$$

where:- H = lateral force

Therefore:-

$$\tan\phi = \frac{Q}{2H}$$

or substituting T for H

$$\tan\phi = \frac{Q}{2T}$$

The critical ϕ value for the limiting stability of a Voussoir beam is obtained by substituting QS/8Z into the above relationship. Hence:-

$$\phi crit = \tan^{-1}\left(\frac{4Z}{S}\right) \qquad \text{..... (Eq 5.11)}$$

or:-

$$FS = \frac{S\tan\phi}{4Z} \qquad \text{..... (Eq 5.12)}$$

Equation 5.12 is the equation for limiting stability against sliding for a Voussoir beam. It is of interest to note that for a two block roof, the critical friction angle is independent of block weight, and depends only on the span to thickness ratio of the beam. If the friction angle of the joint is greater than ϕ crit, then sliding cannot occur and failure, if it occurs, will be by crushing or by one of the other failure modes discussed previously

(Chapter 5.2.1). On the other hand, if the friction angle of the joint is less than this critical value sufficient frictional resistance will not be developed and failure will occur by sliding.

The relationship (Eq 5.11) has been plotted in Figure 5.18 in terms of ϕ (critical), span and thickness using one of the empirical approximations for Z (A) presented by Wright (1972) (See also Chapter 5.3.2 i). Voegele (1978) applied a similar approach, but used (incorrectly) the full block thickness rather than the length of the moment arm (Z). It has been shown (Chapter 5.2.3), that the thrust for the system is generated by rotation and is inversely proportional to the length of the lever arm (Z). Thus, the moment or lever arm must be less than the block thickness.

5.6.3. STABILITY IMPLICATIONS FOR A MINE ROOF

One of the most interesting features to arise from this analysis is that it highlights one of the major differences between Voussoir beams and continuous or normal beams. In the preceding Chapter on beam analysis (Chapter 4) it was shown that the stability of a continuous beam was decreased by increasing the span of the opening. For Voussoir beams however, the above analysis shows that, for failure by slipping, the exact opposite can be true. A Voussoir beam can be too short to be stable.

Failure of a Voussoir beam by slippage of one of the blocks is a result not of excessive deflection of the beam, but rather of insufficient deflection. By increasing the span of such a Voussoir beam the rotation increases. The rotation of the blocks decreases the moment arm which in turn increases the thrust generated at the contacts. The increase in thrust, by virtue of the additional frictional resistance, therefore increases the factor of safety against slippage of a block from the beam.

The same mechanism also applies in reverse. For example if support is introduced in a jointed mine roof at midspan, the mine roof may be prevented from deflecting fully. In this situation the full frictional resistance at the

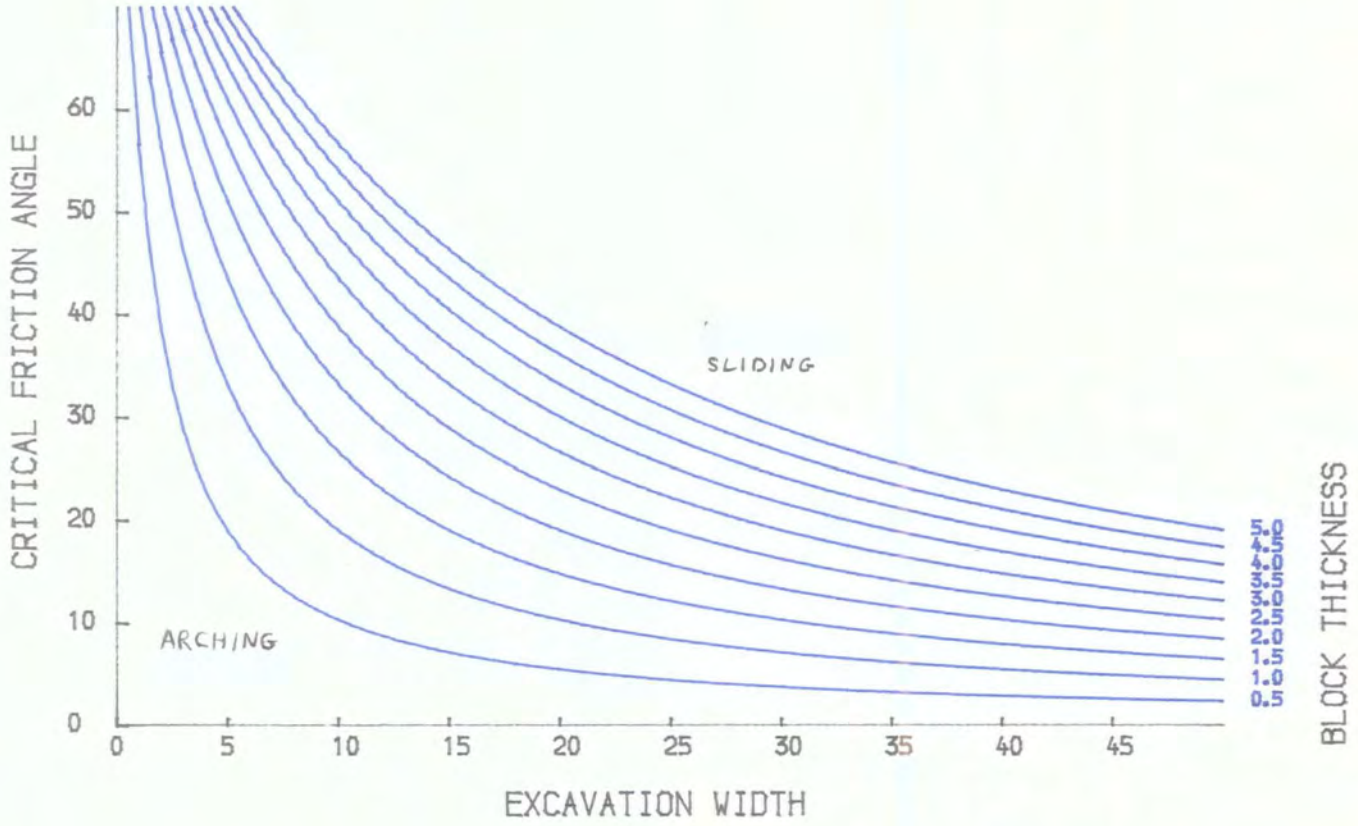

FIG. 5.18 CRITICAL FRICTION ANGLE AS A FUNCTION OF EXCAVATION SPAN AND BLOCK THICKNESS

contacts may not develop, and the roof may collapse. Thus, what was initially a perfectly stable mine roof may collapse as a result of providing support in the wrong place.

5.7 ANALYSIS OF VOUSSOIR BEAMS FOR FAILURE BY SHEAR

Potts et al. (1979), used a series of large-scale models to demonstrate that a Voussoir beam could fail as a result of shear through one of the component blocks of the system. They identified contact to contact shear as the main mode of failure for beams with a certain aspect ratio (Fig. 5.19a). However, the present writer considers that in the analysis of the roofs of old mine workings, where the shear strength along the bedding is likely to be much less than the shear strength across the bedding, axial shear, that is shear along the bedding plane, will be of greater importance than corner to corner shear. This mode of failure is illustrated in Figure 5.19b.

The thrust in a Voussoir system operates as a shear couple between the two opposite contact corners. This couple will exert a uniform shear stress across the thickness of the beam. If a plane of weakness, such as a bedding plane, exists anywhere in the beam between the thrust centroids; and this bedding plane has a shear strength less than the stress acting on the plane, shear will take place along this plane of weakness. Once the block shears, the system will be unable to transmit a lateral force down the beam, and the beam will collapse from excessive rotation.

The shear stress acting on the bedding plane will be:-

$$\tau = \frac{2T}{\text{Area of bedding plane}}$$

where:- T = Thrust
τ = shear stress

Thus:-

$$\tau = \frac{2T}{S/2 \times b} = \frac{4T}{S} \quad \text{(for unit breadth)}$$

This equation can be used to calculate the factor of safety against axial shear in a Voussoir beam. Within the block the shear will be opposed by the cohesion

Corner to corner shear

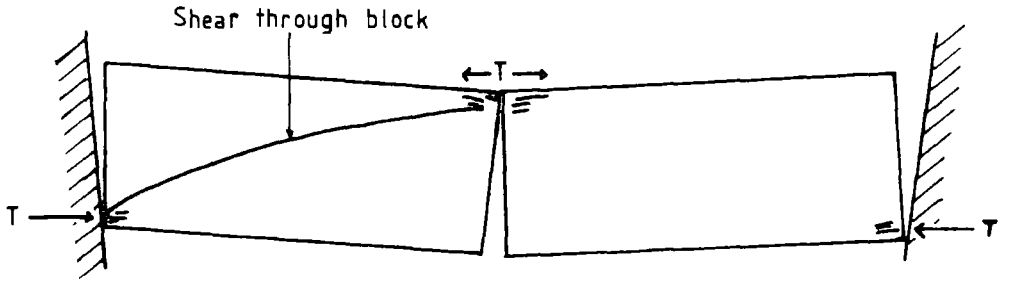

Bending plane shear

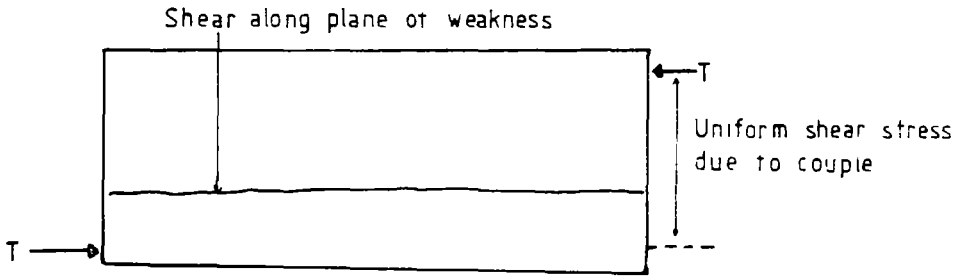

Figure 5.19 Modes of shear failure in a voussoir beam.

and shear strength of the plane of weakness. If the value of this is included within the term C (apparent), the Factor of Safety is given by:-

$$\frac{\uparrow}{FS} = \frac{\frac{4\,T}{S}}{C\ \text{apparent}} = \frac{4\,T}{S\,C}$$

Thus, the force resisting shear is the apparent cohesion along the bedding plane. Because there is no normal force acting across the thickness of the block the $n \tan\emptyset$ term will be zero. However, The c effective term will include a component due to interlock between opposing asperities on the bedding plane. Thus, it is likely that the value for C (effective) will be slightly larger than the tensile strength or cohesion of the bedding plane.

5.8. SUMMARY OF VOUSSOIR BEAM ANALYSIS.

In the preceding chapter an attempt has been made to analyse the diverse approaches of six principal authors namely Evans (1941), Wright and Mirza (1963), Wright (1972), Wright (1973), Potts et al. (1979), and Beer and Meek (1982) who individually over a period of 43 years have made a contribution to Voussoir beam analysis. From a synthesis of this data it has been possible to arrive at a composite theory which is more powerful, versatile and accurate than any of the individual component theories.

A number of errors in the initial theory of Evans (1941) have been identified and isolated. Working solutions to these problems have been obtained by substituting into the relevant areas of the original theory empirical correction factors derived from the work of Wright (1972) and Potts et al. (1979). Three methods of analysis for the failure of Voussoir beams by crushing and elastic buckling are presented. These can cover both 2-D and 3-D situations, and can also predict the effect of dipping beds. The analysis has been extended to cover the effects of additional ground strains, such as those that could be introduced by a subsidence wave from a working underground coal mine.

Two remaining modes of Voussoir failure have also been expanded and described.

An incorrect assumption by Voegele (1978) has been corrected in the analysis for Voussoir slippage, and the correct limit equation is presented. A new mode of shear failure for Voussoir beams has been identified, and a relationship has been developed to analyse for this mode of failure.

In practical terms, the collapse of shallow coal mine workings resulting from the failure of Voussoir beams was found to represent only a small proportion of the observed collapse modes. However, it is difficult to identify failed Voussoirs in the field, and the importance of this mode of failure is probably underestimated, especially in the thicker bedded strata. The analysis technique becomes of greater importance in the analysis of thick competent roof rocks such as limestones, sandstones and ironstones. Thus, the analysis has probably greater application in the analysis of mine workings in these rocks than in the more discontinuous rocks of the Coal Measures.

CHAPTER 6

MECHANISTIC THEORIES

6.1 INTRODUCTION

When characterising or attempting to characterise a rock mass some accommodation has to be made to account for jointing and bedding. It is usual to consider planes of separation parallel to the bedding as horizontally continuous, with the jointing at right angles to this primary set as vertically discontinuous. Such a pattern of bedding and jointing breaks the rock mass into a number of discrete units or blocks. The aspect ratio of a block can be defined as the length of the block divided by its thickness, or in the terms already discussed (Chapter 1 and 3) the effective unit length divided by the effective bed thickness.

Jones and Davies (1929) and Terzaghi (1946, Figure 6.1) both assumed such a model when considering mine roofs, and over the following years this assumption has received tacit approval from numerous authors. However, it should be pointed out that at various times a number of other unit shapes have been proposed and used in theoretical rock mechanics projects. These shapes have included triangular, parallelogram, hexagonal, circular and irregular shaped units (Litiwiniszyn, 1964, Trollope, 1968, Brown, 1972, Maini et al., 1978).

Trollope (1966) stylized the system of mutually perpendicular intersecting sets of discontinuities for his model experiments on the stability of trapezoidal openings in rock. He used blocks with an aspect ratio of 1 (ie. square), stacked to achieve the maximum vertical discontinuity (Fig 6.1). Goodman et al. (1968) used a similar configuration for their finite element analysis of arching in a mine roof, but for numerical and computational reasons they incorporated between the discontinuities 'no thickness' joint elements. Since this time numerous authors have used a similar model at some stage in their analysis of slopes or underground openings (Ergun, 1970, Byrne, 1974, Hocking, 1978, Hittinger, 1978, Stewart, 1981).

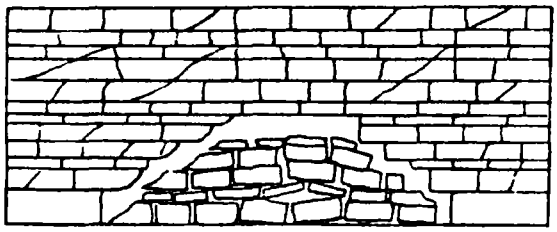

Diagramatic section of a roof fall (After Jones and Davies, 1929)

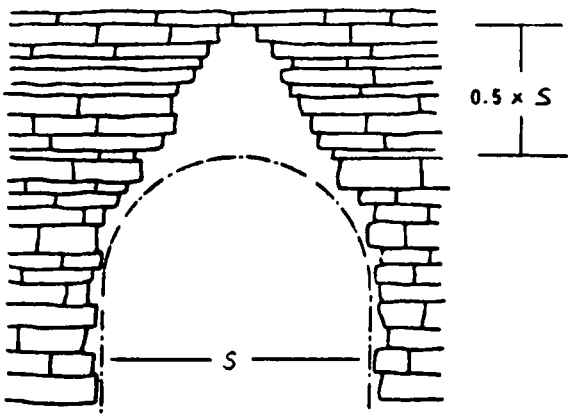

Maximum probable overbreak if no support furnished (Terzaghi, 1946)

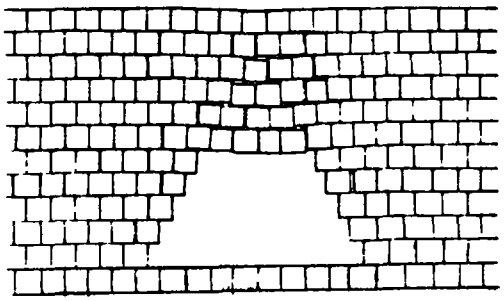

Trollope's Block Jointed Model (Trollope, 1966)

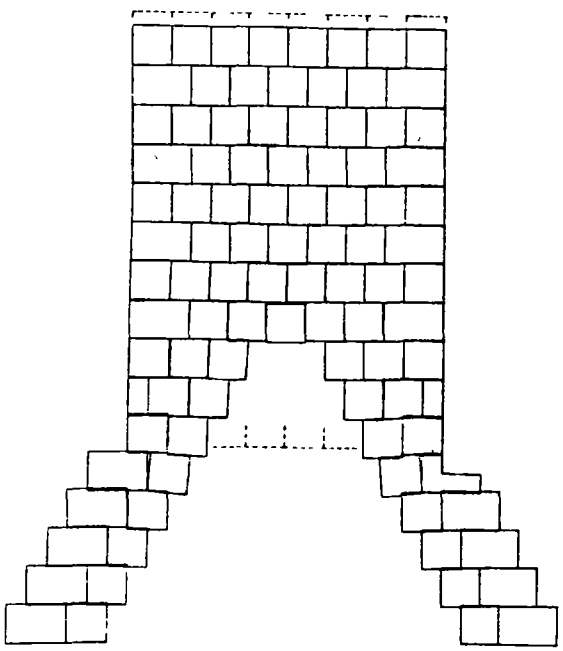

Section used by Goodman et al. (1968)

Figure 6.1 Simplifications used to illustrate or model collapsed mine roofs.

6.2. KINEMATIC CONSIDERATIONS

There is therefore, a long and well established precedent in rock mechanics of considering a rock mass as composed of a number of rectangular elements with the bedding as horizontally continuous and the jointing as vertically discontinuous. Voegele (1978) pointed out that if the rock could be characterised by the spacing of its discontinuities, and the discontinuities dominated the mode of failure, then in an underground mine, the ultimate shape of the unstable arch could be determined from a kinematic consideration of which blocks were free to move into the excavation (Fig 6.1). Under this assumption the possible height of overbreak can be calculated from a knowledge of the relative sizes of the opening, the block length (EUL) and bed thickness (EBT) (See Chapters 1 and 3).

The number of blocks (b) in the bottom row of the roof strata is given by:-

$$b = \frac{S}{EUL}$$

where b= number of blocks in bottom row
S= Span of opening
EUL= Effective unit (block) length
EBT= Effective bed thickness
h= Height of triangular wedge

Assuming that all the blocks are of identical size and have the same aspect ratio it can be shown that the height of the triangular wedge is:-

$$h = b \times EBT$$

In terms of the aspect ratio of the blocks (A), where A = EUL/EBT

$$h = \frac{S}{A} \quad \text{..... (Eq. 6.1)}$$

This relationship (Eq 6.1) has been plotted for a variety of block aspect ratios in Figure 6.2.

These relationships represent kinematic considerations only, and indicate that as the block aspect ratio decreases, the height and hence also the weight of the triangular wedge increase. Voegele (1978) used this model as the basis for the production of a suite of design curves for the ultimate potential load on a tunnel support system. He validated this approach using a computer model which

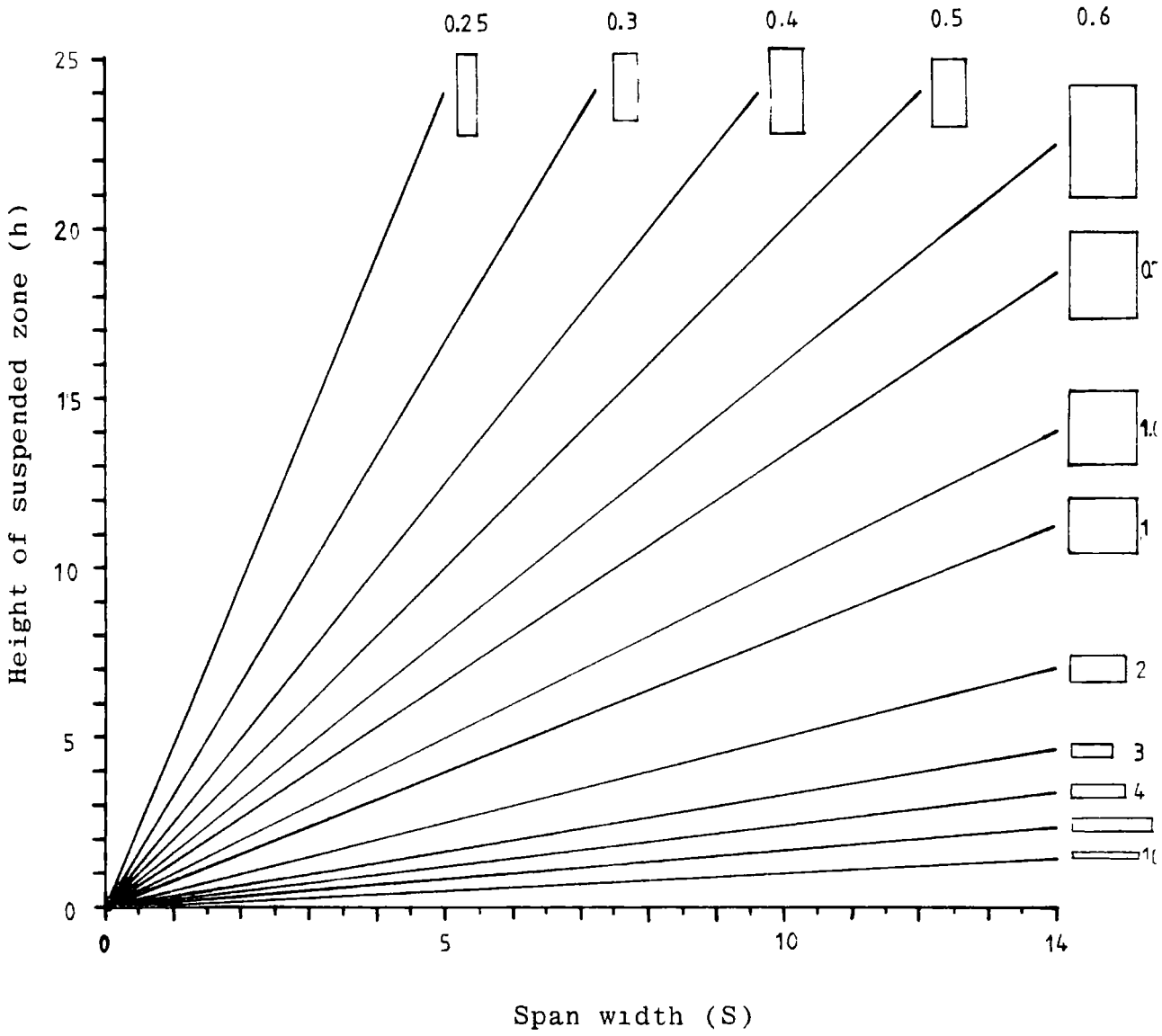

Figure 6.2 Relationship between span width and height of suspended zone.

essentially modelled the same conditions (Rigid block method - computer technique).

6.3. EXTENSION OF THE ANALYSIS TO INCLUDE FRICTIONAL AND COHESIVE FORCES

The analysis of the stability of the blocks constituting the wedge can be extended by considering the cohesion and friction forces acting across the discontinuities.

The total number of blocks (n) making up the wedge can be shown to be equal to :-

$$n = \frac{b}{2}(b + 1)$$

where:-

b= number of blocks in bottom row
= S/EUL
S= Span of opening (m)
EUL= Length of block (m)
EBT= Thickness of block (m)
d= Density (kg/m3)
h= Height of wedge (m)
r= number of rows
wt= weight of wedge (Kg)

The weight of the wedge is:-

$$wt = \frac{S \times EBT}{2}\left(\frac{S}{EUL} + 1\right) \times d$$

The height of the wedge has been shown to be (Eq 6.1):-

$$h = \frac{S}{EUL} \times EBT$$

the number of rows are:-

$$r = \frac{(S / EUL) \times EBT}{EBT} = \frac{S}{EUL}$$

Considering just the effect of the cohesion between the horizontal surfaces or bedding planes. The area over which the cohesion acts (Hor) is:-

$$Hor = r \times EUL$$
$$= S$$

Thus, irrespective of the number of blocks, the total area over which the horizontal cohesion acts is equal to the span of the working.

Considering now the area over which the cohesion acts in the vertical plane (Ver) (For this situation vertical cohesion can include an appropriate value to accommodate any interlock effect, or micro-shear of the discontinuities). For

the full width of the working, the total area for vertical cohesion is:-

$$\text{Ver} = \frac{2\,S}{EUL} \times EBT$$

$$= \frac{2S}{A}$$

$$= 2h$$

Thus, the area over which the vertical cohesion acts will be equal to twice the height of the wedge.

From these relationships, it will be apparent that as the span of the opening increases, the volume, and hence the weight of the wedge, will also increase. But the weight will increase at a faster rate than the cohesion forces along the wedge boundary. Therefore, a point is reached when the weight of the wedge exceeds the cohesion and friction boundary forces, at which point the roof collapses 'en masse'.

The forces resisting collapse will be (for unit breadth roof):-

$$\text{Resisting forces} = \text{horizontal cohesion} + \text{vertical cohesion} + \sigma_n \tan\phi$$

$$= (S \times Ch) + (2h \times Cv) + \frac{H}{2h} \times \tan\phi$$

where H= horizontal thrust

The forces promoting collapse will be:-

$$\text{Promoting forces} = \text{weight of wedge}$$

$$= \frac{S \times EBT}{2} \left(\frac{S}{EUL} + 1\right) \times d$$

where:-
Ch= Horizontal cohesion
Cv= Vertical cohesion

Therefore, the factor of safety (FS) is:-

$$FS = \frac{(S \times Ch) + (2h \times Cv) + \frac{H}{2h} \times \tan\phi}{\frac{S \times EBT}{2} \left(\frac{S}{EUL} + 1\right) \times d} \quad \ldots\ldots\ldots\ldots\ldots\ldots \text{(Eq 6.2)}$$

Taking a simple example and assuming that there is no horizontal thrust (ie. there are no frictional forces), and that the stability of the roof depends

entirely on the horizontal and vertical cohesion, then, for any given parameters, a graph can be plotted of the reduction in the factor of safety with increasing opening span (Fig 6.3).

Hassani et al. (1979) measured typical cohesion values of between 14 and 35 KN/m2 for natural joints in Coal Measures mudstones. Using the relationship derived above (Eq 6.2, Fig 6.3) it can be seen that for the given working geometry a cohesion value of 25kN/m2 predicts a stable span of about 8m. This of course assumes the complete absence of any horizontal forces. If horizontal forces are present, these would tend to increase the factor of safety and hence the length of the stable span. Weathering or time dependent effects can be considered in terms of a reduction in the cohesion value (Chapter 1). If this approach is taken the effect of weathering on the stability of the opening is graphically illustrated by the relationship in Figure 6.3. Any decrease in the cohesion value directly affects the length of the stable span, and some idea of the effect of progressive weathering or deterioration on the stability of the roof can be obtained.

Values for other cohesion values and working spans can easily be calculated, but it must be remembered that the relationship assumes the roof fails 'en masse' rather than by progressive deterioration and spalling. Field observations would suggest that this latter mode of deterioration is the more common.

6.4. ANALYSIS OF BLOCK ASPECT RATIOS

During the field investigations an estimate was made of the average thickness of the collapsed roof material (effective bed thickness Chapter 3, Fig 3.6). At the time it was noticed that the thickness of the block appeared to be related to its length (EUL). To test this hypothesis three opencast sites were chosen for further study. From each site a large number of rock fragments were measured from the collapsed roof sequence above the old workings. Three rock types were chosen, and the location and general size of the blocks are summarised in Table 6.1. and 6.2

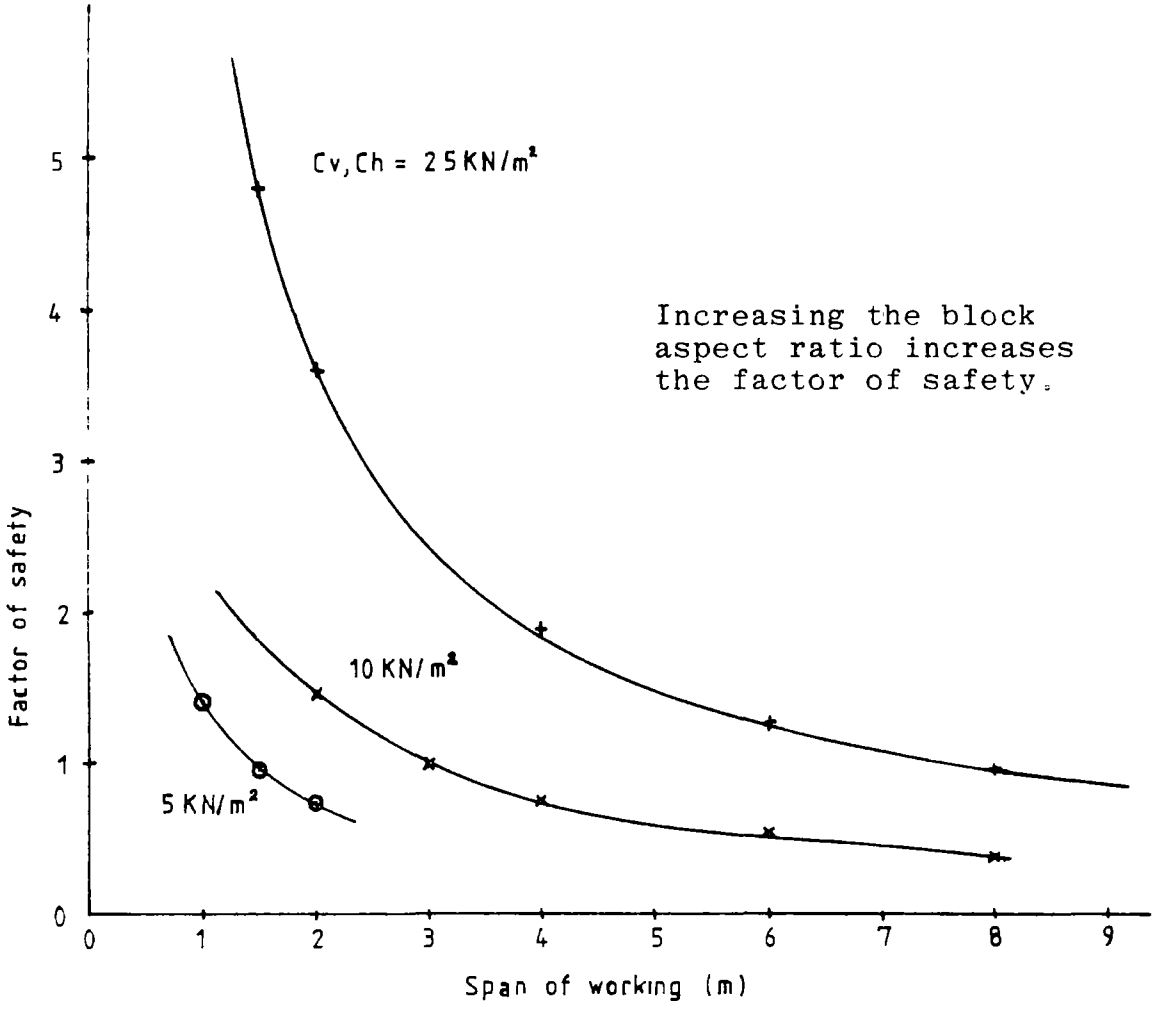

Block Aspect ratio of 2 : Block length (EUL) = 0.1m
Block thickness (EBT) = 0.05m
Density = 2600 Kg/m²
C = Cohesion (vertical and horizontal)
Friction not included

Figure 6.3 Variation in factor of safety with width of working for various cohesion values.

TABLE 6.1 LOCATION AND BASIC STATISTICS OF ROCK TYPES USED TO DETERMINE BLOCK ASPECT RATIOS.

Rock Group	Location OC. site	No. Samp.
Sandstone	Pit House	176
Siltstone	Esh Winning	52
Mudstone	Tow Law	108

TABLE 6.2 SUMMARY STATISTICS FOR BLOCK ASPECT RATIOS.

All Data

		Min	Max	Mean	SD
Length (l)	mm	12.0	2250	316.7	330.7
Breadth (b)	mm	10.0	900	205.5	186.3
Thickness (t)	mm	1.0	350	64.1	65.4
l/t aspect.		0.7	42.5	6.15	3.85
b/t aspect.		1.0	27.5	4.20	2.68
$\sqrt{l \times b}$	mm	16.1	1219	25.1	236.0

Pit House - Sandstone

		Min	Max	Mean	sd	median	Percentiles 2.50	97.5
Length (l)	mm	70.00	2250.0	468.70	384.10	300.00	100.00	1500.0
Breadth (b)	mm	50.00	900.0	298.50	207.90	220.00	70.00	800.0
Thickness (t)	mm	15.00	350.0	93.80	71.50	65.00	16.00	280.0
l/t aspect.		1.87	12.0	5.29	1.86	5.00	2.55	9.4
b/t aspect.		1.21	10.0	3.60	1.45	3.33	1.50	7.1
$\sqrt{l \times b}$	mm	59.20	1219.0	369.00	265.60	275.70	74.20	1020.0

Esh Winning - Siltstone.

		Min	Max	Mean	sd	median	Percentiles 2.50	97.5
Length (l)	mm	12.00	550.0	134.70	106.60	120.00	17.00	350.0
Breadth (b)	mm	10.00	330.0	97.80	66.90	90.00	13.00	250.0
Thickness (t)	mm	2.00	250.0	31.80	42.30	20.00	2.00	140.0
l/t aspect.		0.07	16.5	6.97	3.50	6.57	0.24	16.0
b/t aspect.		1.00	12.0	4.73	2.36	4.33	1.07	12.0
$\sqrt{l \times b}$	mm	16.10	340.0	110.20	74.70	98.00	18.20	250.0

Tow law - Mudstone.

		Min	Max	Mean	sd	median	Percentiles 2.50	97.5
Length (l)	mm	30.00	800.0	156.70	125.00	110.00	32.00	400.0
Breadth (b)	mm	17.00	350.0	105.70	76.30	80.00	20.00	300.0
Thickness (t)	mm	1.00	200.0	31.40	33.50	20.00	2.00	100.0
l/t aspect.		2.00	42.5	7.16	5.68	5.60	2.54	30.0
b/t aspect.		1.50	27.5	4.92	3.89	4.07	1.80	23.3
$\sqrt{l \times b}$	mm	24.50	529.0	127.60	94.70	99.00	27.40	346.0

The primary motive for recording the length, breadth and thickness of a sample of blocks from an opencast site was to obtain an idea of the average block aspect ratios for typical Coal Measures rocks. For this purpose it was not necessary to record a statistically random sample of blocks, but it was necessary to investigate a representative and wide range of block sizes. Therefore, the mean values of the block thicknesses do not exactly correspond to the average effective bed thicknesses (EBT) assessed at the time of the investigation of the old workings (Table 3.1).

Various simple correlation exercises were carried out on the three measured variables (ie. length, breadth and thickness) and various combinations thereof. The results of this analysis showed that the thickness of the block correlated slightly better with the square root of the surface area of the block (ie. length x breadth) ($r=0.92$), than it did with either the length ($r=0.88$) or breadth ($r=0.91$) on their own. (Rank order correlations carried out on combined data $n=336$, sign. $> 99.9\%$). For this reason and to summarise the data, thickness vs. root area have been chosen to illustrate the relationships (Figs. 6.4, 6.5, and 6.6).

An exhaustive statistical analysis of the data revealed some interesting points concerning the inter-relationships between the variables. The average aspect ratio for a block remained remarkably constant irrespective of its absolute thickness or length. However, as would be expected, the range of variation in the aspect ratio increased with the increase in the absolute dimensions. From this observation it would therefore, appear to be perfectly valid to consider the idea of 'typical aspect ratios' for Coal Measures rocks. The aspect ratios calculated from the field data are summarised in Table 6.2.

Once it had been established that the aspect ratio did not vary with the thickness of the block, an analysis was undertaken of the variation between the ratios for the three rock groups. For statistical reasons, both Kruskall Wallis and Median tests were performed on the rock groups. These tests make few assumptions about the distribution of the data within the samples and are hence

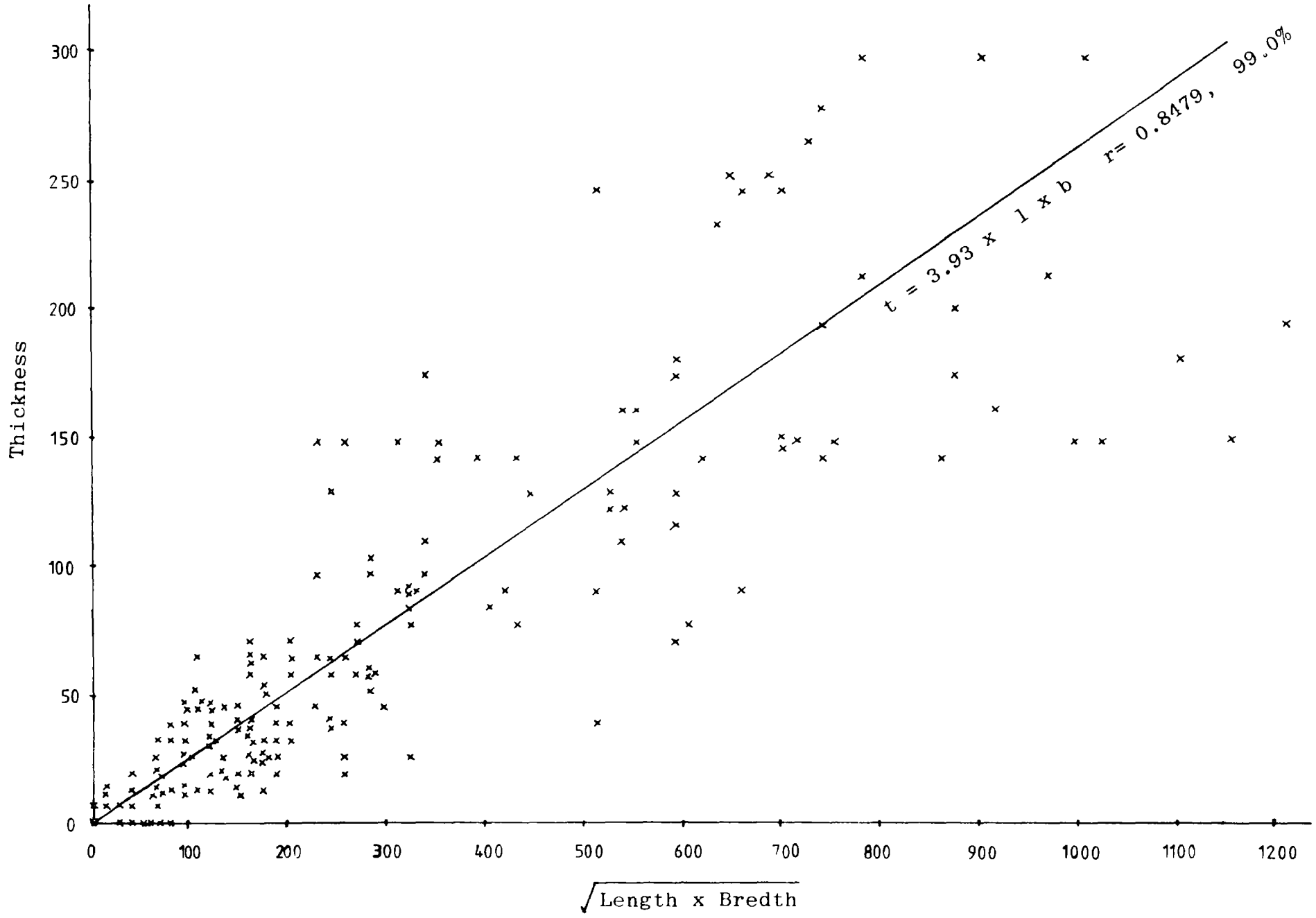

Figure 6.4 Relationship between thickness and square root of

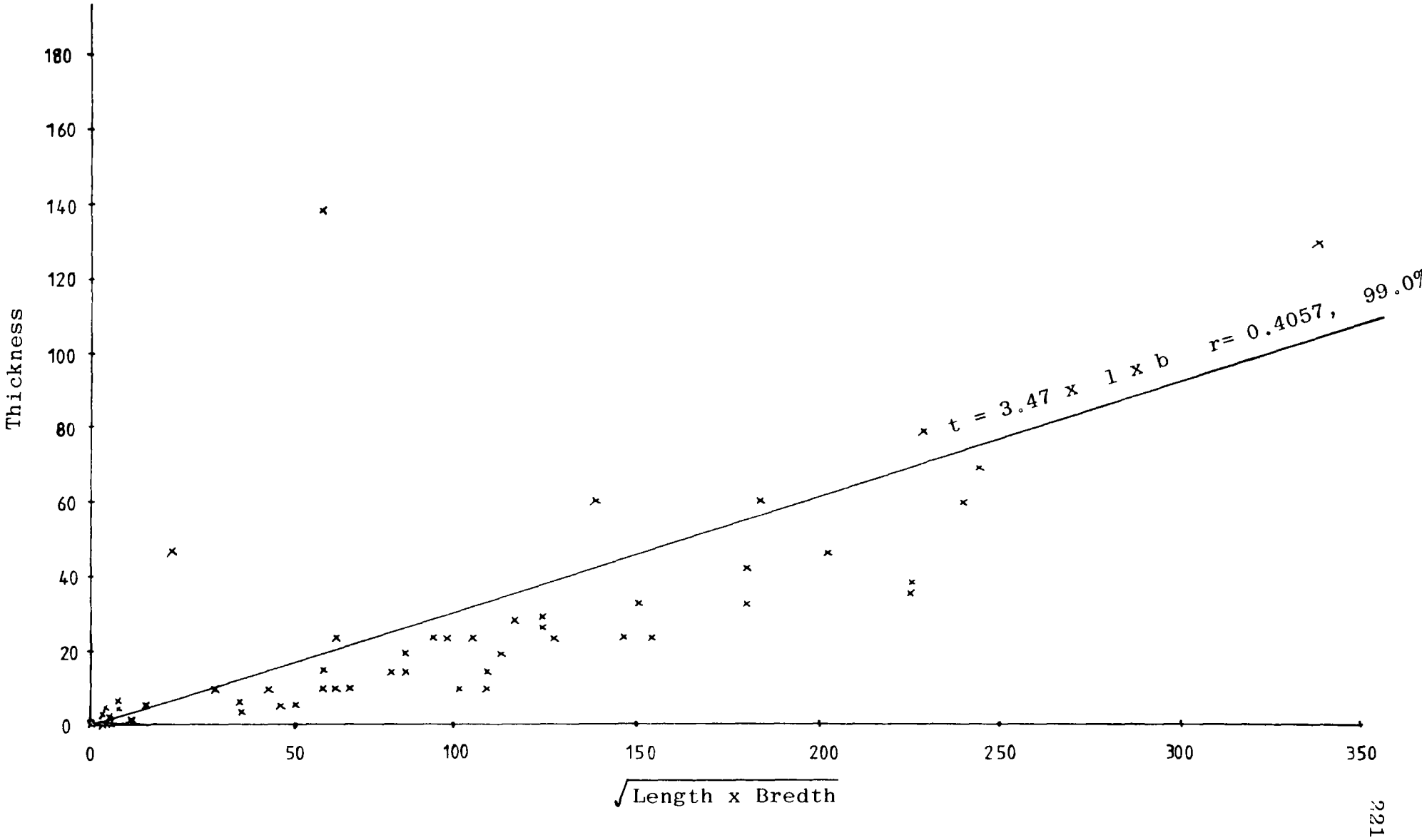

Figure 6.5 Relationship between thickness and square root of area for siltstone blocks : Esh Winning OC site.

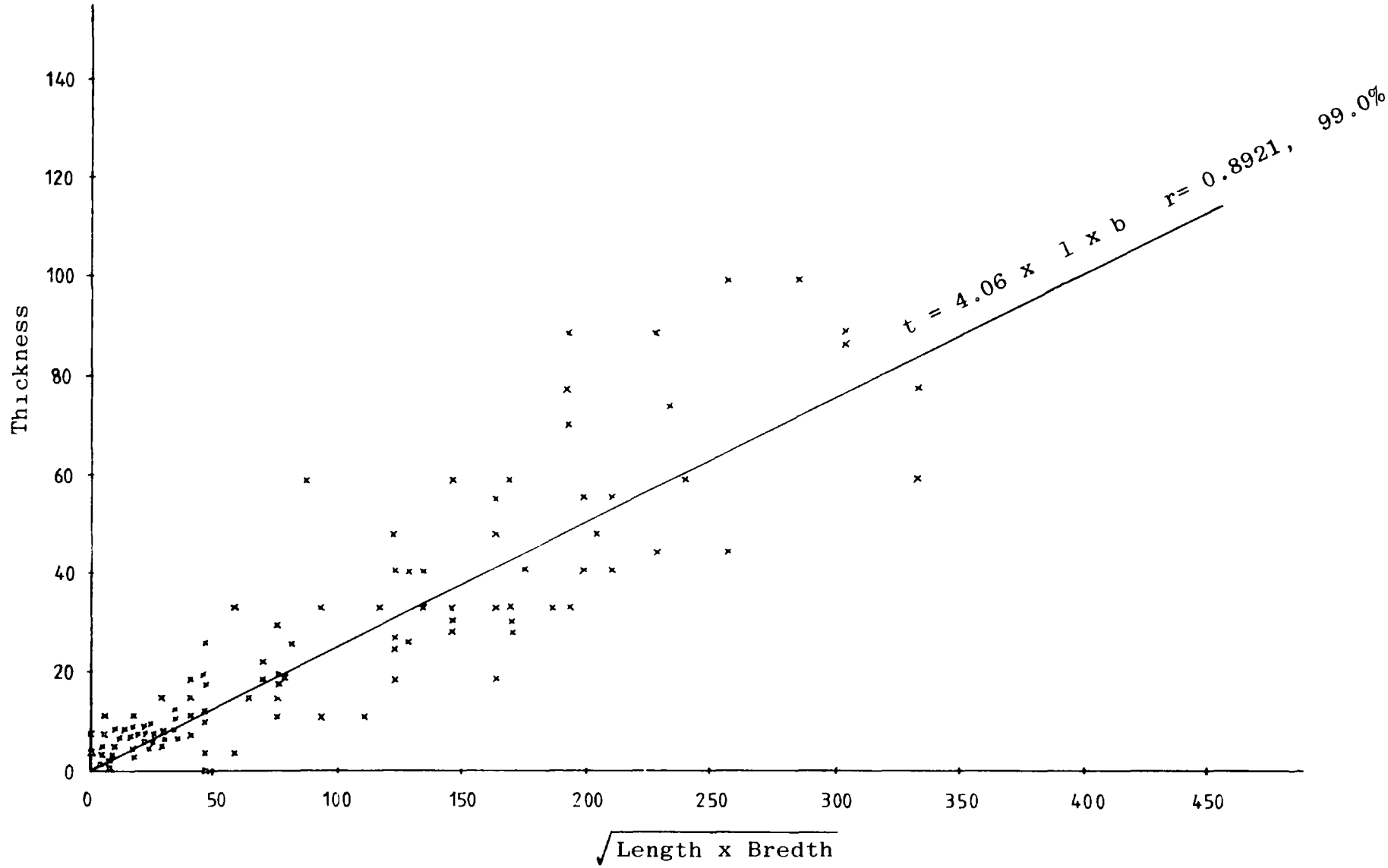

Figure 6.6 Relationship between thickness and square root of area for mudstone blocks : Tow Law OC site.

more appropriate in this case than the analysis of variance test.

The results from the statistical tests are summarised in Table 6.3. The statistical analysis of both the length/thickness and the breadth/thickness (two different block aspect ratios) showed that there was no statistically significant difference between the aspect ratios of the siltstone and mudstone. However, it did suggest that there was a significant difference between the aspect ratio of these rocks and the sandstone.

TABLE 6.3. INTER-RELATIONSHIP BETWEEN THE ASPECT RATIOS FOR THE DIFFERENT ROCK TYPES TESTED.

Length/Thickness block aspect ratio.

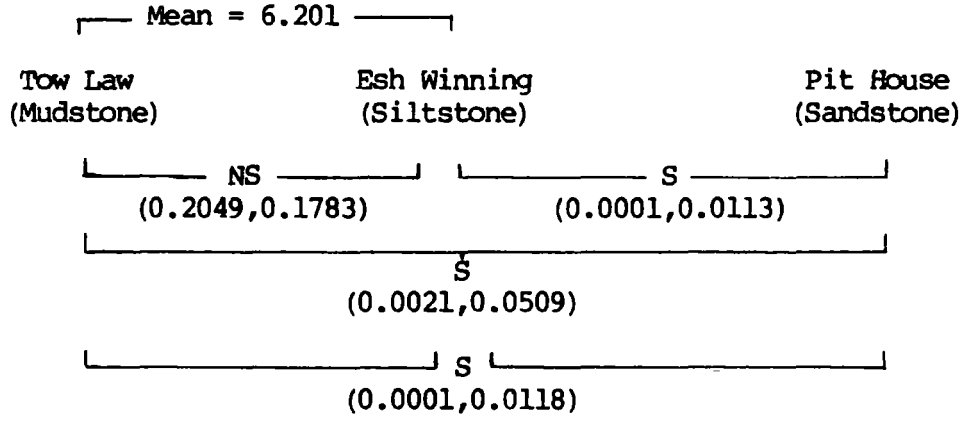

Breadth/Thickness block aspect ratio

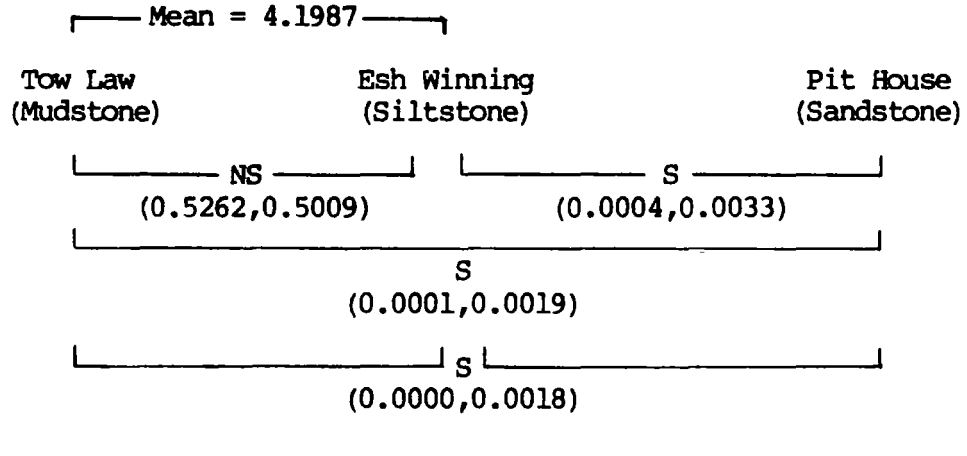

S = Significant difference ie. >95.0%
NS = No significant difference

(0.0000,0.0018) = First statistic refers to the Kruskall Wallis test while the second statistic refers to the Median test. Significance level obtained by eg. 1 - 0.0018 x 100 = 99.8%.

Thus, the data suggest that blocks of sandstones are, relatively speaking, generally short and fat with an average aspect ratio (length/thickness, Median) of about 5. In contrast the mudrocks have slightly longer and thinner blocks with aspect ratios (length/thickness, Median) of about 6.2 (Table 6.3).

6.5. FAILURE MECHANISMS IN JOINTED MODELS

The validity of the theoretical relationship relating block size and collapse height (Chapter 6, Fig 6.2, Eq 6.1), can be assessed by using this relationship with the average block aspect ratio (Table 6.2) to predict the height of collapse for the 'average old working'. If the relationship predicts a reasonable height for the arch, then the theoretical approach is valid. On the other hand if the relationship does not estimate a reasonable collapse height, then some explanation for the discrepancy must be sought. Reference to Table 6.3 will show that the average block aspect ratio for a mudrock is about 6. An old working with an average span width of about 2m and an effective bed thickness of 0.062m (Table 3.1) predicts a collapse height of about 0.34m. This value is substantially less than the average value of 1.25 x S = 2.5m observed in the field (Chapter 3, Table 3.1). Therefore, it must be concluded that one or more of the assumptions made during the derivation of the relationship are invalid.

To examine this question further, a simple base friction model was developed using a wooden tray and various sized, small blocks of wood and rubber. the blocks of varying, but with each test constant aspect ratios, were loaded into the tray with the bedding horizontally continuous and the jointing vertically discontinuous (see Fig. 6.8). Packing was placed between the side of the tray and the blocks so that the horizontal pressure acting on the system could be controlled. The tray was then tilted to an angle of about 60 degrees from the horizontal and an excavation was simulated by removing one block. The remaining blocks were then allowed to consolidate and reorientate as necessary after which the height of the arch or disturbed zone was measured. When all measurements were complete a further block was excavated and the whole procedure repeated.

This sequence was carried out until boundary effects were experienced (Toppling and peeling of the blocks from the side of the tray).

The results of a typical experiment are presented in Figure 6.7. The experiments were repeated for a variety of block aspect ratios and both horizontal and vertical pressures.

During the experiments it was observed that the mechanism of failure of the immediate roof of the excavation appeared to be characterised by three distinct stages:-

TYPE 1 FAILURE (Fig 6.8a). This operated when the width of the opening was small relative to the number of blocks constituting the bottom row. With this type of failure, the numbers of blocks falling out, and hence the height of the arch, corresponded exactly with values obtained from the theoretical relationship developed earlier (Eq 6.1).

TYPE 2 FAILURE (Fig 6.8b). This developed progressively from the first failure type and was characterised by the rotation towards the void of the blocks forming the side of the arch. the blocks overlying these slid on the tilted blocks, thereby moving towards the excavation. This phase was characterised by block chokes. These occurred at or near the arch apex where the blocks interlocked with one another forming a quasi-stable mass which prevented further movement.

TYPE 3 FAILURE (FIG 6.8c). This was the final stage of the development of instability and was characterised by the failure of the chokes formed during the previous stage. At this point the capacity of the arch apex to transmit horizontal forces by 'arching action' broke down, and the arch apex buckled. This resulted in the deterioration of the sides of the arch which ultimately led to mass instability. The 'arch' shape of the excavation was lost and developed vertical sides. Unfortunately, insufficient blocks were available to progress the model further, but it appeared that ultimately the vertical hole would ravel back to an appropriate stable angle.

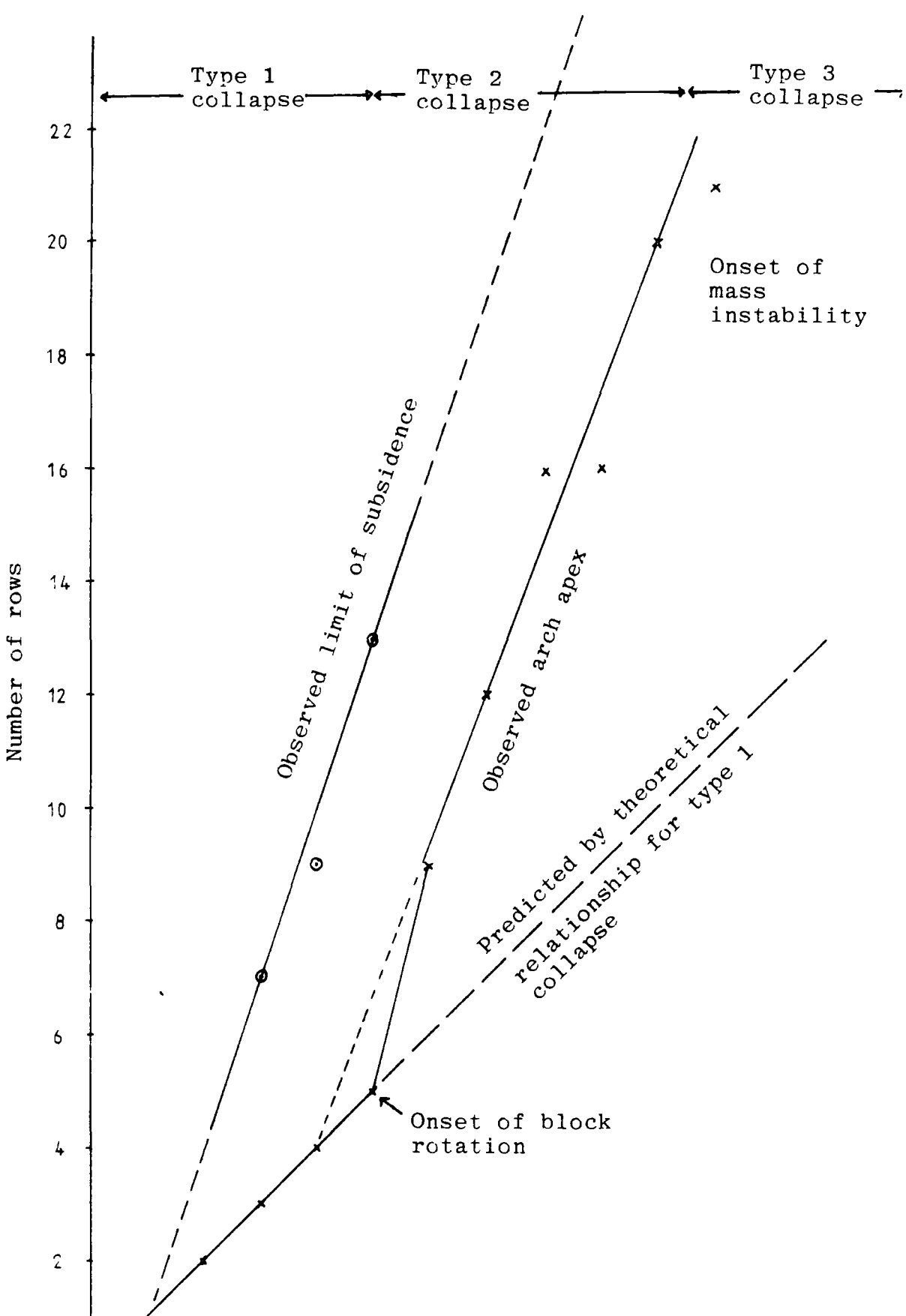

Figure 6.7 Observed relationship between height of suspended zone and number of blocks removed (span of working

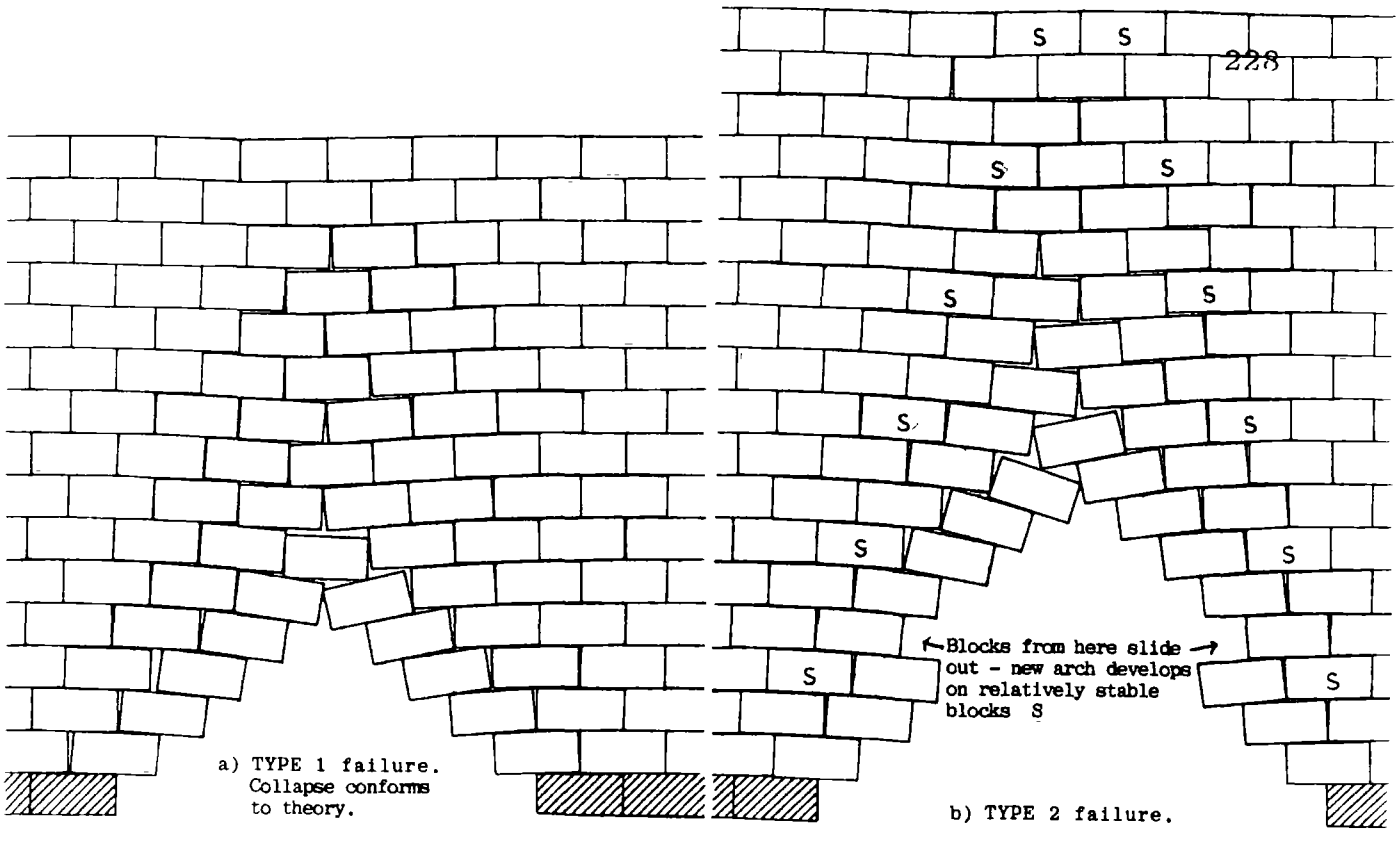

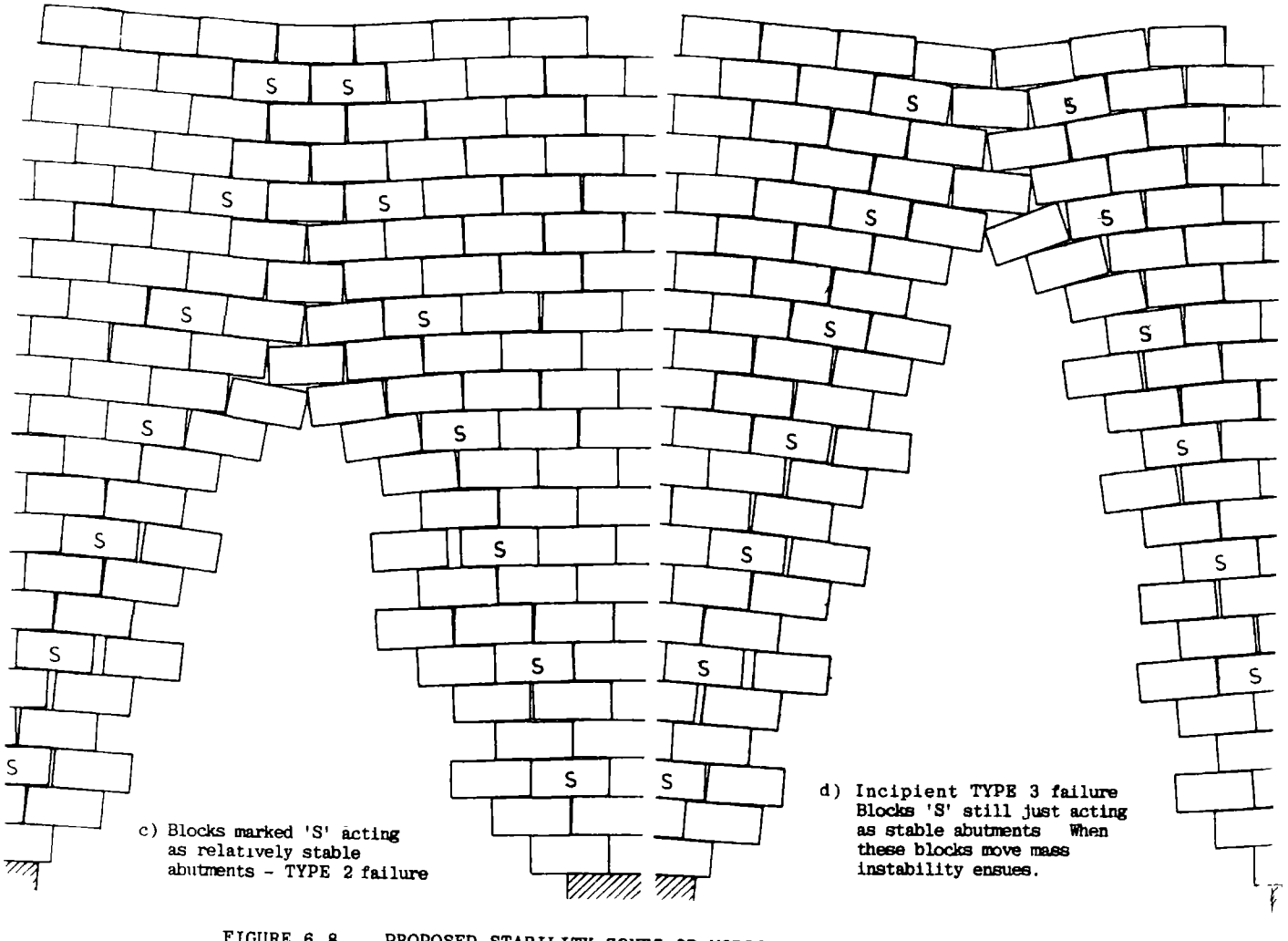

FIGURE 6.8 PROPOSED STABILITY ZONES OR MODES OF FAILURE FOR BLOCK JOINTED SYSTEMS.

This observed sequence is thus essentially identical to the one that was suggested in Chapter 1 as a basis for the classification of old workings. In the field, the majority of old workings are represented by the first two stages of failure. Workings with roof rocks of sandstone or fairly massive mudstone dominate the stage 1 type failures.

During the experiments the degree of instability and the point of transition from one failure stage to another was found to vary with a number of factors.

1 FRICTION ANGLE. The friction angle between the discontinuities affected the point at which sliding of the overlying blocks begins to develop. Thus, the onset of stage 2 and stage 3 type failures will be directly related to the shear strength of the discontinuities. Figure 6.9 and 6.10 are computer simulations and illustrate the effect of varying friction angle on the development of failure.

2 ASPECT RATIO. When the aspect ratio of the blocks was large (ie the blocks were long and thin, the mode of failure progressed rapidly from a type 1 to a type 2 failure. However, because of the interlock effect that developed between the long slabs at the apex of the arch, the onset of the stage 3 type failure was delayed. In contrast when the aspect ratio was low, ie. the blocks were short and fat, the mode of failure progressed from a stage 1 type failure almost directly into a stage 3 type failure. In these cases, mass instability was usually brought about by the buckling of the sides of the arch into the excavation.

3 HORIZONTAL FORCES. Very high horizontal forces were found to stabilise the model excavation. This was because the high horizontal pressure closed the discontinuities, which meant that the beds acted as beam columns (see Chapter 4). These would not fail until the weight of the blocks overcame the effect of the horizontal pressure. A high horizontal force was observed to increase the stability. This was shown by the delayed development of the type 2 and type 3 failure modes. Openings in experiments using a zero or low horizontal force were however, considerably less stable. In these instances failure progressed

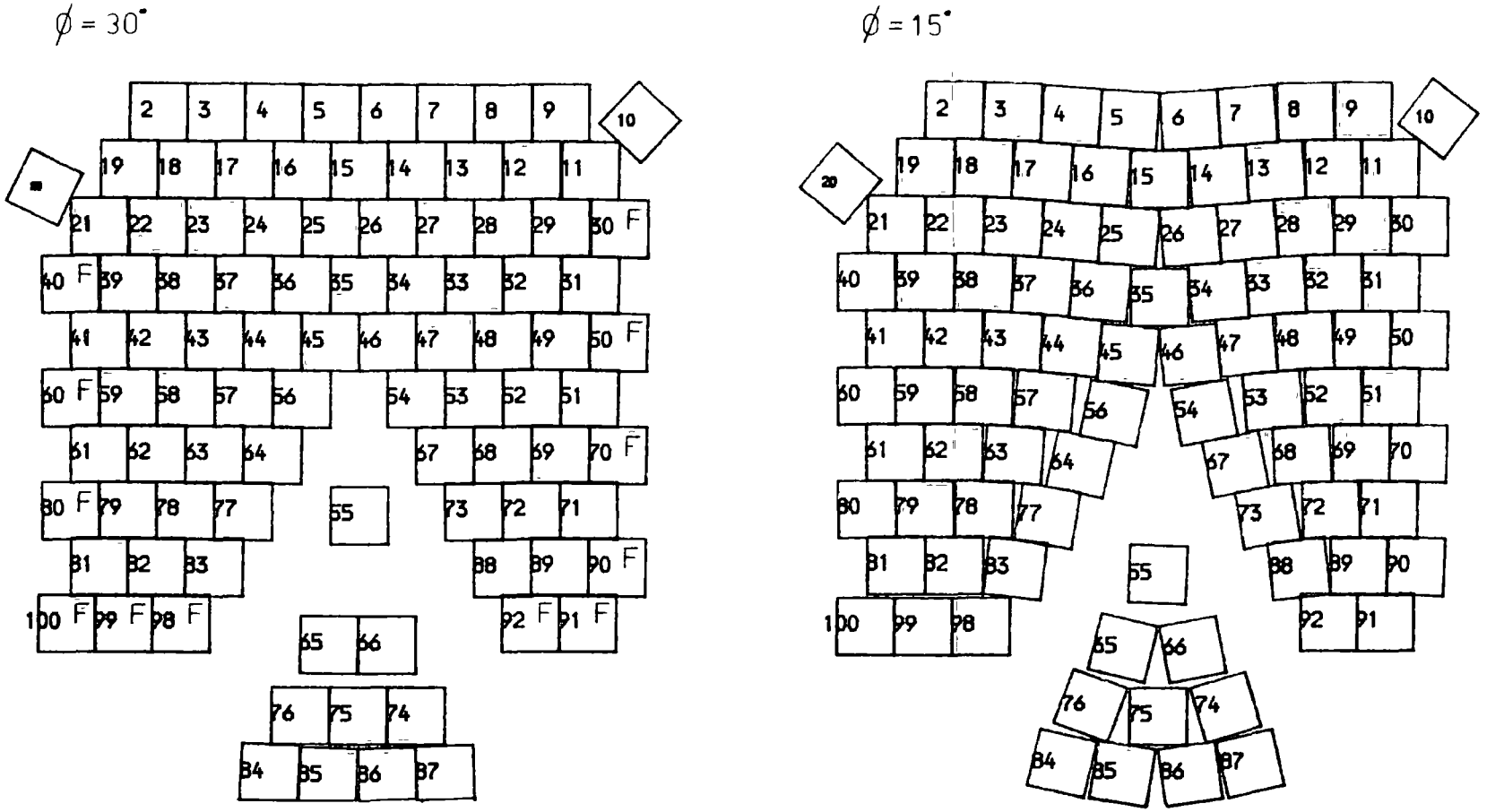

FIGURE 6.9 COMPUTER SIMULATION OF THE EFFECT OF CHANGING THE FRICTION ANGLE ON THE DEVELOPMENT OF COLLAPSE. BLOCK ASPECT RATIO = 1

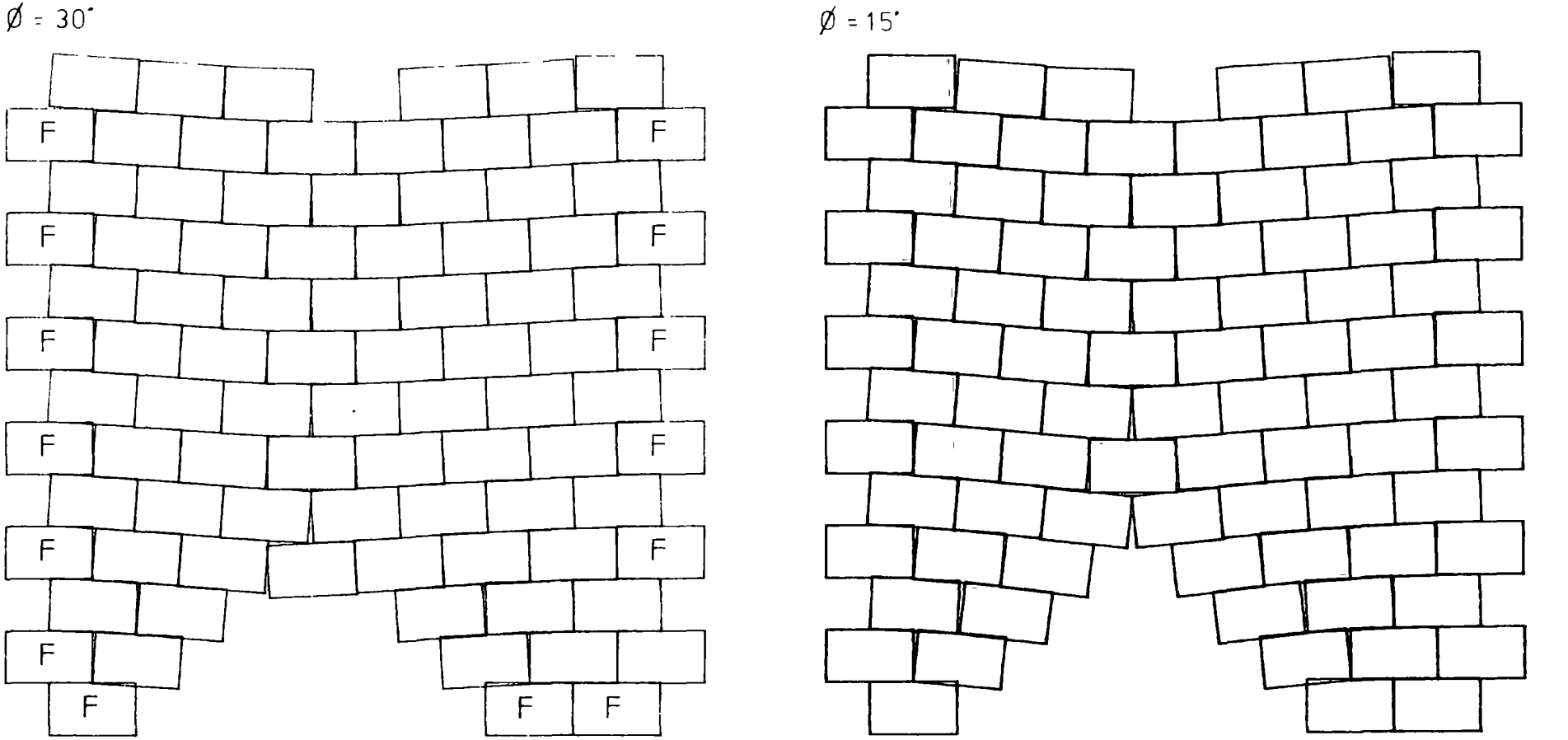

Blocks marked F are fixed and unable to move. The equivalent blocks in the adjacent simulation are also fixed (but not marked)

Overlapping blocks represent high stress contacts

FIGURE 6 10 COMPUTER SIMULATION OF THE EFFECT OF CHANGING THE FRICTION ANGLE ON THE DEVELOPMENT OF COLLAPSE
BLOCK ASPECT RATIO = 2

rapidly through the various stages to mass instability.

4 VERTICAL FORCES. High vertical forces increased the stability of the opening. The effect that both the horizontal and vertical forces had on the stability of the opening can be explained by considering the discontinuities. In a loosely packed and poorly restrained mass the blocks are able to rotate, but to rotate they need space in both the horizontal and vertical direction. This space comes from the discontinuities. If the discontinuities are wide and open, then the blocks can rotate significantly and this promotes the onset of the stage 2 type failure. However, it the blocks cannot rotate, either because of the high horizontal forces eliminating the discontinuity spaces, or because of large vertical forces, then only the unsupported kinematic wedge is able to drop out and rotation will not take place. By analogy therefore, in the field one would expect (theoretically anyway) that old workings in ground with high horizontal forces would be more stable and exhibit less collapse than workings in loose or disturbed ground. (See Chapter 10 for comments on collapse locations with respect to residual stresses in the Appalachia coalfield). Similarly it would be expected that workings at depth should be more stable than surface workings. Unfortunately, for both of these hypotheses, there was insufficient field evidence to reach any conclusion.

The model was developed to gain an insight into the modes of failure of an underground opening. The inter-relationship between void span, collapse height, block aspect ratio, horizontal/vertical force fields, and vertical and horizontal friction angles are complex but could be modelled numerically. Such a numerical approach is usually referred to as the discrete element or discrete block method, and was first described by Cundall (1971). Since this date numerous authors have attempted a solution to the problem, but to the present writer's knowledge, nearly all have been unsuccessful in producing a program that exactly models the correct inter-block contact forces and failure path. The present writer spent a considerable amount of time developing and correcting one of the original versions of the Cundall program. However, the programming problems were immense and although results were obtained, the model must be

considered suspect for quantitative use. In any event the attempt was superseded by the release of a 'correct and working' version of the program Maini et al. 1978). This version of the program had been completely re-written and considerably extended by a group of programmers under the direction of Dr. Cundall. The present writer obtained a version of this program and loaded it onto the Durham computer. Unfortunately, this program was also found to be fatally flawed Rouse (1982), Watson (1983) and therefore, an accurate quantitative computer simulation of a collapsing old working using this technique has proved to be impossible to obtain at this time. However, many qualitative simulations have been produced and these appear to endorse the observations made during the model studies described above. Figures 6.9 and 6.10 were all produced using the present writer's considerably modified version of the Cundall (1971) program. The rigid block technique is still being developed in a few countries, and is actively being pursued at both Durham University and Imperial College.

6.6. QUALITATIVE EVALUATION OF TEST RESULTS

While the results from the base friction experiments could not be used in a quantitative way, they can be used in a qualitative way. During the experiments it was observed that there were two zones of 'movement'.

1 A zone of primary movement which has been discussed already. This is the height of the unstable zone and is characterised by the type 1,2 and 3 modes of failure.

2 A zone of subsidence or ground lowering. This developed in all the models examined and appeared as a zone of movement well above the height of the unstable zone. The development of the subsidence zone was however, limited by the same controls as the zone of instability. In other words, high horizontal forces, high friction angles and short spans reduced the height of the subsidence zone whereas, low horizontal forces, low friction angles and long spans promoted the full development of the subsidence profile.

An explanation for the observed mechanism is illustrated in Figure 6.11. At first just the wedge of unstable, unsupported blocks falls out (Type 1 failure). Block A is fixed and stable. Block (a) rotates on the corner of A. This provides a force upwards (2) on to block (d). This is transmitted to block B. Meanwhile block (c) also rotates and slides forward towards the excavation. Further rotation about the top corner of block (a) is prevented by contact with block B. This contact has the effect of rotating block B AWAY from the opening rather than towards it. This has the effect of stabilising the edge of the arch at this point, and block B provides a sound footing from which the failure in the next layer can develop. The block progression A,B,C,D,E therefore, marks the boundary of the stable zone or 'zone of arching'. The onset of a type two failure is when the blocks start to rotate a significant amount. When this happens some blocks may slip out, blocks (c) and (e) are particularly susceptible. If these blocks fall out it effectively increases the span of the arch apex, in which case blocks (f), (g), and (h) are unsupported and will also fall out.

The experimental results illustrate this theoretical progression (Fig 6.7). The onset of the type 2 failure is marked by the sudden increase in the height of the arch.

Mass instability develops either when the apex of the arching zone breaks the surface, or when there are insufficient horizontal or vertical forces acting on the apex of the zone of arching to maintain its stability. If the apex of the arch buckles, the complete system collapses.

6.7. PRACTICAL APPLICATION OF THE KINEMATIC RELATIONSHIP

The mechanism of collapse has been shown to be more complicated than that envisaged and used by Voegele (1978). However, if the initial assumption concerning the nature of jointing and the aspect ratio of the blocks are correct, the basic relationship that he suggested should still be valid after some modification. For the situation illustrated in Figure 6.8 where the vertical jointing has the maximum vertical discontinuity, a type 1 failure will

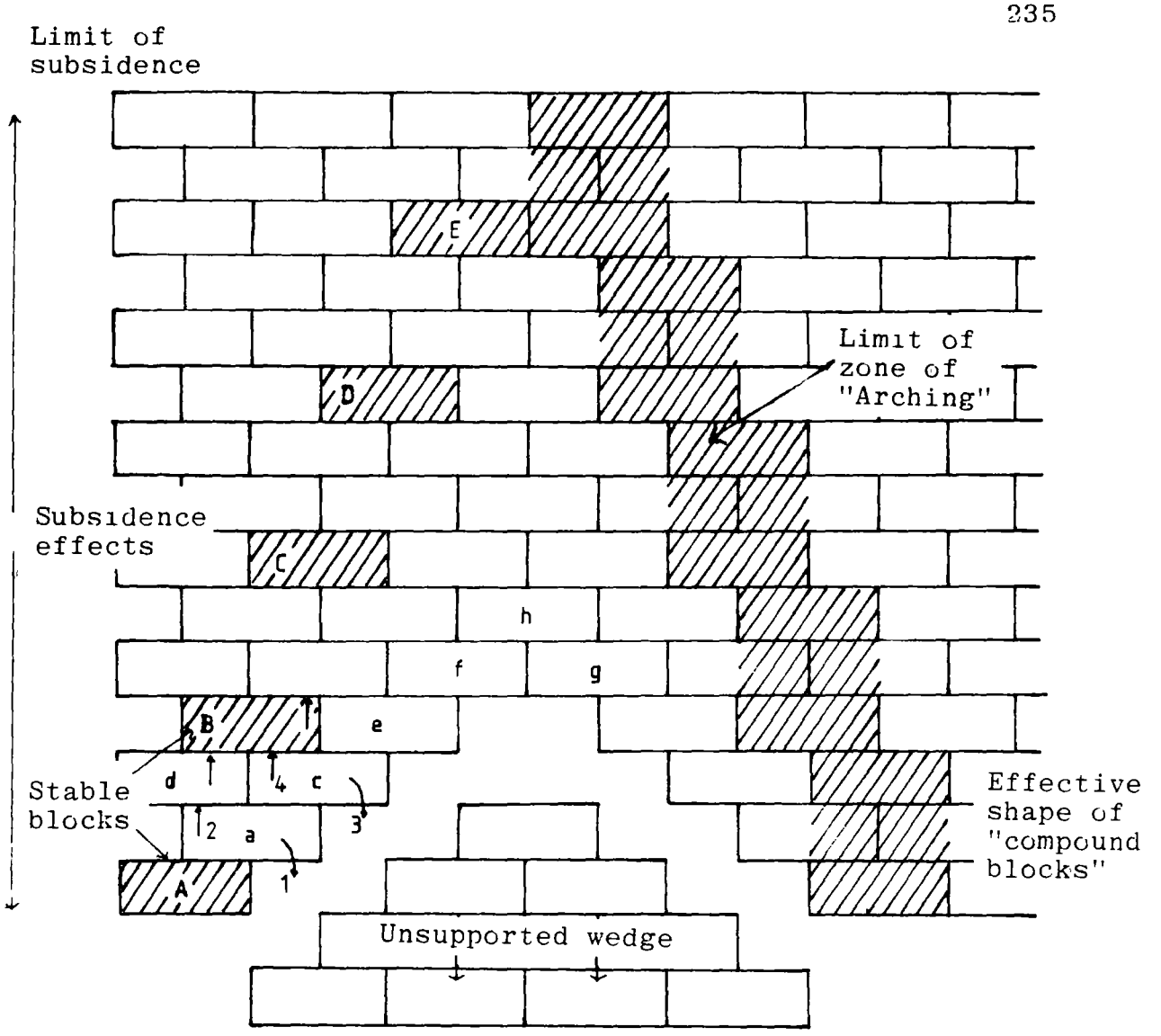

Unstable blocks = a,c,e.

Figure 6.11 Mechanism of collapse of a block jointed system.

still be characterised by the relationship:-

$$h = \frac{S}{A}$$

The height of the zone of subsidence can also be be characterised. Study of Figure 6.7 suggests that the stabilising effect of blocks A,B,C,D, and E can be seen in terms of composite blocks, each comprising three normal sized blocks. These composite blocks therefore, effectively have a block aspect ratio of 1/3 the true value. Thus, the relationship can be modified to predict the maximum height above the working that any subsidence effect would be noticed.

$$h(sub) = \frac{3S}{A}$$

Experimental observations on the models suggest that the coefficient actually varies between 2 to 3. The value increases as the span increases, or the forces or friction angle decrease.

A type 2 collapse reaches a height mid-way between the height of the kinematic wedge and the limit of subsidence. Experimental observations suggest that the effect is equivalent to dividing the block aspect ratio by between 1.5 to 2. As noted above, the higher figure represents the wider spans and lower friction angles. Hence:-

$$h = \frac{1.5 \text{ to } 2\ S}{A} \quad \text{..... (Eq 6.3)}$$

It is interesting to note that when this correction is applied to the calculation performed earlier, again using the average block thickness and aspect ratio obtained from field data (Table 6.2), a slightly more realistic collapse height is obtained. viz:- (h=0.7m). However, this value still falls short of the observed average collapse height of 2.5m. These average values of a 2.5m collapse for a 2m wide working can be used in a back analysis of the type 2 relationship (Eq 6.3). Substituting the values indicates that the operating block aspect ratio lies somewhere between 1.2 and 1.6. Only two conclusions can

be drawn from this:-

a). The rock units in the roof are acting together as short thick blocks, and that these subsequently break down after the unit has collapsed into the excavation. If this is the case then the value of recording the aspect ratios of loose blocks on an opencast site is called into doubt (see Denby et al., 1982). These authors recorded typical block thicknesses and volumes for Coal Measures rocks. It is therefore, pertinent to contemplate how one would obtain reliable data for input into a discrete element computer program, or a finite element program with joint elements.

b). The alternative conclusion is that the theoretical model which assumes that the jointing is vertically discontinuous (Fig 6.8) is invalid. If this is the case then the validity of a large number of the more advanced computer analyses are cast into doubt.

This point will need further clarification and research before the discrete element computer method can be used with confidence for the modelling of underground openings or slope failures.

6.8. SUMMARY.

A theoretical relationship for predicting the height of the unstable zone based on the kinematic approach used by Voegele (1978) has been found to be too simplistic to be of widespread value. Model studies suggested that the relationship was a good deal more complex and was governed by numerous inter-related factors. These included the discontinuity friction angles, the block aspect ratio, the ratio between the span of the working and the block length, and the applied horizontal and vertical forces.

Two zones of movement have been recognised from the model study. A zone of primary movement which includes the kinematic wedge of Voegele, and a zone of 'limited subsidence'. Within the zone of primary movement, three modes of failure were differentiated and approximate relationships have been derived to predict their height or influence.

Running parallel to this approach was a data gathering exercise aimed at obtaining accurate information on the distribution and relationships between block thicknesses, length and breadth. These data revealed that the average aspect ratio for a sandstone was significantly lower than for a siltstone or mudstone. The aspect ratios for these latter rock types were statistically indistinguishable, and had a combined average aspect ratio of about 6:1.

Predicted collapse heights, based on the aspect ratio data gathered in the field, have not been found to tally with field observations. This suggests that the rock units may split and break down once they are released from the rock mass (ie. they split to form long and thin plates). If this is the case then the practical value of recording block sizes in the field is called into doubt. Alternatively, the established theoretical model for characterising discontinuous rock masses does not hold true for Coal Measures strata. If this is the case then the validity of several computer techniques is called into question. Further research is needed to clarify this issue.

CHAPTER 7

ARCHING THEORIES

7.1 INTRODUCTION.

In perfectly elastic rock, the height of the destressed zone above the working and the magnitude of the roof load are independent of the depth at which the working exists. In perfectly plastic rock however, the magnitude of the roof load is directly proportional to the depth of the working. Numerous simple theoretical models have been developed over the years to predict the height and shape of the destressed zone that surrounds a mine or tunnel opening. These can broadly be divided into two groups. Those theories that are independent of depth, and thus consider that the tunnel is within the elastic limit of the surrounding rocks, and those theories that are dependent on depth, and thus recognise some measure of plasticity in the rock mass. Within each group are a broad spectrum of theories, ranging from purely observational and empirical relationships to equations derived entirely from theory. They are all however, characterised by the making of gross assumptions about the nature of the stress distribution and/or the material properties of the superincumbent rock. In their favour is numerical simplicity; they are all generally very quick and easy to use.

Many of the equations obtained from the tunnelling literature were derived to predict roof loads and so do not express the size of the suspended zone in terms of its height. In most cases though, some assumption has been made about the shape of the suspended zone, and it is usually possible to re-phrase the relationship in terms of its height. However, considerable care has to be exercised in differentiating between those theories that predict a suspended zone which is not necessary for the stability of the remaining arch, (ie those that predict a rock-like failure mechanism), and those theories that require the presence of the material in the immediate roof to maintain stability. In spite of the assumptions some of these latter theories can still be of use for comparative purposes and for predicting the additional loads that a 'simple' or

Voussoir beam may be subjected to.

Several of the tunnelling theories assume that the opening has been driven in uniform soil or rock. However, in stratified mineral deposits the roof of an opening is nearly always of a different rock type to the abutments. This can cause problems in that some theories start from the assumption that the failure will initiate by shear from the bottom corners of the abutments and will develop through the abutments at an angle from the horizontal of 45+Ø/2 (Fig 7.1). At roof height these shear failures have the effect of increasing the span over which the rock has to arch. Shear failure through the abutment has not been found to be typical of shallow old workings and very little evidence of this type of failure has been seen in the field by the writer, even though many hundreds of workings were examined. Therefore, all theories that include abutment shear have been re-derived and are presented below in a modified form which assumes that the arching action is restricted to just the width of the working.

A detailed discussion on each theory is considered to be outside the scope of this work and has thus been omitted. However, each relationship has been checked to ensure that it is correct and gives reasonable answers. The dimensions and terms shown in Figure 7.2 have been used throughout the Chapter, and the angle between the horizontal and apex of the suspended zone (angle alpha), has been calculated for every theory. This is so that a comparison can be made between the angles predicted by theory, and those observed in the field (Chapter 3).

7.2. THEORIES NEGLECTING THE EFFECT OF DEPTH.

Engesser (1882) used the analogy of arching action in a masonry arch as the underlying principle for his theory (Szechy, 1970). He arbitrarily assumed, on the basis of the conditions for the equilibrium of the arch, that the minimum specific pressure would occur when the angle beta, between the end tangent of the load carrying arch and the horizontal, equalled the angle of internal friction for the rock (Fig 7.3).

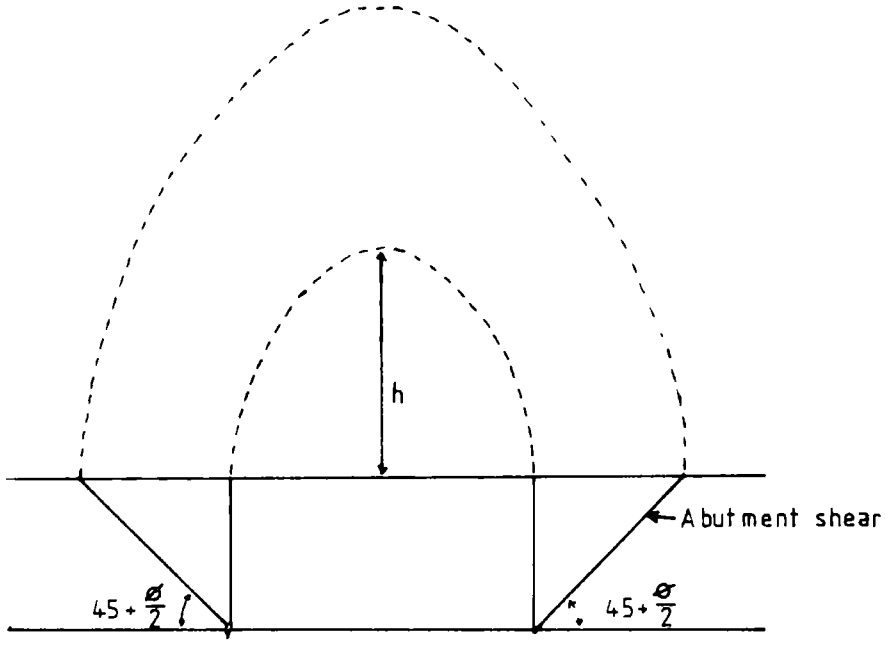

Figure 7.1 Effect of shear failure in the abutment.

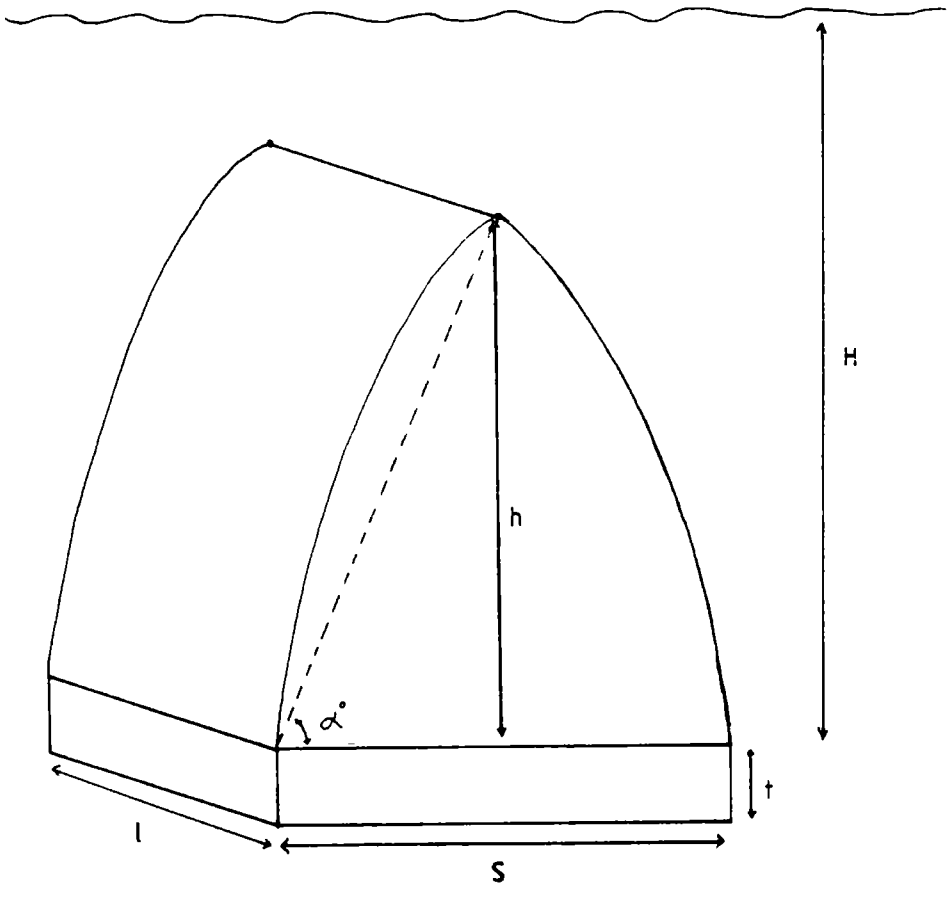

H = Depth of the top of the coal from the surface
t = Thickness of coal seam
h = Height of collapse, or height of suspended zone
S = Span of working
l = Length of working
α = Alpha angle, angle from horizontal to apex of arch (irrespective of shape)

Figure 7.2 Nomenclature used for arching theories.

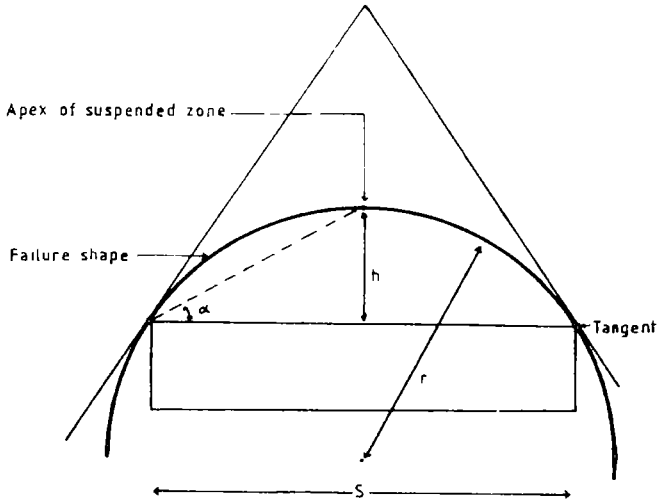

$$h = \frac{\tan\phi \; S}{4}$$

$$r = \frac{S \; (\; \tan\phi + 2\tan(90-\phi))}{4}$$

Figure 7.3 The theory of Engesser (1882), after Szechy (1970).

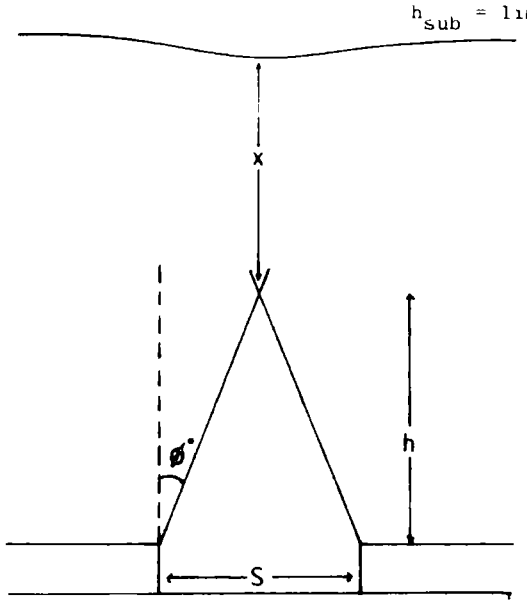

$$h = \frac{S}{2 \tan\phi}$$

$$h_{sub} = \frac{S}{2 \tan\phi} + X$$

Where X = 5 - 10m

Figure 7.4 The theory of Bierbaumer (after Szechy (1970).

The theoretical results were apparently checked against some results obtained from experiments on a sandy soil and Engesser found that there was fair agreement provided that the depth from the surface was greater than 1.5 times the span of the opening. The shape of the failure surface was found to be an arc of a circle whose radius is defined by r in Figure 7.3. Engesser's relationship is probably invalid for the prediction of the height of the destressed zone because it assumes that the material is still present and has not dropped out of the destressed zone. However, of all the forthcoming relationships this relationship predicts the lowest value for the height of the suspended zone.

The relationship in Figure 7.4 has been attributed to Biermbaumer (Szechy, 1970), but appears also to have been proposed by a number of other authors. The relationship is of interest because it recognises that while the simple relationship may represent the height of the unstable zone above the tunnel, subsidence will probably occur beyond this maximum value. Thus, the equation is modified by the addition of a nominal additional height (X). In practice X is said to vary between 5 and 10m (Szechy, 1970). The shape of the failure surface is assumed to be linear.

Jones and Davies (1929) presented a summary of their observations on roof behaviour in British coal mines. They found that roof falls were invariably limited in height, with the majority of the arches extending between about 1 and 3m into the roof. Arches in excess of about 4.5m were considered exceptional. Judging from their description of the mining methods, the roadways were between 3.6 to 5.4m in width. They also concluded the failure surface was typically stepped along the sides, 'In the manner of a stairway viewed from below'.

Rabcewicz (1944), (after Szechy, 1970) used the analogy of a silo with a slot in the bottom in his theory (Fig. 7.5). He observed that at the midspan of the opening a small wedge-shaped mass of soil or rock would drop out of the roof into the cavity. The collapse would then progressively spread upwards and outwards in the shape of a pointed arch until the half arches became capable of

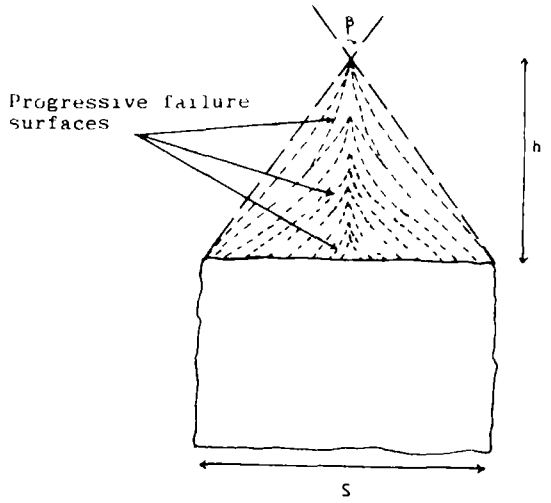

$$h_{max} = \frac{S}{2\tan\frac{\beta}{2}} \cong \frac{S}{2\sin\phi}$$

or taking $\phi = 35^{\circ}$ $h = 0\ 875$
$\alpha = 60^{\circ}$

Figure 7.5 The theory of Rabcewicz (1944), after Szechy (1970).

Ultimate overbreak if no support installed

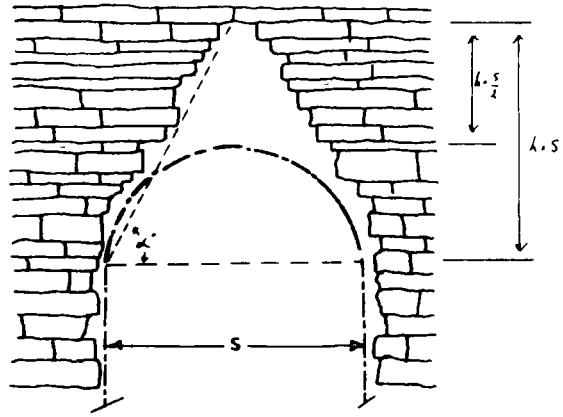

$h = \frac{S}{2}$ for semi-circular roof (Terzaghi 1946)

h = S for flat roof

h = S

$\alpha = 63^{\circ}$

Figure 7.6 The theory of Terzaghi (1946).

supporting each other. Rabcewicz (1944) noted that the angle β varied proportionally with the cohesion of the particular roof material and suggested that the height of collapse could be approximated by the relationship given in Figure 7.5. The shape of the failure surfaces are approximately linear.

Terzaghi (1946), on the basis of considerable experience in rock and soil tunnelling, noted that a peaked roof would develop above a roadway driven in thin strata weakened by many joints. For a semi-circular tunnel he considered that the overbreak would rarely, if ever, exceed a height of more than half the span of the working above the top of the tunnel. For flat roofed openings the height of maximum overbreak would be greater and can be seen to be equal to the span of the working (Fig 7.6). The theory assumes a linear collapse envelope.

Irving (1946), (after Isaacson 1962) took the outline of the destressed zone to be semi-circular and predicted the height of the potential collapse zone to be:-

$$h = 0.5 \times S$$

Where h = height of collapse
S = span width

This would therefore, provide an alpha angle of 45 degrees.

Protodyakonov (after Szechy, 1970) assumed that the arch which develops above a cavity will be unstable until the stresses along the line of the arch are purely compressive and free from bending. The arch produced under these assumptions approximates quite closely to a parabola (Fig 7.7). Note the origin, values and direction of the X and Y axis.

The theory was developed for cohesionless materials but can be used for cohesive soils and rocks by using an appropriate strength coefficient. The condition as well as the type of rock must be taken into account when selecting a value for the strength coefficient and typical values are presented in Table (7.1). In many ways this method shows some similarities to the rock mass classification methods (Bieniawski, 1979, 1981)

The only restriction imposed on the use of the equations is for cavities where the angle of internal friction is less than 40 degrees, and where the overburden

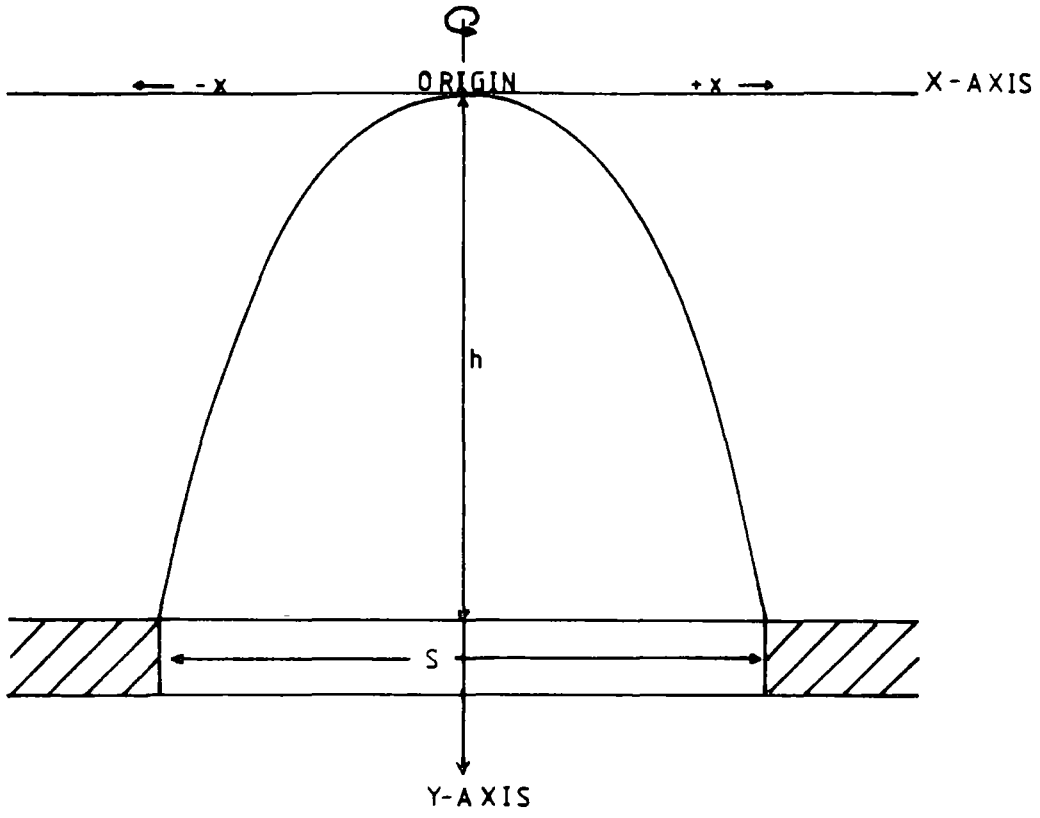

$$h = \frac{S}{2\tan \phi}$$

$$h = \frac{S}{2f}$$

$$y = \frac{2x^2}{Sf}$$

$$p = \frac{1}{3}\, y\, \frac{b^2}{\tan \phi}$$

$$f = \tan \phi + \frac{c}{\sigma_c} \quad \text{(cohesive soils)}$$

$$f = \frac{\sigma_k}{100} \quad \text{(rocks)}$$

Where : c = Cohesion
σ_c = U.C.S.
σ_k = Cube strength = U.C.S.
p = Load / unit length

Figure 7.7. The theory of Protodyakonov, after Szechy (1970).

Category	Strength grade	Denotation of rock (soil)	Unit weight (kg/m³)	Crushing strength σ_l (kg/cm²)	Strength factor f
I	Highest	Solid, dense quartzite, basalt and other solid rocks of exceptionally high strength	2800 3000	2000	20
II	Very high	Solid, granite, quartzporphyr, silica shale Highly resistive sandstones and limestones	2600–2700	1500	15
III	High	Granite and alike Very resistive sand- and limestones Quartz Solid conglomerates.	2500–2600	1000	10
IIIa	High	Limestone, weathered granite Solid sandstone, marble. Pyrites	2500	800	8
IV	Moderately strong	Normal sandstone	2400	600	6
IVa	Moderately strong	Sandstone shales	2300	500	5
V	Medium	Clay-shales Sand- and limestones of smaller resistance. Loose conglomerates.	2400–2800	400	4
Va	Medium	Various shales and slates Dense marl.	2400–2600	300	3
VI	Moderately loose	Loose shale and very loose limestone, gypsum, frozen ground Common marl Blocky sandstone, cemented gravel and boulders, stoney ground	2200–2600	200–150	2
VIa	Moderately loose	Gravelly ground. Blocky and fissured shale, compressed boulders and gravel, hard clay.	2200–2400	–	1 5
VII	Loose	Dense clay Cohesive ballast Clayey ground	2000–2200	–	1 0
VIIa	Loose	Loose loam, loess, gravel	1800–2000	–	0 8
VIII	Soils	Soil with vegetation, peat, soft loam, wet sand.	1600–1800	–	0·6
IX	Granular soils	Sand, fine gravel, upfill	1400–1600	–	0 5
X	Plastic soils	Silty ground, modified loess and other soils in liquid condition	–	–	0 3

Table 7.1 Typical values for Protodyakonov's strength coefficient

depth is less than 2.5 times the span of the working. In such situations arching does not occur. This observation therefore, provides a guide to the minimum depth that an old working must be at to be considered stable.

Protodyakonov's basic equation is identical to that proposed by Biermbaumer whose relationship is presumed to be the earlier of the two.

Mohr (1956), suggests that the rock surrounding an opening can be considered as an isotropic homogeneous elastic media. Under these rather far-fetched assumptions, the theory of elasticity can be used to predict the stress distribution around the opening. From the stress distribution, and with the use of a suitable failure criteria, Mohr predicted that the de-stressed zone around a tunnel would have the shape and size of the smallest ellipse that could enclose the tunnel with an axis ratio in proportion to the in-situ stress field.

Figure 7.8 shows the relationship diagrammatically and gives a table of height to width ratios for different Poisson ratio values. Alternatively, the relationship can be expressed in terms of the stress ratio (K):- which for practical purposes may be approximated by the relationship for normally consolidated clays, namely:-

$$Ko = (1 - \sin \phi) \qquad \text{(see Bishop, 1958).}$$

Barcza and Von Willich (1958), collected data on the size and shape of strata domes in the South African gold mines. The height to span ratios for the seven values, obtained from a depth of 1330m, varied between 0.383 and 0.917. The average value was found to be 0.63, and can be used to predict the height of collapse. This theory gives the following relationship for the height of the destressed zone:-

$$h = 0.63\ S \qquad \text{Angle alpha} = 51.5 \text{ degrees}$$

Obviously, the circumstances in which these observations were made are very different to those of shallow coal mine workings in Britain. However, if the rock is perfectly elastic and still within the elastic limit at this depth, the height to width ratio observed by these authors should be similar to those

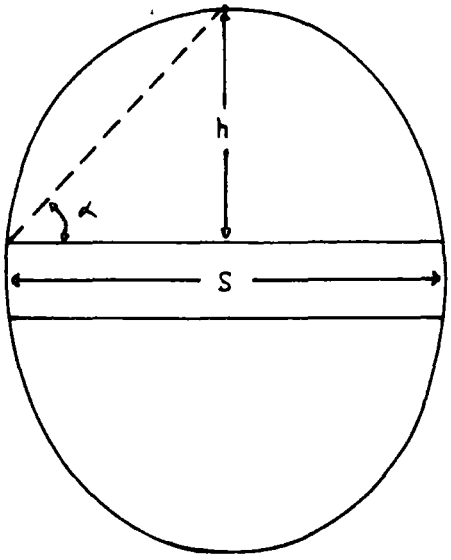

ν	h
0.20	2.00S
0.25	1.50S
0.30	1.00S
0.40	0.75S
0.50	0.50S

$$h = \frac{1 - \nu}{V} \frac{S}{2}$$

or $h = 2KS$

ν = Poisson's ratio

$$K = \frac{\sigma_3}{\sigma_1}$$

Figure 7.8 The theory of Mohr (1956).

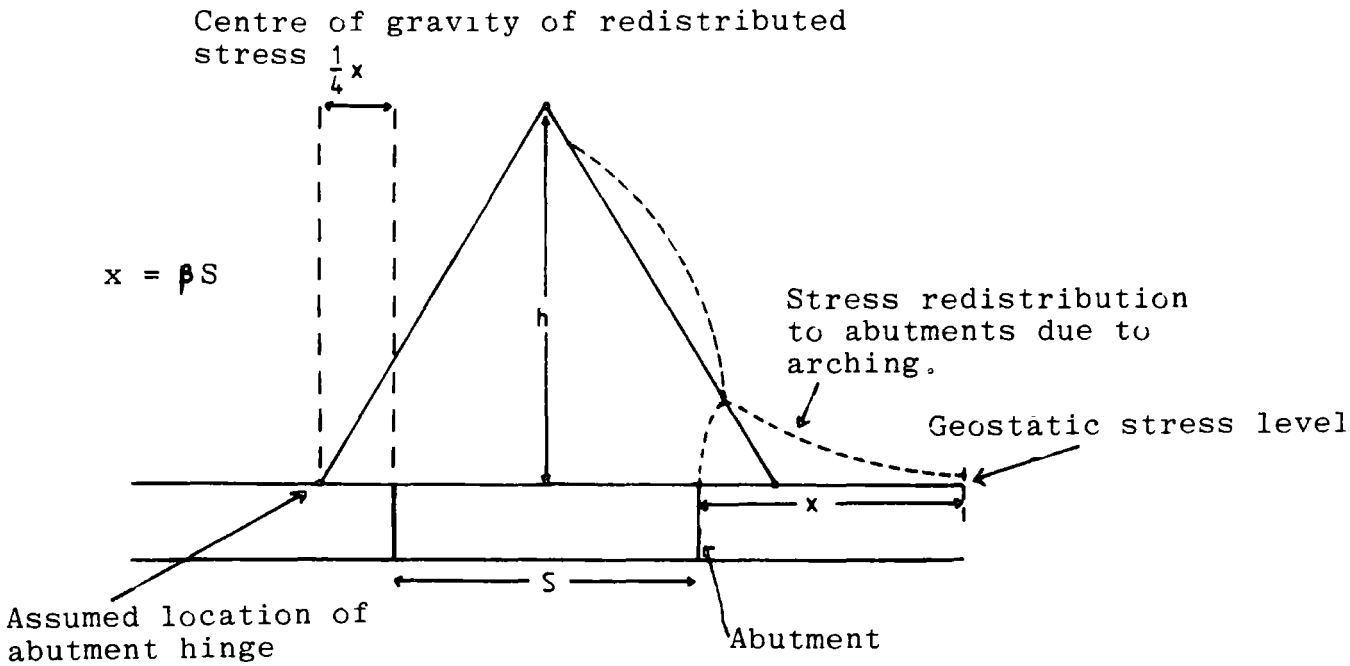

1. For a clamped beam or solid rock :

$$h = \left[1.13\left(1 + \frac{\beta}{2}\right)^2 - 0.5\right]S$$

2. For a simply supported beam or loose soil :

$$h = \left[1.13\left(1 + \frac{\beta}{2}\right)^2 - 0.39\right]S$$

Figure 7.9 The theory of Szecny (1963).

expected for old coal mine workings. No reference was made to the shape of the failure surface but the use of the term strata dome suggests some degree of curvature to the failure surface.

Szechy (1966), used a static beam analogy for his theory and provides two equations for predicting the limit of overbreak. The first equation (Fig 7.9), assumes that the roof is clamped to the abutments, and is of most value for problems involving old workings. The second equation (Fig 7.9), is recommended for use in loose soil or similar situations, where the roof could be considered to be simply supported. The relationship is thus, of little value for predicting the height of migration for old workings.

Of all the theories reviewed, this theory of Szechy (1966), provides the greatest estimate for the height of collapse.

Ackenheil and Dougherty (1970), based their theory on observations made in the Pennsylvania coalfield. They considered that the maximum angle of break, for the failure surface, from the vertical would be equal to 15 degrees. Thus the height of collapse is predicted as:-

$h = 2 \times s$ angle alpha = 75°

This theory also assumes a linear failure surface and derives from strata largely of Mississippian age with a high proportion of strong rock (limestone).

Wilson (1980) attributes the relationship in Figure 7.10 to Airey (1974). He suggests that the strata buckle and fracture at an angle to the vertical equal to the angle of internal friction. In fact the relationship is identical to that proposed by Biermbaumer and Protodyakonov which have already been reviewed.

Peng (1978) analysed the results from accident reports supplied for 22 roof falls, at roadway intersections in the Pittsburg seam (Pennsylvania). He noted that the roof above most of the falls assumed a rough dome shape with an irregular bottom, and defined the width of the opening as the average of the maximum and minimum dimensions of the openings at the roof line (Fig 7.11). These average width values were plotted against the measured collapse height and

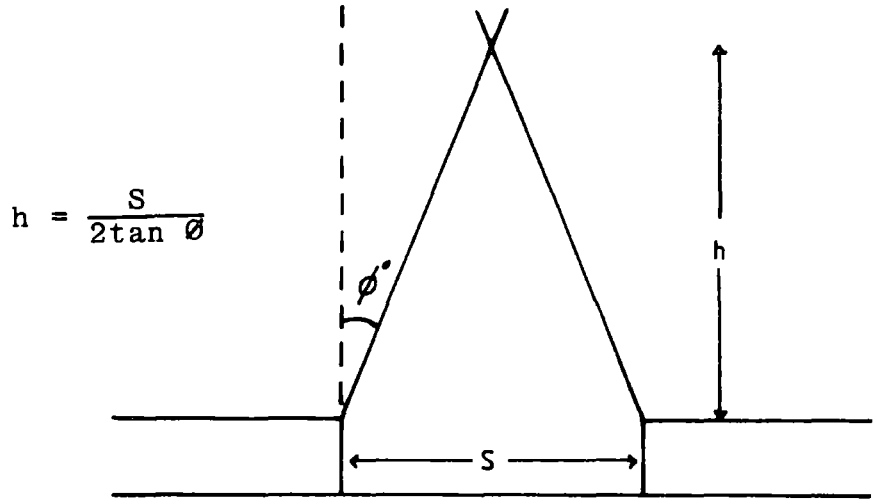

Figure 7.10 The theory of Airey (1974), after Wilson (1980).

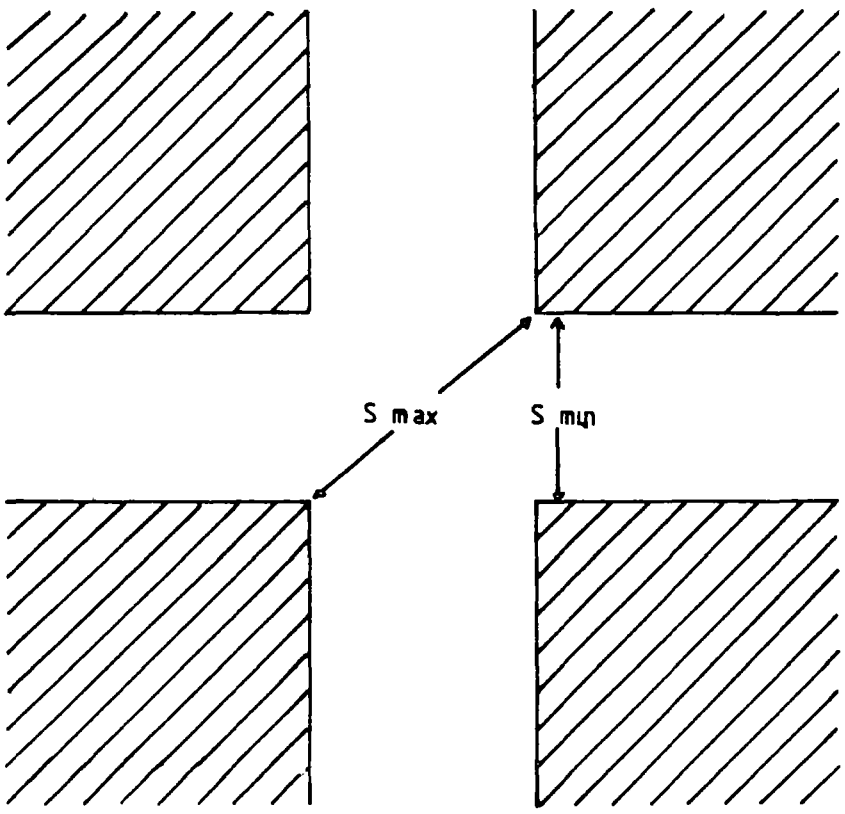

$$S_{av} = \sqrt{S_{max} \times S_{min}}$$

$$h = 0.37\ S_{av}$$

Figure 7.11 The observations of Peng (1978).

a regression line was computed for the data (see Fig 7.11).

The equation was obtained from a study of roadway intersections, and will therefore, give an incorrect answer if applied to a long roadway. However, the intention of the equation is to average the width of the opening and provided that the relationship is still valid if just the width of the roadway is used, the equation can be used to predict the likely height of collapse.

Tandanand and Powell (1982). This theory was originally applied to estimate the height of caving above a longwall face, but is equally valid theoretically for predicting caving above an old working. The theory assumes that the failure surface is a paraboloid and that the failure originates, not at the edge of the abutment, but at a small distance into the pillar. For practical purposes however, this distance is ignored.

The relevant equations and values for the height of collapse are given in Figure 7.12. The height of collapse will be seen to increase as K or Θ, and thus ϕ decrease.

7.3. THEORIES INCLUDING THE EFFECT OF DEPTH

The following theories take some account of the depth of the working beneath the surface and thus recognise in some measure plasticity in the rock mass.

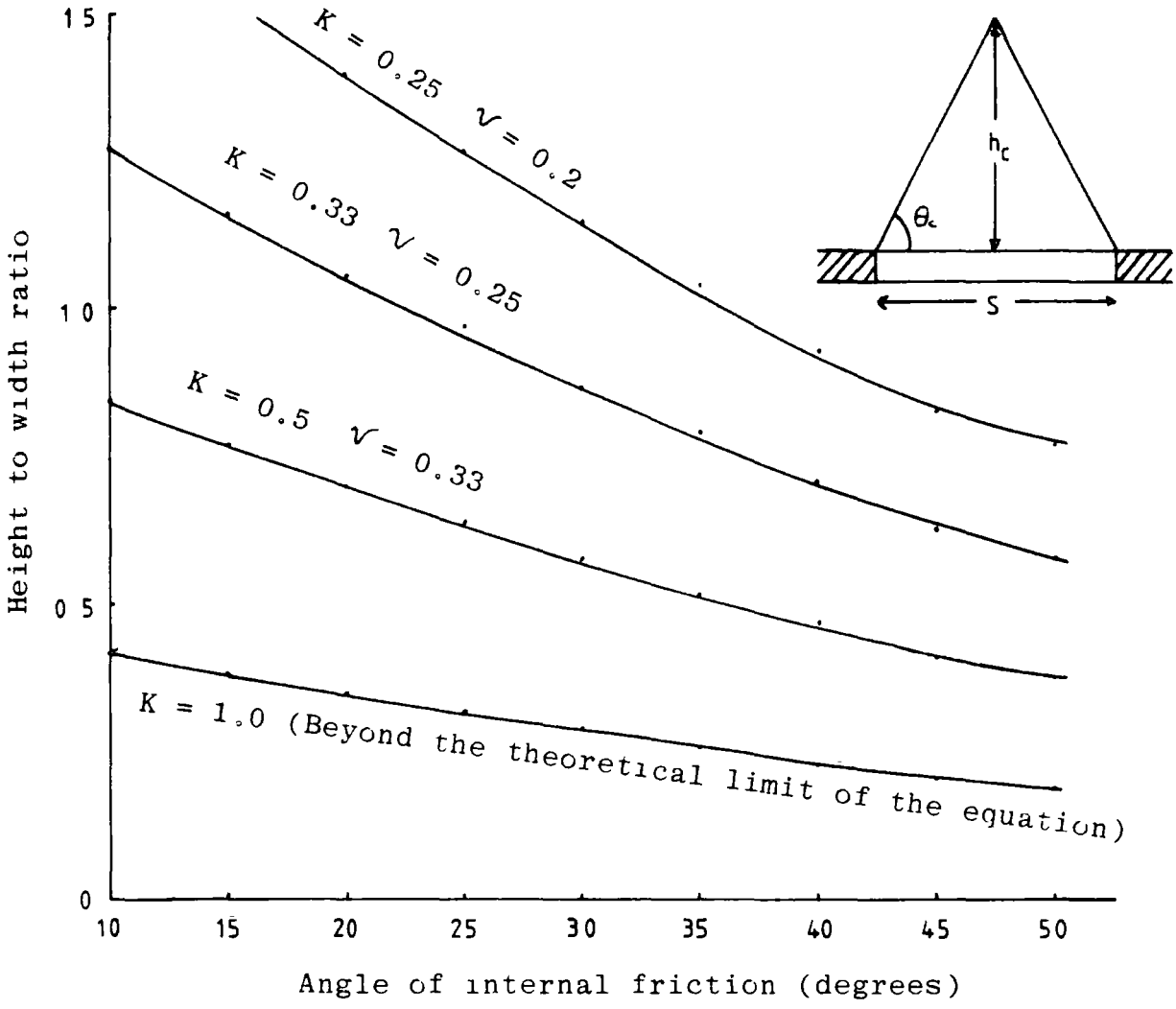

$$h_c = \frac{S}{2K \tan \Theta_c}$$

$$\Theta = 45 + \frac{\emptyset}{2} \qquad K = \frac{\sigma_1}{\sigma_3} \text{ or } \frac{\nu}{1-\nu}$$

Figure 7.12 The theory of Tandanand and Powell (1982).

Biermbaumer (1913), (after Szechy, 1970). This theory was developed during the construction of the great Alpine tunnels, and assumes that the tunnel is acted upon by a mass of rock bounded by a parabola of height

$$h = \delta H$$

The δ value, referred to by Szechy as the reduction coefficient, is proportional to both the depth and the width of the opening. Szechy gives the δ value as

$$\delta = 1 - \frac{\tan \phi \times \tan^2 (45 - \phi/2) \times H}{S + 2t \times \tan (45 - \phi/2)}$$

where ϕ = angle of internal friction
S = Span of opening
t = height of collapse
H = depth from surface

Like many of the theories, this one assumes that failure takes place within, or through, the abutments. If the abutments are considered as solid and un-deformable the equation for δ can be simplified to:-

$$\delta = 1 - \frac{\tan \phi \times \tan^2 (45 - \phi/2) \times H}{S}$$

Szechy (1970) provides a table of calculated heights of collapse for two typical tunnel dimensions using several different depths and angles of internal friction. Unfortunately many of the values given in the table differ from the results obtained from the equation. Some of the values are very close, but as the depth from the surface and the angle of friction increase, the heights of collapse predicted by the equation diverged more and more from the listed values. The derivation of the equation was checked and found to be satisfactory which implies that the table is incorrect. However, inspection of the relationship will show that if the span of the opening is narrow with respect to its depth, the coefficient may become negative. Therefore, this equation, and thus the relationship derived from it, by the present writer for rigid abutments, must be considered to be highly suspect.

Terzaghi (1946). This rock pressure theory was originally developed for cohesionless dry granular soils. However, the theory can be applied to fragmented rock and can also be extended to cover cohesive materials.

Provided that the tunnel is at a sufficient depth, the theory suggests that the majority of the weight of the overlying strata is redistributed to the surrounding soil. The body of rock which transfers the load is referred to as the ground arch (Fig 7.13). For the ground arch to develop, The roof of the opening must deform sufficiently to be able to carry the load P.

If a value of unity is assumed for the stress ratio K, the equation is seen to be very similar to that obtained by Protodyakonov, Biermbaumer, and Airey (see previous sections). However, the method of failure proposed by the two theories is completely different. Protodyakonov's theory predicts a stable dome and falling wedge, whereas Terzaghi's theory requires the roof of the void to deform sufficiently to promote the development of the ground arch and yet to remain sufficiently strong to carry the load P discussed above.

If the roof fails, the material above will cave into the void until the void is completely filled. The failure will propagate from the abutment to the ground surface forming a shear plane at an angle of $45+\emptyset/2$. This theory therefore predicts that there will be no limit to the height of collapse in cohesionless material and is thus more in keeping with longwall subsidence theory. The theory may be of value for the prediction of loads acting on the immediate roof rock where it differs from the bulk of the overburden, as for example where a sandstone forms a massive roof beam.

Balla (1963), arbitrarily assumed that the roof material would break out into the cavity along failure surfaces formed by arcs of circles which started at the upper corners of the rectangular cavity. The origin for these arcs is at roof height and at some depth into the opposite abutment. The radius for these failure surfaces is defined so that at the apex of the roof the tangents to the arcs will form an angle to the horizontal of $45-\emptyset/2$ (Fig 7.14).

The load acting on the roof of the tunnel depends on both the depth from the

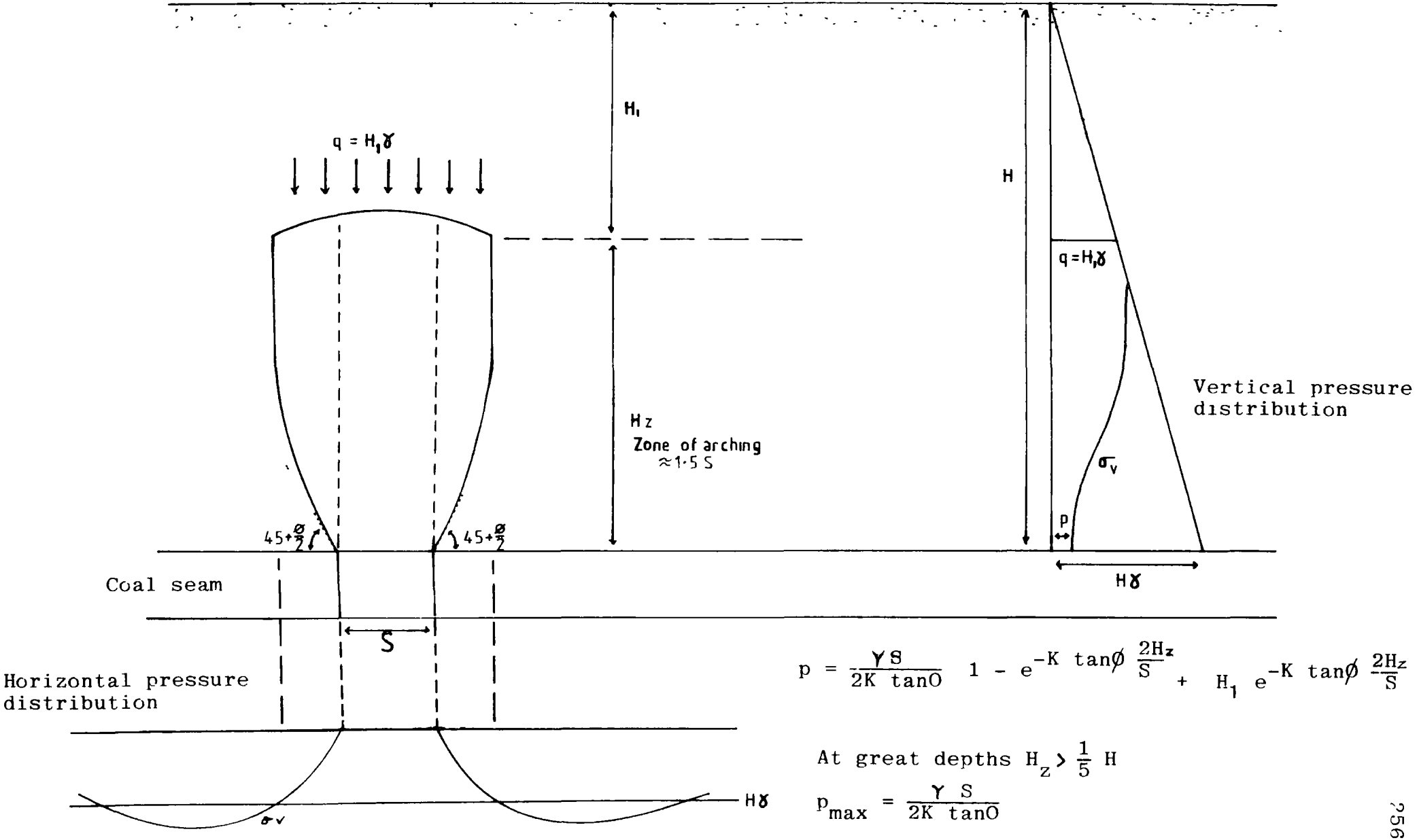

$$p = \frac{\gamma S}{2K \tan\phi}\left(1 - e^{-K \tan\phi \frac{2H_z}{S}}\right) + H_1 e^{-K \tan\phi \frac{2H_z}{S}}$$

At great depths $H_z > \frac{1}{5} H$

$$p_{max} = \frac{\gamma S}{2K \tan\phi}$$

Figure 7.13 The soil theory of Terzaghi (1946).

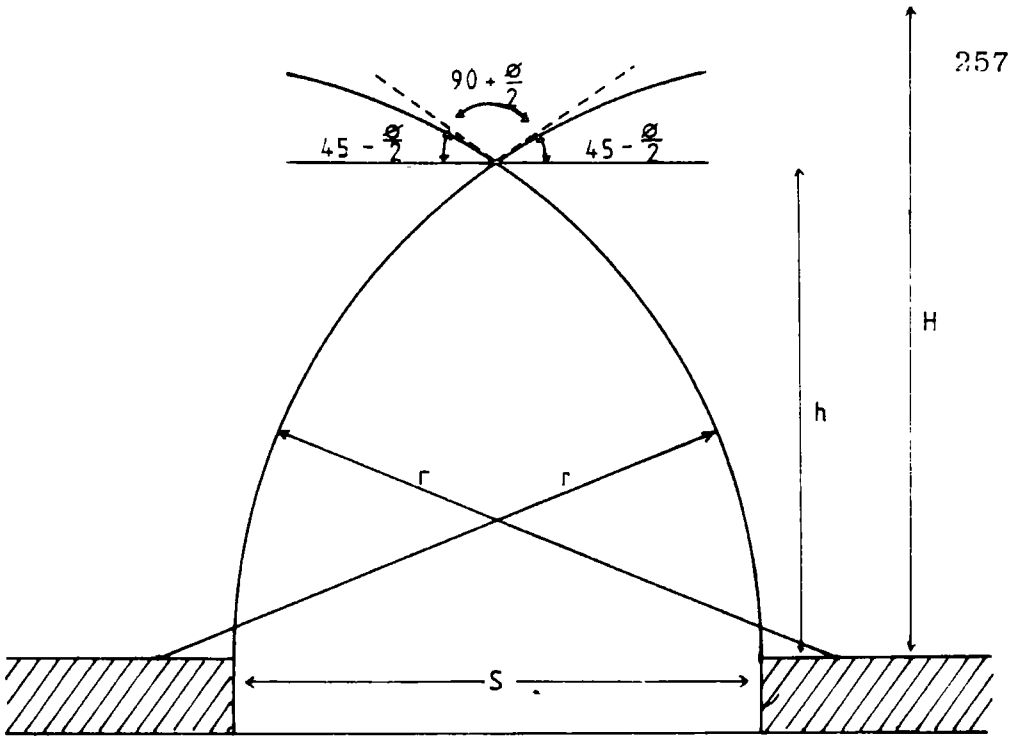

ø	h=Sx	r=Sx	F_H	F_B	F_C
10	1.072	1.572	0.6814	0.1502	1.8066
20	0.960	1.460	0.4145	0.2577	1.6084
30	0.866	1.366	0.2109	0.3277	1.3667
35	0.824	1.324			
40	0.785	1.285	0.0757	0.3671	1.1016
50	0.714	1.214	0.0333	0.3774	0.9667

$$h = \tan\left(\frac{135 + \frac{\phi}{2}}{2}\right) \frac{S}{2}$$

$$r = \frac{S}{2}\left(1 + \tan\left(\frac{135 + \frac{\phi}{2}}{2}\right)\right)$$

$$\text{load } p = H_y\left[F_H + \frac{S}{H} F_B - \frac{c}{H_y} F_C\right]$$

Figure 7.14 The theory of Balla (1963).

ø	h = S x	r = S x
10	1.072	1.572
20	0.96	1.460
30	0.866	1.366
35	0.824	1.324
40	0.785	1.285
50	0.714	1.214

S = span of opening

h = height of arch

r = radius of curvature of arch

TABLE 7.2

HEIGHT TO WIDTH RATIOS FOR VARIOUS VALUES OF ø, CALCULATED USING THE THEORY OF BALLA (1963)

surface, and the angle of internal friction, whereas the shape of the destressed zone is just dependent on the angle of friction, and is independent of depth. Table 7.2 gives equivalent height to width ratios and alpha angles calculated for a number of different values of internal friction.

The theory of Denkhaus (1958) is claimed to be an extension of a theory of Fenner (1938), (Fenner's theory is very similar to the theory later proposed by Mohr (1956) which has been reviewed in the previous section). The theory assumes that the rock mass is homogeneous, isotropic and perfectly elastic and that the optimum shape for the de-stressed zone is an ovoid or an ellipse. The fracture zone or dome that develops within this rock mass assumes a shape whereby at the boundary neither the tensile stresses nor the compressive stress exceeds the strength of the rock mass. The axis ratio for the ellipse corresponding to these assumptions can be obtained from the following formulae.

$$\frac{2h}{S} = \frac{\left(1 + \frac{\sigma t}{wH}\right)}{2K} - 0.5 \qquad \text{or} \qquad \frac{2h}{S} = \frac{2}{\left(K - 1 + \frac{\sigma c}{w H}\right)}$$

where K = ratio of lateral to vertical rock pressure prior to excavation
σt = Uniaxial tensile strength
σc = Uniaxial compressive strength
h = Height of collapse
S = Span
H = depth from surface
w = Unit weight

The ellipse will adopt the greatest of the two ratios obtained from these equations.

At first sight the equations seem quite reasonable but when the functions are plotted (Fig 7.15), their limited value becomes obvious.

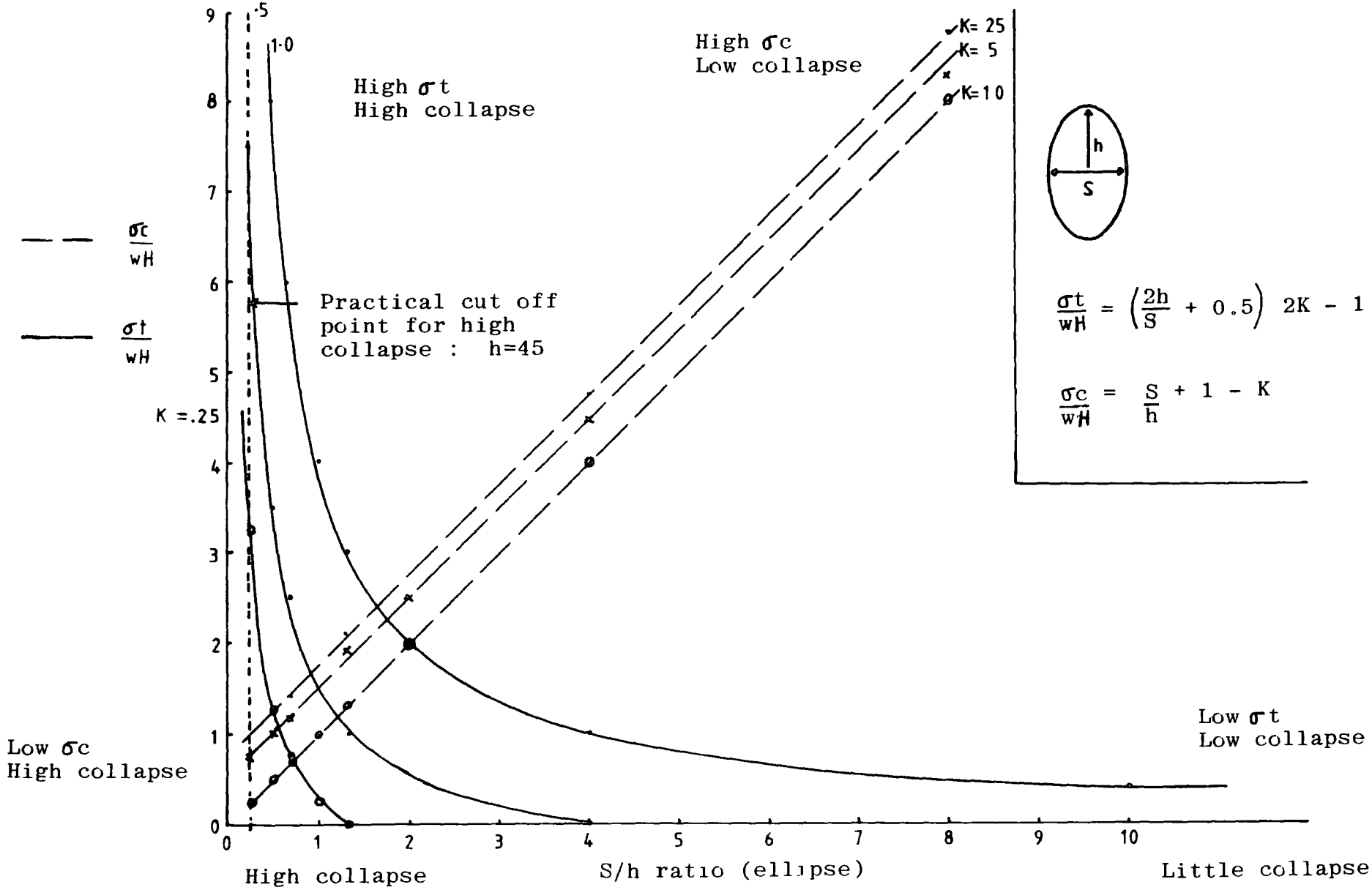

Figure 7.15 The theory of Denkhaus (1958).

Take for example a typical siltstone with the following properties:-

Compressive strength (UCS) = 26.5 MN/m2
Tensile strength = 2.65 MN/m2
Density = 2.65 Mg/m3
Stress Ratio = 0.5

The ratios $\frac{\sigma c}{w} = 1000$ $\frac{\sigma t}{w} = 100$

remembering that it is the largest h/S ratio that is the smallest S/h ratio that is taken one can obtain from the tensile strength a possible $\sigma t/wH$ value of between 0.75 and 10. This is equivalent to a depth of between 133m and 100m. In other words, as the depth of the working increases the height of collapse decreases until at 100m, there is no collapse. It is obvious that the range of heights possible do not even approximate to natural conditions and hence this theory is of no obvious practical value.

Denkhaus (1964). This theory for the shape and size of the destressed zone, is based on the equilibrium of forces at the dome boundary. In treating the problem Denkhaus draws a distinction between two situations:- (Fig 7.16)

Situation 1. Where the rock is sufficiently cohesive. In this situation, the core of the dome will not separate from the dome boundary until the weight of the core exceeds the cohesive resistance along the dome boundary. At this critical point, the whole core will collapse en-masse leaving behind the stable dome boundary. The relationship between the span and height of the dome for this situation is given by Denkhaus (1964) as:-

$$S = \left(\frac{8 \times \sigma c \times h}{w} \times \left(1 - \frac{h}{H}\right) \right)^{1/2}$$

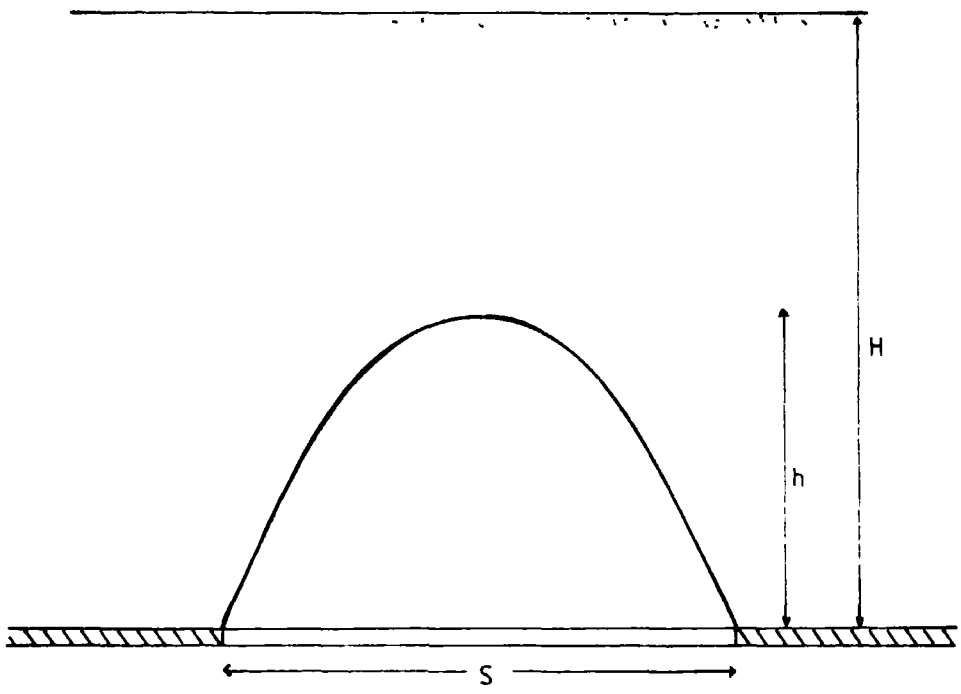

Situation 1. Sufficient cohesion.

$$S = \sqrt{\frac{8\,\sigma_c\,h}{w}\left(1 - \frac{h}{H}\right)}$$

$$h_{max} = 0.5\,H$$

$$S_{max} = \sqrt{\frac{2\,\sigma_c\,H}{w}}$$

Situation 2. Insufficient cohesion.

$$S = \sqrt{\frac{8\,\sigma_c\,H}{w}\left(\frac{h}{H} - 1\right)\ln\left(1 - \frac{h}{H}\right)}$$

$$h_{max} = 0.63\,H$$

$$S_{max} = \sqrt{\frac{2.96\,\sigma_c\,H}{w}}$$

Figure 7.16 The theory of Denkhaus (1964).

From this, the largest possible height for the dome to remain stable and the corresponding span will be :-

$$h_{max} = 0.5 \times H$$

$$S_{max} = \left(\frac{2 \times \sigma c \times H}{w}\right)^{1/2}$$

where S = span
h = height of dome
H = depth
w = specific weight
σc = UCS

Situation 2. Where the rock has insufficient cohesion. With this, small portions of the core separate from the dome boundary at short intervals while the span of the opening is increased. The relationship between the span and height of the dome is given by Denkhaus (op cit) and all subsequent authors as:-

$$\left(\frac{8 \times \sigma c \times H}{w} \times \left(1 - \frac{h}{H}\right) \log \left(1 - \frac{h}{H}\right)\right)^{1/2}$$

and the corresponding maximum height and span becomes:-

$$h_{max} = 0.63 \times H$$

$$S_{max} = \left(\frac{2.96 \times \sigma c \times H}{w}\right)^{1/2}$$

In Denkhaus's original paper there are three references to the main equation for the cohesionless situation. Unfortunately it would appear that a typographical error was made in the equation quoted in the main body of the text. This error has been found to have been repeated by all the subsequent authors who have quoted this theory (eg Wright, 1973, Adler, 1968). The error has been corrected in the equation presented below. However, this is not the only mistake in the paper. Denkhaus provides some values for dome spans and heights of collapse calculated in a worked example for the second situation of insufficient cohesion. While recalculating these values it became obvious that natural logs, rather than logs to base 10, had to be used in the text example. Assuming that Denkhaus used the correct version of the equations in his worked example then the equation for the situation where there is insufficient cohesion, when corrected, should be:-

$$S = \left(\frac{8 \times \sigma c \times H}{w} \left(\frac{h}{H} - 1 \right) \times \ln \left(1 - \frac{h}{H} \right) \right)^{1/2}$$

In spite of the corrections made, the equations are of little practical value. This was in fact pointed out by Denkhaus himself, after he had tried unsuccessfully to use his equations in the back analysis of some South African collapse data. The values for the compressive strength of the rock that he predicted from the analysis were only a fraction (1/450) of the observed strength of the rock. This led him to conclude that:-

> 'The rigid dome concept contains too many oversimplifications to lend itself to quantitative analysis'

Regretfully this statement has been overlooked by later authors and his theory including the two mistakes has become well entrenched in the literature.

7.4. COMPARISON OF ARCHING THEORIES

The theories from which it is possible to obtain a height for the 'suspended zone', are summarised in Table 7.3. As discussed at the beginning of the Chapter (7.1), the theoretical validity of the use of some of these relationships, is doubtful. Many of the theories are ambiguous on questions relating to whether the stability of the 'arch' is dependent on the presence of the 'arch core' material, or on how much movement is tolerated.

For purposes of comparison, the equations have been summarised and are presented, along with typical predicted values for the height to width ratio, in Table 7.3. The values have been calculated for a typical angle of internal friction (Ø) of 35 degrees. These height to width ratios are directly comparable with the field observations summarised in Chapter 3.4.3 (Table 3.1, Figs 3.30, 3.31)

With one or two notable exceptions (Engesser, 1882, Szechy, 1966, and Ackenheil et al. 1970), most of the equations, more or less, predict a similar height for the suspended zone. The range of values compare favourably with the typical old

Investigator	h:S ratio	Equation α°	Relationship	Assumed conditions	Slope	Required ϕ for h:S ratio 1.15	Required ϕ for h:S ratio 1.27
Engessor (1882)	0.175	19.3	$h = \frac{\tan\phi\, S}{4}$	H > 1.5	Arc of a circle	77.7°	78.9°
Bierbaumer*	0.71+x	54.6	$h = \frac{S}{2\tan\phi} + x$	Additional 'x' for max.subs.	Linear	23.5°	21.5°
Rabcewicz (1944)	0.87	60	$h = \frac{S}{2\sin\phi}$		Linear	25.8°	23.2°
Terzaghi (1946)	1	63	$h = S$		Linear		
Irving (1946)	0.5	45	$h = \frac{S}{2}$		Semi-circular		
Protodyakonov*	0.71	54.6	$h = \frac{S}{2\tan\phi}$ or $\frac{S}{2f}$		Parabola	23.5° (UCS=43.5MN/m^2)	21.5°
Mohr (1956)	0.85	60	$h = 2k_o S$ or $h = \frac{(1-\nu)}{\nu}\frac{S}{2}$		Ellipse	25.2°	21.4°
Bariza & Von Willich (1958)	0.63	51.5	$h = 0.383\, k\, 0.417\, S$ (av 0.635)		Dome		
Szechy (1963)	2	75	$h = 2S$		Parabola		
Ackenheil & Dougherty (1970)	2	75	$h = 2S$		Linear		
Airey (1974)*	0.714	55	$h = \frac{S}{2\tan\phi}$		Linear	23.5°	21.5°
Peng (1978)	0.37	37	$h = 0.37\, S$		Dome		
Tandanand et al (1982)	0.52	46	$h = \frac{S}{k\tan\theta}$	K=0.33	Parabola	15° (k=0.33)	10° (k=0.33)
Balla (1963)	0.824	67.5	$h = \tan\left(\frac{135+\frac{\phi}{2}}{2}\right) \times \frac{S}{2}$		2 Intersecting arcs of circles	$>10^{\circ}$	

*Same relationship, $\alpha = 90-\phi$. h = height of arch. S = span of working. ϕ = angle of friction.
α = angle to apex of arch from horizontal.

TABLE 7.3

SUMMARY OF ARCHING THEORIES THAT CAN BE USED TO PREDICT ARCH HEIGHT

working 'observed height to width ratios' presented in Chapter 3.4.3 (Median= 0.63, mean=0.72 Table 3.1). However, it will be recalled (Chapter 3.3.3) that these observed height to width ratios include many arches which have bridged, and so have not fully developed. With a friction angle of 35 degrees, the typical 'theoretical height to width ratio' is greater than most of the values suggested by theory.

This observation is not very surprising when it is considered that the majority of the relationships were derived to predict rock pressure and not the height of collapse. The difference lies in the fact that many of the rock pressure theories were calibrated against measured roof loads in tunnels. The material loading the structure will be, to a certain extent, self-supporting and therefore, the observed loads would be expected to be lower than the equivalent height of the destressed zone.

An alternative explanation, for the discrepancy between the observed and calculated heights of collapse, could be that the average observed angle of friction, taken as 35 degrees, was too high. To examine this hypothesis, a back analyses has been carried out on those theoretical approaches which incorporate friction angle. The typical 'field' observed values were used to derive the required angle of friction (Table 7.3).

The values predicted, for the angle of friction, are much lower than those used in the initial analysis, and vary from about 10 to 26 degrees. The relationship of Protodyakonov is interesting as it predicts, in addition to the angle of friction, the compressive strength of the rock. By his relationship this should equal 43.5 MN/m2. The value is somewhat greater than the average strength determined for the arch rock (25.7 MN/m2, Table 3.1), but it is still realistic.

7.5. SUMMARY

The theoretical validity of the use of some of the equations presented above is in doubt because of the assumptions made concerning the mode of failure. Many of the theories are ambiguous on whether the presence of the material within the

suspended zone is required for the arch to develop.

The theory of Denkhaus (1964) was found to contain two typographical errors which have been repeated by all subsequent authors consulted. These errors have been corrected in this thesis, but in spite of these corrections the relationships would appear to be of limited value.

Some of the remaining theories can provide a useful initial estimate for the height of the average collapse, but only if a low angle of internal friction is used in the calculation. Of the theories reviewed, the relationship $h = S/(2 \tan\phi)$ (Protodyakonov, Biermbaumer, (after Szechy, 1970) and Airey, 1974), would seem to have the greatest potential value. The relationship observed by Terzaghi (1946) ($h = S$) is also of value, but takes no account of the angle of internal friction of the rock.

The relationship of Szechy (1966) and Ackenheil et al. (1970) ($h = 2S$), provides an estimate of the maximum height of collapse, but these values fall short of the relationship of $h = 2.68\ S$, based on field observations, and proposed earlier in the thesis (Chapter 3.4.3).

In general all the theories underestimate the height of collapse, and this may be due, either to the fact that most of the theories were not specifically designed to predict collapse heights, or because the chosen angle of internal friction was too big. Typical values, for the angle of internal friction, that were required to provide the correct collapse height, range from 10 to 26 degrees. Spears and Taylor (1972) show that ϕ=26 degrees probably represents the minimum peak strength of a weathered Coal Measures shale. Anything lower would (logically) be a post peak value and hence it can only be concluded that theoretical arching approaches are not really appropriate for typical Coal Measures cyclothemic rocks.

CHAPTER 8

BULKING THEORY

8.1 REVIEW OF BULKING THEORY

Unlike the previous theories, bulking is not dependent on the span of the old working. For this reason it has become very popular for predicting the maximum height of collapse where the width of the working is unknown. In nearly all practical situations a generalised idea of the coal thickness can usually be gleaned from the literature; and this is really all that is required as a starting point in an analysis.

When the unstable roof of an old mine working collapses, the rock fragments will occupy a larger volume than the original intact rock. The increase in volume is referred to as bulking, and if the situation of a progressively collapsing mine roof is projected to its logical end, the bulked rock debris will eventually choke the working thus preventing any further collapse. Bulking theories can therefore be used to predict the maximum height to which a collapse will occur.

The factors affecting the height of collapse are:-

1. The initial void height, usually taken as the seam thickness.

2. The bulking factor of the collapsing rock.

3. The shape of the collapse

Unfortunately, the term bulking factor does not have a unique definition, and many different authors have used slightly different definitions in their analyses. All however, use some relationship between the volume of the rock before and after collapse.

An increase in volume can be considered as a decrease in density. As density is defined as ' weight per unit volume ', the bulking factor can be defined either in terms of an increase in volume or a decrease in density. Both methods are currently used, and gave identical results. In the following sections. The

volumes and densities cited below will be used for comparison purposes and to aid comprehension.

Vf= volume of broken rock. eg. 130 cubic units
Vi= volume of intact rock. eg. 100 cubic units
df= equivalent density of broken rock. eg. 2.6 Mg/m3
di= equivalent density of intact rock. eg. 2.0 Mg/m3

The earliest reference to a bulking factor that the present writer could find is by Rhiza (1882), (Shadbolt, 1977). However, it is extremely unlikely that Rhiza was the first to recognise the phenomena.

Rhiza actually refers to the bulking factor as the coefficient of volume increase. This by implication he defined as:-

$$a = \frac{Vf - Vi}{Vi}$$

For example, using the typical values given above the coefficient of volume increase a = 0.3

The maximum height for collapse is thus:-

$$h = \frac{t}{a}$$

h= Maximum height of collapse
t= seam extraction height

or using the typical values suggested above:

$$h = 3.33\ t$$

It is of interest to note that the coefficient of volume increase is identical in definition to the more modern term void ratio used in soil mechanics.

Fayol (1885) in his treatise on subsidence, published a table of bulking factors for various rock aggregates subjected to different loads (Table 8.1). These tests were designed to investigate the effect of depth on stowed mine waste.

	Rocks previously crushed or broken Volume remaining under pressure of:			
	1422 psi = 546 yds	2844 psi = 1092 yds	7100 psi = 2730 yds	14220 psi = 5460 yds
Clay	1.00	0.90	0.75	0.70
Shale	1.28	1.16	1.10	0.97
Sandstone	1.36	1.25	1.20	1.05
Coal	1.50	1.25	1.18	1.09

TABLE 8.1

BULKING FACTORS SUGGESTED BY FAYOL (1885) (adapted from Hughes (1904) p 184).

Fayol's bulking factor was defined as:-

$$B = \frac{\text{Volume of broken rock}}{\text{Volume of intact rock}} = \frac{Vf}{Vi}$$

or

$$B = 1.3 \quad \text{(For the typical values)}$$

The bulking factors in Table 8.1 are substantially the same as those used today, and his work is one of the source references for subsidence engineering.

Price et al. (1969) are a frequently quoted source for bulking factors. They defined B in the same terms as Fayol (ie. B=1.3, for typical values). The height of collapse is therefore:-

$$h = \frac{t}{B - 1} = 3.33\ t$$

These authors also gave two average bulking values which they suggested were appropriate for old workings

B= 1.5 for sandstones
B= 1.2 for soft shales and mudstones

These values are similar to the values suggested previously by Fayol. Unfortunately, the factors predict widely differing heights for the collapse of a working. The values represent the extremes and therefore, where the roof rocks consist of mixed lithologies, they have proved inadequate. (see Geddes, 1976).

Thorburn and Reid (1977) defined the bulking factor as:-

$$B = \frac{Vf - Vi}{Vi} = 0.3$$

and the height of collapse as:-

$$h = \frac{t}{B} = 3.33\ t$$

This is therefore the same definition and equation as proposed by Rhiza.

Piggott and Eynon (1977) follow the same trend and although developing the bulking theory somewhat further (see Chapter 8.3.2) use the same definition as Rhiza viz.

$$B = \frac{Vf - Vi}{Vi} = 0.3$$

$$h = \frac{t}{B} = 3.33\ t$$

Sutherland, Schuler and Benzley (1981), who incorrectly claim that Munson and Benzley (1980) were the first to derive the bulking relationship, completely break with the two established definitions. They define the bulking factor as:-

$$B = \frac{Vi}{Vf} = 0.7$$

This is the reciprocal of the bulking factor of Fayol (1885) and Price et al. (1969).

Lastly, Tincelin (1958) uses the alternative density relationship method mentioned previously. His relationship for the height of collapse is:-

$$h = t \left(\frac{\frac{di}{df}}{1 - \frac{di}{df}} \right)$$

If the relationship inside the brackets is regarded as the bulking factor, then:

$$\frac{\frac{di}{df}}{1 - \frac{di}{df}} = 3.33$$

This is equivalent to $\frac{1}{0.3}$ or $\frac{1}{B - 1}$ according to Rhiza's definition of B,

and

$$h = 3.33\ t$$

From the above summary it has been shown that all the equations are essentially variations on a theme proposed initially many years ago and recorded first by Rhiza. Purely for convenience the present writer defines the bulking factor as:-

$$B = \frac{\text{Volume of broken strata}}{\text{volume of intact strata}} = \frac{Vf}{Vi} \qquad \text{eg 1.3}$$

The coefficient of volume increase is taken as:-

$$a = B - 1 = \frac{Vf - Vi}{Vi} \qquad \text{eg 0.3}$$

8.2. DESIGN FORMULAE BASED ON BULKING THEORY.

Various recommended design formulae have been suggested from bulking theory. Price et al. (1969), from the bulking factors quoted above, suggested that the maximum height of collapse above an old working would be equal to 5t in mudstones or shale, and 2t in sandstones. Taylor (1975) using the average measured bulk density for colliery tip materials of 2.0 Mg/m3 and a value of 2.24 Mg/m3 for intact rock (measured from a complete cyclothem near Rotherham) predicted a maximum height of h=8t (B≈1.125). However, Walton and Taylor (1977) from observations on opencast sites suggested that a maximum value of h=7t may be more appropriate.

At this stage it must be emphasised that such simple formulae are only valid if the old working has completely choked. While it may be possible to make measurements of collapse heights and seam thicknesses from situations such as Opencast sites (see Figs. 3.33 and 3.34), these are valueless and misleading if the control on the height of the collapse is not bulking. This must be the case when there is a void above the collapse pile. In such a situation some other factor, such as arching, must be controlling the height of collapse, and therefore the ratio of 'height of collapse/thickness of seam' will not reflect any measure of bulking and will be irrelevant.

The height of collapse of the old working predicted by the above bulking theories assumes that the collapse will have vertical sides. For this reason they are not directly applicable to arches which close to afford some degree of self-support (Walton and Taylor, 1977). Recognising this oversight, Piggott and Eynon (1977) developed the theory of bulking to take into account the shape of the collapsing zone.

These authors recognised three failure geometries

8.2.1. RECTANGULAR COLLAPSE (Fig. 8.1).

The formula derived for this group are identical to the equations presented above. The theory assumes that the sides of the collapse are vertical, and predicts the maximum height of collapse to be:-

$$h = \frac{3t}{B - 1}$$

or inserting typical values $h = 3.33\ t$

8.2.2. WEDGE COLLAPSE (Fig. 8.1).

This assumes that the sides of the collapse zone corbel over the void. In cross section the wedge collapse is triangular which means that the volume of intact rock released into the void progressively decreases as the void migrates upwards. A given volume of material is required to choke the void and therefore the collapse migrates much higher into the roof than for the situation of rectangular collapse. The relationship was shown to be (Piggott and Eynon, 1977):-

$$h = \frac{2t}{B - 1}$$

or using our chosen values $h = 6.66t$

Figure 8.1 Failure geometries recognised by Piggott and Eynon (1977).

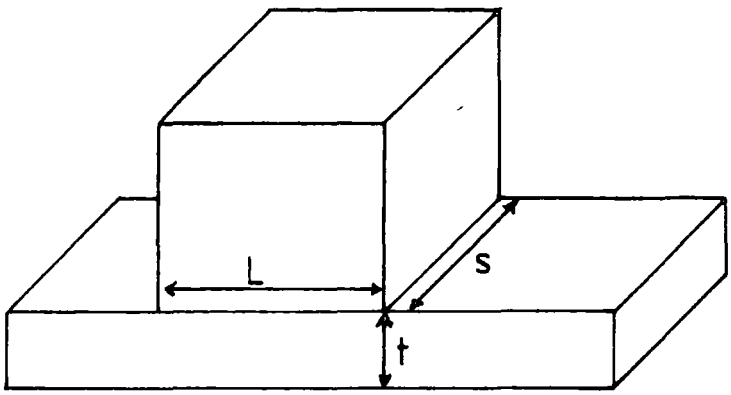

$$h = \frac{t}{B-1}$$

a) Rectangular collapse above a mine roadway.

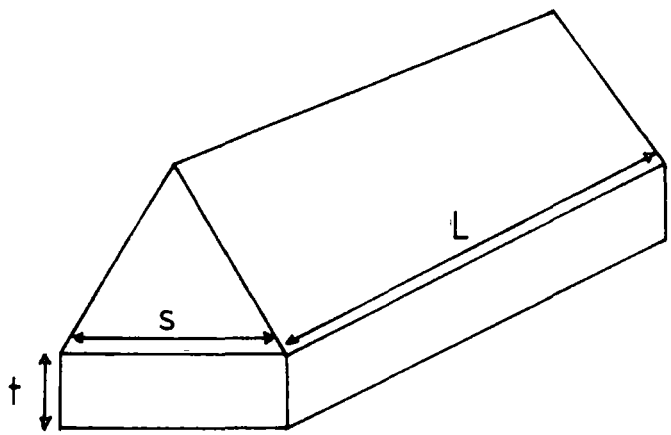

$$h = \frac{2t}{B-1}$$

b) Wedge collapse above a mine roadway.

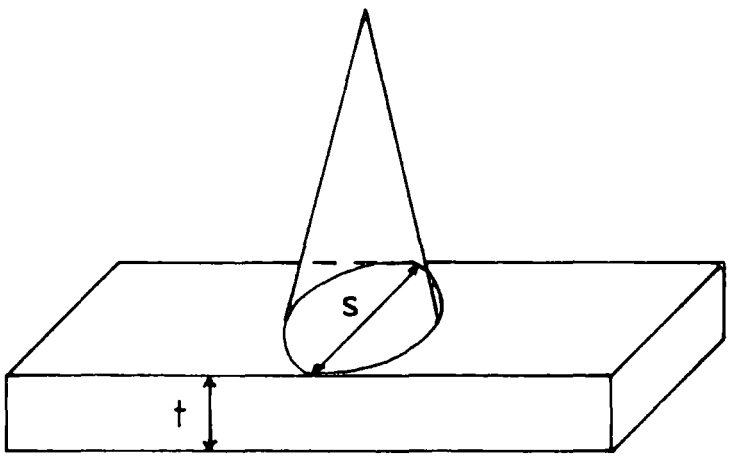

$$h = \frac{3t}{B-1}$$

c) Conical collapse above a mine roadway.

8.2.3. CONICAL COLLAPSE (Fig. 8.1).

This was said to occur typically at roadway intersections or at intermittent points along a roadway. An argument similar to that applied to wedge collapse indicates that the value of the intact rock released, decreases even faster than 2or wedge failures. Thus conical collapses can potentially migrate even higher into the roof than either wedge or rectangular shaped collapses. The relationship was shown to be:-

$$h = \frac{3t}{B - 1}$$

or using typical values, h = 10 t

This work by Piggott and Eynon led them to define a 'safe depth' for old workings. Quoting from their paper:-

> " For near surface foundations, an 'a priory' problem must be considered to exist where old mine workings are present at depths of less than ten times the extracted thickness below rockhead - The interface between solid strata and any surface unconsolidated deposits."

This value of ten times the extracted thickness has been widely adopted and used as a safety cut-off by a number of people, (Higginbottom, 1984, Parry, 1984). In view of the serious implications of defining a 'safe depth' it is worthwhile to examine the assumptions made in the analysis.

Assumptions are made in the following areas of the analysis :-

1. The bulking factor
2. The type of collapse
3. The volume of void into which collapse can occur
4. The shape of the collapse zone

In the following sections each of these will be dealt with in turn to examine

whether they are realistic. Where the assumptions fall short, the theory is developed further to overcome the shortcomings.

8.3. SHORTCOMINGS IN BULKING THEORY AND ITS DEVELOPMENT.

8.3.1. THE BULKING FACTOR.

Usually the bulking factor is considered as having a unique value for a Particular rock type, but in fact the bulking factor is an umbrella term concealing a large number of complex inter-related variables. It is unusual for a mine roof in stratified rock to collapse suddenly. Rather, the roof collapses progressively layer by layer. This has been demonstrated by numerous authors with the aid of models (Brook, 1977, Sutherland et al., 1983), and is self-evident when old workings are examined on an opencast site. The true bulking factor for a rock may be considered as the sum of the individual bulking factors for the different rock units involved multiplied by a number of complex variables which include particle size, consolidation parameters, time, stress and so forth . These can be summarised by:-

$$B = \frac{\sum_{\text{first bed (ie. initiation)}}^{\text{last bed(n) (ie. total collapse)}} (\text{Initial vol. change} \times f1 \times f2 \times f3 \times f4 \times f5)}{n}$$

where f relates to 'function of' the following:-

f1 = time
f2 = global stress
f3 = (consolidation characteristics x depth of collapse pile)
f4 = scale effect and thickness of rock unit
f5 = mechanical properties

and n = number of rock units involved.

From this relationship it might be expected that the bulking factor would vary throughout the thickness of the bulked pile. Such a variation can be appreciated if the effect of just one variable such as block orientation is considered.

When the mine roof first starts to break-down, blocks of certain dimensions fall through the height of the void until they hit the floor. The blocks fall

independently and unstressed. If they fall through a distance equal to several of their characteristic dimensions then the probability of achieving a random orientation is great, and the introduction of void space will be at a maximum. As the roof progressively collapses however, the blocks will fall through less and less height. When a block falls through a distance of the same order as its characteristic dimensions, then the probability of achieving a random orientation is much less and the introduction of void volume will be at a minimum (Sutherland and Schuler, 1981).

Sutherland et al. (1983) modelled the bulking process for two model configurations with the aid of a centrifuge and using silica sand and natural ash-fall tuff as modelling materials. They observed the change in the height of collapse with increasing g forces and measured the relative change in the void height with the progressive collapse of the layers. Figure 8.2 shows the void loss expressed as a percentage, and the change in the bulking factor (as defined for this work) with the increasing number of layers involved. It will be noted that for configuration 1 the thicker tuff beds did not break and the void was 'bridged'.

The graph of bulking factor against number of broken layers illustrates nicely the point made earlier that the bulking factor is likely to vary as the collapse proceeds and the size of the void changes. Such experimental work suggests that to have any confidence in the maximum heights predicted by bulking theory, the bulking factor should be determined from a situation directly analogous to the collapse pile in an old working. It further suggests that perhaps there should be some consolidation term included in the bulking expression. This topic will be returned to later when numerical values for the bulking factor are discussed (Chapter 8.4.1).

8.3.2. COLLAPSE LOCATIONS AND TYPES OF COLLAPSE.

Piggott and Eynon (1977) combined the effects of shape and location, and suggested that conical or rectangular shaped failures would be common at roadway intersections or at intermittent points along the roadways, whereas wedge shaped

Figure 8.2 Area loss and bulking factor for broken layers (after Sutherland et al).

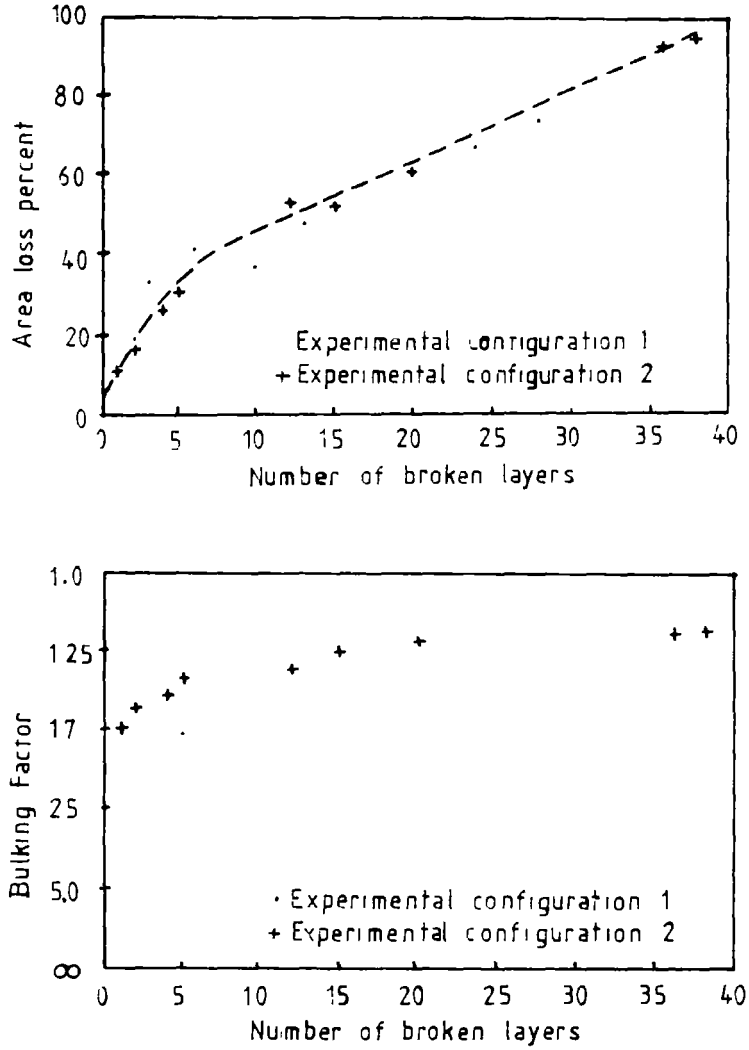

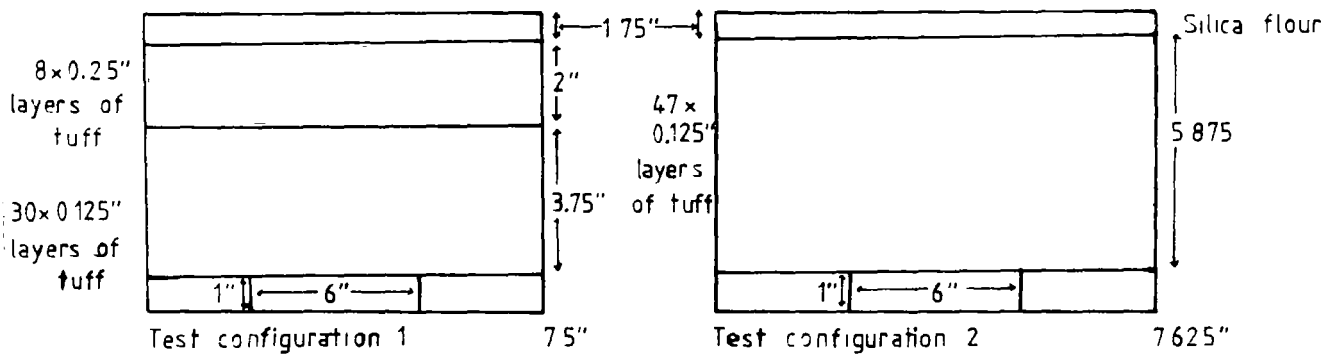

failures would prevail where a complete roadway had collapsed. While such a generalisation can be useful, this writer believes that a better understanding of the problem can be achieved by differentiating between the location of the collapse and the shape of the failure surface. When this distinction is made it is necessary to define and consider the different locations in a mine layout where collapse can occur.

There are four positions in a typical mine layout where collapse can occur (Fig. 8.3). Each location is characterised by the number of free ends to the potential collapse.

A free end may be thought of as a means of access or escape from the fall, thus a roadway collapse has two free ends, one at either end of the collapse, whereas a collapse at the end of a heading has only one free end. The number of free ends will be referred to by the value n. Thus a heading has a n value of 1, whilst an intermittent roadway collapse has a n value of 2.

a. HEADING COLLAPSE (Fig. 8.3). These are rare but occur when the roof collapses at the face of a heading. They are characterised by having one free face, ie. n=1.

b. INTERMITTENT ROADWAY COLLAPSE (Fig. 8.3). These are fairly common and usually occur at weak points in the roof. Such weak points may be due to geological reasons, poor mining technique or robbing of the support pillar at that point. The falls have a length equal to about the span of the roadway, so in plan view they have a nearly square base section. They have two free faces so n=2.

c. TROUGH COLLAPSE OR COMPLETE ROADWAY COLLAPSE (Fig. 8.3). This is the ultimate collapse stage for most mines. Trough collapse is a greatly elongated version of intermittent roadway collapse and when fully developed has no free faces, ie n=0.

d. INTERSECTION COLLAPSE (Fig. 8.3). This is arguably the most common position for collapse to occur in an old working (Chapter 10.3), and may be due

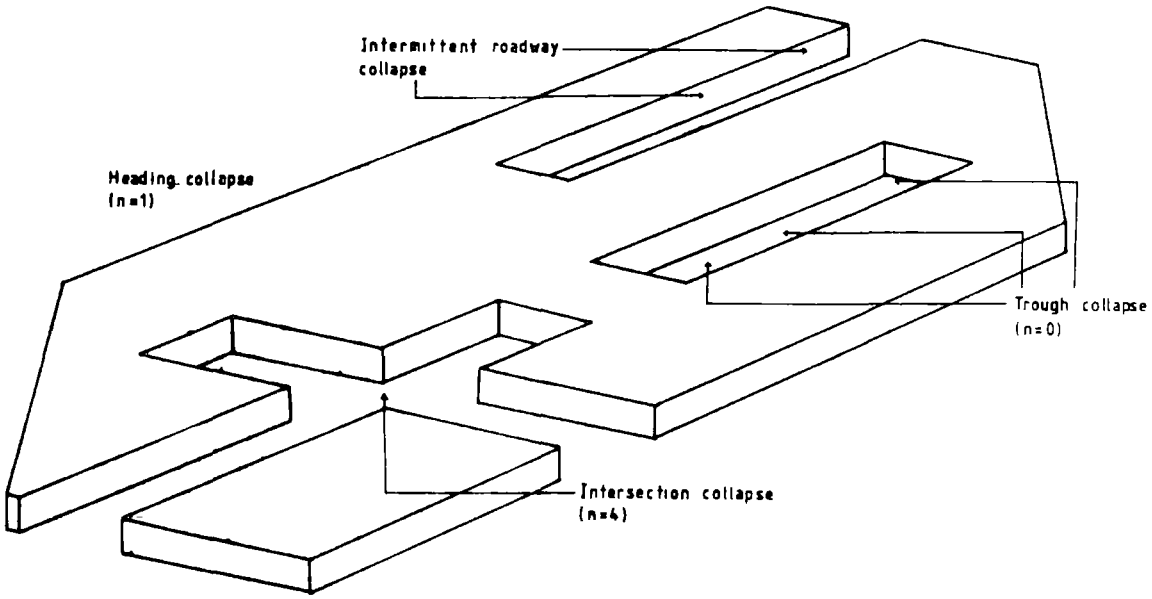

Figure 8.3 Possible locations for roof collapse.

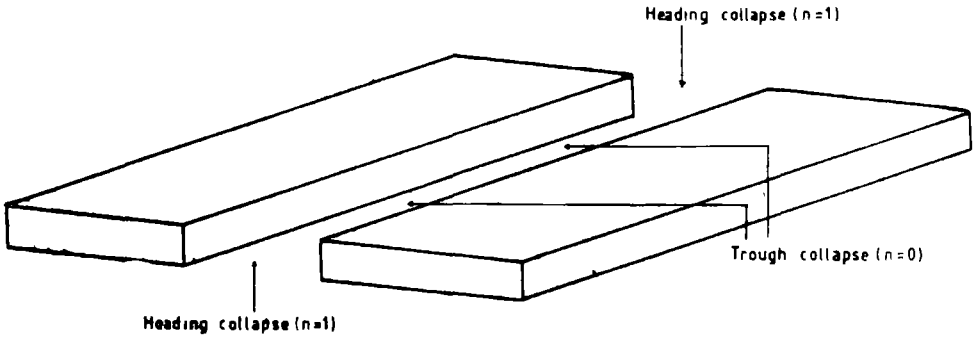

Figure 8.4 Combination of different failure types.

to one of the following reasons:- Firstly, the roof has the maximum span at this point while the corners of the pillars offer the least support for the roof, and secondly the three dimensional effect of any geological discontinuities is exaggerated at an intersection. These collapses have four unbounded faces into which collapse can occur, ie. n=4.

e. OTHER COLLAPSE GEOMETRIES. Other intersection shapes will produce other n values, eg. a triple junction will have an n value of 3 and so on.

The above types of failure can occur together: for instance it will be fairly obvious that an intermittent roadway collapse is equivalent to two heading collapses back to back. However, the most common mix of failure types occurs with trough failures. It is unusual for trough collapses to be completely confined and if a roadway is infinitely long and part collapsed, the collapse structure will be a trough collapse bounded at either end by a heading collapse (Fig. 8.4).

8.3.3. VOLUME OF VOID ASSUMED BY THE CLASSIC BULKING MODEL.

The effect on the maximum height of collapse that is produced by a change in the shape of the collapsing zone has been discussed previously (Chapter 8.2.1 to 8.2.3), where it was shown that conical collapses migrated higher than rectangular collapses. Unfortunately the original theory and the two extensions by Piggott and Eynon all make the assumption that the base area into which the bulked strata falls, has exactly the same dimensions as the base area of the collapse zone in the roof. In practical terms it assumes that the void into which the roof collapses is bounded by walls of the same dimensions as the base of the collapse zone. In a mining environment, except in the situation of trough or complete roadway collapse, this is patently not so. Take for example a simple situation of a single mine roadway. Practical observation suggest that collapse will not be initiated simultaneously at all points along the roadway but that some areas will collapse while others remain stable.

Observations show that some of the collapsed material will run under the roof of

the stable sections at either end of the collapse as in Figure 8.5. This volume is ignored by current theory, yet the volume can be significant. The extreme situation, is the equation for conical collapse (Fig. 8.6). The theory suggests that the shape of the collapse zone will be conical and therefore, the base area for the collapse will be circular in shape. While this may be acceptable, the assumption that the collapsing material will only fill the volume of a cylinder at the base of the collapsing cone is clearly not true. The theory greatly underestimates the realistic area available for the bulked material. This failure to approximate the correct area for the bulked strata must throw into doubt the value of all the current bulking theories.

8.3.4. DEVELOPMENT OF THE BULKING THEORY: VOLUME.

The shortcomings in the theory described above can be overcome. There are in fact two problems. The first is the volume of the void below the mine roof into which the collapse takes place. The second is the volume of bulked material that can be accommodated as run-in beneath the stable roof sections adjoining the fallen area . The first of these problems is best eliminated by re-defining the equations and correcting the initial assumptions. This is dealt with in a later section (Chapter 8.3.5). The remaining problem, dealing with the volume of material that can be accommodated under the roof of the stable sections of the mine, is most conveniently dealt with by considering it in terms of an increase in the initial height of the void.

a. ACCOMMODATION OF RUN-IN BY THE CALCULATION OF APPARENT VOID HEIGHT.

The apparent height of the void can be defined as:-

$$t\ (\text{apparent}) = t\ (\text{true}) + t\ (\text{run-in})$$

where t (true)= worked height of seam

Figure 8.7 shows a typical cross-section through the edge of a collapse. The material that runs in under the roof forms a stable slope at an angle to the horizontal equal to the angle of internal friction of the fragmented material. In the Figure the area of the material involved in one roadway wedge is:-

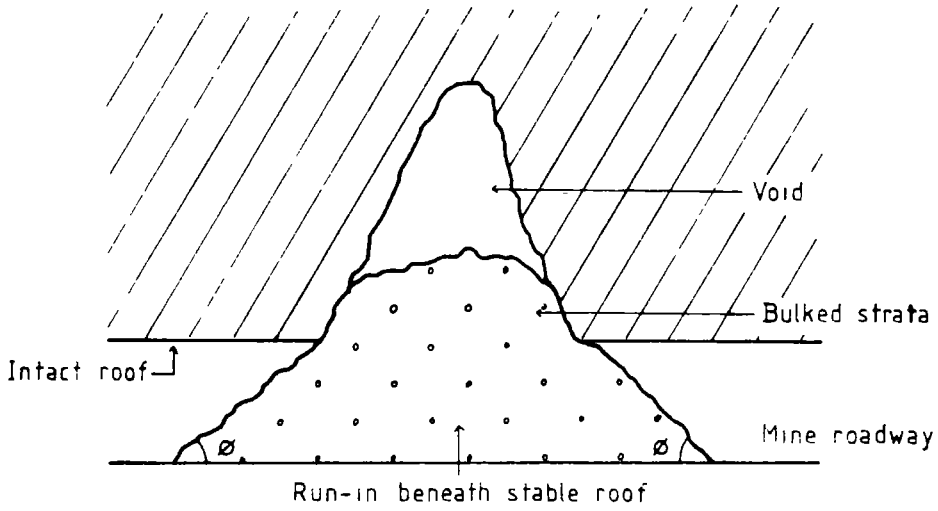

Figure 8.5 Run-in beneath areas of stable roof.

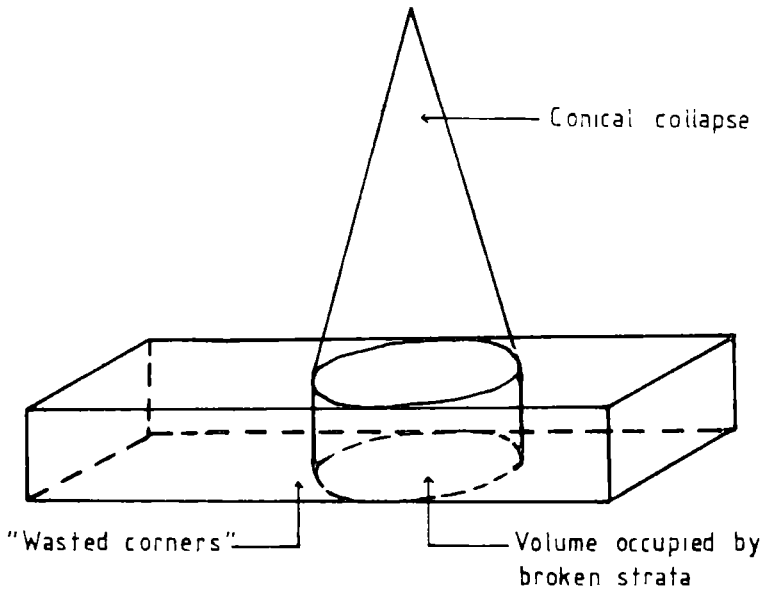

Figure 8.6 Shape of failure assumed by Piggott and Eynon (1977) - Conical collapse

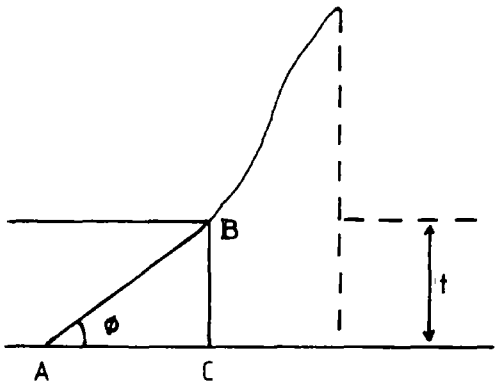

Figure 8.7 Cross-section through typical collapse.

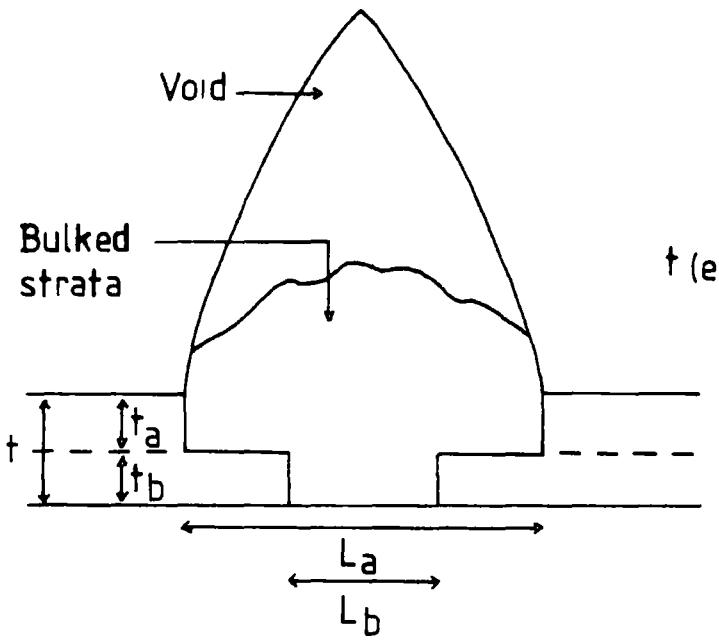

Figure 8.8 Equivalent height of extraction for a part worked seam.

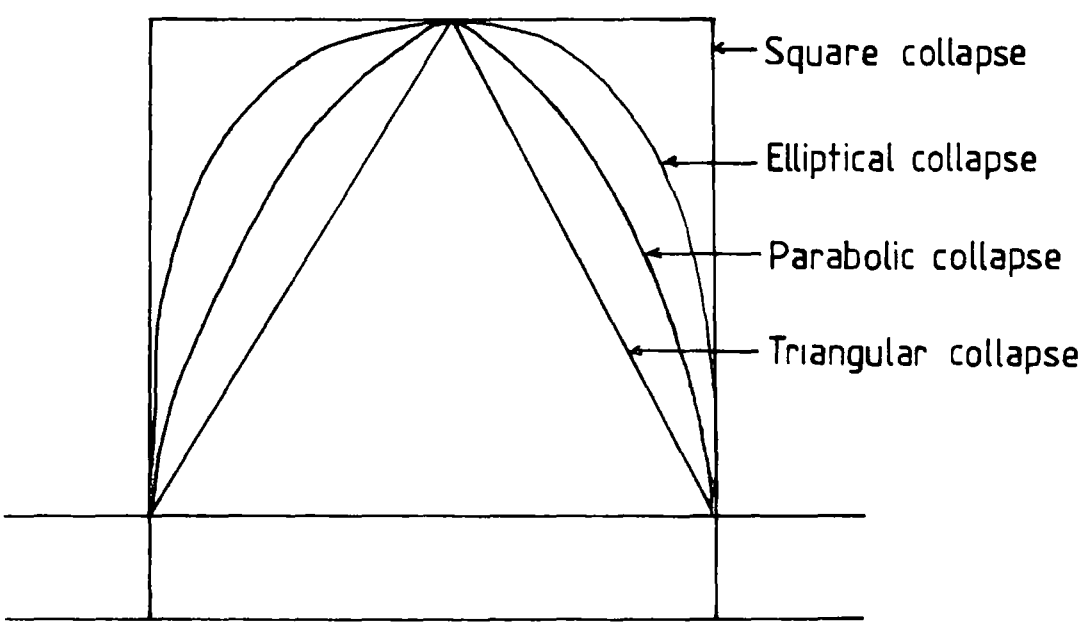

Figure 8.9 Shape of potential collapse structures.

$$\frac{BC \times AC}{2} = \frac{t^2}{2 \times \tan\emptyset}$$

In three dimensions the volume will be the area of the triangle (above) times the span (S) or breadth of the old working. Thus:-

$$\text{volume of one roadway wedge} = \frac{S \times t^2}{2 \times \tan\emptyset}$$

Under the assumption that all the roadways involved with the collapse have similar dimensions, the equation for the total volume of the potential void is:-

V(tot) = volume of void at base of fall + n x volume of roadway wedge

where n is the number of roadways or free-faces to the collapse structure as defined above. Substituting dimensions into the above relationships the equation becomes:-

$$V(tot) = L \times S \times t + \left(\frac{S \times t^2}{2 \times \tan\emptyset} \right)$$

where: L = length of fall $\approx$ breadth
S = span of old working
t = seam thickness
$\emptyset$ = angle of internal friction

dividing this value by the cross section of the base of the fall gives the apparent void height:-

$$t(apparent) = \frac{L \times S \times t + \frac{nS \times t^2}{2 \times \tan\emptyset}}{L \times S}$$

When the dimensions of the roadway of the collapse are known to be different the relationship becomes:-

$$t(apparent) = t + \frac{n1 \times t^2}{b1 \times 2 \times \tan\emptyset} + \frac{n2 \times t^2}{b2 \times 2 \times \tan\emptyset}$$

where n1= number of roadways of width b1
n2= number of roadways of width b2

b. MAXIMUM VALUES FOR t(APPARENT). The maximum obtainable value for t (apparent), or to put it another way, the maximum volume of collapse material

that can be accommodated as run-in under the stable roof, will be when the height of the seam is equal to, or greater than, the breadth of the working. Translating this into an old working situation it follows that if bulking is taken as the limiting criterion, workings in minerals such as limestone, gypsum and ironstone are potentially more dangerous than workings in coal measures. This is because, in the former case, the extracted seam heights are usually of the same order as the span of the workings whereas, in coal, the seam is usually thin compared to the span of the workings.

To prove that the effect of run-in has a significant effect on the potential volume for the collapsed rock, a collapse at an intersection of two roadways (ie. n=4) is used as an example. It will be assumed that the widths of the two roadways are the same at 2m . The angle of repose for the material will be taken as 45 degrees, and the height of the seam, or the true height of the void, will also be taken as 2m . Using the last equation developed above:-

$$t\ (\text{apparent}) = 2 + \left(\frac{4 \times 2 \times 2}{2 \times 2 \times \tan 45}\right) = 6\text{m}$$

This very large increase in the apparent height of the seam over the true height vividly shows the shortcomings of previous approaches. Piggott and Eynon(1977) would have predicted the above situation the maximum height of collapse to be 10 x 2m, or 20m. By just considering the effects of run-in, this value is increases from 20m to a value of 10 x 6m or 60m: a threefold increase . For most coal mine workings the effects are not as dramatic as this, since this example illustrates the worst case in which the span width is equal to the seam thickness.

c. PART-WORKED SEAMS. Care should be exercised in seams which have been part worked, that is where the top leaf of the coal seam has been worked over a greater area than the bottom leaf (Fig.8.8, Plate 8). In these situations the area of extracted seam must be used rather than the height of the seam. The relationships for this condition are given in Figure 8.8.

8.3.5. DEVELOPMENT OF BULKING THEORY: THE SHAPE OF THE FAILURE ZONE.

a. INTRODUCTION.

1. TWO-DIMENSIONS. The original approaches to bulking assumed that, in three-dimensions, the shape of the failure zone would be rectangular. Considering just the first two dimensions (ie. by taking a vertical section across the roadway), a rectangular collapse will have a square or oblong profile. Piggott and Eynon developed the theory to cater for a triangular section, which is represented by a cone in three-dimensions. While triangular section collapses do occur, square or oblong collapse shapes are rare, except perhaps where jointing controls the collapse mechanism. Observations in the field, and a study of the pertinent literature suggest that, in addition to triangular collapse shapes, arch-shaped collapses are also common. Two arch shapes have been suggested from the arching literature reviewed in Chapter 7; these are an elliptical shape and a parabolic shape.(Fig. 8.9).

For a given initial void volume a square or oblong collapse shape will migrate upwards the least distance, followed by an elliptical, then parabolic, and finally by a triangular collapse. A triangular collapse shape thus bulks at the slowest rate and hence migrates the furthest.

2. THREE-DIMENSIONS. When the collapse structures are projected into three dimensions, the new axis length can either be of about the same length as the span or breadth of the working, as in an intersection and heading collapse, or it can have a length far in excess of its breadth as in trough or total roadway collapse.

Taking the trough case first. A square or oblong collapse shape becomes rectangular in three-dimensions , while an elliptical shape becomes an elliptical tube, and a parabolic shape a parabolic tube. Finally a triangular shape becomes a triangular tube or, more correctly, a wedge. Alternatively, if the length of the collapse is short (short-based collapse), the shape will approximate to a cube (or rectangle), a triangular ellipsoid, a paraboloid or a cone respectively.

Piggott and Eynon (1977) chose the cone as a representation for their limited area collapse. This is the extension of a triangle into three dimensions. However, the problems with the circular base area which have been discussed, limit the value of their equation. Any equation for limited area collapse must approximate reality. When a roof collapses the edges of the collapse are usually at right angles to the pillars. Therefore, the base area of the collapse would probably start as a square or rectangle, but would soon change in section as the corners become rounded off and the collapse becomes dome shaped. In any event the area into which the collapse occurs (ignoring run-in effects) will have a square or rectangular section.

In the following section, equations for collapse are developed for cone, paraboloid and triaxial ellipsoid collapse shapes. All assume that the area into which the roof collapses will be rectangular and NOT of the same base area as the structure. Run-in has been treated as an increase in apparent thickness of the seam and so is not included in the following derivations. (see Chapter 8.3.4.). The equations for the developed shapes are summarised in Table 8.2.

b. CONICAL COLLAPSE (Fig. 8.10).

$$\text{Volume of intact beds} \quad Vi = \frac{\pi \times S^2}{4} \times \frac{h}{3}$$

where h = height of collapse
L = length of collapse _ s smallest square to enclose a circle diameter s
S = span of working
t = apparent seam height
B = Bulking factor

Total volume of collapse zone $Vf = Vi + (L \times s \times t)$ or $Vf = Vi + (s \times s \times t)$

$$\text{but} \quad B - 1 = \frac{Vf - Vi}{Vi}$$

$$\text{hence} \quad B - 1 = \frac{12\ t\ S^2}{\pi S^2 h} = \frac{12\ t}{\pi h}$$

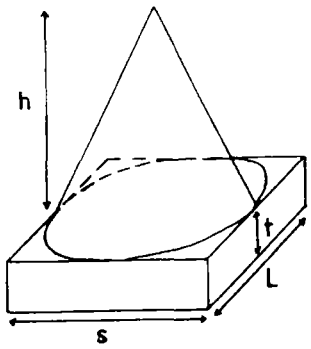

Conical collapse

$s = L$

$h = \frac{3{\cdot}82t}{B-1}$

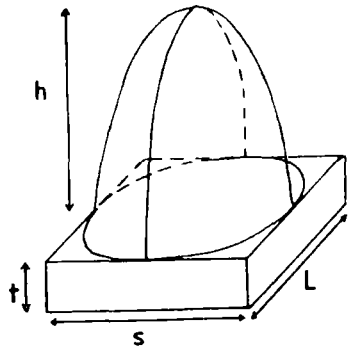

Parabolic collapse

$s \simeq L$

$h = \frac{2{\cdot}0t}{B-1}$

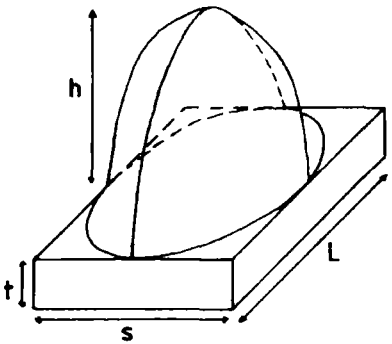

Triaxial ellipsoid collapse

$s \neq L$

$h = \frac{1{\cdot}91t}{B-1}$

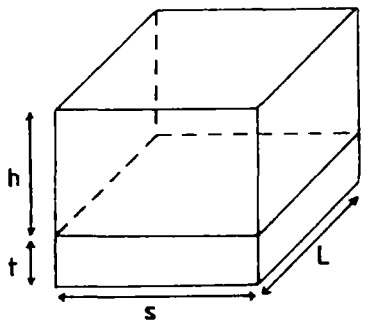

Rectangular collapse

$s \neq L$

$h = \frac{t}{B-1}$

Figure 8.10 Collapse shapes and heights for localised failures.

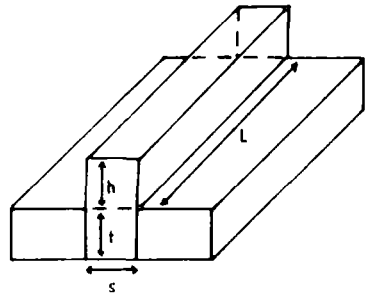

Rectangular collapse

$h = \frac{t}{B-1}$

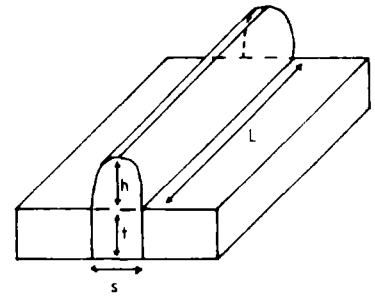

Elliptical collapse

$h = \frac{1{\cdot}27t}{B-1}$

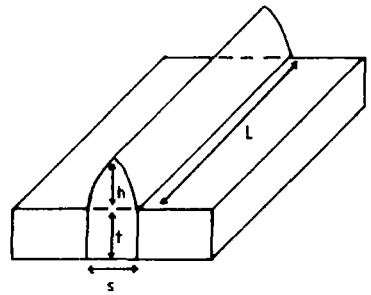

Parabolic collapse

$h = \frac{1{\cdot}5t}{B-1}$

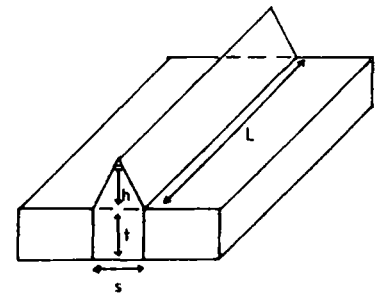

Wedge collapse

$h = \frac{2t}{B-1}$

Figure 8.11 Collapse shapes and heights for trough type failures.

	h =	Typical value assuming B = 1.3 h =
Short based collapses		
1. Rectangular collapse	$\frac{t}{B-1}$	3.33t
2. Conical collapse	$\frac{3.82t}{B-1}$	12.73t
3. Paraboloid collapse	$\frac{2t}{B-1}$	6.67t
4. Triaxial elipsoid collapse	$\frac{1.91t}{B-1}$	6.37t
Trough collapse		
1. Rectangular collapse	$\frac{t}{B-1}$	3.33t
2. Wedge collapse	$\frac{2t}{B-1}$	6.67t
3. Parabolic section	$\frac{1.5t}{B-1}$	5t
4. Eliptical section	$\frac{1.27t}{B-1}$	4.23t

h = Height of collapse
B = Bulking factor
t = Effective seam (void) height.

N.B. Remember that none of the relationships cater for the additional volume of material that will run-in beneath the stable areas of the roof. This volume depends on the location of the collapse and is accounted for by using the effective seam height rather than the true seam height.

TABLE 8.2

SUMMARY OF PREDICTED HEIGHTS OF COLLAPSE FOR DIFFERENT FAILURE GEOMETRICS

$$\text{or} \qquad h = \frac{3.82\ t}{B - 1} \qquad \text{cf.} \quad \frac{3\ t}{B - 1} \text{ (Piggott and Eynon, 1977)}$$

Using a typical value for the bulking factor of 1.3

$$h = 12.73 \times t \qquad \text{cf.} \quad h = 10t$$

Even before taking the effect of run-in into account Piggott and Eynon's (1977) approach would thus seem to underestimate the potential height of collapse. Relationships for the other collapse shapes discussed above are derived below.

c. PARABOLOID COLLAPSE (Fig. 8.10). Under the assumption that the base area of the collapse is rectangular, ie. L x S , an approximate, but sufficiently accurate, relationship can be derived by using similar arguments to those outlined above for conical collapse. Thus:-

volume of a paraboloid = half base area x height

therefore,

$$h = \frac{2t}{B - 1}$$

or

$$h = 6.67\ t \qquad (B=1.3)$$

d. TRIAXIAL ELLIPSOID COLLAPSE (Fig. 8.10). Making similar assumptions concerning the base area as above:-

$$\text{volume of a triaxial ellipsoid} = \frac{4}{3} \times \pi \times h \times \frac{S}{2} \times \frac{L}{2}$$

Where these terms represent (in the ellipsoid and old working):
S = diameter of one of the shorter axes of the ellipsoid ≈ span of working
L = diameter of one of the shorter axes of the ellipsoid ≈ length of working
h = radius of the long axis of the ellipsoid ≈ height of collapse

$$\text{volume of a half triaxial ellipsoid} = \frac{1}{2} \times \frac{4}{3} \times \pi \times h \times \frac{S}{2} \times \frac{L}{2} = \frac{\pi hSL}{6}$$

$$h = \frac{6\ t}{(B - 1) \times \pi} = \frac{1.91\ t}{B - 1}$$

or for a bulking factor of 1.3

$$h = 6.37t$$

e. TROUGH TYPE COLLAPSE. If the shapes are projected into a trough type collapse situation, equations can be derived using similar arguments for all the section shapes discussed (Fig. 8.11). These equations are summarised in Table 8.2.

f. SUMMARY. The following tables have been constructed (Tables 8.3 and 8.4) to illustrate the effect of combining both the newly defined failure geometries and the effect of the location. The first table (Table 8.3) assumes a coal seam height of 1.5m and standard working width of 3.0m. The potential height of collapse for various locations have been calculated using suitable apparent heights based on an angle of repose of 45 degrees and a bulking factor of 1.3 (found to be reasonable -see Chapter 8.2.4.).

TABLE 8.3 TABLE OF PREDICTED HEIGHTS OF COLLAPSE.

		Collapse Geometries				
	n	rectangular / square	elliptical	parabolic	triangular / conical	apparent height
Trough	0	5.0	6.35	7.5	10.0	1.50
Heading	1	6.25	11.90	12.5	23.9	1.875
Intermittent Roadway	2	7.5	14.33	15.0	28.7	2.25
Intersection	4	10.0	19.10	20.0	38.2	3.00

Values for a seam height of 1.5m and a working width of 3m, where n = number of free ends.

TABLE 8.4. NORMALISED TABLE OF PREDICTED HEIGHTS FOR A SEAM HEIGHT : WIDTH RATIO OF 0.5.

		Collapse Geometries				
	n	rectangular / square	elliptical	parabolic	triangular / cone	apparent height
Trough	0	3.3	4.2	5.0	6.7	1.00
Heading	1	4.2	7.9	8.3	16.0	1.25
Intermittent Roadway	2	5.0	9.60	10.0	19.1	1.50
Intersection	4	6.7	12.7	13.3	25.5	2.00

where n = number of free ends

The second table (Table 8.4) has been normalised with respect to the initial height of the seam. This gives values in terms of a seam height to thickness ratio. These values would obviously hold for any situation with a similar span height to width ratio. The values show that the commonly used maximum value of 10 x seam thickness is far from what may be expected assuming bulking to be an important control. The worst situation is given by the conical failure, where for the seam height to width ratio used a collapse of 25.5 times the extracted seam thickness is predicted.

8.3.6. PREDICTION OF VOID BRIDGING.

Using the worst situation, discussed above (ie. the conical failure zone), Figure 8.12 shows that the rate of closure of the arch will be very slow. This provides progressively smaller gaps suitable for bridging. Therefore, if within the strata above the void there is a bed which is more competent than others and which has blocks of a significantly greater size than the other beds, one of these blocks may bridge across the gap and arrest the void at a lower level than that predicted.

For a suitably orientated block, the height above the coal seam that the void might be arrested at, is given by:-

$$h\,(crit) = h - \frac{(l \times b)^{1/2}}{S} \times h$$

where: l = length of block
b = breadth of block
S = span of working
h = height of collapse

Using the previous example, let a thin sandstone horizon with well-developed regular jointing occur at 24.2m above the seam. Let the spacing of the joints in the x and y planes have a mean value of 0.5m with a standard deviation of 0.2m . Will the sandstone arrest the void ? If it will not arrest the void, then what is the probability of a larger than normal block bridging the gap.

$$h\,(crit) = h - \frac{(l \times b)^{1/2}}{S} \times h$$

$$h\,(crit) = 31.8 \text{ metres}$$

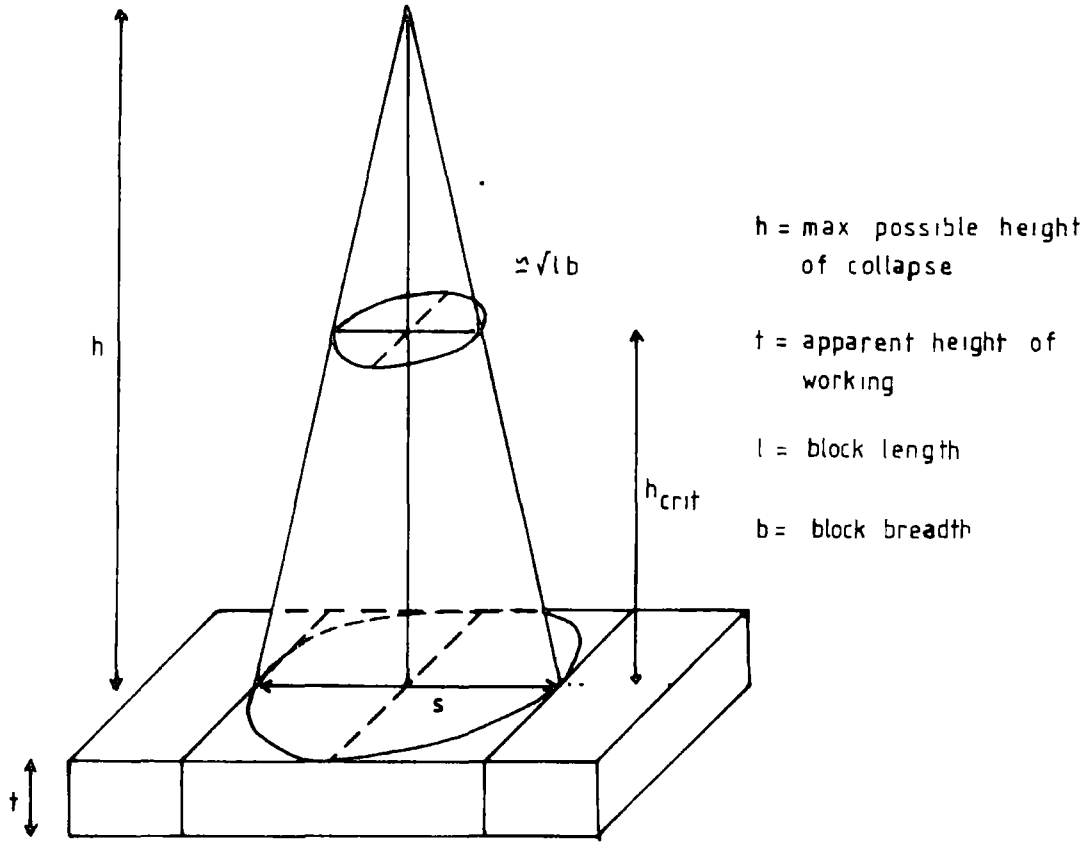

Figure 8.12 Shape of failure zone predicted by bulking theory for the example in the text.

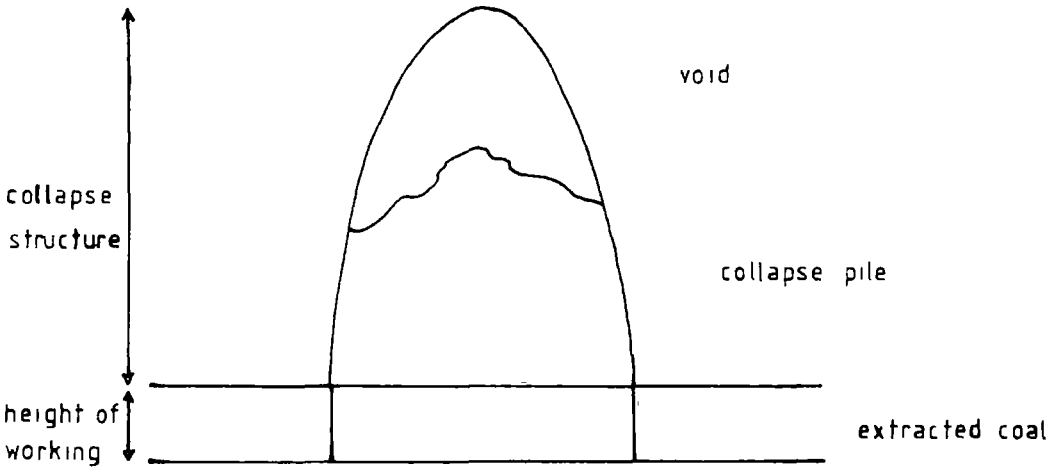

$$\text{Bulked area} = \frac{\text{Area of extracted coal + Area of collapse pile - Area of void}}{\text{Area of extracted coal}}$$

$$\text{Bulking Factor (F)} = 1 + \left[\frac{1}{\text{Bulked area}}\right]$$

Figure 8.13 Calculation of bulking factor from photographs of old workings.

A block 0.5m x 0.5m will only just span the void at 31.8m and therefore it is unlikely to at 24.2m height, where the width of the arch is greater.

Knowing the mean size of the block and the standard deviation:

50.00 %	of the blocks are larger than	0.5m
13.50 %		0.7m
2.25 %		0.9m
0.01 %		1.1m

Hence, substituting into the previous equation for h(crit), shows the size of block required to span the working is:-

$$24.2 = 38.2 - \frac{(l \times b)^{1/2}}{3} \times 38.2$$

the block size = l x b = 1.1

Thus the probability of the collapse being arrested by bridging is about 0.01% or 1 case in 10,000.

8.4. VALUES FOR BULKING FACTOR.

8.4.1. SOURCES AND VALUES FOR BULKING FACTORS.

There are four sources for bulking factors for use in the predictive model generated above. These can be summarised under the following headings.

1. Bulking factors obtained from the literature
2. Bulking factors derived from collapse piles within old workings
3. Bulking factors calculated from measurements made from photographs of bulked old workings
4. Bulking factors derived from suitable analogous situations

a. LITERATURE VALUES. The values obtainable from the literature have already been reviewed at various points in the foregoing text, and therefore will not be discussed further.

b. FIELD VALUES FROM WITHIN OLD WORKINGS. To the writer's knowledge Challinor

(1976) is the only person to have made any measurements of the actual bulking factor for collapsed arch infill. These measurements were made on the Cowsley opencast site using a large (1ft cubed) sampling tin. Challinor obtained a bulking factor of between 1.37 and 1.42 for the silty shale which comprised the core of the collapse pile.

c. VALUES CALCULATED FROM MEASUREMENTS MADE FROM PHOTOGRAPHS OF BULKED WORKINGS. Numerous photographs of old workings taken during the course of the field study showed partially bulked old workings, thus it was decided to use this data to derive typical bulking factors for different locations.

Forty four photographs of well-developed and clear old workings from ten opencast sites were selected from the field records. These old workings varied in the degree of bulking they exhibited from only partially bulked to completely choked. However, care was taken not to include any workings which were known to have been stowed prior to abandonment. Figure 8.13 shows a diagrammatic sketch of a typical old working.

The individual areas of the component parts of the structures were measured with the aid of a planimeter, from tracings of the areas of working and collapse made from the photographs. For this information a bulking factor was calculated for each of the 44 workings, using the formulae developed in Figure 8.13 (Table 8.5).

This data yielded a mean bulking factor or 1.3979 with a standard deviation of 0.145 (n=44). Unfortunately there was insufficient data from either the different locations or for each rock type to make a valid statistical breakdown of the bulking factor, on a basis of location or rock type. However, a trend could be seen for a variation of the bulking factor with the rock type.

Siltstones appear to have a Bulking factor of about	1.35
Mudstones	1.4
Sandstones	1.5

It must be stressed however, that these values are only a very rough guide.

d. BULKING FACTOR VALUES DERIVED FROM AN ANALOGOUS SITUATION, EG. COLLIERY TIPS.

Taylor (1975) was the first to use this technique deriving an average bulking factor of 1.12 for discards from the relative densities of discard and solid rock. He used the then modal bulk density value for colliery tips of 2.00 Mg/m3 and a value of 2.24 Mg/m3 for the bulk density of solid rocks. This value was obtained by measuring the density of a complete cyclothem sequence near Rotherham.

8.2.4. CALCULATION OF BULKING FACTORS FROM COLLIERY TIP DATA.

a. NCB-DURHAM DATA BASE. Since this date an NCB research contract has enabled information on material properties of colliery discards located across the country to be collated. For a little over two years the present writer was employed on this collation study (see Taylor, 1984).

The data base holds over 270,000 pieces of information on 149 tips and provides a unique opportunity to investigate the bulking factor, and analyse for any variations or trends that may occur across the country.

The bulking factor is not a variable which is directly measurable, and so is not included in the NCB-Durham data base. However, dry density and specific gravity are values recorded and on the supposition that an intact sequence of rocks will have a dry density very close to the specific gravity of the rock fragments, the bulking factor may be defined as:-

$$\text{Bulking factor} = \frac{\text{Specific Gravity}}{\text{Dry density}}$$

The NCB-Durham data base is actually composed of three semi-independent data bases of which only one need concern the present thesis.

The U100 data base is the largest source and is founded around the material properties of discard measured from U100 samples obtained from boreholes in tips and lagoon embankments.

The depths from which the samples were obtained have been recorded and thus it is possible to make some assessment of the variation of bulking factor with

depth. It should therefore be possible to check the validity of the 'variable bulking factor' of Sutherland et al. (1981). Additionally, the inter-relationships between bulking and any of the 77 other variables stored in the data base can be examined not only for individual cases but also on a tip, or, more conveniently considering the number of tips involved, a coalfield basis.

The NCB-Durham data base was analysed at Durham using the Michegan Interactive Data Analysis System (MIDAS, 1976). The system has a wide range of data manipulative and statistical analysis features incorporated into an interactive package, and has proved ideal for analysing the enormous quantity of data.

b. JUSTIFICATION FOR THE CALCULATION OF BULKING FACTORS FROM COLLIERY TIP DATA.

It must be emphasised that the NCB-Durham data base is only of value providing that the assumptions made concerning the bulking factor (ie. that it can be derived from the specific gravity and dry density) is valid.

The analysis of the field photograph data yielded an overall average bulking factor value of 1.3979 (Table 8.5). This value is probably quite an accurate estimate of the bulking factor for arch infill. The accuracy of this value is endorsed by the observation that the value lies within the range measured by Challinor (1976) and also is not unreasonable in relation to previous literature estimates. The values for the bulking factors obtained from the photographs can thus be used as an independent check on the validity of the assumptions that need to be made to utilise the NCB-Durham data base.

In fact the bulking factor from the data base was found to have a mean value of 1.3976 (SD= 0.2065 n=577), (Fig. 8.14). The difference of 0.0004 is not statistically significant (t-test). However, the validity of the t-test in this situation is called into doubt as an F-test on the variances of the two estimates suggested that the variances were not equal. In addition, tests for skewness and kurtosis suggested that the data base estimate for the bulking factor was not distributed quite 'normally'. In consequence and as a check on the t-test, a range of appropriate non-parametric comparison statistics were carried out on the two estimates for the bulking factor. Both the Mann-Whitney

Arch Ref. No.	Location	Rock Type	Bulking Factor
0208	CF	SM	1.38
0411	LC	M	1.56
0414	A	SS/Sh	1.282
0416	A	"	1.309
0418	A	"	1.286
0422	A	SS/Sh	1.457
0425	A	"	1.398
0607	I	"	1.344
0606	I	"	1.452
0613	I	"	1.286
0808	I	SS/Sh	1.356
0811	I	"	1.177
0872	I	"	1.227
0814	I	"	1.258
0814	I	"	1.212
0816	I	SM	1 258
0819	I	"	1.291
1022	LC	M	1.606
1031	LC	"	1.769
1126	I	S	1.752
1135	I	S	1.392
1329	I	"	1.329
1324	I	ShM	1.538
1322	I	"	1.556
1427	TL	S	1.388
1425	TL	"	1.422
1705	I	SM	1.345
1710	I	"	1.386
1713	I	"	1.299
1715	I	ShM	1.362
1719	I	"	1.611
2018	B	SS	1.61
2314	P	"	1.372
2314	P	"	1:488
2314	P	"	1.31
2309	P	SS	1.455
RKT	Pe	S M	1.317
2221	M	ShM	1.188
2821	M	SS	1.217
2024	B	SM	1.424
C1	SA	SM	1.411
C5	SA	"	1.357
C7	SA	"	1.486
C8	SA	"	1.669
n= 44			$\tilde{x}$ = 1.398 SD = 0.1446

Locations:CF=Coalfield Farm; LC=Low Close; A=Acclington; I= Ibbetsons; T=Tow Law; B=Blindwells; P=Pit House; Pe= Pethburn; M=Maes-y-Marhog; SA=St. Andrews.

Rock Types: SS=Sandstone; S=Siltstone; SM=Silty Mudstone; SS/Sh=Silty Shale; ShM=Shaley Mudstone; M=Mudstone.

TABLE 8.5

BULKING FACTORS DETERMINED FROM PHOTOGRAPHS OF OLD WORKINGS

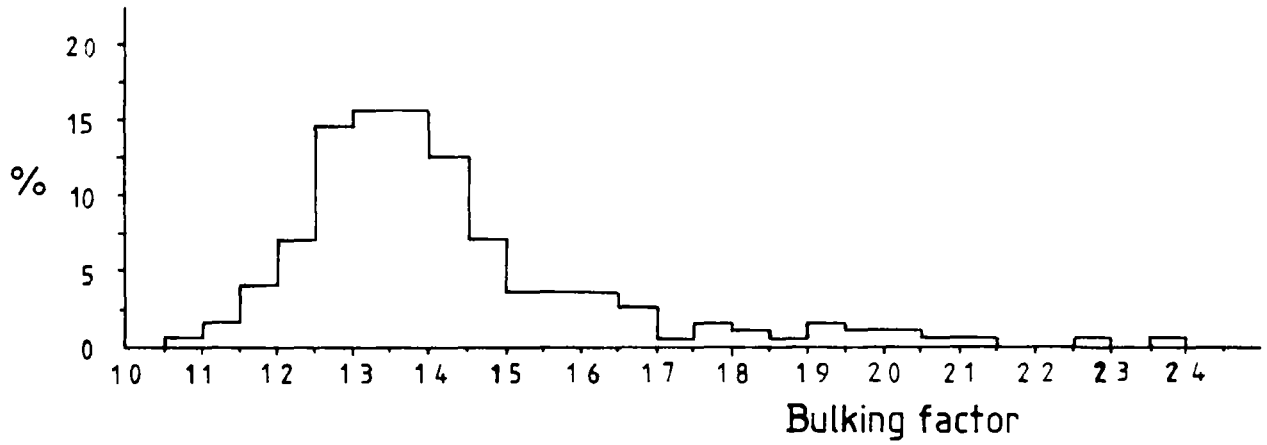

Figure 8.14 Variation in bulking factor.

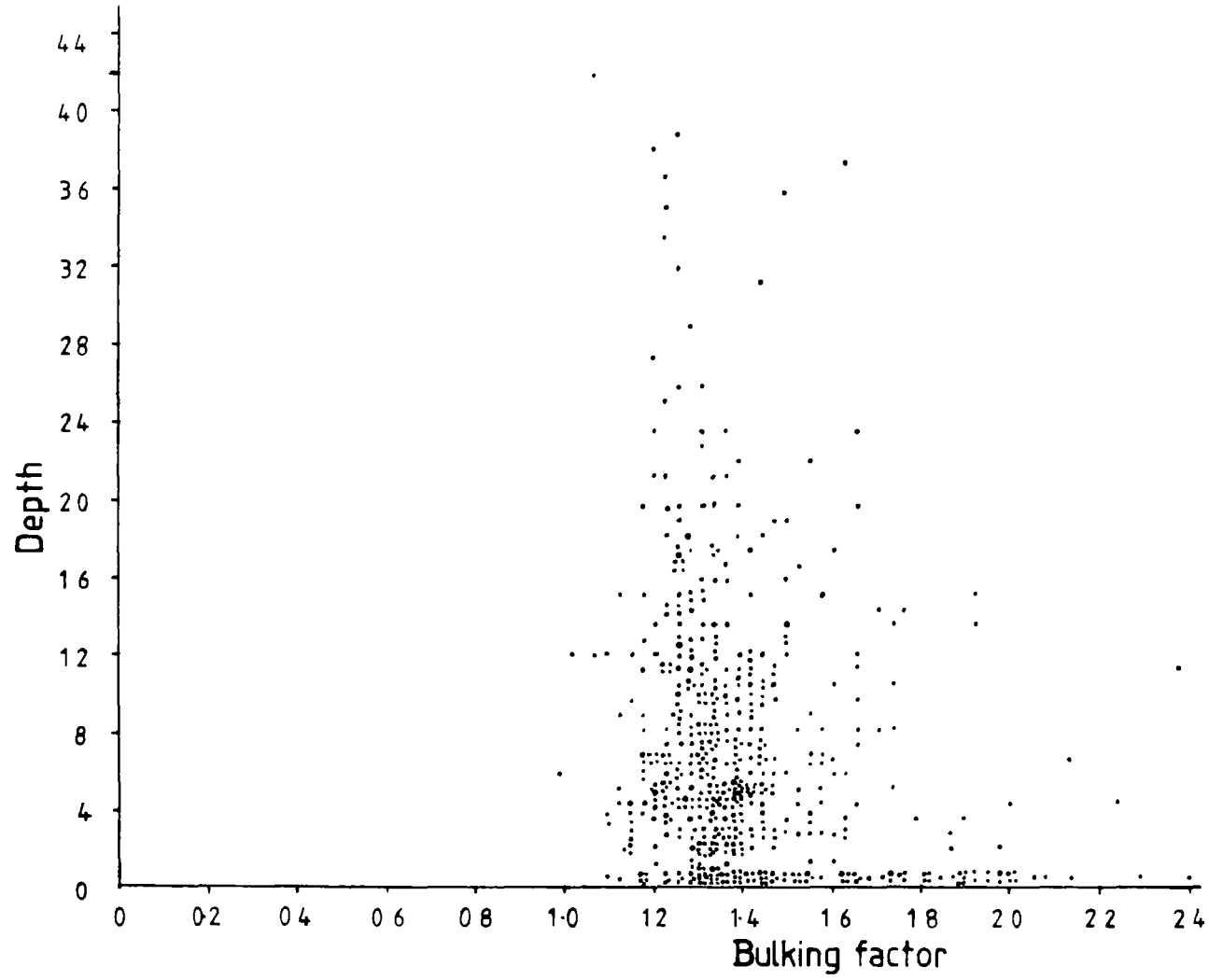

Figure 8.15 Variation in bulking factor with depth.

U and Median tests endorsed the initial t-test results and show that there is no significant difference between the mean or median values. For this reason the NCB-Durham data base values for bulking factor can be used with some confidence for further analysis of regional variations and correlations in the bulking factor.

c. CORRELATION OF BULKING FACTOR WITH OTHER VARIABLES. It was suspected that bulking factor would correlate with a number of other variables held on the data base. To test this hypothesis, product moment and rank order correlation coefficients were obtained for the most likely variables. Of the many possible variables that could have been chosen, those which reflected some aspect of the material 'intactness', (ie particle size, sorting coefficient, clay % and ash content) were expected to correlate best. In fact no other strong correlations were found, apart from the correlations which were to be expected to be highly significant; between such variables as the bulking factor and void ratio (r=0.9997), dry density (r=-0.7890), specific gravity (r=0.2720) and moisture content(r=0.4200). Of those variables mentioned above, it is interesting to note that the bulking factor gains most of its variation from changes in the dry density rather than specific gravity. As the dry density is derived from the bulk density, the inter-relationship between the moisture content and the bulking factor is only to be expected.

The absence of a strong relationship between the bulking factor and particle size was surprising. The particle size is recorded as the size of the fragments representing 25%, 50% and 75% of the sample. The bulking factor correlated negatively with all three variables with the correlation coefficient and statistical significance dropping from a maximum for P75% of r= -0.12 (sign = 0.01 or 99%). This relationship represents only 3.5% of the variation in bulking factor, and is much less than was expected. The negative correlation is however,logical because the more the material is broken down the greater the number of voids that will be created.

The bulking factor was also expected to correlate negatively with the sorting coefficient. The argument being that the greater the degree of sorting, the

greater the potential density for the spoil, and hence the lower the bulking factor. A negative correlation was found (r=-0.08) but the correlation coefficient failed to reach even the 0.1 (90%) significance level, so it must be concluded that there is no evidence to suggest that the bulking factor is related to the degree of sorting of the spoil. No other meaningful or significant inter-relationships were found between the bulking factor and the other variables examined, namely ash% and clay%.

d. CORRELATION OF BULKING FACTOR WITH DEPTH. Figure 8.15 shows a scattergram of the variation of bulking factor with depth. It will be noticed that as the depth in the tip increases the bulking factor does not decrease, but the variation or range of values does decreases. This trend is well shown in Figure 8.16 where the above data have been split by depth into 0.5m groupings. The mean for each group was then plotted against the depth at which it occurred. No overall trend of decreasing bulking factor with depth is discernible. Thus, any variation in the bulking factor attributable to depth of burial in a collapse pile, as experimentally reported by Sutherland et al., (1981), must occur within the top 0.5m or so, or be reduced by the effect of time and consolidation. From this it can be concluded that it is probably reasonable to use a single bulking factor.

8.4.3. REGIONAL VARIATION IN BULKING FACTOR.

Several of the physical properties of discard have been found to vary regionally (Taylor, 1984), and it was suspected that there may also be a regional variation in the bulking factor. To test this hypothesis the NCB-Durham data base was examined on an NCB Area basis. NCB Areas approximate fairly well to the main geological coalfields and have been used in the past for studies of regional variation in the physical properties of discards (eg. Taylor, 1975, 1984). On this basis the country was divided up into thirteen areas, these were:-

Scotland	N. East	Western	Barnsley
Doncaster	S. Yorkshire	N. Yorkshire	N. Derbyshire
N. Nottingham	S. Nottingham	S. Midlands	Kent
S. Wales			

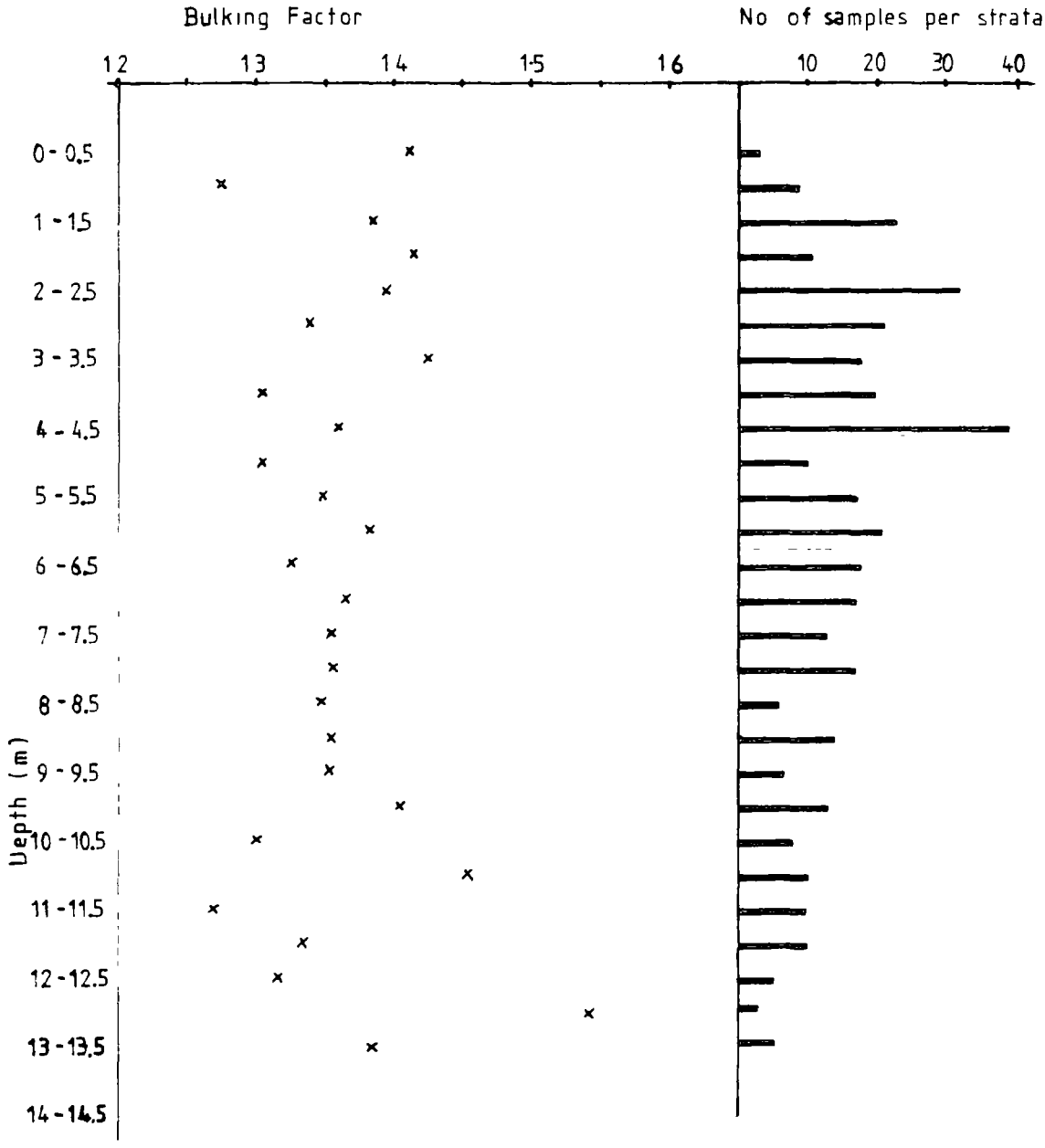

Figure 8.16 Variation of mean bulking factor with depth.

A range of both parametric and non-parametric comparative statistical techniques were employed in the analyses, as the normality of the populations of some of the variables, especially at Area level, could not be taken for granted.

Regional variations in the data were first sought using the analyses of variance test. This parametric test uses the F-test to analyse for the equality of the regional means. The analysis technique assumes that the population variances are the same for all the groups tested. This assumption can itself be tested using the F-test on the population variances. Where the criteria for the analysis of variance test were not met, or where skewed data was suspected, the Median and Kruskall-Wallis tests were also performed. These are equivalent non-parametric statistical tests, and make few assumptions about the distribution of the data.

Regional variation was first sought in the key variables specific gravity and dry density, because of the dependence of the bulking factor on these variables. A variation in the specific gravity would reflect a difference in the proportion of the component minerals in the rocks of the cyclothem, whereas a variation in dry density would reflect a variation in the 'intactness' of the discard, or a variation in the void space. This variation could itself be due to either material differences or to differences in mining or placement techniques. The values for specific gravity and dry density will not necessarily vary together in which case any regional variations in the bulking factor may appear to be independent of both variations in specific gravity and dry density.

In the following sections the statistical significance of the variations is quoted using the following format sign 0.0000, 0.0000. The first value refers to the difference between the means of the groups, while the second value refers to the difference between the variances of the groups. Very low values indicate that there is a strong difference between the measured groups. To be more specific. If the value for the significance was 0.0001, this would mean that the probability of obtaining such a result by chance is 0.0001, or (to put it another way) there is a 1 in 10,000 chance that the variables are the same. A

significance value of 0.0000 thus means that there is less than a 1 in 10,000 chance that the variables are the same.

a. REGIONAL VARIATION IN SPECIFIC GRAVITY. Six hundred and eighty seven determinations of the specific gravity (S.G.) of the discard fragments were used for the analyses. These values, distributed between the thirteen NCB Areas, had an overall mean value of 2.3067 Mg/m3 (SD. 0.1986 n=687, Fig. 8.17). Appropriate statistical tests suggested that there was a highly significant difference between the means and variances of the regional groups, ie. there was regional variation in the specific gravity.

The mean S.G. for the different Areas varied between 1.98 to 2.41 Mg/m3. Table 8.6 shows the order of variation in the parameter. Various linear combinations of the Areas based on geological and numerical similarity were tested to see which grouping produced the most coherent divisions. Of the combinations tested, the groupings shown in Table 8.6 emerged as the best.

The country can broadly be divided into four regions; the low S.G. Areas of Scotland, N. East, Kent and S. Wales form a strong group and have little similarity (sign 0.0000, 0.0000) with the adjacent low-intermediate S.G. group. This group, comprising Doncaster, S. Yorkshire, and N. Yorkshire and the next (high-intermediate) group consisting of the N. Derbyshire, Barnsley, and N. Nottingham Areas merge with one another. They are statistically distinguishable as separate groups, but the individuals on the edge of the groups show leanings to both groups. This suggests the possible existence of gradational boundaries rather than fixed groupings, and perhaps suggests that the groupings are more imaginary than real.

The groupings obtained for the specific gravity were compared to the groupings found previously for other parameters (Taylor, 1984). It is of interest to note that the S.G. groups are almost identical to those obtained for strength variations in discard. In these, strength was found to correlate positively with the angle of internal friction, and Taylor (1974) has also demonstrated the relationship between high coal content (reflected by low S.G.) and high shear

n	Mean ($\bar{x}$)	SD	Median (M)	Area	
9	1.9767	0.3038	1.8900	Kent)	Gp1 $\bar{x}$=2.1984
85	2.1977	0.2205	2.1600	S. Wales)	SD=0.2328 n=164
23	2.2030	0.1755	2.2000	Scotland)	M=2.18
47	2.2400	0.2471	2.2200	N. East)	
57	2.2989	0.1473	2.2600	Doncaster)	Gp2 $\bar{x}$=2.3034
105	2.3045	0.1694	2.3100	S. Yorks)	SD=0.1690 n=227
65	2.3057	0.1875	2.3200	N. Yorks)	M=2.30
12	2.3275	0.1879	2.3400	N. Derbys*)	Gp3 $\bar{x}$=2.3518
96	2.3468	0.1745	2.3800	Barnsley)	SD=0.1829 n=199
91	2.3603	0.1922	2.4000	North Nottingham)	M=2.39
23	2.3883	0.2166	2.4200	Western)	Gp4 $\bar{x}$=2.4046
15	2.3992	0.0688	2.4200	S.Midland*)	SD=0.1401 n=97
59	2.4123	0.1157	2.4450	South Nottingham)	M=2.42
687	2.3067	0.1986	2.3400	All	

*Positions of these areas transposed for strength groupings.

TABLE 8.6

REGIONAL VARIATION FOR SPECIFIC GRAVITY

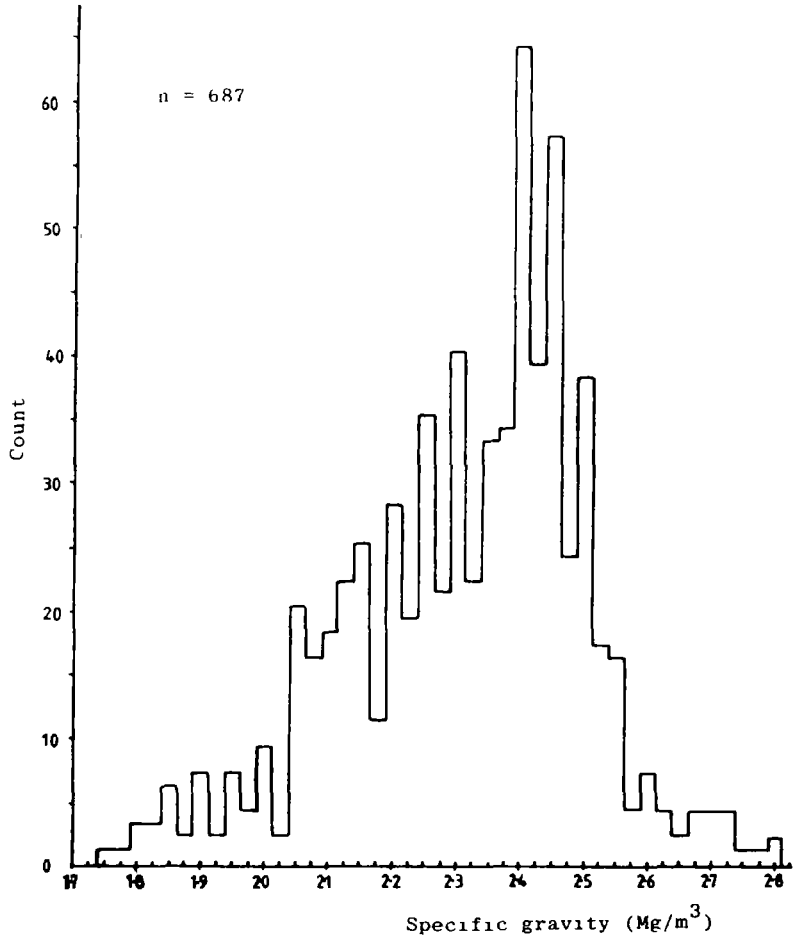

Figure 8.17 Distribution of specific gravity.

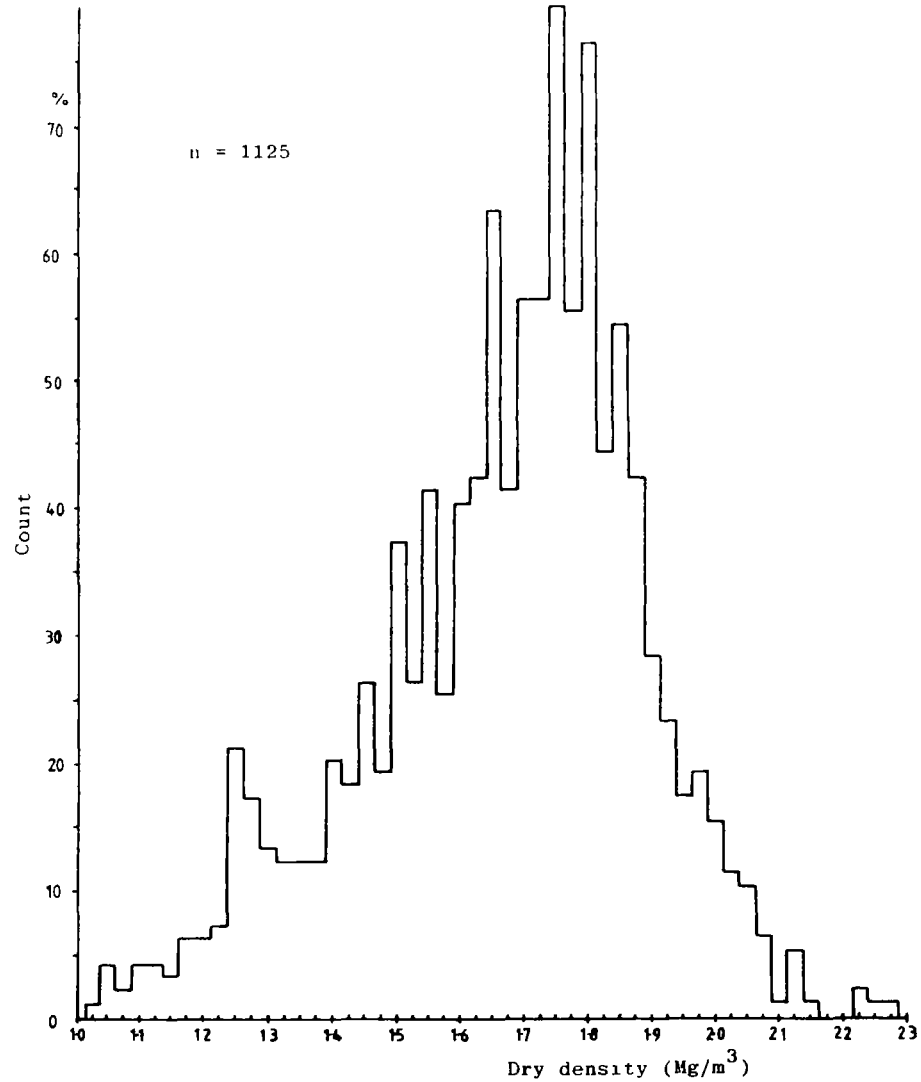

Figure 8.18 Distribution of dry density.

strength. This inter-relationship is probably the foundation for the similarity between the S.G. and strength groupings.

b. REGIONAL VARIATION IN DRY DENSITY. An analysis similar to that performed with the specific gravity was carried out on 1133 dry density results. The variable had an overall mean value of 1.6667 Mg/m3 (sd= 0.2226; Fig. 8.18). Once again appropriate statistical tests strongly suggested regional variation for this variable. Table 8.7 shows the Areas in order of increasing dry density. A comparison with Table 8.6 shows that dry density does not vary systematically with specific gravity. Indeed, no previously recognised groupings such as strength, S.G., or particle size (Taylor, 1984) matched the variation. Various groupings were attempted but while group 1 was fairly distinctive, the distinction between the other groups appeared gradational and was far from clear cut. As with the specific gravity, the end members showed strong differences, but graded into one another towards the centre. The four groups shown in Table 8.7 appear to be best approximations to the data, but the divisions between adjacent groups 2 and 3, and 3 and 4 are indistinct.

c. REGIONAL VARIATION IN BULKING FACTOR. With the strong indication of regional variation in the values for specific gravity and dry density, it was not surprising to find that the bulking factor also showed strong evidence of regional variation A total of 597 assessments of the bulking factor, with a mean value of 1.3936 (sd= 0.2045 n=597, Table 8.8), were used in the following analysis. There is a small difference between the number of samples and the mean value for the bulking factor quoted in this section, compared to the values given previously in the text. This variation is due to the use of a slightly different data split. However, any statistics quoted previously for the validity of the use of the NCB-Durham data base bulking factors have also been proved to apply equally well to this alternative estimate.

The bulking factor was analysed for regional variation in a similar fashion to that employed for specific gravity and dry density, Table 8.8 shows the NCB Areas ranked according to the mean bulking factor. A comparison with Tables 8.6 and 8.7 shows that the variation in bulking factor does not fit any of the

Dry Density

n	Mean ($\bar{x}$)	SD	Median (M)	Area	
12	1.5392	0.2446	1.5400	S. Midlands	Gp1
19	1.5603	0.1566	1.5070	Kent)	Gp2 $\bar{x}$=1.5742
39	1.5679	0.2455	1.5350	Scotland)	SD=0.21375 n=190
132	1.5781	0.2121	1.5700	N. Yorks)	
96	1.6391	0.2272	1.6980	Doncaster)	
161	1.6491	0.2531	1.7100	S. Yorks)	Gp3 $\bar{x}$=1.6604
82	1.6763	0.2590	1.7140	N. East)	SD=0.2429 n=468
129	1.6804	0.2308	1.7200	Barnsley)	
37	1.7051	0.1971	1.7140	Western)	
97	1.7083	0.1799	1.7310	N. Derbys.)	Gp4 $\bar{x}$=1.7111
160	1.7123	0.2086	1.710	S. Wales)	SD=0.2002 n=390
96	1.7143	0.2093	1.7600	North)	
				Nottingham)	
73	1.7314	0.1034	1.7280	South Nottingham	Gp5
1133	1.6667	0.2226	1.707	All	

TABLE 8.7

REGIONAL VARIATION FOR DRY DENSITY

Bulking Factor

n	$\bar{x}$	SD	Median	Area	Level of significance* between areas (mean)	
9	1.1860	0.1282	1.1878	Kent		
					0.0914	4
58	1.2774	0.1203	1.2544	S. Wales		
					0.0835	
21	1.3609	0.0966	1.3626	Western		
					0.0192	5
57	1.3801	0.1697	1.3388	Doncaster	0.0081	1
56	1.3882	0.0713	1.3900	S.Nottingham		
					0.0134	
91	1.4016	0.2027	1.3481	N.Nottingham	0.0003	2
70	1.4046	0.2471	1.3128	Barnsley		
					0.0013	
30	1.4059	0.207	1.3367	N.East		
					0.0105	
59	1.4164	0.2093	1.3403	N.Yorkshire	0.0026	3
100	1.4190	0.2426	1.3409	S.Yorkshire		
					0.0232	
23	1.4422	0.235	1.4188	Scotland		
					0.025	6
11	1.4672	0.1907	1.4270	N.Derbyshire		
					0.1489	
12	1.6161	0.249	1.5871	S.Midlands		
597	1.3936	0.2045	1.34	All		

Level of significance between groupings

Groups	Mean	Variance
1 and 2	0.3968	0.0000
2 and 3	0.54	0.53
1 and 3	0.159	0.000
6	0.950	0.210
4, 5, 6	.0000	.0000

*Below value of 0.05 significant difference.
Above value of 0.05 no significant difference.

TABLE 8.8

REGIONAL VARIATION IN BULKING FACTOR

previously noted trends. This is not altogether surprising considering that both S.G. and dry density showed different trends. From the correlation coefficient it was noted that about 62% of the variation in the bulking factor could be attributed to variation in the dry density, while only about 7.5% was due to variation in specific gravity. The trends in bulking factor show little similarity to those in dry density which suggests that perhaps the bulking factor should be considered as a unique variable in its own right.

Grouping of the data proved even more of a problem than had been the case for the dry density, While once again the end members showed strong disassociations, adjacent Areas (on a ranking basis) were often statistically indistinguishable. This suggests that the distribution of the bulking factor is best considered as a gradational series rather than as groupings of like Areas.

Without more research into the variation it is difficult to explain the patterns of variation that have emerged in the bulking factor. However, the variation is probably the result of a complex inter-relationship of spoil mineralogy, induration and coal content. Figure 8.19 shows the patterns of variation across the country for all three variables, S.G., dry density, and bulking factor. An increase in the number of the shading represents an increase in the value of the variable.

The implications of the regional variation in bulking factor for the collapse potential of old workings are far reaching. The data suggest that if bulking was the limiting factor for collapse then voids would be expected to migrate to a higher level in areas such as South wales and Kent, than in areas such as Scotland or N. Derbyshire. Unfortunately there is insufficient field evidence to confirm or deny this hypothesis at the present time.

8.5. SUMMARY.

The bulking equations in widespread use at the present time have been shown to be rather simplistic and, from a theoretical viewpoint to greatly underestimate the potential height of the collapse zone. The relationships have been

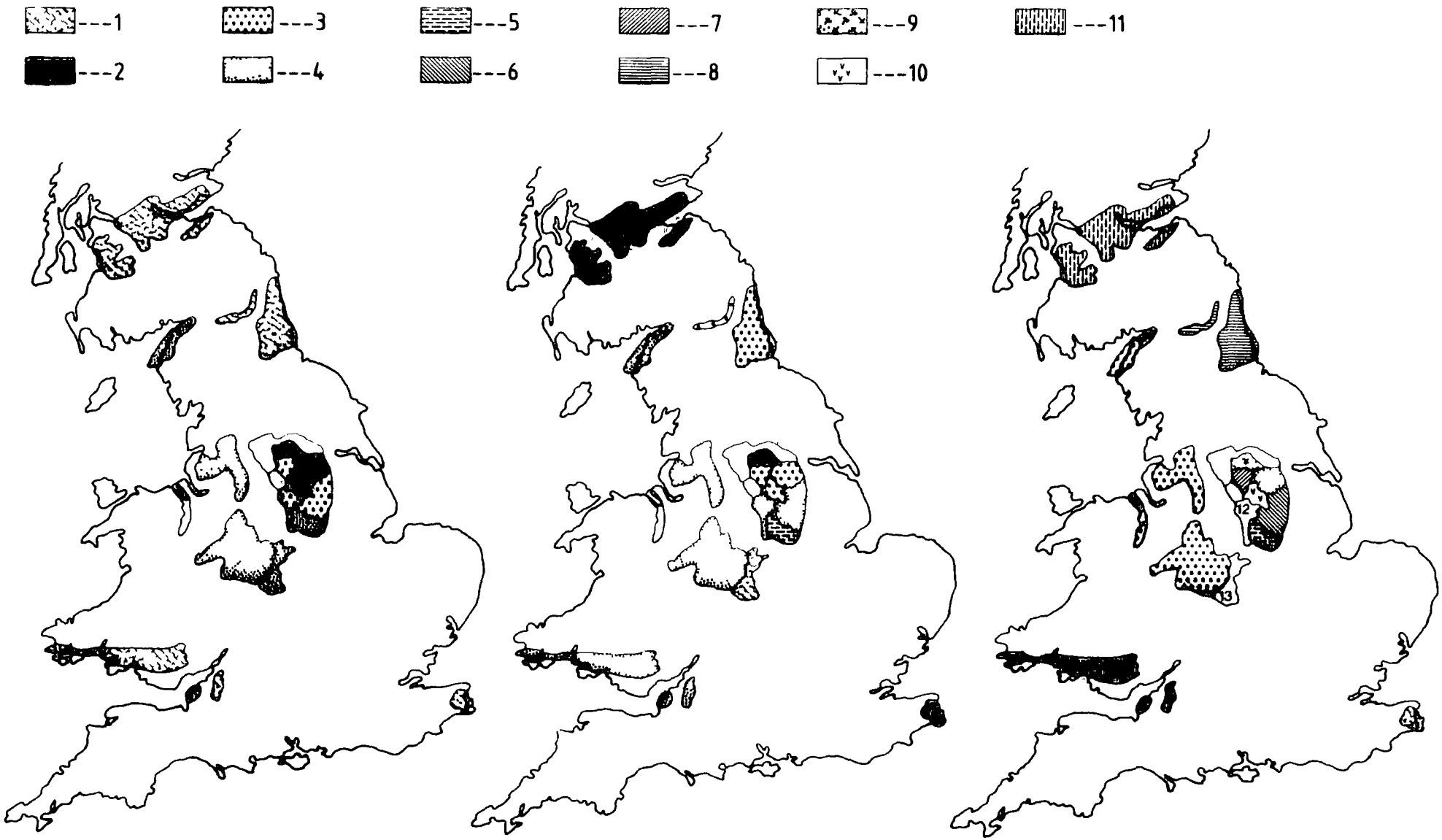

Figure 8.19 Comparison of regional patterns of variation for specific gravity, dry density and bulking factor.

rederived to overcome some of the simplifications of the earlier theories and in the proposed relationships the location in the mine of the collapse has been separated from the shape of the failure or collapse surface. The choice of mine location for the collapse overcomes the effects of 'run-in' of fragmented material beneath a stable portion of the roof. This additional volume can significantly affect the maximum potential height for a collapsing working and must be considered as a serious omission from the previous theories.

Typical values for the bulking factor of Coal Measures rocks have been established from an analysis of field (photographic) data. The values obtained from this analysis have been found to be statistically indistinguishable from the bulking factors calculated from colliery tip data. This observation has been used as justification for the use of this larger body of tip data to analyse for regional variation in the bulking factor.

The results from an analysis of this data show that the bulking factor does not correlate particularly well with any of the other variables investigated eg. particle size, sorting coefficient, ash content etc. However, regional variation in bulking factor was found with regions such as S. Wales and Kent having a significantly lower bulking factor than areas such as Scotland and N. Derbyshire.

Because no field evidence has been seen of old workings collapsing to the sorts of heights predicted by the proposed relationships it must be concluded that the majority of old workings arch before they bulk, and bulking relationships must therefore be considered as limiting collapse heights.

CHAPTER 9

THE SHAPE OF COLLAPSE STRUCTURES ABOVE OLD WORKINGS.

9.1. INTRODUCTION.

The literature review presented in Chapter 8 represents a summary of most of the work done on the potential height of migration of collapse structures. Implicit in any theory of collapse is some hypothesis on the shape of the collapse structure. The shapes of the failure surface in the afore-mentioned review have varied from a linear to a semi-circular envelope. To the writer's knowledge there has been no quantitative assessment of the shape that most nearly approximates to the average failure surface. Indeed it is questionable as to whether there is a 'typical shape' of arch.

To answer these and many other questions a number of field photographs were selected. The criterion used, as with bulking, were that the photographs should show well-developed collapse structures above old workings. Twenty six photographs from 8 opencast sites, representing 4 different rock types, were selected from forty or so suitable short listed collapse structures. Many of these photographs were also used for the assessment of bulking factors (Chapter 8). The detail of their location, shapes and other data will be found in Table 9.1.

The problem was to numerically assess which, if any, of the suggested mathematical models provided the best fit to the observed collapse profile. To achieve this aim it was necessary to digitise the arches and numerically compare the observed shape against the mathematical model.

9.2. DATA ACQUISITION.

9.2.1. INTRODUCTION.

Each old working can, for the purpose of the analysis, be considered as two half arches, back to back. Two possible lines of research extend from this

OLD WORKING REF.No.	O.S SITE LOCATION	ROCK TYPE	FULL ARCH ½-WIDTH (m)	LEFT HALF-ARCH ANALYSIS No.	BEST FIT	LINEAR EQUATION (y=Mx)	PARABOLA EQUATION A	POWER EQUATION ($Y=ax^n$) ($n=0.7446$)	APEX ANGLE degrees	RIGHT HALF-ARCH ANALYSIS No	BEST FIT	LINEAR EQUATION (y=Mx) A	PARABOLA EQUATION A	POWER EQUATION ($y=ax^n$) ($n=0.7446$)	APEX ANGLE degrees
0607	Ibbetsons	SS/Sh	2.04	1	Pow	2.44	144.48	7.8518	66.7	2	Lin.	2.52	156.84	8.1401	68.3
0613	Ibbetsons	SS/Sh	2.11	3	P/P	2.49	152.87	8.0364	68.1	4	Par.	2.53	150.44	8.2128	68.5
0816	Ibbetsons	Mud.	2.15	5	Par.	3.19	253.71	10.3276	72.6	6	P/P	3.12	243.02	10.1077	72.2
1329	Ibbetsons	SS	1.10	7	Pow.	2.18	118.62	7.0617	65.3	-	-	-	-	-	-
1135	Ibbetsons	Mud.	1.03	9	Pow.	2.03	99.95	6.5308	63.8	10	Pow.	1.91	90.94	6.1832	62.3
1425	Tow Law	Silt.	1.16	11	Par.	2.04	104.01	6.6126	63.9	12	Lin.	2.27	128.44	7.3483	66.2
1705	Ibbetsons	Mud.	1.05	13	Par	2.22	121.97	7.1783	65.8	14	Pow.	2.32	131.52	7.4726	66.7
2018	Blindwells	SS	0 71	15	Pow.	2.52	153.49	8.0929	68.3	16	P/P	2.37	140.49	7.6850	67.1
2116	Tow Law	Mud.	1.47	17	Pow	2.48	148.75	7.9671	68.0	18	Pow.	2.39	141.08	7.7202	67.3
C36	Cowsley	Mud.	2.65	19	Pow	2.27	126.11	7.3173	66.2	20	Pow.	2.18	117.53	7.0464	65.3
C48	Cowsley	Mud.	1.06	21	L/Pow	2.56	155.68	8.1920	68.7	22	Lin	2.41	145.31	7.8159	67.5
0814 (1)	Ibbetsons	SS/Sh.	2.25	23	Pow	3.03	230.25	9.8385	71.8	24	Lin	2.91	211 57	9.4310	71.0
0814 (2)	Ibbetsons	SS/Sh.	1.95	25	Par.	3.30	264.4	10.6217	73.2	26	Par	3.05	232.00	9.8758	71.8
2221 (1) *	Maes-y-Marhog	Mud.	3.90	27	Par	2.68	180.08	8.7008	69.6	28	Par.	2.58	166.52	8.3668	68.8
2221 (2) *	Maes-y-Marhog	Mud.	3.74	29	Par.	3.42	286.06	11.0207	73.7	30	Pow.	3.61	325.79	11.7030	74.5
2314 (1) *	Pit House	SS	1.21	31	Lin.	2.27	129.08	7.3664	66.2	32	Lin	2.20	120.77	7.1254	65.5
2314 (2)	Pit House	SS	0.97	33	L/Pow	2.27	128.63	7.3536	66.2	34	Lin	2.68	175.66	8.6361	69.5
0414 *	Acclington	SS/Sh	1.92	35	Pow	2.60	168.66	8.4205	68.9	36	Lin.	2.40	143.70	7.7724	67.4
0416 *	Acclington	SS/Sh	0.70	37	P/P	3.58	320.62	11.6099	74.4	38	Pow.	2.73	175.21	8.7152	69.9
0811 *	Ibbetsons	SS/Sh.	1.79	39	Par.	3.74	348.87	12.1106	75.0	40	Pow.	3.67	329.28	11.8238	74.7
0819 *	Ibbetsons	Mud.	1.44	41	Lin.	4.15	421.82	13.3827	76.5	42	Pow.	3.38	285.18	10.9439	73.5
1322	Ibbetsons	Mud.	0.75	43	L/Pow.	2.11	109.44	6.8164	64.7	44	Lin	2.40	144.38	7.7098	67.4
1427 *	Tow Law	Silt.	0.67	45	Par.	2.32	134.10	7.5083	66.6	46	Par.	2.24	125.74	7.2705	66.0
1635 *	Ibbetsons	Mud.	1.00	47	Par.	2.43	147.4	7.8719	67.6	48	Par.	2.42	145.92	7.8323	67.5
2024 *	Blindwells	SS	0.49	49	Par.	2.93	213.12	9.4887	71.2	50	Lin.	3.48	303.48	11.2592	74.0
RKT	Pethburn	Silt.	1.38	51	Par.	2.67	178.69	8.6672	69.5	52	P/P	3.58	319.65	11.5923	74.4

* = Corrected for Bridging dead space.

Rock abbreviations

Mud. = Mudstone
Silt = Siltstone
SS = Sandstone
SS/Sh = Interbedded sandstone, ironstone & shale

Fit abbreviations & totals

Lin	= Linear	11
L/Pow.	= Linear or Power	3
Pow.	= Power	16
P/P	= Power or Parabola	5
Par.	= Parabola	16
		51

Table 9 1 Location and shapes of arches chosen

assumption. Firstly, the two arches can be considered as 2 separate assessments of the arching capacity for the given situation, which can be summed to provide the average shape for the arch. In other words, the average shape for pairs of half arch collapse structures would be assessed. Alternatively, it can be argued that as one half of the arch has no influence on the other arch (ie. one half arch is completely independent of the other), each arch furnishes two independent assessments of the arching capacity of the rock type. Therefore every complete arch yields two separate arching assessments.

The latter assumption was followed, and as shown later, this proved to be a wise choice. The data base thus consisted of 51 half arches which were independently compared against the numerically developed models described below.

9.2.2. PHOTO CORRECTION.

Two problems were encountered with the data acquisition from the photographs. The first was that only 16 of the 26 collapse structures had completely collapsed, the remaining 10 collapses had been bridged at some high point in the arch. The purpose of the analysis was to investigate the curvature of the collapse structures therefore, the inclusion of the bridged shape would only confuse the issue. In order to remove the bridging effect from the 10 structures, perpendiculars were dropped from the point of bridging down to what previously would have been the roof of the old working and the arch shape enclosed by the perpendicular was then digitised. This procedure effectively reduces the apparent width of the old working. Figure 9.1 shows the elimination of the dead space from a typical old working.

Justification for the inclusion of partly bridged arches into the data set was obtained at the end of the analysis when a chi-squared test showed there was no evidence to suggest (sign 0.8) that the bridged data had a different distribution of arch shapes than the remaining main body of data.

The second problem, parallax, has been discussed earlier in Chapter 2.5.1. While much of the error can be eliminated by a careful choice of the initial

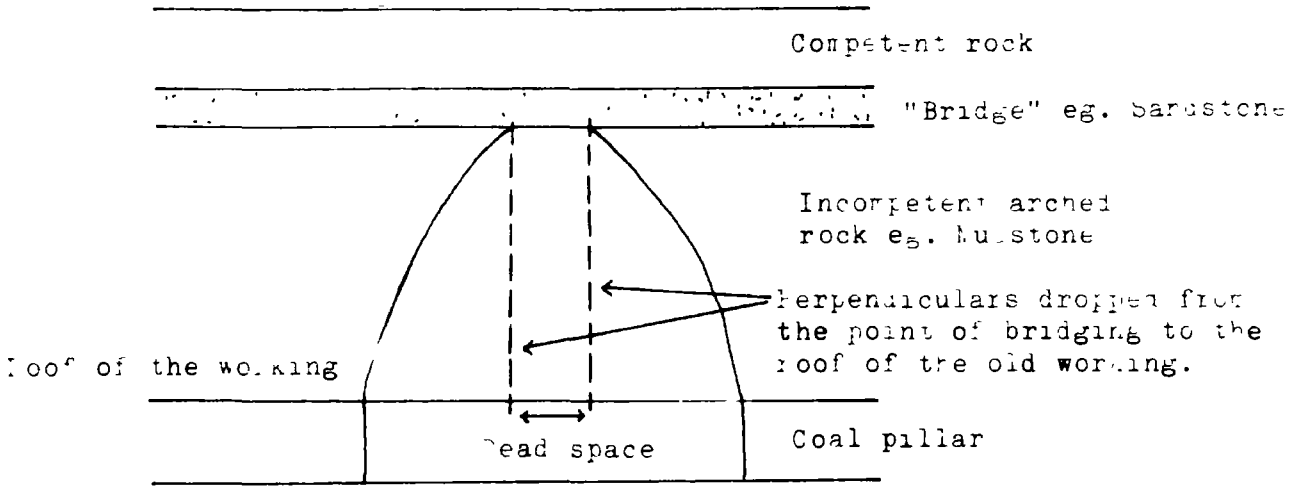

Figure 9.1 Elimination of dead space during digitisation.

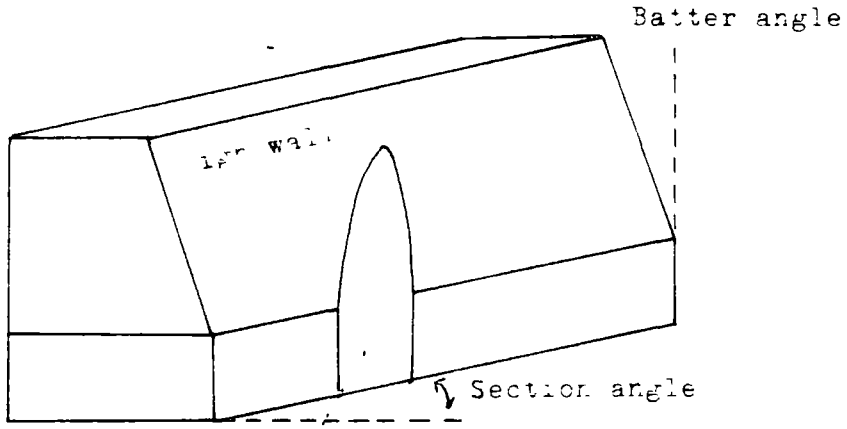

Figure 9.2 Parallax errors due to high wall orientation.

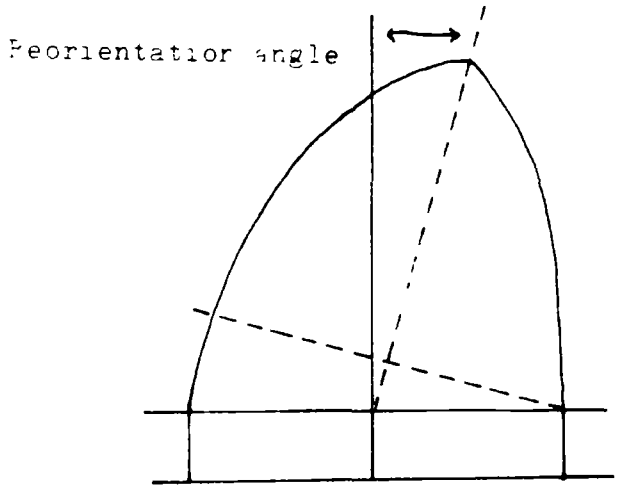

The arch line is assumed to be symmetrical and a crude correction can be made by re-orientation of the axis.

Figure 9.3 Crude correction of parallax errors.

location for taking the stereo-photographs, parallax due to the high wall 'batter angles' and oblique high wall sections cannot be completely overcome. These parallax errors distort the two different halves of the arches to different degrees. The ideal method of overcoming these errors (Fig. 9.2) would be to digitise the shape, and then warp the data numerically to correct for the parallax. An alternative, but numerically less stringent method is to re-define the axis of the arches to accommodate and average out, the parallax (Fig. 9.3).

This method was adopted and proved to be reasonably effective, but in any future work an attempt to numerically warp the data is strongly recommended.

9.2.3. DIGITISING AND SUBSETTING THE DATA.

The digitiser used, produced a stream of X-Y co-ordinates at a pre-selectable time increment. Thus the speed at which the shape was digitised and the time increment selected on the digitiser, dictated the accuracy with which the shape would be characterised. As each arch was photographed at a slightly different distance, their sizes differed. Thus for different arches, the raw data from the digitiser was not directly comparable. Even after adjusting the digitised arches to the same scale, the increments at which the arch had been characterised differed. These problems were overcome in the following manner. The digitiser was set at the maximum resolution (minimum time step), and each arch was digitised. Each half arch was represented by about 300 to 500 X-Y co-ordinates. These were scaled with respect to the X-axis and corrected to a standard origin. The origin of the scaled data lay at (0,0) and the apex of the arch lay at (X-max,Y-max), where X-max was assigned a value of 100. The 400 or so data points for each arch were then sampled to produce Y co-ordinates for every one increment of X, (ie. a subset of 100 X-Y co-ordinates were selected from the data so that each point could then be directly compared with points from other corrected arch data).

Inevitably, especially in the smaller of the arches, there were holes in the data sets, but the high resolution of the subset data ensured that a fair

representation of the arch shape was produced and that there was an adequate quantity of data for any comparisons performed on the shapes.

With the raw data now scaled and reduced to a standard form, it becomes possible to compare the different shapes and also obtain the 'average' shape for an old working. The arches shown in Figures 9.4a to 9.4g have been recreated from the scaled subset data.

9.3. DATA MANIPULATION.

9.3.1. SHAPE REDUCTION.

Statistical techniques were employed to find which mathematical relationship provided the best approximation to the shape of the old workings. The statistics of a straight line are considered easier to use than those of a curve and therefore the data were manipulated to remove the effects of the curvature prior to the comparison. Initially three common shapes with regular mathematical functions were chosen. These were a linear or straight line failure surface, a parabolic failure surface and an elliptical failure surface. These three mathematical functions covered almost all of the shapes proposed in the literature.

Figure 9.5 shows the three proposed shapes for the failure surface of the collapse structure. The following equations derived from the general equations for the shapes involved, will provide a Y co-ordinate varying from 0 to Y-max for a given X co-ordinate value.

The equation for the linear surface is:

$$Y = m X \qquad \text{where } m = \frac{Y\text{-max}}{X\text{-max}}$$

A parabolic relationship is represented by:

$$Y^2 = 4 a X \qquad \text{where } a = \frac{Y\text{-max}^2}{4 \times X\text{-max}}$$

$$Y = (4 a X)^{1/2}$$

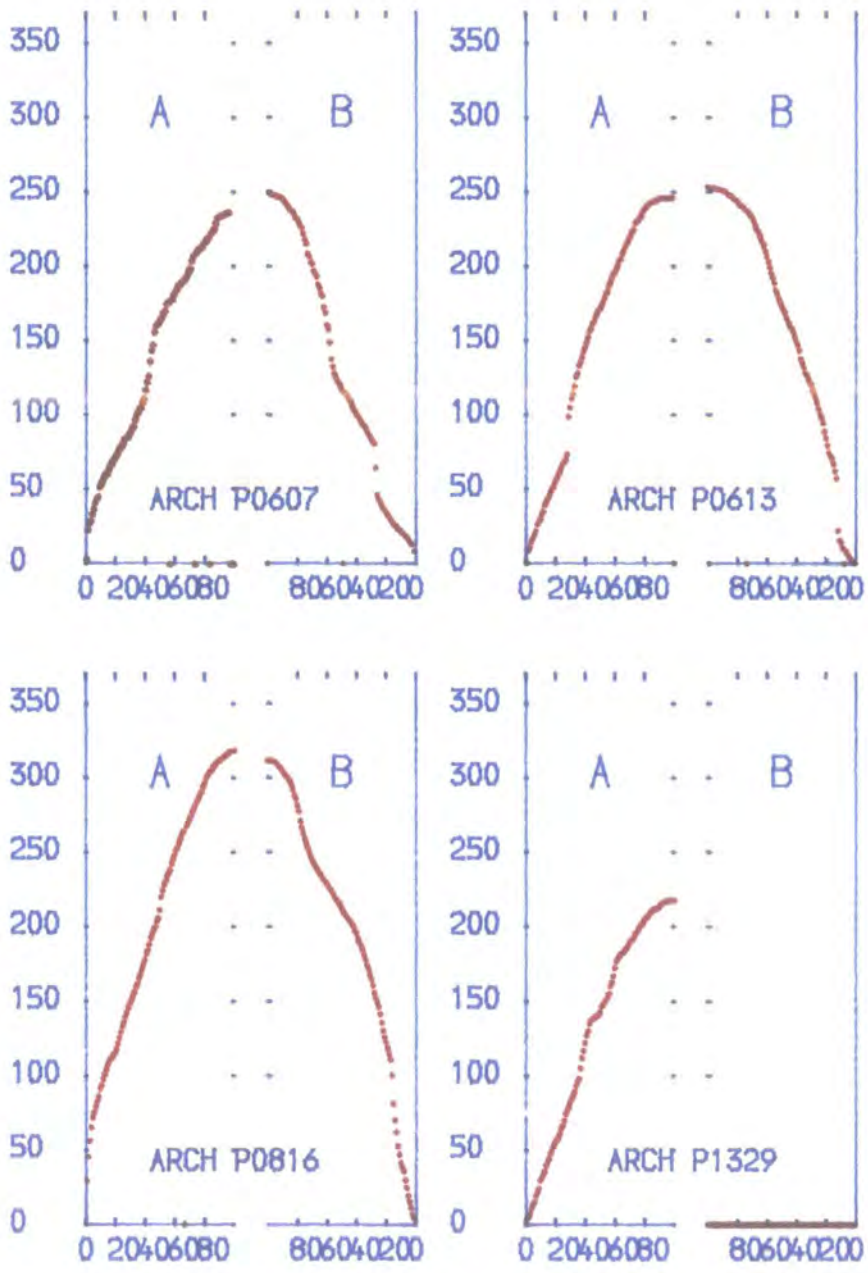

FIG 9.4a SCALED ARCH PROFILES

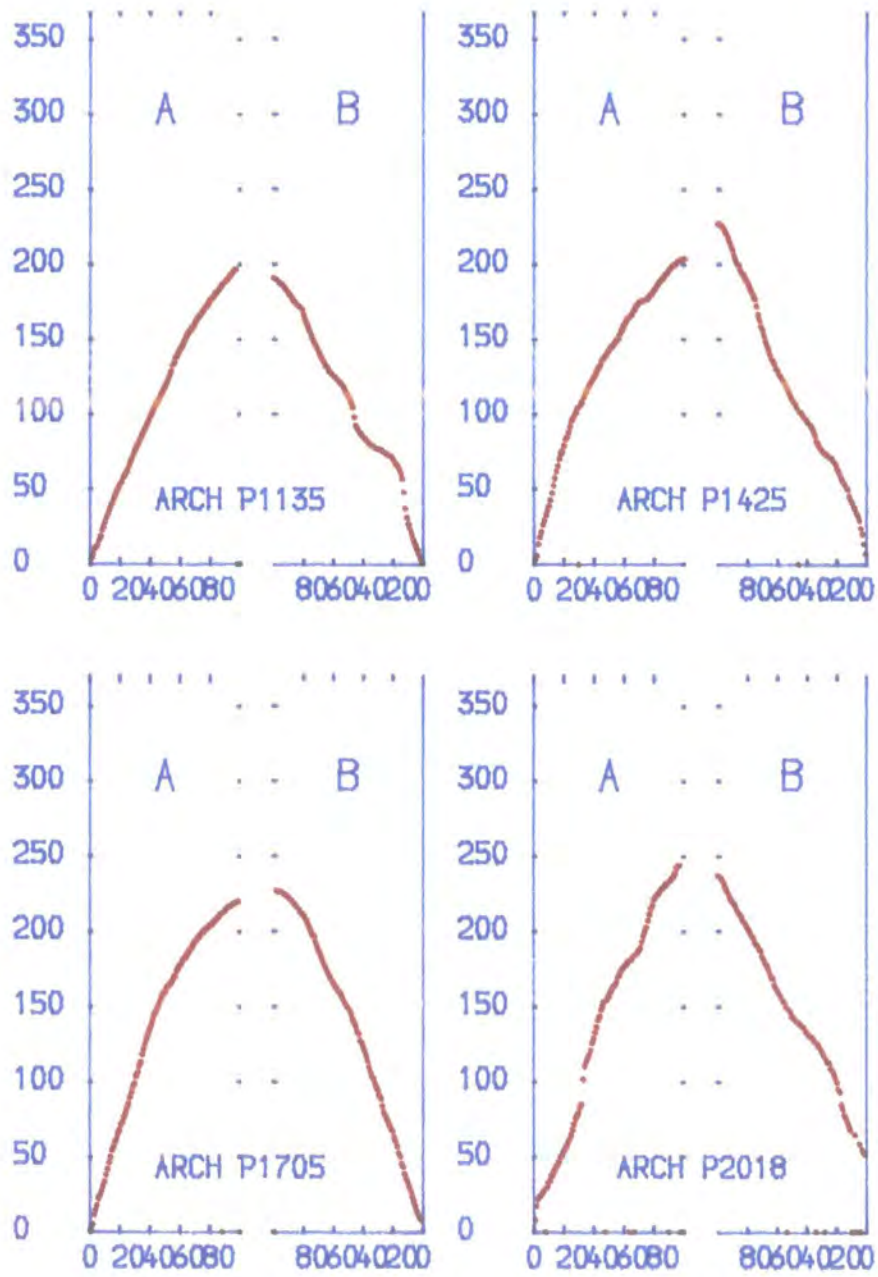

FIG 9.4b SCALED ARCH PROFILES

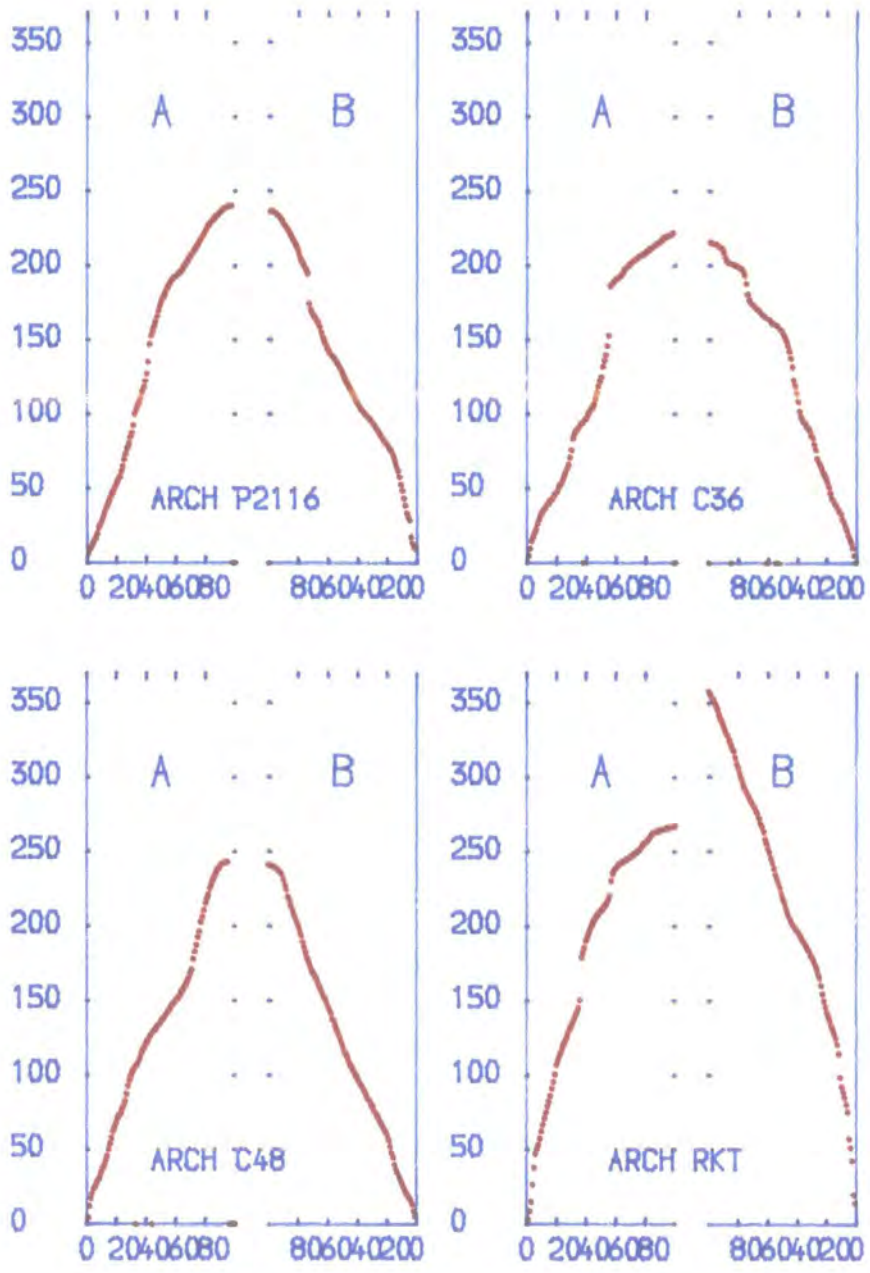

FIG 9.4c SCALED ARCH PROFILES

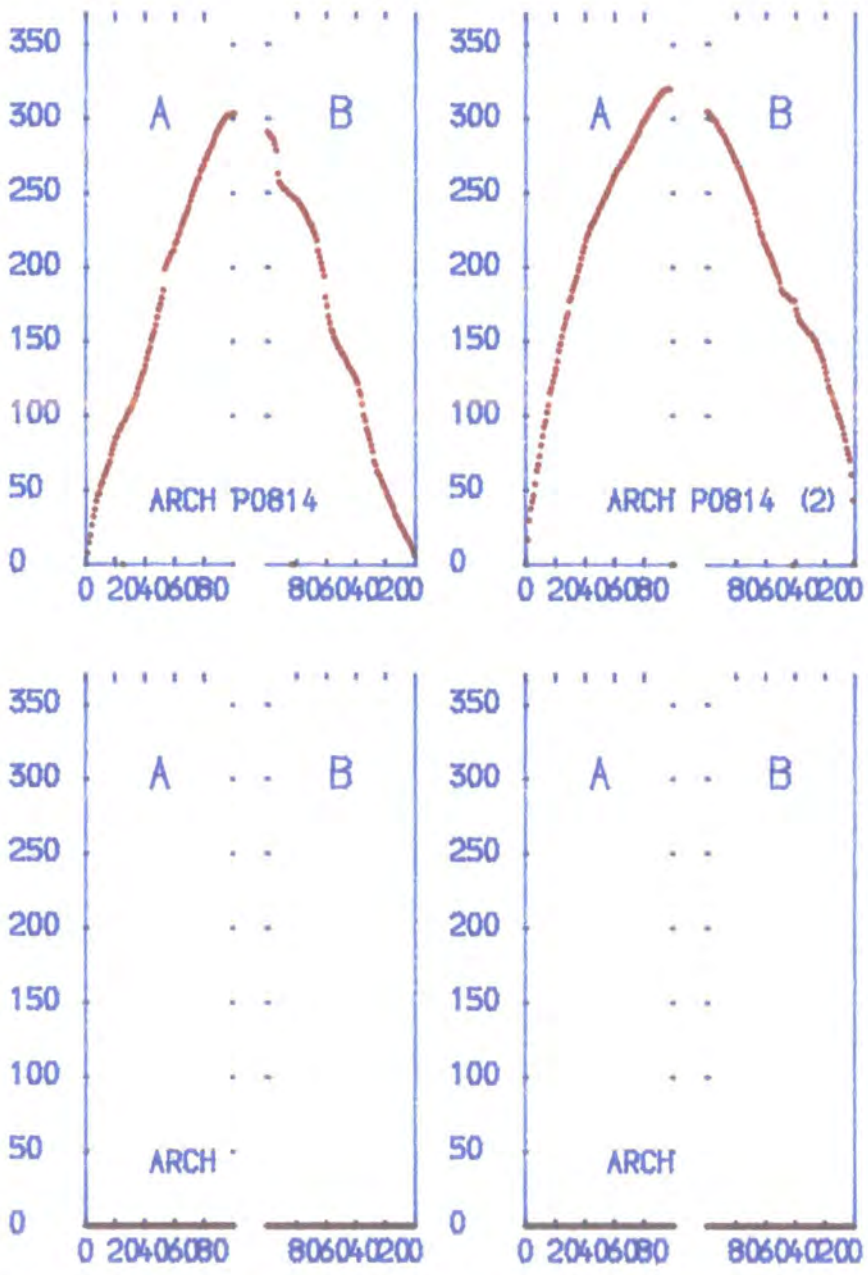

FIG 9.4d SCALED ARCH PROFILES

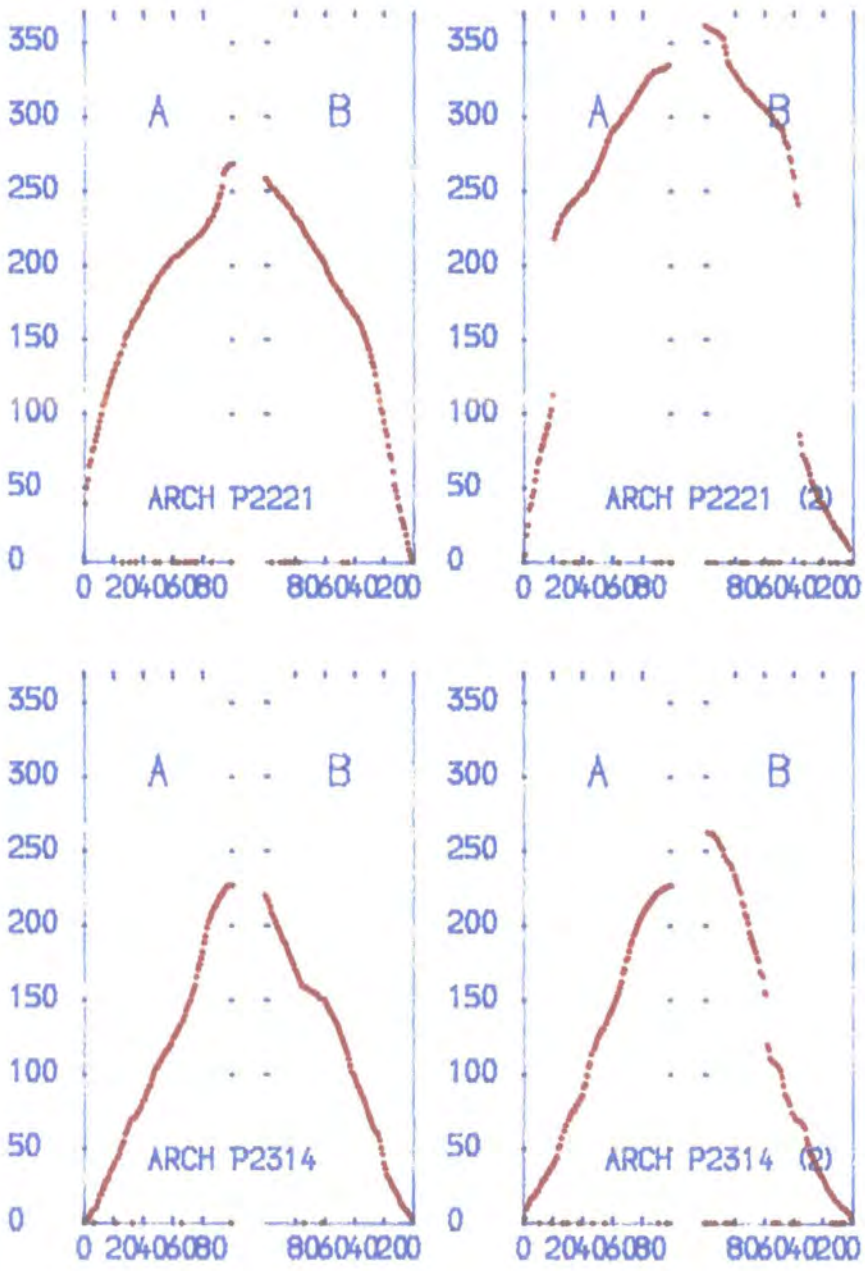

FIG 9.4e SCALED ARCH PROFILES

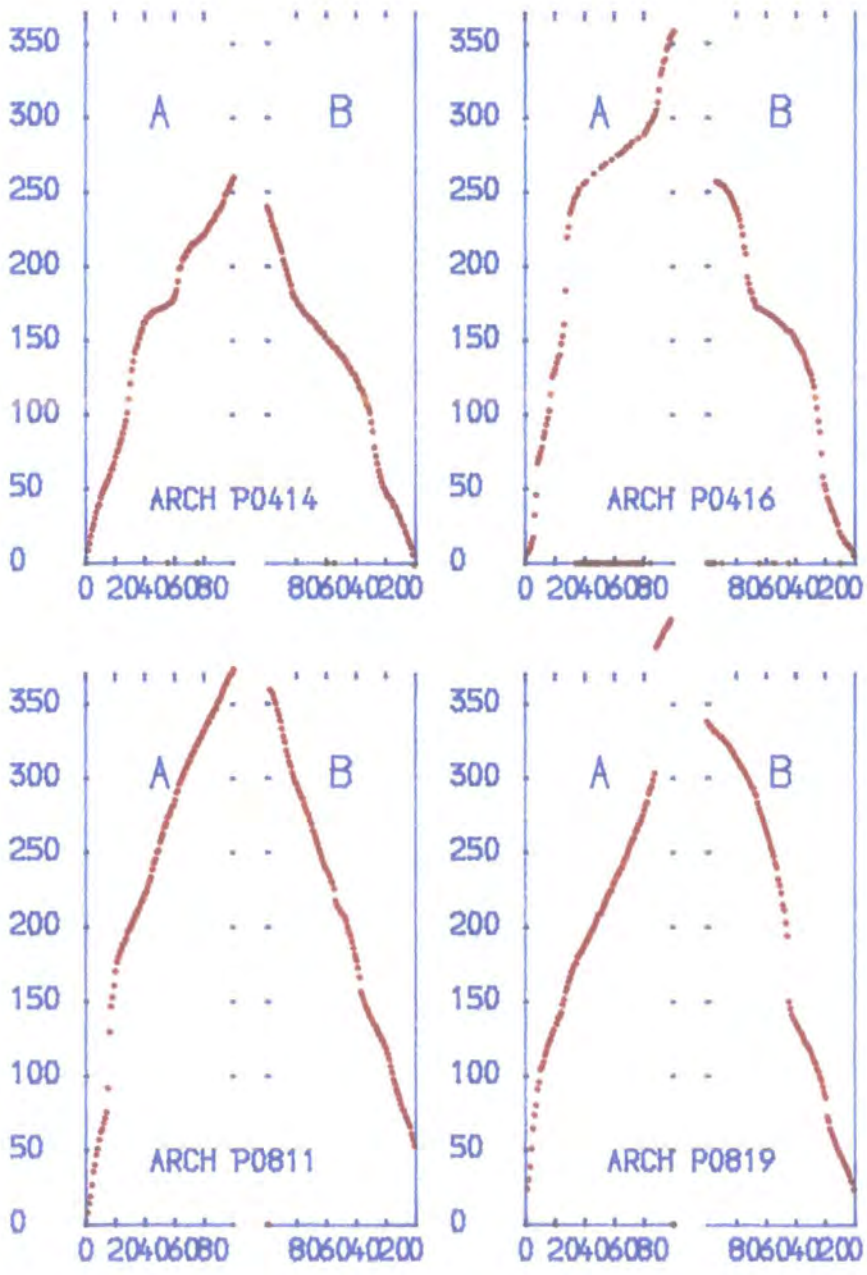

FIG 9.4f SCALED ARCH PROFILES

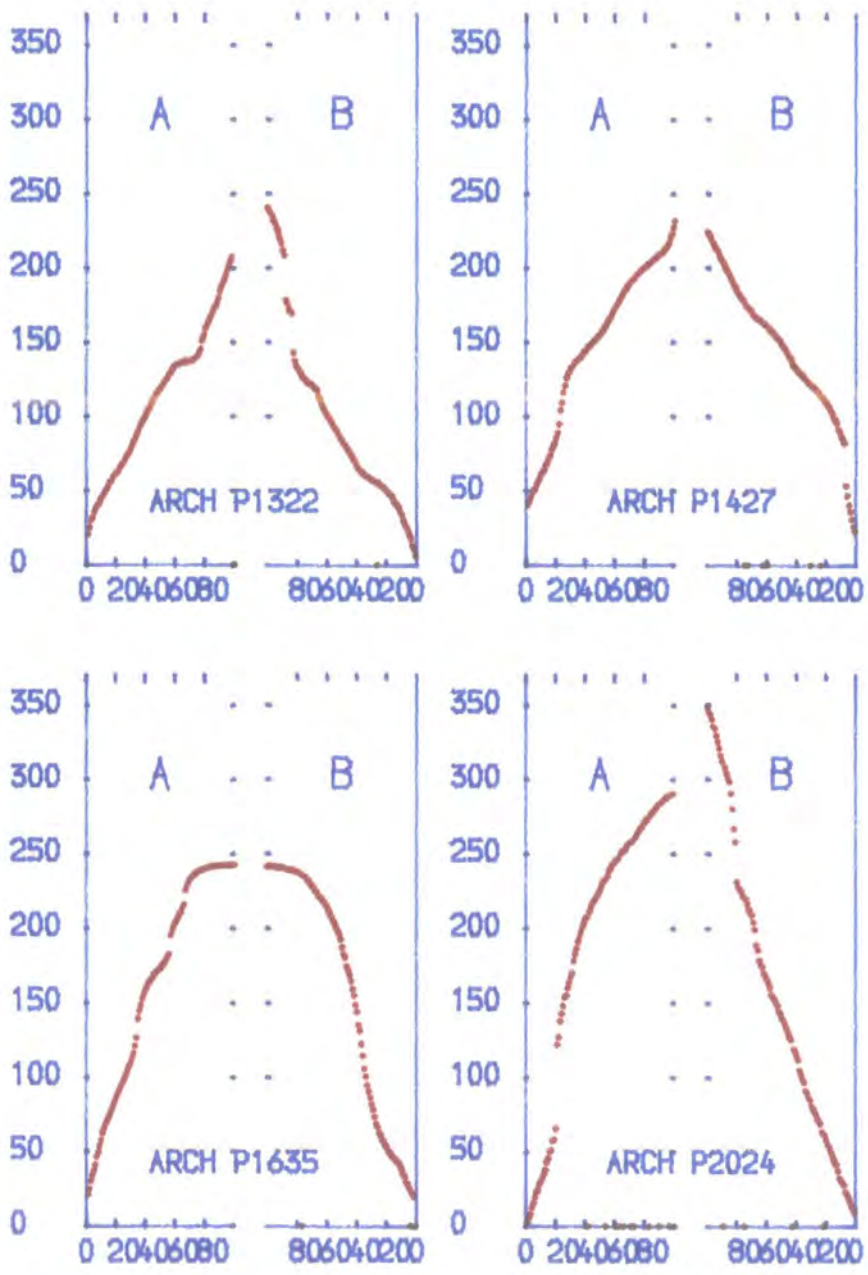

FIG 9.4g SCALED ARCH PROFILES

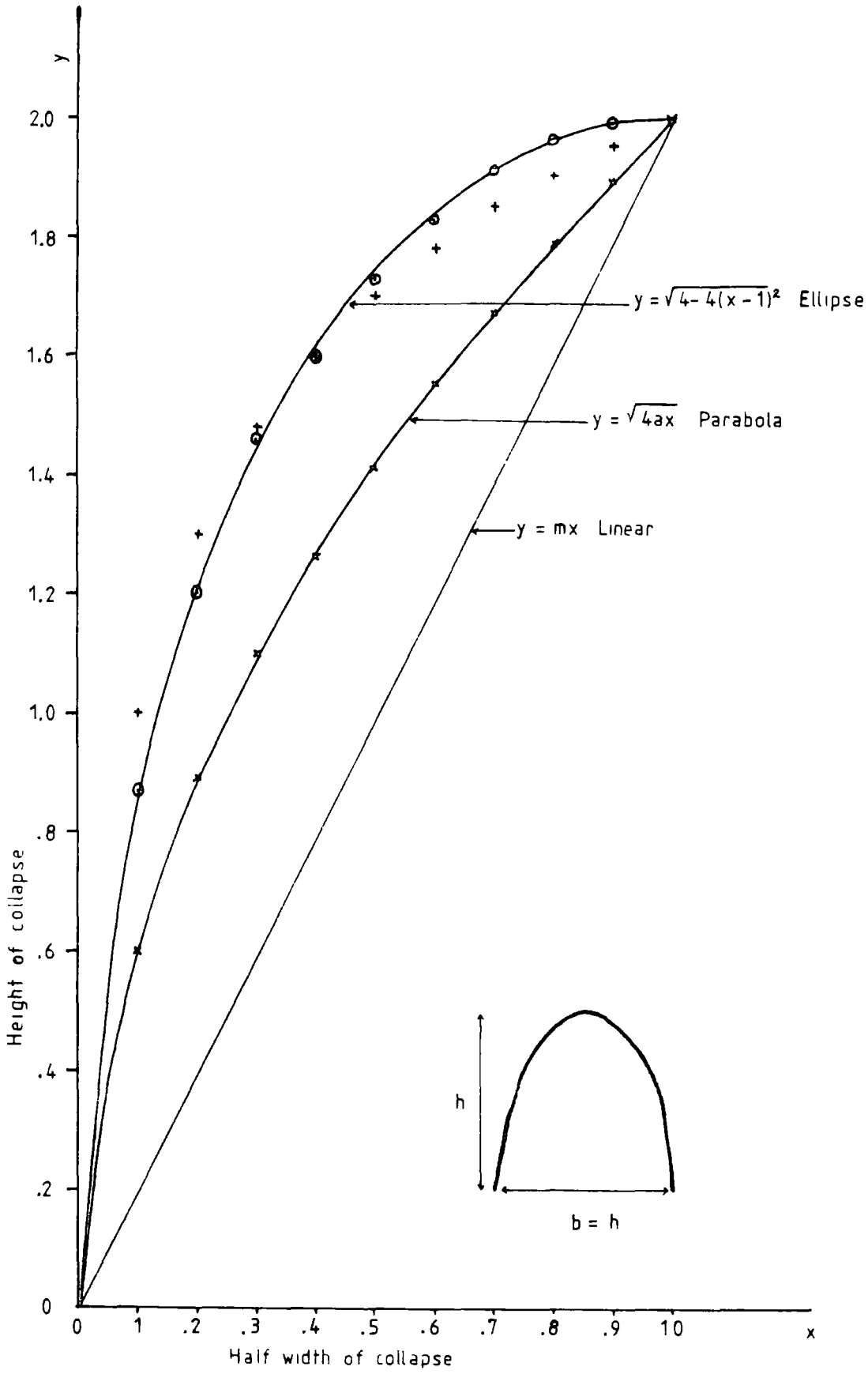

Figure 9.5 Proposed shapes for failure envelopes.

The ellipse is represented by the equation:

$$Y = \left(c^2 \left(1 - \frac{(d - X)^2}{d^2} \right) \right)^{1/2} \qquad \text{where } c = \text{Y-max},\ d = \text{X-max}$$

Before approaching the field data, it is first necessary to find the difference between the theoretical shape derived above and a straight line. That is, for each theoretical shape, the quantity required to remove the effect of curvature and produce a straight line. Once acquired , these differences can be subtracted from the field data. The resulting points from the three reductions can then be analysed for their closeness of fit to a straight line of equation $Y = m X + c$. The reduced data set which most closely approximates to a straight line will indicate which of the proposed shapes provided the closest fit to the field data.

Reference to Figure 9.6 will show that the difference between a parabola and a straight line, ie. the 'parabolic element' of the shape is represented by "dp" (Fig. 9.6). This value is equal to:-

$$dp = YP - YL$$

$$dp = (4\ a\ X(i) - m\ X(i))^{1/2}$$

Similarly the difference between an ellipse and a straight line is represented by "de" (Fig. 9.6) and is equal to:

$$de = YE - YL$$

$$de = \left(\text{Y-max}^2 \times \left(1 - \frac{(\text{X-max} - X(i))^2}{\text{X-max}^2} \right) \right)^{1/2} - m\ X(i)$$

Obviously the difference between a straight line and a straight line is zero. Thus, there is no reduction required for a linear fit, and 'dl' = 0.

To determine which mathematical function best approximates to the field data

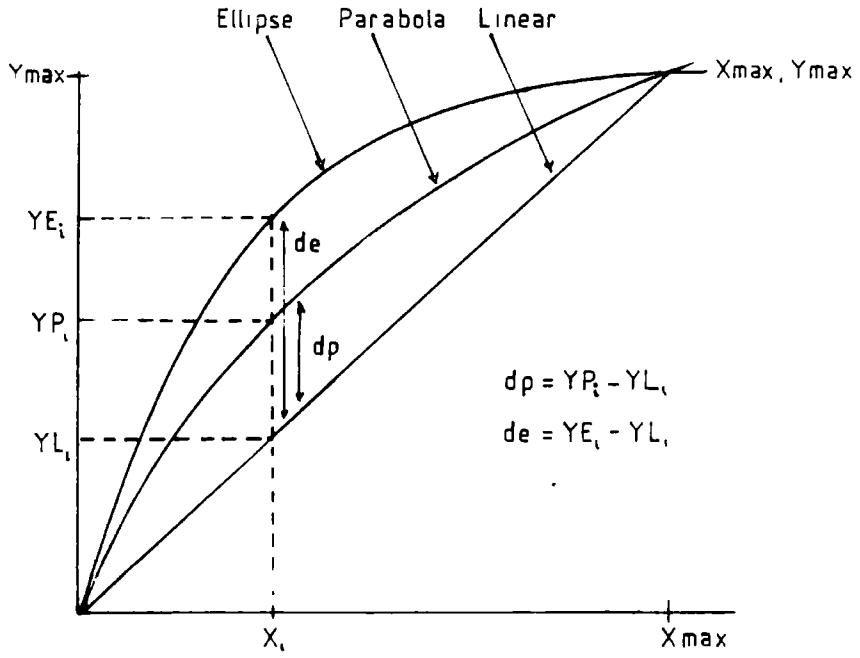

Figure 9.6 Nomenclature for curve reduction.

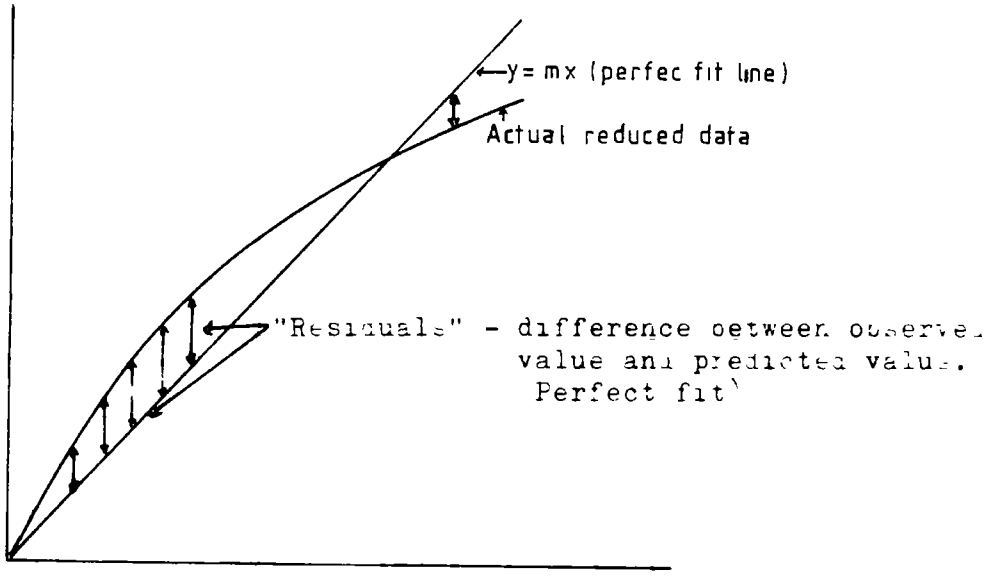

Residuals are:-

$$r(par)_1 = Y(par)_1 - mX_1$$

or $$r(ellip)_1 = Y(ellip)_1 - mX_1$$

Figure 9.7 Determination of residuals from perfect fit.

'de', 'dp' and 'dl' were subtracted in turn from the Y co-ordinate for every X value. For the elliptical and parabolic functions the reductions for X are:-

Elliptical reduction for X:

$$Y(elip)(i) = Y(i) - \left(Y\text{-max} \times \left(1 - \frac{(X\text{-max} - X(i))^2}{X\text{-max}^2} \right) \right)^{1/2} - m\,X(i)$$

and for the parabolic reduction:

$$Y(par)(i) = Y(i) - \left(4\,a\,X(i) \right)^{1/2} - m\,X(i)$$

As 'dl' is zero the field data remains unchanged for the linear reduction.

When the reduction for each shape is complete the 'Yi' reduced values for each shape are plotted in turn against their corresponding X value. If the original shape of the old working was a perfect ellipse then when 'Y(elip)i' is plotted against 'Xi' a straight line would result with an equation:

$$Y = m\,X \qquad \text{where} \quad m = \frac{Y\text{-max}}{X\text{-max}}$$

If the shape of the old working was a perfect parabola then when 'X' is plotted against 'Y(par)i', a straight line would result with the m value as above.

Similarly if the shape of the old working was a perfect triangle, ie. the failure surface were not curved at all, then when 'Y(lin)i' was plotted against 'Xi', a straight line would result.

Obviously it is extremely unlikely that the field data will exactly fit one of the above shapes, therefore a choice between which reduced data set best approximates to a straight line must be done statistically.

9.3.2. STATISTICAL MODEL.

At first sight it may appear that the decision between which of the reduced data sets most closely approximates to a straight line can be obtained by simply

comparing the correlation coefficients 'r'. While this value is a measure of linearity, and is used later in the analysis, it is not necessarily a measure of the closeness of fit to the line 'Y=mX' where (m=Y-max/X-max). A comparison between the reduced data can only be made by looking at the residuals from the perfect fit, that is the difference between the observed and the predicted value.

Figure 9.7 illustrates this point. The residuals are obtained by subtracting the reduced values, for each shape, from a straight line. The mean of the residuals and the standard error of the estimate are then calculated for each fit. These are given by:-

$$\text{Mean} = \frac{\Sigma \text{ residuals}}{n} \qquad \text{S.E.} = \left(\frac{\Sigma(\text{residuals}^2)}{n}\right)^{1/2}$$

A perfect fit would have a mean value of 0 and a standard error of 0. However, a perfect fit is unlikely, and the best fit will have a mean value close to 0 and a small standard error. The standard error gives some measure of how well the theoretical shape fits the field data, and it has the same property as the standard deviation in that it is used to express the spread of data around the mean. Figure 9.8 shows four possible examples for the reduced data and their relationships to the perfect fit line. The third example is obviously the best fit. Following this the fourth and second examples are reasonably good fits, while the first example, in spite of its zero mean and high 'r' value, is obviously not a good fit, as indicated by the high value for the standard error.

In practice the difference between the different fits is not so clear cut. Thus, Snedecor's F and the Student t-test may be used to help choose between the distributions of the residuals for the various fits.

Firstly, the F-test is used to compare the variances of the distributions of the two sets of residuals. If the F-test shows that there is no significant difference between the variances of the residuals, then it is theoretically justified to use the t-test to check whether the mean residual value for one fit

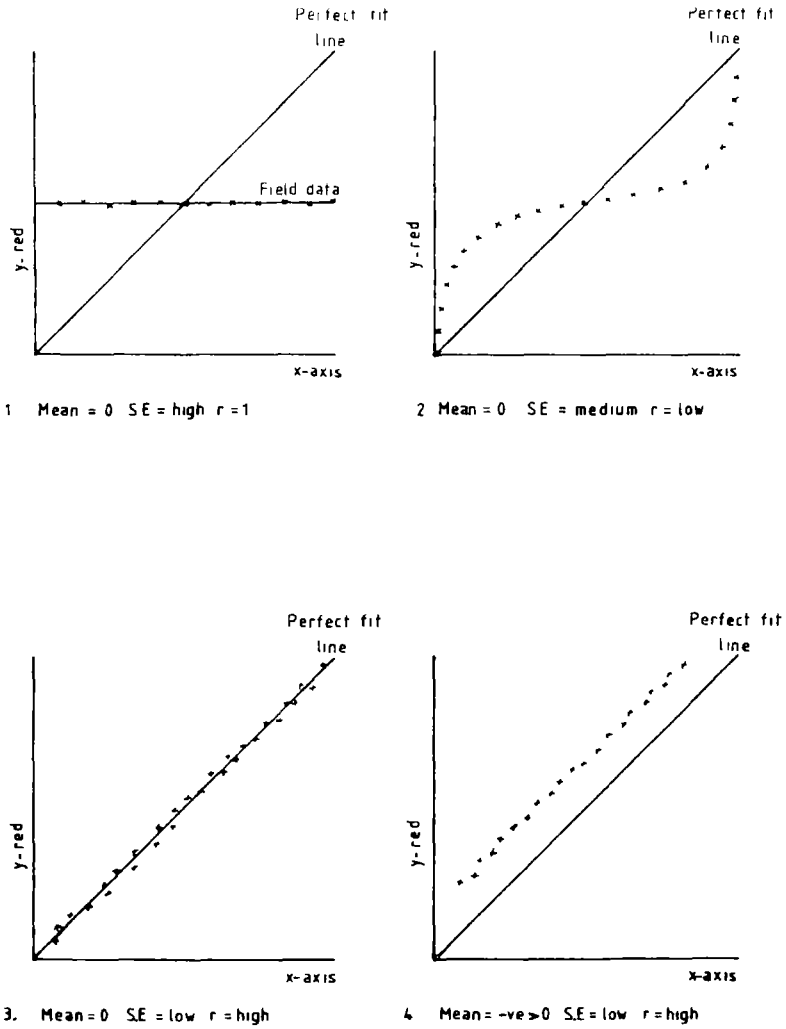

Figure 9.8 Possible relationships between the perfect fit and the reduced data.

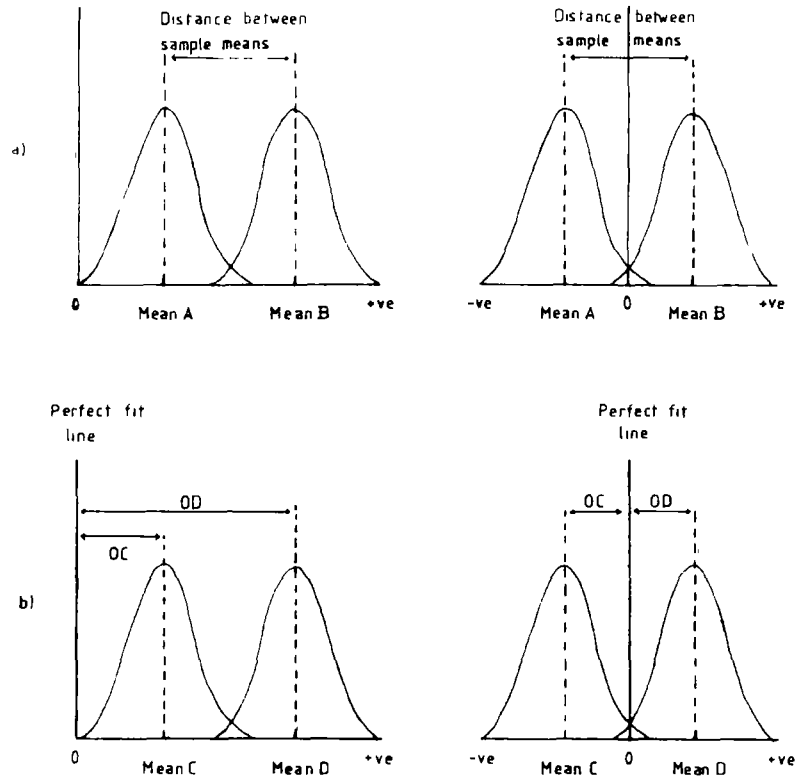

Figure 9.9 Statistical reasons for the adaption of the t-test.

is significantly different from the mean residual for the other fit.

The t-test is generally used to compare the distance between sample means, and hence the sign of the mean is important (Fig. 9.9a). However, for the purpose of this exercise it is necessary to establish whether or not the distance between the sample means and the perfect fit line are significantly different. Because it is the residuals being dealt with , the means will not necessarily fall on the same side of the perfect fit line, thus one may be positive, while the other is negative (Fig. 9.9b).

For the present purpose the means must fall on the same side of the perfect fit line so that the t-test can compare between the distances of the two means from the perfect fit line. The simplest way to achieve this, when calculating the Student t value, is to ignore the sign of the residual mean. Numerically this effect can be obtained by using, in place of the mean residual values, the root of the square of the means. The top line of the t-test is therefore modified to read:

$$t = \frac{\left(\left(m_i \right)^2 \right)^{1/2} - \left(m \right)^2 \right)^{1/2}}{\left(\frac{\sigma_i^2}{n} + \frac{\sigma_2^2}{n} \right)^{1/2}}$$

9.3.3. COMPUTER PROGRAM AND OUTPUT.

Because of the specialised nature of the analysis no propriety statistical packages, in a convenient form, offered suitable analysis techniques, and so a program was written, based on the foregoing text, to compare the shapes of the field data against the theoretical shapes (Appendix 3). Typical output from the program is shown in Table 9.2 which is divided into three sections. The top third provides information relating to the fit of the residuals from the relevant equations above. The middle third gives the levels of significance between the residuals of the different fits, and the final section gives the coefficients for the equations used to obtain the residuals. It is hoped that a guided interpretation of this output will aid comprehension of the previous and

RESULTS FOR ARCH No. 52

ANALYSIS OF RESIDUALS FROM APPROPRIATE FIT

ANGLE TO APEX OF ROOF : 74.4°

	Linear	Parabola	Ellipse	Power
Number	100	100	100	100
Mean	-41.2352	18.2875	60.7100	-15.0753
S.E.	46.7935	20.7088	65.6870	20.1538
R(t)	0.988 64.3	0.997 118.3	0.984 54.7	0.996 110.0 DF = 98

t AND F TESTS OF SIGNIFICANCE

Between	t	DF	F	DF
Linear/Parabola	4.4845	198	5.1058	99,99
Parabola/Ellipse	-6.1954	198	10.0612	99,99
Linear/Ellipse	-2.4147	198	1.9705	99,99
Linear/Power	5.1345	198	5.3909	99,99
Parabola/Power	1.1116	198	1.0558	99,99
Ellipse/Power	6.6417	198	10.6229	99,99

COEFFICIENTS FOR EQUATIONS

Linear	Parabola	Ellipse		Power	
M	A	A	B	a	n
3.58	319.65	100	357.8	11.5923	0.7446

TABLE 9.2

TYPICAL OUTPUT FROM PROGRAM 'SHAPETEST'

forthcoming text. In the example (Table 9.2), a fourth theoretical fit, the power fit is also used (this will be discussed in detail later, Chapter 9.4.3).

Study of the output (Table 9.2), shows in this case the lowest mean residual can be identified as the parabolic fit, but the power fit also has a low mean value. Before a decision can be made on whether or not the difference between the mean value is statistically significant, the variances of the two distributions must be checked to ensure that they are both from the same underlying population. It will be remembered that the t-test can only be used providing that this assumption is valid. The F statistic in the output (Table 9.2) tests this hypothesis. The appropriate F value for the difference between the parabola and a power fit is 1.06 in this case.

TABLE 9.3 SIGNIFICANCE LEVELS FOR THE F AND t TESTS.

significance level		t	DF
0.001	0.1%	3.2905	198
0.050	5.0%	1.9600	198
significance level		**F**	**DF**
0.025	2.5%	1.9000	99,99
0.050	5.0%	1.6300	99,99

Table 9.3 contains extracts from appropriate tables of significance for the F and t tests (Snedecor and Cochran, 1980). Consulting Table 9.2 it will be seen that the F ratio of 1.06 for the differences between the parabolic fit and the power fit fails to reach the 5% significance value, which is equivalent to 1.63 (Table 9.3). Thus there is no significant difference between the variances of the parabolic and power curves. This means that the t-test can now be used to test whether the difference between the residual means of the two fits is statistically significant.

The t-test value for the difference between the means of the residuals from the power and parabola fits is 1.1116 (Table 9.2). Reference to Table 9.3 shows that the t-test value fails to reach the 5% significance level. Thus it can be said with a high degree of confidence, that the data for arch no. 52 are equally well represented by either a power fit or by a parabolic fit, but it is

definitely not well represented by either the linear or elliptical fit. The coefficients for the curves are given at the bottom of the output, while the angle to the apex also referred to as 'alpha angle' (Chapter 3.3.2) is given as 74.4 at the top of the output. It will be noted that the correlation coefficient 'r' for the parabola is slightly higher than for the power equation, intimating that the parabola fit provides the most linear fit. However, the difference between the two coefficients of determination (r squared) shows that the variation represents only about 0.4% of the data, or less than one point on the graph, which is obviously not an important difference. The t-tests on the significance of the correlation coefficients (r), show that all the correlation coefficients are highly significant (as would be expected).

Output from the program can also include the residuals from the best fit. These data are not presented in the thesis, but can be used as an additional assessment of the goodness of fit between the chosen shape and the field data. If the fit were good the residuals would plot on a straight line (high r value). However, if the fit were poor, then the residuals would show some degree of curvature. To test whether the residual line is straight or not, a stepwise polynomial regression can be carried out on the Y values versus X values of the residuals. A first order polynomial is a straight line , a second order polynomial is curved and has one break in slope, while a third order polynomial has 2 breaks in slope, and so on. By doing an F-test on the reduction in the residual mean square due to a successive order for the polynomial, it is possible to determine whether the reduction in the sum of squares is significant or not. A significant reduction in the sum of squares indicates that the residual data are better represented by a curve than a straight line. This implies that while the shape chosen by the above analysis may be the best fit, it is still not very good.

9.4. STATISTICAL INTERPRETATION.

9.4.1. INITIAL ANALYSIS.

The criteria developed above were used to group the 51 half arches into one of

the three best fit groups; parabola, linear, or undifferentiated parabola/linear. The division was done using a significance level of 0.05 (95% confidence level). To put this another way, there had to be a greater than 1 in 20 chance (sign <0.05) that the half arch was best represented by the chosen shape for it to be classified into that group. If there was less than a 1 in 20 chance then the arch was classified as a borderline case and it was allocated to the undifferentiated linear/parabola group.

None of the arches were well-represented by an ellipse so this shape can be considered to be rare. Eight of the half arches could have been equally well represented by either a parabola or a linear fit (undifferentiated), while the remaining 43 were fairly evenly distributed between the linear and the parabola fit. In fact a Chi-squared test on the shapes showed that linear and parabola fits were equally common. This therefore, implied that there was no single shape which could be said to be the 'typical' arch shape.

The data were broken-down further and analysed in a similar fashion to look for any differences between the left hand arches and the right hand arches. Here, the Chi-squared test indicated that there was probably a significant difference (1.5%) between the relative frequency of the different shapes on either side of the arch. The data suggested that left hand arches tended to be more parabolic and the right hand arches more linear.

This possible statistical difference cannot be explained on a geomechanical basis. If the difference is a real one then the most likely sources of error will be either parallax errors in the initial photographs, or poor data correction. This is why in Chapter 9.2.2, it was suggested that for future work numerical warping should be attempted in place of the more crude axis rotation.

However, it was suspected that the difference between the right hand and left hand half arches may be more apparent than real. Such a difference could arise if the majority of the arches fell between the linear and parabolic best fits. If this were the case then a slight parallax error could push the half arch to one side or the other of the dividing line and thus create a large apparent

difference between the two sides. To check this hypothesis and to characterise a 'typical arch' shape the average shape for all the arches was calculated.

9.4.2. CALCULATION OF THE AVERAGE ARCH SHAPE.

a. METHOD 1: 'MEAN DATA'. The field data consist of 51 half arch profiles where the height of the arch at every increment of X is known. the average arch shape can therefore be calculated by finding the average height of the arch at every increment of X and then characterising the shape of all the averages.

The mean and standard deviation for the Y co-ordinate at every increment of X were therefore, calculated and are plotted in Figure 9.10. Statistical tests of skewness and kurtosis showed that the distribution of Y co-ordinates was possibly not perfectly normal (sign 0.05), so median values for the Y co-ordinate were also calculated (Fig. 9.10). The positive skew to the data suggested that there is more variation in the arches that migrate higher than average, than in those that collapse to less than average.

The statistical advantages of using the mean and standard deviation over the median values are well known. Because the possibility of a normal distribution of the Y co-ordinates could not be completely ruled out, and as the positive skewness of the data would tend to overestimate rather than underestimate the height of the collapse anyway, the mean and standard deviation have been used in the remaining part of this analysis.

For reasons that will become obvious (see Chapter 9.4.3), a power function was chosen in preference to a polynomial function to characterise the shape of the mean curve. In addition to an equation for the mean shape, data points representing the upper and lower first and second standard deviations, ie. data points defining 2.5%, 16%, 84%, and 95% of the data were calculated and are shown in Figure 9.11. Back analysis of these shapes using the program 'SHAPETEST' (Appendix 3) showed that the mean curve and upper one and two standard deviation curves were best represented by power or parabolic functions, while the lower one and two standard deviation curves were best represented by

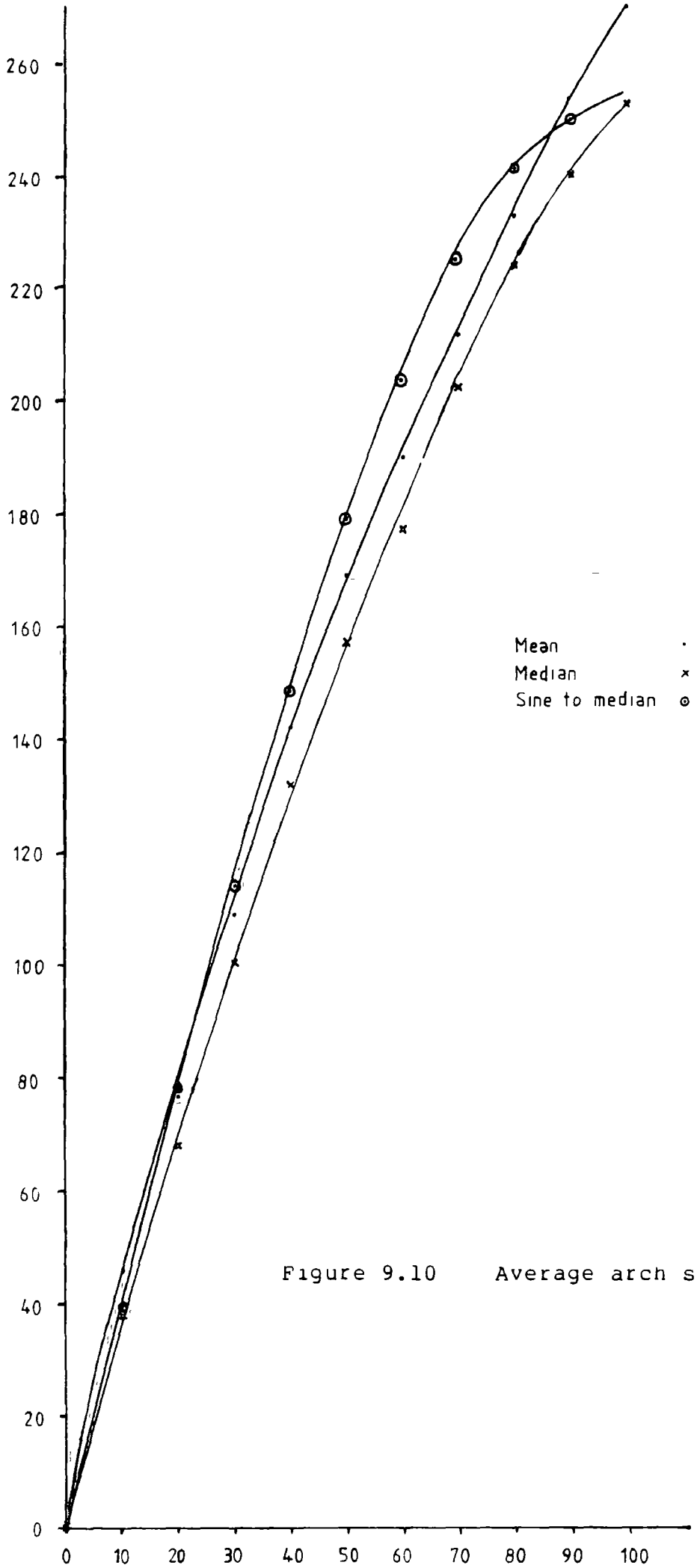

Figure 9.10 Average arch shapes.

linear fits. Appropriate equations to characterise the data were generated and the equations are given in Table 9.4, The form of the equations is shown in Figure 9.11.

TABLE 9.4. POWER FUNCTIONS COMPUTED FOR THE MEAN ARCH AND THE UPPER AND LOWER TWO STANDARD DEVIATIONS.

% of data lying above line		a	n	H : W ratio*	r	apex angle(alpha)
2.5%	Upper 2x s.d.	27.8933	0.5651	1.88 : 1	0.9959	75.1
16.0%	Upper 2x s.d.	17.9102	0.6281	1.61 : 1	0.9969	72.7
50.0%	Mean	8.8614	0.7446	1.37 : 1	0.9986	69.9
84.0%	Lower 1x s.d.	2.2897	1.0000	1.14 : 1	0.9994	66.3
97.5%	Lower 2x s.d.	1.5864	1.0000	0.79 : 1	0.9897	57.7

*H : W = equivalent to the height of working divided by its width.

$$Y = a X^{n}$$

TABLE 9.5. POWER FUNCTIONS COMPUTED FROM ALL DATA.

Total number of points= 4877

	log a	S.E.a	n	r
Mean	0.80254	0.09048	0.81903	0.9033

$$y = 10^{(\log a + S.E.\ a)} \times X^{n}$$

$$\text{eg. mean line} = 6.3466 \times X^{0.8190}$$

b. METHOD 2: 'ALL DATA'. There is an alternative method of obtaining the average shape of the arch profile. By this alternative method, all the X-Y co-ordinate data are fed into a regression program with the object of finding the equation of the line that best represents all the data. This method gives an equal weighting to every Y coordinate irrespective of its X value in contrast to the previous method which gave equal weighting to just the average Y coordinate for a given X value. A power type regression analysis was used, as the results from the initial analysis suggested that the data could either be represented by a straight line or by a curve. The power regression was achieved by using a linear regression analysis on the log (base 10) values of the X-Y

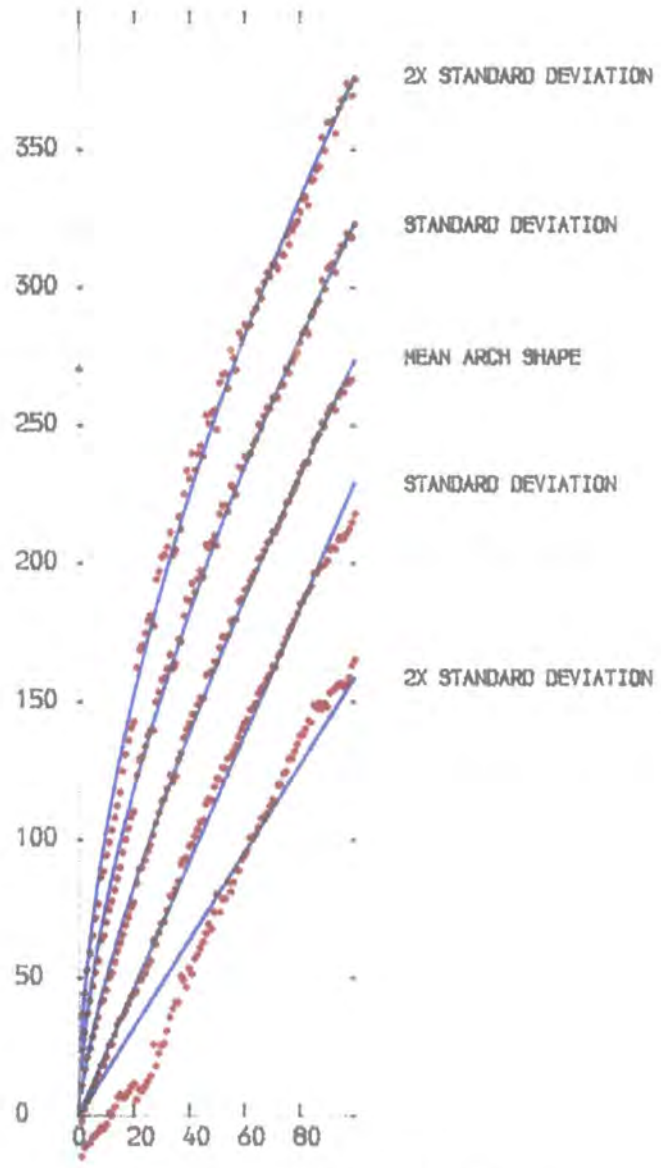

FIG 9.11 AVERAGE ARCH SHAPE CALCULATED FROM MEAN Y COORDINATES

co-ordinate pairs for all of the 57 half arches. The result of the regression analysis was to produce a different power equation to that obtained from the previous curve fitting exercise on the mean values. The new equation generated is given in Table 9.5 and has been plotted in Figure 9.12. The old mean equation shows greater curvature and a more pronounced arch shape than the new 'all data' equation.

It is worthwhile at this stage to recall why an average shape for arches is being considered. The purpose of the curve fitting exercise was twofold. First, it was to characterise the shape of the average arch, and second it was to produce another 'type' curve mid-way between the parabola and linear fits already examined. The statistical validity of the equation is of little concern at this stage, because the half arch data can be tested or back analysed to check which of the equations for the 'typical arch shape' does in actual fact fit the data best.

In the search for other mathematical relationships to characterise the average shape of the data, two other simple functions were also investigated. The log (base 10) curve proved to lie beyond that of the ellipse and was rejected, while the sine curve, although showing a good fit towards the centre of the data, flattened off too much towards the apex of the arch and hence was also rejected.

9.4.3. RE-ANALYSIS OF THE DATA.

The equation of an ellipse, a parabola and a straight line are all simple functions which give varying degrees of curvature to a line pinned at X-min, Y-min (the origin), and X-max, Y-max (the maximum). The equation for a curve fitting exercise, whether it be a power function or a polynomial function, will give the average shape of the data starting at the average origin and finishing at the average maxima. To compare the fitting characteristics of a new function to the previously tried functions, requires that the newly chosen function can also be scaled. In the power function,

$$Y = a X^{2}$$

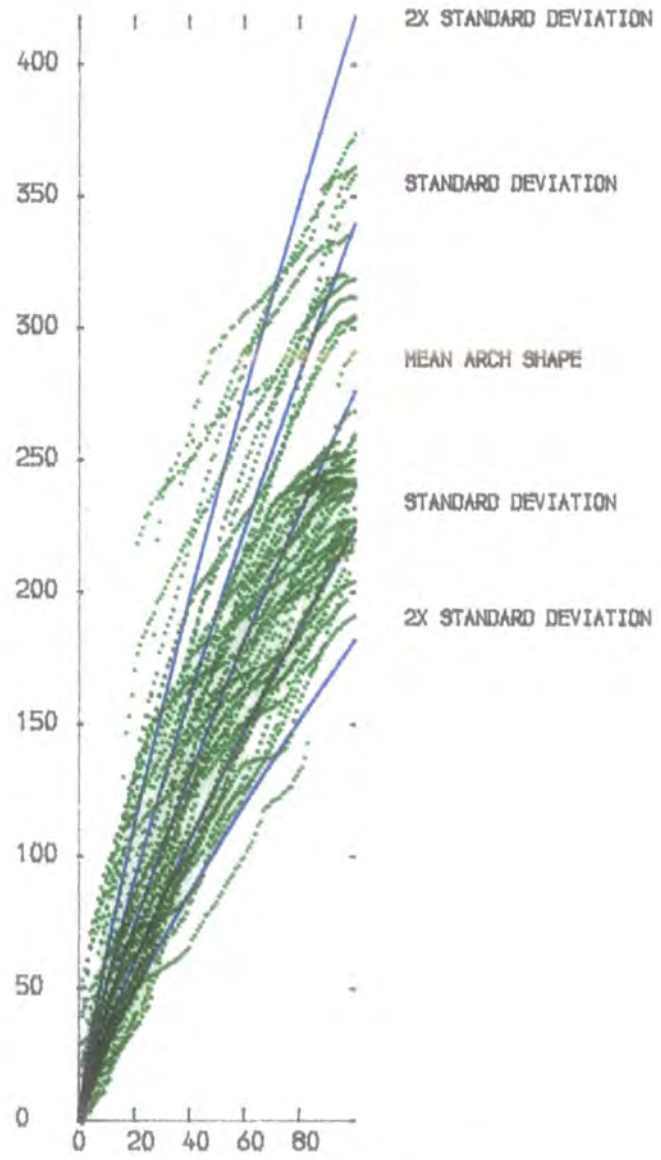

FIG 9.12 AVERAGE ARCH SHAPE CALCULATED FROM ALL THE DATA

the constant 'a' controls the gradient of the line while, the constant 'n' controls the curvature. By retaining the 'n' constant but scaling the 'a' constant relative to the individual X-max and Y-max values for the half arches, the power function will assume the same properties as the other functions, namely that a degree of curvature midway between a parabola and a straight line will be produced on a line fixed at the origin and at X-max, Y-max.

A similar procedure as that described above on a polynomial function is by no means as simple as the manipulation of a power function, especially in the higher order polynomials. It is for this reason, and for its ease in use, that the power function was chosen in preference to a polynomial for the curve fitting exercise.

The analysis procedure and program described at the beginning of the Section was extended to include a power function. Using the half arch data the program was run twice. The first run used the 'scaled' power function derived from the means of the Y co-ordinates, while the second run used the scaled 'all data' equation.

Once more the arches were grouped according to which function best represented their shape. As expected, the undifferentiated linear/parabola group of the previous analysis disappeared to form the core of the new power group. This central group however, also stole fairly evenly from both of the previous linear and parabolic groupings.

At this stage a choice had to be made between which of the power functions represented the data best. The two power functions were in many cases often statistically indistinguishable. However, the power function based on the mean of the Y co-ordinate data fitted slightly more of the half arches than that based on all the data. Therefore, the latter (all data equation) was abandoned. The number of equations with which to characterise the arches had thus been reduced to four. The ellipse, the parabola the power (mean) and the linear functions.

9.4.4. INTERPRETATION.

In accordance with the first analysis, a significance level of 0.05 was chosen as the cut-off point for border-line cases. The number of possible fits had increased to 4 thus there could be four 'good fit groups' and three undifferentiated border-line groups. In fact, as no half arches were well characterised by a elliptical shape the numbers of possible groups reduced to only 5. these groups were, in order of increasing curvature, linear, linear-power, power, power-parabola and parabola.

The group frequencies and the shapes of the individual half arches, their relevant equations and apex angles are all summarised in Table 9.1.

The detailed breakdown of the shape groupings (Table 9.1) shows that there are only 8 half arches that could not be classified into one of the 3 major groups (linear, power and parabolic). This is exactly the same number of unclassifiable arches as were obtained in the initial analysis which distributed the arches between linear and parabolic shaped arches only. However, the number of groups has been increased by one from 2 to 3. This implies that the data have stood up well to the more sophisticated analysis and suggests that the data increment chosen at the start of the analysis was satisfactory (Chapter 9.2.3).

The distribution of the 51 half arches between the groups in the re-analysis of the data shows that over 70% of the half arches exhibit some measure of curvature. However, in terms of an 'average shape', the arches were fairly evenly distributed between the three major shapes (linear, power and parabolic). In fact a Chi-squared test showed that there was absolutely no evidence (sign 0.2) to suggest other than that the three shapes were equally common. In other words there was no evidence to suggest that the majority of arches were linear rather than power or parabolic in shape. However, as the power shape does fall approximately mid-way between the parabolic and linear fits it would seem appropriate to use this relationship as the 'average shape'.

Turning to the difference between the two sides of the arch, the new analysis

has tended to confirm the results of the previous analysis, namely, that there is (just) a possible significant difference between the right hand and left hand arches. However, the level of significance is less than in the previous analysis. As with the previous analysis the right hand arches tended to be slightly more linear than left hand arches.

9.4.5. CORRELATION BETWEEN ARCH SHAPE AND OTHER VARIABLES.

Field observations (Chapter 2) suggested that there might be some relationship between the geomechanical properties of the rocks and the shape of the collapse structure. To test whether or not a trend could be observed a rank order correlation matrix and numerous scatter plots were produced between the shape, ranked in order of increasing curvature, and other variables.

The variables used in the above analysis were chosen to represent a broad range of the variables held on the old working data base. They included the site location, the rock type, the half width of the working and the relative height of collapse of the arch (actual or bridged height).

The rock types were ranked according to their supposed strength and durability, as it was these properties which were expected to be reflected in the shape of the arch. From the half width of the working it was hoped to see whether the widths of the working influenced the final shape. Likewise, the height of the old working was included for similar reasons. The site location for each arch was included to check whether of not the site, and also indirectly many other variables such as depth, stress environment, age, water-table and so on, influenced the shape of the collapse structure.

No statistically significant relationships whatsoever, were found between the arch shape and any of the other variables chosen. In fact the highest correlation coefficient obtained in the rank order correlation was only 0.17 (sign < 0.1).

To check further whether of not there was any systematic variation between the arch shape and any of the other variables, a non-parametric analysis of variance

test was performed. This indicated that the different arch shapes were evenly distributed between the various sites, and that there was no evidence to suggest that one site had a higher proportion of one arch shape than any other site.

Similar analyses were performed on the remaining three variables and as expected the tests showed that the different arch shapes were evenly distributed between the variables. There was no evidence to suggest that one rock type, width of working or height of collapse was preferentially associated with one arch shape rather than another.

These negative results were somewhat unexpected and suggest that there is probably no single variable which will control the shape of an old working, Indeed, the impression gained is that to accurately predict the shape is be extremely difficult.

9.5. SUMMARY.

The analytical techniques developed above proved sensitive enough to statistically recognise and allocate field arch data into one of four groups (linear, power, parabolic or ellipse) of theoretical shapes. Indeed, the technique proved successful in highlighting possible flaws in the interpretation of the original data (eg. parallax errors).

Statistical analyses of the data have shown clearly that the majority of arches exhibit some degree of curvature but there is no such thing as a 'typical arch' profile. Parabolic arches are no more common than linear arches. In fact the shapes of the arches vary almost uniformly between these two limit shapes. Elliptically shaped arches are however, rare, but are still a valid shape to include in a bulking analysis because they would probably be quite common if the effect of bridging had not been removed from the present data.

Several different mathematical functions were tried and eventually rejected in favour of a power function for the characterisation of the 'average' shape. However, the inclusion in the text of the equations for the average shaped arch

does not imply that this is the 'typical' arch shape.

Finally no one factor could be found which controlled the shape of an arch. the conclusion drawn is that the shape of an arch seems to be virtually independent of all other measured variables.

CHAPTER 10

PLAN STUDIES.

10.1. PROBABILITY ANALYSIS OF CHIMNEY CAVES.

10.1.1. INTRODUCTION.

Problems arising from collapsing old workings are not the sole perogative of shallow coal mines. Metalliferous mines can suffer from an equivalent problem where a zone or highly localised caving can develop in the hanging wall of a stope. Such a collapse can migrate through hundreds of metres of strata towards the surface and, if it breaks the surface, can cause localised subsidence holes. Numerous terms such as sinkholes, funnelling, piping and chimney caving have been applied to such phenomena which, although quite well known, have received little attention in the literature (Brauner, 1973).

The Mufilira mine disaster in 1970 (Sandy et al., 1976) highlighted the problem of chimney caving. In this tragedy a chimney cave migrated through about 500m of rock to break surface beneath a mine tailings lagoon. The lagoon liquefied and within fifteen minutes about 680,000 cubic metres of tailings had drained through the chimney cave into the mine workings below, trapping and drowning 89 miners.

10.1.2. ANALYSIS TECHNIQUES.

While chimney caving in metal mines is beyond the scope of this thesis, the approach to the problem taken by Goel and Page (1982) is of interest because of its potential application in the field of shallow surface coal mine collapse. These authors used data on the number and distribution of chimney caves from one known mining area and attempted to predict (using a probability model) the number of incidents of chimney caving in an area of new mining. To the writer's knowledge this in the first paper which has attempted to predict the likelihood of a subsidence event occurring above mine workings.

Goel and Page considered that the number of chimney caves per unit area should

be a function of the ratio of the height of the chimney cave to the height of the void.

$$\frac{\text{number of chimney caves}}{\text{plan area of extraction}} = f\left(\frac{\text{height of chimney cave}}{\text{height of void}}\right)$$

They suggested that if the function in the above relationship could be determined from field data the relationship could be used for prediction purposes.

The thickness of the ore deposit varied in the initial study area dealt with by Goel and Page. Therefore, they used the ratio of 'height of cave / height of void' as a dimensionless geometric parameter. This value was contoured and the area between the contours was measured with the aid of a planimeter. The plan was thus contoured in terms of lines of equal 'cave height/ void height'. To obtain the second of the geometric parameters, a tracing of the surface expression of 66 chimney caves was superimposed on to the plan and a count was made of the number of chimney caves reaching the surface within the different contour intervals. The number of caves was divided by the plan area of the contour interval to obtain a cave frequency per unit area for a given 'height of cave/height of void' ratio. A graph (Fig. 10.1) was then constructed to see whether there was any relationship between the two variables and to determine whether the initial theory was valid.

Goel and Page were therefore suggesting that the frequency of chimney collapses should be a function of the thickness of cover above the workings, and that as the depth of cover increases, the incidence of chimney failures breaking surface should become less and less common. They plotted their results in terms of the dimensionless ratios described above and did indeed find a relationship (see Fig. 10.1).

The potential value of land underlain by mine workings depends on the potential damage that may occur from any collapse. An area which has a very high incidence of chimney caves will of necessity be sterilised. However, there must be a cut-off point between land that must be sterilised and land where limited

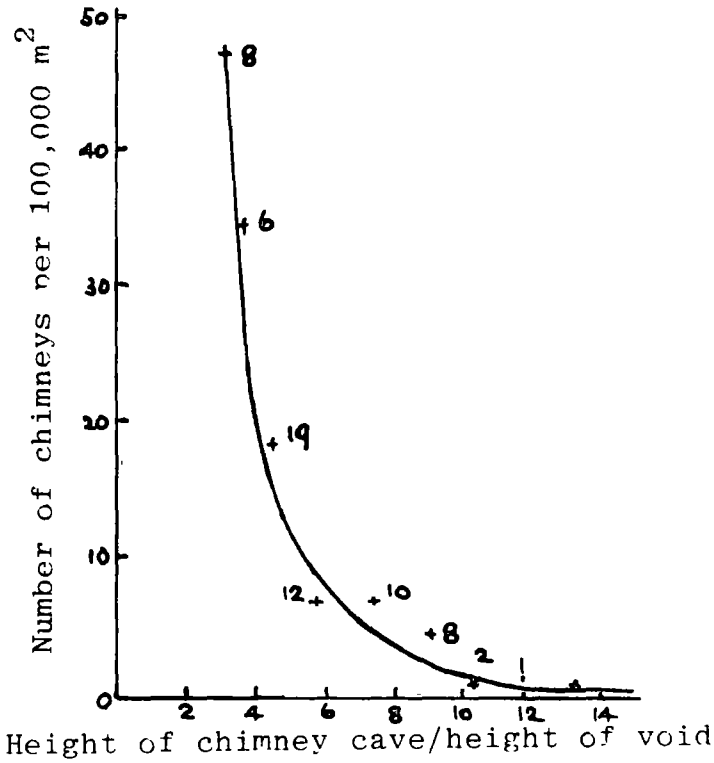

Figure 10.1 Relationship between frequency of chimney caves and depth to workings (after Goel and Page, 1982).

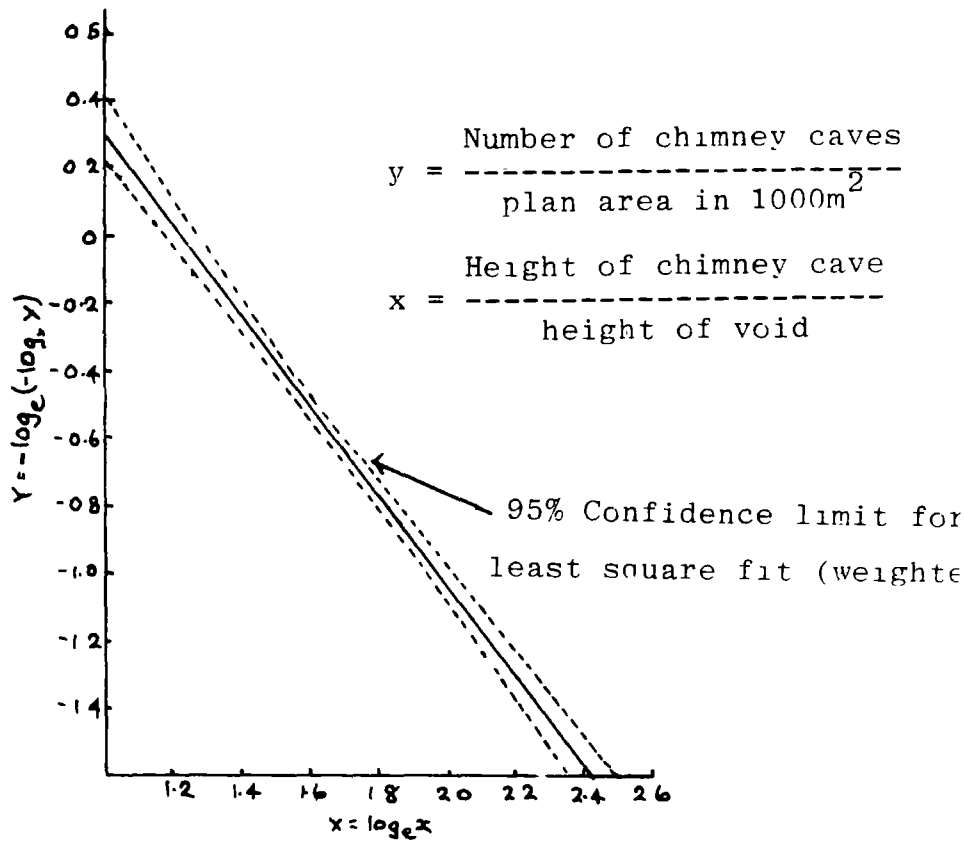

Figure 10.2 Relationship between frequency of caves and depth to workings after the transformation of the scales.

development can occur. This is the situation for old coal mine workings and was also the situation for Goel and Page. They pointed out that the value of any prediction exercise lay with predicting the frequency of collapses for marginal land where the value of the independent parameter, the height of cave/ height of void, was high. In this region of the graph (Fig. 10.1) the curve is asymtotic and therefore difficult to interpolate. However, by using a suitable axis transformation it is possible to linearise the full length of the curve and so greatly ease the problems of interpolation and extrapolation.

Goel and Page (1982) justified the use of Gumbel's theory of extremes (Gumbel, 1967) to linearise their data. This method has widespread use in hydrology for the prediction of such events as extreme tide heights, and the return periods for intense rain storms, and has apparently been widely applied to a number of other sciences.

When their data were replotted on Gumbel's extreme value paper, the results showed some evidence of a linear relationship. A weighted least squares fit was chosen to characterise the data; the graph and relationships developed are shown in Figure 10.2. Goel and Page used the least squares estimates for the relationship to extrapolate the data to an area of new mining. The probable frequency of collapse events in the new area (assuming identical conditions) is the number of chimney caves per unit area predicted from the equation, multiplied by the area of new ground which is being investigated.

10.1.3. RELATIONSHIP WITH BULKING.

Before applying their technique to shallow surface mine workings it is worthwhile to digress briefly and consider the implications of the relationships described above.

The ratio between height of chimney cave and height of void has already been met

with previously in Chapter 8. From bulking theory the following relationship obtains:

$$h = \frac{t}{B - 1} \quad \text{or} \quad h = \frac{t}{a}$$

where

B = Bulking factor
a = Coefficient of volume increase
h = Height of collapse
t = Height of void or seam

This is the original equation relating height of collapse to the bulking factor. Reorganisation of the equations shows that the ratio taken by Goel and Page is the reciprocal of the coefficient of volume increase.

It was shown in Chapter 8 that the height of collapse predicted is not directly related to the bulking factor, but is a function of it, vis:

$$h = f\left(\frac{t}{B - 1}\right)$$

The function f depends on the shape of the assumed failure surfaces. Furthermore, extension of the theory suggested that the height of the void was an inappropriate value to use and that the value defined in the text as 'apparent height of void or apparent seam height' would be more appropriate. This was defined as:

$$t(app) = f\left(t\right)$$

t(app) = apparent height of void
t = actual height of void

The apparent void height is a function of the true void or seam height, and was found to be dependent on the underground working layout and the volume of material that could be accommodated as 'run-in' under the areas of stable roof surrounding the collapse. The run-in was in turn taken to be related to the angle of internal friction for the material and the width of the working.

The height of collapse was therefore shown to be more complicated than

originally thought, and equal to:

$$h = f2\left(\frac{f1(t)}{B-1}\right)$$

f1= working layout and width function
f2= function of shape assumed for failure surface

For the present purposes this may be reorganised and expressed in similar terms to the ratio of Goel and Page (1982).

$$\frac{h}{t} = f3\left(\frac{1}{B-1}\right)$$

f3= general function comprising f1 & f2

In this form the ratio of height of collapse to void height is related to the bulking factor by a third (new) function which combines the effects of failure shape, underground layout and the run-in effect.

In applying their relationship to another location Goel and Page thus used a purely bulking criterion to define collapse. Their relationship assumes that no other limiting criteria need to be taken into account.

10.1.4. INTER-RELATIONSHIP BETWEEN ARCHING, BULKING AND VOID MIGRATION.

Field observations suggest that in most Coal Measures rocks, arching is the dominant control (see Chapter 3.5). It is believed that this is because the height of the void is usually significant, such that an old working will usually have arched before it can bulk. For old coal mine workings, two graphs of potential collapse height can be drawn. One graph with arching used as the limiting criterion (Fig. 10.3a) and another for the situation with bulking as the limiting criterion (Fig. 10.3b). Exactly the same arguments could be applied to such an arching curve as have been applied to the bulking curve. In an arching situation the probability of a high vaulted arch will be less than for a normal height arch. Therefore, a similar distribution of collapses would be expected. This trend can be seen in the histogram of the ratio of theoretical maximum height of collapse to width of working (Fig. 3.29).

The two approaches are not incompatible rather they compliment one another. In

a. Limiting criteria = Arching

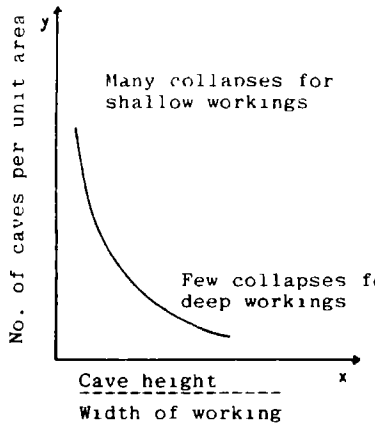

b. Limiting criteria = Bulking

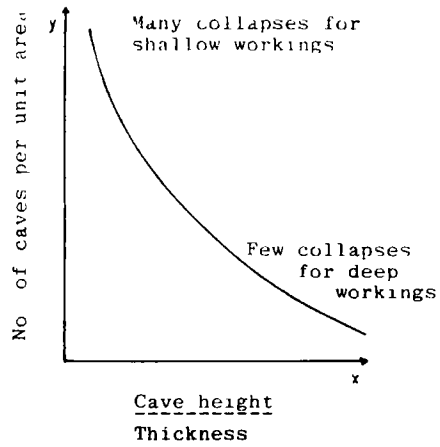

c. Limiting criteria = Arching and Bulking

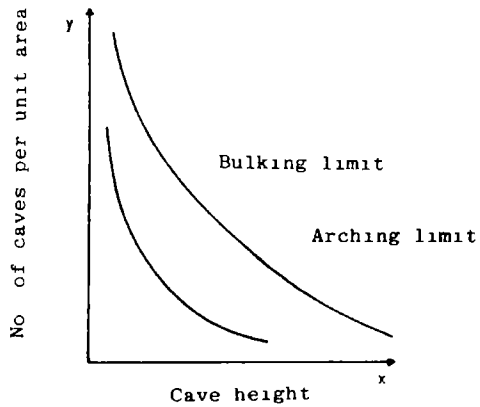

Figure 10.3 Relationship between limiting criteria for a given void height:width ratio.

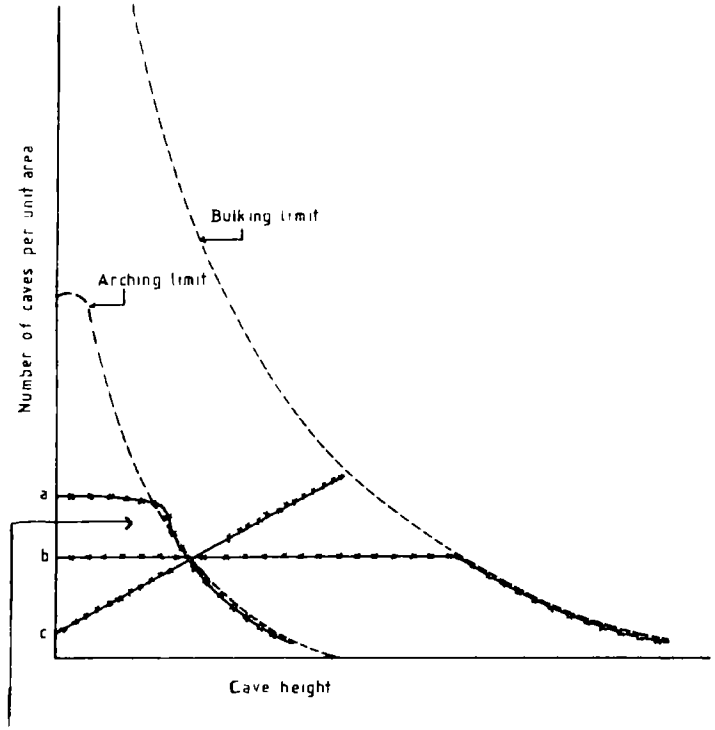

Voids with greater width than standard - at a given depth arching acts as dominant control

Figure 10.4 Possible theoretical relationships between frequency of caves and height of collapse.

most Coal Measures situations the rocks are significantly competent, and the workings sufficiently high, yet narrow, to make arching the dominant control. However, where the rocks are incompetent, or where the ratio of seam height to span width is very low, arching may fail to take place, and then bulking may become the ultimate controlling factor. The two graphs can be superimposed (Fig. 10.3a) to provide a theoretical frame-work within which to classify collapsed old workings. The composite graph implies that bulking is the ultimate limiting criterion, but there are situations when not even bulking will apply. These are situations where the variables and controls on bulking contained within the function f3 in the above relationship are for some reason inappropriate. These variables were shown to be:-

a. Bulking factor
b. Shape
c. Effective seam height

a. BULKING FACTOR. If the material fails to bulk there will obviously be no limiting height to the collapse . Such a situation occurs in longwall mining or in certain joint controlled collapse situations where there is little relative rotation of the rock fragments, so that the introduction of void space is negligible. In this situation there will be no limiting height to the collapse (see Chapter 8).

b. SHAPE. The shape of the failure zone does not decide whether or not the bulking control will be applicable but it does control the relative position of the graph in the X-axis, rectangular-type collapses will be closer to the origin than conical collapses.

c. EFFECTIVE SEAM HEIGHT. The third control on bulking was demonstrated to be the effective seam height. In this the material was assumed to run in beneath the stable roof at an angle equal to the angle of repose for the rock. The effective void height will thus increase as the friction angle of the debris decreases. If the debris behaves plastically and the material is extruded along the roadways, or the debris is continually removed by running water or a similar mechanism, the effective void height will tend towards infinity and bulking will

no longer be a limiting factor. This and other relationships can be represented on the composite graph for the two limiting conditions (Fig. 10.4).

Line a, (Fig. 10.4) represents the situation for a dipping coal seam where initially nearly all the voids break through to the surface as there is insufficient depth for arching to develop. At a critical depth, arching becomes the dominant control and the frequency of subsidence events tails off. This profile is considered as typical of old coal mine workings.

Line b, (Fig. 10.4) represents a situation where arching does not control the collapse of the working but where bulking does take place to limit the height of collapse. In such a situation the incidence of subsidence events decreases once the bulking line is reached. These were the circumstances implied by the Goel and Page (1982) analysis. If the incidence of collapse continued beyond the bulking line, but maintained the same horizontal gradient, then bulking could not be a controlling function. In practice such a profile might be expected from a collapsing old working where the debris was being removed by either gravity or by running water. Such a situation contrasts with the following case line c.

Line c, (Fig. 10.4) represents a situation where the incidence of collapse increases with the depth of the cover. This is suggested as a plastic type failure with the extrusion of the material into the roadways of the workings. As the depth of cover increases, the forces acting on the roadway plugs increase and so the effective void height increases.

10.2. APPLICATION OF GOEL AND PAGE'S ANALYSIS TECHNIQUE TO SHALLOW MINE WORKINGS.

10.2.1. INTRODUCTION.

While no-one would suggest that the results obtained by Goel and Page (1982) would be directly applicable to shallow mine workings, one might expect to observe a similar trend, whether or not the trend is due to either arching or bulking. To analyse for this situation requires details of subsidence incidents

on a plan basis rather than on a section basis as dealt with so far.

Unfortunately the present writer was unable to obtain sufficient field data relating the incidence of surface subsidence to the depth of the seam for a single coal mining situation. However, information was made available on subsidence events for two of the British Steel Companies old ironstone mines. The BSC Survey Department, had prepared potential hazard maps for a few of their old mines as a precautionary move after a number of subsidence incidents. These maps were constructed by superimposing the observed incidents of surface collapse on to the abandonment plan for the mine. The writer was allowed to have copies of all plans and borehole information relating to two sites on the understanding that none of the detailed plans provided by BSC were published. In compliance with this request, no detailed plan of the Thingdon workings has been included in the thesis.

These Jurassic ironstone mines are overlain by argillaceous rocks which resemble some Coal Measures horizons. For this reason the comparison between the ironstone mines and coal mines was considered fair, even though the workings were larger and higher than the majority of coal-mining situations. From the outset of the investigation, the history and distribution of subsidence events above the Thingdon mine suggested that the collapse mechanisms in operation were perhaps, not going to be typical of Coal Measures rocks. Thus, the following analysis is presented as a method of assessing collapses and for looking for variables which may affect the location of the collapse structures, rather than as an analysis of a typical 'Coal Measures' type collapse.

10.2.2. THINGDON MINE.

a. GENERAL DESCRIPTION. The Thingdon mine underlies an area of approximately 222 acres (0.89 square kilometres) on the outskirts and to the south south east Finedon, about 5 miles south of Kettering (N.G. SP 922717). The mine was wrought by Wellingborough Iron Ore Company from the early 1920's until abandonment in October 1947. The mine produced iron ore from the Jurassic Northampton Ironstones, which in this area can be divided into three units. The

total thickness of the ironstone varies across the site from about 9 ft. (2.7m) to a maximum of 17 ft. (5.2m), but in most places only the middle horizon of ironstone has been worked. Mine records suggest that the height of the working averaged about nine feet plus or minus one foot (2.7m + or - 0.3m).

The geological succession (Fig. 10.5) is straightforward. The ironstone is unconformably overlain by the Lower Estuarine Series which consist of between 20 to 24 ft. (6.1m to 7.3m) of thin interbedded blue-grey sandy silts and clays. These in turn are overlain by a variable thickness of a creamy yellow, weathered, rubbly, oolitic limestone; the Lincolnshire Limestone. Finally, the limestone is unconformably overlain by a variable thickness of boulder clay.

The succession dips very gently (0.5 degrees) to the south east, while the topography decreases from the SSE. to NNW. Thus, the thickest roof cover is in the SSE. of the mine where it reaches a maximum of just over 90 ft. (27.4m). The cover decreases towards Finedon in the NNW. where it is only about 20 ft. (6.1m).

Survey information was available for the floor of the mine, and isopachytes were constructed for this level rather than the roof, as there was no information available on the detailed variation in the working height. This should be borne in mind in the following discussion where a distinction is made between depth of cover or height of collapse, and isopachyte values.

Figure 10.6a shows a generalised section through the site from which it will be seen that the thickness of boulder clay varies significantly across the site.

The method of mining employed was entirely pillar and stall. Figure 10.7 shows a representative area of the mine.

It appears from plan information that the initial workings were driven about 16 ft. (4.9m) wide at between 50 ft. to 80 ft. (15.2m to 24.4m) centres. This gave an initial average extraction ratio of about 30 to 40%. At a later date some of these areas were systematically reworked. This was achieved by driving a new 16 ft. (4.9m) roadway through the centre of the old pillar. Such

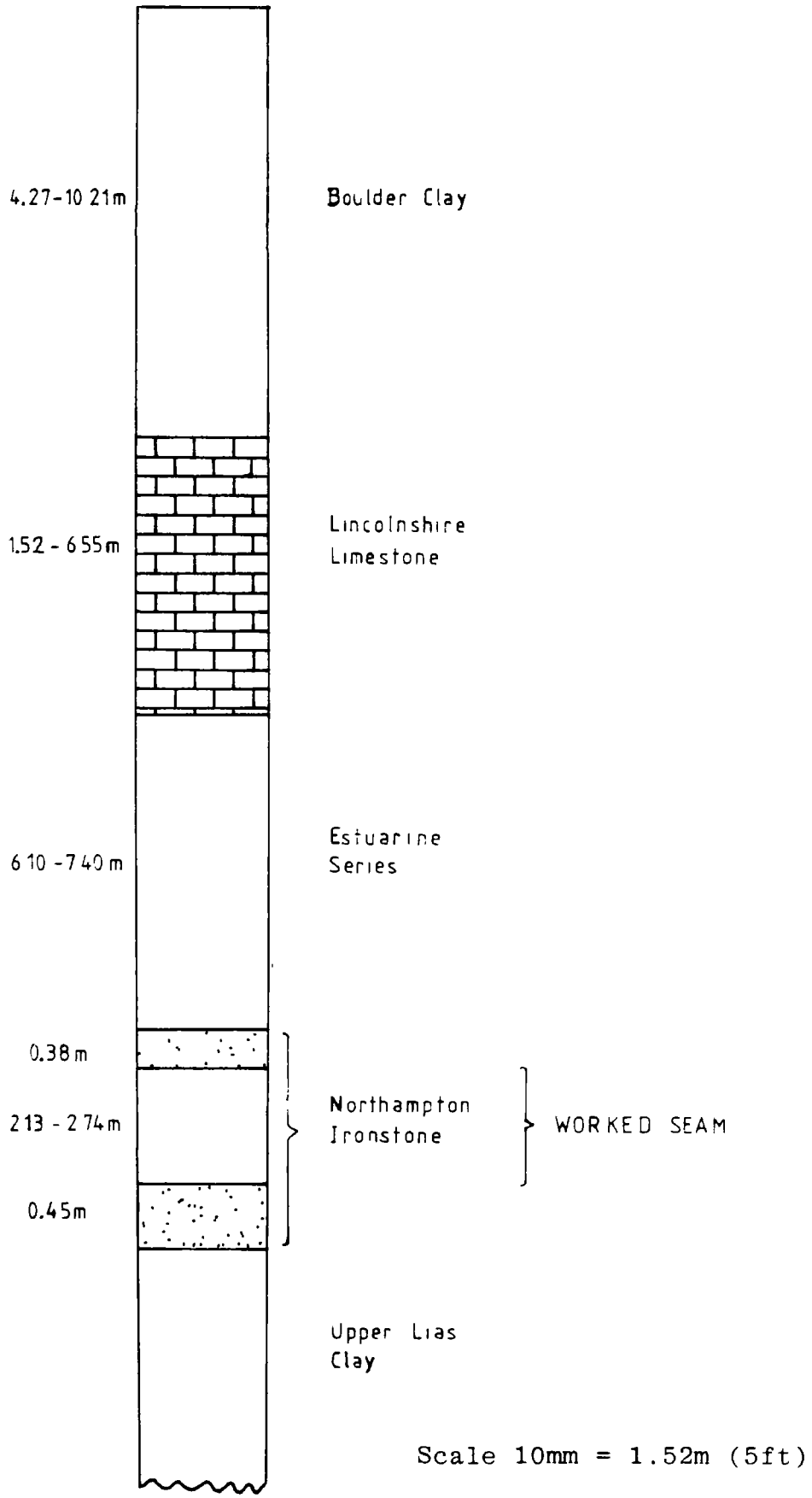

Figure 10.5 General stratigraphic sequence for the Thingdon Mine.

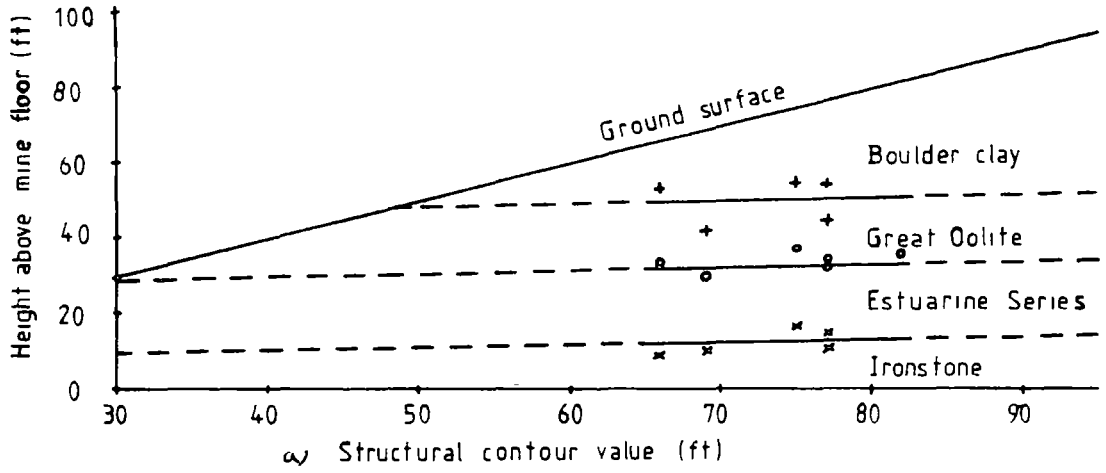

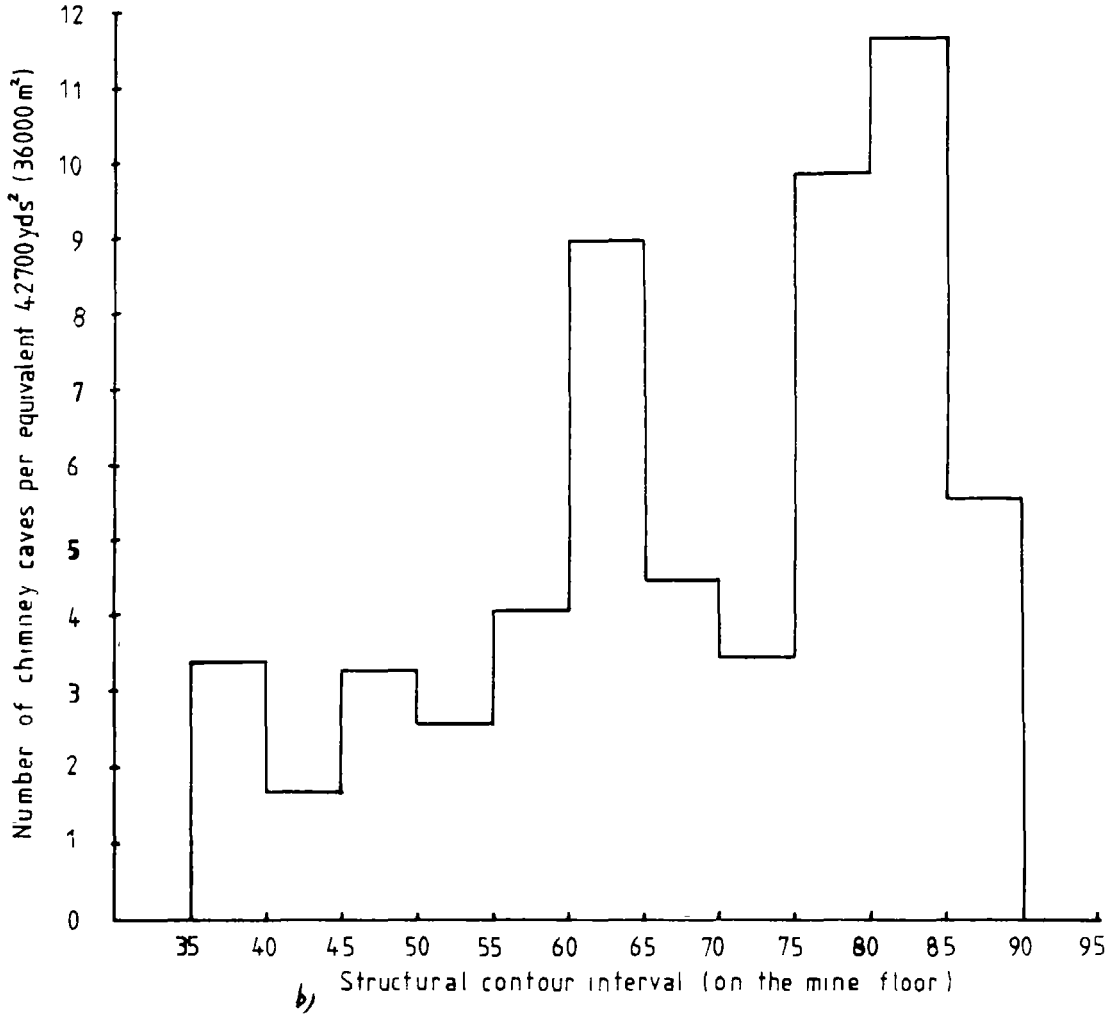

Figure 10.6 Variation in the number of chimney collapses with the change in depth to the base of the ironstone.

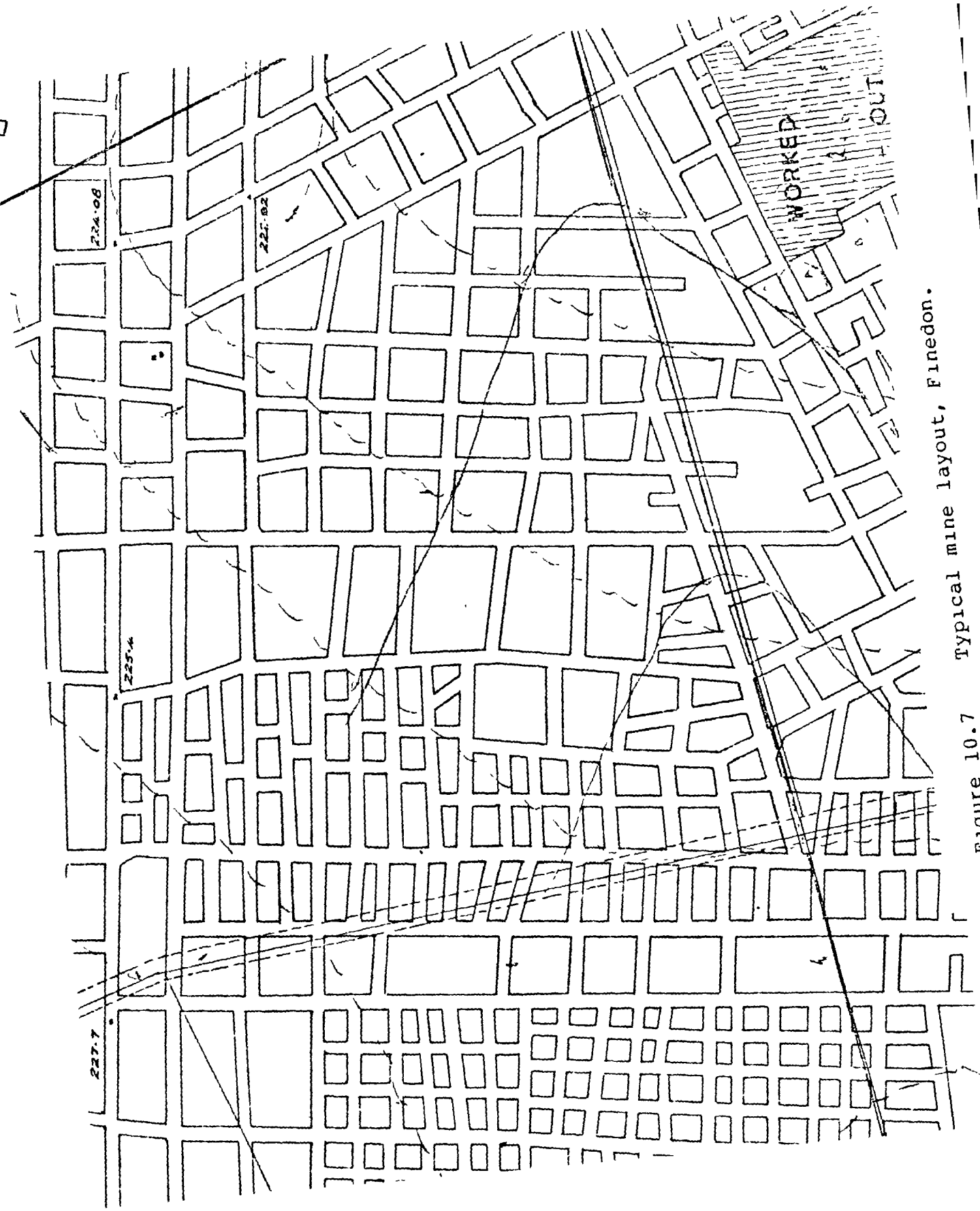

Figure 10.7 Typical mine layout, Finedon.

'Jenkin's' raised the extraction ratio for the area to between 40 to 50%. Finally some areas were further worked by splitting the pillars once more. By this method an extraction ratio of between 60 to 70% was achieved. In one or two small areas the pillars had been completely removed, but such areas represent only a fraction of the total area.

Since abandonment in 1947 the workings had partly flooded, and the information available included some observations on the water level in the mine (Fig. 10.8) The principal information available was on the location of 118 subsidence events which had occurred prior to 1970. These had been catalogued in 1975 and for a period of three years detailed records had been kept on the surface state of some of the collapses. From these records the typical subsidence event, as seen from the surface, started with the development of a small depression or hole with near-vertical sides. This rapidly deepened and often became waterlogged. Within a few months the sides of the hole had run-in creating a waterfilled crater, up to 30 ft. (9.1m) deep and with slippery sides. These were potentially lethal to a grazing animal.

Numerous of these holes had been filled with hardcore by BSC in an attempt to level the site, but the records show that in subsequent years many of these filled holes had suffered further significant subsidence.

The risk was not confined entirely to livestock as the following extract from a local paper suggests.

> "Subsidence caused by underground ironstone workings caused the Finedon Town v Raundstown United counties football league match to be postponed yesterday.
>
> Three seasons ago during a game a hole appeared in the pitch large enough to take a double-decker bus."

b. INTERPRETATION. Goel and Page (1982) contoured their base map in terms of lines of equal 'height of collapse/height of void'. At the Thingdon mine the working height was taken as constant at nine feet and as, initially at any rate, there was no thought of using the information at another location, it is a reasonable assumption to simplify the approach and contour the map in terms of

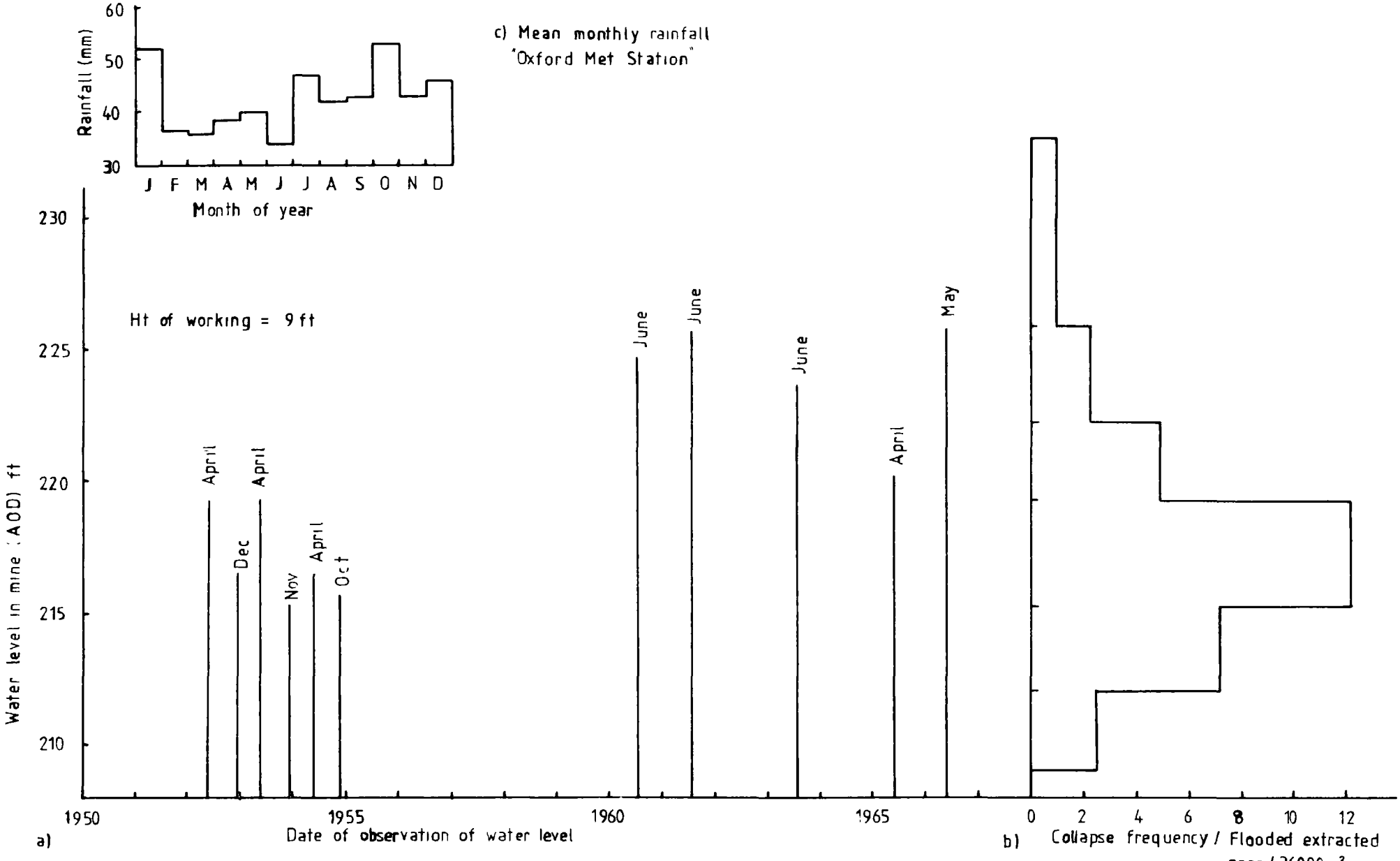

Figure 10.8 Fluctuations in water table and incidence of surface subsidence events.

just height of collapse. This is effectively the same as the isopachytes already constructed.

Goel and Page (op. cit.) were however, not faced with a problem of varying extraction ratios. The frequency of surface subsidence per unit area is directly related to the extraction ratio. One would be surprised if an area with no workings collapsed, so increasing the number of workings beneath the area must increase the chances of collapse. To eliminate this component, the percentage extraction must be taken into account in order that the frequency of collapse per unit area can be truly related to the height of collapse. This can be done by dividing up each of the inter-isopachyte areas on the map into sub-areas of equal working density. Each of the strips between the isopachytes were thus sub-divided according to the extraction ratio obtained in the mine workings below. These areas were measured and the area was then adjusted to a standard percentage extraction by the relationship below:-

$$\text{Equivalent sub-area} = \frac{\text{\% extraction}}{\text{reference \% extraction}} \times \text{area of the sub-area}$$

The average extraction ratio across the site was 41% and this was used as the reference percentage extraction. Inter-isopachyte sub-areas of high extraction were thus scaled up to an equivalent sized area worked at an extraction ratio of 41%, while areas of low extraction were similarly scaled down by the technique.

The adjusted areas for each of the inter-isopachyte sub-areas were summed for each inter-isopachyte area to arrive at a gross equivalent area. Once the adjusted area between the isopachytes had been computed, Goel and Page's procedure of counting the number of collapses per inter-isopachyte area could then be carried out and the second variable. The 'number of caves/equivalent area of collapse', could be derived.

The procedure is therefore, similar to that used by Goel and Page except that it has been adjusted for the specific problems of variable extraction pillar and stall workings.

The relationship between the two variables obtained for the Thingdon mine has been plotted as a histogram (Fig. 10.6b) . This is a more appropriate method of displaying the information than the graph (Fig. 10.1) of Goel and Page. It will be noticed that the relationship is completely different to that found by the above authors. Instead of showing a decreasing incidence of collapse with increasing cover the histogram shows a completely opposite effect of an increasing incidence of collapse with depth.

The histogram has purposefully been plotted beneath the stratigraphic section so that a direct assessment can be made of the effect or otherwise of the overlying strata on the frequency of collapse.

Referring back to the different possible theoretical interpretations of such a graph it is suggested that had the control been purely arching, then the frequency of collapse would have tailed-off at a structural contour value of about 40. This represents a 'height of collapse/width of working' ratio of about 2. The 'top-end' collapses represent a height to width ratio of about 5, which, from field observations, have been shown to be rare (Fig. 3.28).

The control could be one of bulking as the maximum ratio of collapse height to void thickness for the site is only about 9:1. The expected bulking ratio for this situation, using the relationships developed in Chapter 8 would be about 17:1. (Using a working width of 16 ft., B.F.=1.35, Phi=30 degrees, and a parabaloid shaped intersection-type collapse. Apparent void height=26.5 ft., n=4). The observed ratio is therefore still well within the average maximum bulking estimate. However, if the control were simple and the depth of cover had no effect, then one would expect a similar frequency of collapses irrespective of depth. This is not the case, and there are two possible explanations.

Firstly, the depth of burial may be affecting the mechanism of collapse. At the shallow depths involved the ironstone pillars will certainly not have failed. Therefore, the Estuarine Series could be deforming plastically and pushing the roof in. In such a situation the forces on the roof would increase and hence

the incidence of collapse would also increase with an increase in the cover depth.

The alternative theory is that bulking is not taking place, either because the debris piles are consolidating, ie. the bulking factor is about unity, or because the run-in is deforming plastically and being extruded along the roadways. There is some evidence to support this latter theory in that the size and depth of the craters as reported by the surveyors do not show any evidence of decreasing with increasing depth of cover (Fig. 10.9). This would be expected if the controlling factor was bulking.

c. EFFECTS OF MINE FLOODING ON THE FREQUENCY OF COLLAPSE. Isobaths (lines joining points of equal depth of water) were constructed on the mine plan from survey information and information on the fluctuations of the water level in the mine supplied by BSC. The observations on the depth of flooding were made in some cases twice a year, but there is insufficient data to decide whether or not the water level fluctuates with the seasons. The median annual rainfall for the Oxford Meteorological station (Ordnance Survey, 1967) (insert c, Fig. 10.8) suggests that any seasonal variation would not be great. However, there does appear to be a significant variation in water levels on a yearly basis.

It is possible, though doubtful, that the workings are slowly filling. After all the first water levels were recorded 11 years after abandonment of the mine. If it is assumed that the water levels do fluctuate this would be expected to have an effect on the frequency of collapses. Beck et al. (1975) have reported a higher than expected incidence of collapses around the edge of what they term mine pools. These observations were made above abandoned pillar and stall mine workings in the Appalachian coal fields, USA.

It was suspected that a similar mechanism may be effecting the distribution of caves for the Thingdon mine. To check this, a variation of the analysis technique used previously was adopted. The area between the isobaths, the inter-isobath area, was divided into sub-areas of equal percentage extraction. The correction functions described above were applied to each inter-isobath

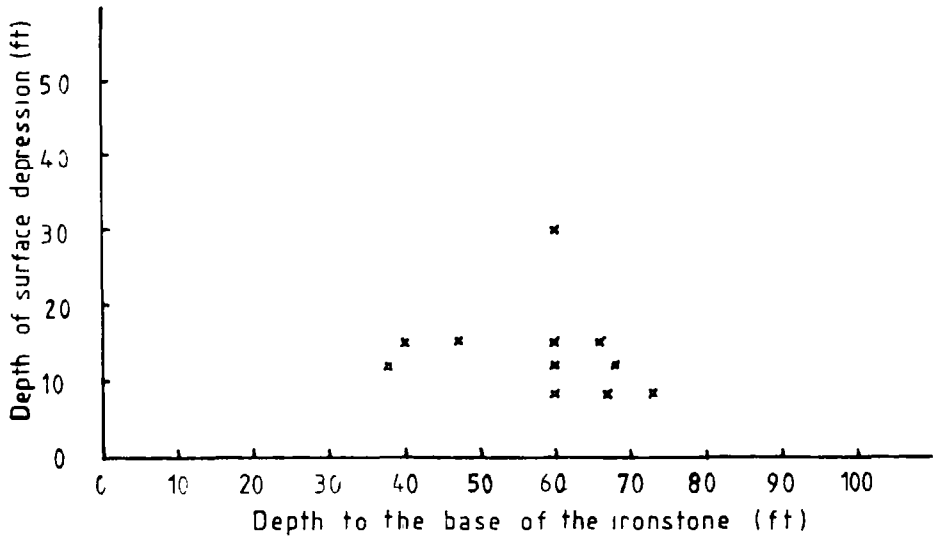

Figure 10.9 Relationship between the depth of surface depressions and the depth to the base of the ironstone.

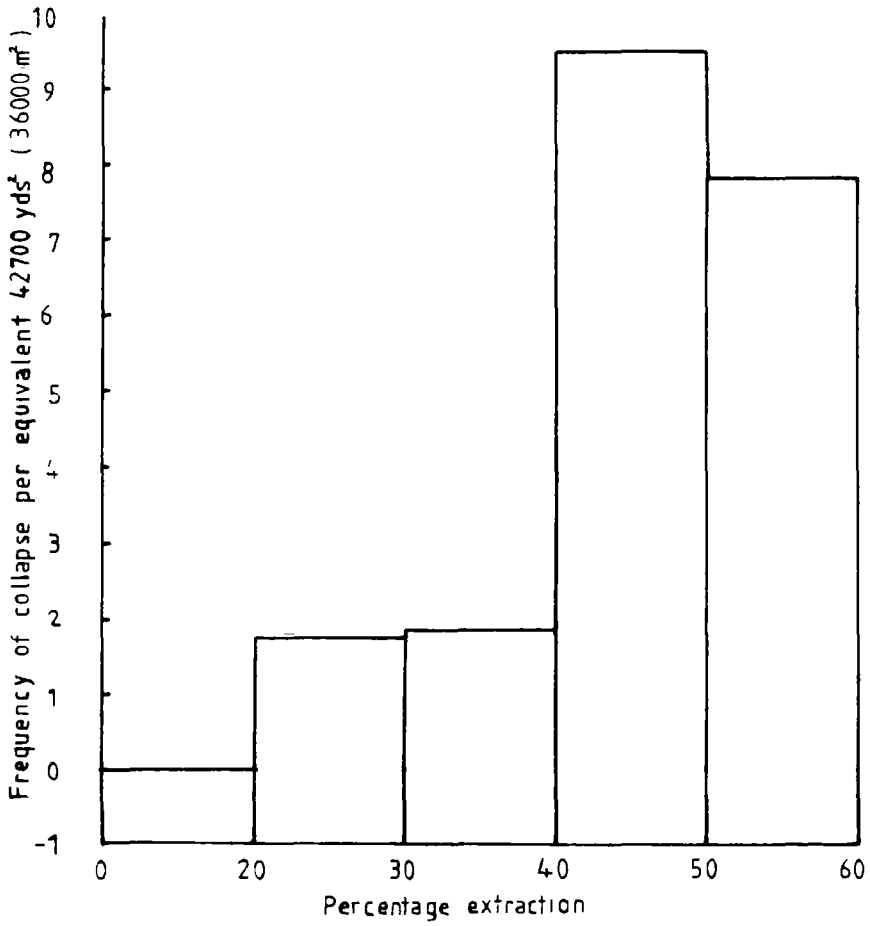

Figure 10.10 Frequency of caves as a function of % extraction.

sub-area in turn, to compensate for differing percentages of extraction. When this had been achieved the total sum for the equivalent areas between each pair of isobaths was then calculated. The number of collapses per inter-isobath area were counted and divided by the equivalent isobath area. In this way an observed collapse frequency per unit equivalent isobath area was obtained. This has been plotted as a histogram alongside the fluctuations in the depth of water recorded by BSC (Fig. 10.8).

The histogram suggests that the maximum frequency of collapses coincides with the area on the edge of the 'average depth mine pool'. This result is therefore in keeping with the observations of Beck et al. (1975) and in line with the suggestion of Gray et al. (1977). One would expect alternating flooding and drying to be very testing on an old working collapse system. Apart from the flushing and softening effects that moving water would have on the collapse base, the material would also be fluctuating between an effective and a total stress condition.

d. EFFECTS OF EXTRACTION RATIOS ON THE FREQUENCY OF COLLAPSES. Finally, it was suspected that a further control on the frequency of collapse may be the percentage extraction. In other words, it was suspected that areas with a higher extraction ratio would have more collapses than areas with a low extraction ratio. To examine this hypothesis the map was contoured in terms of lines of equal working density. The area between each contour was measured and once again corrected to an equivalent percentage extraction working area using the relationship developed above. The number of collapses within these areas were totalled and divided by the equivalent percentage extraction area to obtain the frequency of collapses per equivalent % extraction area. These were plotted as a histogram (Fig. 10.10). The results confirm the suspicion that the number of caves initiated per unit area increases as the percentage extraction rises.

It would be dangerous to read too much into the dramatic increase in the incidence of collapse for extraction ratios greater than 40%. This is because other factors have been shown to have some effect. However, this critical value of 40% represents areas of the mine where secondary or tertiary working had

taken place. The effect of splitting the support pillars has obviously led to deteriorating roof conditions.

e. SUMMARY. This analysis has shown that unlike Goel and Page's metalliferous mine, the incidence of collapse is not controlled by one simple factor such as bulking. At least three semi-independent controls have been isolated. The evidence suggests that at the Thingdon mine more collapses are initiated per unit roof area in areas of high extraction than in areas of low extraction. From initiation, the mechanism of collapse that develops is not typical of collapsing coal-mine workings, as evidenced by the increase in subsidence events with increasing depth. It is considered that plastic failure of the collapse pile is probably enhanced by cyclic flooding. This, coupled with weak, incompetent roof rocks, combines to form chimney caves which are not arrested by any of the overlying strata. The outlook for the land overlying these workings is bleak: there is no evidence that depth will function as a limiting control. Consequently, subsidence events are likely to continue to be as common as at present.

10.2.3. HOLWELL MINE.

a. GENERAL DESCRIPTION. The deductions, arrived at above were made entirely from the distribution of collapse locations and local field evidence, and it is interesting to compare them with the other area of old ironstone workings which lies 35 miles to the north of Finedon at Holwell near Melton Mowbray (N.G. SK 741236). This area became the subject of evidence presented by Clements (1982) on behalf of the Leicestershire and Rutland Trust for Nature Conservation at the Vale of Belvoir Public Inquiry. Clements (op cit) presented as part of his evidence to the enquiry an underground layout for the Holwell mine with, superimposed on top, the underground locations of areas of roof collapse as surveyed in 1978/80. The present writer combined this information with the surface expression of collapses recorded by BSC to produce a unique map depicting both underground as well as surface collapses (Fig. 10.12).

The important point to make is that the two mines are quite similar and have,

geotechnically speaking, similar roof rocks. This is inspite of the fact that the ironstones are from different stratigraphic horizons. The Holwell ironstones form part of the Marlstone Rock which is Middle Lias in age, and thus stratigraphically lower than the Northampton Ironstones of Finedon.

Geologically, the overburden consists of very finely laminated bituminous shales, 'paper shales', which on drying split into well-defined, very thin, sheets. A mineralogical analysis of some samples shows a high percentage of calcium carbonate in the rock. This is not surprising considering the depositional environment. When dry the shale was brittle, but when the moisture content was increased the shale became very flexible. In the field some horizons showed evidence of mud flow.

The geological succession is presented in Figure 10.11, and a description of the mine as given by Clements (1982) is summarised below.

The galleries are approximately 4m (13 ft.) high by 3m (9.8 ft.) wide. There is approximately 0.6m to 1m of Marlstone left in the roofs of the galleries. Above this there is a combined maximum thickness of about 15m of Upper Lias Clay and Boulder Clay. The galleries are supported by cross-ties of railway lines (or similar girders) at about 0.3m to 0.6m below the roof, with the ends seated in notches a few centimetres deep in Marlstone walls. Between these cross-ties and the roof there is a loose packing of further girders and timbers. At major gallery intersections and other points of weakness there were formerly vertical timber supports, these are now largely rotted or otherwise ineffectual.

Although there are many signs of collapse of the roof, this is largely confined to the intersections. Here the blocks of the Marlstone roof drop out, followed progressively by higher and higher parts of the overlying clays, forming a cone shaped projection towards the surface. These clays tend to flow along the galleries. Finally, the surface falls in to produce a conical depression in the land surface. A recent example of one of these depressions was approximately 10m in diameter, and 5m in depth. It should be noted that many of the intersections shown on the map (Fig. 10.12) consist only of a small 'window'

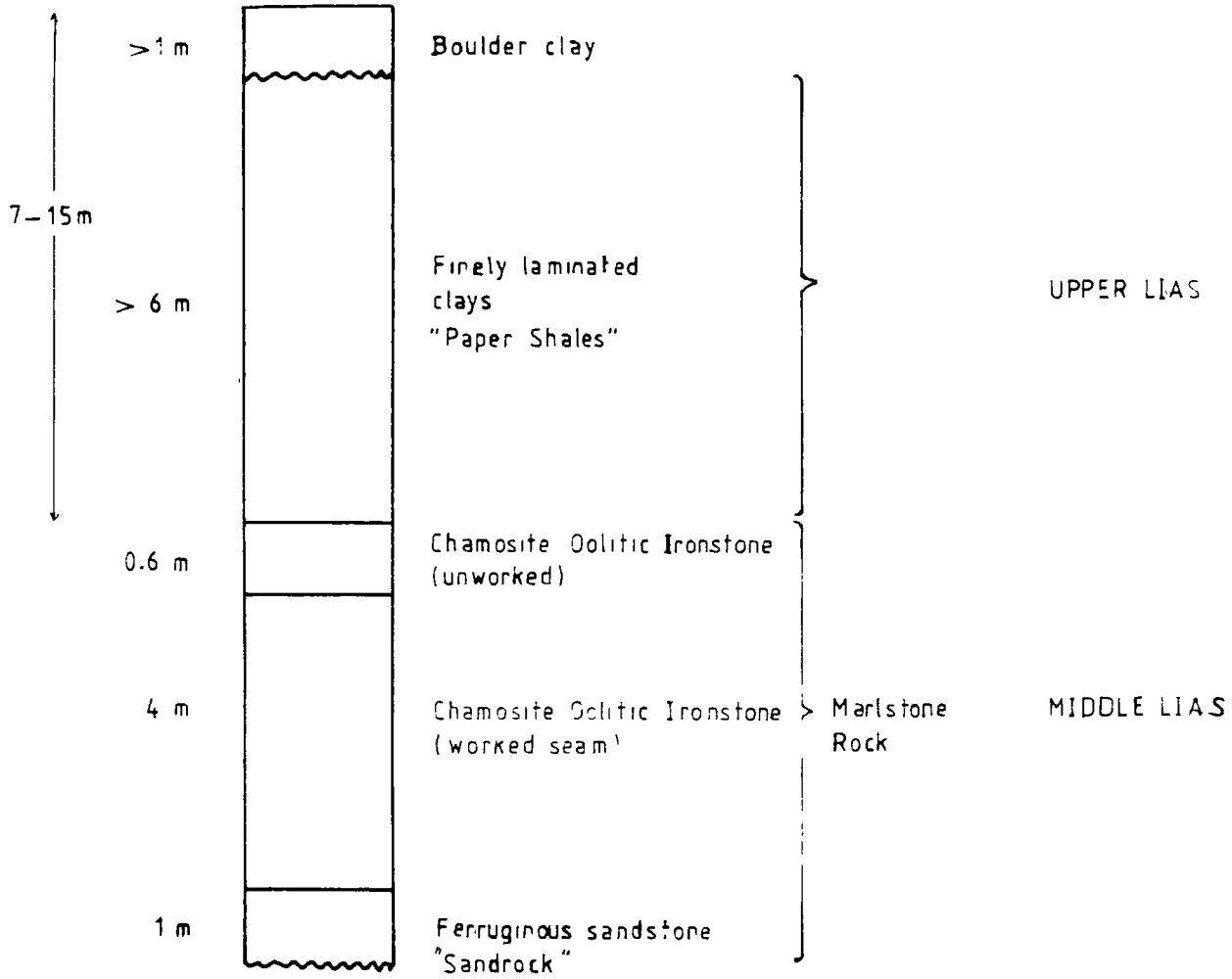

Figure 10.11 General stratigraphic sequence for the Holwell Mine.

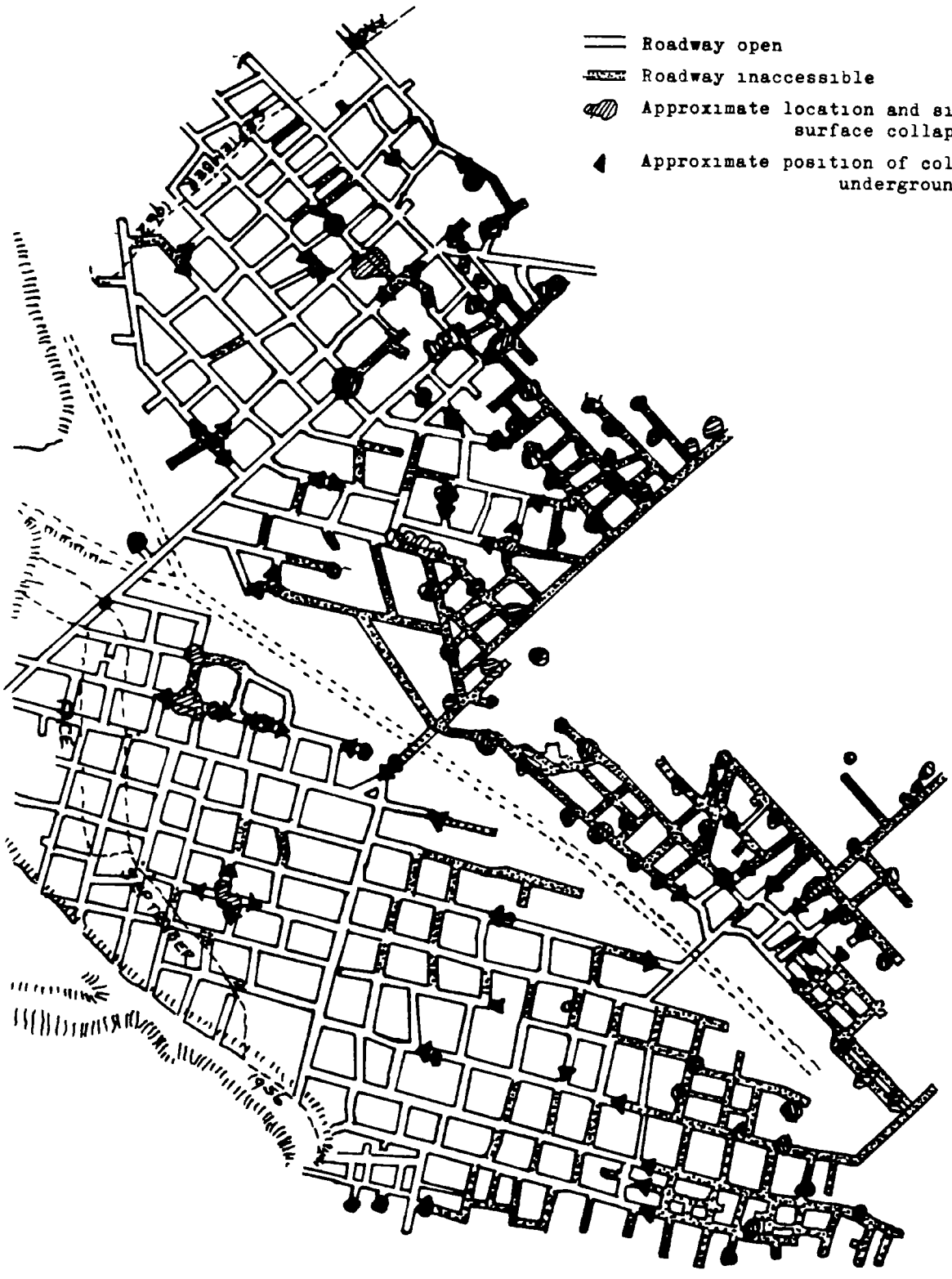

Figure 10.12 Relationship between surface and subsurface collapse structures at the Holwell Mine.

from a main driveway into an adjacent stall. The main galleries themselves seem to be fairly stable and should, undisturbed, maintain this position for a long time.

b. SUMMARY. The mechanism of failure suggested by Clements (1982) for the Holwell mine fits the observations and deductions made independently from a study of the frequencies and locations of collapses at the Finedon mine. The modified technique of Goel and Page would therefore seem to be of some value in areas of old workings where an explanation of the mode of failure is required.

The implication of the observed mode of failure for the two ironstone workings described above is that roof rocks which are finely laminated do not arch as well as thicker rock units. this observation is in keeping with the concept of scale introduced in Chapter 1.

10.3. LOCATION OF COLLAPSES.

10.3.1. INTRODUCTION.

In a Chapter 8 collapse structures were classified into four groups depending on their location relative to the mine layout. These were:-

1. Intersection collapse
2. Intermittent roadway collapse
3. Complete roadway collapse
4. Heading collapse.

It was demonstrated that if bulking was the controlling factor for the height of collapse, the location of the collapse would effect the ultimate height to which a void could migrate. This classification of collapses applies equally to all collapsed mines whether the limiting controls are bulking, arching or whatever. If the limiting control was arching, the height of collapse would be expected to be greatest above an intersection collapse because of the greater span across the diagonal of the intersection. Thus, both arching and bulking predict higher void migration above intersections than above roadways. It would be useful to look at the relative frequency of the different collapse structures to see whether one type of collapse is more common than another.

The overwhelming impression gained from viewing collapse structures in the high walls of opencast coal sites is that all collapses are some form of roadway collapse, whether it be intermittent or complete roadway collapse. Indeed of the 151 workings recorded during the investigation, only two were classified initially as being possible intersection collapse structures. This observation is in marked contrast to the mining engineering literature in which intersections are frequently referred to as areas with a high probability of collapse (Singh, 1981, Peng, 1978). There is therefore, an obvious discrepancy between these two differing observations that needs to be resolved.

The problem is best approached by a study of plans of partially collapsed old workings on which have been superimposed surface subsidence events. The problem then reduces to whether the frequency of collapses at the different locations is greater or less than would be expected. Such a problem dealing with relative frequencies is ideal for statistical analysis using the Chi-squared test. The problem is however, deciding on the distribution of collapse frequency one would expect!

There are two approaches that can be used to obtain an estimate of the expected frequency of collapse, these are:-

a. ROOF AREA. The distribution of collapses could be proportional to the area of the roof exposed. This is fairly logical because one might expect that as the area of roof exposed increases, there should be a corresponding increase in the probability of the initiation of a collapse.

b. NUMBER OF LOCATIONS. This alternative suggests that the expected frequency of collapse is not related to roof area but is proportional to the number of different locations in the mine. Thus, an area with six roadways and two intersections would have an expected collapse frequency in the ratio of 3:1.

10.3.2. THEORETICAL PREDICTION OF EXPECTED COLLAPSE FREQUENCIES.

a. ROOF AREA. The percentage extraction for an area of regular pillar working can be found from the following relationship (Fig. 10.13):

$$\%\text{extraction} = \frac{\text{worked area}}{\text{total area}} \times 100$$

$$= \frac{L \times W - (Ps \times Ns \times Pb \times Nb)}{L \times W} \times 100$$

W = Width of old working area
L = Length of old working area
S = Span of working in X-axis
B = Span of working in Y-axis
Ps= Width of pillar in X-axis
Pb= Width of pillar in Y-axis
Ns= Number of pillars or roadways in W
Nb= Number of pillars or roadways in L

The total roof area of the intersections (I) will be:-

$$I = (S \times B) \times Ns \times Nb$$

The roof area for the roadways in the X-axis is:-

$$(Ps \times L) \times Ns$$

therefore, the total roof area for all the X-axis roadways will be:-

$$RX = Ps \times B \times Ns \times Nb$$

and the roof area for all the roadways in the Y-axis will be:-

$$RY = Pl \times S \times Nb \times Ns$$

Therefore, the total area worked is:-

$$Aw = \text{Intersection} + \text{Roadway-X} + \text{Roadway-Y}$$

$$= I + RX + RY$$

From these relationships can be obtained the ratios of the different collapse locations, and the percentage of the total area underlain by each collapse

location. These are:-

Ratios of the different collapse locations expressed as a percentage

Intersection	Roadway-X	Roadway-Y
$\frac{I}{\%ext \times L \times S}^2 \times 100$	: $\frac{RX}{\%ext \times L \times S}^2 \times 100$	: $\frac{RY}{\%ext \times L \times S}^2 \times 100$

Figure 10.14 shows a graph of the change in the intersection ratio as a function of increasing extraction.

The different parts of a mine layout can also be expressed in terms of the percentage of the total surface area that they underlie. These percentages are:-

Intersection	Roadway-X	Roadway-Y
$\frac{I}{L \times S}^2 \times 100$	: $\frac{RX}{L \times S}^2 \times 100$	: $\frac{RY}{L \times S}^2 \times 100$

Figure 10.14 shows a graph of the change in the area underlain by intersections as a function of increasing extraction.

If Figure 10.13 is taken as an example, using the dimensions:-

W = 12	Pt = Ps = 2
L = 15	Nb = 5
S = B = 1	Ns = 4

The % extraction will be 55.6, while the proportions of collapse expected on the basis of just roof area are:-

Intersections	Roadway-X	Roadway-Y
20%	40%	40%

Thus it can be suggested that if the roof area was the control on collapse only 20% (Fig. 10.14) of the collapses would occur at intersections.

Finally it can be shown using the above equations for total area that only 11.1% of the ground surface over the worked area is underlain by intersections, while 44.4 % is underlain by roadways in the X and Y directions. Because the pillar working is square, half this figure represents the area for each of the X and Y

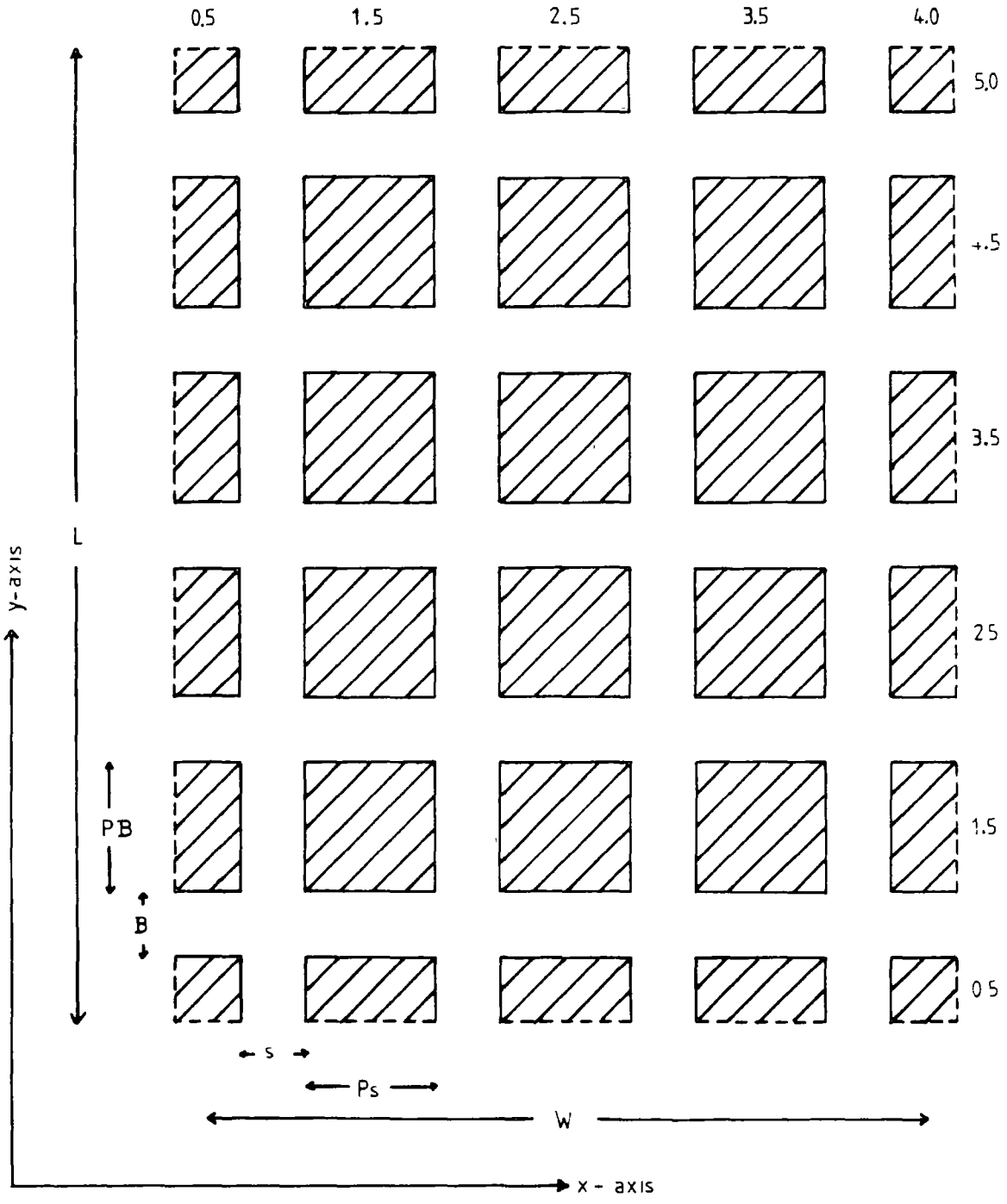

Figure 10.13 Nomenclature used for the calculations of working ratios.

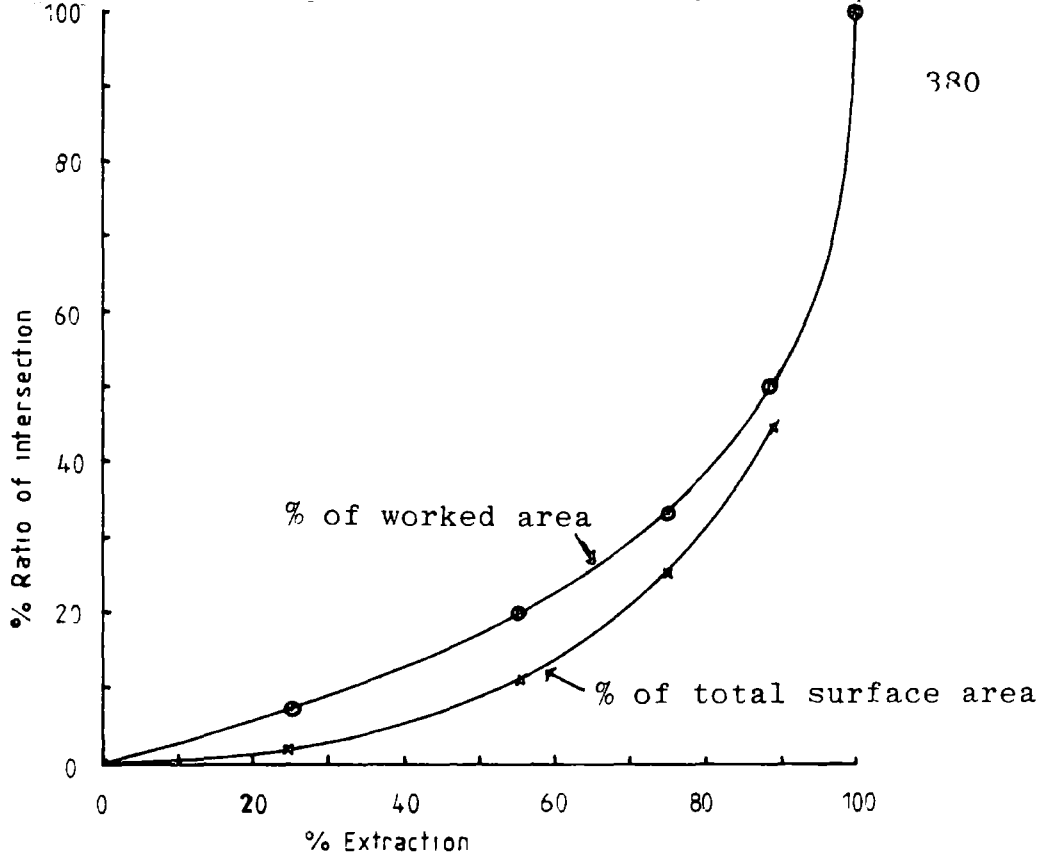

Figure 10.14 Percentage increase in intersection roof area for both total area and worked area as a function of % extraction.

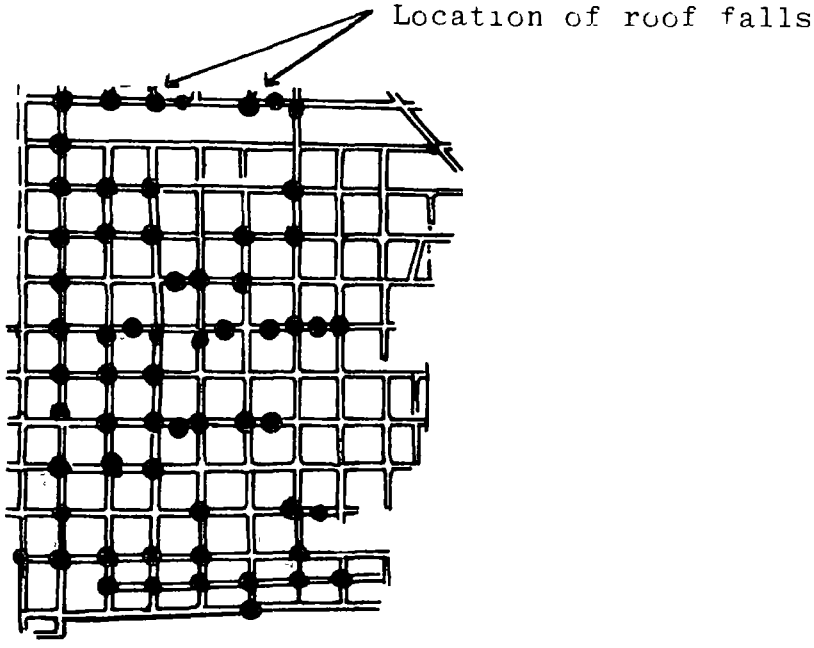

Figure 10.15 Incidence of roof collapse in the Dishergarh seam, India.

roadway roof areas respectfully.

b. NUMBER OF LOCATIONS. From the foregoing calculations it will be obvious that for a regular pillar layout as shown in Figure 10.13, the number of intersections must equal the number of X-roadways which must in turn equal the number of Y-roadways. Therefore if the control on collapse was the number of locations, or incidentally if the collapses occurred completely randomly, the expected ratios would be:-

Intersection	Roadway-X	Roadway-Y
33.3%	33.3%	33.3%

A position has now been reached where an area of collapse can be considered in order to test whether either of the controls suggested above effect the frequency of collapses at the surface.

10.3.3. COMPARISON OF PREDICTED AND EXPECTED COLLAPSE FREQUENCIES.

Plans relating the underground mine layout to the incidence of collapse were available for four locations. Of these it was decided not to use the Finedon example discussed earlier because other factors had already been shown to affect the location of collapses. However, more importantly, the survey data on the surface expression of the collapses at Finedon were insufficiently precise to be able to accurately distinguish between intersection or roadway collapse for the locations of the falls. A similar reason precluded the use of the other ironstone mine example at Holwell, but the overwhelming impression gained from the plan (Fig. 10.12) (Clements, 1982) is that the collapses are preferentially concentrated at the roadway intersections. This impression is confirmed by Clements (1982) who surveyed the workings and in evidence given to the Vale of Belvoir Inquiry stated that -" although there were many signs of collapse of the roof, the collapses are largely confined to the intersections".

Two other sites were considered and these are described below:-

a. ROOF FALLS IN THE DISHERGARH SEAM, INDIA. Singh (1981) presented an

underground layout of a panel in the Dishergarh seam with an indication of the locations of areas of fallen roof (Fig. 10.15). The expected frequency of roof falls under the assumption that the frequency of roof falls is proportional to the roof area can be calculated for this situation (Fig. 10.15) using the formulae developed above. The results obtained for the division of collapses are:-

Intersection	Roadway-X	Roadway-Y
11 %	43 %	46 %

The observed frequencies of collapse at the appropriate locations were, however:-

51	1	9

From the observed distribution the impression is that the collapses were preferentially concentrated at the intersections. A Chi-squared test confirmed this observation giving a significance level of well below 0.001. In other words, if the frequency of collapse was directly related to the roof area, then the observed distribution of roof falls would have been expected to occur less than once in every 1000 panels. However, Singh did not comment on this particular panel as being particularly unusual and it may thus be assumed that in this case the collapses were preferentially concentrated at intersections.

The data were also analysed to see whether the apparently large difference between the number of recorded collapses in the X and Y roadway were statistically significant. The Chi-squared test suggested that the collapses were probably concentrated preferentially along the Y-axis. The level of the significance was only 0.03. This means that a large difference in the frequency of collapse in the X and Y directions might be expected in 3 out of every 100 panels. The difference is statistically possibly significant and could be due to one of two reasons. The first reason may be because the local stress field is greater in the Y-direction. this would mean that the roadways in the X-direction were more stable because the roof rocks were clamped. The second reason could be related to the relative orientation of the coal cleat to the

roadways. This subject has been discussed in greater depth in Chapter 1.

A similar analysis was performed on the above data to see whether the frequency of collapses were related to the number of intersections, X-roadways and Y-roadways. Once again the Chi-squared test suggested that there was preferential concentration (sign << 0.001) at intersections.

b. LOCATION OF COLLAPSES AT ELDON, CO. DURHAM. Eldon is a small pit village to the northeast of Bishop Auckland which has been troubled by a number of subsidence events during the past few years. The NCB in evidence for a recent court case involving a disputed subsidence claim, produced a potential hazard map. This map was constructed by superimposing the underground mine layout on to a map of the surface subsidence events (Fig. 10.16, Walton, 1983). Thirty four claims had, over the years, been made against the NCB. Twenty two were in the writers view directly related to the effects of mining subsidence, and these were analysed to see whether there was any relationship between frequency of collapse and either roof area or number of locations. Because the analysis involved only a few collapses, and as the layout was a little complicated, the areas of the roadways, intersections, triple 'T' junctions, two-way intersections, NW/SE roadways and NE/SW roadways were accurately measured instead of estimating the areas using the equations described above. The location of each subsidence event was then assigned to one of these five groups, and a number of Chi-squared tests were performed to analyse the distribution.

The statistical tests suggest that the observed distribution and frequency of the collapses are definitely not (sign 0.001) proportional to the roof areas of the collapse locations, but they are possibly related (sign $\approx$ 0.1) to the ratio of collapse locations. When data was grouped into intersections and roadways only, then the incidence of collapses is definitely not (Sign 0.001) in proportion to the roof areas and probably not (0.025) related to the number of locations. From this it can be inferred that at Eldon collapses are preferentially located at the intersections.

The data were further analysed to examine which, if any, of the three types of

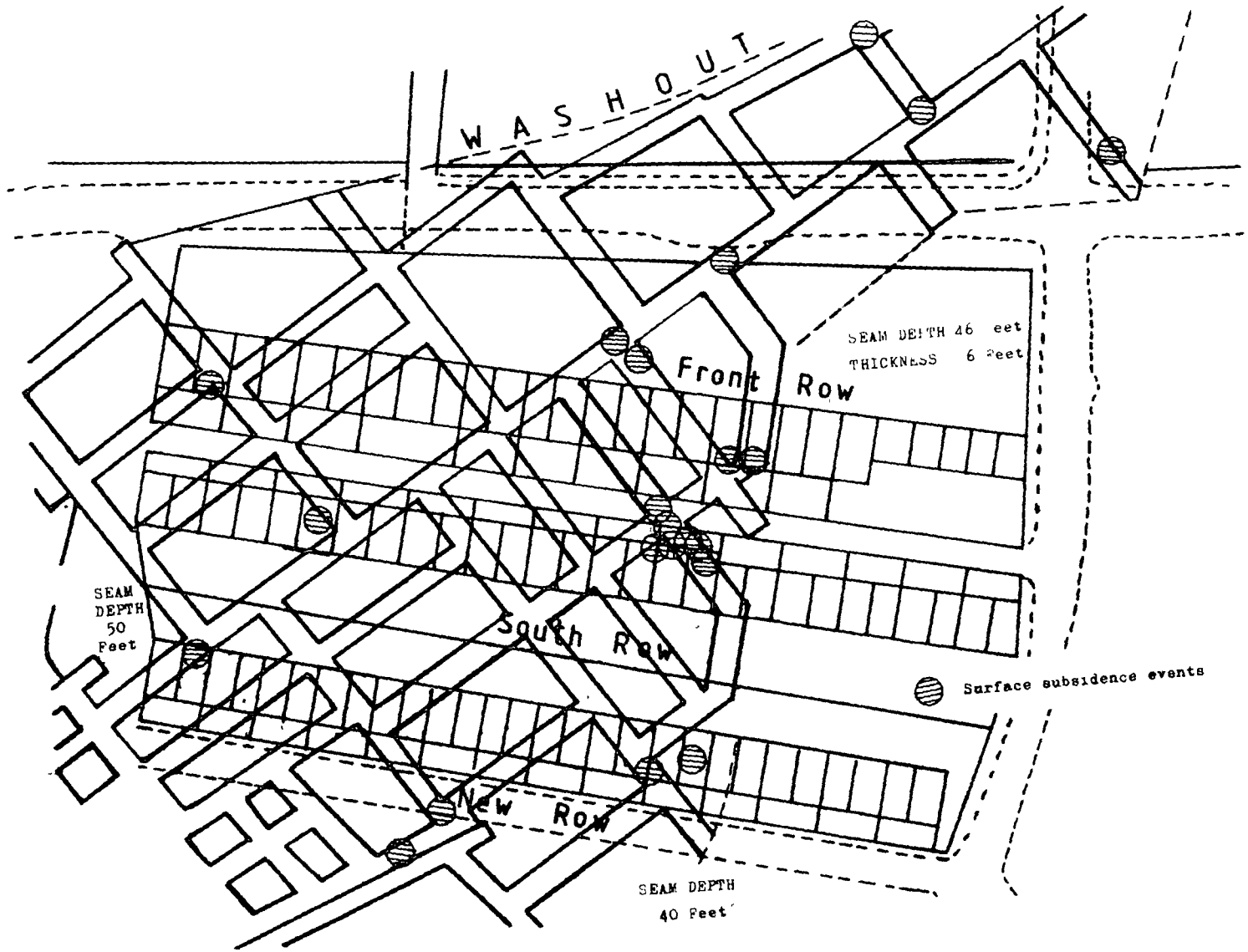

Figure 10.16 Relationship between surface and subsurface collapse structures above the Eldon Mine, Co.Durham.

intersections were more likely to collapse. The Chi-squared test showed that there was no difference between the different types of intersections and that one type was as likely to collapse as another.

Finally, no difference could be found between the frequencies of collapse of the roadways in the NW/SE direction and those in the NE/SW direction. Therefore, at this shallow depth, there is no evidence to suggest that cleat or any other directional property exerts any influence to concentrate collapses in one roadway direction rather than another.

10.4. SUMMARY.

Arching and bulking are seen as complementary approaches to the same problem with each representing the limit solution. Whether or not an old working bulks or arches depends on the relative size of the span width and the void height. A narrow opening in a thick seam is likely to arch before it bulks in contrast to a wide opening in a thin seam which may well bulk before it can arch. For either situation, the incidence of surface collapse should decrease with depth. However, in certain circumstances it doesn't and the relationship between the frequency of collapse incidents per unit area and depth of working has been shown to be of potential use for characterising 'unusual' collapse situations. The distribution of the variables for the 'unusual' collapses at Finedon contrast strongly with the more normal relationship presented by Goel and Page (1982). Further analysis of the Finedon example has led to the conclusion that this failure was atypical and probably due to the squeezing of roof debris along the roadways. This process has been greatly facilitated by the effects of water.

All the evidence presented above, although admittedly limited, suggests that intersections are more likely to collapse than roadways. It follows from this that the observations made on opencast sites in this respect are incorrect. Assuming an average extraction ratio for old workings on an opencast of say 45%, one would expect (Fig. 10.14) that at least 8 or 9 % of the workings seen in section in the high wall would be intersection collapses. This percentage would

represent a figure of about 15 intersection collapses out of the 151 cases documented in Chapter 2. However, it will be recalled that only 2 intersection collapses were initially recognised in the data. In the light of this analysis, the photographs were re-examined once more looking more specifically for additional intersection collapses. The search was rewarded with the identification of a further 3 possible intersection collapses. However, the total number is still considerably less than would have been expected, and it must be accepted that opencast sites do offer a biased view of the distribution of collapsed old workings.

The reason for the bias is almost certainly due to the effect that the old workings have on both the highwall and investigator's ability to distinguish one type of collapse from another. The high wall is more likely to be unstable above intersections than above roadways running orthogonal to the face. It is assumed that additional collapse debris at intersections must mask the nature of the working and therefore makes identification and interpretation of the collapse location more difficult.

CHAPTER 11

CONCLUSIONS

A review of the engineering geology literature dealing specifically with the collapse of old workings has revealed only three semi-quantitative techniques for predicting the stability, or height of collapse of an old working. Of these techniques, only one deals with the stability of the immediate mine roof, while the remaining two are concerned with predicting the height of the suspended zone. The techniques are:-

Concern of analysis	Method	Notes	Presented by (among others)
Prediction of roof collapse	Clamped beam analysis, (Chapter 4).	Analysis of single body loaded layer - no additional horizontal or vertical forces considered. Failure based on tensile strength of rock in question.	Taylor (1975), Wardell and Wood (1965)
Prediction of height of collapse zone	Bulking equations (Chapter 8).	Uses bulking factors for rock to determine max. height to which collapse could migrate before void chokes. Some consideration of rock type	Price et al. (1969) Piggott et al. (1977) Taylor (1975), Higginbottom (1984)
	Observational/ semi-statistical approach. (Chapter 8 & 3)	Uses coefficients that act as multipliers to either seam thickness or working width - based on observations made in the field	Walton and Taylor (1977), Thorburn and Reid (1977).

In addition to these approaches there are one or two 'rule of thumb' or 'golden rules' which have been found to be satisfactory in some cases. These rules include (Carter, 1984):-

a). The Concept of a Safe Depth. This is an old and hotly disputed theory. Those in favour argue that collapsing old workings do not pose a threat provided that they are below a certain 'safe' depth. Beyond this safe depth it is suggested that either the pillars will have crushed out or the void will have choked or bulked. In either case the workings will not pose a threat to surface development. The values suggested have varied between 100m to less

than 20m with about 60m as a norm (Cameron, 1956). It should be noted that bulking theory implies a safe depth (see Chapter 8).

b). The Pillars Don't Fail Rule. This is a widely held belief and is in slight conflict with the previous theory. Field evidence (Chapter 3) has indicated that pillar failure at shallow depths are rare. However, there are numerous examples of pillar failure in the literature (see Galloway, 1835, and Carter, 1980). As a categorical statement this 'rule' is therefore highly dangerous. Pillar collapse must be considered as site specific, particularly in areas of workings with high extraction ratios, and with an apparently strong roof rock.

c). The Age of Workings Rule. It is a widely held belief that workings over one or two centuries old will have completely collapsed, and all settlement will have ceased. No field evidence (Chapter 3) has been found to substantiate this claim, and so this 'rule' must also be considered dubious.

In contrast to the literature specific to the collapse of old mine workings, the literature of mining and tunnelling engineers is full of semi-quantitative and qualitative techniques for predicting the stability of mine headings and tunnels. During this investigation an attempt has been made to bring together and review the majority of the available simple analysis techniques.

The applicability of the analysis techniques depends on the size and geometry of the working. To be able to choose the most appropriate analysis technique it is, to a certain extent, necessary to predict the likely mode of failure. In Chapter 1, a framework was suggested within which it has proved possible to classify old workings and the methods of analysis (Figure 1.7). This was achieved by considering the span of the working in relation to the thickness of the bedding and the separation of joints and other discontinuities. From the classification a clear distinction emerges between:-

a). Those theories that may be used to predict the stability of the immediate roof (eg. beam and Voussoir beam theory).

b). Those theories that may be used to predict the height of the suspended

zone (under the assumption that the immediate roof has failed).

STABILITY OF THE IMMEDIATE ROOF.

Field observations have shown that it is rare for mine roofs to be devoid of fractures or joints. Therefore, beam analysis, which assumes an intact and unfractured roof, must be considered to be of limited practical value. There are however, situations where such an analysis is of value, for example where the mine is overlain by a strong sandstone bed or where there is a large working span and the roof rocks act in conjunction with one another to form a pseudo-beam. The principal criticism to beam analysis arises from the assumption that if the beam cracks the roof has failed. It is a well-established observation that cracked beams can be stable and therefore, Voussoir beam analysis is probably of more value.

Voussoir beam analysis (Chapter 5) has been developed and extended to cover 3-D situations and dipping roofs. This was achieved by using the empirical observations of Wright (1972,1973) to correct mistakes in the original theory of Evans (1941). The analysis that this produces can cope with all the recognised modes of failure for a Voussoir beam, namely crushing of the contacts, elastic buckling, slippage of the blocks from the beam, or shear of the blocks. However, the assumptions behind the analysis are still somewhat simplistic, and the analysis technique will not be of much value where the rock is heavily fractured. Its optimum application would appear to be in situations where the roof is cut by few but well-developed joints. For this reason its general application would probably be more appropriate for the analysis of workings in other minerals such as limestone, ironstone, and sandstone, rather than in Coal Measures rocks.

The stability of the mine roof can be also be considered from a kinematic or mechanistic viewpoint (Chapter 6). This approach links the analysis techniques discussed above with the second group of theories which predict the height and stability of the suspended zone. Model studies have shown that the kinematic approach is a good deal more complex than the theory would suggest. Where there

are more than 3 or 4 blocks in the bottom, row block rotation and sliding become important controls on the failure mechanism. The validity of the approach was also questioned when it was found that the collapse heights the theory predicted, based on the aspect ratio data gathered in the field, could not be made to tally with the field observations of old workings (Chapter 3). This suggests that either the assumptions made in the model are wrong, or that a serious rethink will have to be made with respect to the gathering of field data on the size and aspect ratios of blocks.

THEORIES THAT PREDICT THE HEIGHT OF THE SUSPENDED ZONE

In Chapter 10, the general relationship between arching and bulking was considered. It was concluded that the two approaches should not be viewed in isolation but rather as complementary failure mechanisms. Both mechanisms operate, and the choice of which analysis technique to use will usually depend on the relative size of the span of the working and the height of the void. An old working with a large span relative to its void height is likely to bulk before it can arch (Plate 8). In contrast a working with a short span relative to the void height will probably arch before it can bulk. In the vast majority of collapse situations, arching has been found to be the dominant control on the collapse. However, for design purposes, it could be argued that both arching and bulking should be taken into account when predicting the maximum height of collapse. If this were done the theory that provided the greatest estimate of the collapse height should be used.

Most of the arching theories reviewed in Chapter 7 were shown to underestimate the average height of collapse, and for this reason their practical use is limited. Of the theories considered, those of Protodyakonov and Biermbaumer (Szechy, 1970) are probably of most practical value. In general the failure of the arching theories to predict the correct collapse height probably stems from the fact that the theories were designed to be used to predict roof loads and not collapse heights. The absence of a truly satisfactory arching relationship, for use in predicting the collapse height, is not serious because field results

can be used in its place.

In the past, bulking theory has proved popular, principally because the only information that is required to obtain an estimate of the height of collapse is the thickness of the extracted horizon. Development of the theory by the present writer has shown that the simplistic approach adopted by early authors is incorrect. These theories take no account of the volume of material that can run in beneath the stable roof adjacent to the collapse. The theories therefore, significantly underestimate the potential height of collapse. However, the relationships have been used satisfactorily for a number of years. Evidence has been presented (Chapter 3) that suggests that the reason why these mistakes were not spotted earlier is that the collapse heights predicted by the relationships are approximately equal to the limiting height for arching. There is evidence that the seam height is related to the span of the working, which in turn will predict the collapse height.

The subtle and hitherto unsuspected inter-relationships that have emerged are the result of an analysis of 181 collapsed old workings from 18 different opencast sites across Britain. These data include observations from two other independent sources, and all the workings examined during the project lay between a depth of 1 and 75m from the ground surface. It is worthwhile emphasising that the observations made by the present writer encompass and endorse the observations from earlier studies. A statistical analysis of the field data has shown that nearly 99.5% of all old workings (at sufficient depth) collapse to a height of less than (2.68 x the span of the opening). Only one example in Coal Measures rocks is known where this was not the case (this was a collapse not measured by the present writer).

It follows from this that any collapse structure that migrates to a greater height must be atypical. Three atypical situations involving old pillar and stall workings are recognised:-

1). Where the opening width is too great for arching to develop (eg. soil or longwall type failure)

2). Where bulking controls the collapse height (ie. in those situations where arching is not operating).

3). Where voids migrate beyond the bulking limit.

The Thingdon ironstone mines offer an excellent case history of an atypical collapse (Chapter 10). These collapses fall into the third category and are controlled by neither arching nor bulking. It is suggested that at this site the collapsed roof debris, weakened by water, is being extruded along the mine roadways by the weight of the collapsed roof debris above. A technique has been developed, using the frequency of surface subsidence features, by which such atypical collapse mechanisms can be differentiated from the more normal subsidence features.

Both arching and bulking theories make some assumptions about the shape of the failure surface. A statistical analysis (Chapter 9) of 26 typical arches, each furnishing 2 independent approximations of the failure shape, clearly showed that the majority of 'arches' exhibited some degree of curvature. However, there was no evidence to suggest that there was such a thing as a 'typical' arch profile. In fact the shapes of the arches varied almost uniformly between a linear and parabolic profile. Finally, the shape of the arch seemed to be independent of virtually all the measured variables such as rock type, span width and location.

P L A T E 1. Old working systems

Photo 1a. Ibbetsons OC. site, Burnhope, Co. Durham, 14/4/78, (5/4 seam)

View from the high wall showing remnant 19th C. coal pillars exposed in the coaling cut. The shape of the pillars indicates the mine was worked using the 'Newcastle' system. Note that the seam has two leaves, and that the top leaf has been partially worked. This suggests partial pillar robbing ('working the broken') possibly on retreat. The areas of robbed pillar were not marked on the abandonment plan. In addition the mine plan was miss-orientated by approximately 12 degrees.

Photo 1b. Blindwells OC. site, Lothian, Scotland. 4/7/79, (Parrot seam)

View from the high wall showing remnant 19th C. pillars exposed in the coaling cut. The shape of the pillars suggests the mine was worked by the Scottish technique of 'stoop and room'. The achieved extraction ratio was approximately 80%.

Photo 1a.

Photo 1b.

PLATE 1

P L A T E 2. Potential problems that can arise from old workings

Photo 2a. Low Close OC. site, Cumberland. 11/5/78, P ref=33.4

A fully laden coal truck which broke through 1.3m of mudstone cover into old workings in the Metal and Cannel seams below. The Crow seam was being extracted at the time of the incident.

Photo 2b. Lindel, Barrow in Furness, Cumberland. 22/9/1892

Crown hole that developed beneath a railway engine. The engine (no. 0-6-0-115) was lost (and never recovered), but the crew jumped clear. The workings were in ironstone.

Photo 2c. West Brandon OC. site, Co Durham. 1977, (5/4 seam), P ref=1.36

High wall collapse and instability resulting from the presence of old workings. To the left of the roadway, small toppling failures can be seen to be developing in the rocks above the stowed gob. To the right of the roadway, the high wall collapse is due to a roadway running oblique and towards the face. Note the persistence of the vertical jointing. The workings date from about 1956.

Photo 2d. Co. Durham, (courtesy of Mr. G. Walton)

Crown hole that developed beneath the back yard of a terraced house in Co. Durham. The coal seam was about 15m from the surface.

Photo 2a.

Photo 2b.

Photo 2c.

Photo 2d.

PLATE 2.

P L A T E 3

Photo 3a. Tow Law OC. site, Co Durham. 18/9/78, (Busty's seam), P ref=14.25

Pair of stereo-photographs showing typical arch development above an old working. The photo on the left has been enhanced to bring out the important features. However, the old working had already been highlighted in the field using white spray paint. The shaded area in the left hand photo represents the remnant coal pillar. The old working has bulked. Staff length = 4.9m.

Photo 3b. Ibbetsons OC. site, Co Durham. 19/5/78, (5/4 seam), P ref=8.5

Two examples of Voussoir beams. The working on the left has had partings and waste material from the adjacent haul road dozed into the entrance.

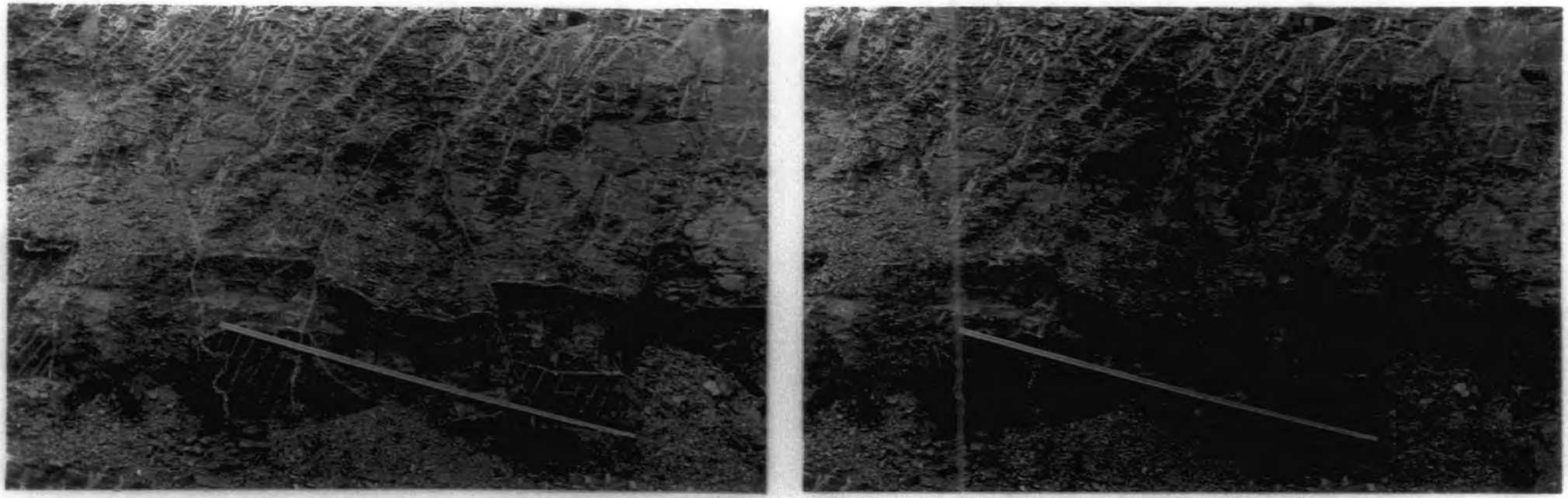

Photo 3a.

Photo 3b.

PLATE 3.

P L A T E 4

Photo 4a. Ibbetsons OC. site, Co. Durham. 19/5/78 (5/4 seam), P ref=8.14

Pair of stereo-photographs showing void migration. The working on the right has bulked, whereas the void on the left is still migrating. The shaded area in the left hand photo represents the coal seam. The staff is 4.9m long.

Photo 4b. Ibbetsons OC. site, Co Durham. 19/5/78, (5/4 seam), P ref=8.08

Pair of stereo photographs showing collapse structures. The collapse to the right of the photo (at the end of the roadway) is thought to be the remains of an intersection collapse (ie. where the two roadways cross one another). The collapse to the centre and right of the photo is a roadway collapse seen in section. The face of the high wall runs almost down the center of this roadway. The staff is 4.9m long.

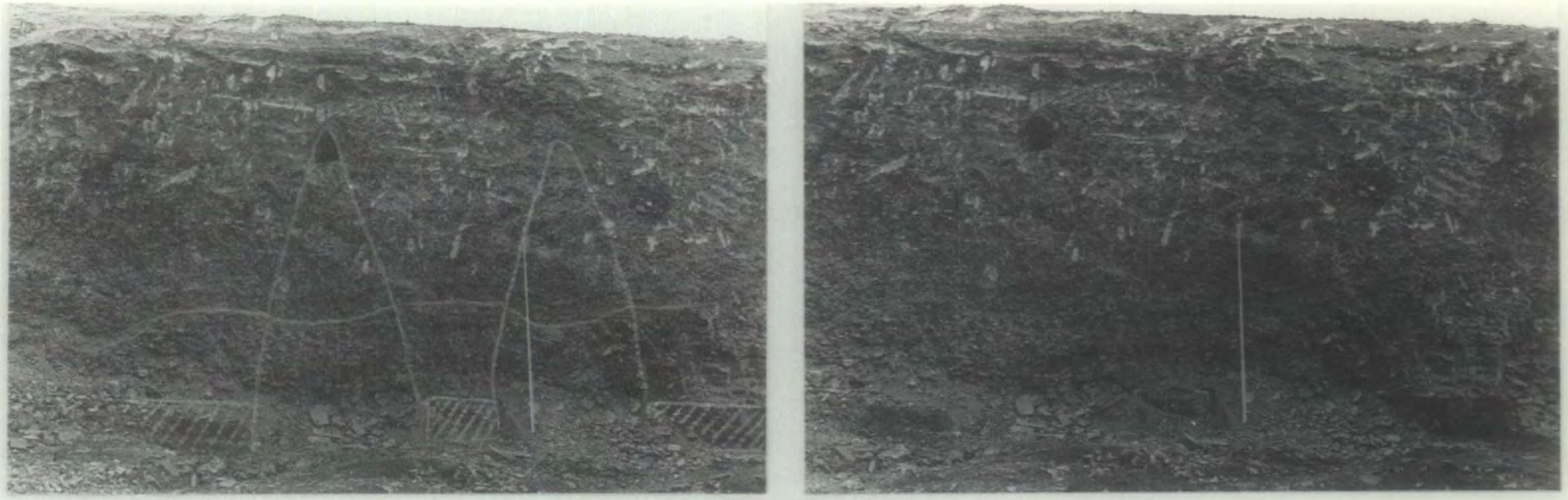

Photo 4a.

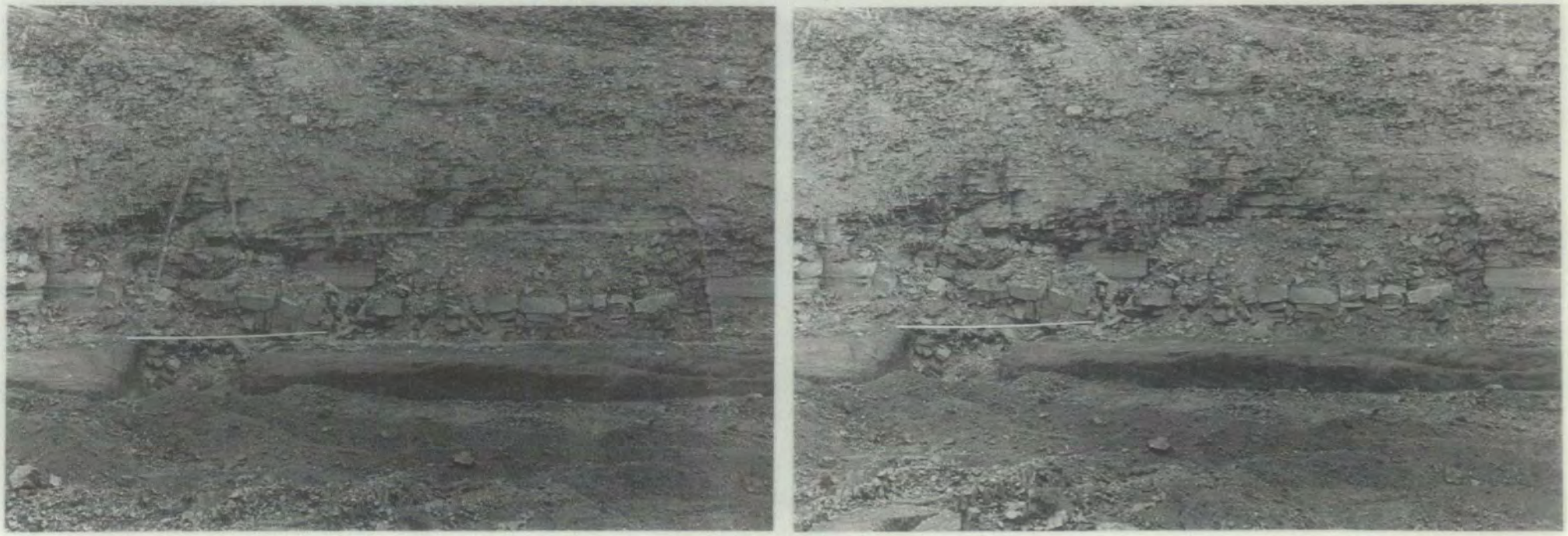

Photo 4b.

PLATE 4

PLATE 5

Photo 5a. Ibbetsons OC. site, Co Durham. 27/6/78, (High Main), P ref=11.36

Typical old working collapse. Note that the remains of some of the propping within the working is still successfully supporting part of the roof. Also of interest is the poorly jointed but fragmented nature of the mudstone roof.

Photo 5b. Ibbetsons OC. site, Co Durham. 19/5/78, (5/4 seam), P ref=9.34

Semi-stable old working. Note the regular and well developed jointing in the roof. Staff is 4.9m long.

Photo 5c. Ibbetsons OC. site, Co Durham. 11/10/78, (High Main), P ref=17.05

Typical old working collapse structure that has been masked by clay, silt and sand washed down the face from the bench above. This is quite a common occurrence especially on high walls that have been exposed for some time.

Photo 5d. Ibbetsons OC. site, Co Durham. 12/9/78, (5/4 seam), P ref=13.24

Rather unusual collapse structure in that the roof rocks are very finely bedded or laminated. Similar modes of failure are predicted to have occurred in the initial stages of the failure at the Thingdon ironstone Mine, Northamptonshire. Note also the slight evidence of floor heave beneath the bottom leaf of the coal. The cleat in the coal is particularly well developed in this instance, The working is in a 'bordwise' direction.

Photo 5a.

Photo 5b

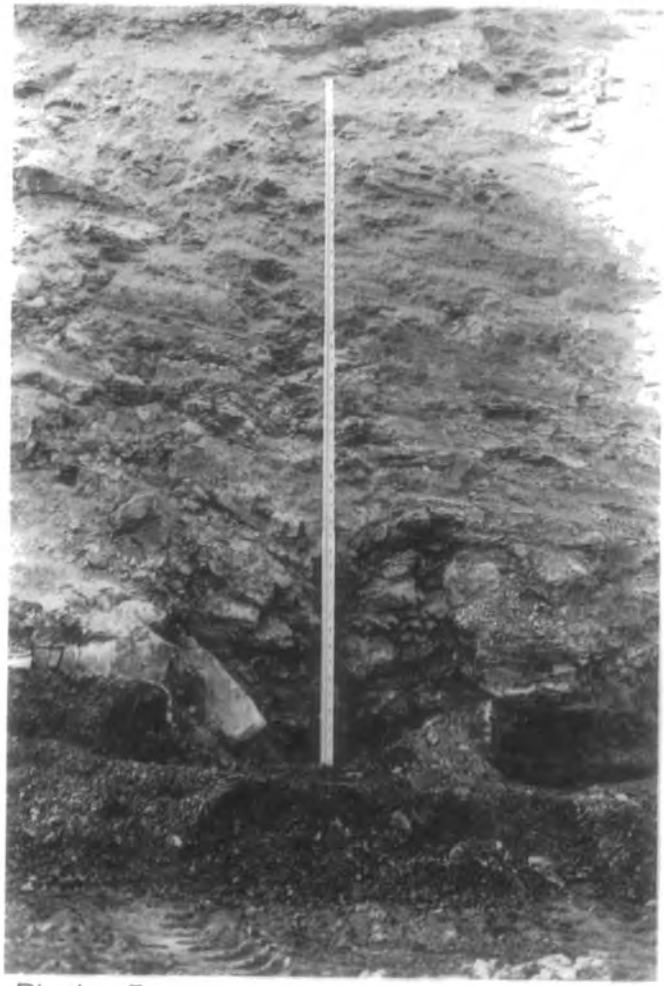

Photo 5c.

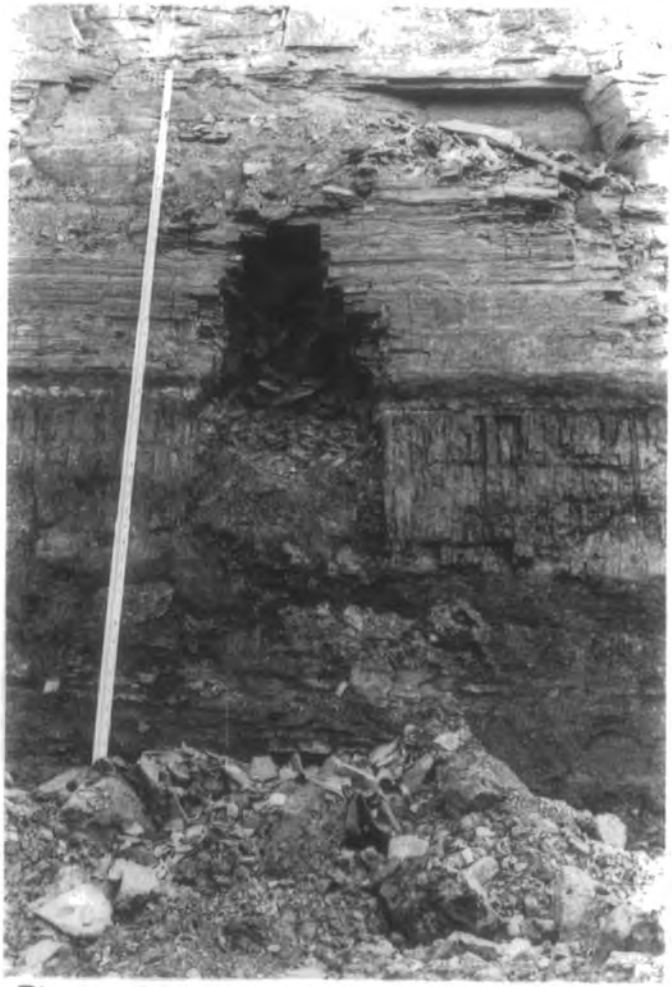

Photo 5d.

PLATE 5

P L A T E 6

Photo 6a. West Brandon OC. site, Co Durham. 10/10/78, P ref=16.18

Joint controlled collapse. The effect of heavy and persistent jointing dominates the mode of failure. The staff is 4.9m long

Photo 6b. Maes y Marhog OC. site, S Wales. 31/7/79, (Bluers seam), P ref 22.21

Two massive collapses seen in section in the high wall. The bench is approximately 15m high (there is a second bench behind the one with the collapse structures). The collapse on the right is 13.6m high and has a base of 8.73m. The collapse on the left is 12.8m high and has a base of 18.0m.

Photo 6c. Debrora OC. site, Co Durham. 14/8/79, P ref=22.24

This photograph illustrates the situation where the old working is too wide and too close to the surface for 'arching' to develop. The result is sub-vertical shears running up towards the surface.

Photo 6d. Coalfield Farm OC. site, Leicestershire. 16/3/78, (Yard seam) P ref=5.05

Typical example of mid 18th C. longwall face. The face was back-stowed with small and inferior coal. To the right of the photo is a roadway pillar left to support the access roads. The access road to the right of the pillar, beyond the photograph, was infact still open. Note the degree of settlement of the stowed material evidenced by the curvature of the old pit prop (near the right hand margin). Staff is 4.9m long.

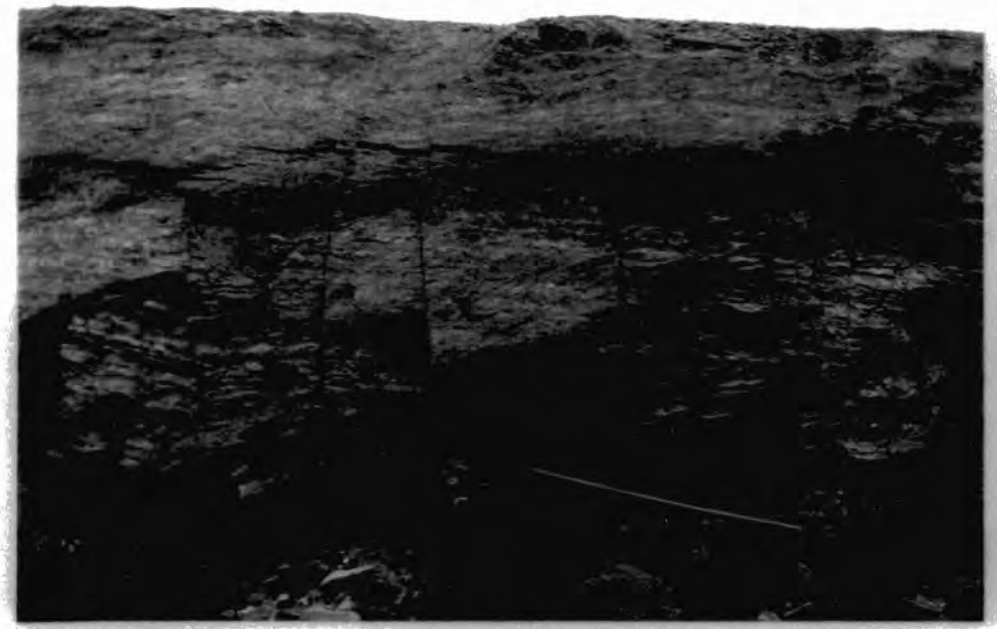

Photo 6a.

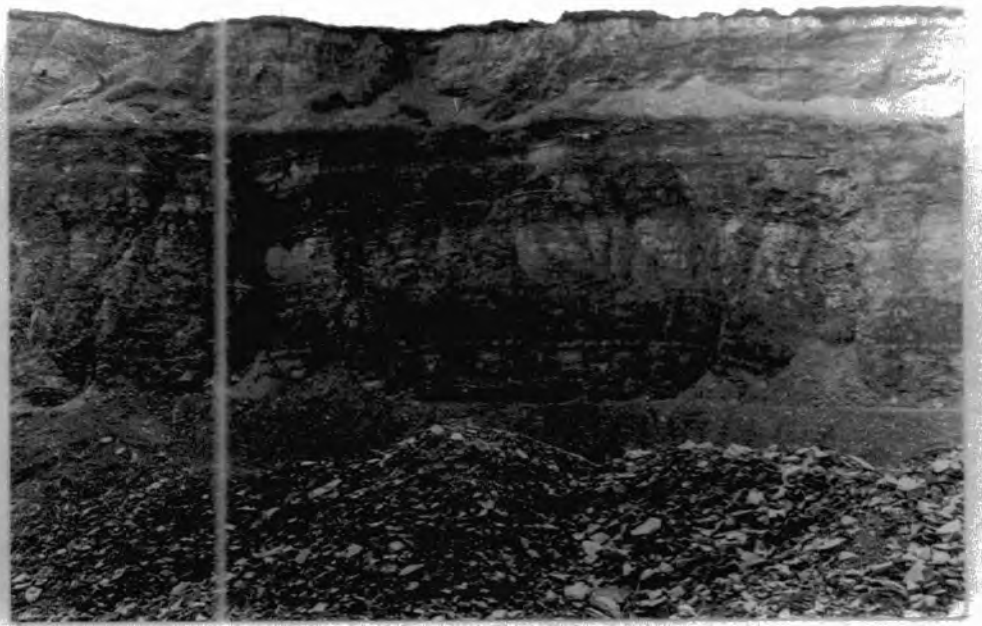

Photo 6b.

Photo 6c.

Photo 6d.

PLATE 6

P L A T E 7

Photo 7a/b. Ibbetsons OC. site Co Durham. 19/5/78, (5/4 seam), P ref=8.19

Pair of stereo photographs showing arch development in a silty mudstone. Note Voussoir type failure of the lower, massive layers. The photograph on the left has been enhanced to show the arch limits. The staff is 4.9m long.

Photo 7c/d. Tow Law OC. site, Co Durham. 28/6/79, (Busty's), P ref=19.27

Unusually high collapse. The coal seam is 1m below the bed marked M. The estimated position and width of the old working has been added to the left hand photo. It is thought that this might represent an intersection collapse structure. The staff is 4.9m long.

Photo 7a.

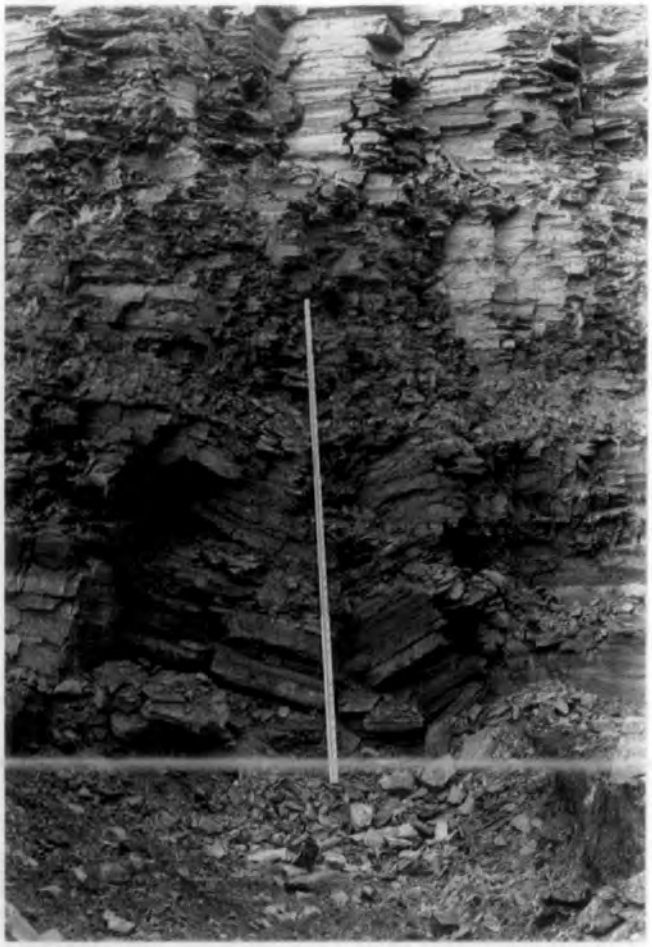

Photo 7b.

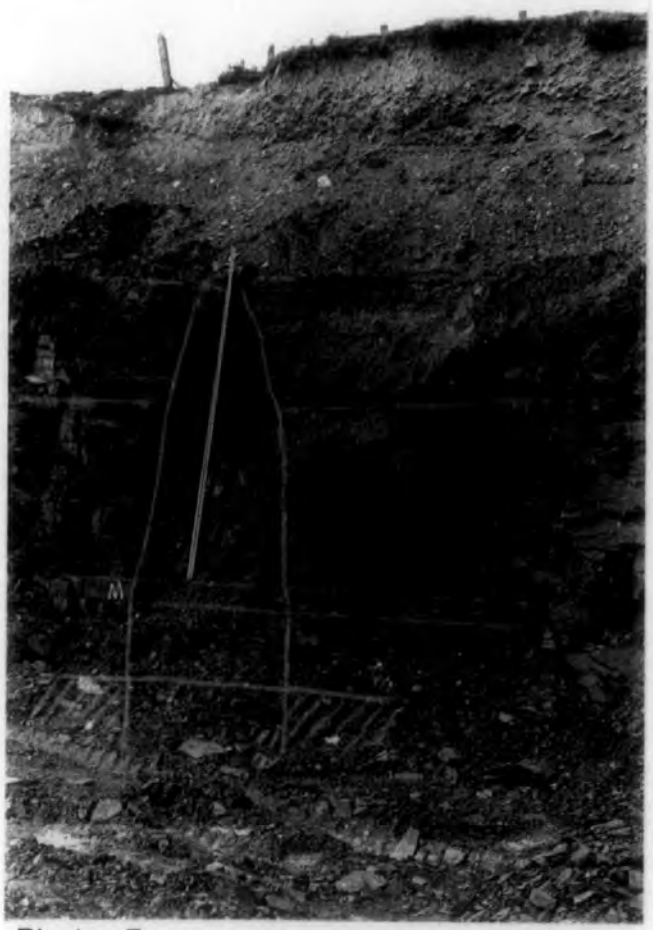

Photo 7c.

Photo 7d.

PLATE 7

P L A T E 8

Photo 8a/b. Pit House OC. site Co Durham. 22/8/79, (5/4 seam), P ref=23.14

Interesting multiple collapse structure possibly brought about by retreat pillar robbing. The adjacent workings were developed in the bottom leaf of the two leaf seam. The top leaf was left to provide a sound roof. On retreat the pillar separating the workings was worked and the void back filled. Three collapse structures have therefore developed. One above each of the roadways, and one above the total structure. The roadway collapse structures are limited by arching, the overall structure is limited by bulking (see Chapter 10). The staff is 4.9m long.

Photo 8c. West Brandon OC. site, Co Durham. 2/11/77, (5/4 seam), P ref=1.42

Beam action in a roof of alternating shale and coal. A small quantity of waste and partings material has been dozed into the workings.

Photo 8d. Ibbetsons OC. site, Co Durham. 11/10/78, (High Main), P ref=16.36

Same bench as photo 5c. The Pillar pattern has been highlighted with spray paint. The staff is 4.9m high.

Photo 8a.

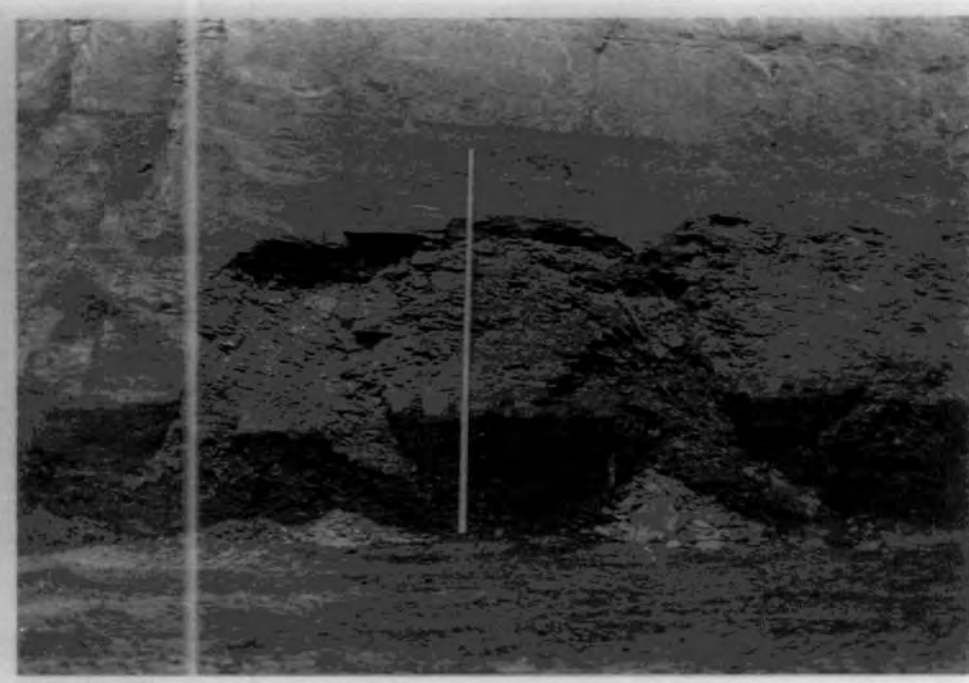

Photo 8b.

Photo 8c.

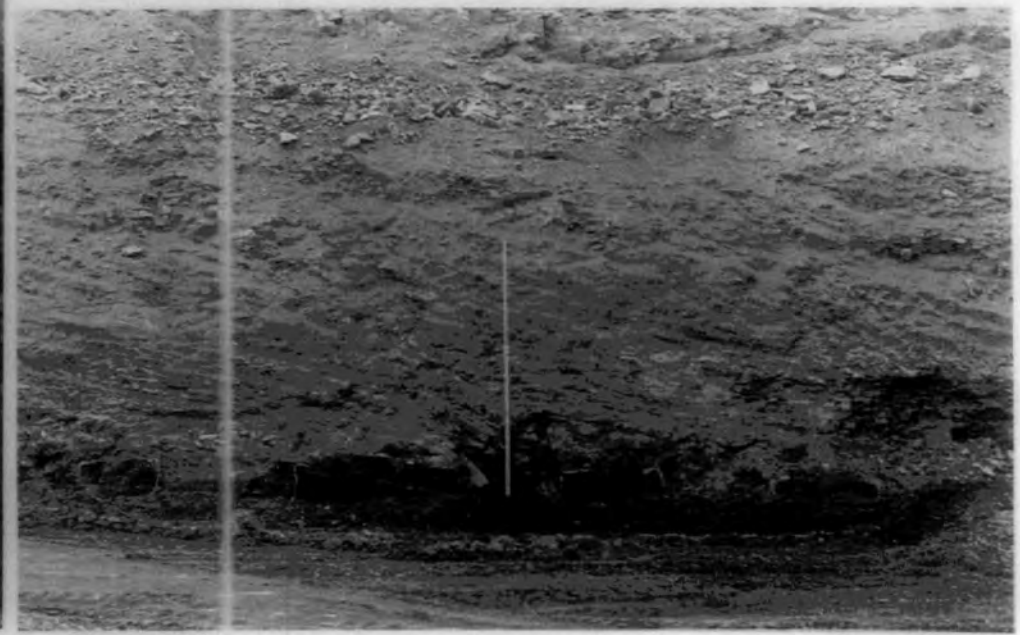

Photo 8d.

PLATE 8

REFERENCES

Ackenheil, A.C. and Dougherty, M.T. (1970), "Recent developments in grouting for deep mines", J. Soil Mechs. and Found. Div., ASCE, 96 No. SMI, pp251-261.

Adler, L and Sun, M.C. (1968), "Ground control in bedded formations", Bull. 28, Research Div., Virginia Polytechnic Inst. Blacksburg 24061, Dec. 1968, pp1-266.

Adler, L. (1973), "A coordinated approach - Preliminary and integrated analysis - roof and ground control", Ch.13, Inst. Mining Engineering Handbook, Soc. Min. Eng., AIME., Vol. 1, Chairman, Cummins, A.B., ed. Givin.I.A., New York.

Airey, E.M. (1974), "The derivation and numerical solution of equations relating to stresses around mine roadways", Ph.D Thesis, Dept. Maths., Univ. Surrey.

Allen, J.C.M, and Robertson, C.W. (1984), "The use of rock mass quality Q in the analysis of engineering properties of rock in areas of abandoned shallow workings", Proc. Int. Conf. on construction in areas of abandoned mine workings, Edinburgh.

Allum, J.A.E., (1966), "Photogeology and regional mapping" Pergamon Press, London, pp1-107.

Anon, (1977), Report by the Geological Society Engineering Group Working Party on "The description of rock masses for engineering purposes", QJEG., Vol. 10, pp355-388.

Aughenbaugh, N.B. (1981), "Effects of humidity on ground control in mining and tunnelling", Effects of moisture on ground control in mining and tunnelling. Soc.Min.Eng., AIME, Mini Symp., No.81-M & E-04, pp15-20.

Balla, A. (1963), "Rock pressure determined from shearing resistance", Proc. Int. Conf. Soil Mech., Budapest, pp461.

Barcza, M., and Von Willich, G.P.R. (1958), "Strata movement measurements at Harmany Gold Mine", Pap. Ass. Min. Mngrs. S. Afr., Vol. 1958/59, pp447-464.

Barker, R.M., and Hatt, F. (1973), "Joint effects in bedded formation roof control", New Horizons in rock mechanics, 14th Symp. on Rock Mech., Penn. State Univ., pp247-261.

Barton, N., Lien R. and Lunde, J. (1974), "Analysis of rock mass quality and support practice in tunnelling, and a guide for estimating support requirements", Internal Report to Norwegian Geotechnical Institute (54206, 19 June).

Beck, W.W. and Russnow, A.L. (1975), "Relationship between underground mine pools and subsidence in the N.E. Pennsylvania Anthracite fields", Pennsylvania Dept. of Environment resources, Harrisburg, ARC. 73 111 2553, pp1-411.

Beer, G. and Meek, J.L. (1982), "Design curves for roofs and hanging-walls in bedded rock based on 'Voussoir' beam and plate solutions", Trans. Inst. Min. Met. (Sect.A), 91, ppA18-22.

Bieniawski, Z.T. (1979), "The geomechanics classification in rock engineering applications", Int. Soc. Rock Mech. Int. Congress Rock Mech. Montreaux, Vo. 2, pp41-48.

Bieniawski, Z.T. (1981), "Estimating safe roof spans in coal mines using rock mass classifications", Proc. 11th Annual Inst. on Coal Mining Health, Safety and Research, Blacksburg, Virginia, pp181-187.

Biermbaumer (1913), Quoted by Szechy, K. (1970).

Bishop, A.W. (1958), "Test requirements for measuring the coefficient of earth pressure at rest", Brussels Earth Conference.

Brauner, G. (1973), "Subsidence due to underground mining 1. Theory and practice in predicting surface deformation", U.S. Dept. of Interior, Bureau of Mines Information Circular/1973, IC 8571.

Briggs, H. (1929), "Mining subsidence", Publ. Edward Arnold.

Brook, N. (1977), "A method of overcoming both shape and size effects in the point load test", Proc. Conf. on Rock Engineering, Newcastle, Attewell P.B., ed., pp53-70.

Brook, N. (1977), "Model studies of mine roadway deformation", The Mining Engineer, pp375-384.

Brook, N. (1980), "Size Correction for Point Load testing", Int. J. Rock Mech. Min. Sci., Vol. 17, pp231-235.

Brown, E.T. and Hudson, J.A. (1972), "Progressive collapse of simple block-jointed systems", Aust. Geomechanics Jour., Vol. G2, No.1, pp49-54.

Bucky, P.B. (1934), "Effect of approximately vertical cracks on behaviour of horizontally lying roof strata", Trans. A.I.M.E., Vol. 109, p212.

Byrne, R.J. (1974), "Physical and numerical models in rock and soil slope stability", Ph.D Thesis, James Cook Univ., N. Queensland.

Callon, M.J. (1874), "Cours d'Exploitation des Mines", Paris.

Cameron, D.W.G. (1956), "The menace of present day subsidence caused by ancient mineral operations", J. R. Inst. Chart. Surv. (Scottish Supplement), 19, Part 3, pp159-171.

Carter, P., Jarman, D., Sneddon, M. (1980), "Mining subsidence in Bathgate, a town study", Proc. 2nd Int. Conf. Ground Movements and structures, UWIST, Ed. Geddes, J.D., Pentech Press.

Carter, P.G. (1984), "Case histories which break the rules", Proc. Int. Conf. on construction in areas of abandoned mine workings, Edinburgh, pp20-29.

Caudel, R.D. and Clark, G.B. (1955), "Stress around mine openings in some simple geologic structures", Univ. of Illinois Eng. Exp. Stat. Bull., No.430, pp1-42.

Challinor, P.G. (1976), "The mode of collapse of room and pillar coal mine workings", Dissertation, M.Sc., Advanced course in Egnineering Geology, University of Durham.

Clements, R.G. (1982), "Proof of evidence given on behalf of Leicestershire and Rutland Trust for Nature Conservation", Vale of Belvoir Public Inquiry.

Cundall, P.A. (1971), "A computer model for simulating progressive large scale movements in blocky rock systems", Proc. Sump. Rock Fracture (ISRM), Nancy, paper 11-8.

Denby, B., Hassani, F.P. and Scoble, M.J. (1982), "The influence of water on the shear strength of Coal Measures rock discontinuities in surface mining", Proc. 1st Int. Mine Water Congress, Budapest, Vol. A, pp334-345.

Denkhaus, H.G. (1958), "The application of the mathematical theory of elasticity to problems of stress in hard rock at great depth", Pap. Ass. Min. Mngers., S. Afr., Vol. 1958/59, pp271-310.

Denkhaus, H.G. (1964), "Critical review of strata movement theories and their application to practical problems", J. of South Afr. Inst. Min. Met., Vol. 64, No.8, pp310-332.

Department of the Environment, (1976), "Reclamation of derelict land - procedure for locating abandoned mine shafts", Report by Ove Arup & Ptns., Planning Regional and Minerals Directorate, DOE., London.

Dunn, M. (1852), "Winning and working of coal" (2nd Ed.), Dunn and Dodsworth, Newcastle.

Engesser, (1882), Quoted by Szechy, K. (1970).

Ergun, I. (1970), "Stability of underground openings in jointed media", Ph.D Thesis, University of London.

Evans, W.H. (1941), "The strength of undermined strata", Trans. Inst. Min. Met., Vol. 50, pp475-500, discussion pp501-532.

Farmer, I.W. (1968), "Engineering Properties of Rocks", London - Spon Ltd.

Fayol, H. (1885), "Notes sur les mouvements de terrain", Bulletin de la Societe de l'Industrie Minerale, St. Etienne.

Fenner, R. (1938), "Untersuchungen zur Erkenntnis des Gebirgdruckes", Gluckauf, Bd, 74, pp681-695, 705-715.

Fielding, C.R. (1982), "Sedimentology and stratigraphy of the Durham Coal Measures and comparison with other British coalfields", Ph.D Thesis, University of Durham.

Galloway, R. (1835), "Annals of coal mining and the coal trade", Vol. 1 and 2, Colliery Guardian Co. London. Repub. David and Charles, 1971.

Geddes, J.D. (1977), Questions session 11, "Proc. conf. on large ground movements and structures", UWIST, Cardiff, pp984-989.

Getzler, Z., Gellert, M. and Eitan, R. (1970), "Analysis of arching pressures in ideal elastic soil", J. Soil Mech. Found. Div., ASCE., pp1357-1372.

Goel, S.C. and Page, C.H. (1982), "Chimney caving above underground mines", Int. J. Rock Mech. Min. Sci., Vol. 19, pp325-337.

Goodman, R.E., Taylor, R.L. and Brekke, T.L. (1968), "A model for the mechanics of jointed rock", J. Soil Mechs. and Found. Div., ASCE., SM3, V. 94, pp637-658.

Gray, R.E., Bruhn, R.W. and Turka, R.J. (1977), "Study and analysis of surface subsidence over the mined Pittsburg coal bed", Gai Consultants Inc., Monroeville, P.A. July, Burmines-OFR-25-78.

Greenwell, G.C. (1855), "On the working of thin seams of coal with observations on longwall and bord and pillar work", Trans. N.England. Inst. Min. Eng., V.4, pp193-201.

Gumbel, E.J. (1967), "Statistics of extremes", Columbia Univ. Press, New York.

Halbaum, H.W.G. (1905), "The great planes of strain in the absolute roof of mines", Trans. Inst. Min. Eng.

Hall, P. (1977), "The investigation and treatment of abandoned mineral workings in the Coal Measures", M.Sc. Dept. Earth Sciences, Leeds University.

Hall, R.C. (1910), "The strength of mine roofs", Mines and Minerals, V. 30.

Hassani, F.P., Whittaker, B.N. and Scoble, M.J. (1979), "Strength characteristics of rocks associated with opencast mining in the U.K.", 20th U.S. Symp. on Rock Mech. Austin, Texas, June 4-6, pp347-355.

Hedley, J. (1851), "A practical treatise on the working and ventilation of coal mines", J. Weale, London.

Henry, J. (1975), "An unusual case of failure in old oil-shale workings at Pumpherston, West Lothian, Scotland", Minerals and the Environment, Vol. 5, pp24-31.

Higginbottom, I. (1984), "Methods of development in areas of ancient shallow coal mining", Proc. Int. Conf. on Construction in areas of abandoned mine workings, Edinburgh, Supplement to paper, pp115-118.

Hittinger, M. (1978), "Numerical analysis of toppling failures in jointed rock", Ph.D. Thesis, University of California, U.S.A.

Hocking, G. (1978), "Analysis of toppling:sliding mechanisms for rock slopes", Proc. 19th U.S. Symp. on Rock Mech., pp288-295.

Hoek, E. and Brown, E.T. (1980), "Underground excavations in rock", Institution of Mining and Metallurgy, London.

Hofer, K.H. and Menzel, W. (1964), "Comparative study of pillar loads in potash mines established by calculation and by measurements below ground", Int. J. Rock Mech. Min. Sci., V. 1, pp181-198.

Holland, J. (1841), "The history and description of Fossil Fuel, the collieries and coal trade of Great Britain", Whittaker & Co., 1841, Sheffield. Reprint:Frank Cass, 1968, London

Hughes, H.W. (1904), "A text book on coal mining", 5th Ed. 1904, Charles Griffin, London 1904, 1st Ed. 1892.

Humphrey, W.S. and Stanislaw, J. (1979), "Economic growth and energy consumption in the U.K. 1700-1975", Energy Policy, V. 7, Pt. 1, pp29-42.

Irving, C.J. (1946), "Some aspects of ground movement", J. Chem. Met. and Mining Soc. of S. Africa, Vol.XLVI.

Isaacson, E. de St.Q. (1962), "Rock Pressure in Mines", Mining Publications Ltd., London, 2nd Ed., pp1-260.

Jennings, J.E. (1966), "Building on the dolomites in the Transvaal", The Civil Engineer in South Africa.

John, K.W. (1962), "An approach to rock mechanics", J. Soil Mech. Found. Div., ASCE., V. 88, N4.

Jones, O.T. and Davies, E.L. (1929), "Pillar and stall working under a sandstone roof", Trans. Inst. Min. Engrs., V. 76, pp313-329.

Ladeira, F.L. and Price, N.J. (1981), "Relationship between fracture spacing and bed thickness", J. Struct. Geol., V. 3, N2, pp179-183.

Langland, R.T. (1978), "Analytical modeling of coal mine roof behaviour", Calif. Univ. Lawrence Livermore Lab., UCRL 52586, Oct., pp1-99.

Litiwiniszyn, J. (1964), "On certain linear and non-linear strata theoretical models", Fourth Symp. on Strata Control and Rock Mech., Columbia Univ.

Littlejohn, G.S. (1979), "Subsurface stability in areas underlain by old coal workings", Ground Engineering, Vol. 12, No.2, pp22-30.

Littlejohn, G.S. (1979), "Consolidation of old coal workings", Ground Engineering Vol. 12, No.4, pp15-21.

Maini, T., Cundall, P., Marti, S., et al (1978), "Computer modelling of jointed rock masses", Dames and Moore, N.T.I.S., (Technical Report - U.S. Army Engineer waterways experiment station - N-78-4). pp1-396.

Maxwell, G.M. (1971), "The investigation of subsurface hazards due to abandoned coal mines", Ph.D Thesis, University of Strathclyde.

Merril, R.H. (1954), "Design of underground mine openings - oil shale mine, Rifle, Colorado", U.S. Bureau of Mines, report of investigations 5089, pp1-56.

Merril, R. (1957), "Roof span studies in limestone", U.S. Bureau Mines Rept. Invest., 5348:38pp.

MIDAS, (1976), "Documentation for MIDAS", Fox, D.J., Guire, K.E., Statistical research laboratory, Univ. Michigan, 3rd Ed.

Mohr, F. (1956), "Influence of mining on strata", Mine and Quarry Engineering, Vol. 22, (4).

Morley, A. (1953), "Strength of Materials", London:Longmans, Green and Co. Ltd., 11th Ed.

Munson, D.E. and Benzley, S.E. (1980), "Analytic subsidence model using void-volume distribution functions", Proc. 21st U.S. Rock Mech. Symp., Rolla.

National Coal Board, (1975), "Subsidence Engineers Handbook", London.

Nef, J.U. (1932), "The Rise of the British Coal Industry", Vol. 1 and 2, George Routlidge, London.

Nichols, T.C. (1980), "Rebound its nature and effect on engineering works", Q.J.E.G., Vol. 13, No. 3, pp133-152.

Nishida, T., Esaki, T., Kameda, N. and Aoki, K. (1981), "Cave-in due to mining at shallow depths", Proc. Int. Symp. on Weak Rock, Tokyo, pp707-712.

Obert, L., Duvall, W.L. and Merril, R.H. (1960), "Design of underground openings in competent rock", USBM, Bull.567.

Parry, H.J. (1984), "Coping with Fife's mineworking heritage - a difference approach", Proc. Int. Conf. on construction in areas of abandoned mineworkings", Edinburgh, pp162-177.

Peng, S.S. (1978), "Coal mine ground control", New York:Wiley

Piggott, R.J. and Eynon, P. (1977), "Ground movements arising from the presence of shallow abandoned mine workings", Proc. Conf. on large ground movements and structures, UWIST, Cardiff, pp749-780.

Potts, E.L.J., Szechi, A., Watson, S.H. and Mottahed, P. (1979), "The evaluation of the design criteria for underground roof strata considered as a linear arch structure", Int. Soc. Rock Mech., Int. Congress Rock Mech., Montreaux, Vo. 2, pp531-538.

Price, N.J. (1966), "Fault and joint development in brittle and semi-brittle rock", Pergamon Press.

Price, D.G., Malkin, A.B. and Knill, L.J. (1969), "Foundations of multi-storey blocks on coal measures with special reference to old workings", Q.J.E.G., Vol. 1., pp271-322.

Rabcewicz, L. (1944), "Gebirgsdruck und Tunnelbau", Springer, Vienna.

Rhiza, F. (1882), "Subsidence due to mining operations", Zeit fur Berg und Huttenwesen XXX Jahrgang.

Ross-Brown, D.M., and Atkinson, K.B. (1972), "Terrestrial photogrammetry in Open Pits:1 Description and use of the photo-theodolite in mine surveying", Trans. I.M.M., A205-213, Vol. 81.

Rouse, K. (1982), "A computer program for modelling jointed rock mass behaviour", Unpublished M.Sc Thesis, University of Durham.

Sandy, J.D., Piesdd, D.D.A., Fleischer, V.D., and Forbes, P.J. (1976), "Failure and subsequent stabilisation of No. 3 dump at Mufulira Mine", Trans. I.M.M., Vol. 85, ppA144-A162.

Shadbolt, C.H. (1977), "Mining subsidence - Historical review and State of the Art", Proc. Conf. on large Ground Movements and Structures, UWIST, Cardiff, Ed. Geddes,pp705-748.

Singh, J.C., and Saluja, S.S. (1982), "Extracting a honey-combed thick coal seam", Coal, Gold and base minerals of Southern Africa, May 1982, Vol. 30 P 5, pp52-56.

Singh, R.D. (1981), "A study of the stability of roof rocks in coal mines in India", Proc. Int. Symp. on weak rock, Tokyo, pp909-914.

Smailes, A.E. (1935), "The development of the Northumberland and Durham coalfield", The Scottish geographical magazine, Vol. 57, No. 4., July.

Smith, T.J. (1976), "Consolidation and other geotechnical properties of shales with respect to age and composition", Ph.D Thesis, University of Durham.

Snedecor, G.W., and Cochran, W.G. (1980), "Statistical Methods", (7th Ed.), IOWA State University Press, Iowa.

Spears, D.A. and Taylor, R.K. (1972), "The influence of weathering on the composition and engineering properties of in situ Coal Measures rocks", Int. J. Rock Mech. Min. Sci., Vol. 9, pp729-756.

Stephansson, O. (1971), "Stability of single openings in horizontally bedded rock", Eng. Geol., No. 5, pp5-71.

Stewart, I.J. (1981), "Numerical and Physical modelling of underground excavations in discontinuous rock", Ph.D Thesis, University of London.

Sutherland, H.J. and Schuler, K.W. (1981), "A review of subsidence prediction research conducted at Sandia National Laboratories", Proc. Workshop on surface susbidence due to underground mining, Nov. 30-Dec. 2, Morgantown: W.V. Univ., Ed. S. Peng.

Sutherland, H.J., Schuler, K.W. and Benzley, S.E. (1981), "Observations and analytic calculations of strata movement above idealised mine structures", Proc. 7th annual underground coal conversion symp., Fallen Leaf Lake, CA, Sept., pp221-233 (see Sutherland et al, 1983).

Sutherland, H.J., Schuler, K.W. and Benzley, S.E. (1983), "Numerical and physical simulations of strata movement above idealised mine structures", In Situ, Vol. 7, pt.1, pp87-113. (N.B. identical to Sutherland et al 1981.)

Szechy, C. (1966), "Approximate determination of rock pressure on the basis of a statistical analogy", Int. Symp. on Rock Mech., Budapest, pp521.

Szechy, K. (1970), "The art of tunnelling", Akademiai Kiado, Budapest, ppl-891.

Tandanand, S. and Powell, (1982), "Consideration of overburden lithology for subsidence prediction", Workshop on surface subsidence due to underground ming, Ed. Peng. S.S. and Harthill, M., W. Virginia Univ., Morgantown, U.S.A., ppl7-33.

Taylor, R.K. (1974), "Influence of coal content on peak shear strength of colliery shales", Geotechnique, Vol. 24, N4, pp634-688.

Taylor, R.K. (1975), "Characteristics of shallow coal-mine workings and their implications in urban redevelopment areas", In 'Site investigations in areas of mining subsidence', Bell F.G. ed. London, Newnes-Butterworths, ppl25-148.

Taylor, R.K. (1983), Personal communication.

Taylor, R.K. (1984), "Composition and engineering properties of British colliery discard", N.C.B., Hobart House, ppl-236 (in press).

Terzaghi, K. (1946), "Introduction to tunnel geology", in Rock tunnelling with steel supports, by Proctor and White (Commercial Shearing and Stamping Co., Youngstown, Ohio).

Thorburn, S. and Reid, W.M. (1977), "Incipient failure and demolition of 2 storey dwellings due to large ground movements", Proc. Conf. on large Ground Movements and Structures, UWIST, Cardiff.

Tincelin, E. (1958), "Pressions et deformations de terrain dans les mines de fer de Lorraine", Jouve Editeurs, Paris, 284.

Trollope, D.H. (1966), "The stability of Trapezoided opening in rock masses", Felsmechanic, V. 4, N3, pp232-242.

Trollope, D.H. (1968), "The mechanics of discontinua or clastic mechanics in rock problems", in Rock Mechanics in Eng. Practice, Stagg and Zienkiewicz, ed. John Wiley, London.

Voegele, M.D. (1978), "An interactive graphics based analysis of the support requirements of excavations in jointed rock masses", Ph.D Thesis, University of Minnesota.

Walton, G. (1983), Personal communication.

Walton, G. and Atkinson, T. (1978), "Some geotechnical considerations in the planning of surface coal mines", Trans. Inst. Min. Met., V. 87, ppA147-A172.

Walton, G. and Taylor, R.K. (1977), "Likely constraints on the stability of excavated slopes due to underground coal workings", Proc. Conf. on rock engineering, Newcastle, Attewell P.B., ed., pp329-349.

Wardell, K. and Wood, J.C. (1965), "Ground instability arising from old shallow mine workings", Proc. Midland Soil Mech. and Found. Soc., Vol. 7, paper No. 36, pp5-30.

Wardell, K. and Eynon, P. (1968), "Structural concept of strata control and mine design", Trans. Inst. Min. Metall. V. 77, ppA125-138.

Watson, C. (1983), "A program designed to model the behaviour of discontinuous rock masses", Unpublished M.Sc Thesis, University of Durham.

Wickens, E.H. and Barton, N.R. (1971), "The application of photogrammetry to the stability of excavated rock slopes", Photogramm Rec.7, April 1971, pp46-54.

Wiggil, R.B. (1963), "The effects of different support methods on strata behaviour around sloping excavations", J. S. Afr. Inst. Min. Metall., Vol. 63, pp391-426.

Willis, A.J. (1980), "Old Coal Workings - client, consultants and contractor", Ground Engineering, Vol. 13, No. 8, pp22-24, 39.

Wilson, A.H. (1980), "A method of estimating the closure and strength of lining required in driveages surrounded by a yield zone", Int. J. Rock Mech. Min. Sci., Vol. 17, N6, pp349-355.

Wright, F.D. and Mirza, M.B. (1963), "Stress distribution around a vertical crack in a mine roof beam", Trans. AIME., Vol. 226, pp174-179.

Wright, F.D. (1972), "Arching action in cracked roof beams", 5th Int. strata control conf., London (NCB), paper 29, pp1-9.

Wright, F.D. (1973), "Roof control through beam action and arching", Mining Engineering Handbook, Soc. Min. Eng. AIME., Vol. 1, Chairman Cummins, A.B., Ed. Given I.A., New York., Ch.13, pp80-96.

Appendix 1.

CODINGS FOR FIELD DATA

FIELDWORK DATE (Day,month,year)

LOCATION The country is divided into eleven different coalfields within which each opencast site has a unique code:-

Coalfield/Region		Sites within Region	
Ayrshire	1- 5	Benbain	1
Midlothian	6-10	Blindwells	6
Northumberland	11-15	Acclington	11
Durham	16-29	St.Andrews	12
Cumbria	30-35	Ibbetsons	16
Yorkshire	36-40	Tow Law	18
Nottinghamshire	41-45	West Brandon	19
Leicestershire	46-50	Pit House	20
Shropshire/Welsh Borderlands	51-55	Esh	21
North Wales	56-60	Tanners Hall	22
South Wales	61-65	Cowsley	23
		Low Close	30
		St.Aidens	36
		Park Meadow	41
		Morrels	42
		Coalfield Farm	46
		Maesgwyn	61
		Maes-y-Marchog	62

PHOTOGRAPH REFERENCE No.

APPROXIMATE AGE OF WORKING (Year) If value for abandonment given, e.g.1735, it is written as 1735. If age uncertain e.g. 18th.century, the value is coded as 1700. The 00 at end indicates century adjustment.

VISUAL CONDITION

1 Excellent
2 Good
3 Medium
4 Poor

DEPTH FROM SURFACE (m)

SEAM NAMES These are divided into the same coalfield/regional groupings as the site locations. However, the value for each seam within the region does not necessarily coincide with the site code, as one site often has old workings in to or more seams.

Penevene Low	1	Hutton	22
Blindwells seam	6	Busty	23
Acclington seam	11	Metal	30
Brockwell	12	Top Soft	36
Five Quarter	16	Piper	41
High Main	17	Silkston Main	42
Tow Law seam	18	Yard	46
Five Quarter	19	Upper Law Main	47
Five Quarter	20	Cornish	61
Bottom Busty	21	Bluers	62

SEAM THICKNESS (m) Recorded as the extracted seam thickness not the total thickness

SEAM CONDITION

1 Strong Cleat
2 Moderate Cleat
3 Slight Cleat
4 No Cleat

MAIN ROCK TYPE

01	Conglomerate	08	Siltstone
02	Sandstone	09	Silty Mudstone
03	Quartz Sandstone	10	Seat Earth
04	Argillaceous Sandstone	11	Coal
05	Mudstone	12	Coal Shale
06	Shaly Mudstone	13	Sandstone & Shale
07	Shale	14	Boulder Clay

ROCK COLOUR

Hue		Shade		Colour	
1	Light	1	Pinkish	1	Pink
2	Dark	2	Reddish	2	Red
		3	Yellowish	3	Yellow
		4	Brownish	4	Brown
		5	Olivish	5	Olive
		6	Greenish	6	Green
		7	Blueish	7	Blue
		8	Greyish	8	White
				9	Grey
				10	Black

e.g 2.7.9 = Dark Blueish Grey

GRAIN SIZE

1	Greater than 60mm	Very Coarse
2	2mm - 60mm	Coarse
3	60μm - 2mm	Medium
4	2um - 60μm	Fine
5	Less than 2μm	Very Fine

BED THICKNESS

1	Greater than 2m	Very thick	5	0.02m - 0.06m	Very thin
2	0.6m - 2m	Thick	6	6mm - 20mm	Thickly laminated
3	0.2m - 0.6m	Medium			
4	0.06m - 0.2m	Thin	7	2mm - 6mm	Thinly laminated

MINERALOGY In order of decreasing abundance

1	Illite	6	Dolomite & Ankerite
2	Kaolinite	7	Siderite
3	Quartz	8	Pyrite
4	Feldspar	9	Carbon & others
5	Calcite		

QUARTZ TO CLAY RATIO %

MOISTURE CONTENT %

ROCK STRENGTH Unconfined Compressive Strength MN/m^2

METHOD OF STRENGTH ASSESSMENT

1	Guesstimate	4	Triaxial/UCS
2	Point Load	5	Other methods
3	NCB Cone indentor	6	Beam bending

STATE OF ROCK WEATHERING

1	Fresh	4	Highly
2	Slightly	5	Completely
3	Moderately	6	Residual Soil

EFFECTIVE BED THICKNESS Average thickness of the collapse blocks derived from the most important of the roof rocks

JOINT FREQUENCY

1	Extra wide, greater than 2m	4	Moderately wide	0.06 - 0.2m
2	Very wide 0.6m - 2m	5	Moderately narrow	0.02m- 0.06m
3	Wide 0.2m - 0.6m	6	Narrow	0.006- 0.02m

JOINT CONDITION (2 variables)

1	Very open	1	Iron staining
2	Open	2	Clay infill
3	Closed	3	No infill
4	Imperceptible	4	Weathered

JOINT VERTICAL EXTENT

1	Greater than 2m	3	0.5 - 1m
2	1 - 2m	4	0 - 0.5m

BRIDGE ROCK TYPE	Same Groups as previously defined
BRIDGE ROCK COLOUR	" " " " "
GRAIN SIZE	" " " " "
BED THICKNESS (BRIDGE)	" " " " "
BRIDGE ROCK STRENGTH	" " " " "
DEGREE OF BRIDGE WEATHERING	" " " " "
EFFECTIVE BED THICKNESS (BRIDGE)	" " " " "
BRIDGE WIDTH (m)	See Fig. for definition
BRIDGE THICKNESS (m)	See Fig. for definition
JOINT FREQUENCY	Same groups as previously defined
JOINT CONDITION	" " " " "
ARCH HEIGHT (MIGRATED) (m)	See Fig. for definition
THEORETICAL ARCH HEIGHT (m)	" " " "
ANGLE OF ARCH APEX FROM HORIZONTAL	See Fig. for definition
WIDTH OF OLD WORKING	" " " "
RATIO OF HEIGHT OF COLLAPSE TO WIDTH OF WORKING:	$\frac{h}{s}$

DEGREE OF BRIDGING OF ARCH (Void arresting properties of next rock unit)

1	Complete	i.e. no further collapse likely
2	Partial	Possibly some further collapse
3	None	Collapse highly probable

TYPE OF OLD WORKING INFILL

1	Totally stowed on abandonment	5	Partially stowed, pit props in place
2	Partially stowed on abandonment	6	No stowing, but pit props in place
3	No stowing	7	Floor heave
4	Totally stowed, pit props in place	8	Heavy ochre deposit

EVIDENCE OF FLOODING IN OLD WORKINGS (before opencast operations)

1	Total Flooding
2	Partial flooding
3	No flooding

DEGREE OF COLLAPSE OF OLD WORKINGS (See text for details)

1	Total	90 - 100%	4	Superficial	5 - 30%
2	Considerable	60 - 90%	5	None	0 - 5%
3	Partial	30 - 60%			

PERCENTAGE COLLAPSE (See main text for details)

ADDITIONAL COMMENTS - Card Reference number

THICKNESS OF PILLAR (m) (distance between old workings)

PERCENTAGE EXTRACTION (% of seam taken as a volume on plan basis)

RATIO OF SPAN WIDTH TO SEAM THICKNESS $\frac{S}{t}$

MISSING VALUES Coded as 00's

REPEAT VALUES (for bridge variables) **Coded as 99's**

```
C
C ***************************************************************************
C
C
C ***************************************************************************
C                                                                       .
C
C     PROGRAMME VALIDAT G.F.G.GARRARD 27/3/79.
C
C
C ***************************************************************************
C
C ***************************************************************************
C
C
C     COMPILED VERSION OF MAIN PROGRAM  VALIDAT AT VALICOM
C
C      BACKUP PROGRAM VALITIDY
C
C
C ***************************************************************************
C
C
C    THIS PROGRAM READS CASEWISE, A DATA MATRIX OF 47 VARIABLES.
C    THESE VARIABLES (LISTED AT THE END OF THE PROGRAM) ARE SUFFICIENT
C    TO CHARACTERISE MOST OLD WORKINGS ENCOUNTERED.  MANY OF THE
C    PARAMETERS USED TO DESCRIBE THE OLD WORKINGS ARE CODED INTO
C    ORDINAL GROUPINGS.
C
C    THIS PROGRAM DECODES THE MATRIX AND, FOR EACH CASE, PRINTS ONE
C    PAGE OF INFORMATION IN A STANDARD FORM WHICH, IT IS HOPED,
C    PRESENTS THE RAW DATA IN AN EASILLY UNDERSTOOD MANNER.
C
C    IN THE DATA MATRIX 0'S STAND FOR MISSING DATA AND 9'S FOR
C    REPEATED DATA.  FOR EXAMPLE : THE MAIN ROCK TYPE MAY BE A
C    SANDSTONE (CODED AS 02) BUT THE BRIDGE ROCK TYPE ABOVE MAY
C    ALSO BE SANDSTONE IN SUCH A CASE, RATHER THAN CODING THE
C    BRIDGE ROCK TYPE AS 02 AGAIN IT IS CODED AS 99.
C
C    DATAMEDDLER IS A COMPLEMENTARY PROGRAM TO THIS ONE.  ITS PURPOSE IS
C    TO READ THE RAW DATA, CONTAINING 9'S, AND REASIGN THE ORIGINAL
C    VALUES IN THEIR PLACE.
C
C
C
C     ARRAY DECLARED AND STATIC DATA INPUT FROM HERE
C
      LOGICAL*1 M1(1)
      DATA M1 /'*'/
      REAL*8 COLLAP(3,5)
      REAL*8 OWFLOD(1,3)
      REAL*8 OWFL(2,8)
      REAL*8 ARCHBR(1,3)
      REAL*8 VERTEX(1,4)
      REAL*8 AJCOND(1,4), BJCOND(2,4)
      REAL*8 AJFREQ(1,6)
      REAL*8 WEATH(2,6)
      REA ,*8 AMETH(2,6)
      REA ,*8 AMIN(2,9)
      REA ,*8 GRAIN(1,5)
      REA ,*8 BTHICK(3,7)
      REA ,*8 HUE(1,2), SHADE(1,8), COLOUR(1,10)
      REA ,*8 ROCK(02,14)
      REA ,*8 SCON(2,4)
      REA ,*8 SEAM(2,62)
      REA ,*8 VISUAL(1,4)
      REA ,*8 ALOCN(02,62)
      DAT \ ALOCN /'BENBAIN', ' ', 8*' ', 'BLINDWEL', 'LS', 8*' ',
     1     'ACCLINGT', 'ON', 'ST.ANDRE', 'WS', 6*' ', 'IBBETSON', 'S',
     2     ' ', '    ', 'TOW LAW', ' ', 'WEST BRA', 'NDON', 'PIT HOUS',
     3     'E', 'ESH WINN', 'ING', 'TANNERS ', 'HALL', 'COWSLEY', ' ',
     4     12*' ', 'LOW CLOS', 'E', 10*' ', 'ST AIDEN', 'S', 8*' ',
     5     'PARK MEA', 'DOW', 'MORRELS', ' ', 6*' ', 'COALFIEL',
     6     'D FARM', 28*' ', 'MAESGWYN', ' ', 'MAES Y M', 'ARC HOG'/
      DAT \ VISUAL /'EXCELENT', 'GOOD', 'MEDIUM', 'POOR'/
      DAT \ SEAM /'PENEVENE', 'LOW', 8*' ', 'PARROT', ' ', 8*' ',
     1     'UNKNOWN', ' ', 'BROCKWEL', 'L', 6*' ', 'FIVE QUA', 'TER',
     2     'HIGH MAI', 'N', '? BUSTYS', ' ', 'FIVE QUA', 'TER',
     3     'FIVE QUA', 'TER', 'BOTTOM B', 'USTY', 'HUTTON', ' ',
     4     'BUSTY', ' ', 12*' ', 'METAL', 11*' ', 'TOP SOFT', ' ',
     5     8*' ', 'PIPER', ' ', 'SILKSTON', ' MAIN', 6*' ', 'YARD', ' ',
     6     'UPPER LO', 'W MAIN', 26*' ', 'CORNISH', ' ', 'BLUERS', ' '/
      DAT \ SCON /'STRONG C', 'LEAT', 'MODERATE', ' CLEAT', 'SLIGHT C',
     1     'LEAT', 'NO CLEAT', ' '/
      DAT \ ROCK /'CONGLOME', 'RATE', 'SANDSTON', 'E', 'QUARTZ S',
     1     'ANDSTONE', 'ARGILLAC', 'EOUS S.S', 'MUDSTONE', ' ',
     2     'SHALEY ', 'MUDSTONE', 'SHALE', ' ', 'SILTSTON', 'E',
     3     'SILTY MU', 'DSTONE', 'SEAT EAR', 'TH', 'COAL', ' ',
     4     'COAL SHA', 'LE', 'SANDSTON', 'E^SHALE', 'BOULDER ', 'CLAY'/
      DAT \ HUE /'LIGHT', 'DARK'/
      DAT \ SHADE /'PINKISH', 'REDDISH', 'YELOWISH', 'BROWNISH',
     1     'OLIVISH', 'GREENISH', 'BLUISH', 'GREYISH'/
      DAT \ COLOUR /'PINK', 'RED', 'YELLOW', 'BROWN', 'OLIVE', 'GREEN',
     1     'BLUE', 'WHITE', 'GREY', 'BLACK'/
      DAT \ GRAIN /'V COARSE', 'COARSE', 'MEDIUM', 'FINE', 'V.FINE'/
      DAT \ BTHICK /'VERY THI', 'CK', '   >2 M ', 'THICK', ' ',
     1     '60CM-2 M', 'MEDIUM', ' ', '20 -60CM', 'THIN', ' ',
     2     '6 - 20CM', 'VERY THI', 'N', '2 - 6 CM', 'THICKLY',
     3     'LAMINATE', ' 6 -20MM', 'THINLY L', 'AMINATED', ' 2 -6 MM'/
      DAT \ AMIN /'ILLITE', ' ', 'KAOLINIT', 'E', 'QUARTZ', ' ',
     1     'FELDSPAR', ' ', 'CALCITE', ' ', 'DOLOMITE', ' ', 'SIDERITE',
     2     ' ', 'PYRITE', ' ', 'CARBON +', ' OTHERS'/
      DAT \ AMETH /'GUESTIMA', 'TE', 'POINT LO', 'AD', 'CONE IND',
     1     'ENTO R', 'TRIAXIAL', ' U.C.S.', 'VARIOUS', ' ', 'BEAM BEN',
     2     'DING'/
      DAT \ WEATH /'FRESH', ' ', 'SLIGHTLY', ' ', 'MODERATL', 'Y',
     1     'HIGHLY', ' ', 'COMPLETL', 'Y', 'RESIDUAL', 'SOIL'/
      DAT \ AJFREQ /'EX WIDE', 'V. WIDE', 'WIDE', 'MOD WIDE', 'MOD NARO',
     1     'NARROW'/
      DAT \ AJCOND /'V. OPEN', 'OPEN', 'CLOSED', 'V CLOSED'/
      DAT \ BJCOND /'IRON STA', 'INING', 'CLAY INF', 'ILL', 'NO INFIL',
     1     'L', 'WEATHERE', 'D'/
      DAT \ VERTEX /'<2M', '1-2M', '0.5-1M', '0-0.5M'/
      DAT \ ARCHBR /'COMPLETE', 'PARTIAL', 'NONE'/
      DAT \ OWFL /'TOTALLY ', 'STACKED', 'PARTIALY', ' STACKED',
     1     'NO STACK', 'lNG', 'TOT STAK', ' + PROPS', 'PART STA',
     2     'K+ PROPS', 'NO STACK', ' + PROPS', 'FLOOR HE', 'AVE',
```

```
     3     'OCHER', ' '/
      DATA OWFLOD /'TOTAL', 'PARTIAL', 'NONE'/
      DATA COLLAP /'TOTAL', ' ', '90-100%', 'CONSIDER', 'ABLE',
     1     '60-90%', 'PARTIAL', ' ', '30-60%', 'SUPERFIC', 'IAL',
     2     '10-30%', 'NONE', ' ', '0-10%'/
C
C     END OF STATIC DATA
C
C
C     NUMBER OF OLD WORKINGS = NO INPUT HERE
C
      READ (5,10) NO
   10 FORMAT (I3)
      DO 1060 JNO = 1, NO
C
C     VARIABLE DATA READ IN FROM HERE
C
   20   READ (5,M1) J1, J2, J3, R4, J5, J6, R7, J8, R9, J10, J11, J12,
     1       JJ12, JJJ12, J13, JJ13, J14, J, K, L, M, N, R15, J16, R17,
     2       J18, J19, R20, J21, J22, JJ22, J23
        READ (5,M1) J24, J25, JJ25, JJJ25, J26, JJ26, R27, J28, R29,
     1       R30, R31, J32, J33, JJ33, R34, R35, J36, R37, R38, J39,
     2       J40, J41, J42, J43, J44, J45, J46, R47
C
C     END OF VARIABLE DATA
C     PROGRAMME BEGINS HERE
C
        WRITE (6,1080) J1
        WRITE (6,1070) ALOCN(1,J2), ALOCN(2,J2)
        WRITE (6,1090) J3
        WRITE (6,1100) R4
        K5 = J5 / 100
        JJ5 = J5 - (K5*100)
        JAGE = K5 + 1
        IF (K5 .EQ. 00) GO TO 30
        IF (JJ5 .EQ. 00) GO TO 40
        WRITE (6,1120) J5
        GO TO 50
   30   WRITE (6,1110)
        GO TO 50
   40   WRITE (6,1130) JAGE
   50   CONTINUE
        IF (J6 .EQ. 0) GO TO 60
        WRITE (6,1140) VISUAL(1,J6)
        GO TO 70
   60   WRITE (6,1560)
   70   CONTINUE
        IF (R7 .EQ. 000) GO TO 80
        WRITE (6,1150) R7
        GO TO 90
   80   WRITE (6,1570)
   90   CONTINUE
        IF (J8 .EQ. 00) GO TO 100
        WRITE (6,1160) SEAM(1,J8), SEAM(2,J8)
        GO TO 110
  100   WRITE (6,1580)
  110   CONTINUE
        IF (R9 .EQ. 000) GO TO 120
        WRITE (6,1170) R9
        GO TO 130
  120   WRITE (6,1590)
  130   CONTINUE
        IF (J10 .EQ. 0) GO TO 140
        WRITE (6,1180) SCON(1,J10), SCON(2,J10)
        GO TO 150
  140   WRITE (6,1600)
  150   CONTINUE
        IF (J11 .EQ. 0) GO TO 160
        WRITE (6,1190) ROCK(1,J11), ROCK(2,J11)
        GO TO 170
  160   WRITE (6,1610)
  170   CONTINUE
        IF (J12 .EQ. 0) GO TO 180
        IF (JJJ12 .EQ. 0) JJJ12 = 10
        WRITE (6,1200) HUE(1,J12), SHADE(1,JJ12), COLOUR(1,JJJ12)
        GO TO 190
  180   WRITE (6,1620)
  190   CONTINUE
        IF (J13 .EQ. 0) GO TO 200
        WRITE (6,1210) GRAIN(1,J13)
        GO TO 210
  200   WRITE (6,1630)
  210   CONTINUE
        IF (JJ13 .EQ. 0) GO TO 220
        WRITE (6,1220) BTHICK(1,JJ13), BTHICK(2,JJ13), BTHICK(3,JJ13)
        GO TO 230
  220   WRITE (6,1640)
  230   CONTINUE
        IF (J14 + J .EQ. 0 .AND. K + L .EQ. M) GO TO 240
        WRITE (6,1230) AMIN(1,J14), AMIN(2,J14), AMIN(1,J), AMIN(2,J),
     1  AMIN(1,K), AMIN(2,K), AMIN(1,L), AMIN(2,L), AMIN(1,M),
     2  AMIN(2,M), AMIN(1,N), AMIN(2,N)
        GO TO 250
  240   WRITE (6,1650)
  250   CONTINUE
        IF (R15 .EQ. 00) GO TO 260
        WRITE (6,1240) R15
        GO TO 270
  260   WRITE (6,1660)
  270   CONTINUE
        IF (J16 .EQ. 00) GO TO 280
        WRITE (6,1250) J16
        GO TO 290
  280   WRITE (6,1670)
  290   CONTINUE
        IF (R17 .EQ. 000) GO TO 300
        WRITE (6,1260) R17
        GO TO 310
  300   WRITE (6,1680)
  310   CONTINUE
        IF (J18 .EQ. 0) GO TO 320
        WRITE (6,1270) AMETH(1,J18), AMETH(2,J18)
        GO TO 330
  320   WRITE (6,1690)
  330   CONTINUE
        IF (J19 .EQ. 0) GO TO 340
        WRITE (6,1280) WEATH(1,J19), WEATH(2,J19)
        GO TO 350
  340   WRITE (6,1700)
  350   CONTINUE
```

```
      IF (R20 .EQ  000) GO TO 360
      WRITE (6,1290) R20
      GO TO 370
360   WRITE (6,1710)
370   CONTINUE
      IF (J21 .EQ. 0) GO TO 380
      WRITE (6,1300) AJFREQ(1,J21)
      GO TO 390
380   WRITE (6,1860)
390   CONTINUE
      IF (J22 + JJ22 .EQ. 0) GO TO 400
      WRITE (6,1310) AJCOND(1,J22), BJCOND(1,JJ22), BJCOND(2,JJ22)
      GO TO 410
400   WRITE (6,1720)
410   CONTINUE
      IF (J23 .EQ. 0) GO TO 420
      WRITE (6,1320) VERTEX(1,J23)
      GO TO 430
420   WRITE (6,1730)
430   CONTINUE
      IF (J24 .EQ. 0 .OR. J24 .EQ. 9 .AND. J11 .EQ. 0) GO TO 440
      IF (J24 .EQ. 99) GO TO 450
      WRITE (6,1330) ROCK(1,J24), ROCK(2,J24)
      GO TO 460
440   WRITE (6,1610)
      GO TO 460
450   WRITE (6,1740) ROCK(1,J11), ROCK(2,J11)
460   CONTINUE
      IF (JJJ25 .EQ. 0) JJJ25 = 10
      IF (J25 .EQ. 0 .OR. J25 .EQ. 9 .AND. J12 .EQ. 0) GO TO 470
      IF (J25 .EQ. 9) GO TO 480
      WRITE (6,1340) HUE(1,J25), SHADE(1,JJ25), COLOUR(1,JJJ25)
      GO TO 490
470   WRITE (6,1620)
      GO TO 490
480   WRITE (6,1750) HUE(1,J12), SHADE(1,JJ12), COLOUR(1,JJJ12)
490   CONTINUE
      IF (J26 .EQ. 0 .OR. J26 .EQ. 9 .AND. J13 .EQ. 0) GO TO 500
      IF (J26 .EQ. 9) GO TO 510
      WRITE (6,1350) GRAIN(1,J26)
      GO TO 520
500   WRITE (6,1630)
      GO TO 520
510   WRITE (6,1760) GRAIN(1,J13)
520   CONTINUE
      IF (JJ26 .EQ. 0 .OR. JJ26 .EQ. 9 .AND. JJ13 .EQ. 0)
     1    GO TO 540
      IF (JJ26 .EQ. 9) GO TO 530
      WRITE (6,1220) BTHICK(1,JJ26), BTHICK(2,JJ26), BTHICK(3,JJ26)
      GO TO 550
530   WRITE (6,1770) BTHICK(1,JJ13), BTHICK(2,JJ13), BTHICK(3,JJ13)
      GO TO 550
540   WRITE (6,1640)
550   CONTINUE
      IF (R27 .EQ. 0 .OR. R27 .EQ. 999 .AND. R17 .EQ. 0)
     1    GO TO 560
      IF (R27 .EQ. 999) GO TO 570
      WRITE (6,1360) R27
      GO TO 580
560   WRITE (6,1680)
      GO TO 580
570   WRITE (6,1780) R17
580   CONTINUE
      IF (J28 .EQ. 0 .OR. J28 .EQ. 9 .AND. J19 .EQ. 0) GO TO 590
      IF (J28 .EQ. 9) GO TO 600
      WRITE (6,1370) WEATH(1,J28), WEATH(2,J28)
      GO TO 610
590   WRITE (6,1700)
      GO TO 610
600   WRITE (6,1790) WEATH(1,J19), WEATH(2,J19)
610   CONTINUE
      IF (R29 .EQ. 0 .OR. R29 .EQ. 9999 .AND. R20 .EQ. 0)
     1    GO TO 620
      IF (R29 .EQ. 9999) GO TO 630
      WRITE (6,1380) R29
      GO TO 640
620   WRITE (6,1710)
      GO TO 640
630   WRITE (6,1800) R20
640   CONTINUE
      IF (R30 .EQ. 0000) GO TO 650
      WRITE (6,1390) R30
      GO TO 660
650   WRITE (6,1810)
660   CONTINUE
      IF (R31 .EQ. 0000) GO TO 680
      IF (R31 .EQ. 9999) GO TO 670
      WRITE (6,1400) R31
      GO TO 690
670   WRITE (6,1830)
      GO TO 690
680   WRITE (6,1820)
690   CONTINUE
      IF (J32 .EQ. 0 .OR. J32 .EQ. 9 .AND. J21 .EQ. 0) GO TO 700
      IF (J32 .EQ. 9) GO TO 710
      WRITE (6,1300) AJFREQ(1,J32)
      GO TO 720
700   WRITE (6,1840)
      GO TO 720
710   WRITE (6,1850) AJFREQ(1,J21)
720   CONTINUE
      IF (J33 .EQ. 0) GO TO 730
      IF (J33 .EQ. 9 .AND. J22 .EQ. 0) GO TO 730
      IF (J33 .EQ. 9) GO TO 740
      WRITE (6,1310) AJCOND(1,J33), BJCOND(1,JJ33), BJCOND(2,JJ33)
      GO TO 750
730   WRITE (6,1860)
      GO TO 750
740   WRITE (6,1870) AJCOND(1,J22), BJCOND(1,JJ22), BJCOND(2,JJ22)
750   CONTINUE
      IF (R34 .EQ. 0000) GO TO 760
      WRITE (6,1410) R34
      GO TO 770
760   WRITE (6,1880)
770   CONTINUE
      IF (R35 .EQ. 0000) GO TO 780
      WRITE (6,1420) R35
      GO TO 790
780   WRITE (6,1890)
790   CONTINUE
```

```
      IF (J36 .EQ. 00) GO TO 800
      WRITE (6,1430) J36
      GO TO 810
  800 WRITE (6,1900)
  810 CONTINUE
      IF (R37 .EQ. 0000) GO TO 820
      WRITE (6,1440) R37
      GO TO 830
  820 WRITE (6,1910)
  830 CONTINUE
      IF (R38 .EQ. 0000) GO TO 840
      WRITE (6,1450) R38
      GO TO 850
  840 WRITE (6,1920)
  850 CONTINUE
      IF (J39 .EQ. 0) GO TO 860
      WRITE (6,1460) ARCHBR(1,J39)
      GO TO 870
  860 WRITE (6,1930)
  870 CONTINUE
      IF (J40 .EQ. 0) GO TO 880
      WRITE (6,1470) OWFL(1,J40), OWFL(2,J40)
      GO TO 890
  880 WRITE (6,1940)
  890 CONTINUE
      IF (J41 .EQ. 0) GO TO 900
      WRITE (6,1480) OWFLOD(1,J41)
      GO TO 910
  900 WRITE (6,1950)
  910 CONTINUE
      IF (J42 .EQ. 00) GO TO 920
      WRITE (6,1490) COLLAP(1,J42), COLLAP(2,J42), COLLAP(3,J42)
      GO TO 930
  920 WRITE (6,1960)
  930 CONTINUE
      IF (J43 .EQ. 00) GO TO 940
      WRITE (6,1500) J43
      GO TO 950
  940 WRITE (6,1970)
  950 CONTINUE
      WRITE (6,1510) J44
      IF (J45 .EQ. 00) GO TO 960
      WRITE (6,1520) J45
      GO TO 970
  960 WRITE (6,1980)
  970 CONTINUE
      IF (J46 .EQ. 00) GO TO 980
      WRITE (6,1530) J46
      GO TO 990
  980 WRITE (6,1990)
  990 CONTINUE
      IF (R47 .EQ. 0000) GO TO 1000
      WRITE (6,1540) R47
      GO TO 1010
 1000 WRITE (6,2000)
 1010 CONTINUE
C
C     CALCULATED INFORMATION
C
      IF (R20 .EQ. 0 .OR. R37 .EQ. 0) GO TO 1020
      J48 = R37 * 100 / R20
      WRITE (6,2010) J48
      GO TO 1030
 1020 WRITE (6,2020)
      J48 = 0
 1030 CONTINUE
      IF (R29 .EQ. 9999 .AND. J48 .EQ. 0) GO TO 1040
      IF (R29 .EQ. 0 .OR. R37 .EQ. 0) GO TO 1040
      J49 = R37 * 100 / R29
      IF (R29 .EQ. 9999) GO TO 1050
      WRITE (6,2030) J49
      GO TO 1060
 1040 WRITE (6,2020)
      GO TO 1060
 1050 WRITE (6,2030) J48
 1060 CONTINUE
C
C     PROGRAMME ENDS HERE
C
C     FORMAT STATEMENTS BEGIN HERE
C
 1070 FORMAT (' OPENCAST SITE.', 16X, 2A8)
 1080 FORMAT ('1FIELDWORK DATE.', 15X, I6)
 1090 FORMAT (' PHOTO REFERENCE NUMBER.', 7X, I4)
 1100 FORMAT (' STRENGTH REFERENCE NUMBER.', 4X, F5.2)
 1110 FORMAT (1X, 'APPROX. AGE OF WORKING.', 7X, 'UNKNOWN')
 1120 FORMAT (1X, 'APPROX. AGE OF WORKING.', 7X, I4)
 1130 FORMAT (1X, 'APPROX. AGE OF WORKING.', 7X, I2, 'TH.CENTURY.  ')
 1140 FORMAT (' VISUAL CONDITION.', 13X, A8)
 1150 FORMAT (' APPROX. DEPTH  OLD WORKINGS.', 2X, F5.2)
 1160 FORMAT (' SEAM NAME.', 20X, 2A8)
 1170 FORMAT (' SEAM THICKNESS.(M).', 10X, F5.2)
 1180 FORMAT (' SEAM CONDITION.', 15X, 2A8)
 1190 FORMAT (' MAIN ROCK TYPE.', 15X, 2A8)
 1200 FORMAT (' MAIN ROCK COLOUR.', 13X, 2A8, 1X, A8)
 1210 FORMAT (' GRAIN SIZE.', 19X, A8, 1X, 'GRAINED.')
 1220 FORMAT (' BED THICKNESS.', 16X, 3A8)
 1230 FORMAT (' MINERALS IN ORDER OF ABUNDANCE.', /' ', 6(2A8))
 1240 FORMAT (' QUARTZ TO CLAY RATIO.', 9X, F4.2)
 1250 FORMAT (' MOISTURE CONTENT PER CENT.', 4X, I2)
 1260 FORMAT (' ROCK STRENGTH MN/SQ.M.', 7X, F7.2)
 1270 FORMAT (' STRENGTH METHOD OF ASSESMENT. ', 2A8)
 1280 FORMAT (' DEGREE OF WEATHERING.', 9X, 2A8)
 1290 FORMAT (' EFFECTIVE BED THICKNESS.(CM). ', F7.2)
 1300 FORMAT (' JOINT FREQUENCY.', 14X, A8)
 1310 FORMAT (' JOINT CONDITION.', 14X, A8, 2X, 2A8)
 1320 FORMAT (' JOINT VERTICAL EXTENT.', 8X, A8)
 1330 FORMAT (' BRIDGE ROCK TYPE.', 13X, 2A8)
 1340 FORMAT (' BRIDGE ROCK COLOUR.', 11X, 2A8, 1X, A8)
 1350 FORMAT (' GRAIN SIZE.', 19X, A8, 1X, 'GRAINED.')
 1360 FORMAT (' BRIDGE ROCK STRENGTH MN/SQ.M. ', F7.2)
 1370 FORMAT (' DEGREE OF WEATHERING.', 9X, 2A8)
 1380 FORMAT (' EFFECTIVE BED THICKNESS.(CM).', F7.2)
 1390 FORMAT (' WIDTH OF BRIDGED SPAN.(M).', 2X, F7.2)
 1400 FORMAT (' THICKNESS OF BRIDGE.(CM).', 3X, F7.2)
 1410 FORMAT (' ARCH HEIGHT. (M) (MIGRATED).', F7.2)
 1420 FORMAT (' THEORETICAL ARCH HEIGHT.(M).', F7.2)
 1430 FORMAT (' ANGLE,DEGREES FROM HORIZONTAL', 2X, I2)
 1440 FORMAT (' WIDTH OF OLD WORKING.(M).', 3X, F7.2)
 1450 FORMAT (' HEIGHT   WIDTH RATIO ', 7X, F7.2)
```

```
1460 FORMAT (' DEGREE OF BRIDGING OF ARCH.', 3X, A8)
1470 FORMAT (' TYPE OF O.W. INFILL.', 10X, 2A8)
1480 FORMAT (' FLOODING IN OLD WORKINGS.', 5X, A8)
1490 FORMAT (' DEGREE OF COLLAPSE.', 11X, 3A8)
1500 FORMAT (' PERCENTAGE COLLAPSE.', 10X, I2)
1510 FORMAT (' ADDITIONAL COMMENTS CARD.', 4X, I3)
1520 FORMAT (' THICKNESS OF PILLAR (METERS). ', I2)
1530 FORMAT (' PERCENTAGE EXTRACTION.', 9X, I2)
1540 FORMAT (' SPAN WIDTH : SEAM THICKNESS.', F7.2)
1550 FORMAT ('+', 29X, ' UNKNOWN')
1560 FORMAT (' VISUAL CONDITION.', 12X, ' UNKNOWN')
1570 FORMAT (' APPROX. DEPTH OF OLD WORKINGS.UNKNOWN.')
1580 FORMAT (' SEAM NAME.', 19X, ' UNKNOWN')
1590 FORMAT (' SEAM THICKNESS.', 14X, ' UNKNOWN')
1600 FORMAT (' SEAM CONDITION.', 14X, ' UNKNOWN')
1610 FORMAT (' BRIDGE ROCK TYPE.', 13X, 'UNKNOWN')
1620 FORMAT (' BRIDGE ROCK COLOUR.', 11X, 'UNKNOWN')
1630 FORMAT (' GRAIN SIZE.', 18X, ' UNKNOWN')
1640 FORMAT (' BED THICKNESS.', 15X, ' UNKNOWN')
1650 FORMAT (' MINERALS IN ORDER OF ABUNDANCE.', /30X,
    1       ' INFORMATION UNAVAILABLE.')
1660 FORMAT (' QUARTZ TO CLAY RATIO.', 8X, ' UNKNOWN')
1670 FORMAT (' MOISTURE CONTENT PER CENT.', 3X, ' UNKNOWN')
1680 FORMAT (' ROCK STRENGTH MN/SQ.M.', 7X, ' UNKNOWN')
1690 FORMAT (' STRENGTH METHOD OF ASSESMENT. UNKNOWN')
1700 FORMAT (' DEGREE OF WEATHERING.', 8X, ' UNKNOWN')
1710 FORMAT (' EFFECTIVE BED THICKNESS.', 5X, ' UNKNOWN')
1720 FORMAT (' JOINT CONDITION.', 13X, ' UNKNOWN')
1730 FORMAT (' JOINT. VERTICAL EXTENT.', 6X, ' UNKNOWN')
1740 FORMAT (' BRIDGE ROCK TYPE.', 12X, ' AS ABOVE', 2X, 2A8)
1750 FORMAT (' BRIDGE ROCK COLOUR.', 10X, ' AS ABOVE', 2X, 3A8)
1760 FORMAT (' GRAIN SIZE.', 18X, ' AS ABOVE', 2X, A8)
1770 FORMAT (' BED THICKNESS.', 16X, 'AS ABOVE', 2X, 3A8)
1780 FORMAT (' BRIDGE ROCK STRENGTH MN/SQ.M. AS ABOVE', 2X, F7.2)
1790 FORMAT (' DEGREE OF WEATHERING.', 8X, ' AS ABOVE', 2X, 2A8)
1800 FORMAT (' EFFECTIVE BED THICKNESS.', 5X, ' AS ABOVE', 2X, F7.2)
1810 FORMAT (' WIDTH OF BRIDGED SPAN.', 7X, ' UNKNOWN')
1820 FORMAT (' THICKNESS OF BRIDGE.', 9X, ' UNKNOWN ASSUME E.B.T')
1830 FORMAT (' THICKNESS OF BRIDGE.', 9X, ' AS E.B.T. ABOVE.')
1840 FORMAT (' JOINT FREQUENCY.', 13X, ' UNKNOWN')
1850 FORMAT (' JOINT FREQUENCY.', 13X, ' AS ABOVE', 2X, A8)
1860 FORMAT (' JOINT CONDITION.', 13X, ' UNKNOWN')
1870 FORMAT (' JOINT CONDITION.', 13X, ' AS ABOVE', 2X, A8, 2X, 2A8)
1880 FORMAT (' ARCH HEIGHT (MIGRATED).', 6X, ' UNKNOWN')
1890 FORMAT (' THEORETICAL ARCH HEIGHT.', 5X, ' UNKNOWN')
1900 FORMAT (' ANGLE,DEGREES FROM HORIZONTAL', ' UNKNOWN')
1910 FORMAT (' WIDTH OF OLD WORKING.', 8X, ' UNKNOWN')
1920 FORMAT (' HEIGHT : WIDTH RATIO.          UNKNOWN')
1930 FORMAT (' DEGREE OF BRIDGING OF ARCH.  UNKNOWN')
1940 FORMAT (' TYPE OF O.W. INFILL.           UNKNOWN')
1950 FORMAT (' FLOODING IN OLD WORKINGS.     UNKNOWN')
1960 FORMAT (' DEGREE OF COLLAPSE.', 10X, ' UNKNOWN')
1970 FORMAT (' PERCENTAGE COLLAPSE.', 9X, ' UNKNOWN')
1980 FORMAT (' THICKNESS OF PILLAR (METERS)  UNKNOWN.')
1990 FORMAT (' PERCENTAGE EXTRACTION.         UNKNOWN')
2000 FORMAT (' SPAN WIDTH : SEAM THICKNESS. UNKNOWN')
2010 FORMAT (' RATIO OF E.B.T. TO O.W. WIDTH', I4, '( MAIN ROCK)')
2020 FORMAT (' RATIO OF E.B.T. TO O.W. WIDTH', ' UNKNOWN')
2030 FORMAT (' RATIO OF E.B.T. TO O.W. WIDTH', I4, '( BRIDGE ROCK)')
C
```

```
C
C     ****************************************************************
C
C                        DATA VARIABLES USED IN PROGRAM
C
C
C                      FIRST READ (CARD 1)
C          PARAMETER              VARIABLE NAME UNITS DATA NO. CODES
C                                                    TYPE COL UN  R
C FIELDWORK DATE                  J1            YRS   I    5
C LOCATION (OPENCAST SITE)        J2                       6
C PHOTO REFERENCE NUMBER          J3                       2
C STRENGTH REFERENCE NUMBER       R4
C APPROX. AGE OF WORKING          J5            YRS   I    4   Y
C VISUAL CONDITION                J6                  O    1   Y
C DEPTH BENEATH THE SURFACE       R7             M    R    3   Y
C SEAM NAME                       J8                       2   Y
C SEAM THICKNESS                  R9             M    R    3   Y
C SEAM CONDITION                  J10                 O    1   Y
C MAIN ROCK TYPE                  J11                      2   Y
C COLOUR (HUE,SHADE,COLOUR)       J12,JJ12,JJJ12           3*1 Y
C GRAIN SIZE                      J13                 I    1   Y
C BED THICKNESS                   JJ13                I    1   Y
C MINERALOGY                      J14,K,L,M,N,O            6*1 Y
C QUARTZ TO CLAY RATIO            R15                 I    2   Y
C MOISTURE CONTENT %              J16            %    R    2   Y
C ROCK STRENGTH (UCS)             R17          MN/M2  R    3   Y
C STRENGTH METHOD OF ASSESMENT    J18                      1   Y
C DEGREE OF WEATHERING            J19                 O    1   Y
C EFFECTIVE BED THICKNESS         R20          CM     R    3   Y
C JOINT FREQUENCY                 J21                 I    1   Y
C J.CONDITION (OPEN,INFILL)       J22,JJ22            O    1+1 Y
C VERTICAL EXTENT     J23                           I    1   Y
C
C                      SECOND READ (CARD 2)
C          PARAMETER              VARIABLE NAME UNITS DATA NO. CODES
C                                                    TYPE COL UN  R
C
C BRIDGE ROCK TYPE                J24                      2   Y  Y
C BRIDGE ROCK COLOUR              J25,JJ25,JJJ25           3*1 Y  Y
C GRAIN SIZE                      J26                 I    1   Y  Y
C BED THICKNESS                   JJ26                I    1   Y  Y
C BRIDGE ROCK STRENGTH            R27          MN/M2  R    3   Y  Y
C DEGREE OF WEATHERING            J28                 O    1   Y  Y
C EFFECTIVE BED THICKNESS         R29          CM     R    4   Y  Y
C BRIDGE WIDTH                    R30            M    R    4   Y
C BRIDGE THICKNESS                R31          CM     R    4   Y  Y=R29
C JOINT FREQUENCY                 J32                 I    1   Y  Y
C J.CONDITION (OPEN,INFILL)       J33,JJ33            O    1+1 Y  Y
C ARCH HEIGHT (MIGRATED)          R34            M    R    4   Y
C THEORETICAL ARCH HEIGHT         R35            M    R    4   Y
C ANGLE DEGREES FROM HORIZ.       J36          DEGR.  R    2   Y
C WIDTH OF OLD WORKING            R37            M    R    4   Y
C HEIGHT(COLLAP):WIDTH RATIO      R38            M    R    4   Y
C DEGREE OF BRIDGING OF ARCH      J39                 O    1   Y
C TYPE OF O.W. INFILL             J40                 O    1   Y
C FLOODING IN OLD WORKINGS        J41                 O    1   Y
C DEGREE OF COLLAPSE              J42                 I    1   Y
C PERCENTAGE COLLAPSE             J43            %    R    2   Y
C ADDITIONAL COMMENTS CARD        J44                      3
```

```
C THICKNESS OF PILLAR          J45              M     R     2    Y
C PERCENTAGE EXTRACTION        J46              %     R     2    Y
C SPAN WIDTH : SEAM THICKNESS  R47              M     M     4    Y
C
C
C
C     ************************************************************
C               *****************************************
C                         ***************************
C                                   ******
      STOP
      END
```

```
C ********************************************************************
C ********************************************************************
C
C                      PROGRAM  DATAMEDDLER
C
C     This program is designed to work on the raw data collected from
C     collapsed old workings.  The program substitutes the bridge
C     variables repeat codes (9,99,999,or 9999), for the correct
C     values, as listed in the master printout.
C
C ********************************************************************
C ********************************************************************
C
C
      READ (5,*) NO
      DO 80 JNO = 1, NO
   10   READ (5,*) J1, J2, J3, R4, J5, J6, R7, J8, R9, J10, J11, J12,
     1       JJ12, JJJ12, J13, JJ13, J14, J, K, L, M, N, R15, J16, R17,
     2       J18, J19, R20, J21, J22, JJ22, J23
        READ (5,*) J24, J25, JJ25, JJJ25, J26, JJ26, R27, J28, R29, R30,
     1       R31, J32, J33, JJ33, R34, R35, J36, R37, R38, J39, J40,
     2       J41, J42, J43, J44, J45, J46, R47
        IF (J24 .EQ. 99) J24 = J11
        IF (J25 .EQ. 9) GO TO 40
   20   IF (J26 .EQ. 9) J26 = J13
        IF (JJ26 .EQ. 9) JJ26 = JJ13
        IF (R27 .EQ. 999) R27 = R17
        IF (J28 .EQ. 9) J28 = J19
        IF (R29 .EQ. 9999) R29 = R20
        IF (R31 .EQ. 9999) R31 = R29
        IF (J32 .EQ. 9) J32 = J21
        IF (J33 .EQ. 9) GO TO 50
   30   WRITE (6,60) J1, J2, J3, R4, J5, J6, R7, J8, R9, J10, J11, J12,
     1  JJ12, JJJ12, J13, JJ13, J14, J, K, L, M, N, R15, J16, R17, J18,
     2  J19, R20, J21, J22, JJ22, J23
        WRITE (6,70) J24, J25, JJ25, JJJ25, J26, JJ26, R27, J28, R29,
     1  R30, R31, J32, J33, JJ33, R34, R35, J36, R37, R38, J39, J40,
     2  J41, J42, J43, J44, J45, J46, R47
        GO TO 80
   40   J25 = J12
        JJ25 = JJ12
        JJJ25 = JJJ12
        GO TO 20
   50   J33 = J22
        JJ33 = JJ22
        GO TO 30
   60   FORMAT (' ', I6, 1X, I2, 1X, I4, 1X, F5.2, 1X, I4, 1X, I1, 1X,
     1         F5.2, 1X, I2, 1X, F5.2, 1X, I1, 1X, I2, 1X, 3(I1,1X),
     2         2(I1,1X), 6(I1,1X), F4.2, 1X, I2, 1X, F6.2, 1X, I1, 1X,
     3         I1, 1X, F5.2, 1X, I1, 1X, 2(I1,1X), I1)
   70   FORMAT (' ', I2, 1X, 3(I1,1X), 2(I1,1X), F6.2, 1X, I1, 1X, F6.2,
     1         1X, F6.2, 1X, F6.2, 1X, I1, 1X, I1, 1X, I1, 1X, F6.2, 1X,
     2         F6.2, 1X, I2, 1X, F6.2, 1X, F6.2, 1X, I1, 1X, I1, 1X, I1,
     3         1X, I1, 1X, I2, 1X, I3, 1X, I2, 1X, I2, 1X, F6.2)
   80 CONTINUE
      STOP
      END
```

```
 21177 19  142  1.05 1956 1  8.00 19  1.30 1 12 2 8 0 5 4
    3 1 7 2 9 4 3.60  0 15.00 1 1  2.50 4 4 3 4
99 9 9 9 9 9 999.00 9 9999.00    0.0  9999.00 9 9 9    0.55
   0.0  65   2.1800    0 0  2 6 3 4  0   1 25  0   1.6800
 21177 19  100  1.05 1956 1  8.00 19  1.30 1 12 2 8 0 5 4
    3 1 7 2 9 4 3.60  0 15.00 1 1  2.50 4 4 3 4
 2 1 6 9 3 3  29.00 1    2.50    0.74   10.00 2 2 1    0.95
   1.55 56   2.1000    0.74 1 6 3 2 61   1 25  0   1.6200
 81177 36  202  7.00 1800 4 75.00 36  1.20 1  5 1 8 9 5 4
    0 0 0 0 0 0 0.0   3  6.00 2 1  0.0  2 0 0 4
99 9 9 9 9 9 999.00 9 9999.00    0.01 9999.00 9 9 9    0.10
   0.10  1   1.1800    0.0  1 7 3 5 99   2  0  0   1.0300
 91177 42  207  0.0     0 2  0.0  42  0.80 2 11 2 8 0 0 0
    0 0 0 0 0 0 0.0   0  0.0  0 2 15.00 0 0 0 0
99 9 9 9 9 9 999.00 9 9999.00    0.01 9999.00 9 9 9    0.10
   0.01  1   1.1600    0.0  1 8 1 5 99   3  0  0   1.4500
101177 46  208  8.10 1890 2  0.0  47  1.20 1  9 1 8 9 5 7
    3 1 2 7 9 4 1.01  5 10.00 2 1 11.00 3 3 3 4
99 9 9 9 9 9 999.00 9 9999.00    0.01 9999.00 9 9 9    1.79
   1.79 74   1.4000    1.79 3 2 2 2 99   4  9  0   1.1700
101177 46  211  8.10 1890 3  0.0  47  1.20 1  9 1 8 9 5 7
    3 1 2 7 9 4 1.01  5 10.00 2 1  9.00 3 3 3 4
99 9 9 9 9 9 999.00 9 9999.00    0.60    9.00 9 9 9    1.08
   2.06 72   1.3400    1.54 2 2 2 3 52   4  9  0   1.1200
251177 30  407 11.00 1880 4 10.00 30  1.20 2  5 1 8 9 5 6
    1 2 3 7 9 4 0.18  0 18.00 2 1  3.00 0 2 1 3
99 9 9 9 9 9 999.00 9 9999.00    0.0  9999.00 9 9 9    0.01
   0.0   0   0.8000    0.0  2 3 1 5  0   5  6  0   0.6700
251177 30  407 11.00 1880 0 10.00 30  1.10 2  5 1 8 9 5 6
    1 2 3 7 9 4 0.18  0 18.00 2 1  3.00 3 2 1 3
99 9 9 9 9 9 999.00 9 9999.00    0.0  9999.00 9 9 9    0.0
   0.0   0   1.7000    0.0  2 3 1 5  0   5  6  0   1.5500
251177 30  411 15.16 1880 1  6.00 30  1.20 2  5 2 8 9 5 5
    1 2 3 7 9 4 0.18  0 17.00 2 3  2.00 0 0 0 0
99 9 9 9 9 9 999.00 9 9999.00    0.75    2.00 9 9 9    1.49
   2.10 59   2.5700    0.82 2 3 1 2 71   5  0  0   2.1400
 51277 11  414 12.14 1800 1 10.00 11  0.90 3 13 0 0 0 0 0
    3 1 7 2 9 4 1.06  4 30.00 2 1 13.00 4 2 3 4
 2 9 9 9 9 9  21.00 1   50.00    1.09   13.00 2 2 3    5.64
   7.07 69   5.3800    1.31 1 3 3 2 80   6  6  0   4.8900
 51277 11  416 12.14 1800 1 11.00 11  0.90 3 13 0 0 0 0 0
    3 1 7 2 9 4 1.06  4 30.00 2 1  6.00 4 2 3 4
 2 9 9 9 9 9  21.00 1   50.00    1.75   50.00 2 2 3    2.98
   5.49 71   3.7800    1.45 1 1 3 3 52   6  6  0   3.4400
 51277 11  418 12.14 1800 1 12.00 11  0.90 3 13 0 0 0 0 0
    3 1 7 2 9 4 1.06  4 30.00 2 1  4.00 4 2 3 4
 2 9 9 9 9 9  21.00 1   50.00    2.09  100.00 2 2 3    2.21
   4.90 68   3.8400    1.26 1 3 3 3 55   6  6  0   3.2000
 51277 11  420 12.14 1800 2 12.00 11  1.00 3 13 0 0 0 0 0
    3 1 7 2 9 4 1.06  4 30.00 2 1  4.00 1 2 3 1
 2 9 9 9 9 9  21.00 1  100.00    1.43  100.00 2 2 3    2.21
   5.22 77   2.4800    2.10 1 3 3 3 42   6  6  0   2.4800
 51277 11  422 12.14 1800 1 12.00 11  0.90 3 13 0 0 0 0 0
    3 1 7 2 9 4 1.06  4 30.00 2 1  6.80 1 2 3 1
 2 9 9 9 9 9  21.00 1   90.00    1.84  100.00 2 2 3    2.20
   4.33 67   3.7300    1 16 1 3 3 3 51   6  6  0   4.1400
 51277 11  425 12.14 1800 2 12.00 11  0.90 3 13 0 0 0 0 0
    3 1 7 2 9 4 1.06  4 30.00 2 1  6.80 1 2 3 1
 2 9 9 9 9 9  21.00 1   90.00    1.09   90.00 9 9 9    2.09
   3.80 72   2 4200    1.57 1 3 3 3 55   6  2  0   2.6900

 51277 11  425 12.14 1800 1 12.00 11  0.90 3 13 0 0 0 0 0
    3 1 7 2 9 4 1.06  4 30.00 2 1  6.80 1 2 3 1
 2 9 9 9 9 9  21.00 1   90.00    1.70   90 00 9 9 9    2.42
   3.90 65   3.7000    1.06 1 3 3 2 62   6  2  0   4.1100
160378 41  539  0.0  1800 4  0.0  41  1.20 3  5 2 8 9 5 7
    0 0 0 0 0 0 0.0   0  0.0  0 0 10.00 2 3 3 4
99 9 9 9 9 9 999.00 9 9999.00    0.54   10.00 0 0 0    0.30
   0.47 32   1.5000    0.31 2 2 3 3 64   7  0  0   1.2500
160378 46  521  8.10 1890 2  0.0  47  1.20 1  9 1 8 9 5 7
    3 1 2 7 9 4 1.01  5 10.00 2 1 10.00 3 2 3 4
99 9 9 9 9 9 999.00 9 9999.00    0.01 9999.00 9 9 9    3.83
   3.83 72   2.5000    1.53 3 0 1 1 99   8 30  0   2.0800
160378 46  505  0.0  1701 1  0.0  46  1.30 2 11 2 8 0 5 2
    0 0 0 0 0 0 0.0   0  0.0  0 1  0.0  4 4 3 4
 6 2 8 9 5 6 999.00 1   30.00    0.0  9999.00 3 3 3    0.0
   0.0  72   0.0       0.0  0 4 1 1  0   9  3  0   0.0
160378 46  502  0.0  1701 1  0.0  46  1.30 2 11 2 8 0 5 2
    0 0 0 0 0 0 0.0   0  0.0  0 1  0.0  4 4 3 4
 6 2 8 9 5 6 999.00 1   30.00    0.0  9999.00 3 3 3    0.61
   0.0  67   1.2200    0.0  2 6 1 3  0   9  3  0   0.9400
140478 16  613 17.19 1800 1  0.0  16  1.40 3 13 2 8 9 4 7
    0 0 0 0 0 0 0.0   3 26.00 2 1 10.00 3 2 1 1
99 9 9 9 9 9 999.00 9 9999.00    0.01 9999.00 9 9 9    4.55
   4.55 69   3.4500    1.32 3 3 3 1 99  10  5  0   2.4600
140478 16  612 17.19 1800 1  0.0  16  1.40 3 13 2 8 9 4 7
    0 0 0 0 0 0 0.0   3 26.00 2 1 10.00 3 2 1 1
99 9 9 9 9 9 999.00 9 9999.00    0.98   10.00 0 0 0    1.74
   4.84 81   1.5300    3.16 2 2 3 3 36  10  5  0   1.0900
140478 16  607 17.19 1800 1  0.0  16  1.70 3 13 2 8 9 4 7
    0 0 0 0 0 0 0.0   3 26.00 2 1 10.00 3 2 1 1
99 9 9 9 9 9 999.00 9 9999.00    0.01 9999.00 9 9 9    4.53
   4.53 66   4.0800    1.12 3 3 3 1 99  10  5  0   2.4000
140478 16  606 17.19 1800 1  0.0  16  1.10 3 13 2 8 9 4 7
    0 0 0 0 0 0 0.0   3 26.00 2 1 10.00 3 2 1 1
99 9 9 9 9 9 999.00 9 9999.00    0.01 9999.00 9 9 9    5.33
   5.33 71   3.7200    1.43 3 3 3 1 99  10  5  0   3.3800
140478 16  604 17.19 1800 3  0.0  16  1.10 3 13 2 8 9 4 7
    0 0 0 0 0 0 0.0   3 26.00 2 1 10.00 2 2 1 1
99 9 9 9 9 9 999.00 9 9999.00    0.58 9999.00 9 9 9    4.39
   5.07 67   4.3000    1.12 3 3 3 2 87  10  5  0   3.9100
140478 16  602 17.19 1800 1  0.0  16  1.40 1  5 2 8 9 4 7
    0 0 0 0 0 0 0.0   3 26.00 2 1 17.00 2 2 3 2
99 9 9 9 9 9 999.00 9 9999.00    0.63 9999.00 9 9 9    0.83
   1.42 62   1.5200    0.93 2 3 3 3 58  10  5  0   1.0900
190578 16  805 17.19 1800 1  0.0  16  1.40 3  9 2 8 9 4 7
    0 0 0 0 0 0 0.0   2 46.00 2 1 10.00 2 2 3 2
99 9 9 9 9 9 999.00 9 9999.00    1.4  9999.00 9 9 9    0.38
   1.49 58   1.8800    0.79 2 6 3 4 26  11  5  0   1.3400
190578 16  807 17.19 1800 2  0.0  16  1.40 2  9 2 8 9 4 7
    0 0 0 0 0 0 0.0   2 46.00 2 1  9.00 2 2 3 2
 2 1 3 9 3 3 117.00 1   60.00    1.32   60.00 2 2 3    1.55
   3.36 70   2.4500    0.63 2 3 3 3 46  11  5  0   1.7500
190578 16  808 17.19 1800 2  0.0  16  1.40 2 13 2 8 9 5 7
    0 0 0 0 0 0 0.0   3 26.00 2 1  9.00 2 2 3 2
99 9 9 9 9 9 999.00 9   35.00    0.01 9999.00 9 9 9    4.68
   4.68 68   3.7000    1.26 3 3 3 1 99  11 10  0   2.6400
190578 16  808 17.19 1800 2  0.0  16  1.40 2 13 2 8 9 5 7
    0 0 0 0 0 0 0.0   3 26.00 2 1  9.00 2 2 3 2
99 9 9 9 9 9 999.00 9   35.00   10.56 9999.00 9 9 9    5 28
  20.60 71  14.2000    1.45 1 3 3 1 26  12 10  0  10.1000
```

```
190578 16  811 17.19 1800 1  0.0  16  1.40 2 13 2 8 7 5 7
    0 0 0 0 0 0 0.0   3 26.00 2 1 10.00 2 2 3 2
99 9 9 9 9 9 999.00 9 9999.00    0.8  9999.00 9 9 9    5.42
   6.97 76   3.5900    1.94 3 3 3 2 78  13 10  0   2.5500
190578 16  812 17.19 1800 2  0.0  16  1.40 2 13 2 8 9 5 7
    0 0 0 0 0 0 0.0   3 26.00 2 1 10.00 2 2 3 2
99 9 9 9 9 9 999.00 9 9999.00    0.01 9999.00 9 9 9    7.70
   7 70 68   6.1000    1.26 3 3 3 1 99  13  5  0   4.3600
190578 16  814 17.19 1800 2  0.0  16  1.40 2 13 2 8 9 5 7
    0 0 0 0 0 0 0.0   3 26.00 2 1 10.00 2 2 3 2
99 9 9 9 9 9 999.00 9 9999.00    0.01 9999.00 9 9 9    6.20
   6.20 73   3.8900    1.59 3 3 3 1 99  13 10  0   2.7800
190578 16  814 17.19 1800 2  0.0  16  1.40 2 13 2 8 9 5 7
    0 0 0 0 0 0 0.0   3 26.00 2 1 10.00 2 2 3 2
99 9 9 9 9 9 999.00 9 9999.00    0.01 9999.00 9 9 9    6.38
   6.38 71   4.5000    1.42 3 3 3 1 99  13 10  0   3.2100
190578 16  816 17.19 1800 2  0.0  16  1.90 2  9 2 8 9 5 7
    0 0 0 0 0 0 0.0   3 26.00 2 1 10.00 2 2 3 2
99 9 9 9 9 9 999.00 9 9999.00    0.01 9999.00 9 9 9    7.67
   7.67 73   4.8000    1.60 3 3 3 1 99  13 10  0   2.5300
190578 16  819 17.19 1800 3  0.0  16  1.40 2  9 2 8 9 5 7
    0 0 0 0 0 0 0.0   3 26.00 2 1  9.00 2 2 3 2
99 9 9 9 9 9 999.00 9 9999.00    1.38   10.00 9 9 9    5.13
   7.12 71   4.9300    1.45 2 3 3 2 72  13 10  0   3.5000
190578 16  821 17.19 1800 3  0.0  16  1.40 2  9 2 8 9 5 7
    0 0 0 0 0 0 0.0   3 26.00 2 1 12.00 2 2 3 2
99 9 9 9 9 9 999.00 9 9999.00    0.01 9999.00 9 9 9    5 54
   5.54 66   4.9400    1.12 3 3 3 1 99  13 10  0   3.5300
210478 30  920  0.0  1880 3  6.50 30  1.00 0  5 2 8 0 5 7
    0 0 0 0 0 0 0.0   0 15.00 1 4 10.00 0 0 0 0
14 2 4 4 4 1  60.00 3    1.00    3.33    1.00 9 9 9    2.24
   2.24 42   4.9700    0.45 1 3 8 2 99  14  7  0   4.9700
190578 30  929 20.00 1880 2  8.00 30  1.00 2  5 2 8 0 5 7
    0 0 0 0 0 0 0.0   0 31.00 2 3  4.00 3 2 1 3
99 9 9 9 9 9 999.00 9 9999.00    0.01 9999.00 9 9 9    0.23
   0.23 25   1.0000    0.23 2 2 1 4 99  14  0  0   1.0000
190578 16  932 17.19 1800 3  0.0  16  1.40 2  9 2 8 9 5 7
    0 0 0 0 0 0 0.0   0 26.00 2 1  3.00 3 3 3 3
99 9 9 9 9 9 999.00 9 9999.00    0.87    0.30 9 9 9    0.87
   1.66 61   1.8300    0.90 2 3 3 3 52  15  0  0   1.3100
190578 16  933 17.19 1800 3  0.0  16  1.40 2  9 2 8 0 5 7
    0 0 0 0 0 0 0.0   0 47.00 2 1  7.00 3 3 3 3
99 9 9 9 9 9 999.00 9 9999.00    2.19   10.00 9 9 9    0.13
   0.13  7   2.1900    0.06 2 3 3 4  1  15  0  0   1.5600
190578 16  935 17.19 1800 1  0.0   1  1.30 3  9 2 8 0 5 7
    0 0 0 0 0 0 0.0   2 47.00 2 1  3.40 2 2 3 2
99 9 9 9 9 9 999.00 9 9999.00    1.84 9999.00 9 9 9    0.28
   1.25 46   2.3800    0.53 1 3 3 4 22  15  2  0   1.8000
 90578 16 1017 17.19 1800 1  0.0  16  1.50 3 13 2 8 9 5 7
    0 0 0 0 0 0 0.0   3 26.00 2 1 10.00 2 2 3 2
99 9 9 9 9 9 999.00 9 9999.00    0.01 9999.00 9 9 9    4.88
   4.88 71   3.4200    1.43 2 3 3 2 99  16  2  0   2.2800
300578 30 1020 20.00 1880 1  7.00 30  1.90 2  5 2 8 0 5 5
    0 0 0 0 0 0 0.0   0 31.00 2 1  5.00 2 3 3 3
99 9 9 9 9 9 999.00 9 9999.00    0.01 9999.00 9 9 9    0.34
   0.34 25   1.4400    0.24 2 3 2 4 99  16  2 75   0.7600
300578 30 1022 20.00 1880 1  7.00 30  1 00 2  5 2 8 0 5 5
    0 0 0 0 0 0 0.0   0 31.00 2 1  5.00 3 2 3 3
99 9 9 9 9 9 999.00 9 9999.00    0.85 9999.00 9 9 9    0.94
   2.07 69   1.5600    1.32 2 3 2 3 47  16  2 75   1.5900
300578 30 1024 20.00 1880 2  7.00 30  1.00 2  5 2 8 0 5 5
    0 0 0 0 0 0 0.0   0 31.00 2 1  5.00 2 2 3 3
99 9 9 9 9 9 999.00 9 9999.00    0.69 9999.00 9 9 9    0.59
   1.16 59   1.4100    0.82 2 3 2 3 51  16  2 75   1.4100
300578 30 1025 20.00 1880 3  7.00 30  0.90 2  5 2 8 0 5 5
    0 0 0 0 0 0 0.0   0 31.00 2 1  4.60 2 2 3 3
99 9 9 9 9 9 999.00 9 9999.00    0.34 9999.00 9 9 9    0.92
   1.37 69   1.0400    1.31 2 3 2 2 67  16  2 75   1.0600
300578 30 1028 20.00 1880 2  7.00 30  0.90 2  5 2 8 0 5 5
    0 0 0 0 0 0 0.0   0 31.00 2 1  4.50 3 2 3 3
99 9 9 9 9 9 999.00 9 9999.00    1.18 9999.00 9 9 9    0.86
   2.10 65   1.9900    1.06 2 3 2 3 41  16  2 75   2.2000
300578 30 1029 20.00 1880 2  7.00 30  0.90 2  5 2 8 0 5 5
    0 0 0 0 0 0 0.0   0 31.00 2 1  5.80 3 2 3 3
11 2 8 0 5 3 999.00 1   15.00    0.73 9999.00 5 4 3    1.02
   2.45 76   1.2500    1.96 1 3 2 3 42  16  2 75   1.3900
300578 30 1031 20.00 1880 2  7.00 30  0.60 2  5 2 8 0 5 5
    0 0 0 0 0 0 0.0   0 31.00 2 1  5.00 3 3 3 3
99 9 9 9 9 9 999.00 9 9999.00    0.78 9999.00 9 9 9    0.67
   2.30 77   1.1000    2.10 2 3 2 3 29  16  2 75   1.8000
310578  1 1034 24.25 1945 2  8.00  1  1.70 3  5 2 8 0 5 4
    2 3 1 7 9 4 0.37  0 17.00 2 1  2.00 4 3 3 4
 2 1 3 8 3 3  47.00 1   15.00    1.15   40.00 2 3 3    0.30
   0.89 46   1.7300    0.52 2 2 2 4 34  17  0  0   1.0200
 70678 16 1125 17.19    0 3  0.0  16  0.80 3  5 2 8 0 5 5
    0 0 0 0 0 0 0.0   0 25.00 1 1  6.00 3 2 3 3
99 9 9 9 9 9 999.00 9 9999.00    1.04   15.00 9 9 9    0.05
   0.40 37   1.2000    0.33 2 3 3 4 12  18  0  0   1.5000
 70678 16 1126 17.19    0 3  0.0  16  1.70 2  9 2 8 0 5 5
    0 0 0 0 0 0 0.0   0 25.00 1 1 10.00 3 2 3 3
 2 1 3 8 0 3  47.00 1   35.00    1.60   60.00 2 2 3    1.98
   6.38 80   2.3200    2.75 3 3 3 3 31  18  0  0   1.3600
 70678 16 1129 17.19    0 3  0.0  16  0.80 3  5 2 8 0 5 5
    0 0 0 0 0 0 0.0   0 25.00 1 1  8.00 3 2 3 3
99 9 9 9 9 9 999.00 9   18.00    1.09 9999.00 9 9 9    1.53
   2.64 64   2.5900    1.02 2 3 3 2 58  18  0  0   3.2400
 70678 16 1131 17.19    0 4  0.0  16  0.80 3  5 2 8 0 5 5
    0 0 0 0 0 0 0.0   0 25.00 1 1  8.00 3 2 3 8
99 9 9 9 9 9 999.00 9   50.00    0.0    50.00 9 9 9    0.0
   0.0  64   2.5800    0.0  2 3 3 2  0  18  0  0   3.2300
270678 16 1135  0.0  1946 2 17.00 17  1.10 2  8 1 8 9 5 5
    0 0 0 0 0 0 0.0   0 30.00 1 1  8.00 4 2 3 4
99 9 9 9 9 9 999.00 9 9999.00    0.01 9999.00 9 9 9    1.84
   1.84 61   2.0500    0.90 0 6 3 1 99  19 20  0   1.8600
270678 16 1136  0.0  1946 1 15.00 17  1.10 1  8 1 8 9 5 5
    0 0 0 0 0 0 0.0   0 30.00 1 1 10.00 4 2 3 4
99 9 9 9 9 9 999.00 9 9999.00    1.49 9999.00 9 9 9    0.80
   6.48 82   1.7000    3.80 2 6 3 3 12  19 20  0   1.5500
270678 21 1139 27.28    0 1 19.00 21  1.10 2  5 2 8 0 5 7
    2 3 1 7 9 4 0.72  0 26.00 2 1  2.00 4 3 3 4
 2 1 8 8 4 4  64.00 1   13.00    1.05   25.00 2 3 3    0.26
   1.22 61   1.3300    0.92 1 3 3 4  0  20  0  0   1.2100
270778 21 1142 27.28    0 4 19.00 21  1.10 2  5 2 8 0 5 7
    2 3 1 7 9 4 0.72  0 26.00 2 1  3.00 4 3 3 4
 2 1 8 8 4 4  64.00 1   13.00    0.0    25.00 2 3 3    0.35
   0.0   0   2.5600    0.0  1 3 3 4  0  20  0  0   2.3300
 30778 18 1216 29.31 1830 3  9.00 18  0.70 2  5 1 6 9 5 6
    0 0 0 0 0 0 0.0   4 24.00 2 5  1.00 4 2 4 4
99 9 9 9 9 9 999.00 9 9999.00    0.01 9999.00 9 9 9    2.39
   2.39 59   2.8700    0.83 0 3 3 1 99  21  0 20   4.1000
```

```
110778  1 1232 24.25 1945 4  9.00  1  1 10 2  5 2 8 0 5 4
    2 3 1 7 9 4 0.37  0 17.00 2 1  2.00 4 3 3 4
 2 1 3 8 3 3  47.00 1   15.00     2.68    50.00 2 3 3     0.0
   0.0   0   0.0         0.0  1 3 3 4  0  22 12  0    0.0
110778  1 1229 24.25 1945 4  8.00  1  1.70 3  5 2 8 0 5 4
    0 0 0 0 0 0 0.0   0 17.00 2 1  2.00 4 3 3 4
 2 1 3 8 3 3  47.00 1   15.00     0.0  9999.00 2 3 3     0.79
   0.0   0   2.2100     0.0  1 5 2 4  0  22  0  0    1.3000
110778  1 1230 24.25 1945 1  9.00  1  1.10 2  5 2 8 0 5 4
    2 3 1 7 9 4 0.37  0 17.00 2 1  2.00 4 3 3 4
 2 1 3 8 3 3  47.00 1   15.00     0.82 9999.00 2 3 3     0.40
   1.29 65    1.1900     1.08 1 3 3 4 31  22 12  0    1.0800
170778 61 1236 32.00     0 3   0.0   61  1.30 0  5 2 8 0 5 5
    0 0 0 0 0 0 0 0.0   1 56.00 2 1  4.00 3 2 3 2
99 9 9 9 9 9 9 999.00 9 9999.00     0.01 9999.00 9 9 9     3.50
   3.5  60    2.5400     1.38 0 0 0 1 98  23  7  0    1.9500
170778 61 1235 32.00     0 4   0.0   61  1.30 0  5 2 8 0 5 5
    0 0 0 0 0 0 0 0.0   1 56.00 2 1  4.00 3 2 3 2
99 9 9 9 9 9 9 999.00 9 9999.00     0.01 9999.00 9 9 9     3.70
   3.7  62    2.5900     1.43 0 0 0 1 98  23  7  0    1.9900
310778 30 1238 26.00 1880 4  6.00 30  1.00 3  6 2 8 0 5 7
    2 3 1 7 9 4 0.37  0 42.00 2 2  6.00 3 3 3 4
99 9 9 9 9 9 9 999.00 9 9999.00     0.01 9999.00 9 9 9     0.22
   0.22 12    2.0400     0.0  1 3 1 4  1  24  0 50    2.0400
310778 30 1240 26.00 1880 1  6.00 30  1.00 3  6 2 8 0 5 7
    2 3 1 7 9 4 0.37  0 42.00 2 2  6.00 3 3 3 4
99 9 9 9 9 9 9 999.00 9 9999.00     0.92 9999.00 9 9 9     0.05
   0.05  6    0.9200     0.0  1 3 1 4  1  24  0 50    0.9200
120978 16 1332  0.0  1946 3 15.00 17  1.00 0  4 0 0 0 0 0
    0 0 0 0 0 0 0 0.0   0 40.00 1 3  6.50 3 3 3 4
99 9 9 9 9 9 9 999.00 9 9999.00     1.83 9999.00 9 9 9     0.01
   0.01  1    1.8300     0.0  2 3 3 4  1  25  0  0    1.8300
120978 16 1329  0.0  1946 1 15.00 17  0.90 1  4 1 8 9 5 5
    0 0 0 0 0 0 0 0.0   0 35.00 1 3  6.50 3 2 3 3
99 9 9 9 9 9 9 999.00 9 9999.00     0.01 9999.00 9 9 9     2.55
   2.55 67    2.2000     1.16 0 5 3 1 98  25  0  0    2.4400
120978 16 1326  0.0  1946 1 15.00 17  0.90 1  4 1 8 9 5 5
    0 0 0 0 0 0 0 0.0   0 35.00 1 3  6.50 3 2 3 3
99 9 9 9 9 9 9 999.00 9 9999.00     0.01 9999.00 9 9 9     0.90
   0.90 47    1.6400     0.53 0 5 3 1 98  25  0  0    1.8200
120978 16 1324  0.0     0 1 22.00 16  1.10 1  6 2 8 0 5 6
    0 0 0 0 0 0 0 0.0   0 30.00 1 1  1.50 3 3 3 4
99 9 9 9 9 9 9 999.00 9 9999.00     0.33 9999.00 9 9 9     1.14
   1.59 70    1.1700     1.36 1 3 3 2 72  26  0  0    1.0700
120978 16 1322  0.0     0 1 22.00 16  1.10 1  6 2 8 0 5 6
    0 0 0 0 0 0 0 0.0   0 30.00 1 1  2.00 3 3 3 4
99 9 9 9 9 9 9 999.00 9 9999.00     0.25 9999.00 9 9 9     1.07
   1.29 60    1.4900     0.86 0 2 3 2 83  26  0  0    1.3500
120978 16 1320  0.0     0 2 22.00 16  1.00 2  6 2 8 0 5 6
    0 0 0 0 0 0 0 0.0   0 30.00 1 1  3.60 3 3 3 3
99 9 9 9 9 9 9 999.00 9 9999.00     0.62 9999.00 9 9 9     1.20
   1.93 67    1.6400     1.61 2 2 3 2 62  26  0  0    1.6100
110978  1 1316 24.25 1945 2 20.00  1  1.10 2  5 2 8 0 5 4
    2 3 1 7 9 4 0.37  0 25.00 1 1 16.00 3 2 3 1
99 9 9 9 9 9 9 999.00 9 9999.00     1.30   40.00 9 9 9     3.50
   8.14 82    2.2800     3.57 3 2 3 2 43  27  0  0    2.0700
180978 18 1430 38.39 1830 2  1.30 18  1.10 3  8 1 5 9 5 7
    0 0 0 0 0 0 0 0.0   4  7.60 2 4  1.50 4 3 4 4
99 9 9 9 9 9 9 999.00 9 9999.00     0.59 9999.00 9 9 9     3.95
   5.86 81    1.8100     3.24 2 2 3 2 67  28  8  0    1.6500
180978 18 1427 38 39 1830 2  8 10 18  1.10 3  8 2 5 9 5 7
    0 0 0 0 0 0 0 0.0   4  7.60 2 4  3.00 3 3 4 4
99 9 9 9 9 9 9 999.00 9 9999.00     0.01 9999.00 9 9 9     1.88
   1.88 65    1.7300     1.06 0 2 3 1 98  27  1  0    1.6200
180978 18 1425 38.39 1830 1  8.50 18  1.10 3  8 2 5 9 5 7
    0 0 0 0 0 0 0 0.0   4  7.60 2 4  4.00 3 3 4 4
99 9 9 9 9 9 9 999.00 9 9999.00     0.01 9999.00 9 9 9     2.57
   2.57 67    2.2000     1.17 0 2 3 1 98  28  1  0    2.0000
101078 19 1607  1.05 1956 2  6.30 19  1.30 2  2 1 6 9 3 3
    2 3 1 7 9 4 0.37  0 30.00 2 1 10.00 3 2 3 2
99 9 9 9 9 9 9 999.00 9 9999.00     0.01 9999.00 9 9 9     1.93
   1.93 59    2.3200     0.83 0 6 3 1 98  29  0  0    1.7200
101078 19 1608  1.05 1956 1  8.00 19  1.30 1 12 2 8 0 5 7
    0 0 0 0 0 0 0 0.0   0 13.00 2 1  1.30 4 3 3 4
11 2 8 0 0 0   7.00 1   20.00     1.93    9.00 9 9 9     0.33
   0.0  90    1.9300     0.0  1 5 3 4  0  29  0  0    1.4800
101078 19 1610  1.05 1956 1 10.00 19  1.30 1 12 2 8 0 5 7
    0 0 0 0 0 0 0 0.0   0 13.00 2 1  1.50 4 3 3 4
11 2 8 0 0 0   7.00 1   20.00     1.50   55.00 9 9 9     0.38
   2.00 65    1.8500     1.09 1 5 3 4 19  29  0  0    1.4200
101078 19 1612  1.05 1956 3 10.00 19  1.00 1 11 2 8 0 5 4
    0 0 0 0 0 0 0 0.0   0  7.50 2 1  1.50 4 3 3 4
 2 1 6 9 3 3  50.00 1   60.00     3.17   60.00 1 2 3     0.73
   2.72 52    4.3300     0.63 3 6 3 4 27  29  0  0    4.3300
101078 19 1614  1.05 1956 3 10.00 19  1.20 2 12 2 8 0 5 7
    0 0 0 0 0 0 0 0.0   0 13.00 2 1  1.50 4 3 3 4
 2 1 6 9 3 3  50.00 1   40.00     2.05  100.00 2 2 3     1.01
   4.80 75    2.6000     2.33 1 6 3 4 21  29  0  0    2.2000
101078 19 1618  1.05 1956 3  8.10 19  1.30 2  2 1 6 9 3 3
    0 0 0 0 0 0 0 0.0   0 30.00 2 1 17.00 2 2 3 1
99 9 9 9 9 9 9 999.00 9 9999.00     0.01 9999.00 9 9 9     2.53
   2.53 36    6.8400     0.37 2 6 3 3  0  30  3  0    5.2600
101078 19 1620  1.05 1956 4  8.10 19  1.30 2  2 1 6 9 3 3
    0 0 0 0 0 0 0 0.0   0 30.00 2 1  9.00 2 2 3 2
99 9 9 9 9 9 9 999.00 9 9999.00     0.01 9999.00 9 9 9     2.78
   5.18 47    5.1800     0.54 0 6 3 2 54  30  0  0    3.9800
101078 19 1623  1.05 1956 1  5.50 19  1.30 2  2 1 6 9 3 3
    0 0 0 0 0 0 0 0.0   0 30.00 2 1 10.00 2 2 3 1
99 9 9 9 9 9 9 999.00 9 9999.00     3.37 9999.00 9 9 9     5.18
  10.78 73    6.6300     1.63 0 6 3 1 45  30  4  0    5.1000
101078 19 1625  1.05 1956 2  5.50 19  1.30 2  2 1 6 9 3 3
    0 0 0 0 0 0 0 0.0   0 30.00 2 1 11.00 2 2 3 1
99 9 9 9 9 9 9 999.00 9 9999.00     0.80 9999.00 9 9 9     1.33
   1.75 24    3.8800     1.32 2 6 3 2 76  30  5  0    2.6000
101078 20 1628  1.05 1956 1 12.00 20  1.60 2  4 1 8 8 3 3
    0 0 0 0 0 0 0 0.0   0 30.00 1 1  8.00 2 2 3 2
99 9 9 9 9 9 9 999.00 9 9999.00     0.01 9999.00 9 9 9     9.85
   9.85 61   11.1000     0.89 0 2 1 1 98  31  0  0    6.9300
111078 16 1635 41.00 1946 2  8.50 17  0.90 2  9 1 8 9 5 5
    0 0 0 0 0 0 0 0.0   0 10.00 1 4  3.00 3 2 4 2
99 9 9 9 9 9 9 999.00 9 9999.00     0.01 9999.00 9 9 9     3.38
   3.38 74    2.0000     1.69 0 5 3 1 98  32  2  0    2.2000
111078 16 1705 41.00 1946 1  8.50 17  0.90 2  9 1 8 9 5 5
    0 0 0 0 0 0 0 0.0   0 10.00 1 4  3.00 3 2 4 2
99 9 9 9 9 9 9 999.00 9 9999.00     0.01 9999.00 9 9 9     2.37
   2.37 66    2.0900     1.13 0 5 3 1 98  32  2  0    2.3200
111078 16 1707 41.00 1946 1  8.50 17  0.80 3  9 1 8 9 5 5
    0 0 0 0 0 0 0 0.0   0 10.00 1 4  2.00 3 2 4 4
99 9 9 9 9 9 9 999.00 9 9999.00     0.01 9999.00 9 9 9     1.69
   1.69 58    2.1500     0.79 0 5 3 1 98  32  2  0    2.6900
```

```
111078 16 1710 41.00 1946 1  8 50 17  1.20 3  9 1 8 9 5 5
    0 0 0 0 0 0 0 0.0   0 10.00 1 4  6.00 3 2 4 3
99 9 9 9 9 9 999.00 9 9999.00    0.01 9999.00 9 9 9    2.83
   2.83 73   1.7700    1.60 0 5 3 1 98  32  3  0   1.4700
111078 16 1713 41.00 1946 1  8.50 17  1.20 0  9 1 8 9 5 5
    0 0 0 0 0 0 0 0.0   0 10.00 1 4  1.50 4 2 4 3
99 9 9 9 9 9 999.00 9 9999.00    1.45 9999.00 9 9 9    2.95
  11.00 82   2.2400    4.90 2 5 3 3 27  32  0  0   1 9000
111078 16 1715  0.0     0 1 22 00 16  1.50 1  6 2 8 0 5 6
    0 0 0 0 0 0 0 0.0   0 30.00 1 1  2.50 4 4 3 4
 2 1 8 8 3 3  50.00 1   40.00    0.64 9999.00 3 2 3    3.35
   4.20 70   3.1000    1.26 1 3 3 2 80  33  0  0   2.0700
111078 16 1718  0.0     0 1 22.00 16  1.20 1  6 2 8 0 5 6
    0 0 0 0 0 0 0 0.0   0 30.00 1 1  1.50 4 3 3 4
 2 1 8 8 3 3  57.00 1   15.00    0.66 9999.00 3 2 3    1.34
   2.40 73   1.4600    1.68 1 3 3 2 56  33  0  0   1.2200
111078 16 1719  0.0     0 1 22.00 16  1.00 1  6 2 8 0 5 6
    0 0 0 0 0 0 0 0.0   0 30.00 1 1  1.50 4 4 3 4
 2 1 8 8 3 3  50.00 1   40.00    0.64 9999.00 3 2 3    1.10
   2.01 71   1.4100    1.43 1 3 3 3 55  33  0  0   1.4100
121078 20 1724  0.0   1950 1 12.00 20  1.00 1 12 2 8 0 5 7
    0 0 0 0 0 0 0 0.0   0 17.00 1 1  2.00 0 0 0 0
11 2 8 0 0 0   0.0  1   30.00    0.54 9999.00 0 0 0    0.29
   1.85 72   1.2000    1.55 1 3 3 4 15  34  5  0   1.2000
121078 20 1726  0.0   1950 1 12.00 20  1.00 1 12 2 8 0 5 7
    0 0 0 0 0 0 0 0.0   0 17.00 1 1  6.40 4 3 3 4
11 2 8 0 0 0   0.0  1 9999.00    0.73   30.00 0 0 0    0.34
   1.37 71   0.9700    1.42 1 3 3 4 25  34  5  0   0.9700
121078 20 1727  0.0   1950 1 12.00 20  1.00 1 12 2 8 0 5 7
    0 0 0 0 0 0 0 0.0   0 17.00 1 1  5.70 4 3 3 4
11 2 8 0 0 0   0.0  1   30.00    1.53 9999.00 0 0 0    0.36
   2.56 71   1.7800    1.44 1 3 3 4 14  34  5  0   1.7800
121078 20 1728  0.0   1950 1 12.00 20  1.00 1 12 2 8 0 5 7
    0 0 0 0 0 0 0 0.0   0 17.00 1 1  5.70 4 3 3 4
11 2 8 0 0 0   0.0  1   30.00    1.35 9999.00 0 0 0    0.64
   2.16 66   1.9400    1.12 1 3 3 4 14  34  5  0   1.9400
121078 20 1730  0.0   1950 3  4.40 20  1.00 1  2 1 8 8 3 3
    0 0 0 0 0 0 0 0.0   0 50.00 1 1 13.00 3 2 3 2
99 9 9 9 9 9 999.00 9 9999.00    0.01 9999.00 9 9 9    3.30
   3.30 70   2.3500    1.40 0 3 3 1 98  34  5  0   2.3500
121078 20 1732  0.0   1950 3  5.00 20  1.00 1  2 1 8 8 3 3
    0 0 0 0 0 0 0 0.0   0 50.00 1 1 10.00 3 2 3 2
99 9 9 9 9 9 999.00 9 9999.00    0.01 9999.00 9 9 9    2.47
   2.47 46   4.7100    0.53 0 3 3 1 98  34  5  0   4.7100
260679 20 1903  0.0   1956 1 10.00 20  1.20 1  4 1 8 9 3 3
    0 0 0 0 0 0 0 0.0   0 20.00 1 1  5.00 2 3 3 3
99 9 9 9 9 9 999.00 9 9999.00    1.34 9999.00 9 9 9    0.75
   2.31 67   1.9900    1.16 2 3 3 3 32   0  0  0   1.6300
260679 20 1906  0.0   1956 1 10.00 20  1.30 1  4 1 8 9 3 3
    0 0 0 0 0 0 0 0.0   0 20.00 1 1  5.00 2 3 3 3
99 9 9 9 9 9 999.00 9 9999.00    0.0  9999.00 9 9 9    0.32
   1.60 58   2.0000    0.80 2 3 3 4 20   0  0  0   1.5400
260679 20 1909  0.0   1956 2 10.00 20  1.30 1  4 1 8 9 4 3
    0 0 0 0 0 0 0 0.0   0 20.00 1 2  7.00 1 2 3 2
99 9 9 9 9 9 999.00 9 9999.00    0.01 9999.00 9 9 9    3.17
   3.17 60   3.6900    0.86 3 6 3 1 99   0  0  0   2.8400
260679 18 1915  0.0   1830 3 11.00 18  1.00 2  5 1 8 0 4 2
    0 0 0 0 0 0 0 0.0   0 20.00 1 1  4.00 3 3 1 3
99 9 9 9 9 9 999.00 9 9999.00    0.86 9999.00 9 9 9    1.38
   2.36 66   2.0600    1.15 2 3 3 3 59   0 10  0   2.0600
260679 18 1918  0.0   1830 3 10.00 18  1 00 2  5 1 8 0 4 2
    0 0 0 0 0 0 0 0.0   0 20.00 1 1  2.50 3 3 1 3
99 9 9 9 9 9 999.00 9 9999.00    1.85 9999.00 9 9 9    0.80
   1.64 61   1.8500    0.89 2 3 3 3 49   0 10  0   1.8500
280679 18 1922  0.0   1830 4 11.00 18  1.00 2  5 1 8 0 4 2
    0 0 0 0 0 0 0 0.0   0 20.00 1 1  4.50 3 3 1 3
99 9 9 9 9 9 999.00 9 9999.00    0.90 9999 00 9 9 9    2.24
   3.36 68   2.6900    1.25 2 3 3 2 80   0 10  0   2.6900
280679 18 1924  0.0   1830 4 11.00 18  1.00 2  5 1 8 0 4 2
    0 0 0 0 0 0 0 0.0   0 20.00 1 1  3.70 3 3 1 3
99 9 9 9 9 9 999.00 9 9999.00    0.69 9999.00 9 9 9    0.94
   1.41 54   2.0600    0.69 2 3 3 2 67   0 10  0   2.0600
280679 18 1927  0.0   1830 3 10.00 18  1.00 2  5 1 8 0 4 2
    0 0 0 0 0 0 0 0.0   0 20.00 1 1  4.00 3 3 1 3
99 9 9 9 9 9 999.00 9 9999.00    0.71 9999.00 9 9 9    5.31
   7.26 80   2.6400    2.75 2 3 3 2 73   0 10  0   2.6400
280679 18 1930  0.0   1830 4 10.00 18  1.00 2  5 1 8 0 4 2
    0 0 0 0 0 0 0 0.0   0 20.00 1 1  5.00 3 3 1 3
99 9 9 9 9 9 999.00 9 9999.00    1.03 9999.00 9 9 9    1.00
   2.05 64   2.0000    1.02 1 3 3 3 49   0 10  0   2.0000
 30779 30 2006  0.0   1880 3 12.00 30  1.10 3  5 2 8 9 4 4
    0 0 0 0 0 0 0 0.0   0 20.00 1 3  3.00 3 2 4 3
99 9 9 9 9 9 999.00 9 9999.00    0.82 9999.00 9 9 9    0.46
   1.09 56   1.4400    0.75 2 3 1 3 43   0  0  0   1.3100
 30779 30 2009  0.0   1880 4  9.00 30  1.10 3  5 2 8 9 4 4
    0 0 0 0 0 0 0 0.0   0 20.00 1 3  3.00 3 2 4 3
99 9 9 9 9 9 999.00 9 9999.00    1.04 9999.00 9 9 9    0.90
   2.92 76   1.5000    1.95 2 3 1 3 31   0  6  0   1.3600
 30779 30 2014  0.0   1880 4  9.00 30  1.10 3  5 2 8 9 4 4
    0 0 0 0 0 0 0 0.0   0 20.00 1 3  3.00 3 2 4 3
99 9 9 9 9 9 999.00 9 9999.00    0.78 9999.00 9 9 9    1.05
   2.20 71   1.5000    1.47 3 3 1 3 48   0  6  0   1.3600
 40779  6 2018  0.0   1830 2  4.70  6  1.30 1  2 1 8 8 3 3
    0 0 0 0 0 0 0 0.0   0 45.00 1 2  7.00 3 2 1 2
99 9 9 9 9 9 999.00 9 9999.00    0.01 9999.00 9 9 9    1.68
   1.68 66   1.4700    1.15 3 3 3 1 99   0  3 70   0.8800
 40779  6 2021  0.0   1830 3  4.70  6  1.30 1  2 1 8 8 3 3
    0 0 0 0 0 0 0 0.0   0 45.00 1 2  7.00 3 2 1 2
99 9 9 9 9 9 999.00 9 9999.00    1.14 9999.00 9 9 9    1.31
   2.21 58   2.8100    0.79 3 3 3 1  0   0  3 70   2.1600
 40779  6 2024  0.0   1830 2  4.70  6  1.30 1  2 1 8 8 3 3
    0 0 0 0 0 0 0 0.0   0 45.00 1 2  7.00 3 2 1 2
99 9 9 9 9 9 999.00 9 9999.00    0.48 9999.00 9 9 9    1.59
   2.24 70   1.6500    1.36 3 3 3 2 71   0  3 70   1.3000
310779 62 2221  0.0   1930 2 40.00 62  2.50 1  6 2 8 0 4 3
    0 0 0 0 0 0 0 0.0   0 25.00 1 1  7.00 2 3 3 3
99 9 9 9 9 9 999.00 9 9999.00    8.34 9999.00 9 9 9   12.80
  24.00 69  18.0000    1.33 2 2 0 3 54   0 16  0   7.2000
310779 62 2221  0.0   1930 2 40.00 62  2.50 1  6 2 8 0 4 3
    0 0 0 0 0 0 0 0.0   0 25.00 1 1  7.00 2 3 3 3
99 9 9 9 9 9 999.00 9 9999.00    1.80 9999.00 9 9 9   13.60
  17.10 76   8.7300    1.96 2 2 0 2 79   0 16  0   3.5000
 50779 18 2030  0.0   1830 3 11.00 18  1.00 2  5 1 8 0 4 2
    0 0 0 0 0 0 0 0.0   0 20.00 1 1  3.00 3 3 1 3
99 9 9 9 9 9 999.00 9 9999.00    0.70 9999.00 9 9 9    1.40
   2.62 74   1.5000    1.75 2 3 3 3 53   0 10  0   0.5800
 50779 18 2108  0.0   1830 4 11.00 18  1.00 2  5 1 8 0 4 2
    0 0 0 0 0 0 0 0.0   0 20.00 1 1  5.00 3 3 1 3
99 9 9 9 9 9 999.00 9 9999.00    0.54 9999.00 9 9 9    2.80
   3.84 75   2.0000    1.92 3 3 3 2 73   0 10  0   2.0000
```

```
 50779 18 2110   0.0   1830 4 11.00 18   1.00 2  5 1 8 0 4 2
    0 0 0 0 0 0 0 0.0    0 20.00 1 1   4.00 3 3 1 3
99 9 9 9 9 9 9 999.00 9 9999.00     0.20 9999.00 9 9 9     1.60
   1 78 61    2.0000     0.89 2 3 3 1 90    0 10   0    2.0000
 50779 18 2112   0.0   1830 4 11.00 18   1.00 2  5 1 8 0 4 2
    0 0 0 0 0 0 0 0.0    0 20.00 1 1   5.00 3 3 1 3
99 9 9 9 9 9 9 999.00 9 9999.00     1.31 9999.00 9 9 9     1.60
   3.12 67    2.7000     1.15 2 3 3 3 51    0 10   0    2.7000
 50779 18 2114   0.0   1830 3 11.00 18   1.00 2  5 1 8 0 4 2
    0 0 0 0 0 0 0 0.0    0 20.00 1 1   4.00 3 3 1 3
99 9 9 9 9 9 9 999.00 9 9999.00     0.79 9999.00 9 9 9     2.20
   3.10 67    2.7000     1.15 2 3 3 2 71    0 10   0    2.7000
 50779 18 2116   0.0   1830 4 11.00 18   1.00 2  5 1 8 0 4 2
    0 0 0 0 0 0 0 0.0    0 20.00 1 1   4.50 3 3 1 3
99 9 9 9 9 9 9 999.00 9 9999.00     0.36 9999.00 9 9 9     3.58
   4.07 70    3.0000     1.36 3 3 3 1 88    0 10   0    2.9800
 50779 18 2119   0.0   1830 4 11.00 18   1.00 2  5 1 8 0 4 2
    0 0 0 0 0 0 0 0.0    0 20.00 1 1   5.00 3 3 1 3
99 9 9 9 9 9 9 999.00 9 9999.00     0.69 9999.00 9 9 9     3.50
   4.28 66    3.7600     1.14 1 3 3 2 82    0 10   0    3.7600
220879 20 2301   0.0   1936 1  9.00 20   1.30 2  4 1 3 9 3 3
    0 0 0 0 0 0 0 0.0    0 30.00 1 2   7.00 2 2 1 1
99 9 9 9 9 9 9 999.00 9 9999.00     1.27 9999.00 9 9 9     1.87
   3.14 64    3.1200     1.00 2 3 3 2 60    0  2   0    2.2600
220879 20 2306   0.0   1936 1  9.00 20   1.20 2  4 1 3 9 3 3
    0 0 0 0 0 0 0 0.0    0 30.00 1 2   7.00 2 2 1 1
99 9 9 9 9 9 9 999.00 9 9999.00     2.45 9999.00 9 9 9     2.32
   8.53 79    3.3600     2.54 2 3 3 2 27    0  2   0    2.8000
220879 20 2309   0.0   1936 1 10.00 20   1.20 2  4 1 3 9 3 3
    0 0 0 0 0 0 0 0.0    0 30.00 1 2   6.50 2 2 1 1
99 9 9 9 9 9 9 999.00 9 9999.00     0.01 9999.00 9 9 9     2.42
   2.42 69    1.8800     1.29 3 3 3 1 99    0  2   0    1.0800
220879 20 2314   0.0   1936 1 10.00 20   1.10 2  4 1 3 9 3 3
    0 0 0 0 0 0 0 0.0    0 30.00 1 2   6.50 2 2 1 1
99 9 9 9 9 9 9 999.00 9 9999.00     0.69 9999.00 9 9 9     2.77
   3.48 65    3.3700     1.03 2 3 3 2 80    0  2   0    3.0600
220879 20 2314   0.0   1936 1 10.00 20   1.10 2  4 1 3 9 3 3
    0 0 0 0 0 0 0 0.0    0 30.00 1 2   6.50 2 2 1 1
99 9 9 9 9 9 9 999.00 9 9999.00     5.11 9999.00 9 9 9     2.25
   6.31 58    7.9000     0.80 3 4 3 1 36    0  2   0    7.2000
220879 20 2314   0.0   1936 1 10.00 20   1.10 2  4 1 3 9 3 3
    0 0 0 0 0 0 0 0.0    0 30.00 1 2   6.50 2 2 1 1
99 9 9 9 9 9 9 999.00 9 9999.00     0.36 9999.00 9 9 9     2.13
   2.60 69    2.0100     1.29 3 3 3 1 82    0  2   0    1.8300
   681 22 2815   0.0   1950 4   0.0   22   0.80 1   6 2 8 0 4 3
    1 3 9 2 7 4 0.23    2 25.00 2 1   3.50 3 3 3 2
99 9 9 9 9 9 9 999.00 9 9999.00     1.23 9999.00 9 9 9     0.82
   1.87 62    2.0000     0.94 2 6 1 3 44    0  3   0    2.5000
   681 22 2818   0.0   1950 4   0.0   22   0.80 1   6 2 8 0 4 3
    1 3 9 2 7 4 0.23    2 25.00 2 1   3.50 3 3 3 2
99 9 9 9 9 9 9 999.00 9 9999.00     0.46 9999.00 9 9 9     1.01
   1.30 51    2.0800     0.63 2 6 1 2 77    0  3   0    2.6000
   681 22 2820   0.0   1950 2   0.0   22   0.80 1   6 2 8 0 4 3
    1 3 9 2 7 4 0.23    2 25.00 2 1   3.50 3 3 3 2
99 9 9 9 9 9 9 999.00 9 9999.00     1.20 9999.00 9 9 9     0.61
   1.63 60    1.9100     0.85 2 6 1 3 37    0  3   0    2.3900
   681 22 2822   0.0   1950 2   0.0   22   0.80 1   6 2 8 0 4 3
    1 3 9 2 7 4 0.23    2 25.00 2 1   4.00 3 3 3 2
99 9 9 9 9 9 9 999.00 9 9999.00     0.73 9999.00 9 9 9     1.05
   1.77 63    1.7800     0.99 3 4 1 5 59    0  3   0    2.2300
   681 22 2825   0 0   1950 2   0 0   22   0.80 1   6 2 8 0 4 3
    1 3 9 2 7 4 0.23    2 25.00 2 1   4.00 3 3 3 2
99 9 9 9 9 9 9 999.00 9 9999.00     1.03 9999.00 9 9 9     1.15
   2.37 67    2.0000     1.18 2 6 1 3 49    0  3   0    2.5000
   681 22 2827   0.0   1950 2   0.0   22   0.80 1   6 2 8 0 4 3
    1 3 9 2 7 4 0.23    2 25.00 2 1   4.00 3 3 3 2
99 9 9 9 9 9 9 999.00 9 9999.00     0.48 9999 00 9 9 9     1 00
   1.41 62    1.5400     0.92 3 4 1 2 69    0  3   0    1 9300
    76 12 9901   0.0      0 3 22.00 12   0.90 0   9 1 8 9 4 4
    0 0 0 0 0 0 0 0.0    0   0.0   0 0 10.00 3 3 1 2
99 9 9 9 9 9 9 999.00 9 9999.00     1.35 9999.00 9 9 9     2.05
   3.30 62    3.5700     0.92 2 3 0 2 62    0  0   0    3.9600
    76 12 9902   0.0      0 3 22.00 12   0.90 0   9 1 8 9 4 4
    0 0 0 0 0 0 0 0.0    0   0.0   0 0  6.00 3 3 1 2
99 9 9 9 9 9 9 999.00 9 9999.00     0.0  9999.00 9 9 9     0.0
   0.0   47   0.0        0.0   0 0 0 0   0   0   0   0.0
    76 12 9903   0.0      0 3 22.00 12   0.90 0   9 1 8 9 4 4
    0 0 0 0 0 0 0 0.0    0   0.0   0 0  5.40 3 3 1 2
99 9 9 9 9 9 9 999.00 9 9999.00     0.40 9999.00 9 9 9     1.02
   1.48 66    1.3000     1.14 2 0 0 2 69    0  0   0    1.4400
    76 12 9905   0.0      0 2 22.00 12   0.90 0   9 1 8 9 4 4
    0 0 0 0 0 0 0 0.0    0   0.0   0 0  7.30 3 3 1 2
99 9 9 9 9 9 9 999.00 9 9999.00     1.22 9999.00 9 9 9     2.18
   5.50 80    2.0200     2.73 2 3 0 3 40    0  0   0    2.2400
    76 12 9907   0.0      0 2 22.00 12   0.90 0   9 1 8 9 4 4
    0 0 0 0 0 0 0 0.0    0   0.0   0 0  5.10 3 3 1 2
99 9 9 9 9 9 9 999.00 9 9999.00     1.70 9999.00 9 9 9     1.25
   2.72 60    3.1500     0.86 2 3 0 3 46    0  0   0    3.5000
    76 12 9908   0.0      0 2 22.00 12   0.90 0   9 1 8 9 4 4
    0 0 0 0 0 0 0 0.0    0   0.0   0 0  8.60 3 3 1 2
99 9 9 9 9 9 9 999.00 9 9999.00     0.56 9999.00 9 9 9     0.66
   0.98 49    1.7100     0.58 2 2 0 2 67    0  0   0    1.9000
    76 23 9920   0.0      0 3 13.00 23   0.60 0   9 1 8 9 4 5
    0 0 0 0 0 0 0 0.0    0   0.0   0 1  9.10 3 3 3 4
99 9 9 9 9 9 9 999.00 9 9999.00     1.41 9999.00 9 9 9     0.67
   2.64 70    1.8900     1.40 2 3 0 2 25    0  0   0    3.1500
    76 23 9923   0.0      0 4 13.00 23   0.60 0   9 1 8 9 4 5
    0 0 0 0 0 0 0 0.0    0   0.0   0 1  7.10 3 3 3 4
99 9 9 9 9 9 9 999.00 9 9999.00     0.0  9999.00 9 9 9     0.0
   0.0   69   0.0        0.0   0 0 0 0   0   0   0   0.0
    76 23 9929   0.0      0 3 13.00 23   0.60 0   9 1 8 9 4 5
    0 0 0 0 0 0 0 0.0    0   0.0   0 1 10.00 3 3 3 4
99 9 9 9 9 9 9 999.00 9 9999.00     0.56 9999.00 9 9 9     1.94
   2.59 67    2.2500     1.15 2 3 0 2 75    0  0   0    3.7500
    76 23 9923   0.0      0 2 13.00 23   0.60 0   9 1 8 9 4 5
    0 0 0 0 0 0 0 0.0    0   0.0   0 1  8.20 3 3 3 4
99 9 9 9 9 9 9 999.00 9 9999.00     0.53 9999.00 9 9 9     1.50
   1.82 51    3.0000     0.61 2 3 0 1 90    0  0   0    5.0000
    76 21 9956   0.0      0 3 23.00 21   1.20 0   5 2 8 0 4 5
    0 0 0 0 0 0 0 0.0    0   0.0   0 1  6.40 3 3 3 4
 4 0 0 0 3 2    0.0   1    15.00     2.00     0.25 2 3 3     1.23
   1.66 48    3.0000     0.55 1 3 0 2 74    0  0   0    2.5000
    76 21 9955   0.0      0 3 23.00 21   1.20 0   5 2 8 0 4 5
    0 0 0 0 0 0 0 0.0    0   0.0   0 1  5.40 3 3 3 4
 4 0 0 0 3 2    0.0   1    15.00     2.00     0.25 2 3 3     1.50
   1.82 51    3.0000     0.61 1 3 0 2 82    0  0   0    2.5000
    76 21 9957   0.0      0 3 23.00 21   1.20 0   4 1 8 9 4 4
    0 0 0 0 0 0 0 0.0    0   0.0   0 1  7.50 3 3 3 4
99 9 9 9 9 9 9 999.00 9 9999.00     1.90 9999.00 9 9 9     0.97
   2.90 64    2.8600     1.01 2 0 0 3 34    0  0   0    2.3800
```

```
   76 21 9962  0.0      0 4 23.00 21  1.20 0  5 2 8 0 4 5
   0 0 0 0 0 0 0 0.0    0  0.0  0 1  5.70 3 3 3 4
4 0 0 0 3 2    0.0  1     0.50     0.74     0.60 2 3 3     0.65
  1.59 69    1.2500     1.28 1 0 0 3 41    0  0  0    1.0400
```

Appendix 2.

Worked example using the relationship for a Voussoir beam suggested by Evans (1941).

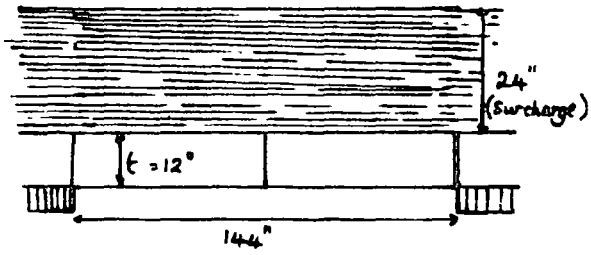

S = Span = 144 inches
t = thickness = 12 inches
w = unit weight = 0.0950056 lb/in^3
n = contact fraction = 0.5 (Evans, 1941)
E = Young's Modulus = 1×10^6 p.s.i.

To accomodate the surcharge load the unit weight of beam is increased; Thus:-
Unit weight of beam + 24" surcharge = $0.0950056 \times 3 = 0.2850168$.

For a given rock strength the maximum stable span is:-

$$S = \sqrt{\frac{8ft\left(n/2 - n^2/6\right)}{w}}$$

In this instance it is the stress at a given span that is required:-

$$f = \frac{S^2 \times w}{8t\left(n/2 - n^2/6\right)} = \frac{144^2 \times 0.2850168}{8 \times 12 \times \left(0.5/2 - 0.5^2/6\right)} = 295.505891 \text{ p.s.i.}$$

Arch height (Z):

$$Z = \left(1 - \frac{2n}{3}\right)t = 8 \text{ inches}$$

Initial length of parabolic arch (L)

$$L = S + \frac{8Z^2}{3S} = 144 + \frac{8 \times 8^2}{3 \times 144} = 145.185185 \text{ inches}$$

Revised length of parabolic arch as a result of elastic bulkling

$$L_1 = S + \frac{8Z^2}{3S} - \left(S + \frac{8Z^2}{3S}\right)\frac{11f}{24E} = 145.185185 - \left(145.185185\right) \times \frac{11 \times 295.505891}{24 \times 1 \times 10^6}$$

$$= 145.1655211 \text{ inches.}$$

Revised height of arch (Z_1) is:-

$$Z_1 = \sqrt{\frac{3S}{8}\left(L_1 - S\right)} = 7.933356091 \text{ inches}$$

If $Z_1 \simeq Z$ then blocks are rigid
$\frac{Z - Z_1}{Z} \times 100 = 0.83\%$

In this case $Z_1 \neq Z$, the difference is:-
In this case iteration continues until the analysis converges (blocks stable) or diverges (elastic rotation)

Stress increase (f_1)

$$f_1 = \frac{Z}{Z_1} = 1.00840046 \text{ p.s.i.}$$

The total linear strain (X_1) is:

$$X_1 = \frac{11f \times f_1}{24E} = 0.000136577 \text{ inches}$$

and the revised length of arch ($L2$) is:

$$L_2 = L - X_1 = 145.1850484 \text{ inches}$$

Revised height of arch (Z_2) becomes:-

$$Z_2 = \sqrt{\frac{3S}{8}(L_2 - S)} = 7.999538414 \text{ inches}$$

If $Z_2 \simeq Z_1$ then blocks are rigid In this case $Z_2 \neq Z_1$; the difference is $\frac{Z_1 - Z_2}{Z_1} \times 100 = -0.83\%$. Therefore, iteration continues.

Stress increase:

$$f_2 = \frac{Z_1}{Z_2} = 0.991726732 \text{ p.s.i}$$

Linear Strain:

$$X_2 = \frac{11f \times f_2}{24E} = 0.000134319 \text{ inches}$$

Revised arch length:

$$L_3 = L - X_2 = 145.1850507 \text{ inches}$$

Revised arch height:

$$Z_3 = \sqrt{\frac{3S}{8}(L_3 - S)} = 7.9995460 \text{ inches}$$

If $Z_3 \simeq Z_2$ the blocks are rigid. In this case $Z_3 \simeq Z_2$, the difference is:

$\frac{Z_2 - Z_3}{Z_2} \times 100 = < 0.0001\%$ Thus, the blocks have stabilised and elastic rotation is not occurring.

The final stress increase at the end of the iteration is calculated

$$f_3 = \frac{Z_2}{Z_3} = 0.999999051 \text{ p.s.i}$$

Therefore, the stress acting at the abutment contact is:-

$$f_{tot} = f \times f_1 \times f_2 \times f_3 = 295.5226593 \text{ p.s.i}$$

(compare this 'maximum value' with the F E stress distribution for this situation given in Figure 5.10, page 183).

The factor of safety (FS) against crushing at the contacts is

$$FS = \frac{7250}{295.52} = 24.53 \qquad (U.C.S. = 7250 \text{ p.s.i})$$

Compare this value with that predicted by Wright (1972, FS=5.9)
Thus, the original equation of Wright (1972) considerably underestimates the contact stresses

WORKED EXAMPLE USING THE RELATIONSHIP FOR A VOUSSOIR BEAM SUGGESTED BY WRIGHT (1972/73)

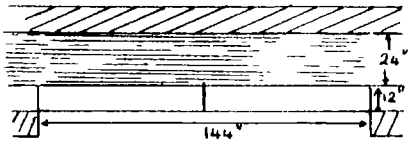

S = Span = 144 inches
t = thickness = 12 inches
E = Young's Modulus = 1×10^6 psi
b = beam depth = nominal value of 1
w = unit weight = 0.0950056 lb/in^3

To accomodate surcharge load due to overlying beds the unit weight is increased by a factor of 3 (≡ wt of beam)

$3 \times w = 0.2850168$

Q is the total uniformly distributed transverse load per unit depth of beam

$Q = S \times b \times t \times w = 492.5$ lb

Initial estimate of height of moment arm (ie distance between thrust centroids)

$$A_0 = 0.72\left(\frac{S}{t}\right)^{0.08} \times t = 10.54 \text{ inches}$$

Initial thrust acting at contacts

$$T_0 = \frac{QS}{8A_0} = \frac{492.5 \times 144}{8 \times 10.54} = 841.08$$

Deflection at mid span due to elastic deformation of beam

$$d_0 = \frac{1.2 A_0 S^{1.78} T}{t^{2.78} E} = 0.07389 \text{ inches}$$

New height of moment arm

$$A_1 = A_0 - d_0 = 10.466$$

This is shorter because beam has deflected more

New thrust

$$T_1 = \frac{QS}{8A_1} = \frac{492.5 \times 144}{8 \times 10.466} = 847.02 \text{ lb}$$

This is increased because beam has rotated more

New deflection calculated for mid point of beam

$$d_1 = \frac{1.2 \times A_0 S^{1.78} T_1}{t^{2.78} E} = 0.074418 \text{ inches}$$

Greater deflection results for increased load due to greater rotation If d_1 is not approximately equal to d_0 then the iteration continues In this case there is a 0.7 % difference Therefore continue

eg difference $= \frac{d_1 - d_0}{d_0} \times 100 = 0.7\%$

New height of moment arm

$$A_2 = A_0 - d_1 = 10.54 - 0.0744 = 10.4656$$

New thrust due to change in length of moment arm

$$T_2 = \frac{QS}{8A_2} = \frac{492.5 \times 144}{8 \times 10.4656} = 847.062 \text{ lb}$$

New deflection due to change in thrust

$$d_2 = \frac{1.2 A_0 S^{1.78} T_2}{t^{2.78} E} = 0.0744215 \text{ inches}$$

If d_2 is approximately equal to d_1 then the iteration need not continue In this case the difference is

$\frac{d_2 - d_1}{d_1} \times 100 = 0.04\%$ This is negligible and means that the beam has stabilised ie it is not deforming elastically

Thus the final (stabilised) height of moment arm

$$A_3 = A_0 - d_2 = 10.46558 \text{ inches}$$

The position of the thrust centroid (a) is -

$$a = 0.294 (t - A_n) = 0.294 (12 - 10.46558)$$

$$a = 0.4511 \text{ inches}$$

The maximum stress at the abutment contact (the most critical contact) is

$$\sigma_{max} = \frac{2T}{3a} = \frac{2 \times 847.062}{3 \times 0.4511} = 1252 \text{ psi}$$

or 8.63 Mn/m^2

If the compressive strength of the sandstone is 7250 psi (50Mn/m^2) then the factor of safety against crushing of contact is -

$$FS = \frac{7250}{1252} = 5.79$$

Therefore the beam is unlikely to fail by crushing of the contacts

Worked example using the relationship for a Voussoir beam developed during the present investigation.

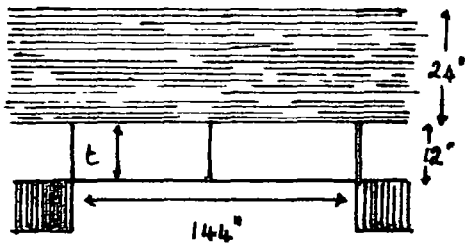

t = thickness of beam = 12"
S = span = 144"
ϕ = angle of friction = 35°
w = unit weight = 0.0950056 lb/in^3

To accomodate the surcharge load the unit weight is increased to $0.0950056 \times 3 = 0.2850168$

The fraction of beam thickness (n) under load is :- (see eq. 5.5)

$$n = 0.882 - 0.63504 \left(\frac{S}{t}\right)^{0.08} = 0.882 - 0.63504\,(12)^{0.08} = 0.107296$$

(c.f. Wright, 1972 $n = 0.5$)

The height of arch (Z) :-

$$= t - (1.133787\, n t) \qquad = 10.54018501 \text{ inches}$$

The critical span is :-

$$S = \sqrt{\frac{4 f n Z}{w}}$$

Therefore, the stress at abutment contact is :-

$$f = \frac{S^2 \times w}{4 n Z} = \frac{144^2 \times 0.2850168}{4 \times 0.107296 \times 10.54018501} = 1306.483 \text{ psi}$$

The initial length of the arch (L) is:-

$$L = S + \left(\frac{8 Z^2}{3S}\right) = 144 + \left(\frac{8 \times 10.54018501^2}{3 \times 144}\right) = 146.057324 \text{ inches.}$$

The total linear strain (X) is :-

$$X = L \times \frac{k f}{E} \qquad \text{where } k = \frac{4 E n t\,(A^2 - Z^2)}{T\,(8Z^2 - 3S^2)} = 0.1553 \text{ (see Section 5.8.2e)}$$

$$= \frac{146.057324 \times 0.1553 \times 1306.483}{1 \times 10^6} = 0.029634 \text{ inches}$$

Thus the revised length of arch is :

$$L_1 = L - X = 146.057324 - 0.029634 = 146.027689 \text{ inches}$$

and the revised height of arch is:-

$$Z_1 = \sqrt{\frac{3S}{8}\,(L_1 - S)} = 10.46399682 \text{ inches.}$$

If $Z_1 \simeq Z$ then blocks are rigid. In this case $Z_1 \neq Z$; the difference is :-

$\frac{Z - Z_1}{Z} \times 100 = 0.723\%$

In this case, iteration continues until the analysis converges or diverges

As the $\frac{Z-Z_1}{t} = 0.00634$ and is less than 0.14, elastic bulking has not occurred and analysis continues.

Stress increase f_1

$$f_1 = \frac{Z}{Z_1} = \frac{10.54018501}{10.46399682} = 1.00728098 \text{ p.s.i}$$

Revised linear strain :

$$X_1 = X \times f_1 = 0.029634 \times 1.00728098 = 0.029849764 \text{ inches}$$

2nd revised length

$$L_2 = L - X_1 = 146.057324 - 0.029849764 = 146.0274742 \text{ inches}$$

2nd revised arch height (Z_2)

$$Z_2 = \sqrt{\frac{3S}{8}(L_2 - S)} = 10.46344153 \text{ inches}$$

If $Z_2 \simeq Z_1$ then blocks rigid. In this case $Z_2 \simeq Z_1$; the difference is :-

$\frac{Z_1 - Z_2}{Z_1} = 0.005306\ \%$

$\frac{Z - Z_2}{t} = 0.00639$ This is less than 0.14. Therefore, elastic buckling has not taken place and the blocks have stabilised

As the blocks have reached equilibrium and elastic bulkling is not taking place, the final stress increase is calculated as:-

$$f_2 = \frac{Z_2}{Z_1} = \frac{10.46344153}{10.46399682} = 0.999946933 \text{ p.s.i.}$$

Therefore, the total stress acting at the abutment contact is :-

$$f_{tot} = f \times f_1 \times f_2 = 1315.92 \text{ p.s.i}$$

The factor of safety (F.S) against crushing at the contact is :-
(ucs = 7250 p.s.i)

$$F.S = \frac{7250}{1315.92} = 5.509 \quad \text{(ie Crushing is unlikely to occur).}$$

This factor of safety is very similar to the value predicted by Wright (1973) and justifies the modifications made to the theory by Evans (1941).

The factor of safety against Voussoir slippage is :-

$$F.S. = \frac{S \tan \phi}{4Z} = \frac{144 \times \tan 35^\circ}{4 \times 10.463} = 2.409 \quad \text{(Eq. 5.12)}$$

Thus the individual Voussoirs will not have slipped.

Assuming the main roof beam has a weaker bedding plane contact with an apparent cohesion (C) of 290 psi (~2 MN/m²) (approximately equivalent to tensile strength), the factor of safety against Voussoir shear is :-

$$F.S. = \frac{SC}{4T} = \frac{144 \times 290}{4 \times 847.2} = 12.33$$

Where $T = \frac{f_{nt}}{2} = \frac{1316 \times 0.107296 \times 12}{2} = 847.2$ p.s.i

(see Ch 5 3.1b)

Therefore, there is little chance of Voussoir failure by shear.

Summary :-

Factors of safety :

against :	Crushing	5.5
	Slippage	2.41
	Shear	12.33
	Elastic rotation	No elastic rotation

Thus the beam is stable under the present loading configuration.

Appendix 3.

```
C                        Program Shapetest              G.F.G. Garrard
C Dec 83.
C
C       This program is designed to read in raw data from the
C       digitised 'half arches'.  The program scales and subsets the
C       data to produce Y values at standard increments of X.  The
C       subset data is then statistically compared with four
C       curverlinear shapes.  The shapes or relationships chosen
C       include linear, elipse, parabola and power fits.  A choice
C       of the best fit can be made from the statistics procuced in
C       the output.
C
C
C
C             Input on unit 5 follows the following format
C
C  line 1        reference no. of arch (I3) , Number of lines in file
C
C   line 2        ref no, Xcoor , Ycoor  (origin of arch base) (Free
C                                                          Format)
C
C   line 3        ref no, Xcoor , Ycoor  (position on X axis
C                                         perpendicularly below apex
C                                         of arch)  (Free Format)
C
C   line 4        ref no, Xcoor , Ycoor  of arch   (Free Format)
C    |              :      :       :
C  End of file      .      :       :
C
C
C
C         Output for the statistics is on unit 6
C
C         Unit 7 contains the following data on the theoretical
C                reduced shapes :-
C
C     Ref no, Xcoor, Ycoor, Ycoor(parabola), Ycoor(elipse), Ycoor(power)
C
C
C         Unit 8 contains data for the scaled residuals (RES) from the
C                theoretical reduced line :-
C
C     Ref no, Xcoor, Ycoor, RESlin, RESpar, RESelip, RESpow
C
C                  ****************************************
C
C
C
      DIMENSION YCOOR(100), YLIN(100), YPARA(100), YELIP(100), YPOW(100)
      IXMAX = 0
      YMAX = 0
      DO 10 INIT = 1, 100
        YCOOR(INIT) = 0.0
        YLIN(INIT) = 0.0
        YPARA(INIT) = 0.0
        YELIP(INIT) = 0.0
        YPOW(INIT) = 0.0
   10 CONTINUE
      READ (5,*) IFILE, ITOT
      READ (5,*) I, XO, YO
      READ (5,*) I2, XOX, YOX
      XTOT = XOX - XO
      ITOT2 = ITOT - 2
   20 DO 40 IN = 1, ITOT2
        READ (5,*) I, XS, YS
        CXS = ((XS - XO)/XTOT) * 100
        CYS = ((YS - YO)/XTOT) * 100
        ICXS = CXS
C     WRITE(7,7)CXS,ICXS
   30   FORMAT (1X, F6.2, 1X, I3)
        IF (ICXS .GT. 100) GO TO 40
        IF (ICXS .LE. IXMAX) GO TO 40
C
C
C ***************************************************************************
C
C    STORING A SUBSET OF THE DATA
C
C
        YCOOR(ICXS) = CYS
        IXMAX = ICXS
        IF (CYS .GT. YMAX) YMAX = CYS
C
   40 CONTINUE
C
C    ******* SORT OUT CONSTANTS TO BE CALCULATED AND INITIALISE VARIABLES
C
      NCOUNT = 0
      SLIN = 0
      SLIN2 = 0
      SPAR = 0
      SPAR2 = 0
      SELIP = 0
      SELIP2 = 0
      SPOW = 0
      SPOW2 = 0
      TOTL = 0
      TOTP = 0
      TOTE = 0
      TOTPOW = 0
      TOTX = 0
      SUMXYL = 0
      SUMXYP = 0
      SUMXYE = 0
      SUMXPO = 0
      XREST = 0
      YRESLT = 0
      YRESPT = 0
      YRESET = 0
      YREPOW = 0
      ACONST = (YMAX**2) / (4*IXMAX)
      RMCONS = YMAX / IXMAX
C
C    ******* POWER CONSTANTS SET HERE  Y=AX**N  A=POWA N=POWN
C
      POWN = 0.7446
      POWINT = IXMAX ** POWN
      POWA = YMAX / POWINT
C
C    ******* DATA MANIPULATION STARTS HERE
C
```

```
      DO 70 IGO = 1, IXMAX
C
C     ******* LINEAR YCOOR LET STRAIGHT THROUGH
C
            IF (YCOOR(IGO) .LT. 0.01) GO TO 70
            NCOUNT = NCOUNT + 1
            YLIN(IGO) = YCOOR(IGO)
C
C     ******* PARABOLIC REDUCTION
C
C
            YTHEOP = SQRT(4*ACONST*IGO)
            DELTAP = YTHEOP - (RMCONS*IGO)
            YPARA(IGO) = YCOOR(IGO) - DELTAP
C
C     ******* ELIPSE REDUCTION
C
            YINT1 = (IXMAX - IGO) ** 2
            YINT2 = IXMAX ** 2
            YINT3 = 1 - (YINT1/YINT2)
            YTHEOE = SQRT(YMAX**2*YINT3)
            DELTAE = YTHEOE - (RMCONS*IGO)
            YELIP(IGO) = YCOOR(IGO) - DELTAE
C
C     ******* POWER REDUCTION
C
            YTHPOW = POWA * (IGO**POWN)
            DELPOW = YTHPOW - (RMCONS*IGO)
            YPOW(IGO) = YCOOR(IGO) - DELPOW
C
C     ******* CALCULATION OF RESIDUALS FROM THEORETICAL LINE
C
            RESLIN = (RMCONS*IGO) - YLIN(IGO)
            SLIN = RESLIN + SLIN
            SLIN2 = RESLIN ** 2 + SLIN2
C
            RESPAR = (RMCONS*IGO) - YPARA(IGO)
            SPAR = RESPAR + SPAR
            SPAR2 = RESPAR ** 2 + SPAR2
C
            RESEL = (RMCONS*IGO) - YELIP(IGO)
            SELIP = RESEL + SELIP
            SELIP2 = RESEL ** 2 + SELIP2
C
            RESPOW = (RMCONS*IGO) - YPOW(IGO)
            SPOW = RESPOW + SPOW
            SPOW2 = RESPOW ** 2 + SPOW2
C
C     ******* TOTALS FOR CORRELATION COEFFICIENTS
C
            TOTL = TOTL + YLIN(IGO)
            TOTP = TOTP + YPARA(IGO)
            TOTE = TOTE + YELIP(IGO)
            TOTPOW = TOTPOW + YPOW(IGO)
            TOTX = TOTX + IGO
            SUMXYL = SUMXYL + (IGO*YLIN(IGO))
            SUMXYP = SUMXYP + (IGO*YPARA(IGO))
            SUMXYE = SUMXYE + (IGO*YELIP(IGO))
            SUMXPO = SUMXPO + (IGO*YPOW(IGO))
C
C     ******* WRITE STATEMENTS - DATA
C
            WRITE (7,50) IFILE, IGO, YLIN(IGO), YPARA(IGO), YELIP(IGO),
     1      YPOW(IGO)
50          FORMAT (1X, I2, ' , ', I3, 4(' , ',F12.5))
C
            WRITE (8,60) IFILE, IGO, YLIN(IGO), RESLIN, RESPAR, RESEL,
     1      RESPOW
60          FORMAT (1X, I3, 2X, I3, 5(2X,F7.2))
C
70    CONTINUE
      FCOUNT = NCOUNT
C
C     ******* CALCULATE MEANS AND STANDARD ERRORS OF RESIDUALS
C
      RMRESL = SLIN / FCOUNT
      RMTESL = RMRESL
      IF (RMRESL .LT. 0.0) RMTESL = 0.0 - RMRESL
      VRESL = SLIN2 / FCOUNT
      SERESL = SQRT(VRESL)
C
      RMRESP = SPAR / FCOUNT
      RMTESP = RMRESP
      IF (RMRESP .LT. 0.0) RMTESP = 0.0 - RMRESP
      VRESP = SPAR2 / FCOUNT
      SERESP = SQRT(VRESP)
C
      RMRESE = SELIP / FCOUNT
      RMTESE = RMRESE
      IF (RMRESE .LT. 0.0) RMTESE = 0.0 - RMRESE
      VRESE = SELIP2 / FCOUNT
      SERESE = SQRT(VRESE)
C
      RMRPOW = SPOW / FCOUNT
      RMTPOW = RMRPOW
      IF (RMRPOW .LT. 0.0) RMTPOW = 0.0 - RMRPOW
      VRPOW = SPOW2 / FCOUNT
      SERPOW = SQRT(VRPOW)
C
C     ******* CALCULATION OF MEANS AND VARIANCE FOR X AND Y REDUCED DATA
C
      YMEANL = TOTL / FCOUNT
      YMEANP = TOTP / FCOUNT
      YMEANE = TOTE / FCOUNT
      YMEAPO = TOTPOW / FCOUNT
      XMEAN = TOTX / FCOUNT
C
      DO 80 I = 1, IXMAX
        IF (YCOOR(I) .LT. 0.001) GO TO 80
        XRES = I - XMEAN
        XREST = XREST + (XRES**2)
C
        YRESL2 = (YLIN(I) - YMEANL) ** 2
        YRESLT = YRESLT + YRESL2
C
        YRESP2 = (YPARA(I) - YMEANP) ** 2
        YRESPT = YRESPT + YRESP2
C
        YRESE2 = (YELIP(I) - YMEANE) ** 2
        YRESET = YRESET + YRESE2
```

```
C
      YREPO2 = (YPOW(I) - YMEAPO) ** 2
      YREPOW = YREPOW + YREPO2
C
   80 CONTINUE
C
      XSD = SQRT(XREST/FCOUNT)
      ALSD = SQRT(YRESLT/FCOUNT)
      PSD = SQRT(YRESPT/FCOUNT)
      ESD = SQRT(YRESET/FCOUNT)
      POWSD = SQRT(YREPOW/FCOUNT)
C
C     ******* CALCULATION OF CORRELATION COEFFICIENT
C
      RLIN = ((SUMXYL/FCOUNT) - (YMEANL*XMEAN)) / (XSD*ALSD)
      RPARA = ((SUMXYP/FCOUNT) - (YMEANP*XMEAN)) / (XSD*PSD)
      RELIP = ((SUMXYE/FCOUNT) - (YMEANE*XMEAN)) / (XSD*ESD)
      RPOWE = ((SUMXPO/FCOUNT) - (YMEAPO*XMEAN)) / (XSD*POWSD)
C
C     ******* SIGNIFICANCE OF CORRELATION COEFICIENT
C
      RTESTL = (RLIN*SQRT(FCOUNT - 2)) / SQRT(1 - RLIN**2)
      RTESTP = (RPARA*SQRT(FCOUNT - 2)) / SQRT(1 - RPARA**2)
      RTESTE = (RELIP*SQRT(FCOUNT - 2)) / SQRT(1 - RELIP**2)
      RTEPOW = (RPOWE*SQRT(FCOUNT - 2)) / SQRT(1 - RPOWE**2)
C
      MDF = NCOUNT - 2
C
C     ******* T AND F TESTS ON MEANS AND SE'S OF RESIDUALS
C
C     ******* T BETWEEN LINEAR-PARABOLA
C
      TLP = (RMTESL - RMTESP) / SQRT((SERESL**2/FCOUNT) + (SERESP**2/
     1FCOUNT))
      IF (VRESL .GE. VRESP) FLP = VRESL / VRESP
      IF (VRESP .GT. VRESL) FLP = VRESP / VRESL
C
C     ******* T BETWEEN PARABOLA-ELIPSE
C
      TPE = (RMTESP - RMTESE) / SQRT((SERESP**2/FCOUNT) + (SERESE**2/
     1FCOUNT))
      IF (VRESP .GE. VRESE) FPE = VRESP / VRESE
      IF (VRESE .GT. VRESP) FPE = VRESE / VRESP
C
C     ******* T BETWEEN LINEAR-ELIPSE
C
      TLE = (RMTESL - RMTESE) / SQRT((SERESL**2/FCOUNT) + (SERESE**2/
     1FCOUNT))
      IF (VRESL .GE. VRESE) FLE = VRESL / VRESE
      IF (VRESE .GT. VRESL) FLE = VRESE / VRESL
C
C     ******* T BETWEEN LINEAR-POWER
C
      TLPOW = (RMTESL - RMTPOW) / SQRT((SERESL**2/FCOUNT) + (SERPOW**2/
     1FCOUNT))
      IF (VRESL .GE. VRPOW) FLPOW = VRESL / VRPOW
      IF (VRPOW .GT. VRESL) FLPOW = VRPOW / VRESL
C
C     ******* T BETWEEN PARABOLA-POWER
C
      TPPOW = (RMTESP - RMTPOW) / SQRT((SERESP**2/FCOUNT) + (SERPOW**2/
     1FCOUNT))
      IF (VRESP .GE. VRPOW) FPPOW = VRESP / VRPOW
      IF (VRPOW .GT. VRESP) FPPOW = VRPOW / VRESP
C
C     ******* T BETWEEN ELIPSE-POWER
C
      TEPOW = (RMTESE - RMTPOW) / SQRT((SERESE**2/FCOUNT) + (SERPOW**2/
     1FCOUNT))
      IF (VRESE .GE. VRPOW) FEPOW = VRESE / VRPOW
      IF (VRPOW .GT. VRESE) FEPOW = VRPOW / VRESE
C
C     ******* DEGREES OF FREEDOM FOR ABOVE
C
      IDFT = (NCOUNT*2) - 2
      IDFF = NCOUNT - 1
      ANGLE = ATAN(RMCONS) * 57.296
C
C     ******* WRITE STATEMENTS - STATISTICS
C
      WRITE (6,90) IFILE
      WRITE (6,100)
      WRITE (6,110) ANGLE
      WRITE (6,120)
      WRITE (6,130) NCOUNT, NCOUNT, NCOUNT, NCOUNT
      WRITE (6,140) RMRESL, RMRESP, RMRESE, RMRPOW
      WRITE (6,150) SERESL, SERESP, SERESE, SERPOW
      WRITE (6,160) RLIN, RTESTL, RPARA, RTESTP, RELIP, RTESTE, RPOWE,
     1RTEPOW, MDF
      WRITE (6,170)
      WRITE (6,180)
      WRITE (6,190) TLP, IDFT, FLP, IDFF, IDFF
      WRITE (6,200) TPE, IDFT, FPE, IDFF, IDFF
      WRITE (6,210) TLE, IDFT, FLE, IDFF, IDFF
      WRITE (6,220) TLPOW, IDFT, FLPOW, IDFF, IDFF
      WRITE (6,230) TPPOW, IDFT, FPPOW, IDFF, IDFF
      WRITE (6,240) TEPOW, IDFT, FEPOW, IDFF, IDFF
      WRITE (6,250)
      WRITE (6,260)
      WRITE (6,270)
      WRITE (6,280) RMCONS, ACONST, IXMAX, YMAX, POWA, POWN
   90 FORMAT ('0', 20X, 'RESULTS FOR ARCH NO. ', I2)
  100 FORMAT (1X, 10X, 'ANALYSIS OF RESIDUALS FROM APPROPRIATE FIT')
  110 FORMAT ('0', 'ANGLE TO APEX OF ROOF', F4.1)
  120 FORMAT ('0', 9X, 'LINEAR', 7X, 'PARABOLA', 7X, 'ELIPSE', 8X,
     1        'POWER')
  130 FORMAT ('0', 'NUMBER', 5X, I3, 12X, I3, 12X, I3, 12X, I3)
  140 FORMAT (1X, 'MEAN', 2X, F11.4, 3X, F11.4, 2(3X,F11.4))
  150 FORMAT (1X, 'S.E.', 2X, F11.4, 3X, F11.4, 2(3X,F11.4))
  160 FORMAT (1X, 'R (T) ', F5.3, 1X, F5.1, 3(3X,F5.3,1X,F5.1), 2X,
     1        'DF=', I3/)
  170 FORMAT ('0', 15X, 'T AND F TESTS OF SIGNIFICANCE')
  180 FORMAT ('0', 'BETWEEN', 16X, 'T', 8X, 'DF', 8X, 'F', 10X, 'DF')
  190 FORMAT ('0', 'LINEAR/PARABOLA', 3X, F11.4, 2X, I3, 3X, F11.4, 3X,
     1        I2, ',', I2)
  200 FORMAT (1X, 'PARABOLA/ELIPSE', 3X, F11.4, 2X, I3, 3X, F11.4, 3X,
     1        I2, ',', I2)
  210 FORMAT (1X, 'LINEAR/ELIPSE', 5X, F11.4, 2X, I3, 3X, F11.4, 3X, I2,
     1        ',', I2)
  220 FORMAT (1X, 'LINEAR/POWER   ', 3X, F11 4, 2X, I3, 3X, F11 4, 3X,
```

```
     1       I2, ',', I2)
230  FORMAT (1X, 'PARABOLA/POWER ', 3X, F11.4, 2X, I3, 3X, F11.4, 3X,
     1       I2, ',', I2)
240  FORMAT (1X, 'ELIPSE/POWER ', 5X, F11.4, 2X, I3, 3X, F11.4, 3X, I2
     1       ',', I2)
250  FORMAT ('0', 17X, 'COEFFICIENTS FOR EQUATIONS')
260  FORMAT (1X, 'COEFFICIENT')
270  FORMAT (1X, 11X, 'M', 13X, 'A', 10X, 'A', 6X, 'B')
280  FORMAT ('0', 9X, F5.2, 8X, F6.2, 7X, I3, 2X, F6.2, 2X, F7 4, 1X,
     1       F6.4)
      STOP
      END
```